



Modelling air quality in the Surat Basin, Queensland

Julie Noonan, Martin Cope, Sarah J. Lawson, Jennifer C. Powell, Suzie Molloy, Marcus Thatcher and Kathryn Emmerson 2019

Final Report for the Gas Industry Social and Environmental Research Alliance (GISERA), Project No G.3

ISBN (print): 978-1-4863-1285-6

ISBN (online): 978-1-4863-1286-3

Citation

Julie Noonan, Martin Cope, Sarah J. Lawson, Jennifer C. Powell, Suzie Molloy, Marcus Thatcher and Kathryn Emmerson, 2019 Modelling air quality in the Surat Basin, Queensland 2019, CSIRO, Australia.

Copyright

© Commonwealth Scientific and Industrial Research Organisation 2019. To the extent permitted by law, all rights are reserved and no part of this publication covered by copyright may be reproduced or copied in any form or by any averages except with the written permission of CSIRO.

Important disclaimer

CSIRO advises that the information contained in this publication comprises general statements based on scientific research. The reader is advised and needs to be aware that such information may be incomplete or unable to be used in any specific situation. No reliance or actions must therefore be made on that information without seeking prior expert professional, scientific and technical advice. To the extent permitted by law, CSIRO (including its employees and consultants) excludes all liability to any person for any consequences, including but not limited to all losses, damages, costs, expenses and any other compensation, arising directly or indirectly from using this publication (in part or in whole) and any information or material contained in it.

CSIRO is committed to providing web accessible content wherever possible. If you are having difficulties with accessing this document please contact csiroenquiries@csiro.au.

Contents

Acknowledgments.....	xiii
Glossary	xiv
Executive summary	xvii
1 Introduction	23
2 The CTM modelling system	26
3 Emission Inventory	31
3.1 Surat Basin anthropogenic emission inventory.....	32
3.2 Australian emissions inventories (including soil, bushfires, vegetation and wider anthropogenic sources)	Error! Bookmark not defined.
3.3 Assumptions, uncertainties and exclusions	38
4 Observational data	43
5 Results and Discussion.....	46
5.1 PM _{2.5}	50
5.2 Ozone.....	73
5.3 Nitrogen Dioxide.....	92
5.4 Carbon Monoxide	113
5.5 Air Toxics.....	127
5.6 Representativeness of observation sites to wider region.....	156
5.7 Implications of model assumptions, uncertainties and exclusions.....	162
5.8 Relationship of the model findings to the monitoring study	164
6 Summary and next steps	165
6.1 Summary of the study findings.....	165
6.2 Significance of this study and next steps	166
7 References	168
Appendix A CCAM meteorological performance.....	174
Appendix B CTM Performance Information	191
Appendix C Sources and methodologies for local anthropogenic emission inventory.....	203
Appendix D CTM-CCAM Time Series Plots.....	217
Appendix E Extra plots: Modelled effect of CSG at various sites	306
Appendix F Extra plots: O ₃ 1-hour averages.....	335

Appendix G Extra Town sites frequency plots 345

Figures

Figure 1.1 Study area including the regional modelling area (source: Lawson et al., 2017b).....	25
Figure 2.1 Schematic diagram showing the CCAM-CTM modelling framework used to simulate interactive emissions, transport and chemical transformation.	27
Figure 2.2 The CTM modelling grids: outer 50 km grid (50 km grid squares) with nested inner grids 9, 3 and 1 km.	29
Figure 2.3 Grids for the CTM modelling system - 3 and 1 km inner model grids and the Surat emissions inventory grid. Gas field sites (green and yellow) are ‘MAQ’ - Miles Airport air quality station, ‘CAQ’ - Condamine air quality station and ‘HAQ’ - Hopeland air quality station. Regional sites (green and yellow) are ‘TAQ’ - Tara Region air quality station, ‘BAQ’ - Burncluith air quality station. ‘Town’ sites (blue) are Chinchilla, Miles township, Roma, Tara township and Warra.....	30
Figure 3.1 Total air emissions for individual pollutants (kg/annum) for the Surat Basin region, from the Surat Basin emissions inventory. Data source: Katestone 2017.	33
Figure 3.2 The Surat Basin Air Emissions Inventory – Source contribution (%) by industry sector or activity (from Katestone 2017). The Source Contribution scale ranges from 0 – 100%.	34
Figure 3.3 The emissions inventory grid as well as nested 3 and 1 km modelling grids. Locations of the modelled CSG-related emission sources are also shown: blue = well areas, high point vent areas, other area sources, pink = stacks, flares, other point sources.....	36
Figure 5.1 The observed and modelled time series of the 1-hour average PM _{2.5} concentrations (µg m ⁻³) at Miles Airport for the modelled year (red = model results with all sources, purple = model results without CSG sources, blue = observations).	51
Figure 5.2 The modelled contributions from the CSG-related emissions to the 1-hour average PM _{2.5} concentrations (µg m ⁻³) at Miles Airport for the modelled year.	52
Figure 5.3 Satellite picture on the 16/9/15 about midday (Terra / MODIS) showing a number of different areas of smoke, small red spots are ‘hot spots’, the blue dot locates Miles township and the Burncluith Air Quality station is indicated by an arrow (NASA Worldview, https://worldview.earthdata.nasa.gov/).	54
Figure 5.4 Spatial plots from the model results with all sources (left) PM _{2.5} (µg m ⁻³) and (right) levoglucosan (smoke tracer) (µg m ⁻³), both are at 06:00 AEST on the 7 th October 2015.	55
Figure 5.5 The modelled contribution from the CSG-related emissions to the 24-hour average PM _{2.5} concentration (µg m ⁻³) at the Gas field and Regional sites shown as a frequency distribution for each season. The x-axis shows the concentration ranges of the contribution from the CSG-related emissions and the y-axis shows the percentage of model hours.	56
Figure 5.6 The modelled contribution from the CSG-related emissions to the 24-hour average PM _{2.5} concentration (µg m ⁻³) at Miles Airport shown as a scatter plot for each season. The x-axis shows the modelled 24-hour average PM _{2.5} concentrations with all sources (µg m ⁻³) and the y-axis shows the contribution from the CSG-related emissions to the 24-hour average PM _{2.5} concentration (µg m ⁻³).	57

Figure 5.7 The maximum 24-hour average PM _{2.5} concentrations (µg m ⁻³) for each month of September 2015 – August 2016 at the Gas field and Regional sites: observed (blue), model results with all sources (red) and model results without the CSG sources (purple).	59
Figure 5.8 The maximum concentration of the 24-hour average PM _{2.5} in each grid square for the model results with all sources during each season (µg m ⁻³). Note that the maximum concentrations shown in each grid square may be from different days during the season. The red arrow indicates the location of the maximum value for the season.	61
Figure 5.9 The maximum concentration of the 24-hour average levoglucosan (smoke tracer) in each grid square for the model results with all sources during each season (µg m ⁻³). Note that the maximum concentrations shown in each grid square may be from different days during the season. The red arrow indicates the location of the maximum value for the season.	62
Figure 5.10 The contribution of the CSG-related emissions to the modelled maximum 24-hour average PM _{2.5} concentration (maximum in each grid square from Figure 5.8) during each season (µg m ⁻³). Note that the concentrations shown in each grid square may be from different days during the season. The red arrow indicates the location of the maximum value for the season. ...	63
Figure 5.11 The maximum contribution of the CSG-related emissions to the modelled 24-hour average PM _{2.5} concentrations during the modelled year (µg m ⁻³). Note that the concentrations shown in each grid square may be from different days during the year. The red arrow indicates the location of the maximum value for the year.	64
Figure 5.12 The locations, marked by red crosses, of the modelled 24-hour average PM _{2.5} concentrations (left) that exceed the air quality objective (25 µg m ⁻³) or (right) that exceed 80 % of the air quality objective (20 µg m ⁻³). All exceedances are when the contribution of the CSG-related emissions is greater than 1 µg m ⁻³	66
Figure 5.13 The modelled maximum 24-hour average PM _{2.5} concentrations (µg m ⁻³) for each month of September 2015 – August 2016 at the Town sites: model results with all sources (red) and model results without the CSG sources (purple).	68
Figure 5.14 The modelled contribution from the CSG-related emissions to the 24-hour average PM _{2.5} concentration (µg m ⁻³) at the Town sites shown as a frequency distribution for each season. The x-axis shows the concentration ranges of the contribution from the CSG-related emissions and the y-axis shows the percentage of model hours.	69
Figure 5.15 The modelled contribution from the CSG-related emissions to the 24-hour average PM _{2.5} concentration (µg m ⁻³) at Miles township shown as a scatter plot for each season. The x-axis shows the modelled 24-hour average PM _{2.5} concentrations with all sources (µg m ⁻³) and the y-axis shows the contribution from the CSG-related emissions to the 24-hour average PM _{2.5} concentration (µg m ⁻³).	70
Figure 5.16 The observed and modelled time series of the 1-hour average O ₃ concentrations (ppb) at Miles Airport for the modelled year (red = model results with all sources, purple = model results without CSG sources, blue = observations).	75
Figure 5.17 The modelled contributions from the CSG-related emissions to the 1-hour average O ₃ concentrations (ppb) at Miles Airport for the modelled year.	76

Figure 5.18 The modelled contribution from the CSG-related emissions to the 4-hour average O ₃ concentration (ppb) at the Gas field and Regional sites shown as a frequency distribution for each season. The x-axis shows the concentration ranges of the contribution from the CSG-related emissions and the y-axis shows the percentage of model hours.	78
Figure 5.19 The modelled contribution from the CSG-related emissions to the 4-hour average O ₃ concentration (ppb) at Miles Airport shown as a scatter plot for each season. The x-axis shows the modelled 4-hour average O ₃ concentrations with all sources (ppb) and the y-axis shows the contribution from the CSG-related emissions to the 4-hour average O ₃ concentration (ppb).....	79
Figure 5.20 The maximum 4-hour average O ₃ concentrations (ppb) for each month of September 2015 – August 2016 at the Gas field and Regional sites: observed (blue), model results with all sources (red) and model results without the CSG sources (purple).	81
Figure 5.21 The maximum concentration of the 4-hour average O ₃ in each grid square for the model results with all sources during each season (ppb). Note that the maximum concentrations shown in each grid square may be from different time periods. The red arrow indicates the location of the maximum value for the season.	83
Figure 5.22 The contribution of the CSG-related emissions to the modelled maximum 4-hour average O ₃ concentration (maximum in each grid square from Figure 5.21) during each season (ppb). Note that the concentrations shown in each grid square may be from different time periods. The red arrow indicates the location of the maximum value for the season.	84
Figure 5.23 The maximum contribution of the CSG-related emissions to the modelled 4-hour average O ₃ concentrations during the modelled year (ppb). Note that the concentrations shown in each grid square may be from different time periods. The red arrow indicates the location of the maximum value for the year.	85
Figure 5.24 The locations, marked by red crosses, of the modelled 4-hour average O ₃ concentrations that exceed 80 % of the air quality objective (64 ppb), when the contribution of the CSG-related emissions is greater than 2 ppb.	87
Figure 5.25 The modelled maximum 4-hour average O ₃ concentrations (ppb) for each month of September 2015 – August 2016 at the Town sites: model results with all sources (red) and model results without the CSG sources (purple).....	88
Figure 5.26 The modelled contribution from the CSG-related emissions to the 4-hour average O ₃ concentration (ppb) at the Town sites shown as a frequency distribution for each season. The x-axis shows the concentration ranges of the contribution from the CSG-related emissions and the y-axis shows the percentage of model hours.....	89
Figure 5.27 The modelled contribution from the CSG-related emissions to the 4-hour average O ₃ concentration (ppb) at Warra shown as a scatter plot for each season. The x-axis shows the modelled 4-hour average O ₃ concentrations with all sources (ppb) and the y-axis shows the contribution from the CSG-related emissions to the 4-hour average O ₃ concentration (ppb).....	90
Figure 5.28 The observed and modelled time series of the 1-hour average NO ₂ concentrations (ppb) at Miles Airport for the modelled year (red = model results with all sources, purple = model results without CSG sources, blue = observations).	95

Figure 5.29 The modelled contributions from the CSG-related emissions to the 1-hour average NO ₂ concentrations (ppb) at Miles Airport for the modelled year.....	96
Figure 5.30 The observed and modelled time series of the 1-hour average NO ₂ concentrations (ppb) at Miles Airport from 1/5/16 00:00 AEST to 12/5/16 00:00 AEST (top panel: red = model results with all sources, purple = model results without CSG sources, mid- blue = observations; bottom panel: green = model results with all model stacks removed, pink = model results with all model ‘Producer 1’ stacks removed, light-blue = model results with all model ‘Producer 2’ stacks removed and dark blue = model results with only the model stack closest to Miles Airport removed).....	97
Figure 5.31 The modelled contribution from the CSG-related emissions to the 1-hour average O ₃ concentrations and the modelled contribution from the CSG-related emissions to the 1-hour average NO ₂ concentration for a sub-set of MAM (ppb) at Miles Airport.	97
Figure 5.32 The modelled contribution from the CSG-related emissions to the 1-hour average NO ₂ concentration (ppb) at the Gas field and Regional sites shown as a frequency distribution for each season. The x-axis shows the concentration ranges of the contribution from the CSG-related emissions and the y-axis shows the percentage of model hours.	98
Figure 5.33 The modelled contribution from the CSG-related emissions to the 1-hour average NO ₂ concentration (ppb) at Miles Airport shown as a scatter plot for each season. The x-axis shows the modelled 1-hour average NO ₂ concentrations with all sources (ppb) and the y-axis shows the contribution from the CSG-related emissions to the 1-hour average NO ₂ concentrations (ppb).....	100
Figure 5.34 The maximum 1-hour average NO ₂ concentrations (ppb) for each month of September 2015 – August 2016 at the Gas field and Regional sites: observed (blue), model results with all sources (red) and model results without the CSG sources (purple).	102
Figure 5.35 The maximum concentration of the 1-hour average NO ₂ in each grid square for the model results with all sources during each season (ppb). Note that the maximum concentrations shown in each grid square may be from different time periods. The red arrow indicates the location of the maximum value for the season.	103
Figure 5.36 The contribution of the CSG-related emissions to the modelled maximum 1-hour average NO ₂ concentration (maximum in each grid square from Figure 5.35) during each season (ppb). Note that the concentrations shown in each grid square may be from different time periods. The red arrow indicates the location of the maximum value for the season.	104
Figure 5.37 The maximum contribution of the CSG-related emissions to the modelled 1-hour average NO ₂ concentrations during the modelled year (ppb). Note that the concentrations shown in each grid square may be from different time periods. The red arrow indicates the location of the maximum value for the year.	105
Figure 5.38 The location, marked by a red cross, of the modelled 1-hour average NO ₂ concentration that exceeds 80 % of the air quality objective (96 ppb).	106
Figure 5.39 The modelled maximum 1-hour average NO ₂ concentrations (ppb) for each month of September 2015 – August 2016 at the Town sites: model results with all sources (red) and model results without the CSG sources (purple).	108

Figure 5.40 The modelled contribution from the CSG-related emissions to the 1-hour average NO ₂ concentration (ppb) at the Town sites shown as a frequency distribution for each season. The x-axis shows the concentration ranges of the contribution from the CSG-related emissions and the y-axis shows the percentage of model hours.....	109
Figure 5.41 The modelled contribution from the CSG-related emissions to the 1-hour average NO ₂ concentration (ppb) at Miles township shown as a scatter plot for each season. The x-axis shows the modelled 1-hour average NO ₂ concentrations with all sources (ppb) and the y-axis shows the contribution from the CSG-related emissions to the 1-hour average NO ₂ concentration (ppb).	110
Figure 5.42 The observed and modelled time series of the 1-hour average CO concentrations (ppb) at Burncluth for the modelled year (red = model results with all sources, purple = model results without CSG sources, blue = observations). (peaks off scale: model, 15/9/15 21:00 = 6302 ppb, OBS 16/9/15 15:00 = 1170 ppb, 25/9/15 08:00 1143 ppb).....	115
Figure 5.43 The modelled contributions from the CSG-related emissions to the 1-hour average CO concentrations (ppb) at Burncluth for the modelled year.....	116
Figure 5.44 The modelled contribution from the CSG-related emissions to the 8-hour average CO concentration (ppb) at the Gas field and Regional sites shown as a frequency distribution for each season. The x-axis shows the concentration ranges of the contribution from the CSG-related emissions and the y-axis shows the percentage of model hours.	117
Figure 5.45 The modelled contribution from the CSG-related emissions to the 8-hour average CO concentration (ppb) at Miles Airport shown as a scatter plot for each season. The x-axis shows the modelled 8-hour average CO concentrations with all sources (ppb) and the y-axis shows the contribution from the CSG-related emissions to the 8-hour average CO concentrations (ppb).....	118
Figure 5.46 The maximum 8-hour average CO concentrations (ppb) for each month of September 2015 – August 2016 at the Gas field and Regional sites: observed (blue), model results with all sources (red) and model results without the CSG sources (purple).	119
Figure 5.47 The maximum concentration of the 8-hour average CO in each grid square for the model results with all sources during each season (ppb). Note that the maximum concentrations shown in each grid square may be from different time periods. The red arrow indicates the location of the maximum value for the season.	120
Figure 5.48 The contribution of the CSG-related emissions to the modelled maximum 8-hour average CO concentration (maximum in each grid square from Figure 5.47) during each season (ppb). Note that the concentrations shown in each grid square may be from different time periods. The red arrow indicates the location of the maximum value for the season.	121
Figure 5.49 The maximum contribution of the CSG-related emissions to the modelled 8-hour average CO concentrations during the modelled year (ppb). Note that the concentrations shown in each grid square may be from different time periods. The red arrow indicates the location of the maximum value for the year.	122

Figure 5.50 The modelled maximum 8-hour average CO concentrations (ppb) for each month of September 2015 – August 2016 at the Town sites: model results with all sources (red) and model results without the CSG sources (purple).....	123
Figure 5.51 The modelled contribution from the CSG-related emissions to the 8-hour average CO concentration (ppb) at the Town sites shown as a frequency distribution for each season. The x-axis shows the concentration ranges of the contribution from the CSG-related emissions and the y-axis shows the percentage of model hours.....	124
Figure 5.52 The modelled contribution from the CSG-related emissions to the 8-hour average CO concentration (ppb) at Warra shown as a scatter plot for each season. The x-axis shows the modelled 8-hour average CO concentrations with all sources (ppb) and the y-axis shows the contribution from the CSG-related emissions to the 8-hour average CO concentration (ppb).....	125
Figure 5.53 The observed (2-week sampling period) and modelled (1-hour average) time series of the formaldehyde concentrations (ppb) at Chinchilla for the modelled year (red = model results with all sources, purple = model results without CSG sources, blue = observations). (peak off scale: model, 16/9/15 21:00 = 15.3 ppb)	129
Figure 5.54 The modelled contributions from the CSG-related emissions to the 1-hour average formaldehyde concentrations (ppb) at Chinchilla for the modelled year.....	130
Figure 5.55 The observed (2-week sampling period) and modelled (1-hour average) time series of benzene concentrations (ppb) at Chinchilla for the modelled year (red = model results with all sources, purple = model results without CSG sources, blue = observations). (peaks off scale: model, 15/9/15 12:00 = 0.5 ppb, 16/9/15 00:00, 05:00, 21:00 = 1.2, 1.2, 3.0 ppb, 7/10/15 06:00 = 0.4 ppb, 10/8/16 07:00, 21:00 = 0.82,0.60 ppb).....	131
Figure 5.56 The modelled contributions from the CSG-related emissions to the 1-hour average benzene concentrations (ppb) at Chinchilla for the modelled year.....	132
Figure 5.57 The modelled contribution from the CSG-related emissions to the 24 -hour average formaldehyde concentration (ppb) at the Gas field and Regional sites shown as a frequency distribution for each season. The x-axis shows the concentration ranges of the contribution from the CSG-related emissions and the y-axis shows the percentage of model hours.	133
Figure 5.58 The modelled contribution from the CSG-related emissions to the 24-hour average benzene concentration (ppb) at the Gas field and Regional sites shown as a frequency distribution for each season. The x-axis shows the concentration ranges of the contribution from the CSG-related emissions and the y-axis shows the percentage of model hours.	134
Figure 5.59 The modelled contribution from the CSG related emissions to the 24-hour average formaldehyde concentration (ppb) at Miles Airport shown as a scatter plot for each season. The x-axis shows the modelled 24-hour average formaldehyde concentrations with all sources (ppb) and the y-axis shows the contribution from the CSG-related emissions to the 24-hour average formaldehyde concentration (ppb).	135
Figure 5.60 The modelled contribution from the CSG related emissions to the 24-hour average benzene concentration (ppb) at Miles Airport shown as a scatter plot for each season. The x-axis shows the modelled 24-hour average benzene concentrations with all sources (ppb) and	

the y-axis shows the contribution from the CSG-related emissions to the 24-hour average benzene concentration (ppb).	136
Figure 5.61 The maximum 24-hour average formaldehyde concentrations (ppb) for each month of September 2015 – August 2016 at the Gas field and Regional sites: model results with all sources (red) and model results without the CSG sources (purple).....	138
Figure 5.62 The maximum 24-hour average benzene concentrations (ppb) for each month of September 2015 – August 2016 at the Gas field and Regional sites: model results with all sources (red) and model results without the CSG sources (purple).....	139
Figure 5.63 The maximum concentration of the 24-hour average formaldehyde in each grid square for the model results with all sources during each season (ppb). Note that the maximum concentrations shown in each grid square may be from different days during the season. The red arrow indicates the location of the maximum value for the season.	141
Figure 5.64 The contribution of the CSG-related emissions to the modelled maximum 24-hour average formaldehyde concentration (maximum in each grid square from Figure 5.63) during each season (ppb). Note that the concentrations shown in each grid square may be from different days during the season. The red arrow indicates the location of the maximum value for the season.	142
Figure 5.65 The maximum concentration of the 24-hour average benzene in each grid square in the model results with all sources during each season (ppb). Note that the maximum concentrations shown in each grid square may be from different days during the season. The red arrow indicates the location of the maximum value for the season.	143
Figure 5.66 The contribution of the CSG-related emissions to the modelled maximum 24-hour average benzene concentration (maximum in each grid square from Figure 5.65) during each season (ppb). Note that the concentrations shown in each grid square may be from different days during the season. The red arrow indicates the location of the maximum value for the season.	144
Figure 5.67 The maximum contribution of the CSG-related emissions to the modelled 24-hour average formaldehyde concentrations during the modelled year (ppb). Note that the concentrations shown in each grid square may be from different days during the year. The red arrow indicates the location of the maximum value for the year.....	145
Figure 5.68 The maximum contribution of the CSG-related emissions to the modelled 24-hour average benzene concentrations during the modelled year (ppb). Note that the concentrations shown in each grid square may be from different days during the year. The red arrow indicates the location of the maximum value for the year.....	146
Figure 5.69 The modelled maximum 24-hour average formaldehyde concentrations (ppb) for each month of September 2015 – August 2016 at the Town sites: model results with all sources (red) and model results without the CSG sources (purple).....	148
Figure 5.70 The modelled maximum 24-hour average benzene concentrations (ppb) for each month of September 2015 – August 2016 at the Town sites: model results with all sources (red) and model results without the CSG sources (purple).....	149

Figure 5.71 The modelled contribution from the CSG-related emissions to the 24-hour average formaldehyde concentration (ppb) at the Town sites shown as a frequency distribution for each season. The x-axis shows the concentration ranges of the contribution from the CSG-related emissions and the y-axis shows the percentage of model hours.....	150
Figure 5.72 The modelled contribution from the CSG-related emissions to the 24-hour average benzene concentration (ppb) at the Town sites shown as a frequency distribution for each season. The x-axis shows the concentration ranges of the contribution from the CSG-related emissions and the y-axis shows the percentage of model hours.....	151
Figure 5.73 The modelled contribution from the CSG-related emissions to the 24-hour average formaldehyde concentration (ppb) at Chinchilla shown as a scatter plot for each season. The x-axis shows the modelled 24-hour average formaldehyde concentrations with all sources (ppb) and the y-axis shows the contribution from the CSG-related emissions to the 24-hour average formaldehyde concentration (ppb).	152
Figure 5.74 The modelled contribution from the CSG-related emissions to the 24-hour average benzene concentration (ppb) at Warra shown as a scatter plot for each season. The x-axis shows the modelled 24-hour average benzene concentrations with all sources (ppb) and the y-axis shows the contribution from the CSG-related emissions to the 24-hour average benzene concentration (ppb).	153
Figure 5.75 Locations of the air quality monitoring sites (green and yellow squares), 'Town sites' (blue) and 'Extra Town sites' (red) on the 1 km modelling grid. Locations of the modelled CSG-related emission sources are also shown, blue = well areas, high point vent areas, other area sources, pink = stacks, flares, other point sources.	156
Figure 5.76 Percentage of model hours in the year where the contribution to the 24-hour average PM _{2.5} concentration due to the CSG-related emission is greater than 0.25 µg m ⁻³ (red) or greater than 0.5 µg m ⁻³ ppb (blue). Note that 0.25 and 0.5 µg m ⁻³ are 1 and 2 % respectively of the 24-hour PM _{2.5} air quality objective.	157
Figure 5.77 Percentage of model hours in the year where the contribution to the 4-hour average O ₃ concentration due to the CSG-related emissions is greater than 2 (or less than -2) ppb (red) or greater than 5 (or less than -5) ppb (blue). Note that 2 and 5 ppb are 2.5 and 6.25 % respectively of the 4-hour O ₃ air quality objective.	158
Figure 5.78 Percentage of model hours in the year where the contribution to the 1-hour average NO ₂ concentration due to the CSG-related emissions is greater than 2.5 ppb (red) or greater than 5 ppb (blue). Note that 2.5 and 5 ppb are 2 and 4 % respectively of the 1-hour NO ₂ air quality objective.....	159
Figure 5.79 Percentage of model hours in the year where the contribution to the 8-hour average CO concentration due to the CSG-related emissions is greater than 6 ppb (red) or greater than 10 ppb (blue). Note that 6 and 10 ppb are 0.07 and 0.1 % respectively of the 8-hour CO air quality objective.	159
Figure 5.80 Percentage of model hours in the year where the contribution to the 24-hour average formaldehyde concentration due to the CSG-related emissions is greater than 0.1 (red)	

or greater than 0.2 (blue) ppb. Note that 0.1 and 0.2 ppb are 0.25 and 0.5 % respectively of the 24-hour formaldehyde air quality objective. 160

Tables

Table 5.1 Air quality objectives used to assess concentrations in this report.....	48
Table 5.2 The observed and modelled annual average concentrations of PM _{2.5} (µg m ⁻³) at the Gas field and Regional sites.	58
Table 5.3 The 8 modelled 24-hour average PM _{2.5} concentrations that exceed the air quality objective (25 µg m ⁻³) and the 8 modelled 24-hour average PM _{2.5} concentrations of the 15 exceedances of 80 % of the air quality objective (20 µg m ⁻³) with the highest contribution of the CSG-related emissions. The contribution (µg m ⁻³) and the percentage contribution of the CSG-related emissions to the exceedances are also included.	65
Table 5.4 The modelled annual average concentrations of PM _{2.5} (µg m ⁻³) at the Town sites.	67
Table 5.5 Eight of the 120 exceedances of 80 % of the air quality objective (64 ppb) for the 4-hour average O ₃ concentrations with the highest contribution of the CSG-related emissions. The contribution (ppb) and the percentage contribution of the CSG-related emissions to the exceedances are also included.	86
Table 5.6 The observed and modelled annual average concentrations of NO ₂ (ppb) at the Gas field and Regional sites.	101
Table 5.7 The two values of modelled 1-hour average NO ₂ concentrations that exceed 80 % of the air quality objective (96 ppb) and the contribution (ppb) and the percentage contribution of the CSG-related emissions to the exceedances.....	106
Table 5.8 The modelled annual average concentrations of NO ₂ (ppb) at the Town sites.....	107
Table 5.9 The annual average modelled concentrations of formaldehyde and benzene (ppb). The six-month-average observations of formaldehyde except at Hopeland where they are 7-month average observations. The annual average observations of benzene (ppb) from 20-22/1/15 to 27-29/1/16 (see Lawson et al., 2018a for discussion of observations).	137
Table 5.10 The modelled annual average concentrations of formaldehyde and benzene (ppb) at the Town sites.....	147

Acknowledgments

This project is supported by the Gas Industry Social and Environmental Research Alliance (GISERA). GISERA undertakes publicly-reported independent research that addresses the socioeconomic and environmental impacts of Australia's natural gas industries. For further information visit www.gisera.org.au.

Our thanks to several people who reviewed and provided feedback on this report including Ashok Luhar (CSIRO) and Hugh Malfroy (Malfroy Environmental Strategies Pty Ltd).

Many thanks to Matt Kernke (Origin), Graeme Starke (formerly of QGC) and Kelsey Bawden (Arrow) for providing emission inventory data.

Data and/or imagery from the following sources was used to identify locations and occurrence of fires in the study region - LANCE FIRMS operated by NASA's Earth Science Data and Information System (ESDIS) with funding provided by NASA Headquarters, and the NASA Worldview application (<https://worldview.earthdata.nasa.gov/>), part of the NASA Earth Observing System Data and Information System (EOSDIS). This report contains modified Copernicus Atmosphere Monitoring Service Information [2015 and 2016] and neither the European Commission nor ECMWF is responsible for any use that may be made of the information it contain.

Glossary

Units of measurement

km – kilometre

$\mu\text{g m}^{-3}$ – micrograms per cubic metre (1 microgram = one millionth of a gram)

ppm – parts per million by volume

ppmC – parts per million of volume of gaseous carbon contained in one million volumes of air

ppb – parts per billion by volume

Nomenclature

Boundary layer – The part of the atmosphere that directly feels the effect of the earth's surface (a few metres to several kilometres deep).

Gas field sites – Miles Airport, Condamine and Hopeland

Gas processing facility – facility which compresses and dries gas

Gathering networks – network of pipes which carry gas and water to treatment and processing facilities

Levogluosan – a chemical product unique to the combustion of wood, can be used as a smoke tracer in a model

Model with all sources – model run with all emission sources *including* the CSG emission sources

Model without CSG sources – model run with all emission sources *excluding* CSG-related emission sources

Pipeline compressor stations – facilities which compress gas along a gas pipeline

Regional sites – Tara Region and Burncluith

Secondary pollutant – a pollutant that is not directly emitted to the atmosphere but formed through reactions between other pollutants in the atmosphere.

Tracer – a gas or particle measurement used as a proxy for other atmospheric constituents not directly measured, or used to indicate the possible impact of a specific pollution source

Water treatment facility – facility which treats produced water from the wells

Wellhead gas and water – gas and water sampled from the separator at an individual CSG wellhead

Abbreviations

APLNG – Australia Pacific Liquefied Natural Gas

BTX – a subset of VOCs including benzene, toluene and xylenes

CAMS – Copernicus Atmosphere Monitoring Service

CCAM – Conformal Cubic Atmospheric Model

CH₄ – methane

CO – carbon monoxide

CO₂ – carbon dioxide

C-SEM – CSIRO smoke emissions model

CSG – Coal Seam Gas

CTM – Chemical Transport Model

DES – Department of Environment and Science

DJF – December 2015, January 2016 and February 2016

DNRME – Department of Natural Resources, Mines and Energy, Queensland

ECMWF – European Centre for Medium-Range Weather Forecasts

EIS – Environmental Impact Statement

EPP – Queensland Environmental Protection (Air) Policy

GMR – Greater Metropolitan Region (NSW)

GPF – gas processing facility

JJA – June, July and August 2016

MAM – March, April and May 2016

NEPM – National Environment Protection Measure

NH₃ – ammonia

NMOC – non-methane organic compound

NO_x – nitrogen oxides, includes nitric oxide (NO) and nitrogen dioxide (NO₂)

NO₂ – nitrogen dioxide

NPI – National Pollutant Inventory

O₃ – ozone

OBS - observations

PM_{2.5} – particles with an aerodynamic diameter of < 2.5 μm

PM₁₀ – particles with an aerodynamic diameter of < 10 μm

PM – particulate matter

SEQR – South East Queensland Region

SON – September, October and November 2015

Texas AMCV - Texas Commission on Environmental Quality air Monitoring Comparison Values

TVOC – total volatile organic compounds

TSP – total suspended particles

VOC – volatile organic compounds

WTF – water treatment facility

Executive summary

The rapid expansion of coal seam gas (CSG) production in the Surat Basin in Queensland in recent years has raised community concerns about the potential impact of the industry on the air quality in the region. The GISERA project G.3 “Ambient air quality, Surat Basin, Queensland” has provided the first comprehensive assessment of air quality in the Surat Basin using an air quality observation network and detailed air quality chemical transport modelling. These studies will inform industry, the community and the government about the potential impact of CSG production on a variety of key air quality parameters in the Surat Basin. This report delivers Task 3 of the project by presenting the air quality modelling component of the study and assessing the overall potential impact of CSG production activities on air pollutants levels in the Surat Basin.

The aims of this air quality modelling study were

1. To assess the impact of CSG operations on ambient levels of nitrogen oxides (NO_x), carbon monoxide (CO), ozone (O₃), volatile organic compounds (VOCs) and particulate matter (PM) in the Surat Basin over an entire year (Sep 2015 –Aug 2016). This differs from the approach used in the monitoring study (Lawson et al 2018 a, b) in which the CSG-related contribution to air pollutants was investigated only during air quality exceedances and other periods of elevated concentrations. The modelling study presented here examines the impact of emissions from a wide range of operational activities associated with the CSG industry in the Surat Basin in 2015-2016 as well as a range of non-CSG sources, both anthropogenic and natural. The model does not include emissions associated with the development of CSG-related infrastructure or infrequent/incidental CSG operational activities.
2. To determine spatial variability of nitrogen oxides (NO_x), carbon monoxide (CO), ozone (O₃), volatile organic compounds (VOCs) and particulate matter (PM) in the Surat Basin to ensure the location of the three Gas field ambient air quality monitoring sites (Lawson et al 2018c) were representative of regional air quality.

This report describes the modelling system and emissions inventory, presents the modelled results and describes model assumptions, uncertainties and limitations of the study.

Method

Air quality modelling was undertaken using the CSIRO Chemical Transport Model (CTM) (Cope et al., 2004, 2014), with meteorology generated using the Conformal Cubic Atmospheric Model (CCAM) (McGregor, 2015). CCAM provides meteorological data, such as wind and temperature, as hourly inputs to the CTM, which then models the interactive emission, transport, chemical transformation and wet and dry deposition of a mixed gas and aerosol phase system. The CTM has been used extensively in Australia by CSIRO for modelling urban- and regional-scale photochemical smog production and smoke impacts, including primary and secondary aerosol mass. (Cope et al., 2004, 2009, 2014, 2019; Emmerson et al., 2016; Galbally et al. 2008; Keywood et al. 2015; Lawson et al., 2017a; Luhar et al., 2008; Meyer et al., 2008).

The model was run with a 50 km spaced outermost grid covering the Australian region, with three nested grids with grid spacing of 9, 3 and 1 km (see Figure 1). The year from September 2015 through to August 2016 was modelled because meteorological and ambient air monitoring data from the sites at Miles Airport, Condamine, Hopeland, Tara region and Burncluith were available for all or part of that time to compare with the model output, and because the year overlapped with the period of highest rate of CSG production in the region at the time. The model simulated the interactive emission, transport and transformations of pollutants in the air over the Surat Basin at 1 km resolution for every hour of the modelled year.

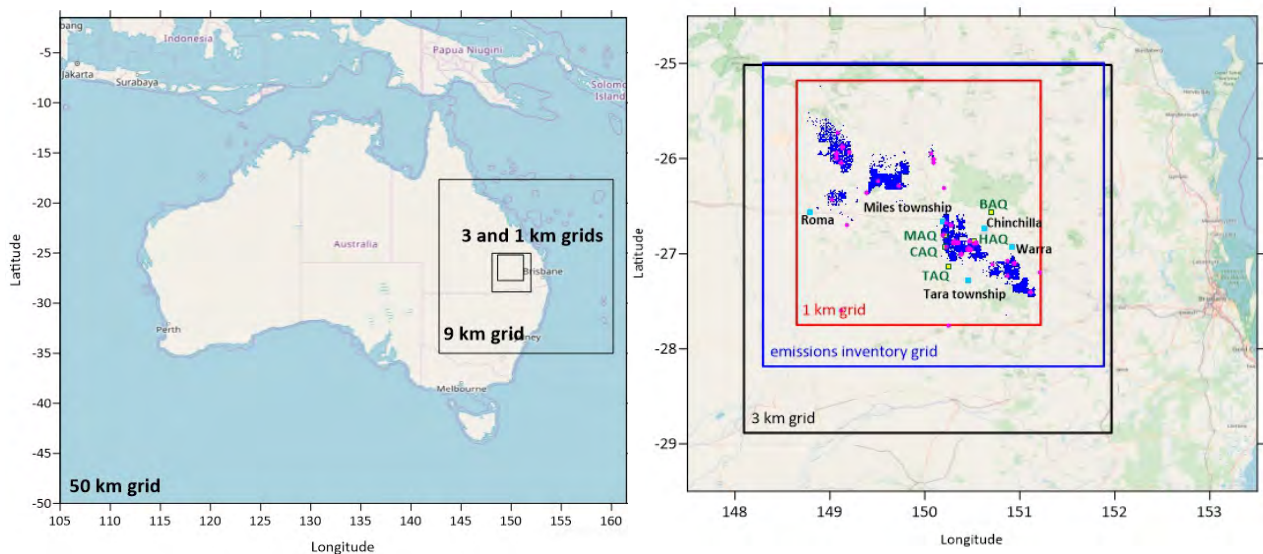


Figure 1. Left: Outermost modelling grid domain (50 km grid spacing) with nested inner grids 9, 3 and 1 km grid spacing; Right: The emissions inventory grid as well as 3 and 1 km nested modelling grids. The CSG-related emission sources are shown as follow: blue = well areas, high point vent areas, other area sources; pink = stacks, flares, other point sources. Monitoring sites are shown as follows the Gas field sites are ‘MAQ’ - Miles Airport air quality station, ‘CAQ’ - Condamine air quality station and ‘HAQ’ - Hopeland air quality station. The Regional sites are ‘TAQ’ - Tara Region air quality station, ‘BAQ’ - Burncluith air quality station.

Katestone Environmental was commissioned to develop an anthropogenic emission inventory (Katestone et al 2017) for the 300 km x 300 km emissions inventory grid (see Figure 1). The inventory was constructed by identifying and mapping sources of pollutants and quantifying the emission rates of pollutants for each source. Sources of pollutants in the study area included a wide variety of natural and man-made (anthropogenic) emissions including the CSG industry, power generation, quarries and mines, agriculture (including feedlots), motor vehicles, domestic and commercial sources, domestic wood heaters, bushfires and prescribed burning, wind-blown dust and vegetation. CSG-related emissions were characterised from the operational activities of Origin Energy, QGC, Arrow, Santos and Other Producers. Direct detailed emission information was obtained from Origin and QGC as the two major CSG producers in the study region at the time. Other sources of information included Queensland Government department and agency databases, Queensland Globe (DNRME 2015a-c), the National Pollutant Inventory (NPI) database, industry Environmental Impact Statements (EIS), and aerial photography. Specific CSG industry-

related emissions in the inventory included but were not limited to: gas processing facility (GPF) emissions including compressors, engines, venting, flares and leaks, water treatment facility (WTF) emissions as well as field emissions including wellhead engines/microturbines, wellhead leaks, water and gas gathering networks and vehicles. Emission data was not validated by CSIRO but was reviewed by a third party to ensure representativeness of emissions.

Results

The impact of CSG operations on ambient levels of air pollutants in the Surat Basin was assessed by comparing the air quality model outputs for model runs with and without the CSG-related emissions included. The modelled pollutant concentrations were compared with observed pollutant concentrations measured at 5 ambient air monitoring stations including 3 Gas field sites (Hopeland, Miles Airport and Condamine) and 2 Regional sites (Tara Region and Burncluth). The Gas field stations were located between 1 and 5 km from gas processing facilities, between 100 – 450 m from operating CSG wells and had 15 - 25 wells within a 2 km radius. The Regional sites were 10-20 km away from major potential CSG-related emission sources (Lawson et al., 2018c). The modelled pollutant concentrations were also compared with air quality objectives including the Air NEPM (2016), the Air Toxics NEPM (2011), the QLD EPP (2008) and the Texas AMCV (2016a).

The modelled concentrations are presented in this report for PM_{2.5}, O₃, NO₂, CO, and formaldehyde and benzene, with toluene and xylene data in the appendix. Of the PM fractions, PM_{2.5} results are shown as this is the PM fraction that has the strongest association with adverse health effects. Formaldehyde and benzene are air toxics in the Air Toxics NEPM and NO₂, CO and O₃ are criteria pollutants included in the Air NEPM.

A summary of findings from this modelling study is as follows:

- The modelled pollutant concentrations agreed reasonably well with the monitoring data from the observation sites. The model was able to broadly reproduce background concentrations, diurnal behaviours, periods of general concentration increase and frequency of peaks. The model was challenged in some cases to reproduce peaks from local fire events (PM_{2.5}), and overestimated the magnitude of local, CSG-related NO₂ events. As such, the modelled contribution of CSG-related sources to NO₂ concentrations in this study are likely to be overestimates.
- Modelled ambient concentrations were in general well below air quality objectives. There were some modelled exceedances of the 24-hour average PM_{2.5} objective and some modelled near exceedances (>80 % of air quality objective) for 1-hour NO₂ and 4-hour O₃ concentrations (Air NEPM (2016), QLD EPP (2008)).

Smoke from vegetation fires resulted in the largest modelled air quality impacts over the region, particularly for PM_{2.5}, CO and O₃. Smoke from vegetation fires was the main contributor to the modelled exceedances of the 24-hour PM_{2.5} air quality objective.

- Where CSG-related emissions contributed to an exceedance of the 24-hour air quality objective for PM_{2.5} (8 occasions in total), CSG emissions contributed at most 4-37 % of the total 24-hour PM_{2.5} concentration. Over the modelled 1 km domain during the modelled year CSG-related emissions contributed to 0.06 % of all the PM_{2.5} exceedances. The

predominant source of PM_{2.5} exceedances in the region is from vegetation fires. When CSG-related emissions contributed to values of PM_{2.5}, O₃ and NO₂ which were >80 % of the relative air quality objective (Air NEPM (2016) and Qld EPP (2008)), CSG-related emissions contributed 6 – 92 %, 3 – 7 % and 99 % to the total concentration respectively.

- The maximum impact of the modelled CSG-related emissions on air pollutant levels tended to be localised and occurred within a few kilometres of emission sources (for example GPFs) particularly for NO₂ and PM_{2.5}. For O₃ the maximum impact of CSG-related emissions was generally to decrease the O₃ concentration near combustion sources (due to reaction of O₃ with NO_x). CSG-related emissions sometimes contributed to higher O₃ concentrations downwind from CSG-related emission source.
- At the Gas field, Regional and at 11 town sites in the region the largest modelled contributions of CSG-related emissions to the 4-hour O₃ concentrations occur most frequently in the summer months. Generally the largest modelled contributions from CSG-related emissions occur for larger O₃ values (i.e. increased peak concentrations). However when the modelled concentrations of O₃ in the region were highest (> 80 % of the air quality objective), CSG-related emissions made a minor (4 ppb) contribution to the total concentration (3 – 7 % of the total 4-hour O₃ concentration).
- The modelled concentrations of air toxics benzene and formaldehyde were very low and well below air quality objectives (Air Toxics NEPM (2011), Texas AMCV (2016a)). The modelled contribution of CSG-related emissions to ambient concentrations of these air toxics was very low to negligible.
- The modelling indicates that the contribution of CSG-related emissions to air pollutant levels was highest at the Gas field sites when compared to the two Regional sites and 11 town sites in the region. As such, air quality data from the Gas field monitoring sites (Lawson et al 2018c) were well-located to experience CSG-related air pollution impacts. These sites are likely to provide a ‘worst case’ regional impact from CSG-related emissions for the period 2015 - 2016.
- Combustion of gas and/or diesel in CSG infrastructure/sources was the likely major source of CSG-related emissions of PM_{2.5}, CO, NO₂, and precursors leading to O₃, rather than fugitive emissions of CSG itself.

The monitoring study reported some elevated levels of larger particle fractions (PM₁₀ and TSP) at Gas field sites likely associated with CSG activities, cattle farming and other agricultural activities (Lawson et al 2018c). However, these activities were identified as local, short lived and unpredictable, and included wheel-generated soil or dust from vehicles, infrequent/incidental CSG operational activities and movement of cattle. As such, emissions of PM₁₀ and TSP from these transient activities could not be captured with the regional modelling system used here.

Significance and next steps

This air quality modelling study has provided the first detailed assessment of the influence of CSG-related operational emissions on air pollutant levels in an unconventional gas region in Australia. This work also provides an understanding of the spatial distribution of pollutant levels over the wider Surat Basin over the course of a year; information that cannot easily be collected through an

observation network of only a few sites. Findings from this study could be used to better understand the contribution that CSG operational activities made to different air pollutant levels in the Surat Basin during 2015-2016 and to inform future policy development in the region. The modelling system developed in this work could be used to assess potential CSG impacts in subsequent years, in which the type and number of emission sources may have changed with the further increases in CSG production over this period. The modelling system could also be used to explore potential CSG impacts on a number of additional air pollutants if required. Further work to investigate the reason/s for the modelled over-prediction of NO₂ in this study could also be undertaken.

1 Introduction

CSG production has rapidly expanded in the Surat Basin in Queensland in recent years and this growth has raised community concerns about the potential impact on the air quality in the region. The GISERA project G.3 “Ambient air quality, Surat Basin, Queensland” provides the first comprehensive assessment of air quality assessment in the Surat Basin Queensland using an air quality observation network and detailed air quality chemical transport modelling. These studies aim to inform industry, the community and the government about the impact of CSG production on a variety of key air quality parameters in the Surat Basin.

Background and purpose of the modelling study

From 2014-2018, a comprehensive ambient air quality monitoring program was undertaken in the Surat Basin near Condamine, Miles and Chinchilla in Queensland, see Figure 1.1 and Section 4 (Lawson et al., 2018c). The monitoring program measured air pollutants in the region and assessed concentrations against air quality objectives. The monitoring program found that air quality in the region is well within relevant air quality objectives for the majority of the time for a wide range of gaseous pollutants that are potentially emitted by CSG activities (Lawson et al., 2018c). When levels of atmospheric particulate matter (PM) occasionally exceeded or approached 24-hour air quality objectives, the main source of PM_{2.5} exceedances (particles with an aerodynamic diameter of < 2.5 µm) was found to be smoke from vegetation fires. For PM₁₀ (particles with an aerodynamic diameter of < 10 µm) and total suspended particles (TSP), the most likely sources of exceedances were due to a combination of emissions from smoke from vegetation fires, CSG activities, regional dust, unsealed roads and cattle farming.

In the present study an air quality model has been used as an additional tool to further explore air quality in the region.

The aims of the present air quality modelling study are:

1. To assess the impact of CSG operations on ambient levels of nitrogen oxides (NO_x), carbon monoxide (CO), ozone (O₃), volatile organic compounds (VOCs) and particulate matter (PM) in the Surat Basin over an entire year. This differs from the approach used in the previous monitoring study (Lawson et al., 2018 a, b) in which the CSG-related contribution was investigated only during air quality exceedances and other periods of elevated concentrations.
2. To determine the spatial variability of NO_x, CO, O₃, VOCs and PM in the Surat Basin to ensure the location of the three Gas Field ambient air quality sites from the air quality monitoring study were representative of air quality within the region.

This report delivers Task 3 of GISERA project G.3 by presenting the air quality modelling component of the study and assessing the overall impact of CSG production activities on ambient levels of primary and secondary air quality parameters in the Surat Basin. The report presented here also describes the modelling tasks, and the assumptions, uncertainties and limitations of the study.

Overview of the air quality model

The area modelled was centred on the Chinchilla-Miles-Condamine region of the Surat Basin (300 km x 300 km), shown in (Figure 1.1), which was also the focus of the ambient air quality monitoring study (Lawson et al., 2018c). The year selected for the Surat Basin modelling study was September 2015 through to August 2016 because meteorological and ambient air monitoring data from Miles Airport, Condamine, Hopeland, Tara Region and Burncluith are available for all or part of that period to compare with model output (Lawson et al., 2018a). While 2016 had the highest rate of CSG production in the Surat Basin to date at the time the modelling commenced (452 petajoules, PJ in June 2016), production increased a further ~30% to 585 PJ by the middle of June 2018 (DNRME 2019).

The air quality modelling system comprises a CSIRO model which generates meteorological fields, coupled with a chemical transport model (Section 2). A detailed emissions inventory for CSG infrastructure, other industry, domestic and commercial activities, motor vehicles and intensive farming for the Surat Basin region was prepared by Katestone Environmental (Katestone (2017)) and is summarised in Section 3.1.

The modelling system is a nested grid system (see Figure 2.2 and Figure 2.3). The large outer grid covers Australia and the smallest inner grid covers the region of interest in the Surat Basin. Each model grid is run separately using the next larger grid for boundary conditions, this ensures pollutants are passed from the outermost grid through to the innermost grid with the passage of weather systems. Each grid needs appropriate emission inventories, and therefore inventories for different regions in Australia are included.

Smoke emissions (due to bushfires and large fuel reduction burns) and natural emissions are included along with the South East Queensland Region (SEQR) inventory. NSW EPA GMR inventory (NSW EPA, 2008) and Victorian inventories are used in the outer grids to include the possible influence of long-range emissions, and these are described in Section 3.2. Air quality and meteorology data sets from the GISERA Surat Basin air quality monitoring network for the years 2015 and 2016 were used to assess the validity of the model output (Section 5).

Presentation of findings

The model simulated the interactive emission, transport and transformations of pollutants in the air over the Surat Basin at 1 km resolution for every hour from September 2015-August 2016. The impact of CSG operations on ambient levels of NO₂, CO, O₃, VOCs and PM_{2.5} in the Surat Basin was then assessed by comparing the air quality model outputs from the model run with all sources including the CSG inventory and a second model run which excluded the CSG inventory. The differences between the model runs allowed an assessment of the potential contribution of CSG sources to air pollutant levels in the region. The potential contribution of CSG related emissions to total pollutant concentrations is provided in Section 5 for each pollutant. A comparison of the modelled pollutant levels between the monitoring sites and at 11 towns in the wider region has been used to assess the spatial representativeness of the air quality monitoring sites (Section 5.6). Implications of model assumptions, uncertainties and exclusions are explored in Section 5.7 and the relationship of the model findings to the monitoring study is presented in Section 5.8. Finally, a summary of this modelling work and possible next steps are presented in Section 6.

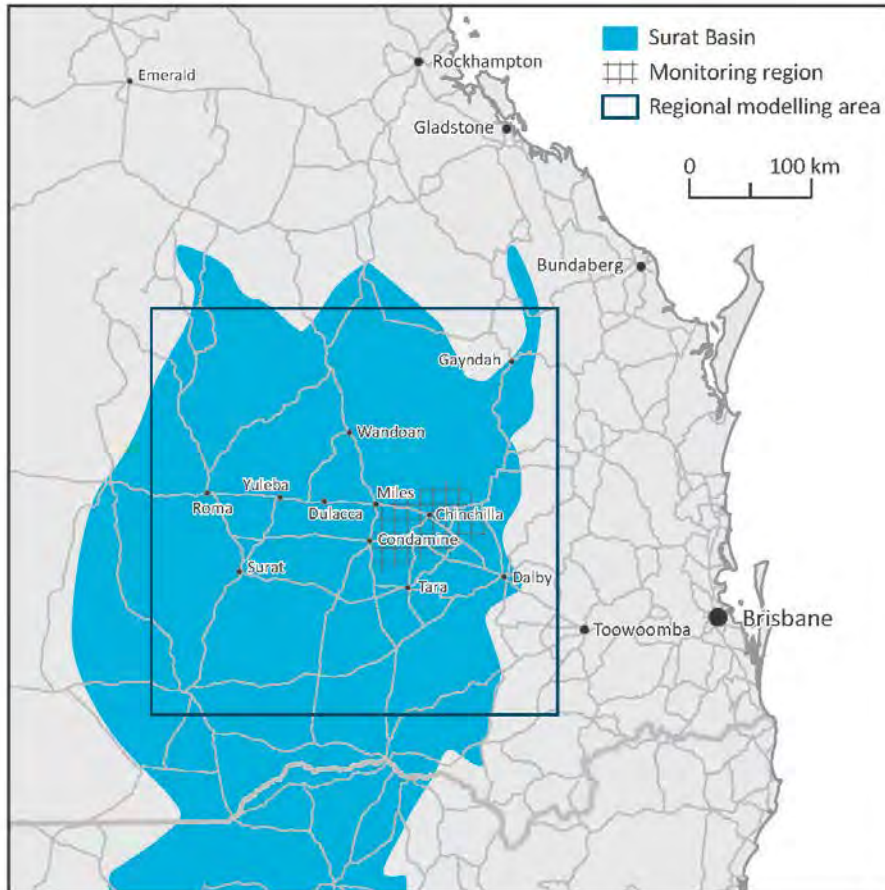


Figure 1.1 Study area including the regional modelling area (source: Lawson et al., 2017b).

2 The CTM modelling system

Background

The CSIRO CTM (Chemical Transport Model) modelling system has previously been used for air quality forecasting (Cope et al., 2004, 2014), shipping emission simulations (Broome et al., 2016), urban air quality (Cope et al., 2014; Galbally et al., 2008), biogenic (Emmerson et al., 2016) and biomass burning studies (Keywood et al., 2015; Lawson et al., 2017a) and for modelling primary and secondary particulate matter from urban and natural sources (Cope et al., 2009).

The CTM has also been used for modelling the potential impacts from a power station in the Latrobe Valley (Azzi et al., 2014) and over the last few years the CTM has formed part of a prototype forecast modelling framework with an emphasis on modelling smoke (Cope et al., 2019).

These modelling studies, involving multiple nested domains, have all been based over the Australian region with the innermost nest (which is usually the region of interest) focussed on different parts of Australia (e.g. Melbourne, Sydney, Tasmania, Latrobe Valley, Northern Territory). Comprehensive emission inventories have been used in most of the studies centred on Sydney and Melbourne. The modelling system has been evaluated for combined meteorological and air pollution prediction performance in previous studies. Most studies present an assessment of the modelling system. Cope and Emmerson (2016) assessed the modelling system by evaluating the performance of O₃, NO₂, NO_x, CO and SO₂ for a year focussed on Sydney. Cope et al. (2017) focussed on the performance of PM_{2.5} in a similar run. Cope et al. (2019) present three examples of the smoke forecasting system with verification of the performance for each example.

This study is focused on the Surat Basin region and like many of the above studies includes outer nests (or grids) that cover larger populated areas of Australia.

Figure 2.1 shows a schematic diagram of the modelling system.

Numerical weather model - CCAM

The numerical weather model used to drive the CTM is CCAM (Conformal Cubic Atmospheric Model) (McGregor, 2015, and references therein). CCAM is a global stretched grid model that can zoom over particular areas of interest, producing high spatial resolution fields of meteorological parameters, such as wind speed, wind direction and temperature, as hourly averages that are then input to the CTM. The data are also used for the prediction of some emissions that are meteorologically mediated such as volatile organic compound (VOC) emissions from vegetation and evaporative emissions from motor vehicles. The meteorological data are also used for calculating plume rise from buoyant industrial sources, advection, diffusion and chemical transformation in the CTM.

CCAM optimises the accuracy of the simulated meteorological fields by nudging the CCAM meteorological fields towards the large-scale features of an observation-based weather analysis, updated at six hourly intervals (ECMWF ERA interim- 80 km resolution). CCAM has 13 vertical levels below 2 km to resolve low level vertical wind shear and temperature inversions. Good resolution of the temperature and wind structure in the lower atmosphere is particularly

important for resolving various meteorological features such as boundary layer growth and nocturnal jets, which all strongly influence air pollution transport and hence the subsequent concentrations. The lowest CCAM-CTM level is 20 m above ground.

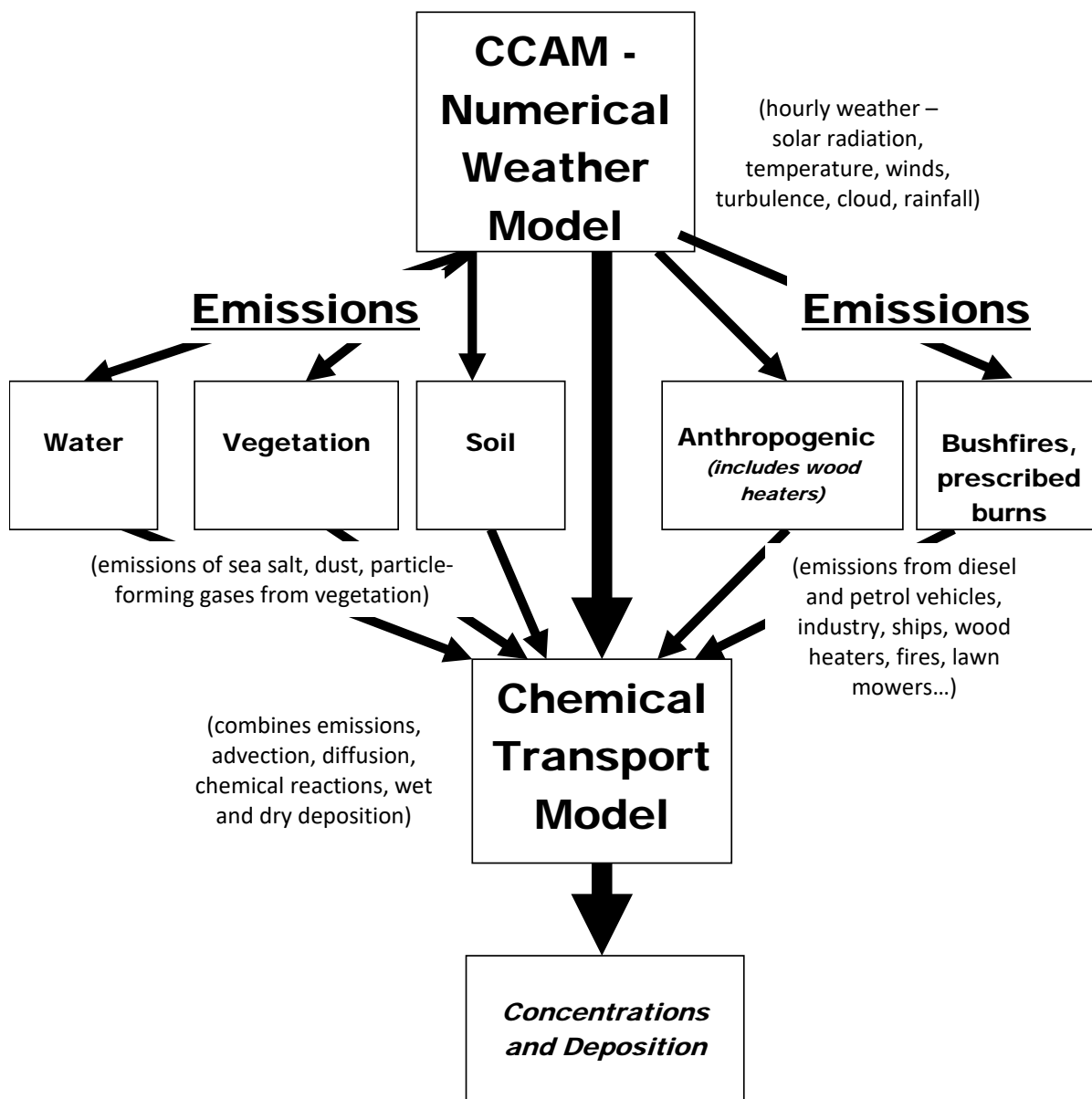


Figure 2.1 Schematic diagram showing the CCAM-CTM modelling framework used to simulate interactive emissions, transport and chemical transformation.

Chemical Transport Model (CTM)

The CTM is an Eulerian (i.e. grid based) model designed to model the interactive emissions, transport, chemical transformation and wet and dry deposition of a gas phase - or a mixed gas and aerosol phase system. It is typically used for modelling urban and regional scale photochemical smog production, including primary and secondary aerosol mass. (A secondary pollutant is not directly emitted to the atmosphere but is formed through reactions between other pollutants in the atmosphere.)

Chemical transformation in the CTM has been designed to enable different photochemical mechanisms. The chemical transformation used in this study is an extended version of the Carbon Bond 5 mechanism (Sarwar et al., 2008) (The CTM version used is 'cb05_aer2_v5p5'.)

As mentioned previously, the modelling system is a nested grid system (see Figure 2.2 and Figure 2.3). The model is run on a larger outer grid first, then the model is run on the next inner grid and so on until the final model run on the innermost grid, depending on the horizontal resolution required. The horizontal resolution of the grids increases with each nest. Each model grid uses the previous larger grid for boundary conditions, this ensures that pollutants lying in the outermost grid are able to be transported from the outermost grid through to the innermost grid with the passage of weather systems. The nested modelling system allows a fine resolution model run (1 km) with the ability to incorporate pollutants from well outside the fine grid region e.g. fine particles can travel long distances across Australia and this type of modelling system allows that to be included.

Further input to the modelling system are emissions. Each model grid needs appropriate emissions from anthropogenic sources (e.g. industrial sources, diesel and petrol vehicles, ships and wood heaters) and natural sources (e.g. bushfires, prescribed burns, wind-blown dust, sea salt aerosol, volatile organic carbon emitted from vegetation and nitric oxides from soils). The various emission sources in this study are described in Section 3 and they provide emission data over the course of the modelled year. Some emission data are constant with time and some vary according to the day, month or year.

For the model runs in this study the CTM is run with a 50 km spaced outer grid covering the Australian region, see Figure 2.2. The large outer grid is used to capture the long-range transport of various species (e.g. PM_{2.5} and O₃). The outermost grid needs initial and boundary conditions and the CTM uses boundary concentrations that are defined on a monthly basis (set by the user). Three nested grids are also run within the 50 km grid, they have a grid spacing of 9, 3 and 1 km. The smallest inner grid covers the region of interest in the Surat Basin with 258 x 258 grid points at 1 km spacing.

Figure 2.3 shows the two inner grids and the emission inventory grid discussed in Section 3. The results presented in this report are from the 1 km grid. For model comparison with data from the air quality observation sites, the CTM predictions are extracted at the nearest grid point to the observation site and at the lowest model level, 20 m above the ground.

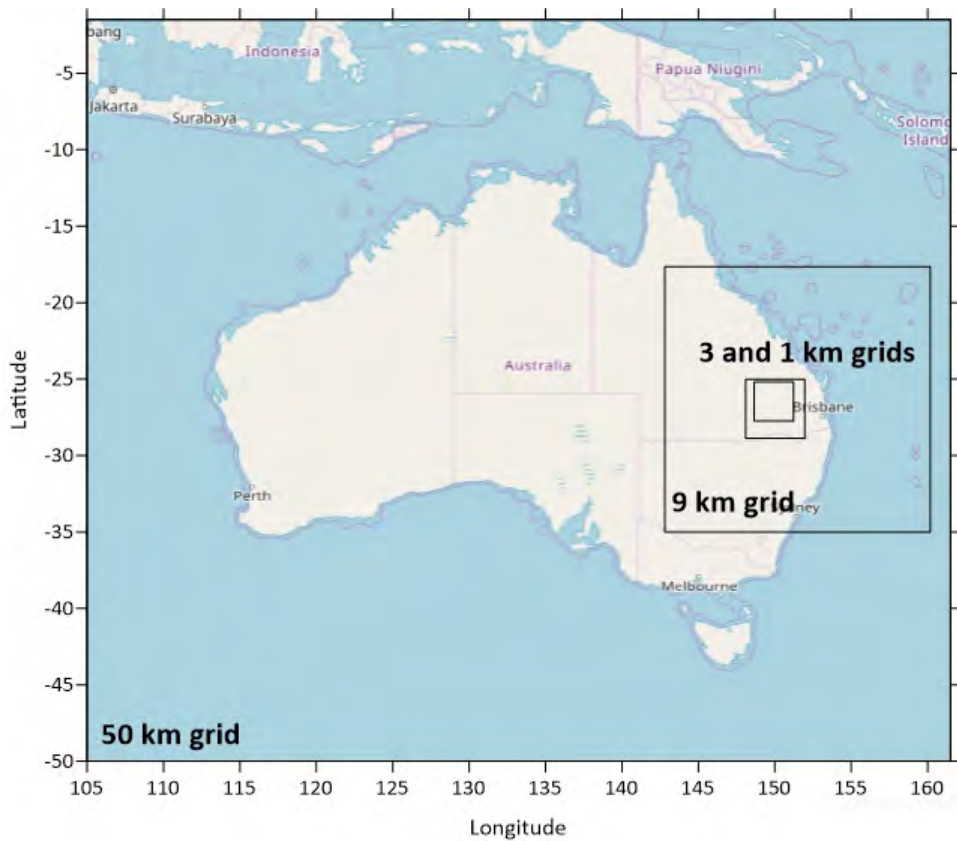


Figure 2.2 The CTM modelling grids: outer 50 km grid (50 km grid squares) with nested inner grids 9, 3 and 1 km.

The performance of the modelling system

The performance of the meteorological model is examined in Appendix A.

To summarise, the results for CCAM indicate that the model is doing well in predicting near-surface temperature and wind direction, perhaps slightly less so for the wind speed particularly at Burncluith (see Figure 2.3 for location). A previous evaluation of simulated CCAM meteorology during 2014 – 2015 in the Surat Basin found similar results (Thatcher, 2016).

Previous evaluations of CCAM have shown the ability of the model to reproduce observed meteorology in Australia. An assessment of CCAM in Sydney over one year showed very good agreement with observations with some minor issues with underprediction of the frequency of very light winds (Cope and Emmerson (2016).

Cope et al. (2014) investigated CCAM performance aloft by comparing model profiles of wind speed, wind direction and temperature with data from commercial aircraft, they found that overall CCAM did well in capturing the nocturnal jet, boundary layer growth due to convection in the morning and the onset of sea breezes which strongly influence air pollution transport.

The results of the statistical analysis in Appendix A and these previous studies give confidence in using CCAM meteorology to drive the CTM in this study.

The analysis of the CTM’s performance in predicting observed pollutant concentrations is shown in Appendix B. The results of the performance analysis are similar to the results for previous studies for PM_{2.5} and O₃ concentrations (Cope and Emmerson, 2016 and Cope et al., 2017) and they

suggest good model performance on the whole. However the model performance for NO₂ is not as good as that for PM_{2.5} and O₃. The model generally overestimates the night-time peaks of NO₂.

Cope and Emmerson (2016) found NO₂ and NO_x to be reasonably well modelled except during the summer season when there was a tendency to overpredict (note, the main emission sources of NO₂ in that study (urban) are likely to be significantly different to the present study).

Overall, the results of the statistical analysis in Appendix B and these previous studies give confidence in the ability of the CTM to predict air pollutant concentrations in this study, with the exception of NO₂ (discussed above and in more detail in Section 5.3.1). The NO₂ concentration predictions in this study are overestimated at the Gas field and Regional sites and most likely overestimated at other locations. As discussed in Section 5.3, the modelled results for other species are unlikely to be significantly affected by the overestimation of NO₂ with the exception of the minimum O₃ concentrations.

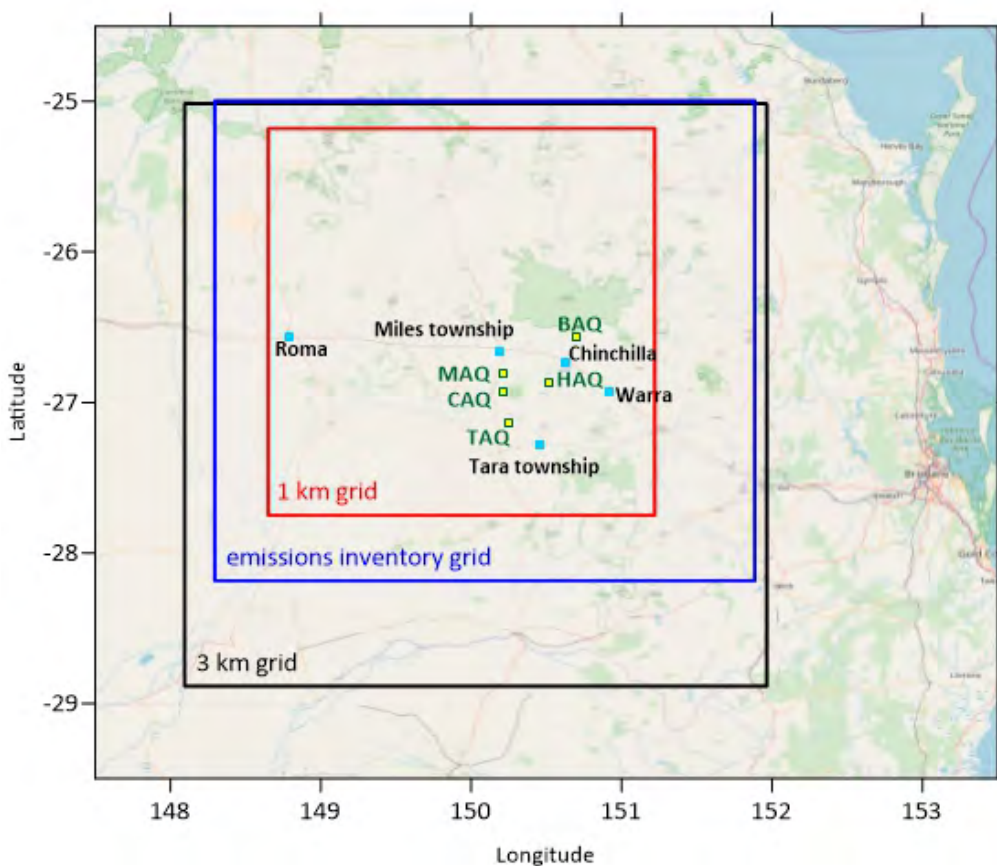


Figure 2.3 Grids for the CTM modelling system - 3 and 1 km inner model grids and the Surat emissions inventory grid. Gas field sites (green and yellow) are ‘MAQ’ - Miles Airport air quality station, ‘CAQ’ - Condamine air quality station and ‘HAQ’ - Hopeland air quality station. Regional sites (green and yellow) are ‘TAQ’ - Tara Region air quality station, ‘BAQ’ - Burncluith air quality station. ‘Town’ sites (blue) are Chinchilla, Miles township, Roma, Tara township and Warra.

3 Emission Inventory

The release of pollutants from sources was represented in the model using an emission inventory. The emission inventory was constructed by identifying and mapping sources of pollutants and quantifying the emission rates of pollutants for each source.

Sources of pollutants in the inventory included a wide variety of natural and man-made (anthropogenic) emissions including the CSG industry, power generation, quarries and mines, agriculture (including feedlots), motor vehicles, domestic and commercial sources, domestic wood heaters, bushfires and prescribed burning, wind-blown dust and vegetation.

The following pollutants were included in the emission inventory; carbon monoxide, nitrogen oxides, particles (PM_{2.5}, PM₁₀, TSP), ammonia (NH₃), VOCs and sulfur dioxide (SO₂). These pollutants were selected because they were identified as being emitted from sources in the study area, and have a potential negative impact on air quality. For some pollutants such as ammonia and sulfur dioxide, the CSG industry was not identified as a major source (Lawson et al., 2017b); for these pollutants, and other sources were likely to be more important including agriculture (ammonia) and power stations (sulfur dioxide). Methane, which makes up about 98 % of CSG in the study area (Lawson et al 2017b) is not directly harmful to human health at ambient concentrations and has no air quality objective; as such, emissions of methane were not included in the air emissions inventory. However, other constituents of CSG which may influence air quality, such as VOCs, were included in the inventory.

The emissions inventory was developed for an area 300 km by 300 km (Figure 2.3), which while larger than the Condamine-Miles-Chinchilla air quality monitoring region, was chosen to ensure that emissions from outside of the monitoring area that can impact air quality, were included in the modelling. The air quality modelling also included the transport of emissions from the South East Queensland region incorporating Brisbane, from NSW and Victoria and from the lower resolution population based full Australian inventory to account for impact of long range transport on local pollutant levels.

Once the emission sources were identified, the emission rates of carbon monoxide, nitrogen oxides, particles (PM_{2.5}, PM₁₀, TSP), ammonia, VOCs and sulfur dioxide were quantified for every square kilometre of the emission inventory grid (Figure 2.3). The inventory was based on 2015/2016 emissions where possible, except for some situations where only 2013/2014 emissions were available at the time, for example emissions from Power Generation and Mines and Quarries (see Appendix C). Where VOC inventory data was available only as total VOCs (TVOC), this data was converted into speciated VOC emissions suitable for input into the CTM using the speciation method from the NSW EPA Greater Metropolitan Region (GMR) Inventory 2008 (NSW EPA, 2008) and / or US EPA SPECIATE database. The SPECIATE is the U.S. Environmental Protection Agency's (EPA) repository of volatile organic gas and particulate matter (PM) speciation profiles of air pollution sources (Simon et al., 2010).

The inventory was developed in two parts. A Surat Basin anthropogenic inventory for sources in the 300 km x 300 km emission inventory grid that were identified and quantified by Katestone

Consulting (see Section 3.1). This very detailed emission inventory quantified sources at a resolution of 1 km x 1 km and was reviewed by a third party prior to being used in the model to independently verify the representation of emissions. The second part of the inventory included emissions from natural sources such as fires, dust and vegetation for the modelling grids and was collated by CSIRO.

Anthropogenic and natural emissions were included in all model grids Australia wide to make sure the modelling system included the impact of long range transport on local pollutant levels (see Section 3.2).

An overview of the Surat Basin anthropogenic inventory as well as the Australia-wide anthropogenic and natural emissions is given below.

3.1 Surat Basin anthropogenic emission inventory

Katestone Environmental consultants was commissioned to develop an anthropogenic emission inventory for the Surat Basin covering an area of 300 km x 300 km. It included the following sources:

- CSG industry sources
- Power Generation
- Mines and Quarries
- Agriculture
- Domestic Wood Heating
- Motor Vehicles

Details of the methodology employed for quantifying the above emission sources is in Appendix C. A broader discussion of CSG-related sources included in the emissions inventory is provided in Section 3.1.1.

A summary of the main air pollutant sources identified in the Surat Basin anthropogenic emission inventory is as follows (reproduced from Katestone 2017)

1. NH₃ and NO_x were identified as being emitted in the largest quantities in the Surat Basin followed by SO_x, PM₁₀ and CO. Total volatile organic compounds (TVOCs) and PM_{2.5} are emitted in the smallest quantities (Figure 3.1) where TVOC is the sum of VOCs.
2. CSG activities were identified as the major contributor to VOCs and CO emissions and an important contributor to NO_x emissions (Figure 3.2)
3. Power stations were identified as the major contributor to SO_x and NO_x emissions (Figure 3.2)
4. Agricultural activities were identified as contributing to the majority of the NH₃ emissions. (Figure 3.2)
5. Coal mine and quarry activities were identified as the major contributor to PM₁₀ emissions. (Figure 3.2). It should be noted that emissions from CSG development activities which are a likely source of PM₁₀ (through earthmoving and other activities) were not included in the inventory.

6. Motor vehicles are the major contributor to anthropogenic PM_{2.5} emissions. (Figure 3.2)

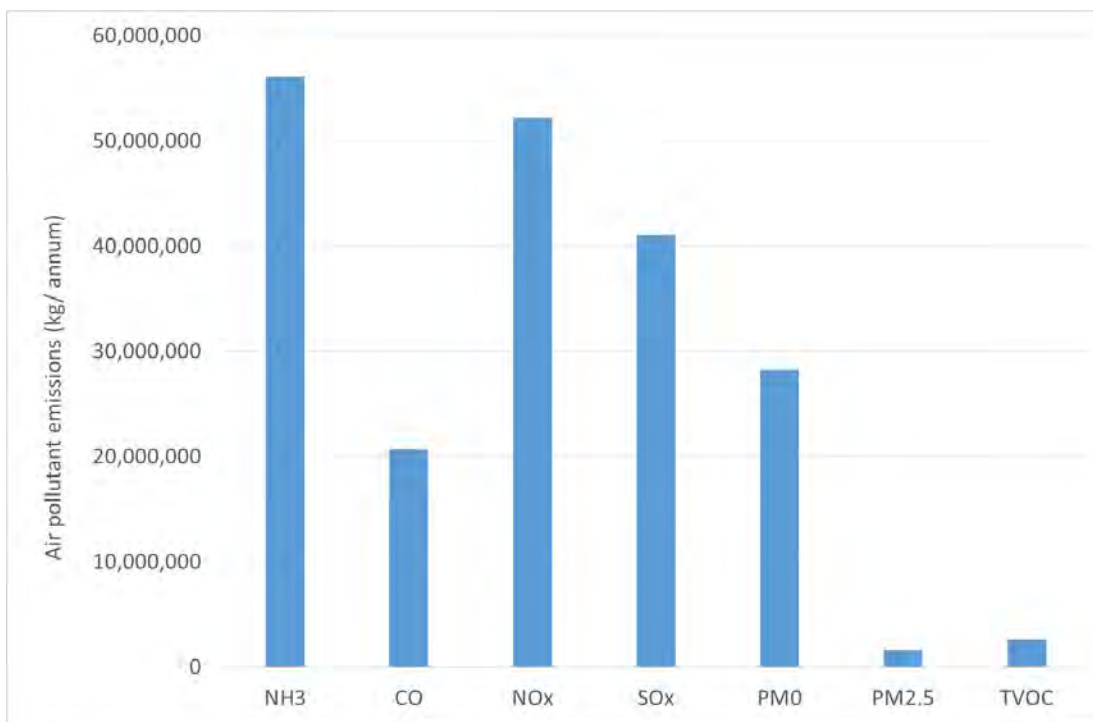


Figure 3.1 Total air emissions for individual pollutants (kg/annum) for the Surat Basin region, from the Surat Basin emissions inventory. Data source: Katestone 2017.

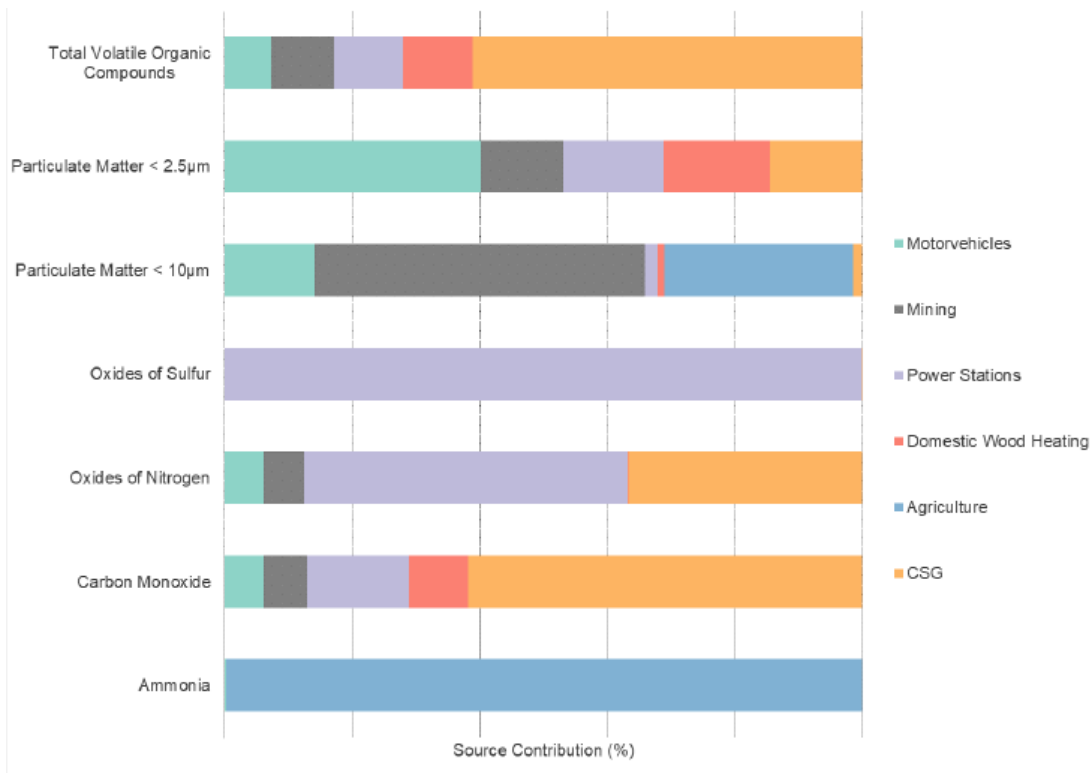


Figure 3.2 The Surat Basin Air Emissions Inventory – Source contribution (%) by industry sector or activity (from Katestone 2017). The Source Contribution scale ranges from 0 – 100%.

3.1.1 Overview of Emissions from Coal Seam Gas (CSG) Extraction and Processing

An overview of how emissions were calculated for CSG-related emissions in the Surat Basin inventory is provided below. This information is summarised and, in some cases, reproduced from a report by Katestone (2017) who compiled the Surat Basin inventory. For further details on the CSG-related emissions see Appendix C.

CSG-related air emissions were characterised from the following CSG producers: Origin Energy, QGC, Arrow, Santos and Other Producers. Note that in 2015 Origin and QGC were the major CSG producers in the study region, and as such, detailed information was obtained from these producers about emission sources and activity rates so that emissions could be represented as accurately as possible (see below).

Emission sources were identified using a range of different information sources, including obtaining information directly from industry, Queensland Government department and agency databases, Queensland Globe (DNRME 2015a-c), the National Pollutant Inventory (NPI) database, industry Environmental Impact Statements, and aerial photography.

Specific emission sources identified from the CSG industry included but are not limited to: GPF emissions including compressors, engines, venting, flares and leaks, WTF emissions and field emissions including wellhead engines/microturbines, wellhead leaks, water and gas gathering networks and vehicles.

CSG-related emissions were categorised as Production or Processing emissions. Production emissions relate to the activities required to extract CSG (raw CSG) from the ground and transport

it to processing facilities. Air emissions may occur from wells and gathering infrastructure located across the Surat Basin. Production emissions include fugitive emissions from planned or unplanned releases of CSG from wells, high-point vents and valves associated with gathering network and infrastructure. Production emissions also include fuel combustion sources such as engines and generators at wells and vehicle usage emissions including road dust.

Processing emissions occur as a result of processing raw CSG to produce saleable natural gas. Activities leading to processing emissions include cleaning and drying of gas, compressing raw CSG at compressor stations, centralised processing plants and water treatment plants. Processing emissions include the fuel combustion sources at compressor stations, processing plants and water treatment plants such as compressor engines, generator engines, boilers and flares. The majority of fuel combustion sources use the processed CSG. In most cases emissions from CSG infrastructure or activities were assumed to be constant across the year except for some Origin emissions which were scaled to monthly fuel/gas consumption.

Detailed production information was provided by Origin and QGC for 2015 for use in calculating their respective air emission inventories. Air emissions data for the year 2015 were provided by Arrow using methods consistent with the NPI reporting requirements. For Santos and the Other Operators, publicly available data were used to estimate the air emissions inventory. Further details used to generate the inventory for each producer are provided in Appendix C including emission sources, as well as the methodology used to distribute emissions spatially and the methodology used to calculate emissions. Figure 3.3 shows areas of identified CSG-related emission sources in the Surat inventory, including wells and high point vents, stacks, flares and other point sources in the modelling domain.

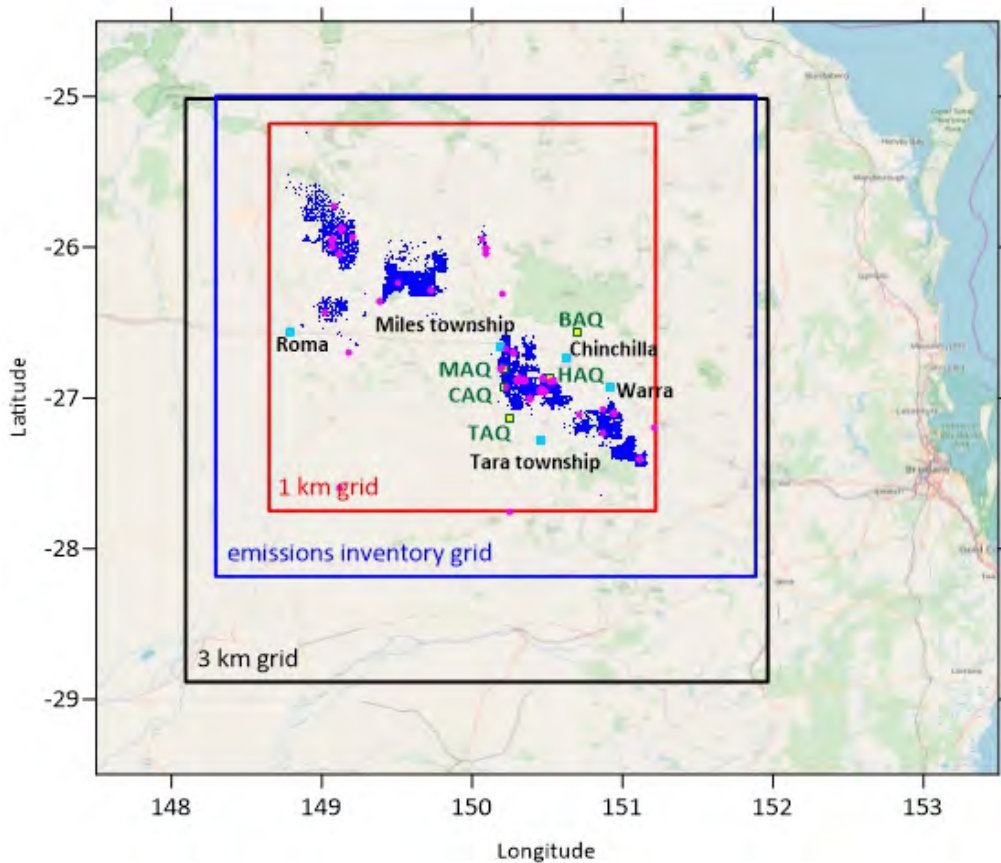


Figure 3.3 The emissions inventory grid as well as nested 3 and 1 km modelling grids. Locations of the modelled CSG-related emission sources are also shown: blue = well areas, high point vent areas, other area sources, pink = stacks, flares, other point sources

3.2 Australian emissions inventories (including soil, bushfires, vegetation and wider anthropogenic sources)

All model grids are run with emissions inventories that include anthropogenic, natural and smoke emissions. Some inventories are at different scales, for instance the population-based inventory for all of Australia is low resolution and provides background anthropogenic emissions suitable for the larger 50 km spacing outer grid.

Types of emissions included in all CTM grids from emission inventories are

- Anthropogenic emissions
 - Industrial, commercial and domestic sources (wood heater emissions)
 - Elevated point source (e.g. power stations)
 - Motor vehicle emissions
- Natural emissions
 - VOC emissions from forest canopies and pasture and grasses

- Natural NO_x emissions from soil and natural landscapes (e.g. forest, shrubland, pastureland, urban, water)
- Natural NH₃ emissions from natural landscapes (forest, shrubland, pastureland, desert)
- Sea salt emissions
- Wind-blown dust emissions
- Mercury emissions from soils and vegetation
- Smoke emissions
 - Bushfires, planned burns

These are discussed in the following sections.

3.2.1 Anthropogenic emissions

Pollutant emission inventories used in the CTM for anthropogenic emissions are listed below. Each grid will use all inventories that fall within its bounds making sure not to double up, coarse emission information is replaced with the most detailed emission information.

- National Scale – used on the CTM outer grid (50 km resolution)
 - population based inventory for all of Australia (low resolution, motor vehicles and commercial and domestic sources), provides background anthropogenic emissions
(<http://www.nepc.gov.au/system/files/resources/9947318f-af8c-0b24-d928-04e4d3a4b25c/files/aaqprcrpttapmphase2200105final.pdf>)
 - shipping emissions prescribed for the entire Australian region (generated as described in Goldsworthy, 2017 and Broome et al., 2016)
- Victoria, 2006, 5km resolution. (Delaney and Marshall, 2011)
- PPR (Port Phillip Region), 2006, 1 km resolution. (Delaney and Marshall, 2011)(https://www.epa.vic.gov.au/air/emissions_inventory/default.asp)
- New South Wales EPA GMR Inventory 2008 (NSW EPA, 2008). Covers greater Sydney, Newcastle and Wollongong regions (GMR) 1 km resolution
- SEQR (South East Queensland Region), updated 2000 inventory. EPA and BBC (2004). Air Emissions Inventory: South East Queensland Region. 1 – 3 km resolution. http://www.epa.qld.gov.au/environmental_management/air/air_quality_monitoring/air_quality_reports/air_emissions_inventory/
- Surat Basin emissions inventory described in Section 3.1, 1 km resolution

3.2.2 Natural emissions

Natural emissions of VOCs, NO_x and NH₃ from vegetation and soils, emissions of sea salt aerosol, emissions of wind-blown dust and re-emission of elemental mercury emissions from soils, vegetation and water are all modelled interactively within the CTM (Cope et al., 2009). For example the CTM includes algorithms for estimating emissions of windblown dust following Lu and Shao (1999) and emissions of NMOCs from vegetation following Azzi et al. (2012). These emissions use the meteorological information within the CTM to produce the emissions as needed during the model run.

All grids include these natural emissions and are all modelled within the CTM.

3.2.3 Smoke emissions

Smoke emissions from vegetation fires are computed nationally using ECMWF CAMS Global Fire Assimilation System data (ECMWF-CAMS) of wildfire combustion rate, wildfire overall flux of burnt carbon and mean altitude of maximum injection. So the 50, 9 and 3 km model grids all use this fire information for smoke emissions in a model run.

For the inner 1 km Surat region model grid local higher resolution fire data is calculated using VIIRS hotspot data (<https://earthdata.nasa.gov/earth-observation-data/near-real-time/firms/viirs-i-band-active-fire-data>).

The CSIRO smoke emissions model (C-SEM) estimates the fluxes of gaseous and aerosol products from the combustion of biomass within a bushfire or planned burn (Cope et al., 2016). VIIRS hot spot data provides the daily locations of hotspots and C-SEM uses this to infer the area burned and the time period for each fire. C-SEM produces time varying emissions by also including estimates of fine and coarse fuel burnt, fuel burning efficiency and emission rates of the smoke related gases and aerosols.

In this study all hot spots were treated as bushfires, not planned burns. It was not possible or practical to sort each hot spot into type of fire due to the enormous quantity of hotspots (can be 30 or more distinct hotspots in one day) and to the lack of information about the underlying source of most hotspots. Testing showed that a good compromise was to assume each hot spot was a bushfire; these assumptions effect the length of time a fire is flaming and smouldering as well as the plume rise. On occasions the CTM may misrepresent some fires which may result in some modelled species, e.g. PM_{2.5} being over/underestimated.

3.3 Assumptions, uncertainties and exclusions

This section discusses assumptions in the emission inventory and modelling system and possible implications for the study's findings.

The modelling system in this study utilises a comprehensive and detailed emissions inventory to represent the release of air emissions from a wide variety of sources. The representation of a wide variety of air pollutants from CSG-related emission sources in the Surat Basin at a spatial resolution of 1 km has been undertaken for the first time in an Australian unconventional gas region. A 1 km methane emission inventory for the Surat Basin was also used as part of inverse

modelling work in the GISERA project Characterisation of Regional Fluxes of Methane in the Surat Basin, Queensland (Luhar et al., 2018).

The emission inventory incorporated the best available emission data, and where possible, detailed source and emission information was obtained directly from the two largest CSG producers in the study area at the time of the study (Origin and QGC) to ensure the most comprehensive and relevant emission data was included. However, all emission inventories include some assumptions and uncertainties in how emissions are represented. For example, when emission inventories are developed, emission factors are used to represent emissions which are in many cases based on estimates rather than based on direct measurements. A discussion of the main assumptions and uncertainties is provided below as well as possible implications for the findings of the study

3.3.1 Emission data assumed correct as received

- The Surat Basin anthropogenic emission inventory data was provided to CSIRO by Katestone and was not validated by CSIRO, however, it was reviewed by a third party to independently verify the representation of emissions
- Emission sources, species and rates provided from the CSG industry were assumed to be correct. Similarly emission sources, species and rates obtained from the NPI and other publicly reported data were assumed to be correct. In many cases the emission rates were based on emission factors rather than direct measurements, as is typical of many air quality emission inventories.

3.3.2 Excluded emissions

- The inventory excludes some emissions that are transitory in nature and difficult to quantify in terms of timing, emission species and rates such as an individual vehicle travelling past on an unsealed road, sudden livestock movement, dust from a seasonal cropping activity (e.g. harvesting) and CSG development or transient operational activities involving earthworks. These types of transitory emissions are not usually included in air quality modelling studies.
- CSG development activities including well drilling and completions, any pipeline or other construction, and any infrequent/incidental operational activities or any sources that are not included in Section 3.1 and Appendix C.
- Other emissions of a transitory nature, including agricultural activities that may release airborne soil such as crop production (ploughing, harvesting) or emissions from livestock not housed in feedlots.
- Fires were identified via satellite hotspots. However, some fires may have been missed where cloud cover obscured the hotspot during the satellite overpass. Also, small or low intensity fires may have not been detected by hotspots. This may result in an underestimation of PM_{2.5} in the region.

- The inventory did not include PM_{2.5} from non-combustion sources such as mining, quarries, as NPI does not require facilities to report non-combustion PM_{2.5}. However the inventory did include PM₁₀ from these sources (which incorporates PM_{2.5}).
- Other minor sources may have been excluded from the inventory for example where NPI reporting thresholds were not exceeded

3.3.3 Temporally variable emissions represented as constant emissions

- In many cases the emission rates from CSG and other sources were assumed to be constant over a given time period (typically constant over a year, or in some cases over a month). This is because emission data is typically reported over timescales of months to years, and because detailed information about activities occurring on finer timescales was not available. Where temporally varying emissions have been assumed constant over months to a year, the absolute emissions have been captured by the inventory, but the way in which they vary over times scales of minutes, hours and days is not captured. As such peaks and troughs (ie variability) in some emissions that occurs on a time scale of days to weeks to days to hours (for example variability in emissions from flaring, variability in emission from wells and HPV) are not captured in the model.

Emissions from all agricultural sources (i.e. feedlots, piggeries, poultry farms) and Mining and Quarry emissions were assumed to be constant over one year. Peaks and troughs in emissions from these sources are not captured in the model.

Some sources had emissions included at a higher (hourly) temporal variability in the inventory, including power stations, smoke from fires, woodheater use and motor vehicles. The temporal variability of emissions from woodheaters and motor vehicles were estimated from methodologies developed for NSW and reasonable assumptions were made in using the methodologies in the Surat Basin (Katestone, 2017).

3.3.4 Representativeness of Emissions for 2015-2016

- The CSG-related emissions inventory was compiled with data for 2015 (Origin and QGC) and 2015/16 reporting year for Santos and Arrow. The period for the model runs was September 2015 to August 2016. It was assumed that the reported CSG-related emissions were representative of the model period.
- In some cases, the most recent reported emission data available was for the year of 2013/14, such as in the case for Mines and Quarries and agricultural emissions. It was assumed that the emission data reported for 2013/14 was representative of the emissions for 2015/16.

3.3.5 Model limitations and assumptions

- As discussed above, transient, irregular, short-lived and one –off emissions have not been included in the inventory as is typical for regional air quality modelling studies. However, even if these events could be included in the inventory, the chemical transport model used in this study would be challenged to accurately resolve the concentrations of PM₁₀ and TSP from nearby and short lived activities, i.e. activities occurring within a kilometre and with a duration of less than a few hours.
- The CTM is driven by the predicted meteorology that drives it. Unless the meteorology is reproduced perfectly there will always be differences, large or small, in the transport of air pollutants. Accumulated errors in time and space in the modelled winds can explain differences in the location of modelled and observed concentration plumes.
- The CTM can only model the emissions as provided, errors or missing information about the characteristics of emissions sources in particular the height of emission release can have large effects on the modelled concentrations.
- The CTM cannot resolve near-source impacts of plumes therefore impacts within a few kilometres of a point emission source may be under or overestimated.

3.3.6 Some additional CSIRO assumptions around emission characterisation

- In some cases, the VOC emission data was provided to CSIRO as TVOC. In these cases, CSIRO used GMR speciation (NSW EPA GMR Inventory 2008 (NSW EPA, 2008)) and / or US EPA SPECIATE database to convert TVOC data into speciated VOC emissions suitable for input into the CTM (Simon et al., 2010). Where TVOC emission data was given for a number of sources with potentially different VOC speciation, VOCs were generally speciated according to the most dominant emission source.
- Actual fires during the study period were identified using hotspots from satellite overpass and smoke emissions estimated. All hot spots were assumed to be bushfires, not planned burns due to a lack of information about the underlying source of each hotspot. This assumption affects the burn characteristics of the fire, pollutants emitted, as well as the plume rise. Testing showed that assuming each hot spot was a bushfire was a good compromise, but there will inevitably be some observed fires that are not represented by the model.
- CSG-related emissions for wells and high point vents were modelled as ground-level area sources, while those for stacks were modelled as elevated point sources with appropriate plume rise. The remaining sources, listed in the CSG inventory as point sources are a mixture of flares, compressors and diesel consumption and most of these are modelled as ‘stacks’ with information provided. Reasonable assumptions were made in distributing emissions between stacks and flares (where this

information was not available for some producers) and in determining stack heights.

4 Observational data

The purpose of this section is to provide background information about the Surat Basin ambient air monitoring study, including aims and findings, and to provide context for the modelling results presented in this report. Monitoring and reporting of air quality data discussed below comprised Tasks 1, 2, 4 and 5 from the GISERA Ambient Air Quality in the Surat Basin project (<https://gisera.csiro.au/project/ambient-air-quality-in-the-surat-basin/>).

Background

From 2014-2018, a comprehensive ambient air quality monitoring program was undertaken in the Surat Basin near Condamine, Miles and Chinchilla in Queensland. The purpose of the monitoring program was to measure and assess air quality in the region, and where possible, assess the impact of CSG-related activities on air quality.

Air quality monitoring data from this period is reported in Lawson et al. (2018a, b), with an overall assessment of air quality in the region reported in Lawson et al. (2018c). From August 2016 – February 2018 preliminary air quality data from the monitoring sites was streamed to the Department of Environment and Science (DES) website under South West Queensland region (<https://www.ehp.qld.gov.au/air/data/search.php>).

Air quality measurements were made at five ambient air monitoring stations including three Gas field sites (Miles Airport, Condamine and Hopeland) and two Regional sites (Tara Region and Burncluith) (Figure 3.3). Gas field stations were located between 1 and 5 km from gas processing facilities, between 100 – 450 m from operating CSG wells and had 15 - 25 wells within a 2 km radius. The Regional sites were 10-20 km away from major potential CSG-related emission sources.

From 2015 - 2018 continuous air measurements were made at four of the ambient air monitoring stations, while continuous measurements were made at the Condamine station from 2016-2017. A review of the CSG composition and CSG-related emission sources in the region (Lawson et al., 2017b) informed the selection of pollutants to be included in the monitoring program. Pollutants selected for continuous measurement included nitrogen oxides (NO_x, including NO₂), carbon monoxide (CO), ozone (O₃) (Gas field and Regional sites) and methane (CH₄), carbon dioxide (CO₂) and particles including PM_{2.5} (particles < 2.5 µm), PM₁₀ (particles < 10 µm) and total suspended particles (TSP) (Gas field sites only). Meteorological parameters including temperature, humidity, solar radiation, wind speed and direction were measured at all sites. In addition to the continuous measurements, 54 individual volatile organic compounds (VOCs) including benzene, toluene and xylene (BTX), aldehydes and hydrogen sulphide were measured over integrated 14-day periods during 2014- 2016 at a network of 10 Passive sampling sites including Chinchilla township as well as Gas field and Regional sites.

Monitoring program outcomes

A key aim of the monitoring program was to compare air pollutant levels with air quality objectives, including those contained in the Queensland Government Environment Protection (Air) Policy (QLD EPP, 2008), the Ambient Air Quality National Environment Protection Measure (NEPM 2016), and the Queensland Government Department of Environment and Science (DES) Nuisance Dust Guidelines for TSP (MFE 2016). Two weekly integrated measurements of VOCs, aldehyde and hydrogen sulfide were assessed against the Air Toxics NEPM (NEPM 2011) and the Queensland Government Air EPP (QLD EPP, 2008). Where no Australian objectives were available, the Texas Commission on Environmental Quality Air Monitoring Comparison Values (AMCV) (Texas 2016a) and Effects Screening Levels (ESLs) were referenced. (Texas 2016b).

There were no exceedances of air quality objectives for any of the gaseous pollutants listed above, including CO, NO_x and O₃ or for individual VOCs, aldehydes and hydrogen sulphide. Concentrations of all these pollutants were well below air quality objectives in almost all cases except for three occasions where the 4-hour average ozone concentration was >80 % of the air quality objective.

Particle concentrations occasionally exceeded 24-hour air quality objectives with seven PM_{2.5} exceedances, three PM₁₀ exceedances and 18 TSP exceedances of 24-hour average air quality objectives at Gas field sites from 2015 - 2018. Annual air quality objectives for particles were not exceeded. Investigation of the 24-hour exceedance events identified smoke from vegetation fires as the main source of PM_{2.5} exceedances, while a combination of vegetation fire smoke and dust from a number of sources including unsealed roads/CSG activities, regional dust and cattle farming were identified as the most likely sources of the PM₁₀ and TSP exceedances. Many of these sources were identified as being typical of other rural areas in Queensland. An additional 48 events were investigated where pollutant concentrations were > 80 % of the air quality objectives (predominantly PM_{2.5}, PM₁₀, TSP events); these were identified as having similar sources to the PM exceedance events described above. It should be noted that the investigations of pollution events focussed on the identified dominant source(s), rather than all possible contributing sources.

CSG-related activities are likely to have contributed to some of the TSP and PM₁₀ 24-hour average exceedance events. This was most likely from the entrainment of soil and dust into the air from vehicles driving on unsealed roads or other CSG development or operational activities, rather than gas or diesel combustion. The source/s of the airborne soil and dust was sometimes difficult to identify, particularly at the Miles Airport and Hopeland sites which during the study were likely influenced both by CSG-related and agricultural activities and vehicle traffic.

Concentrations of VOCs (including BTX) and aldehydes were low and typical of other background rural areas in Australia, and in all cases well below air quality objectives. BTX was detected most frequently and with the highest concentrations in Chinchilla township, with the likely source being motor vehicles, as well as domestic and commercial sources within the town. Hydrogen sulphide was not detected in any sample over the study.

Methane was measured as a tracer for CSG-related activities, as methane comprises ~98 % of CSG composition in the study area (Lawson et al., 2017b). Methane itself does not have an air quality objective as it is not considered to pose a risk to human health in the ambient environment. An investigation of 30 of the largest methane concentration events during the study suggested that the CSG industry likely contributed to 80 % of the largest concentration events observed.

However, none of these methane events were associated with an air quality exceedance for other pollutants measured, including BTX and hydrogen sulphide.

In conclusion, the monitoring program found that air quality in the region is well within relevant air quality objectives for the majority of the study duration for a wide range of gaseous pollutants that are potentially emitted by CSG activities. There were infrequent exceedances of air quality objectives for particles (PM_{2.5}, PM₁₀ and TSP). CSG activities are a likely contributor to infrequent coarse particulate matter (PM₁₀ and TSP) events in the study area along with a range of other regional activities and sources which are typical of rural areas. CSG activities were not identified as a dominant source of infrequently observed fine particle (PM_{2.5}) events in the region, which were mainly the result of smoke from vegetation fires.

Relationship of the monitoring program to the modelling study

The monitoring program has provided the largest contribution to air quality data for the Surat Basin region to date, and gave important information about the levels and sources of air pollutants in the region. Monitoring data has been used in the validation of CSIRO's air quality model as part of this project (see Appendix A and Section 5).

In addition, the air quality model used in this study has been used to investigate the impact of CSG-related emissions on a range of pollutant concentrations by running the model with and without the CSG-related emissions. This provides an estimate of the contribution of the CSG-related emissions to total air pollutant levels over an entire year (Section 5). This differs from the approach used in previous reports (Lawson et al., 2018 a, b) in which the CSG-related contribution was investigated only during pollution events. The model has also been used to investigate how the CSG industry contributes to the pollutant levels over a larger spatial area (258 km by 258 km) than was covered by the monitoring network. Finally the model has been used to assess whether the Gas field monitoring sites were appropriately sited to be representative of the regional air quality (Section 5.6). The modelling system developed in this study could be used to model air quality in the Surat Basin for different emission scenarios in subsequent years, providing the emission rates and sources in the emission inventory were updated for the relevant period.

5 Results and Discussion

In order to investigate the contribution of the CSG industry to the overall pollutant levels in the study area, the model is run in two modes;

- 1) with all sources *including* the CSG industry (denoted by 'all sources'), and
- 2) with all sources *excluding* the CSG industry (denoted by 'without CSG sources' or 'no CSG sources').

The difference between the two model concentration outputs provides an estimate of the contribution of the CSG industry to air pollutant levels. The time period modelled is September 2015 through to August 2016.

In the following sub-sections results are presented for PM_{2.5}, O₃, NO₂, CO, formaldehyde and benzene. Of the PM fractions, PM_{2.5} is selected as this represents the PM fraction that has the strongest association with adverse health effects. PM_{2.5} sources include combustion and secondary formation processes. TSP or PM₁₀ are not presented as these larger size fractions are dominated by large particles that undergo rapid deposition or removal from the air. This means that high PM₁₀ events can be very short lived and localised rather than spatially widespread as in the case of the finer PM_{2.5}.

The VOCs, formaldehyde and benzene are presented as these pollutants are listed as air toxics in the Air Toxics NEPM and NO₂ is presented as it is listed as a criteria pollutant under the Air NEPM (as are CO and O₃).

The data has been presented as follows:

- The observed pollutant concentrations are compared with the modelled pollutant concentrations. The observed and modelled (with all sources and without CSG sources) pollutant concentration data are mostly presented for the Miles Airport monitoring site. Time series plots of observed and modelled data for the other four monitoring sites (Condamine, Hopeland, Tara Region and Burncluith) are in Appendix D. Observations from the Miles Airport monitoring site are selected for comparison with model output because Miles Airport (and Hopeland) generally has the most observations during the modelling time period. Miles Airport is also in close proximity (<2 km) to major CSG infrastructure and had 20 CSG wells within a 2 km radius of the monitoring site, so is likely to be impacted by CSG-related emissions. For CO, Burncluith data are presented as only observations made at Burncluith are relevant due to the sensitivity of the instruments used to measure CO. For the air toxics Chinchilla data are presented as the measurement detection frequency is lower at Miles Airport. More information is provided in the relevant result sections.
- The impact of CSG-related emissions on pollutant levels at each of the 5 monitoring sites (Miles Airport, Condamine, Hopeland, Tara Region and Burncluith) is examined using plots which show the frequency and magnitude of change in pollutant concentrations due to CSG-related emissions (for each season of the year). The change in pollutant

concentrations due to CSG-related emissions is discussed in terms of the relevant air quality objective (Table 5.1).

- The impact of CSG-related emissions on pollutant levels at Miles Airport is examined by plotting modelled average values of pollutant concentrations (all sources) versus the contribution from CSG-related emissions (scatter plots). Scatter plots for the other 4 monitoring sites are provided in Appendix E. The change in pollutant concentrations due to CSG-related emissions is discussed in terms of the relevant air quality objective (Table 5.1)
- The observed and modelled (with all sources and without CSG sources) maximum monthly pollutant concentrations at each of the 5 monitoring sites (Miles Airport, Condamine, Hopeland, Tara Region and Burncluith) are compared to the relevant air quality objectives (Table 5.1).
- To investigate whether an exceedance of an air quality objective occurred in the wider region (outside the monitoring network), modelled pollutant concentrations are presented as spatial plots. These plots show maximum modelled concentrations of pollutants over the region in each grid square of the model domain. Note that each grid square shows the maximum concentration modelled for that grid square *for that entire season. As such the maximum concentration shown in each grid square may be from different time periods.* These maximum concentrations are compared to air quality objectives with appropriate averaging times. The contribution from CSG-related emissions to each maximum grid square concentration is also shown.
- The maximum contribution of CSG-related emissions to each grid cell for the year are shown in spatial plots. These plots differ from the plots above, in that these plots show the maximum contribution of CSG to each grid square *regardless of the absolute concentration or contribution from other sources at the time.*
- The effects of CSG-related emissions on pollutant concentrations are presented in five towns which are the main population centres in the study area (Chinchilla, Miles township, Roma, Tara township and Warra). This data is presented via showing maximum monthly concentrations compared to air quality objectives, frequency of change plots, and scatter plots.
- In Section 5.6 an analysis is undertaken to determine how representative the location of the 5 monitoring sites (Miles Airport, Condamine, Hopeland, Tara Region and Burncluith) were of pollutant levels in the wider region. The modelled pollutant concentrations with and without CSG-related emissions are investigated for an extra 6 towns in the region (11 towns in total) and compared to concentrations and impact of CSG-related emissions at the 5 monitoring sites.
- Results presented as seasonal averages have the following short hand notation – SON = September, October and November 2015, DJF = December 2015, January 2016 and February 2016, MAM = March, April and May 2016 and JJA = June, July and August 2016.

Comparison with Air quality objectives

In the following Sections the modelled concentrations are compared to air quality objectives to assess whether there are any modelled exceedances. The air quality objectives used to assess the pollutant concentrations are presented in Table 5.1 and are based on the values from the QLD EPP (2008), the Air Toxics NEPM (2011), the Air NEPM (2016) and the Texas Commission on Environmental Quality air Monitoring Comparison Values (Texas 2016a). See Lawson et al. (2018a) for a discussion of air quality objectives used in this study.

Table 5.1 Air quality objectives used to assess concentrations in this report.

Air pollutant	Averaging Period	Objective	80 % of the Objective
Ozone	4-hour	80 ppb (one day per year) ^{a,b}	64 ppb
	1-hour	100 ppb (one day per year) ^{a,b}	80 ppb
Nitrogen dioxide	Annual	30 ppb ^{a,b}	
	1-hour	120 ppb (one day per year) ^{a,b}	96 ppb
PM _{2.5}	Annual	8 µg m ⁻³ ^{a,b}	
	24-hour	25 µg m ⁻³ ^{a,b}	20 µg m ⁻³
Carbon monoxide	8-hour	9000 ppb (one day per year) ^{a,b}	7200 ppb
Formaldehyde	Annual	8.9 ppb ^c	
	24-hour	40 ppb ^{a,b}	32 ppb
Benzene	Annual	3 ppb ^{a,b}	

^a NEPM (2016)

^b EPP (2008)

^c Texas AMCV

5.1 PM_{2.5}

Particles are one of the six key air pollutants in the Ambient Air Quality NEPM (NEPM, 2016). The mass of particles with an aerodynamic diameter of <2.5 µm (PM_{2.5}) and the mass of particles with an aerodynamic diameter of <10 µm (PM₁₀) as well as total suspended particles (TSP) were measured at the three Gas field sites (Miles Airport, Condamine and Hopeland). Airborne primary particles are emitted directly from the source (e.g. dust, diesel and smoke emissions), while secondary particulates are formed from reactions of gas phase precursors in the atmosphere. Particles have been identified in the CSG industry EIS as a key pollutant (QGC 2010, APLNG 2010). CSG-related sources include diesel exhaust, combustion and dust emissions, relating mostly to construction activities, along with gas fired boilers, engines and flares. Other sources of particles in the study area include agricultural sources and fires. PM_{2.5} is emitted mainly from combustion (including fuel and fires) and secondary formation.

5.1.1 Modelled effect of the CSG-related emissions at the observation sites

Time series plots of the observed and modelled concentrations of 1-hour average PM_{2.5} at Miles Airport are shown in Figure 5.1. The observations are shown in blue, the model results with all emission sources in red and the model results without the CSG-related emission sources in purple. The time series are presented for different seasons. For comparison purposes and completeness the 1-hour average PM_{2.5} concentration time series for Condamine, Hopeland, Tara Region and Burncluith are shown in Appendix D. In the time series figure it is not always possible to see the two modelled time series, the red (all sources) concentration series is plotted first and then the purple (no CSG sources) series is plotted. Where the values of each series are the same only the last plotted series will be seen, which is the purple one (no CSG sources). Therefore, when red is seen on the plot it is because the two modelled series have different values at that point in time and the difference between the two values is the contribution to the concentration from the CSG-related emissions; this contribution is shown in Figure 5.2 (the contribution for the other sites is shown in Appendix D).

The observed and modelled PM_{2.5} concentrations at Miles Airport show broad agreement, with the model capturing the background values of PM_{2.5} and periods of slightly elevated PM_{2.5}. This is also true at the other Gas field sites (there are no PM_{2.5} observations at the Regional sites).

There are a number of periods of observed elevated PM_{2.5} around 16/9/15, 7/10/15, 5/11/15 and 9-11/8/16 some of which do not appear in the modelled Gas field sites data. The PM_{2.5} event around the 5/11/15 is identified as a regional fire at Miles Airport and Hopeland and the events around 9-11/8/16 are identified as local fires at Condamine and Hopeland in Lawson et al. (2018a). The cause of the event around the 7/10/15, which was accompanied by PM₁₀ and TSP exceedances, is likely to have been a local but unidentified source of airborne soil at Miles Airport. While the event on the 16/9/15 was not analysed in Lawson et al. (2018a) smoke can be seen in the region in a satellite image from the 16/9/15 (Figure 5.3), suggesting that the event on the 16/9/15 is possibly due to smoke from vegetation fires.

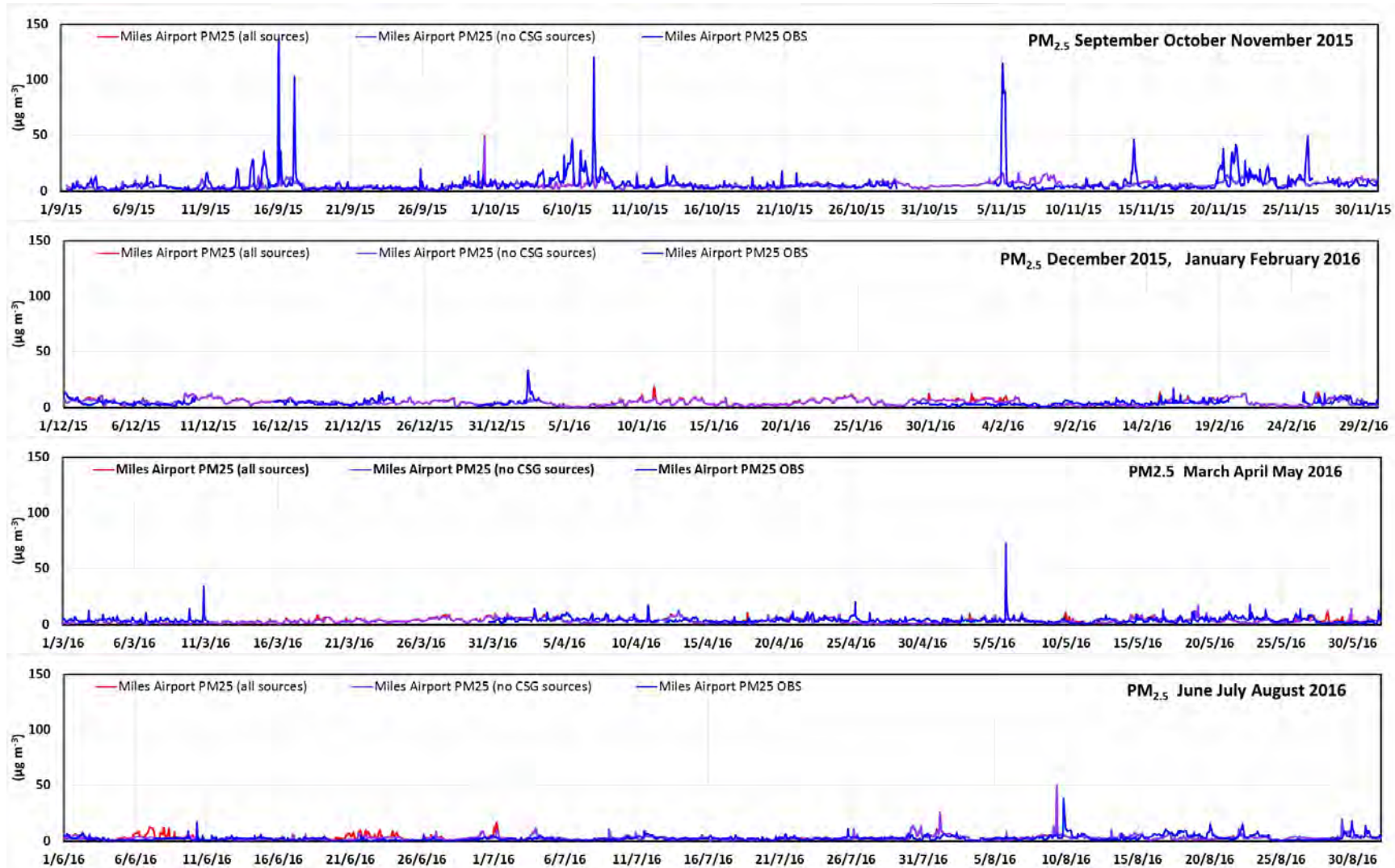


Figure 5.1 The observed and modelled time series of the 1-hour average PM_{2.5} concentrations ($\mu\text{g m}^{-3}$) at Miles Airport for the modelled year (red = model results with all sources, purple = model results without CSG sources, blue = observations).

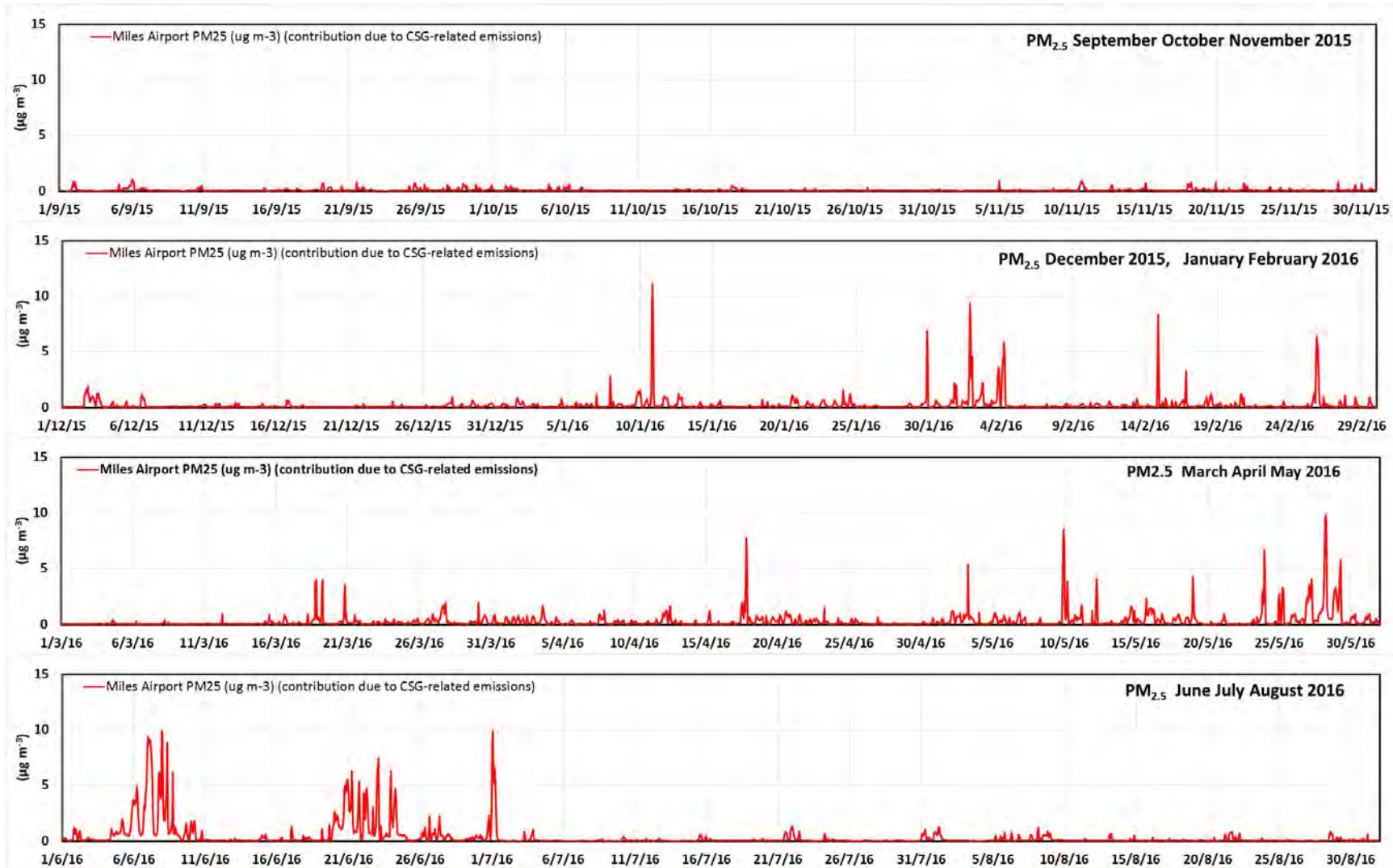


Figure 5.2 The modelled contributions from the CSG-related emissions to the 1-hour average PM_{2.5} concentrations (µg m⁻³) at Miles Airport for the modelled year.

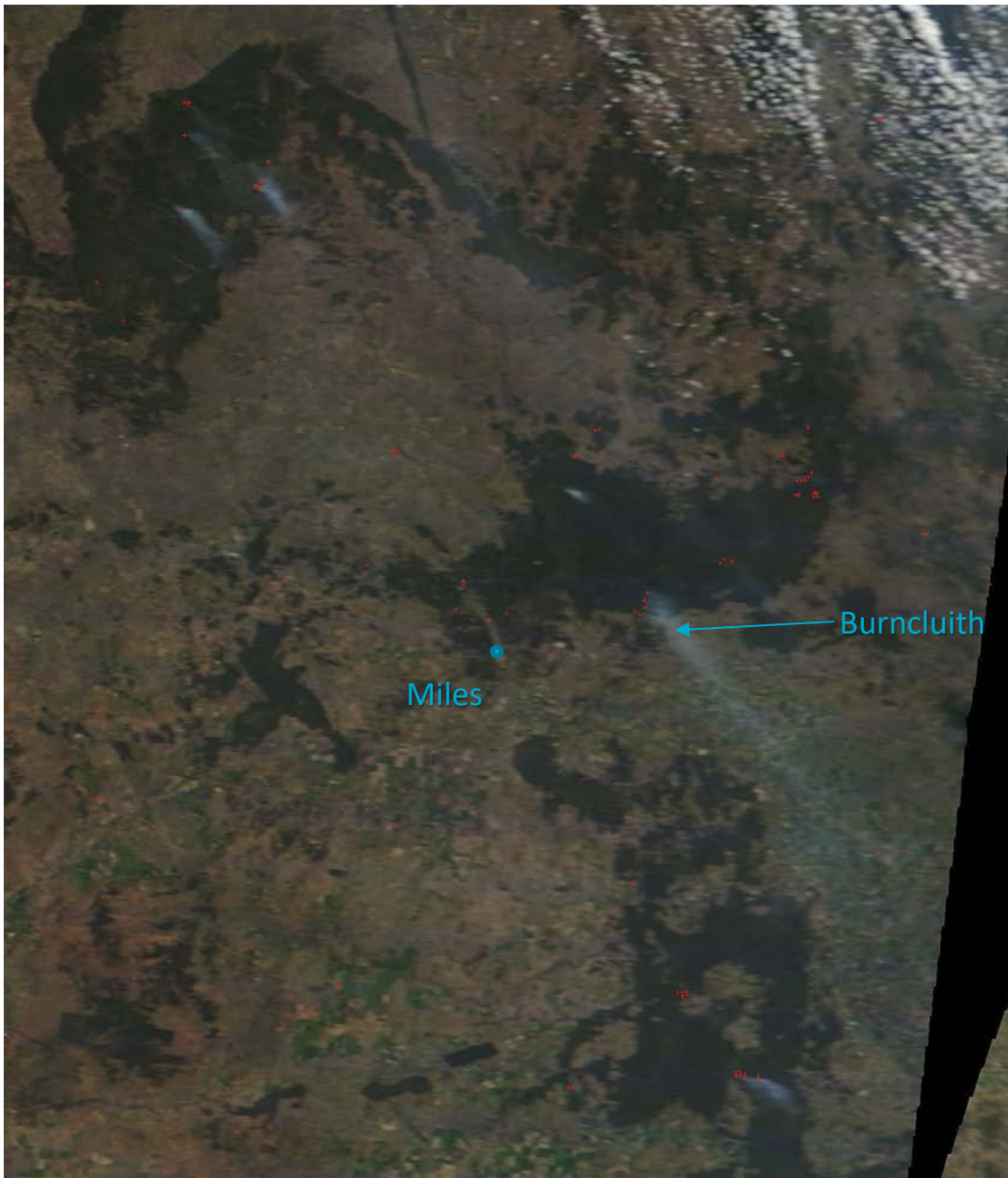


Figure 5.3 Satellite picture on the 16/9/15 about midday (Terra / MODIS) showing a number of different areas of smoke, small red spots are 'hot spots', the blue dot locates Miles township and the Burncluith Air Quality station is indicated by an arrow (NASA Worldview, <https://worldview.earthdata.nasa.gov/>).

Many of the larger and broader observed peaks are due to fires which the model has simulated reasonably well when judged by an analysis of the results in the CSIRO two-dimensional animated system. The model may not produce exact matches in time and space with the observations but for many of the larger peaks associated with fires the model is capturing the fire in the vicinity. An example of this is the model output on 7/10/15 which shows that areas with elevated $PM_{2.5}$ concentrations in the model coincide with the higher concentrations of levoglucosan (Figure 5.4). Levoglucosan is a chemical product that is unique to the combustion of wood. It is included in the

model's chemistry and can be used as a unique smoke tracer to help identify areas of PM_{2.5} that are associated with biomass burning. The comparison of the plots in Figure 5.4 shows that areas with elevated PM_{2.5} concentrations in the model coincide with areas of elevated levoglucosan concentrations which indicates that the modelled PM_{2.5} concentration is associated with smoke from modelled biomass burning. As Figure 5.4 shows, on the 7/10/15 the model produces PM_{2.5} concentrations from fires to the north and north-east of Miles Airport that travel toward Miles Airport but do not reach Miles Airport at the observed time or with the observed value. As such, while a PM_{2.5} concentration plume was not modelled over Miles Airport at the same time as the observations, the model has captured enhanced areas of PM_{2.5} concentration nearby. There are other observed peaks of PM_{2.5} concentration due to smoke from vegetation fires which are not seen in the modelled PM_{2.5} concentration time series at the observation sites for the reasons given above. Accumulated errors in time and space in model winds can account for differences in the location of modelled and observed PM_{2.5} concentration plumes. Other reasons why observed fires may not be captured in the model are due to missing hot spot data (see Section 3.2.3 for a discussion of hot spots and the CSIRO smoke emissions model (C-SEM)).

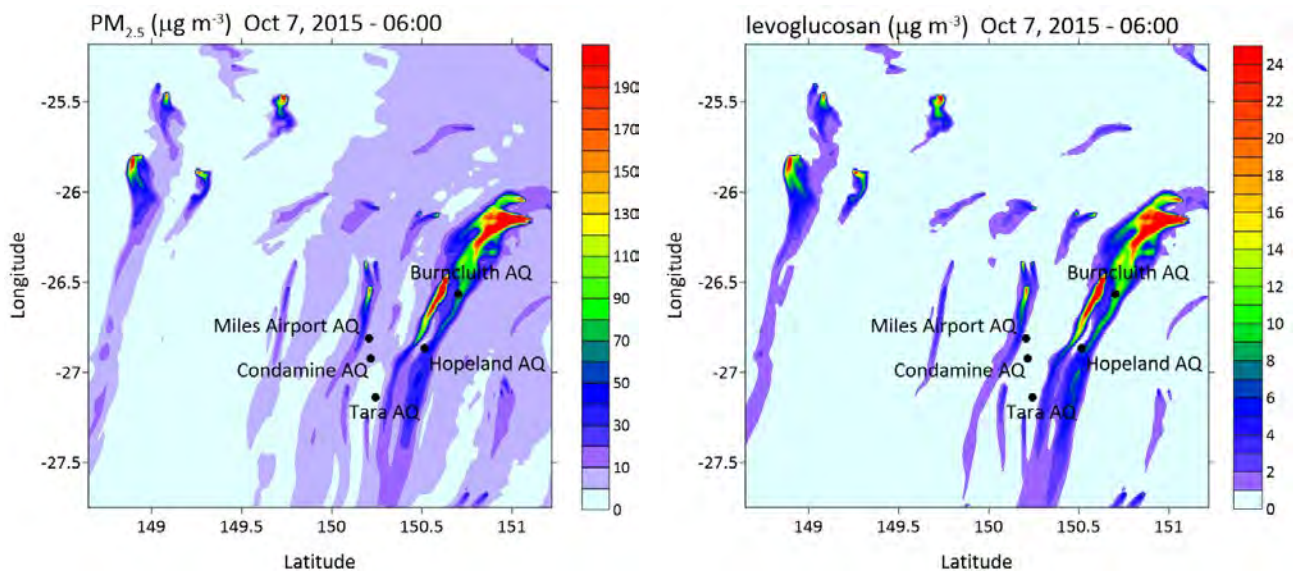


Figure 5.4 Spatial plots from the model results with all sources (left) PM_{2.5} ($\mu\text{g m}^{-3}$) and (right) levoglucosan (smoke tracer) ($\mu\text{g m}^{-3}$), both are at 06:00 AEST on the 7th October 2015.

The model results with all sources time series are similar to the model results without the CSG sources time series at Condamine, Hopeland and the Regional sites (Appendix D). Most differences occur at Miles Airport in June (Figure 5.1 and Figure 5.2), under westerly winds which bring PM_{2.5} concentrations from nearby sources. (Appendix A shows the observed and modelled wind direction time series for Miles Airport).

The modelled contribution from the CSG-related emissions to the 24-hour average PM_{2.5} concentrations at each of the observation sites is presented in Figure 5.5. Each plot shows the percentage of model hours within each season for the modelled contribution from the CSG-related emissions to the 24-hour average PM_{2.5} concentrations.

Mostly there is very little contribution from the CSG-related emissions at any site; on average 97 % of the time the contribution is less than 0.5 $\mu\text{g m}^{-3}$ which is 2 % of the 24-hour $\text{PM}_{2.5}$ air quality objective ($25 \mu\text{g m}^{-3}$, Table 5.1). At most the contribution from the CSG-related emissions to the 24-hour average $\text{PM}_{2.5}$ is less than 5 $\mu\text{g m}^{-3}$. Miles Airport is predicted to have the largest frequency of change due to the CSG-related emissions during DJF, MAM and JJA, however these changes are not large as can also be seen in the time series plots in Figure 5.1 and Figure 5.2.

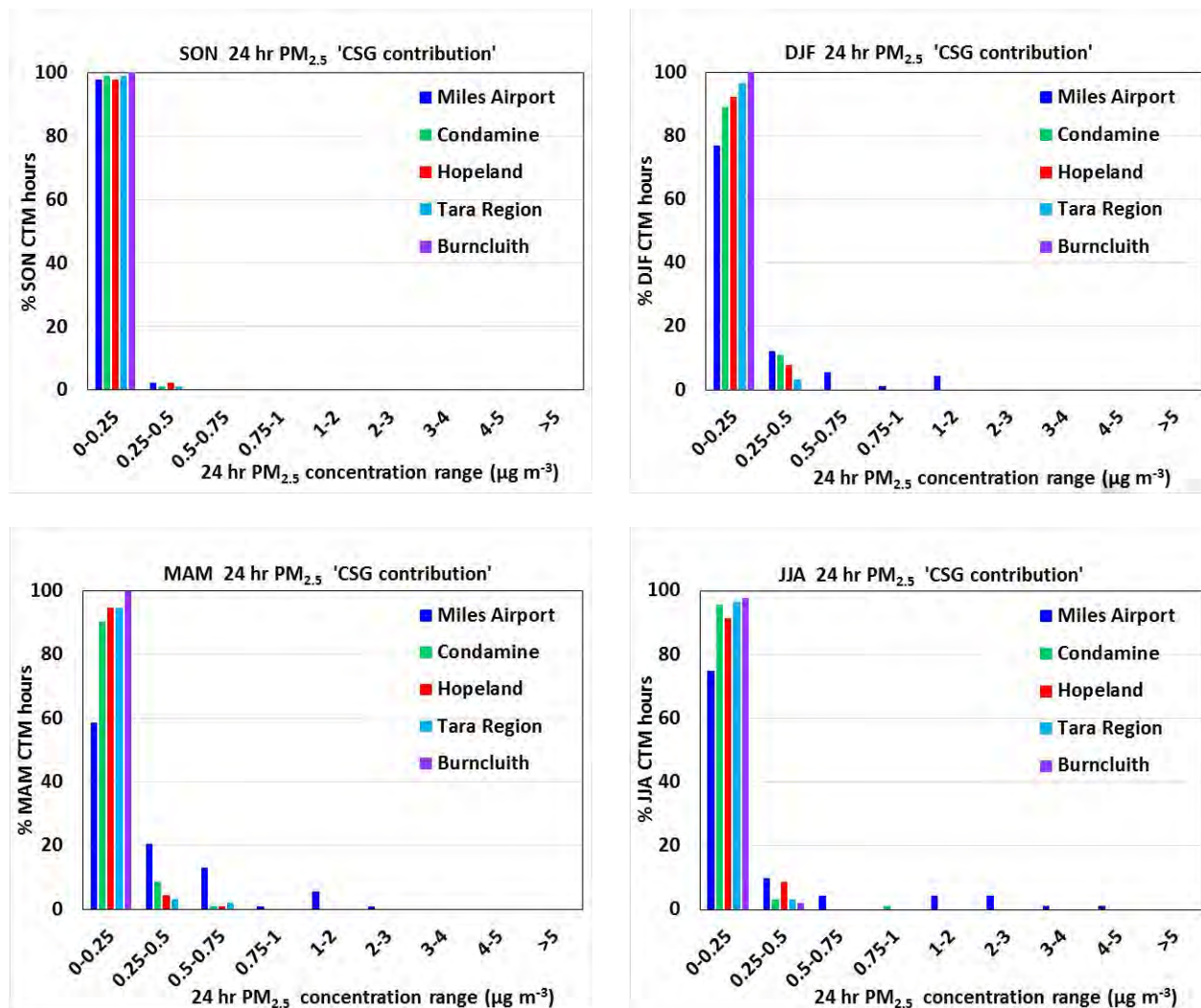


Figure 5.5 The modelled contribution from the CSG-related emissions to the 24-hour average $\text{PM}_{2.5}$ concentration ($\mu\text{g m}^{-3}$) at the Gas field and Regional sites shown as a frequency distribution for each season. The x-axis shows the concentration ranges of the contribution from the CSG-related emissions and the y-axis shows the percentage of model hours.

Figure 5.6 shows plots of the modelled 24-hour average $\text{PM}_{2.5}$ concentrations with all sources against the contribution from the CSG-related emissions to the modelled 24-hour average $\text{PM}_{2.5}$ concentrations at Miles Airport. Those for Condamine, Hopeland, Tara Region and Burncluth are shown in Appendix E. The plots are seasonal and one point is plotted for each modelled day.

At Miles Airport there are small increases in the 24-hour average modelled PM_{2.5} due to the CSG-related emissions during DJF, MAM and JJA. The largest increases (> 2 µg m⁻³) occur during JJA, although as Figure 5.5 shows they occur less than 10 % of the time. The maximum increase in the 24-hour average PM_{2.5} concentration due to the CSG-related emissions is less than 5 µg m⁻³ which is 20 % of the air quality objective for PM_{2.5} (25 µg m⁻³, Table 5.1). At the other Gas field sites and the Regional sites the maximum increase in the modelled 24-hour average PM_{2.5} concentration due to the CSG-related emissions is less than 1 µg m⁻³ (see Appendix E).

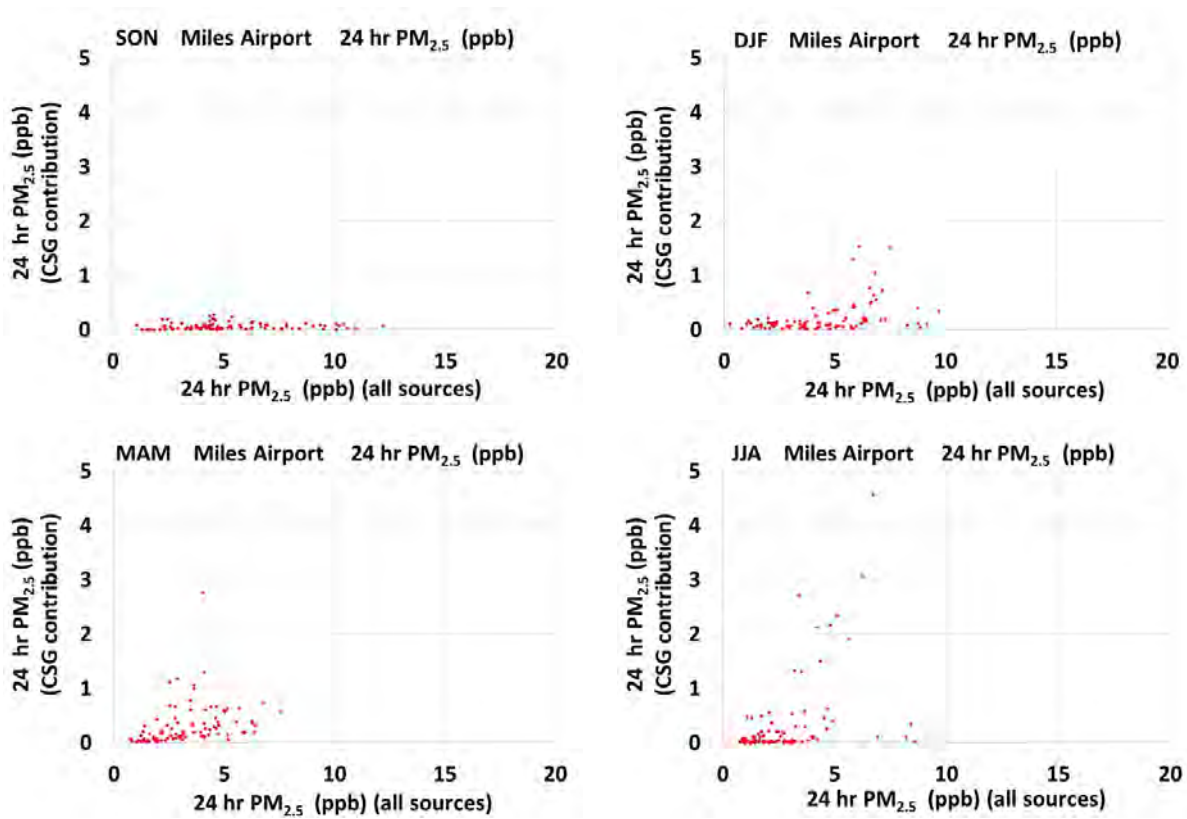


Figure 5.6 The modelled contribution from the CSG-related emissions to the 24-hour average PM_{2.5} concentration (µg m⁻³) at Miles Airport shown as a scatter plot for each season. The x-axis shows the modelled 24-hour average PM_{2.5} concentrations with all sources (µg m⁻³) and the y-axis shows the contribution from the CSG-related emissions to the 24-hour average PM_{2.5} concentration (µg m⁻³).

5.1.2 Comparison with Air Quality Objectives at Observation Sites

In this section the model results are compared to air quality objectives to assess whether there are any modelled exceedances of PM_{2.5} at the Gas field or Regional sites. The air quality objectives used to assess the pollutant concentrations are presented in Table 5.1.

Table 5.2 presents the observed annual average concentrations of PM_{2.5} and those modelled with all sources and without the CSG sources at the Gas field and Regional sites. Note that according to the NEPM (2016), annual observations are only valid for regulatory purposes if at least 75 % of

observations in each calendar quarter are valid. In Table 5.2 annual observations are listed where this is met or almost met with the appropriate percentage listed.

In no instances (modelled or observed) did the annual average PM_{2.5} concentrations exceed the PM_{2.5} annual air quality objective (8 µg m⁻³, Table 5.1). In addition, the modelled annual average PM_{2.5} concentrations with all sources included and those without the CSG sources are almost the same, and similar to the observed where available.

Table 5.2 The observed and modelled annual average concentrations of PM_{2.5} (µg m⁻³) at the Gas field and Regional sites.

Annual average (µg m ⁻³)	Observed PM _{2.5}	Modelled PM _{2.5} (all sources)	Modelled PM _{2.5} (without CSG sources)
Miles Airport	4.2 ^a	3.9	3.6
Condamine	c	3.9	3.8
Hopeland	4.3 ^b	4.0	3.9
Tara Region	nd	3.7	3.6
Burncluith	nd	4.3	4.2

a – PM_{2.5} observations 44 % Jan, Feb, Mar

b – PM_{2.5} observations 64 % Jan, Feb, Mar

c – only 6 months of observations

nd – no data available

Figure 5.7 shows the maximum 24-hour average PM_{2.5} concentrations for each month of the model simulation, at each observation site. The bar plots show the observed values in blue, the model results with all sources in red and the model results without the CSG sources in purple. The dashed horizontal red line shows the value of the air quality objective. The observed values are only shown when at least 75 % of observations are available for the month.

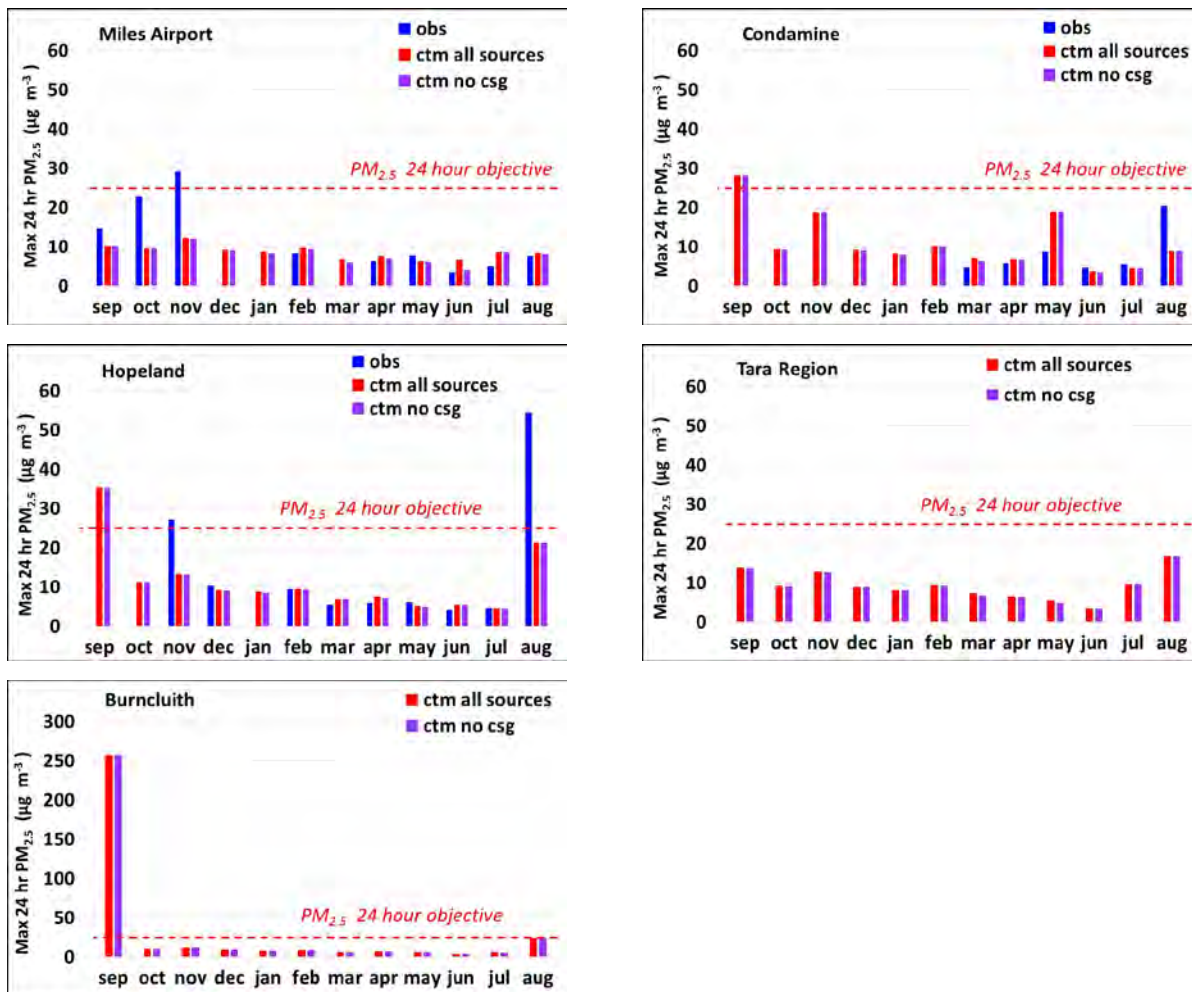


Figure 5.7 The maximum 24-hour average PM_{2.5} concentrations (µg m⁻³) for each month of September 2015 – August 2016 at the Gas field and Regional sites: observed (blue), model results with all sources (red) and model results without the CSG sources (purple).

Observations of the maximum 24-hour average PM_{2.5} concentrations exceed the air quality objective for PM_{2.5} (25 µg m⁻³, Table 5.1) at Miles Airport and Hopeland in November 2015 and at Hopeland in August 2016. The modelled PM_{2.5} concentrations exceed the 24-hour air quality objective at Condamine and Burncluith in September 2015 and at Hopeland on two occasions in September 2015 (on consecutive days with the highest value shown in Figure 5.7). The observed exceedances are discussed in Lawson et al. (2018a), and all of the modelled exceedances are associated with fires but there are no corresponding observations to confirm.

During the modelled year there are no modelled exceedances of the 24-hour average PM_{2.5} air quality objective or 80 % of the air quality objective (Table 5.1) at any of the Gas field or Regional sites when the contribution of the CSG-related emissions to PM_{2.5} is greater than 1 µg m⁻³.

At all sites the maximum modelled 24-hour average PM_{2.5} concentrations for the results with all sources included and for the results without the CSG sources are similar (differences less than 1 µg m⁻³), except for June 2016 at Miles Airport where the maximum 24-hour average PM_{2.5} concentration for the results with all sources included is greater than for the results without the CSG sources by 2.6 µg m⁻³.

The modelled and observed 24-hour average PM_{2.5} concentrations are similar except when there is an observed or modelled fire during the month.

5.1.3 Comparison with Air Quality Objectives for the Region

Figure 5.8 shows spatial plots over the model 1 km grid domain of the modelled maximum 24-hour average PM_{2.5} concentrations with all sources included for each season. Note that each grid square shows the maximum concentration modelled for that grid square *for that entire season*. As such the maximum concentration shown in each grid square may be from different days during the season.

Areas exceeding the 24-hour average PM_{2.5} air quality objective of 25 µg m⁻³ and 80 % of the 24-hour average PM_{2.5} air quality objective of 20 µg m⁻³ (to identify these areas see the coloured scale in Figure 5.8) are predominantly due to modelled fires as can be seen by comparison with a similar plot for the smoke tracer levoglucosan shown in Figure 5.9.

Figure 5.10 shows the contribution, in each grid square for each season, of the CSG-related emissions to the modelled maximum 24-hour average PM_{2.5} concentrations shown in Figure 5.8. Note, this is calculated for each grid square by subtracting the maximum 24-hour average PM_{2.5} concentration for the season in the run without the CSG sources from the maximum 24-hour average PM_{2.5} concentration for the same season in the run with all sources. Importantly, in each grid square the two maximum values that are subtracted may each be from a different day during the season.

The CSG contribution to these maximum values is small over the region, generally less than 1 µg m⁻³ with larger values close to the CSG-related sources. The maximum value (indicated by the red arrow) is 12 µg m⁻³ during MAM and is about 1 km from CSG-related emission sources. Note that the model cannot resolve near-source impacts of plumes well and therefore impacts within a few kilometres of a point emission source may be under or overestimated.

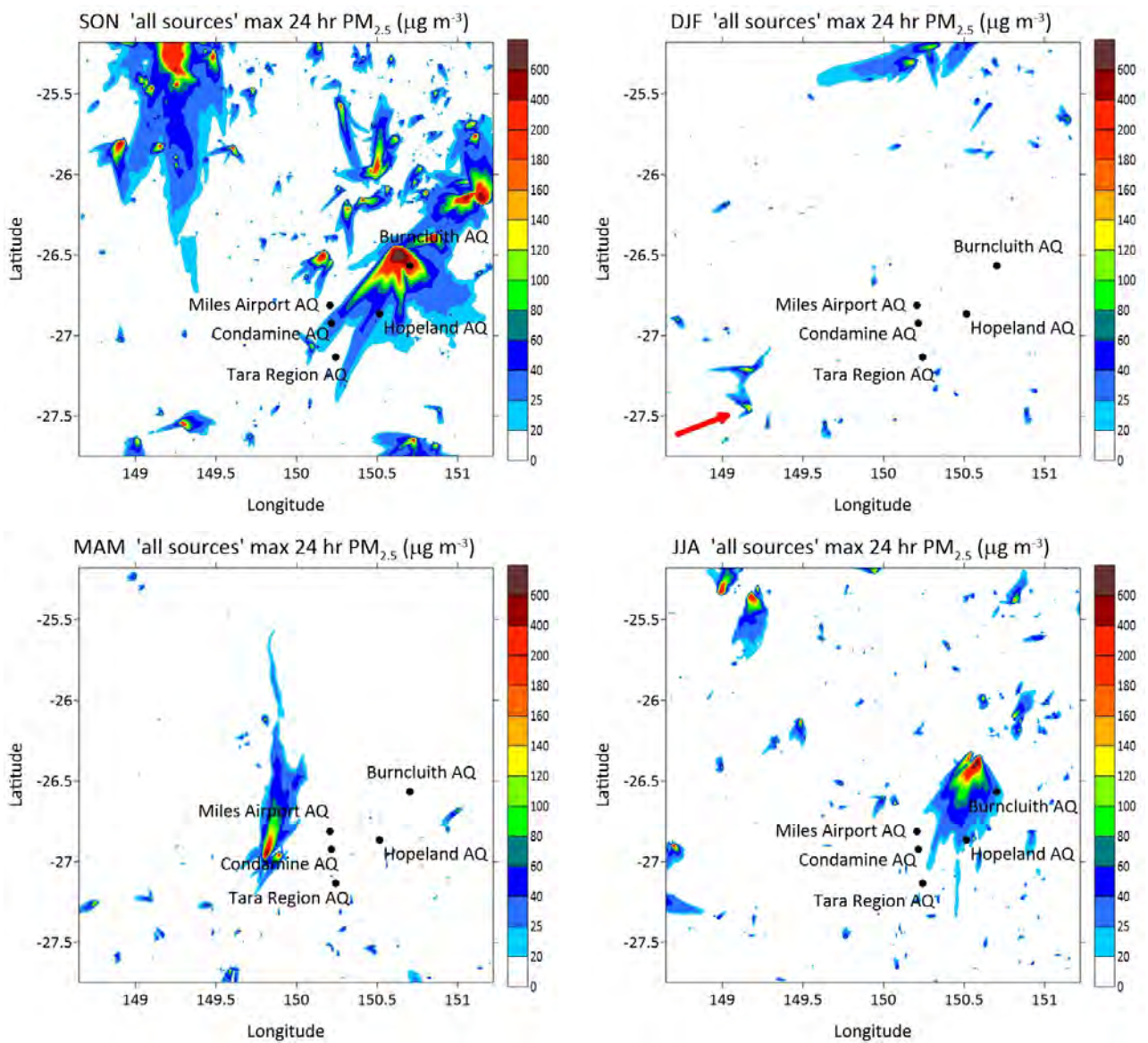


Figure 5.8 The maximum concentration of the 24-hour average PM_{2.5} in each grid square for the model results with all sources during each season ($\mu\text{g m}^{-3}$). Note that the maximum concentrations shown in each grid square may be from different days during the season. The red arrow indicates the location of the maximum value for the season.

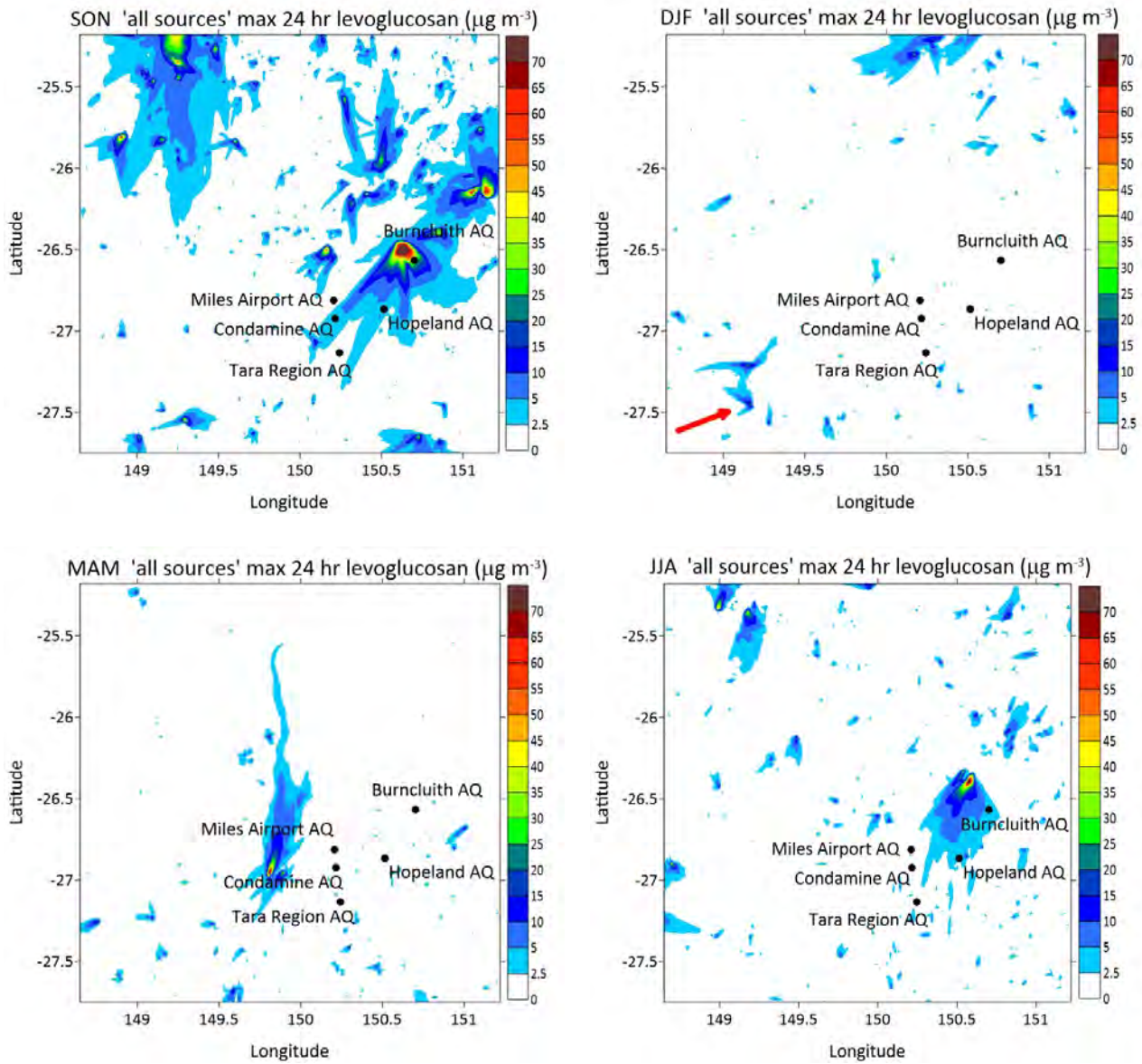


Figure 5.9 The maximum concentration of the 24-hour average levoglucosan (smoke tracer) in each grid square for the model results with all sources during each season ($\mu\text{g m}^{-3}$). Note that the maximum concentrations shown in each grid square may be from different days during the season. The red arrow indicates the location of the maximum value for the season.

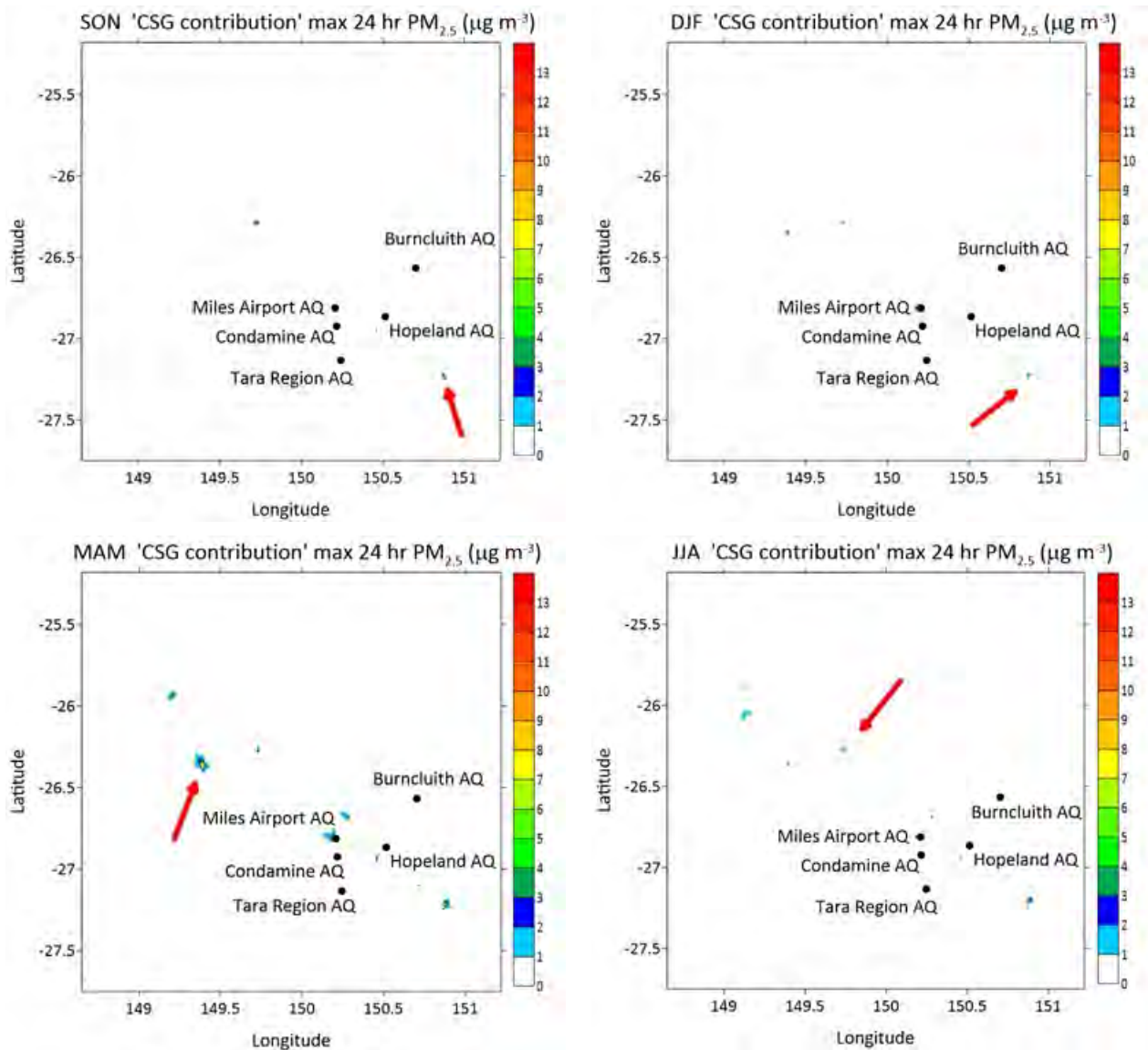


Figure 5.10 The contribution of the CSG-related emissions to the modelled maximum 24-hour average $PM_{2.5}$ concentration (maximum in each grid square from Figure 5.8) during each season ($\mu g m^{-3}$). Note that the concentrations shown in each grid square may be from different days during the season. The red arrow indicates the location of the maximum value for the season.

Figure 5.11 shows the maximum contribution of the CSG-related emissions to the 24-hour average modelled $PM_{2.5}$ concentrations in each grid square for the modelled year. Note, this is calculated in each grid square by subtracting, every day, the 24-hour average $PM_{2.5}$ concentration for the run without CSG sources from that for the run with all sources and then calculating the maximum value for the year from the daily values. Importantly, in each grid square the two values that are subtracted are from the same day in the season. Note this figure is showing the maximum contribution to the $PM_{2.5}$ concentration values whilst Figure 5.10 shows the contribution to the maximum $PM_{2.5}$ concentration values.

Generally, the maximum modelled contributions are less than $1 \mu g m^{-3}$ with larger values close to CSG sources. The largest maximum contribution (indicated by the red arrow) is $22.1 \mu g m^{-3}$ which

is 88 % of the air quality objective ($25 \mu\text{g m}^{-3}$, Table 5.1) and 92 % of the 24-hour average modelled $\text{PM}_{2.5}$ concentration and is located about 1 km from CSG-related emission sources.

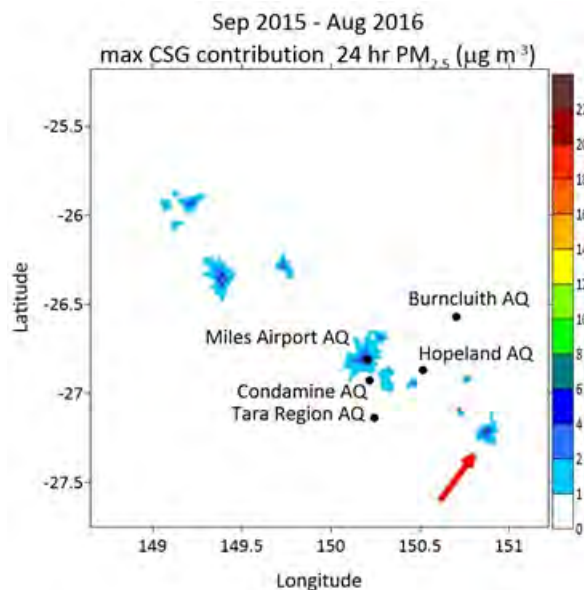


Figure 5.11 The maximum contribution of the CSG-related emissions to the modelled 24-hour average $\text{PM}_{2.5}$ concentrations during the modelled year ($\mu\text{g m}^{-3}$). Note that the concentrations shown in each grid square may be from different days during the year. The red arrow indicates the location of the maximum value for the year.

Over the modelled 1 km grid domain during the modelled year there are 8 exceedances of the 24-hour average $\text{PM}_{2.5}$ air quality objective ($25 \mu\text{g m}^{-3}$, Table 5.1) when the contribution of the CSG-related emissions to $\text{PM}_{2.5}$ concentrations is greater than $1 \mu\text{g m}^{-3}$. There are also 15 exceedances of 80 % of the air quality objective ($20 \mu\text{g m}^{-3}$, Table 5.1). Exceedances are not included if there is already an exceedance before the CSG-related emissions are included.

The 8 exceedances are listed in Table 5.3. Also listed are 8 of the exceedances of 80 % of the air quality objective with the highest contribution of the CSG-related emissions to the 24-hour average $\text{PM}_{2.5}$ concentrations. The contribution and the percentage contribution of the CSG-related emissions to all exceedances are also listed.

The highest 24-hour average $\text{PM}_{2.5}$ exceedance of the air quality objective, which has a contribution from the CSG-related emissions greater than $1 \mu\text{g m}^{-3}$, is $31.5 \mu\text{g m}^{-3}$ with a 37 % ($11.7 \mu\text{g m}^{-3}$) contribution from the CSG-related emissions.

The largest contribution of the CSG-related emissions to the modelled exceedances of 80 % of the air quality objective for 24-hour average $\text{PM}_{2.5}$ is $22.1 \mu\text{g m}^{-3}$ which represents a 92 % contribution. Of the 15 80 % exceedances (not all listed in Table 5.3) the contribution from the CSG-related emissions ranges from $1.0 - 22.1 \mu\text{g m}^{-3}$ which is a 6 – 92 % contribution from the CSG-related emissions to the 24-hour average $\text{PM}_{2.5}$ concentrations.

Table 5.3 The 8 modelled 24-hour average PM_{2.5} concentrations that exceed the air quality objective (25 µg m⁻³) and the 8 modelled 24-hour average PM_{2.5} concentrations of the 15 exceedances of 80 % of the air quality objective (20 µg m⁻³) with the highest contribution of the CSG-related emissions. The contribution (µg m⁻³) and the percentage contribution of the CSG-related emissions to the exceedances are also included.

24- hour PM _{2.5} exceedances (µg m ⁻³)	Contribution of the CSG-related emissions to exceedances (µg m ⁻³)	Percentage contribution of the CSG-related emissions to exceedances	24- hour PM _{2.5} 80 % exceedances (µg m ⁻³)	Contribution of the CSG-related emissions to 80 % exceedances (µg m ⁻³)	Percentage contribution of the CSG-related emissions to 80 % exceedances
31.5	11.7	37	24.1	22.1	92
25.1	9.2	37	23.8	11.6	49
25.4	7.9	31	20.8	10.8	52
27.8	6.5	24	21.7	7.2	33
27.2	5.4	20	20.4	5.5	27
27.2	5.1	19	22.5	5.1	23
25.3	1.6	6	20.7	3.9	19
25.0	1.0	4	23.2	3.4	15

Figure 5.12 (left) shows the location of the modelled 24-hour average PM_{2.5} concentrations that exceed the air quality objective when the contribution of the CSG-related emissions is greater than 1 µg m⁻³. Also shown in Figure 5.12 (right) is the same plot but for exceedances of 80 % of the air quality objective. These 15 exceedances occur at 12 separate locations shown by the red crosses in Figure 5.12 and all occur within a few kilometres of CSG-related emission sources. (Note it may be difficult to see 12 separate locations in the figure as the grid point spacing is 0.01 degrees and a number of the exceedances occur in neighbouring grid squares.)

Over the modelled 1 km grid domain during the modelled year 0.12 % of the possible 24-hour average PM_{2.5} concentrations exceed the air quality objective (see Figure 5.8) and of those 0.06 % include a contribution from the CSG-related emissions greater than 1 µg m⁻³. The predominant source of PM_{2.5} exceedances in the region is from vegetation fires.

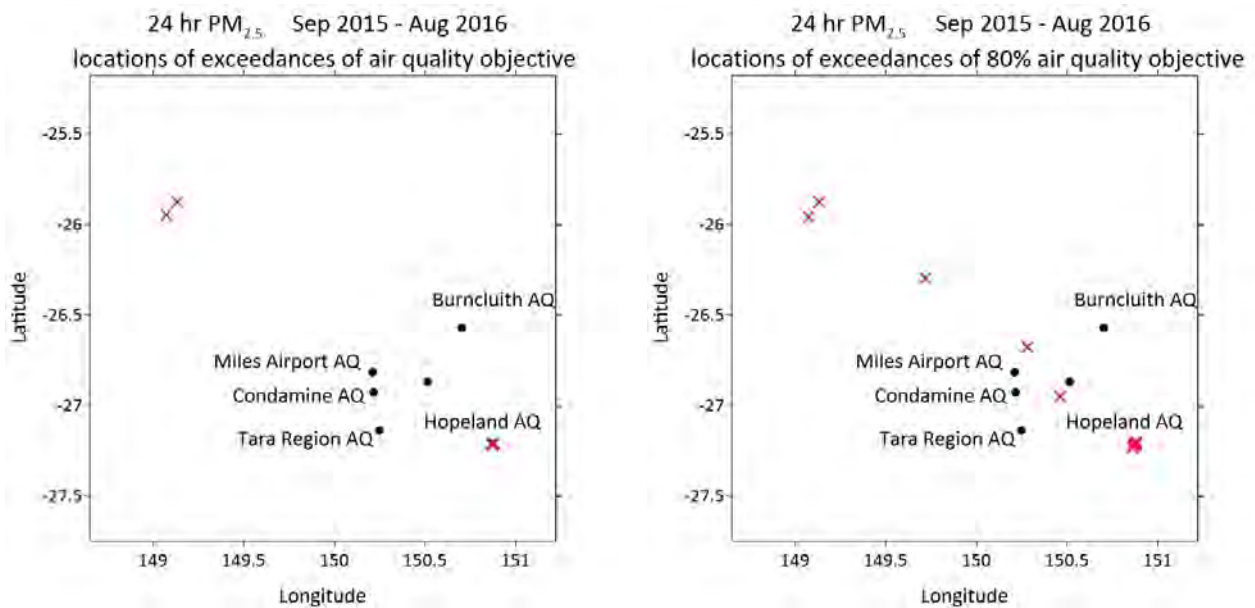


Figure 5.12 The locations, marked by red crosses, of the modelled 24-hour average $PM_{2.5}$ concentrations (left) that exceed the air quality objective ($25 \mu g m^{-3}$) or (right) that exceed 80 % of the air quality objective ($20 \mu g m^{-3}$). All exceedances are when the contribution of the CSG-related emissions is greater than $1 \mu g m^{-3}$.

5.1.4 Modelled effect of the CSG-related emissions on $PM_{2.5}$ levels at Town sites.

Model results are presented for five towns in the model domain to investigate the effects of the CSG-related emissions to $PM_{2.5}$ concentrations over the region. These towns are chosen due to their proximity to the CSG region and / or because they are major population centres in the study area. The towns selected are Chinchilla, Myles township, Roma, Tara township and Warra and their locations are shown in Figure 2.3 they will be referred to collectively as ‘Town sites’.

Table 5.4 presents the annual average concentrations of $PM_{2.5}$ for the model results with all sources and without the CSG sources at the Town sites. All modelled concentrations are well below the annual air quality objective for $PM_{2.5}$ ($8 \mu g m^{-3}$, Table 5.1) and the annual average $PM_{2.5}$ concentrations for model results with and without CSG sources are almost the same.

Table 5.4 The modelled annual average concentrations of PM_{2.5} (µg m⁻³) at the Town sites.

Annual average (µg m ⁻³)	Modelled PM _{2.5} (all sources)	Modelled PM _{2.5} (without CSG sources)
Chinchilla	4.0	4.0
Miles township	3.8	3.7
Roma	3.7	3.6
Tara township	3.7	3.6
Warra	3.8	3.7

Figure 5.13 shows the maximum 24-hour average PM_{2.5} concentrations for each month of the model simulation at the Town sites. The bar plots show the model results with all sources in red and the model results without the CSG sources in purple. The dashed horizontal red line shows the value of the air quality objective.

The modelled maximum 24-hour average PM_{2.5} concentrations exceed the air quality objective (25 µg m⁻³, Table 5.1) at Chinchilla during September 2015 and are associated with a modelled fire. Smoke is observed during this period as discussed in Section 5.1.1. The maximum 24-hour average PM_{2.5} concentrations approach the air quality objective in August 2015 at Chinchilla, Tara township and Warra and are also associated with a modelled fire. Lawson et al., (2018a) identified the observed elevated PM_{2.5} concentrations during this period as local fires at Condamine and Hopeland. Otherwise the maximum 24-hour average PM_{2.5} concentrations are well below the air quality objective.

At the Town sites the modelled maximum 24-hour average PM_{2.5} concentrations with all sources and without the CSG sources are similar (differences less than 1 µg m⁻³).

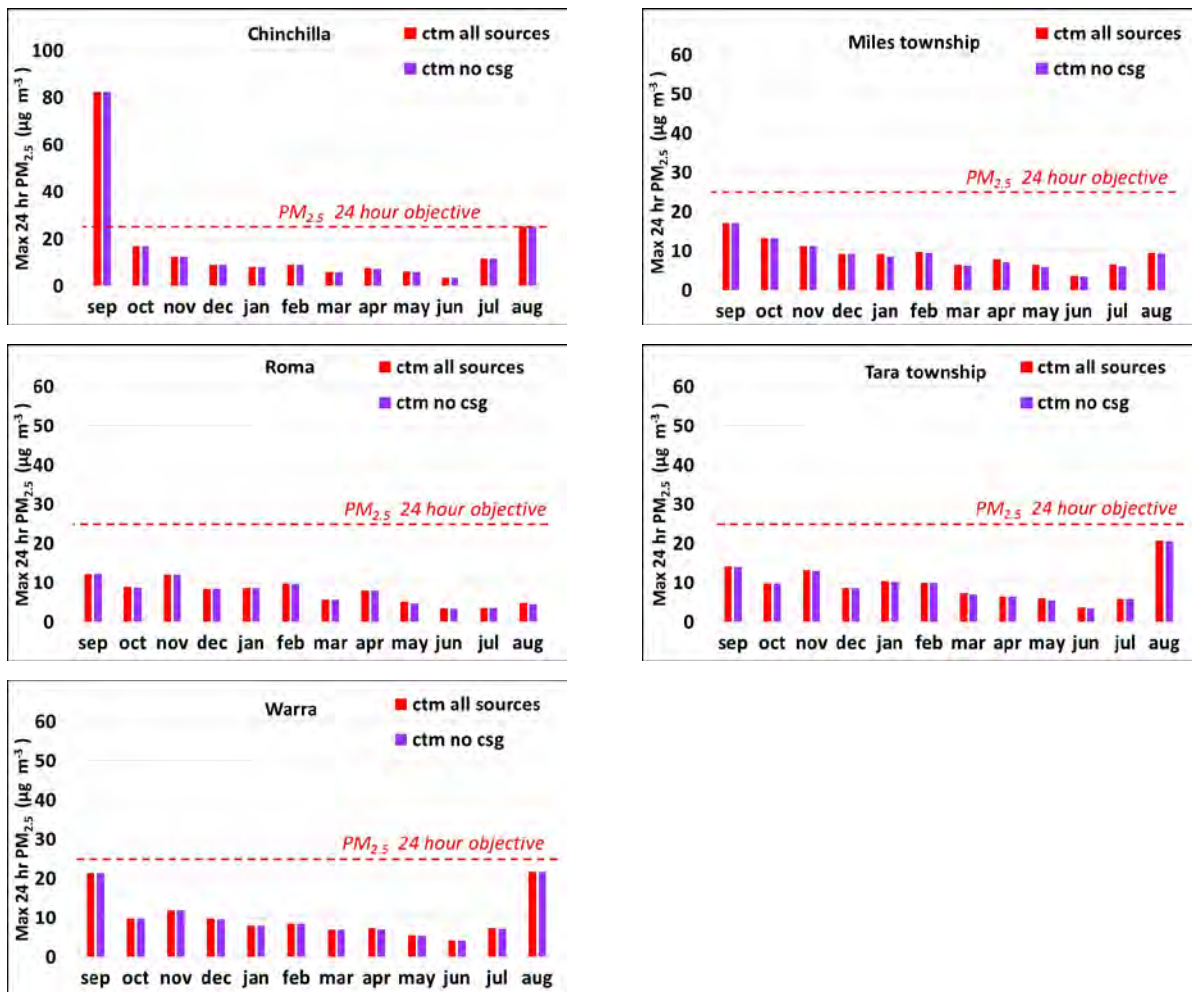


Figure 5.13 The modelled maximum 24-hour average PM_{2.5} concentrations ($\mu\text{g m}^{-3}$) for each month of September 2015 – August 2016 at the Town sites: model results with all sources (red) and model results without the CSG sources (purple).

The modelled contribution from the CSG-related emissions to the 24-hour average PM_{2.5} concentrations at each of the Town sites is presented in Figure 5.14. Each plot shows the percentage of model hours within each season for the modelled contribution from the CSG-related emissions to the 24-hour average PM_{2.5} concentrations.

Mostly there is very little contribution from the CSG-related emissions at any Town site; on average 99.7 % of the time the contribution is less than $0.5 \mu\text{g m}^{-3}$ which is 2 % of the 24-hour air quality objective for PM_{2.5} ($25 \mu\text{g m}^{-3}$, Table 5.1). Miles township is predicted to have the largest frequency of change due to the CSG-related emissions during MAM, however, these changes are very small (less than $1 \mu\text{g m}^{-3}$).

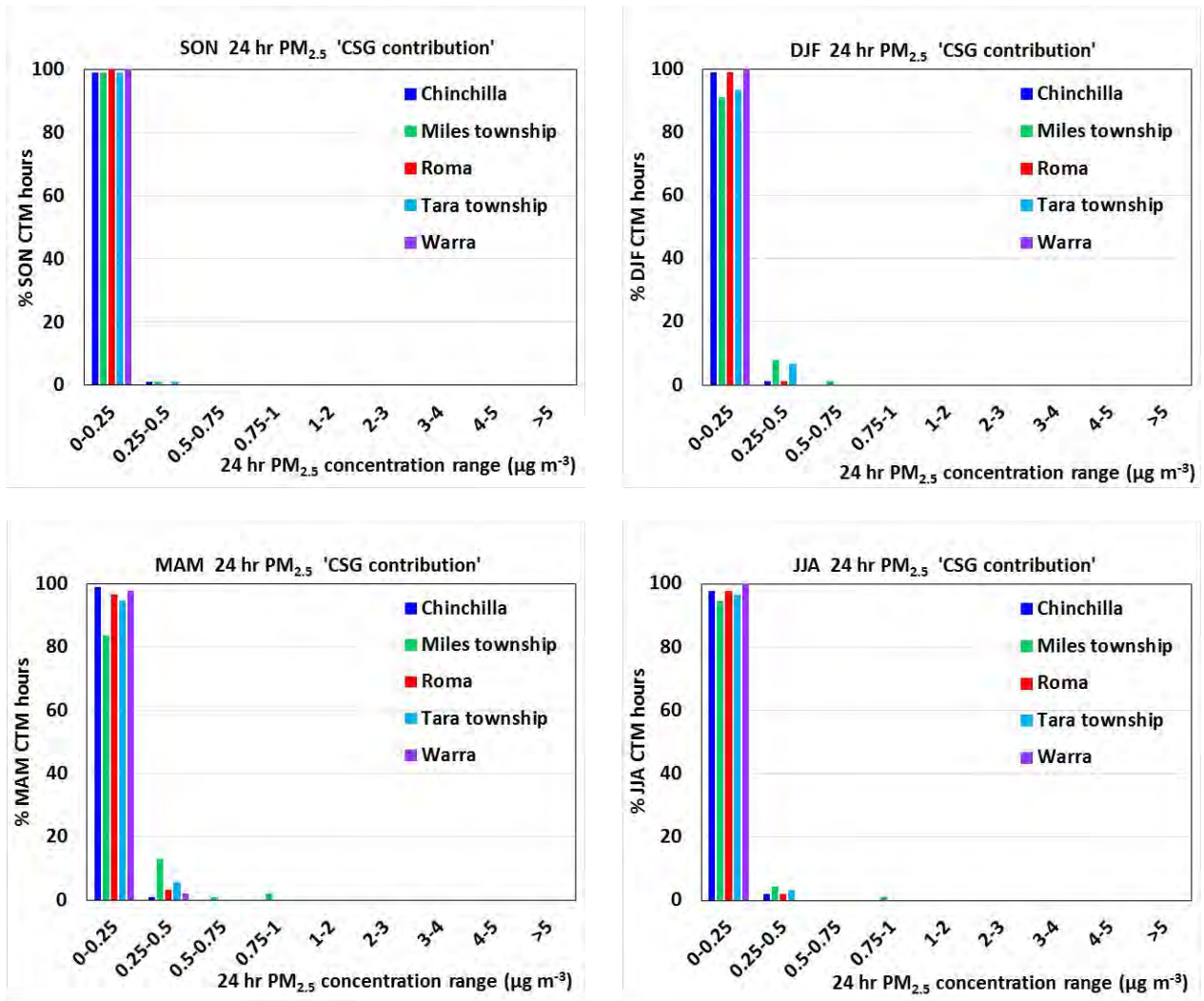


Figure 5.14 The modelled contribution from the CSG-related emissions to the 24-hour average PM_{2.5} concentration (µg m⁻³) at the Town sites shown as a frequency distribution for each season. The x-axis shows the concentration ranges of the contribution from the CSG-related emissions and the y-axis shows the percentage of model hours.

Figure 5.15 shows plots of the modelled 24-hour average PM_{2.5} concentrations with all sources against the contribution from the CSG-related emissions to the modelled 24-hour average PM_{2.5} concentrations at Miles township, one of the Town sites. Those for the other Town sites are shown in Appendix E. The plots are seasonal and one point is plotted for each modelled day.

There is very little increase (< 1 µg m⁻³) in the 24-hour modelled PM_{2.5} concentrations due to the CSG-related emissions at Miles township and this result is typical for the other Town sites (see Appendix E).

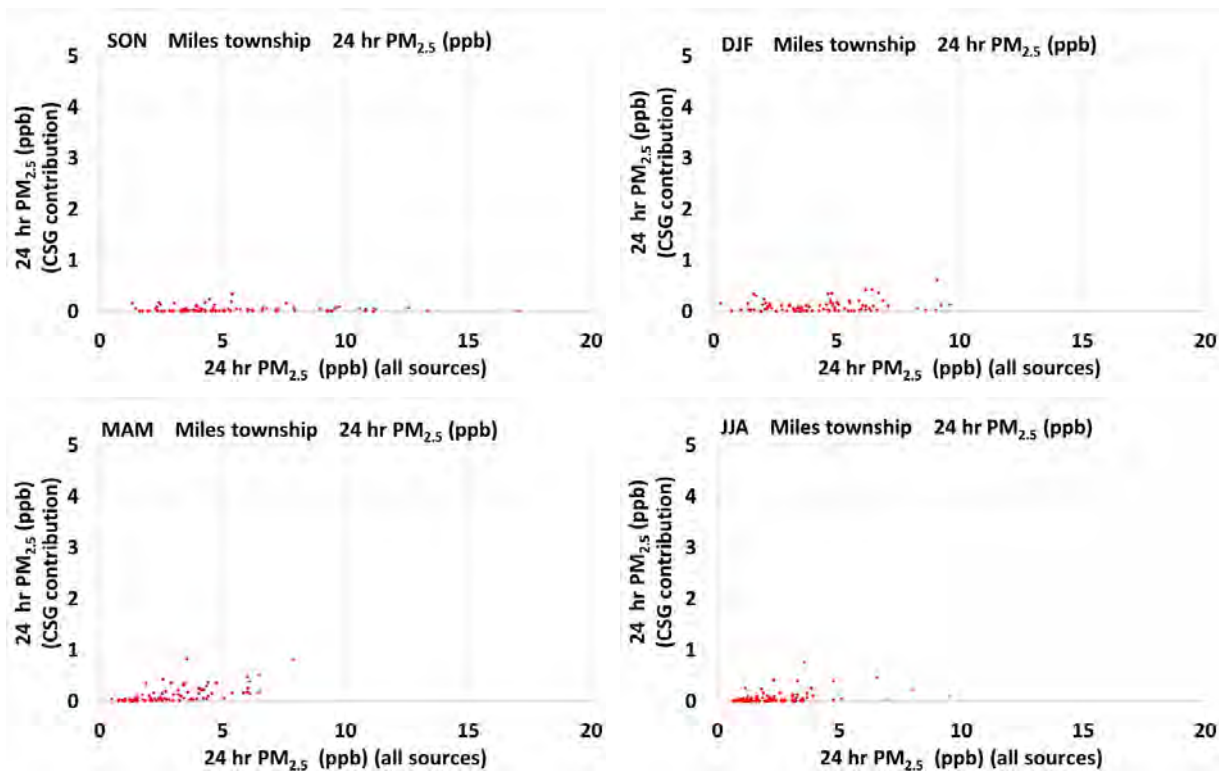


Figure 5.15 The modelled contribution from the CSG-related emissions to the 24-hour average $PM_{2.5}$ concentration ($\mu g m^{-3}$) at Miles township shown as a scatter plot for each season. The x-axis shows the modelled 24-hour average $PM_{2.5}$ concentrations with all sources ($\mu g m^{-3}$) and the y-axis shows the contribution from the CSG-related emissions to the 24-hour average $PM_{2.5}$ concentration ($\mu g m^{-3}$).

5.1.5 Summary

The impacts of CSG activity on the 24-hour average $PM_{2.5}$ concentrations modelled in the Surat Basin are summarised below:

Comparison of the model results with the observations

- The observed and modelled time series of $PM_{2.5}$ concentration at the Gas field sites show broad agreement, with the model capturing the background values of $PM_{2.5}$ and periods of slightly elevated $PM_{2.5}$. There are a number of observed larger peaks of $PM_{2.5}$ which the model does not capture at the Gas field sites. Many of the larger and broader observed peaks are due to fires which the model has simulated reasonably well but does not produce exact matches in time and space with the observations.

Contribution of the CSG-related emissions to the modelled 24-hour average $PM_{2.5}$ concentrations

- On average 97 % of the time at the Gas field and Regional sites and 99.7 % of the time at the Town sites the contribution from the CSG-related emissions is less than $0.5 \mu g m^{-3}$ which is 2 % of the air quality objective.
- At the Gas field, Regional and Town sites the largest modelled effect due to the CSG-related emissions on the 24-hour average $PM_{2.5}$ concentrations occurs at Miles Airport. The

maximum increase that can be attributed to the CSG-related emissions at Miles Airport is less than $5 \mu\text{g m}^{-3}$ which is 20 % of the air quality objective. The largest increases ($> 2 \mu\text{g m}^{-3}$) occur at Miles Airport during JJA for less than 10 % of the time. At the other Gas field, Regional and Town sites the maximum increase in the 24-hour average modelled $\text{PM}_{2.5}$ concentrations due to the CSG-related emissions is less than $1 \mu\text{g m}^{-3}$.

- Over the entire model 1 km grid domain during the modelled year the maximum contribution of the CSG-related emissions to the modelled 24-hour average $\text{PM}_{2.5}$ concentrations is $22.1 \mu\text{g m}^{-3}$ which is 88 % of the air quality objective and 92 % of the 24-hour average modelled $\text{PM}_{2.5}$ concentration and occurs about 1 km from CSG-related emission sources.
- Note that the model cannot resolve near-source impacts of plumes therefore impacts within a few kilometres of a point emission source may be under or overestimated.

Contribution of the CSG-related emissions to exceedances of the air quality objective or 80 % of the air quality objective when the CSG-related emissions contribute more than $1 \mu\text{g m}^{-3}$ to the modelled 24-hour average $\text{PM}_{2.5}$ concentrations

- There are no modelled exceedances of the annual average $\text{PM}_{2.5}$ air quality objective at any of the Gas field, Regional or Town sites.
- At the Gas Field, Regional or Town sites there are no modelled exceedances of the 24-hour average $\text{PM}_{2.5}$ air quality objective or 80 % of the air quality objective during any month when the CSG-related emissions contribute more than $1 \mu\text{g m}^{-3}$ to the 24-hour average $\text{PM}_{2.5}$ concentrations.
- Over the entire modelled 1 km grid domain during the modelled year there are 8 exceedances of the 24-hour average $\text{PM}_{2.5}$ air quality objective when the contribution of the CSG-related emissions to $\text{PM}_{2.5}$ concentrations is greater than $1 \mu\text{g m}^{-3}$. There are also 15 exceedances of 80 % of the air quality objective. All exceedances and 80 % exceedances with CSG-related contributions occur within a few kilometres of CSG-related emission sources. The highest 24-hour average $\text{PM}_{2.5}$ exceedance of the air quality objective with a CSG-related contribution is $31.5 \mu\text{g m}^{-3}$ with a 37.2 % ($11.7 \mu\text{g m}^{-3}$) contribution from the CSG-related emissions. Of the 15 80 % exceedances the contribution from the CSG-related emissions ranges from $1.0 - 22.1 \mu\text{g m}^{-3}$ which is a 6 – 92 % contribution from the CSG-related emissions to the 24-hour average $\text{PM}_{2.5}$ concentrations.
- Over the modelled 1 km grid domain during the modelled year 0.12 % of the possible 24-hour average $\text{PM}_{2.5}$ concentrations exceed the air quality objective and of those 0.06 % include a contribution from the CSG-related emissions greater than $1 \mu\text{g m}^{-3}$. The predominant source of $\text{PM}_{2.5}$ exceedances in the region is from vegetation fires.

Relative importance of different sources

- The largest values of the modelled 24-hour average $\text{PM}_{2.5}$ concentrations in the region are attributed to processes other than the CSG-related emissions, in particular, emissions associated with fires. This is in agreement with the monitoring study which found that all $\text{PM}_{2.5}$ exceedances at the Gas field sites are predominantly due to smoke from fires.

5.2 Ozone

Ozone (O_3) is another of the six key air pollutants included in the Ambient Air Quality NEPM (NEPM, 2016). Ground level ozone is a secondary pollutant, meaning that it is not directly emitted to the atmosphere but rather is formed through reactions between other pollutants in the atmosphere. Ozone formation requires the presence of precursors VOCs, nitrogen oxides, and sunlight. The CSG industry emits nitrogen oxides and VOCs primarily from gas and diesel combustion. Venting or fugitive emissions of CSG is an additional source of VOCs, however the predominant VOCs in CSG in the study area (ethane and propane) have a relatively low ozone formation potential. The amount of ozone formation in the study region potential is dependent on a combination of emissions from all potential sources (including CSG-related sources, other anthropogenic sources and natural sources), as well as meteorology.

5.2.1 Modelled effect of the CSG-related emissions at the observation sites

Time series plots of the observed and modelled concentrations of 1-hour average O_3 at Miles Airport are shown in Figure 5.16. The observations are shown in blue, the model results with all emission sources in red and the model results without the CSG-related emission sources in purple. The time series are presented for different seasons. For comparison purposes and completeness the 1-hour average O_3 concentration time series for Condamine, Hopeland, Tara Region and Burncluith are shown in Appendix D. In the time series figure it is not always possible to see the two modelled time series, the red (all sources) concentration series is plotted first and then the purple (no CSG sources) series is plotted. Where the values of each series are the same only the last plotted series will be seen, which is the purple one (no CSG sources). Therefore, when red is seen on the plot it is because the two modelled series have different values at that point in time and the difference between the two values is the contribution to the concentration from the CSG-related emissions; this contribution is shown in Figure 5.17 (the contribution for the other sites is shown in Appendix D).

The observed and modelled O_3 concentrations at Miles Airport (see Figure 5.16) show reasonable agreement in the diurnal pattern of maximum concentrations during the middle of the day (or later in the afternoon) and minimum concentrations during the night-time and early-morning hours. The model also reproduces well the observed time periods with reduced amplitude in the diurnal pattern, such as shown during mid-July in Figure 5.16. Ozone peaks are generally underpredicted or similar to the observed during SON, however in the other seasons the modelled concentrations are similar to or overpredict the observed O_3 concentration peaks. The prediction of the magnitude of the night-time minima is mixed, during MAM and JJA the magnitude of the O_3 concentration minima occasionally tends to be overpredicted (i.e. concentrations are lower). This is possibly due to removal of O_3 due to reaction with (overpredicted) night-time peaks of NO_x which is presented later in Section 5.3.1 (Figure 5.28 shows that NO_2 peaks are generally overpredicted).

At Condamine there are O_3 observations for most of March 2016 and from May through to August 2016. The model tends to mostly overpredict during March and from May onwards the model captures the observed concentration pattern reasonably well (see Appendix D).

Hopeland has observations for most of the year and the model captures the observed concentration variations reasonably well. The O₃ peaks are generally overpredicted or similar to the observations except during JJA while the magnitude of the O₃ minima are generally underpredicted or similar to the observations except during JJA.

At the Regional sites there are O₃ observations for most of JJA and during this period the model tends to overpredict (see Appendix D).

Comparison of the time series for the model results with all sources and the model results without CSG sources in Figure 5.16 and Figure 5.17 (this figure shows the difference between the two modelled series in Figure 5.16) suggests that the CSG activities do not systematically influence the magnitude of the maximum and minimum O₃ concentrations that make up the O₃ diurnal patterns. This is also true for the other Gas field and Regional sites, although the contribution of the CSG-related emissions to O₃ at Burncluith is less than at the other sites (see Appendix D).

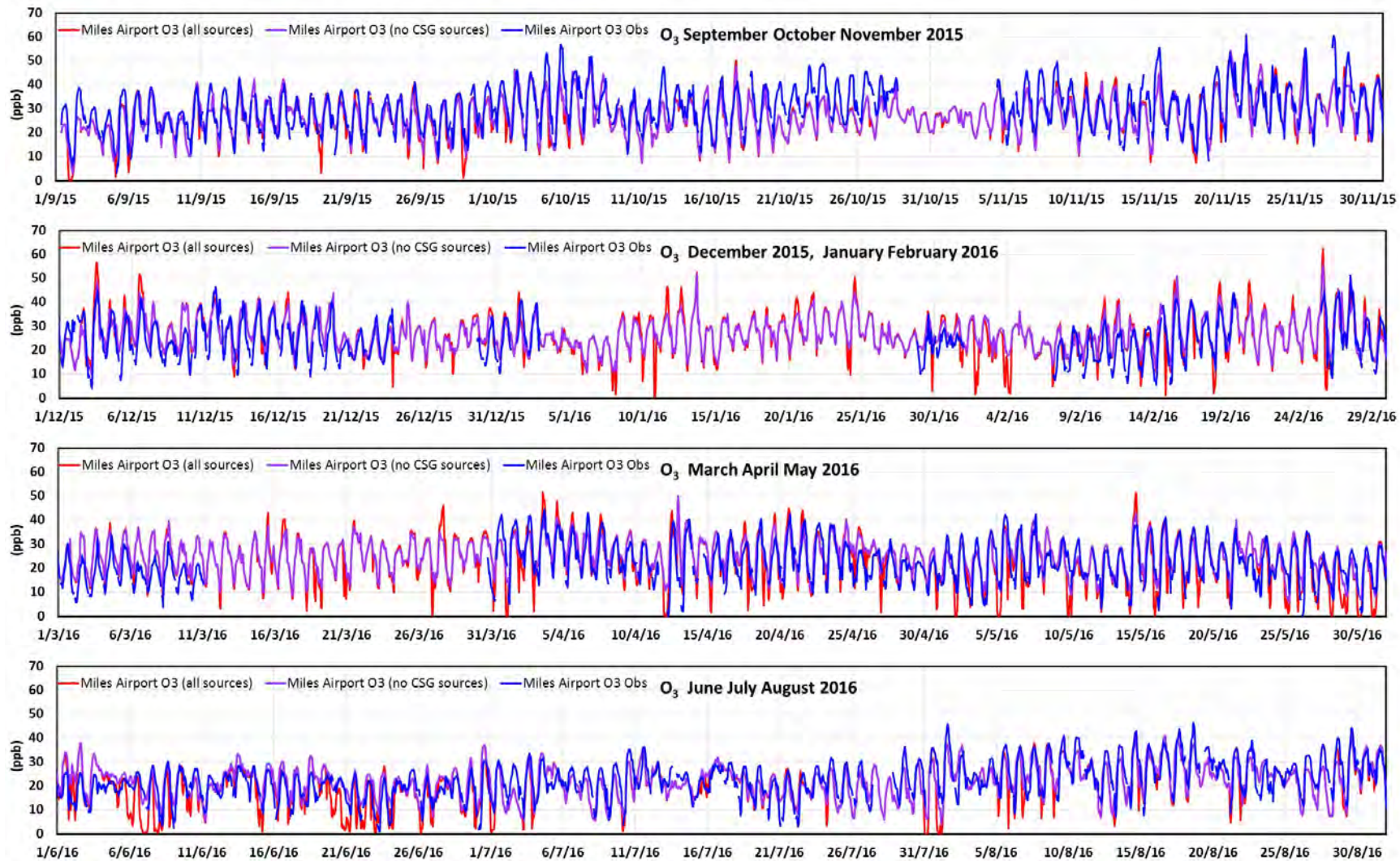


Figure 5.16 The observed and modelled time series of the 1-hour average O₃ concentrations (ppb) at Miles Airport for the modelled year (red = model results with all sources, purple = model results without CSG sources, blue = observations).

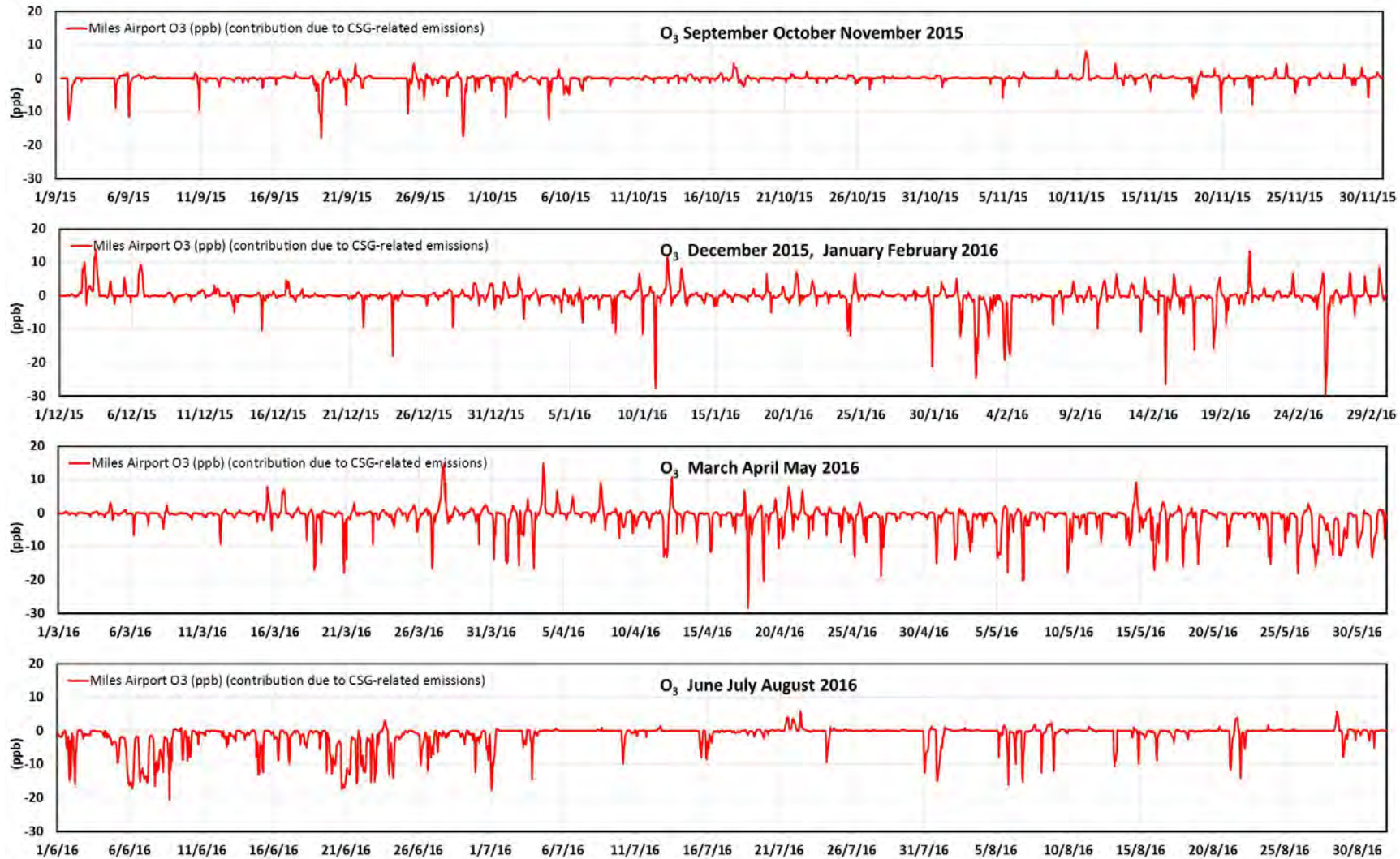


Figure 5.17 The modelled contributions from the CSG-related emissions to the 1-hour average O₃ concentrations (ppb) at Miles Airport for the modelled year.

The modelled contribution from the CSG-related emissions to the 4-hour average O₃ concentrations at each of the observations sites is presented in Figure 5.18. The change for the 1-hour average O₃ concentration is similar and shown in Appendix F. Each plot shows the percentage of model hours within each season for the modelled contribution from the CSG-related emissions to the 4-hour average O₃ concentrations. Note the change in O₃ can be negative or positive.

On average 96 % of the time the contribution from the CSG-related emissions at all sites is within ± 5 ppb which is 6.25 % of the 4-hour O₃ air quality objective (80 ppb, Table 5.1). The smallest frequency of change due to the CSG-related emissions is modelled at Burncluith, while the largest frequency of change due to the CSG-related emissions occurs at Condamine except during JJA.

During SON and DJF the effect of the CSG-related emissions is generally to increase O₃ while during MAM and JJA it is generally to decrease O₃. The largest modelled contributions of the CSG-related emissions to the 4-hour O₃ concentrations occurs most frequently in the summer months.

The frequency of change in the modelled O₃ whether positive or negative is reasonably consistent across the different monitoring sites. This is likely due to O₃ being controlled by regional processes and sources. This is in agreement with the observation study (Lawson et al., 2018c) which found that when elevated O₃ events occurred, they were generally seen at all monitoring sites and are therefore regional in nature.

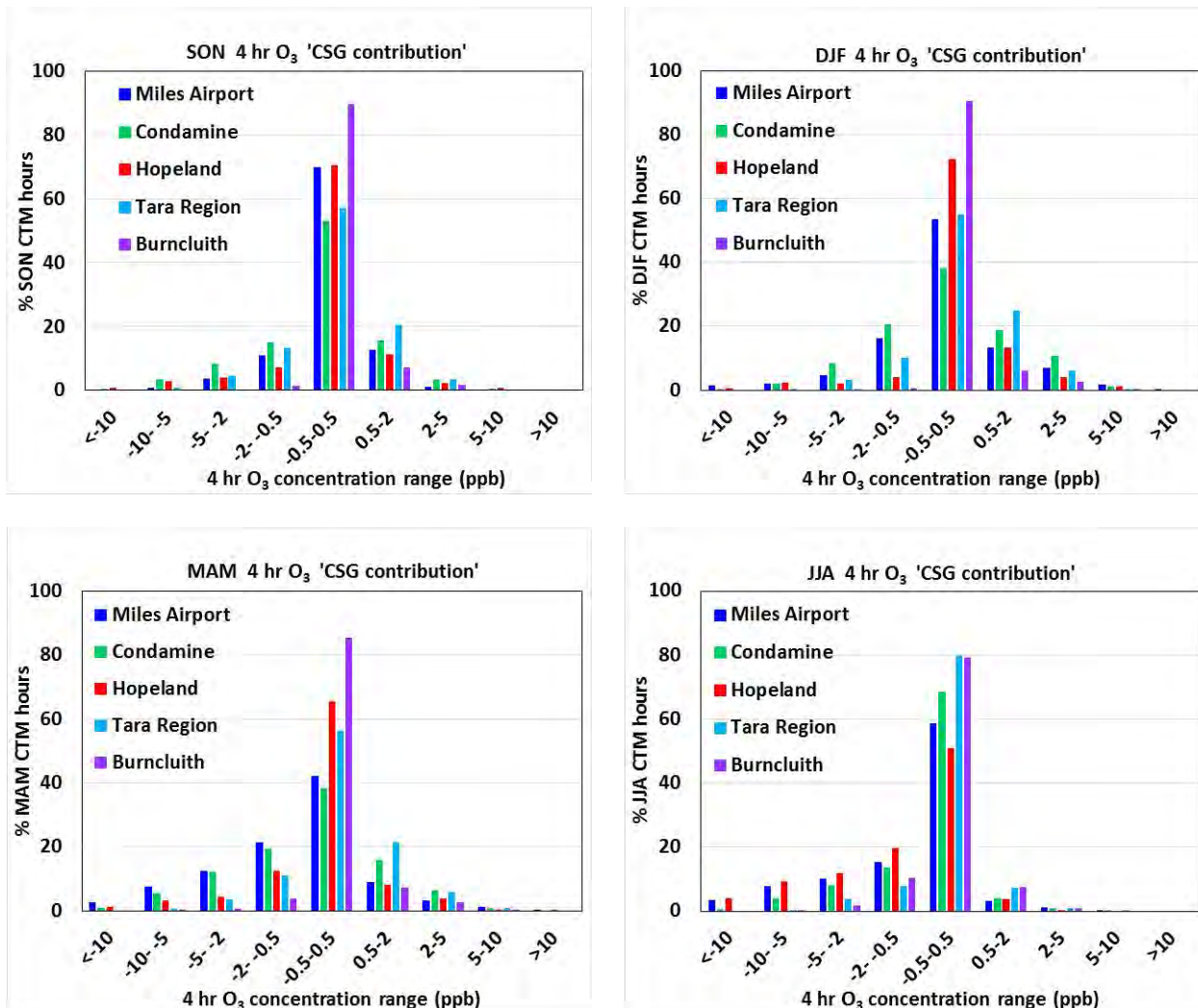


Figure 5.18 The modelled contribution from the CSG-related emissions to the 4-hour average O₃ concentration (ppb) at the Gas field and Regional sites shown as a frequency distribution for each season. The x-axis shows the concentration ranges of the contribution from the CSG-related emissions and the y-axis shows the percentage of model hours.

Figure 5.19 shows plots of the modelled 4-hour average O₃ concentrations with all sources against the contribution from the CSG-related emissions to the modelled 4-hour average O₃ concentrations at Miles Airport. The 1-hour average O₃ concentration plots are similar and are shown in Appendix E. Those for Condamine, Hopeland, Tara Region and Burncluith are also shown in Appendix E. The plots are seasonal and one point is plotted for each four-hourly modelled value. At Miles Airport the largest modelled increases (> 5 ppb) in the 4-hour average O₃ concentrations due to the CSG-related emissions occur mostly for larger O₃ values (i.e. increased peak concentrations) during DJF and MAM, with these increases accounting for up to 30 % of the O₃ value. The maximum increase due to the CSG-related emissions is 13.5 ppb which is 17 % of the 4-hour O₃ air quality objective (80 ppb, Table 5.1).

The largest decreases (< -10 ppb) are modelled to occur mostly for smaller values of the 4-hour average O_3 concentrations (i.e. deepening the minima) during all seasons but more frequently during MAM and JJA as shown also in Figure 5.18. These decreases account for up to 100 % of the 4-hour average O_3 value – e.g. emissions from the CSG-related sources reduce O_3 to zero probably due to removal of O_3 due to reaction with NO_x . The maximum decrease due to CSG-related emission is 23 ppb.

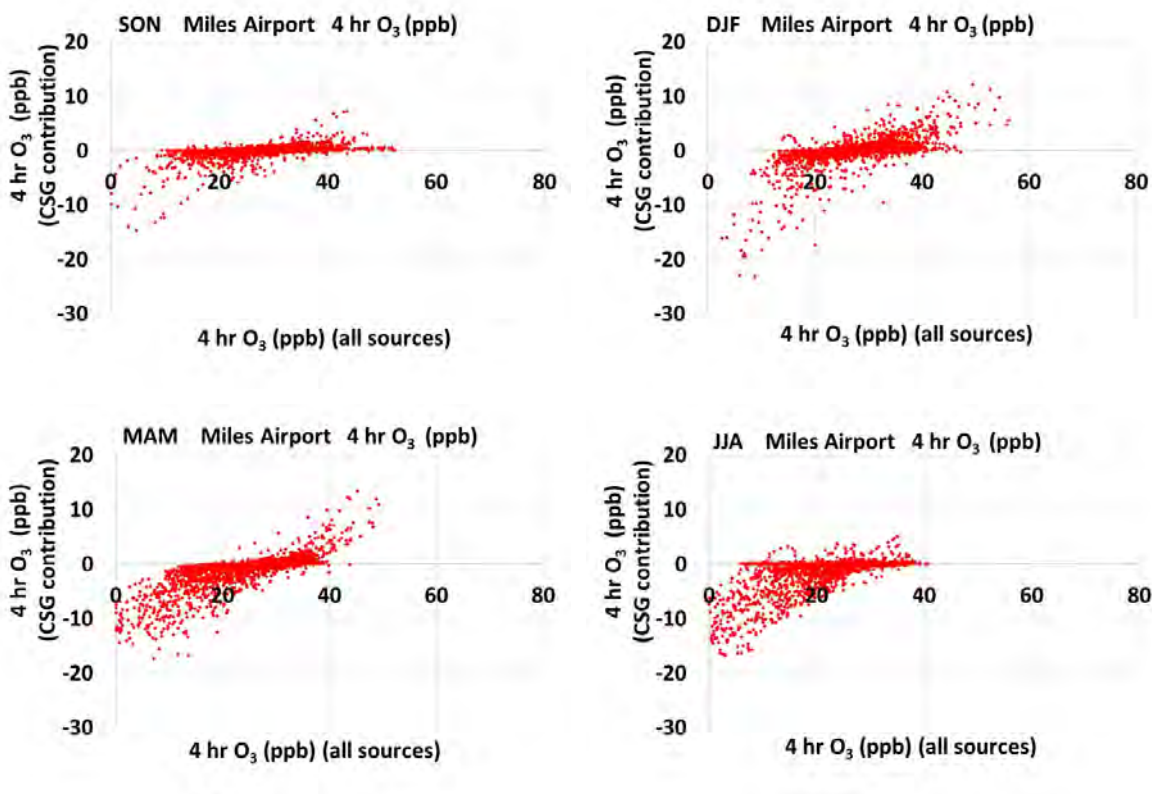


Figure 5.19 The modelled contribution from the CSG-related emissions to the 4-hour average O_3 concentration (ppb) at Miles Airport shown as a scatter plot for each season. The x-axis shows the modelled 4-hour average O_3 concentrations with all sources (ppb) and the y-axis shows the contribution from the CSG-related emissions to the 4-hour average O_3 concentration (ppb).

Similar patterns of higher maxima and deeper minima are modelled for Condamine and Hopeland (see Appendix E). Hopeland has the largest increase in the 4-hour average O_3 concentration due to the CSG-related emissions at 16.5 ppb, which equates to 20.6 % of the 4-hour O_3 air quality objective. Tara Region shows a smaller effect on maximum and minimum values of O_3 and the effect at Burnluith due to the CSG-related emissions is smaller again, reflecting the greater distance from CSG sources.

5.2.2 Comparison with Air Quality Objectives at Observation Sites

In this section the model results are compared to air quality objectives to assess whether there are any modelled exceedances of O₃ at the Gas field or Regional sites. The air quality objectives used to assess the pollutant concentrations are presented in Table 5.1.

Figure 5.20 shows the maximum 4-hour average O₃ concentrations for each month of the model simulation, at the Gas field and Regional sites. Those for the 1-hour average O₃ concentrations are shown in Appendix F. The bar plots show the observed values in blue, the model results with all sources in red and the model results without the CSG sources in purple. The dashed horizontal red line shows the value of the air quality objective. The observed values are only shown when at least 75 % of observations are available for the month.

The 4-hour average O₃ air quality objective (Table 5.1) and 80 % of the 4-hour average O₃ air quality objective are not exceeded by the observed or modelled 4-hour average O₃ concentrations at any site in any month (there are also no exceedances for the 1-hour average O₃ concentrations).

At Miles Airport the maximum modelled values are similar or within 10 ppb of those observed, with the model over and underpredicting. The largest differences between the observed and modelled are seen at Hopeland with the model overpredicting by up to 17 ppb.

December through to May shows greater modelled maximum 4-hour O₃ concentrations for the model results with all sources at Miles Airport, with contributions due to the CSG-related emissions of up to 9 ppb. The results at the other Gas field sites are similar, while at the Regional sites there is less of a difference between the model results with all sources and the model results without the CSG sources, with contributions due to the CSG-related emissions of up to 4 ppb.

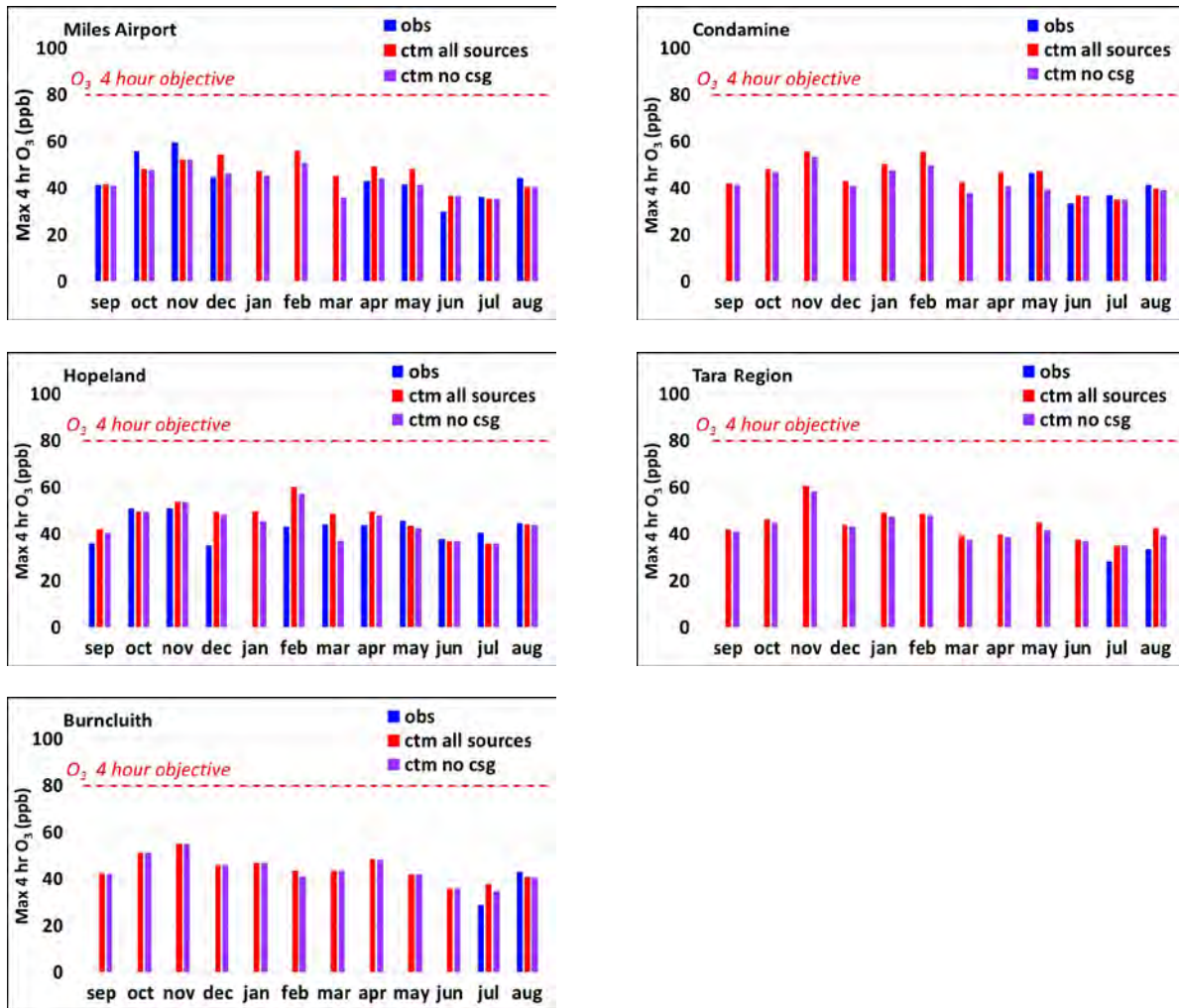


Figure 5.20 The maximum 4-hour average O₃ concentrations (ppb) for each month of September 2015 – August 2016 at the Gas field and Regional sites: observed (blue), model results with all sources (red) and model results without the CSG sources (purple).

5.2.3 Comparison with Air Quality Objectives for the Region

Figure 5.21 shows spatial plots over the model 1 km grid domain of the modelled maximum 4-hour average O₃ concentrations with all sources included for each season. Note that each grid square shows the maximum concentration modelled for that grid square *for that entire season*. As such the maximum concentration shown in each grid square may be from different time periods.

Areas exceeding the 4-hour average O₃ air quality objective of 80 ppb and 80 % of the 4-hour average O₃ air quality objective of 64 ppb are highlighted in the figure (to identify these areas see the coloured scale in Figure 5.21). The SON maximum modelled grid value for the 4-hour average O₃ is 84 ppb which exceeds the air quality objective of 80 ppb. This value occurs close to the eastern grid boundary, a second area with a maximum of 83 ppb occurs in the top north-west of the grid. Both of these areas over 80 ppb are small and are predominantly the result of emissions from modelled fires (compare with the SON smoke tracer levoglucosan in Figure 5.9).

No modelled exceedances of the 4-hour air quality objective for O₃ occur during the other seasons. During SON and DJF there are areas over 80 % of the 4-hour average O₃ air quality objective with a maximum grid value for DJF of 79 ppb.

For the other seasons the maximum grid values are 60 ppb for MAM and 47 ppb for JJA (indicated by the red arrow). The maximum grid value for each season is the same for both model results, i.e. all sources included and without CSG sources. The contribution from CSG-related emissions is negligible to the maximum grid value of the 4-hour average O₃ during each season.

Figure 5.22 shows the contribution, in each grid square for each season, of the CSG-related emissions to the modelled maximum 4-hour average O₃ concentrations shown in Figure 5.21. Note, this is calculated for each grid square by subtracting the maximum 4-hour average O₃ concentration for the season in the run without CSG sources from the maximum 4-hour average O₃ concentration for the same season in the run with all sources. Importantly, in each grid square the two maximum values that are subtracted may each be from a different day and time during the season. Note the change in O₃ can be negative or positive.

The largest CSG contributions occur in the vicinity and/or generally west of the CSG-related emission source area. No CSG-related contribution to the maximum 4-hour average modelled O₃ concentration exceeds 12 ppb (MAM maximum 11.1 ppb, indicated by the red arrow).

Similar spatial plots for the modelled maximum 1-hour average O₃ concentrations are shown in Appendix F. The 1-hour average O₃ results are similar to the 4-hour average O₃ results, however there are no predicted exceedances of the air quality objective of 100 ppb. During SON and DJF there are areas over 80 % of the 1-hour average O₃ air quality objective in similar locations as those for the 4-hour O₃ concentrations.

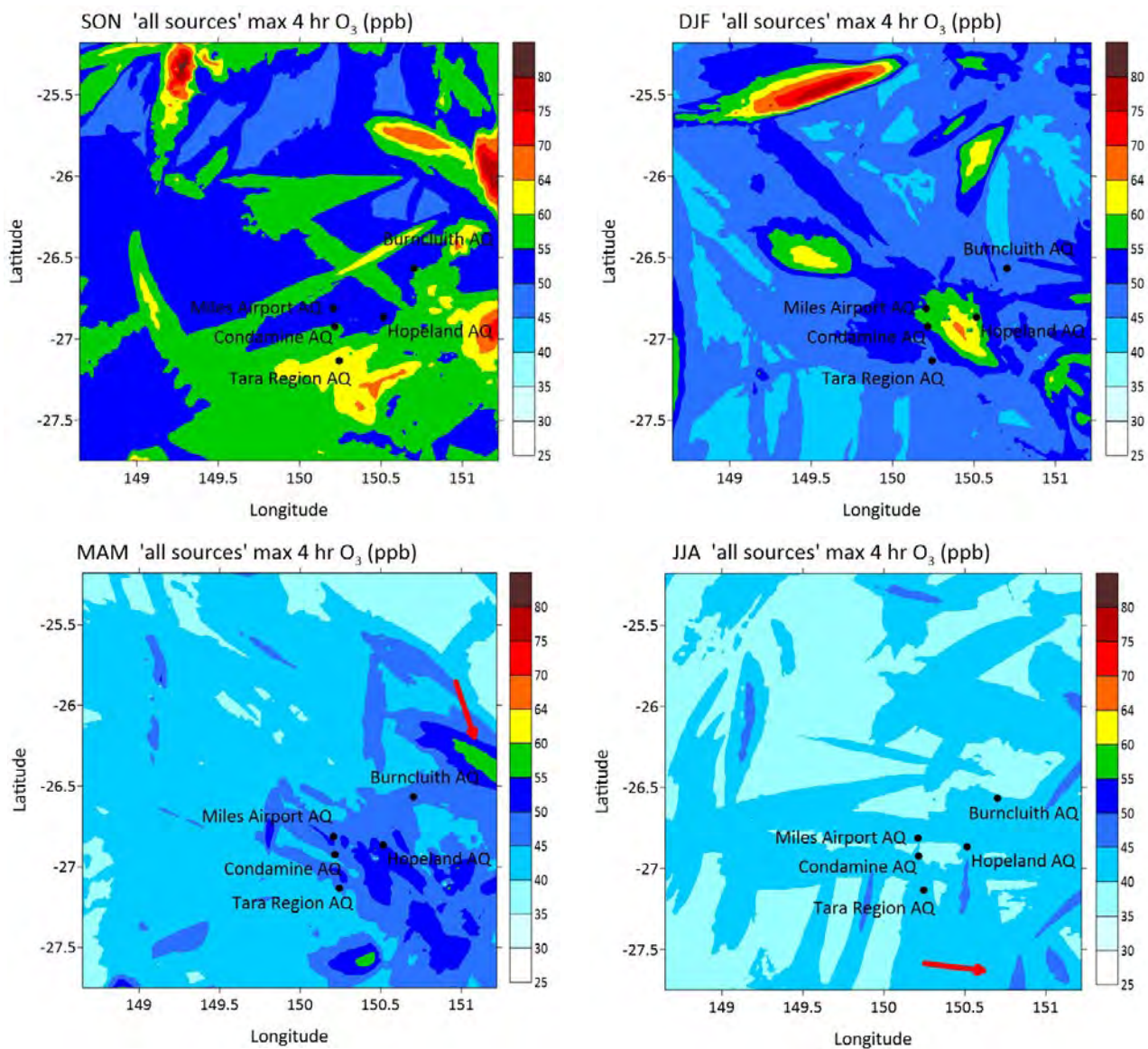


Figure 5.21 The maximum concentration of the 4-hour average O₃ in each grid square for the model results with all sources during each season (ppb). Note that the maximum concentrations shown in each grid square may be from different time periods. The red arrow indicates the location of the maximum value for the season.

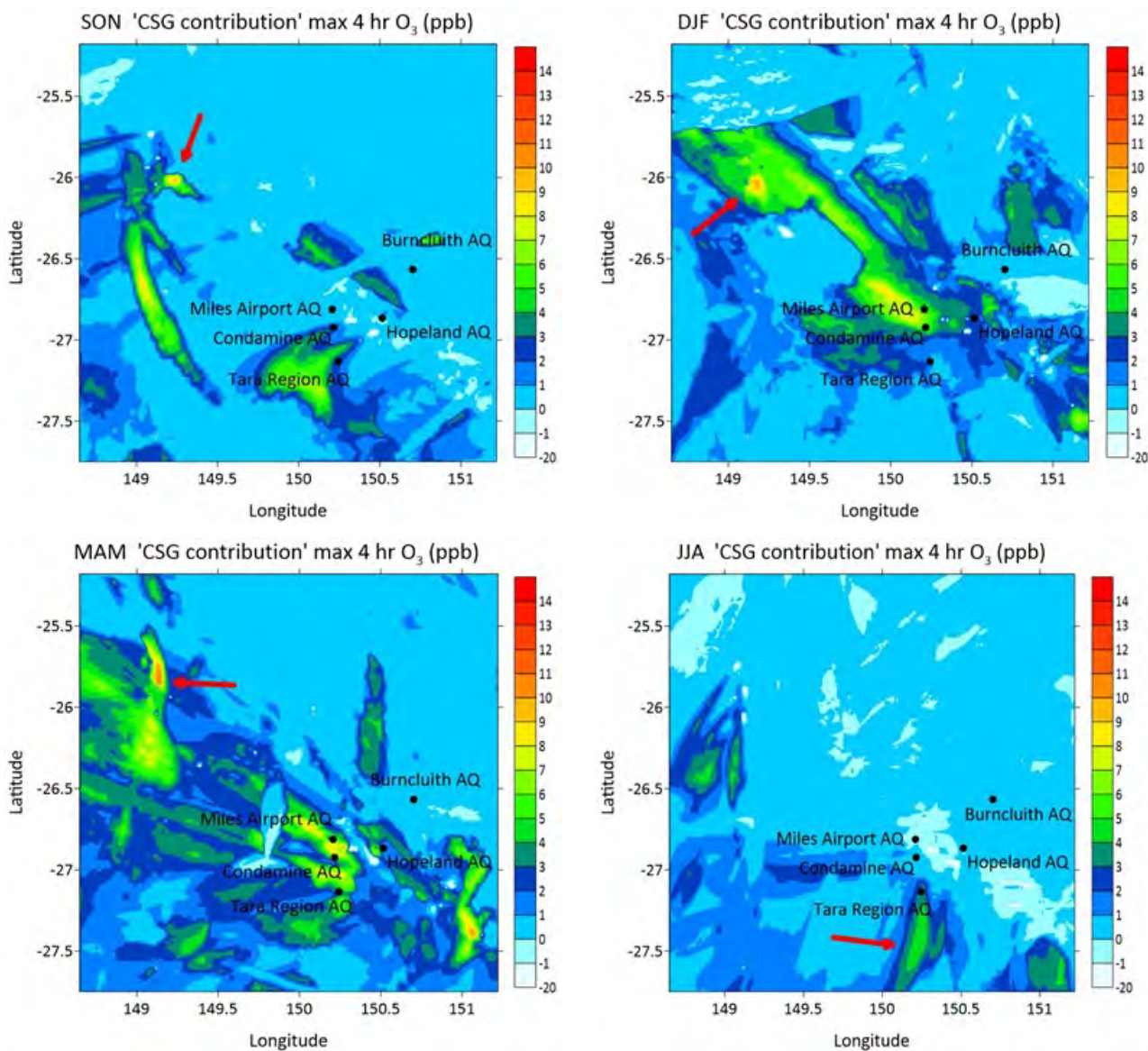


Figure 5.22 The contribution of the CSG-related emissions to the modelled maximum 4-hour average O₃ concentration (maximum in each grid square from Figure 5.21) during each season (ppb). Note that the concentrations shown in each grid square may be from different time periods. The red arrow indicates the location of the maximum value for the season.

Figure 5.23 shows the maximum contribution of the CSG-related emissions to the 4-hour average modelled O₃ concentrations in each grid square for the modelled year. Note, this is calculated in each grid square by subtracting, every hour, the 4-hour average O₃ concentration for the run without CSG sources from that for the run with all sources and then calculating the maximum value for the year from the hourly values. Importantly, in each grid square the two values that are subtracted are from the same day and time in the year. Note this figure is showing the maximum contribution to the O₃ concentration values whilst Figure 5.22Figure 5.37 shows the contribution to the maximum O₃ concentration values.

The equivalent figure for the 1-hour average O₃ concentrations is shown in Appendix F.

Generally the maximum modelled contributions are between 4 – 8 ppb with relatively small areas greater than 12 ppb. The largest maximum positive value is 24 ppb (indicated by the red arrow) which is 30 % of the air quality objective (80 ppb, Table 5.1).

There are also larger areas of negative values close to CSG sources with the largest maximum negative value equal to -39 ppb. Emissions from the CSG-related sources reduce O₃ probably due to removal due to reaction with NO_x.

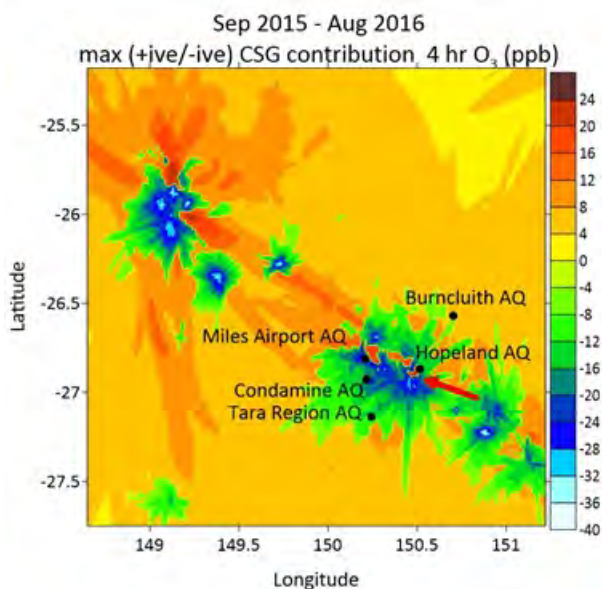


Figure 5.23 The maximum contribution of the CSG-related emissions to the modelled 4-hour average O₃ concentrations during the modelled year (ppb). Note that the concentrations shown in each grid square may be from different time periods. The red arrow indicates the location of the maximum value for the year.

Over the modelled 1 km grid domain during the modelled year there are no exceedances of the 4-hour average O₃ air quality objective (80 ppb, Table 5.1) when the contribution of the CSG-related emissions to the 4-hour average O₃ concentration is greater than 2 ppb but there are 120 exceedances of 80 % of the air quality objective (64 ppb, Table 5.1) when the contribution of the CSG-related emissions to the 4-hour average O₃ is greater than 2 ppb. Exceedances are not included if there is already an exceedance of 80 % of the air quality objective before the CSG-related emissions are included.

Eight of the exceedances of 80 % of the air quality objective with the highest contribution of the CSG-related emissions to the 4-hour average O₃ concentrations are listed in Table 5.5. The contribution and the percentage contribution of the CSG-related emissions to the exceedances are also listed.

The largest contribution of the CSG-related emissions to the modelled exceedances of 80 % of the air quality objective for the 4-hour average O₃ is 4.5 ppb which represents a 7 % contribution to the 4-hour average O₃ concentration of 64 ppb. Of the 120 exceedances (not all listed in Table 5.5) the contribution from the CSG-related emissions ranges from 2 - 4.5 ppb which is a 3 – 7 % contribution from the CSG-related emissions to the 4-hour average O₃ concentrations.

For the 1-hour average modelled O₃ concentrations there are no exceedances of the air quality objective and no exceedances of 80 % of the air quality objective when the contribution of the CSG-related emissions to O₃ is greater than 2 ppb.

Over the modelled 1 km grid domain during the modelled year, 0.00001 % of the possible 4-hour average O₃ concentrations exceed the air quality objective (Figure 5.21) with negligible contributions from CSG-related emissions.

Table 5.5 Eight of the 120 exceedances of 80 % of the air quality objective (64 ppb) for the 4-hour average O₃ concentrations with the highest contribution of the CSG-related emissions. The contribution (ppb) and the percentage contribution of the CSG-related emissions to the exceedances are also included.

4-hour O₃ 80 % exceedances (ppb)	Contribution of the CSG-related emissions to 80 % exceedances (ppb)	Percentage contribution of the CSG-related emissions to 80 % exceedances
64.0	4.5	7
64.3	4.5	7
64.3	4.5	7
64.0	4.4	7
64.4	4.3	7
64.0	4.3	7
64.4	4.3	7
64.3	4.3	7

Figure 5.24 shows the locations of the modelled 4-hour average O₃ concentrations that exceed 80 % of the air quality objective (64 ppb) when the contribution of the CSG-related emissions to the 4-hour average O₃ is greater than 2 ppb. The locations are marked by red crosses (note it may be difficult to see the separate locations in the figure as the grid point spacing is 0.01 degrees and many of the exceedances occur at neighbouring grid squares).

All of the exceedances occur in the southern part of the region with most amongst CSG-related emission sources. The southern cluster of exceedances (including the exceedances on the southern boundary) all occur on the 20th November 2015 and the northern cluster all occur on the 25th February 2016.

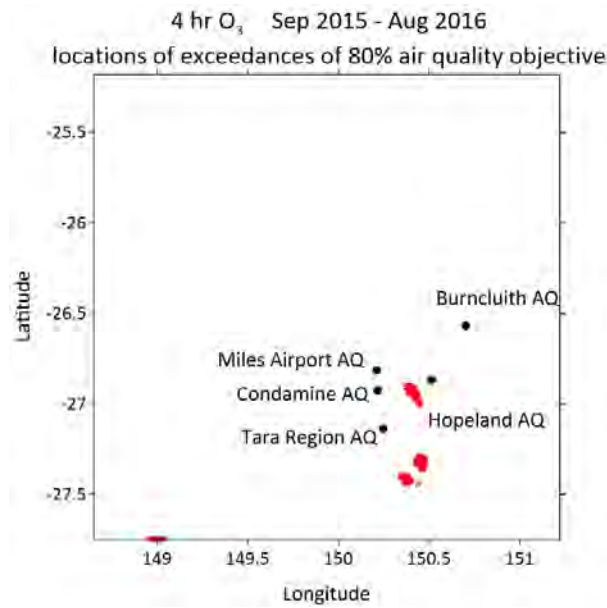


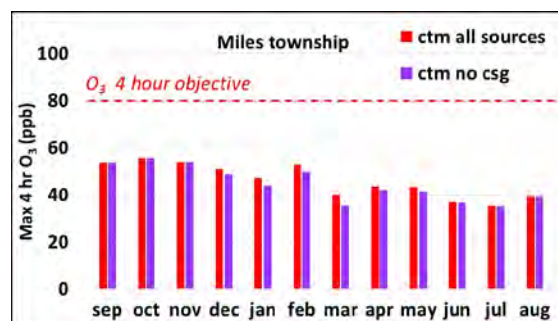
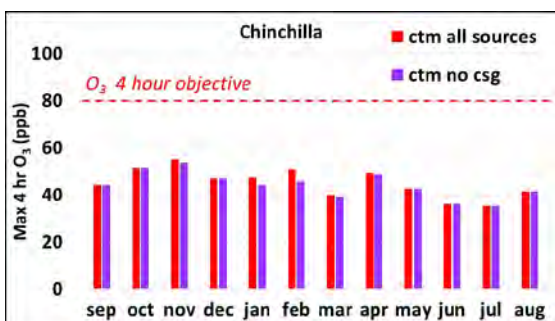
Figure 5.24 The locations, marked by red crosses, of the modelled 4-hour average O₃ concentrations that exceed 80 % of the air quality objective (64 ppb), when the contribution of the CSG-related emissions is greater than 2 ppb.

5.2.4 Modelled effect of the CSG-related emissions on O₃ levels at Town sites

Model results are presented at the Town sites to investigate the effects of the CSG-related emissions to O₃ concentrations over the region. Figure 5.25 shows the maximum 4-hour average O₃ concentrations for each month of the model simulation at the Town sites. Those for the maximum 1-hour average O₃ concentrations are shown in Appendix F. The bar plots show the model results with all sources in red and the model results without the CSG sources in purple. The dashed horizontal red line shows the value of the air quality objective.

The air quality objectives (Table 5.1) are not exceeded by the modelled 4-hour average O₃ or 1-hour average O₃ concentrations at any of the Town sites. Also, 80 % of the air quality objective for O₃ (Table 5.1) is not exceeded by the modelled 4-hour average O₃ or 1-hour average O₃ concentrations when the contribution of CSG-related emissions to O₃ is greater than 2 ppb at any Town site during the modelled year.

The difference between the O₃ maximum monthly values from the model results with all sources and the model results without CSG sources is less than 6 ppb at the Town sites.



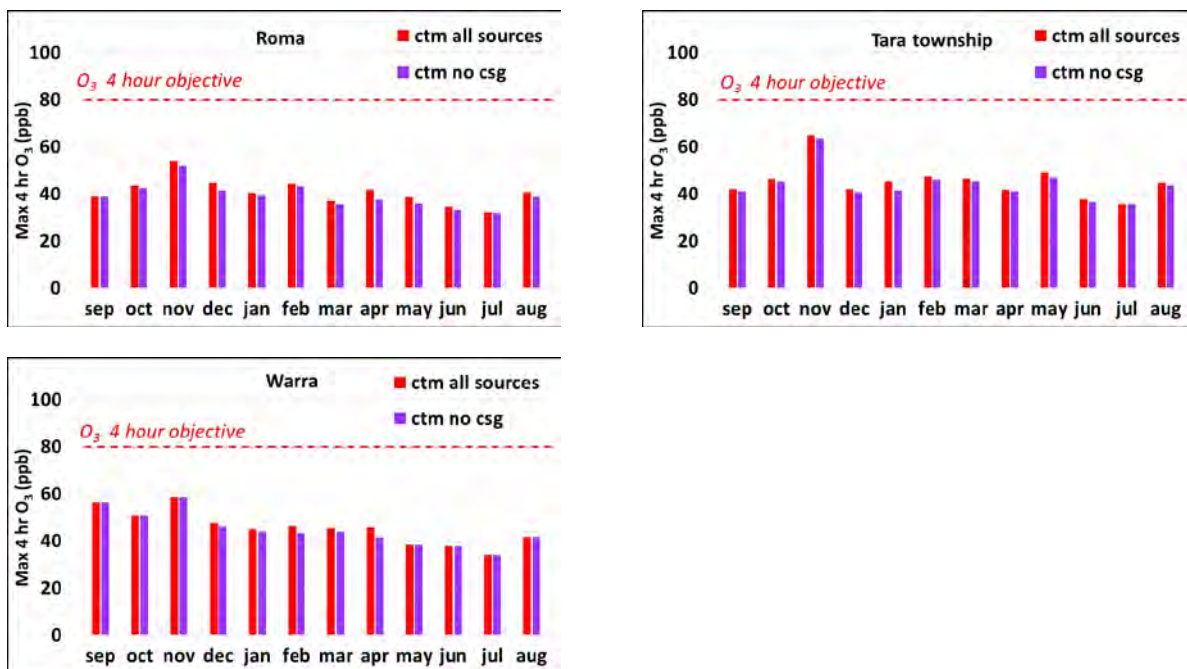


Figure 5.25 The modelled maximum 4-hour average O₃ concentrations (ppb) for each month of September 2015 – August 2016 at the Town sites: model results with all sources (red) and model results without the CSG sources (purple).

The modelled contribution from the CSG-related emissions to the 4-hour average O₃ concentrations at each of the Town sites is presented in Figure 5.26. The contribution for the 1-hour average O₃ concentration is similar and shown in Appendix F. Each plot shows the percentage of model hours within each season for the modelled contribution from the CSG-related emissions to the 4-hour average O₃ concentrations.

On average 99 % of the time the contribution from the CSG-related emissions at the Town sites is within ± 5 ppb which is 6.25 % of the 4-hour O₃ air quality objective (80 ppb, Table 5.1). The lowest frequency of change is at Chinchilla and Warra except during JJA. The largest frequency of change is modelled at Roma in DJF and MAM.

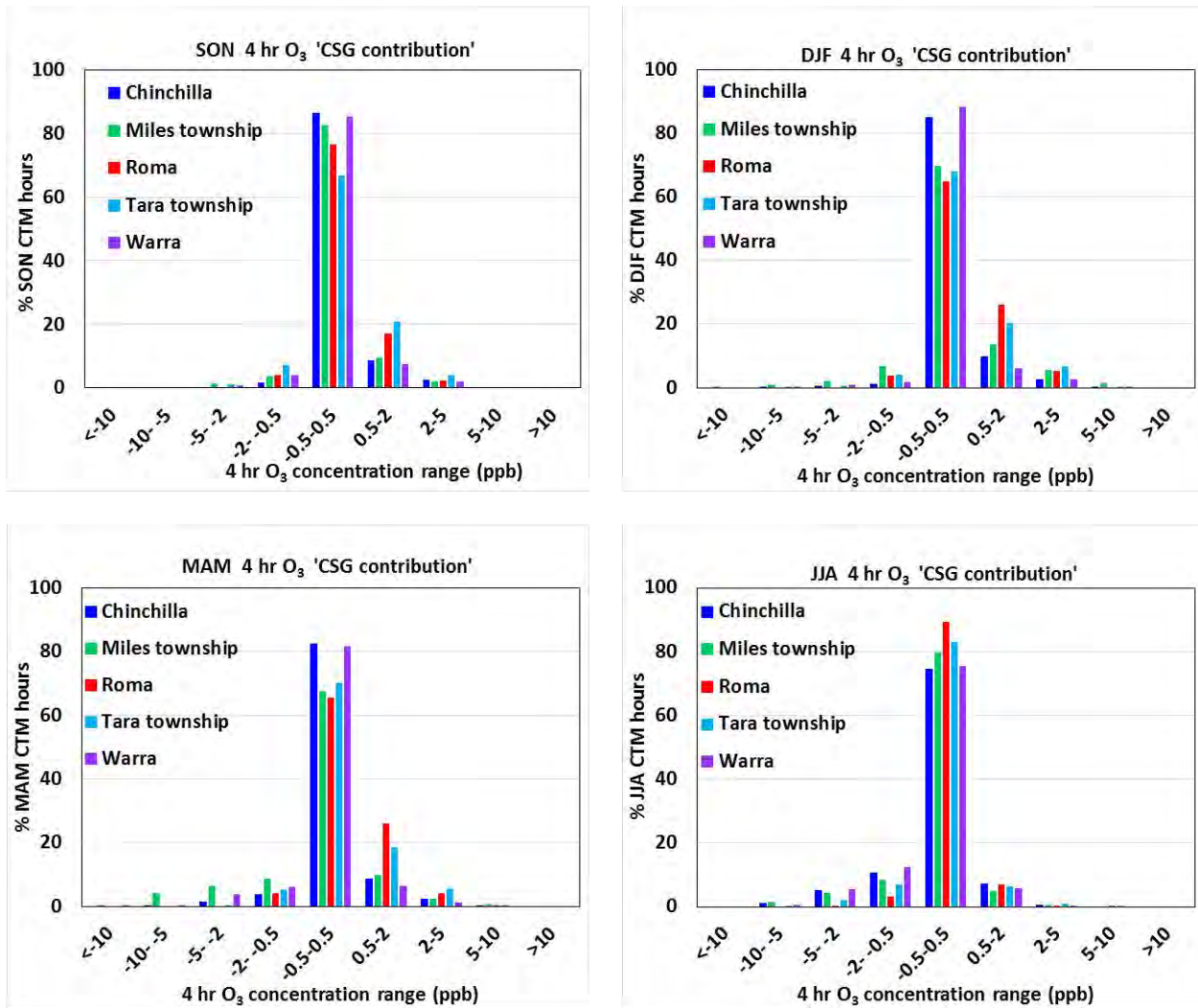


Figure 5.26 The modelled contribution from the CSG-related emissions to the 4-hour average O₃ concentration (ppb) at the Town sites shown as a frequency distribution for each season. The x-axis shows the concentration ranges of the contribution from the CSG-related emissions and the y-axis shows the percentage of model hours.

Figure 5.27 shows plots of the modelled 4-hour average O₃ concentrations with all sources against the contribution from the CSG-related emissions to the modelled 4-hour average O₃ concentrations at Warra, one of the Town sites. The plots are seasonal and one point is plotted for each modelled hour. Results at Warra are representative of those at the other Town sites and those for the 1-hour average O₃ concentrations (plots are shown in Appendix E). The results from Warra are also similar to those at the Gas field and Regional sites. The largest changes in the 4-hour O₃ due to the CSG-related emissions occur at the maximum or minimum values of O₃ concentrations. Of the Town sites Roma shows the smallest changes due to CSG.

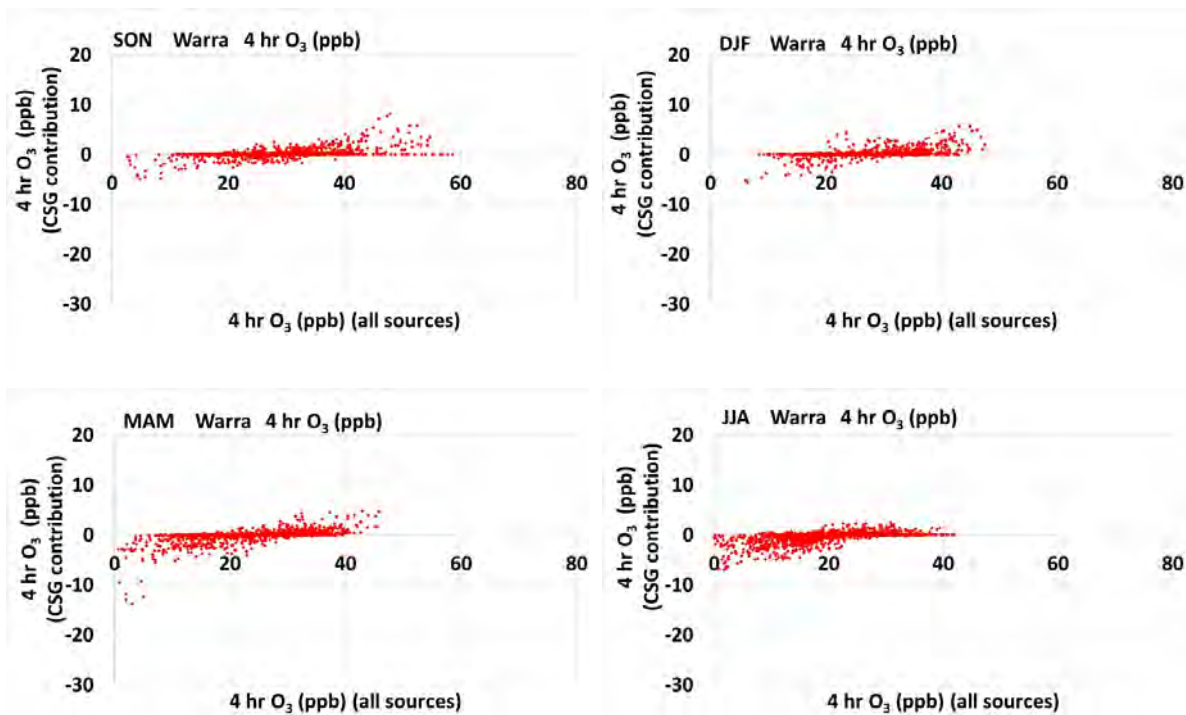


Figure 5.27 The modelled contribution from the CSG-related emissions to the 4-hour average O₃ concentration (ppb) at Warra shown as a scatter plot for each season. The x-axis shows the modelled 4-hour average O₃ concentrations with all sources (ppb) and the y-axis shows the contribution from the CSG-related emissions to the 4-hour average O₃ concentration (ppb).

5.2.5 Summary

The impacts of CSG activity on the 4-hour average O₃ concentrations modelled in the Surat Basin are summarised below:

Comparison of the model results with the observations

- The observed and modelled time series of O₃ concentrations show reasonable agreement in the diurnal pattern of maximum concentrations during the middle of the day or later in the afternoon and minimum concentrations during the night-time and early-morning hours. The model also reproduces well the observed time periods with reduced amplitude in the diurnal pattern. There is some underprediction and overprediction of maxima and minima at various sites.

Contribution of the CSG-related emissions to the modelled 4-hour average O₃ concentrations

- On average 96 % of the time at the Gas field and Regional sites and 99 % of the time at the Town sites the contribution from the CSG-related emissions is within ± 5 ppb which is 5 % of the 1-hour O₃ air quality objective and 6.25 % of the 4-hour objective.
- The smallest frequency of changes are modelled at Burncluth, while the largest frequency of changes occur at Condamine.

- At the Gas field, Regional and Town sites generally the largest modelled increases in the 4-hour average O₃ concentrations due to the CSG-related emissions occur mostly for larger O₃ values (i.e. increased peak concentrations). The largest decreases are modelled to occur mostly for smaller values of the 4-hour average O₃ concentrations (i.e. deepening the minima). These decreases account for up to 100 % of the 4-hour average O₃ value – e.g. emissions from CSG-related sources reduce O₃ to zero probably due to reaction with NO_x.
- The largest modelled contributions of the CSG-related emissions to the 4-hour ozone concentrations occur most frequently in the summer months.
- Hopeland has the largest increase in the 4-hour average O₃ concentrations due to the CSG-related emissions, 16.5 ppb, which equates to 20.6 % of the 4-hour O₃ air quality objective.
- Over the entire model 1 km grid domain during the modelled year the maximum predicted contribution of the CSG-related emissions to the modelled 4-hour average O₃ concentrations is 24 ppb which is 30 % of the air quality objective.

Contribution of the CSG-related emissions to exceedances of the air quality objective or 80 % of the air quality objective when the CSG-related emissions contribute more than 2 ppb to the 4-hour average O₃ concentrations

- At the Gas Field, Regional or Town sites there are no modelled exceedances of the 4-hour average O₃ air quality objective or 80 % of the air quality objective during any month.
- Over the modelled 1 km grid domain during the modelled year there are no exceedances of the 4-hour average O₃ air quality objective (80 ppb, Table 5.1) when the contribution of the CSG-related emissions to the 4-hour average O₃ concentration is greater than 2 ppb, there are 120 exceedances of 80 % of the air quality objective (64 ppb, Table 5.1) when the contribution of the CSG-related emissions to the 4-hour average O₃ is greater than 2 ppb.
- Over the entire modelled 1 km grid domain during the modelled year there are no exceedances of the 4-hour average O₃ air quality objective but there are 120 exceedances of 80 % of the air quality objective with a contribution from CSG-related emissions. Of the 120 exceedances the contribution from the CSG-related emissions ranges from 2 - 4.5 ppb which is a 3 – 7 % contribution to the 4-hour average O₃ concentrations.
- Over the modelled 1 km grid domain during the modelled year 0.00001 % of the possible 4-hour average O₃ concentrations exceed the air quality objective (Figure 5.21) with negligible contributions from the CSG-related emissions.

Relative importance of different sources

- The modelled maximum 4-hour average O₃ concentrations exceed the air quality objective of 80 ppb at a few small areas within the model 1 km grid domain during SON. These modelled exceedances are predominantly the result of emissions from modelled fires.

5.3 Nitrogen Dioxide

Nitrogen dioxide (NO₂) is one of the six key criteria air pollutants included in the Ambient Air Quality NEPM (NEPM, 2016). Nitrogen oxides (NO_x) include nitric oxide (NO) and nitrogen dioxide (NO₂) and are gases produced from fuel combustion, including diesel, biomass and gas, coal, as well as natural processes. Nitrogen oxides are a key pollutant identified in CSG industry Environmental Impact Statements (EIS) (QGC 2010, APLNG 2010). CSG-related sources include combustion of gas via flaring and gas combustion engines and diesel engine emissions. Nitrogen oxides are also a precursor of tropospheric ozone.

5.3.1 Modelled effect of the CSG-related emissions at the observation sites

Time series plots of the observed and modelled concentrations of 1-hour average NO₂ at Miles Airport are shown in Figure 5.28. The observations are shown in blue, the model results with all emission sources in red and the model results without the CSG-related emission sources in purple. The time series are presented for different seasons. For comparison purposes and completeness time series at Condamine, Hopeland, Tara Region and Burncluith are shown in Appendix D. In the time series figure it is not always possible to see the two modelled time series, the red (all sources) concentration series is plotted first and then the purple (no CSG sources) series is plotted. Where the values of each series are the same only the last plotted series will be seen, which is the purple one (no CSG sources). Therefore, when red is seen on the plot it is because the two modelled series have different values at that point in time and the difference between the two values is the contribution to the concentration from the CSG-related emissions; this contribution is shown in Figure 5.29 (the contribution for the other sites is shown in Appendix D).

Comparison of the observed and modelled 1-hour average NO₂ concentrations at Miles Airport (see Figure 5.28) shows the background NO₂ is mostly captured by the model (except during SON), whereas the modelled NO₂ overestimates many of the observed peak values. Importantly even though the magnitude of the peaks is overestimated the frequency and timing of a number of the peaks are captured by the model. Comparing the time series during SON with that during MAM shows the model reproduces the increased frequency of the peaks as observed but less so in the other seasons. The comparison at Condamine (see Appendix D) is similar to that at Miles Airport. At Hopeland, the observed NO₂ time series has fewer and smaller peaks than at the other Gas field sites and the model overestimates the magnitude of these peak values particularly during JJA. At the Regional sites there are NO₂ observations for most of JJA and the observed and modelled peaks are smaller compared to those at the Gas field sites. However, the model still overestimates the magnitude of the peaks.

Figure 5.28 and Figure 5.29 show that the predicted NO₂ concentration peaks are larger when the CSG-related emission sources are included. Also, the model results with the CSG-related emission sources generally overestimate the observed NO₂ peaks while the model results without the CSG-related emission sources often underestimate the observed NO₂ peaks. This is also true at Condamine but not at Hopeland. The Regional sites have mixed results.

The overprediction of the NO₂ peaks when all sources are included and the underprediction of the NO₂ peaks when no CSG sources are included suggests that some level of CSG-related emissions is needed in the model to reproduce the observed NO₂ concentration pattern.

To investigate the overprediction of the modelled NO₂ peaks various model checks have been completed and suggest the overprediction of the modelled NO₂ peaks is not a problem with the chemistry component in the model. The NO₂ concentration at stack emission locations is about 15 – 20 % of NO_x as expected, the NO_x/CO ratios at the same locations are within the range of the NO_x/CO ratios for the various emission sources at the location (noting there can be area sources and stacks in the same model grid box).

To investigate what emission sources are contributing to the predicted NO₂ concentrations a few extra model runs for a small time slice are performed. The model is run from 1/5/2016 to 12/5/2016 a period where there are a number of observed NO₂ peaks (see Figure 5.28 Figure 5.30). The top panel in Figure 5.30 shows the model results at Miles Airport for the runs with and without the CSG sources and the observations. As previously stated the run without the CSG sources generally underestimates the peaks in the 1-hour NO₂ observations while the run with all sources generally overestimates the peaks in the 1-hour NO₂ observations.

A model stack is a modelled elevated emission source with plume rise. For the following tests various combinations of the modelled CSG-related emissions stacks are removed from the all sources model run, the model is re-run and the results are shown in the bottom panel of Figure 5.30. The green trace is the result with all the model stacks removed so area sources like CSG wells are still present, the pink trace is the result with all the model 'Producer 1' stacks removed, the light-blue trace is the result with all the model 'Producer 2' stacks removed and the dark blue trace is the result with only the model stack closest to Miles Airport removed. (Note where only dark blue and pink lines are seen in between the 'dark-blue peaks' the green and light-blue lines are underneath the dark-blue lines. Within the second dark-blue peak from the left the green and light-blue lines are underneath the pink line.)

Comparing the dark blue line (model results when the model stack closest to Miles Airport is removed) in the bottom panel of Figure 5.30 with the red line (model results with all sources) in the top panel of Figure 5.30 shows that the last peak in the all sources time series (red line) is not seen when the stack closest to Miles Airport is removed, therefore the modelled stack closest to Miles Airport is the main source for the 'last' modelled NO₂ concentration peak in the top panel. Importantly, even though this modelled stack is within a few kilometres of Miles Airport it is not having a significant effect on the NO₂ concentrations at Miles Airport in this time period. The other modelled peaks in the time series trace are mostly due to a combination of sources as can be seen by the different coloured lines within the peaks in the bottom panel. During this time period all the CSG-related emission sources are contributing to the modelled 1-hour NO₂ concentration. While this sensitivity test is only a small time slice of the modelled year it is reasonable to assume that similar patterns would occur for the rest of the year and the modelled concentration at Miles Airport will generally be a combination of the CSG-related emission sources from different producers interacting with the local meteorology. It is unlikely that a particular emission source is responsible for the modelled overprediction of NO₂. Similar results are observed at the other Gas field sites.

The observed and modelled NO₂ peaks mostly occur at night when the boundary layer can be shallow and stable. Modelled emissions from the stacks can be trapped in the lowest model layer with resulting increased concentrations. It is possible that more modelled levels near the surface may resolve some of these peaks but it is also possible that the effective height of release (i.e. physical height plus plume rise) of the CSG-related emissions may not be correctly represented in the model.

In summary the predicted concentrations of NO₂ from the all sources run is mostly larger than the observed and there are a number of possible reasons why the model overestimates the CSG-related NO₂ peaks: 1) NO_x emissions may be overestimated at some CSG-related emission sources, 2) the effective height of release of some CSG-related emissions may not be correctly represented in the model, 3) the time pattern of release of some CSG-related emission sources may not be correctly represented in the model and/or 4) the height of the night-time boundary layer may not be correctly represented in the model.

The overprediction of the NO₂ peak concentrations is most likely contributing to the overprediction of the magnitude of the night-time minima of O₃ concentrations (i.e. sometimes the predicted O₃ concentrations are lower than the observed concentrations, see Figure 5.16). Figure 5.31 shows the modelled contribution from the CSG-related emissions to the 1-hour average O₃ concentration (blue line) and the modelled contribution from the CSG-related emissions to the 1-hour average NO₂ concentration (red line) for a sub-set of MAM (a shorter time period is plotted so more detail is visible). The modelled contribution peaks of NO₂ concentration coincide with the negative contribution peaks of O₃ concentration, also the larger the NO₂ concentration peak the larger the magnitude of the O₃ concentration minimum. However, when the contribution to O₃ is positive the contribution to NO₂ is very small.

Therefore, in this study the overprediction of NO₂ peak concentrations is unlikely to have a significant effect on the modelled day-time maximum O₃ concentrations. The day-time maximum O₃ concentrations are predominantly determined by the photochemistry.

In this study, the NO₂ concentration predictions are most likely overestimated at other locations in addition to the Gas field and Regional sites. The modelled results for other species are unlikely to be greatly affected with the exception of the minimum O₃ concentrations as discussed above.

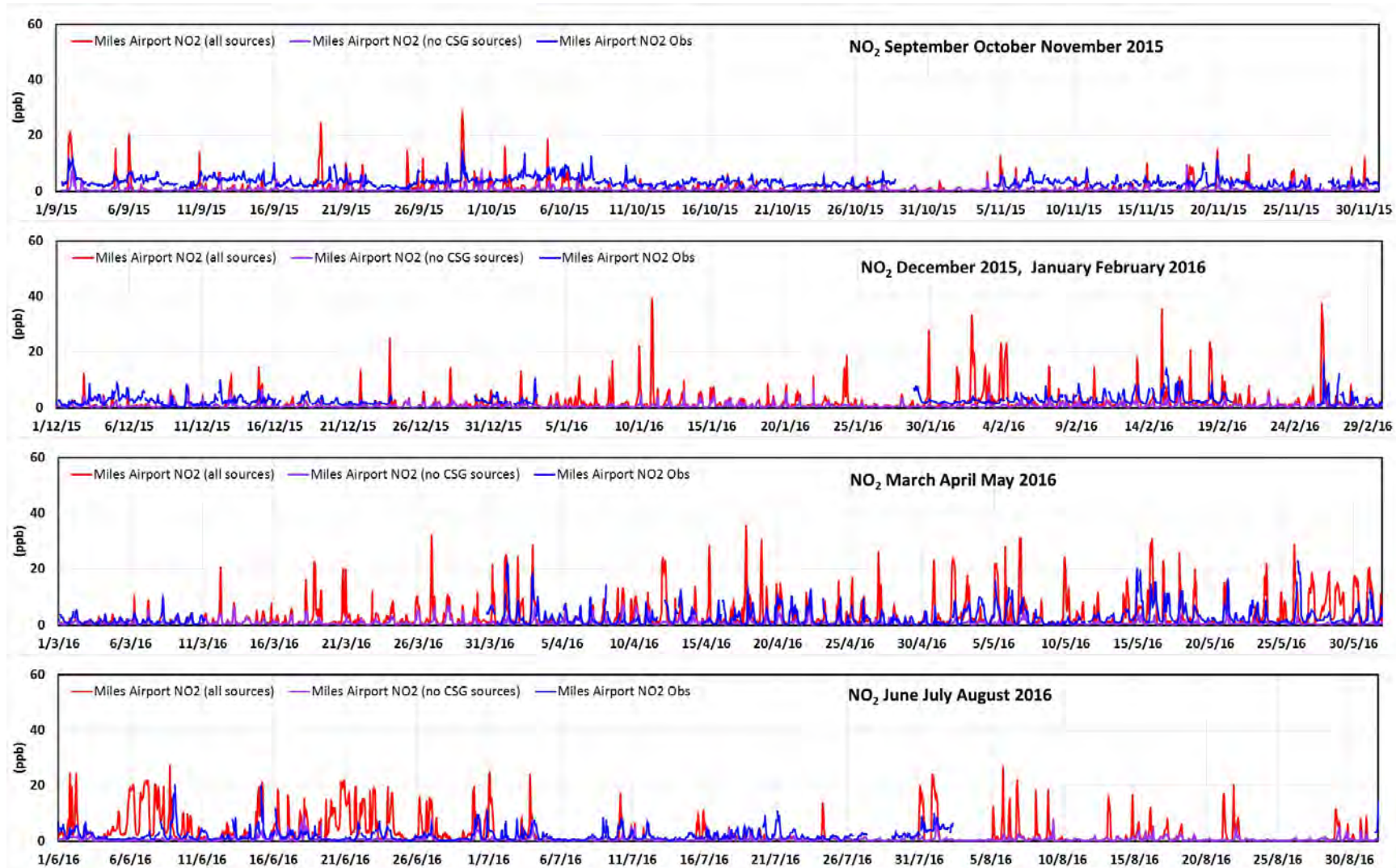


Figure 5.28 The observed and modelled time series of the 1-hour average NO₂ concentrations (ppb) at Miles Airport for the modelled year (red = model results with all sources, purple = model results without CSG sources, blue = observations).

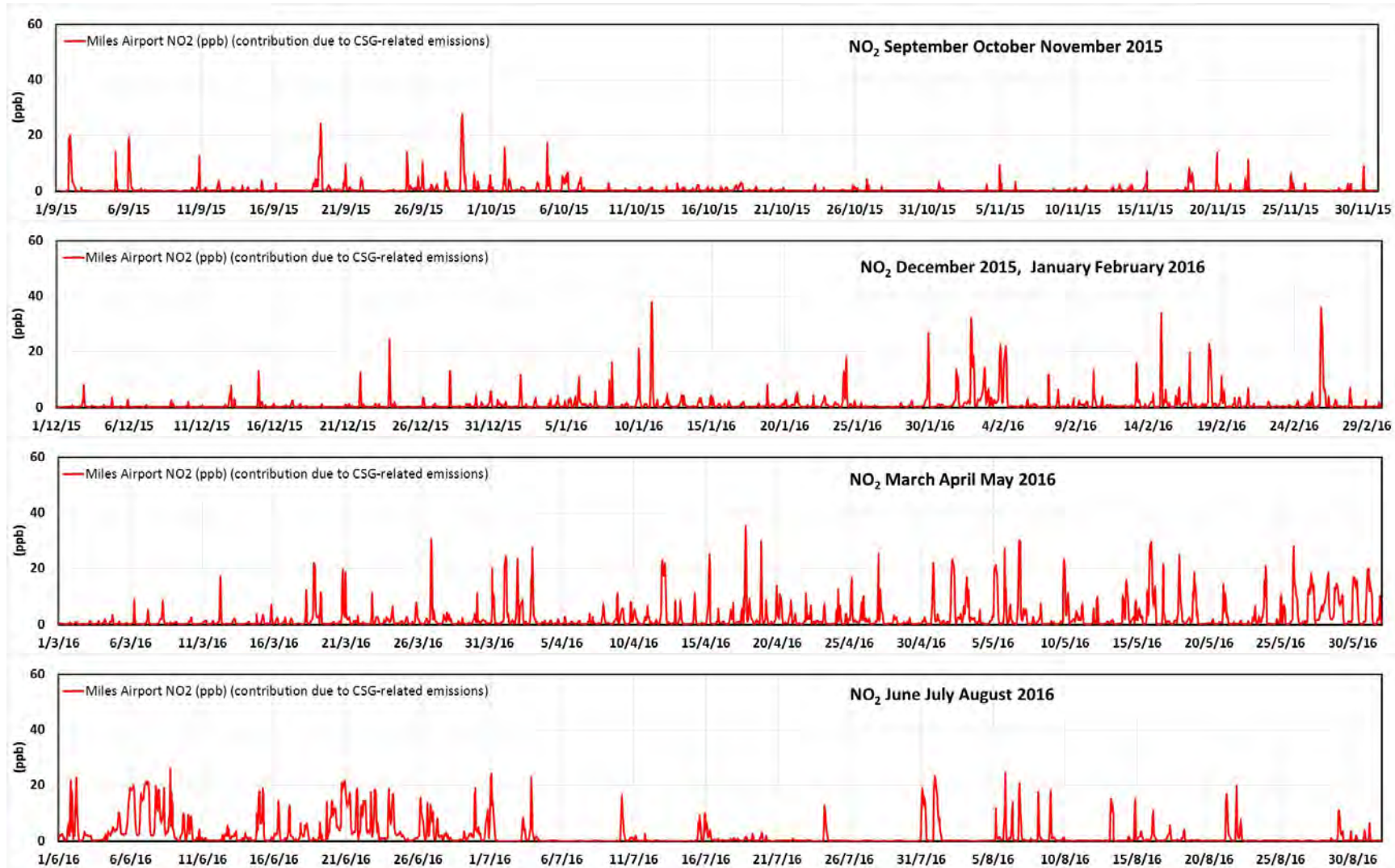


Figure 5.29 The modelled contributions from the CSG-related emissions to the 1-hour average NO₂ concentrations (ppb) at Miles Airport for the modelled year.

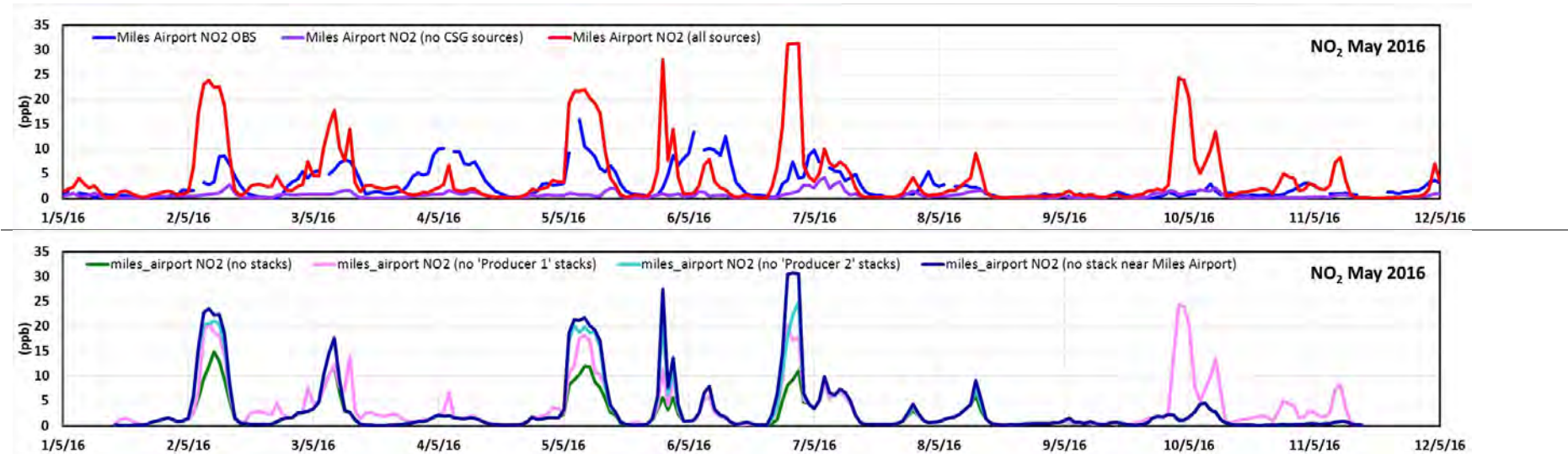


Figure 5.30 The observed and modelled time series of the 1-hour average NO₂ concentrations (ppb) at Miles Airport from 1/5/16 00:00 AEST to 12/5/16 00:00 AEST (top panel: red = model results with all sources, purple = model results without CSG sources, mid- blue = observations; bottom panel: green = model results with all model stacks removed, pink = model results with all model 'Producer 1' stacks removed, light-blue = model results with all model 'Producer 2' stacks removed and dark blue = model results with only the model stack closest to Miles Airport removed).

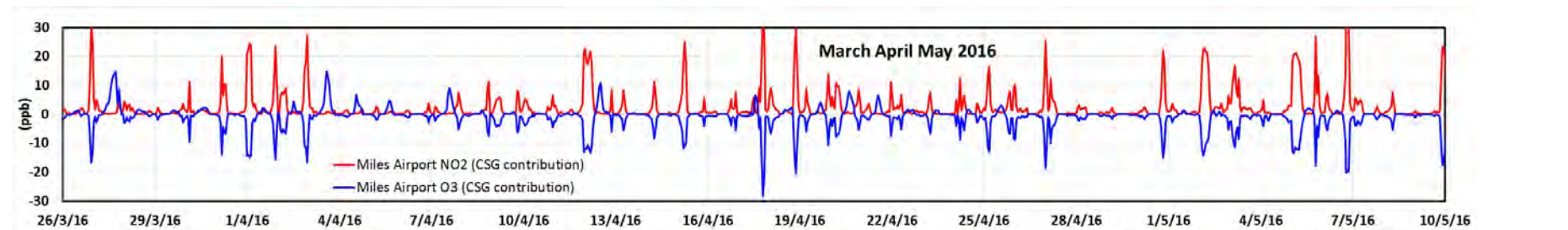


Figure 5.31 The modelled contribution from the CSG-related emissions to the 1-hour average O₃ concentrations and the modelled contribution from the CSG-related emissions to the 1-hour average NO₂ concentration for a sub-set of MAM (ppb) at Miles Airport.

The modelled contribution from the CSG-related emissions to the 1-hour average NO₂ concentrations at each of the observation sites is presented in Figure 5.32. Each plot shows the percentage of model hours within each season for the modelled contribution from the CSG-related emissions to the 1-hour average NO₂ concentrations.

On average 95 % of the time the contribution from the CSG-related emissions at all sites is less than 5 ppb which is 4 % of the 1-hour air quality objective for NO₂ (120 ppb, Table 5.1). The lowest frequency of change due to the CSG-related emissions is modelled at Burncluith which is furthest from the major CSG sources, while the largest frequency of change occurs at the Gas field sites and particularly during MAM and JJA.

Due to the model overestimating the 1-hour average NO₂ concentrations as discussed above these results are also most likely an overestimate.

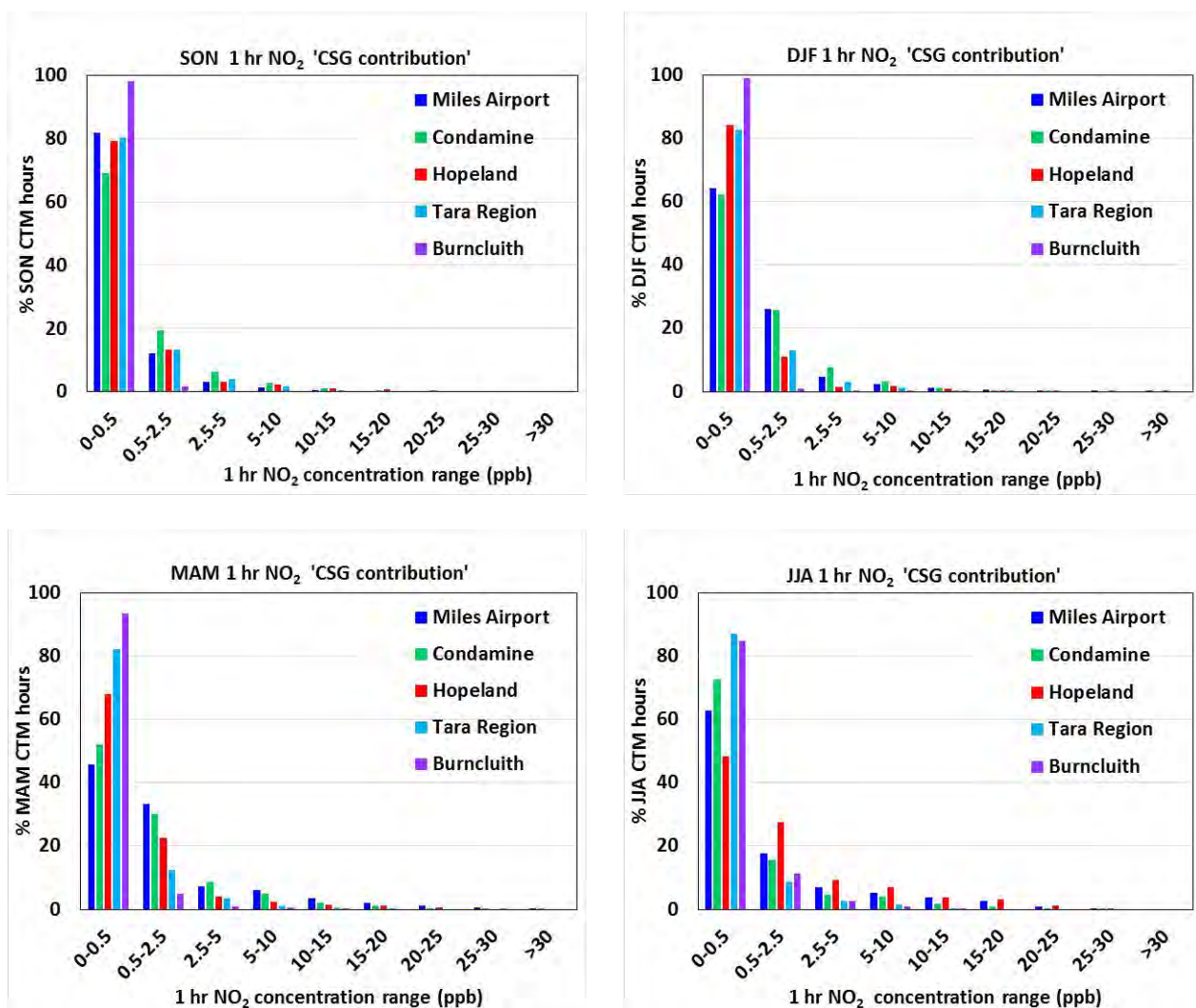


Figure 5.32 The modelled contribution from the CSG-related emissions to the 1-hour average NO₂ concentration (ppb) at the Gas field and Regional sites shown as a frequency distribution for each season. The x-axis shows the concentration ranges of the contribution from the CSG-related emissions and the y-axis shows the percentage of model hours.

Figure 5.33 shows plots of the modelled 1-hour average NO₂ concentrations with all sources against the contribution from the CSG-related emissions to the modelled 1-hour average NO₂ concentrations at Miles Airport. Those for Condamine, Hopeland, Tara Region and Burncluith are shown in Appendix E. The plots are seasonal and one point is plotted for each hourly modelled value.

At Miles Airport, and the other Gas field and Regional sites, when the modelled contributions are greater than about 10 ppb they account for (mostly) greater than 85 % of the 1-hour average NO₂ concentration value. The largest increases (> 30 ppb) at Miles Airport occur during DJF and MAM with the maximum contribution to the 1-hour average NO₂ concentration due to the CSG-related emissions equal to 38 ppb which is 32 % of the air quality objective for NO₂ (120 ppb, Table 5.1) and 97 % of the 1-hour modelled NO₂ concentration value. The largest contribution at any site is 41 ppb at Condamine which is 34 % of the air quality objective for NO₂ and 97 % of the 1-hour modelled NO₂ concentration value.

The smallest contribution due to the CSG-related emissions is modelled at Burncluith during all seasons.

Due to the model overestimating the 1-hour average NO₂ concentrations as discussed above these results are also most likely an overestimate.

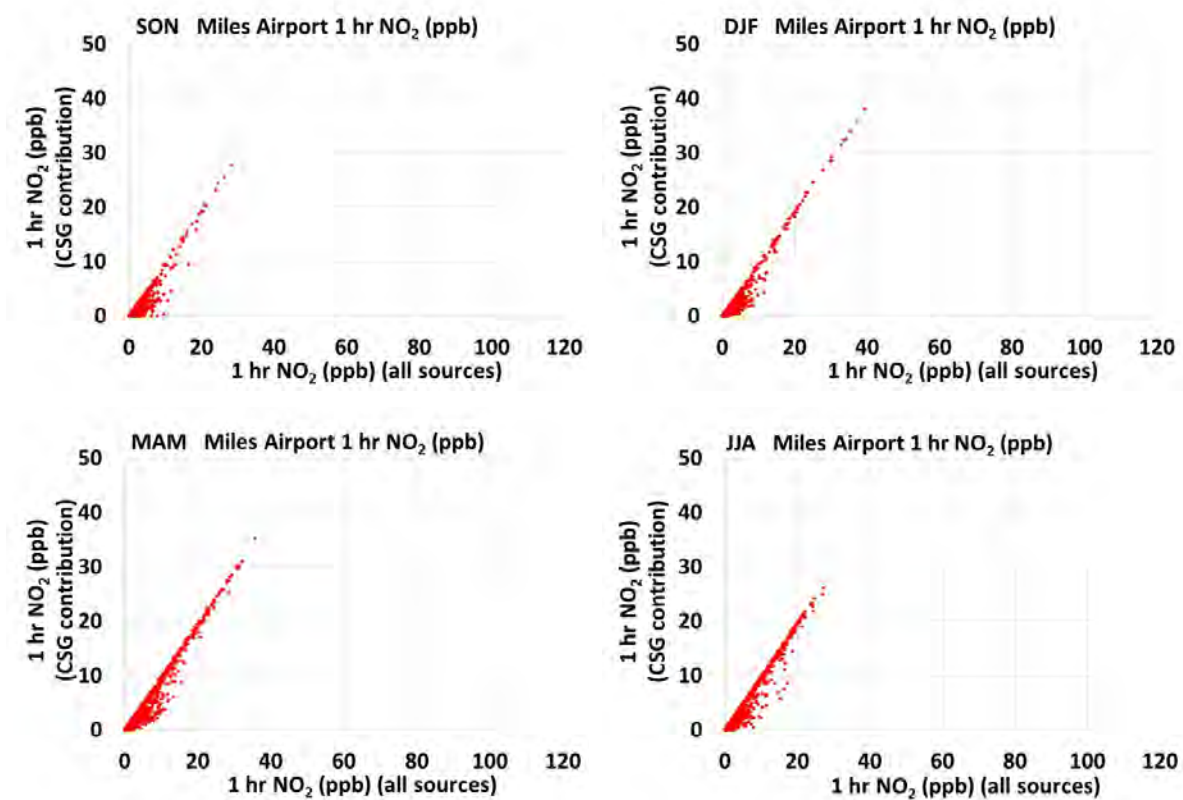


Figure 5.33 The modelled contribution from the CSG-related emissions to the 1-hour average NO₂ concentration (ppb) at Miles Airport shown as a scatter plot for each season. The x-axis shows the modelled 1-hour average NO₂ concentrations with all sources (ppb) and the y-axis shows the contribution from the CSG-related emissions to the 1-hour average NO₂ concentrations (ppb).

5.3.2 Comparison with Air Quality Objectives at Observation Sites

In this section the model results are compared to air quality objectives to assess whether there are any modelled exceedances of NO₂ at the Gas field or Regional sites. The air quality objectives used to assess the pollutant concentrations are presented in Table 5.1.

Table 5.6 presents the observed annual average concentrations of NO₂ and those modelled with all sources and without the CSG sources at the Gas field and Regional sites. Note that according to the NEPM (2016), annual observations are only valid for regulatory purposes if at least 75 % of observations in each calendar quarter are valid. In Table 5.6 annual observations are listed where this is met or almost met with the appropriate percentage listed.

All annual average NO₂ concentrations are well below the annual air quality objective and in no instances (modelled or observed) did the concentrations exceed the NO₂ annual air quality objective (30 ppb, Table 5.1). At the Gas field sites the modelled annual average NO₂ concentration with all sources included are at least twice as large as those without CSG-related sources but are almost the same as the observed values where available. At the Regional sites there is not enough observed data to compare with the model results but the modelled annual

average NO₂ concentrations with all sources are larger than those without CSG-related sources by up to 84 %, but smaller than the annual average NO₂ concentration values at the Gas field sites.

Table 5.6 The observed and modelled annual average concentrations of NO₂ (ppb) at the Gas field and Regional sites.

Annual average (ppb)	Observed NO ₂	Modelled NO ₂ (all sources)	Modelled NO ₂ (without CSG sources)
Miles Airport	2.7 ^a	2.6	0.7
Condamine	b	1.9	0.7
Hopeland	2.2	2.4	1.1
Tara Region	c	1.1	0.6
Burncluith	c	0.7	0.5

a – NO₂ observations 41 % Jan, Feb, Mar and 63 % Jun, Aug, Sep

b – only 6 months of observations

c – only 3 months of observations

Figure 5.34 shows the maximum 1-hour average NO₂ concentrations for each month of the model simulation, at each observation site. The bar plots show the observed values in blue, the model results with all sources in red and the model results without the CSG sources in purple. The dashed horizontal red line shows the value of the air quality objective. The observed values are only shown when at least 75 % of observations are available for the month.

The 1-hour average NO₂ air quality objective (120 ppb, Table 5.1) and 80 % of the 1-hour average NO₂ air quality objective (96 ppb, Table 5.1) are not exceeded by the observed or modelled 1-hour average NO₂ concentrations at any site in any month.

At all sites except Burncluith the modelled maximum 1-hour average NO₂ concentration values for the results with all sources included are generally larger than the concentrations from the model results without the CSG-related sources. The observed maximum 1-hour average NO₂ concentrations are generally in-between the values from the two model runs except at Hopeland where the model results without CSG-related sources are closer to the observed values.

Due to the model overestimating the 1-hour average NO₂ concentrations as discussed in Section 5.3.1 these results are also most likely an overestimate.

The largest contribution due to the CSG-related emissions is 32 ppb at Miles Airport which is 25 % of the air quality objective for NO₂ (120 ppb, Table 5.1). The maximum 1-hour average NO₂ concentration occurs at Burncluith during September and is 51 ppb with less than 1 % contribution from the CSG-related emissions and is predominantly due to a modelled fire.

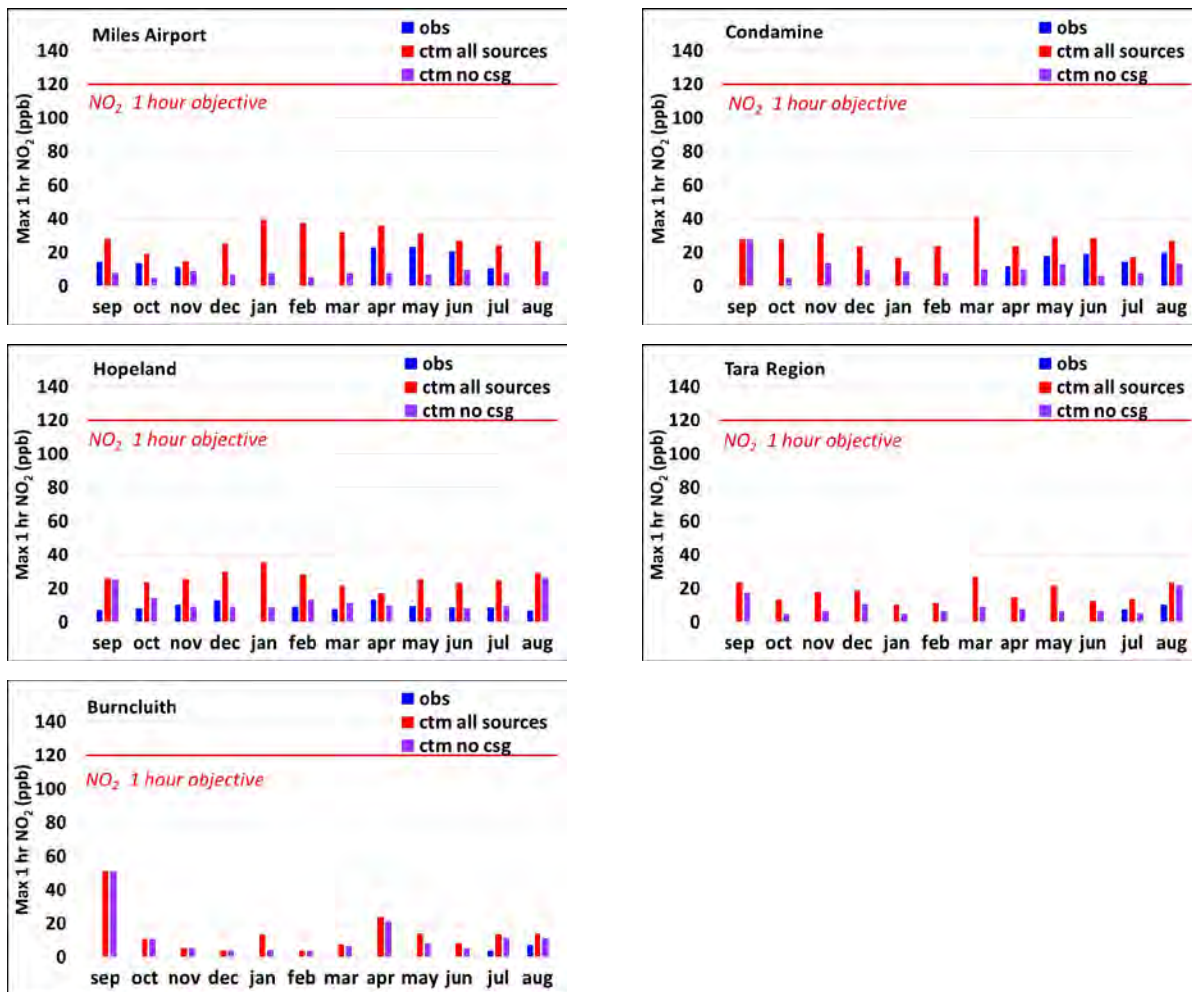


Figure 5.34 The maximum 1-hour average NO₂ concentrations (ppb) for each month of September 2015 – August 2016 at the Gas field and Regional sites: observed (blue), model results with all sources (red) and model results without the CSG sources (purple).

5.3.3 Comparison with Air Quality Objectives for the Region

Figure 5.35 shows spatial plots over the model 1 km grid domain of the modelled maximum 1-hour average NO₂ concentrations with all sources included for each season. Note that each grid square shows the maximum concentration modelled for that grid square *for that entire season*. As such the maximum concentration shown in each grid square may be from different time periods.

The 1-hour average NO₂ air quality objective of 120 ppb is not exceeded anywhere in the modelled domain during any season and the areas of largest NO₂ values in the model domains are close to CSG-related emission sources with maximum values (indicated by the red arrows) of 104 ppb during SON, 74 ppb during DJF, 88 ppb during MAM and 71 ppb during JJA. There are no easily visible areas exceeding 80 % of the 1-hour average NO₂ air quality objective of 96 ppb in Figure 5.35 but they occur during SON, are very small and are discussed below.

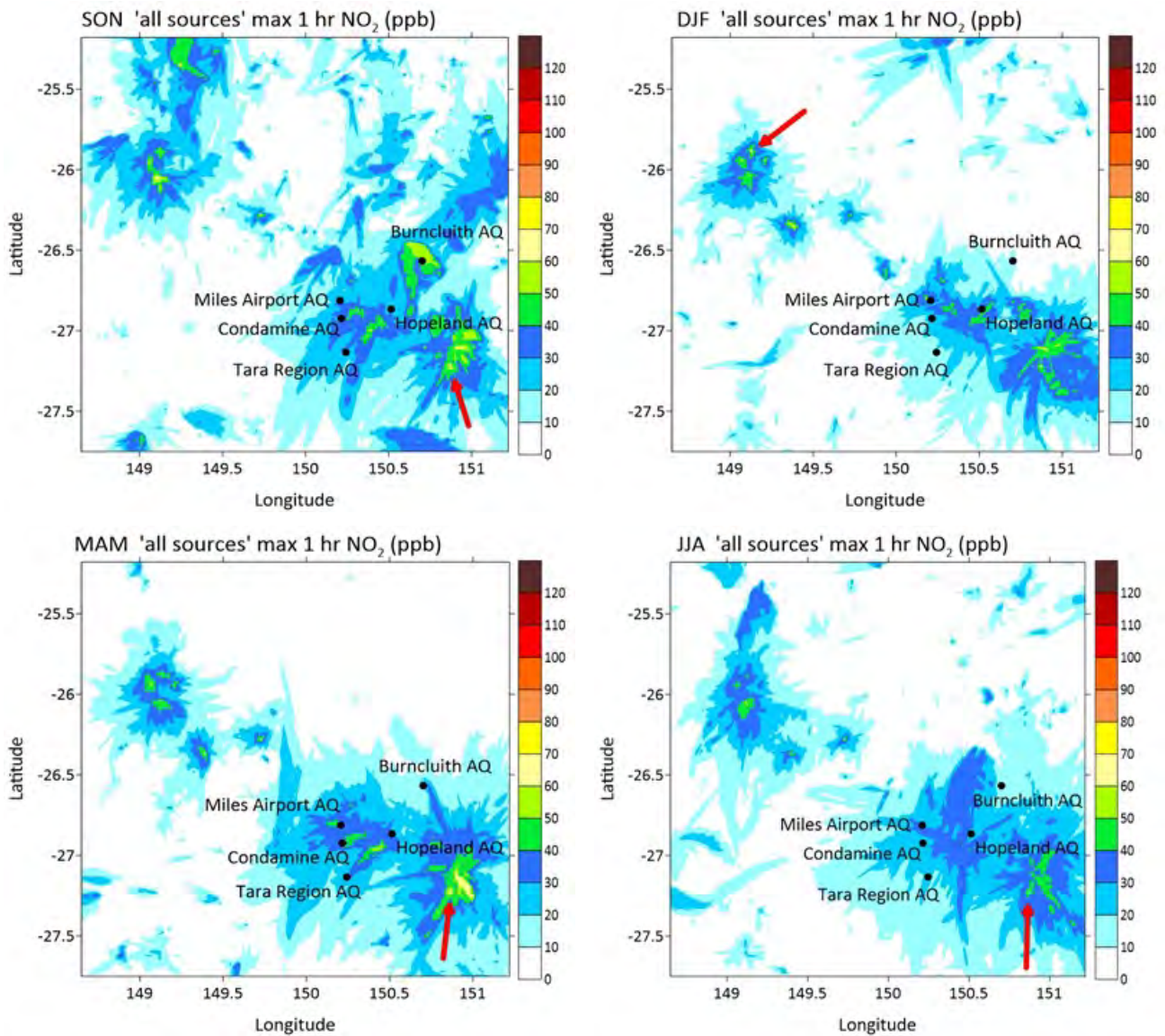


Figure 5.35 The maximum concentration of the 1-hour average NO_2 in each grid square for the model results with all sources during each season (ppb). Note that the maximum concentrations shown in each grid square may be from different time periods. The red arrow indicates the location of the maximum value for the season.

Figure 5.36 shows the contribution, in each grid square for each season, of the CSG-related emissions to the maximum modelled 1-hour average NO_2 concentrations shown in Figure 5.35. Note, this is calculated for each grid square by subtracting the maximum 1-hour average NO_2 concentration for the season in the run without CSG sources from the maximum 1-hour average NO_2 concentration for the same season in the run with all sources. Importantly, in each grid square the two maximum values that are subtracted may each be from a different day and time during the season.

The largest CSG contributions to these maximum values occur close to CSG sources. The maximum values (indicated by the red arrows) are 65 ppb during SON, 71 ppb during DJF, 59 ppb during MAM and 62 ppb during JJA and all are within 1 km of CSG-related emission sources. Note that the model cannot resolve near-source impacts of plumes therefore impacts within a few kilometres of a point emission source may be under or overestimated.

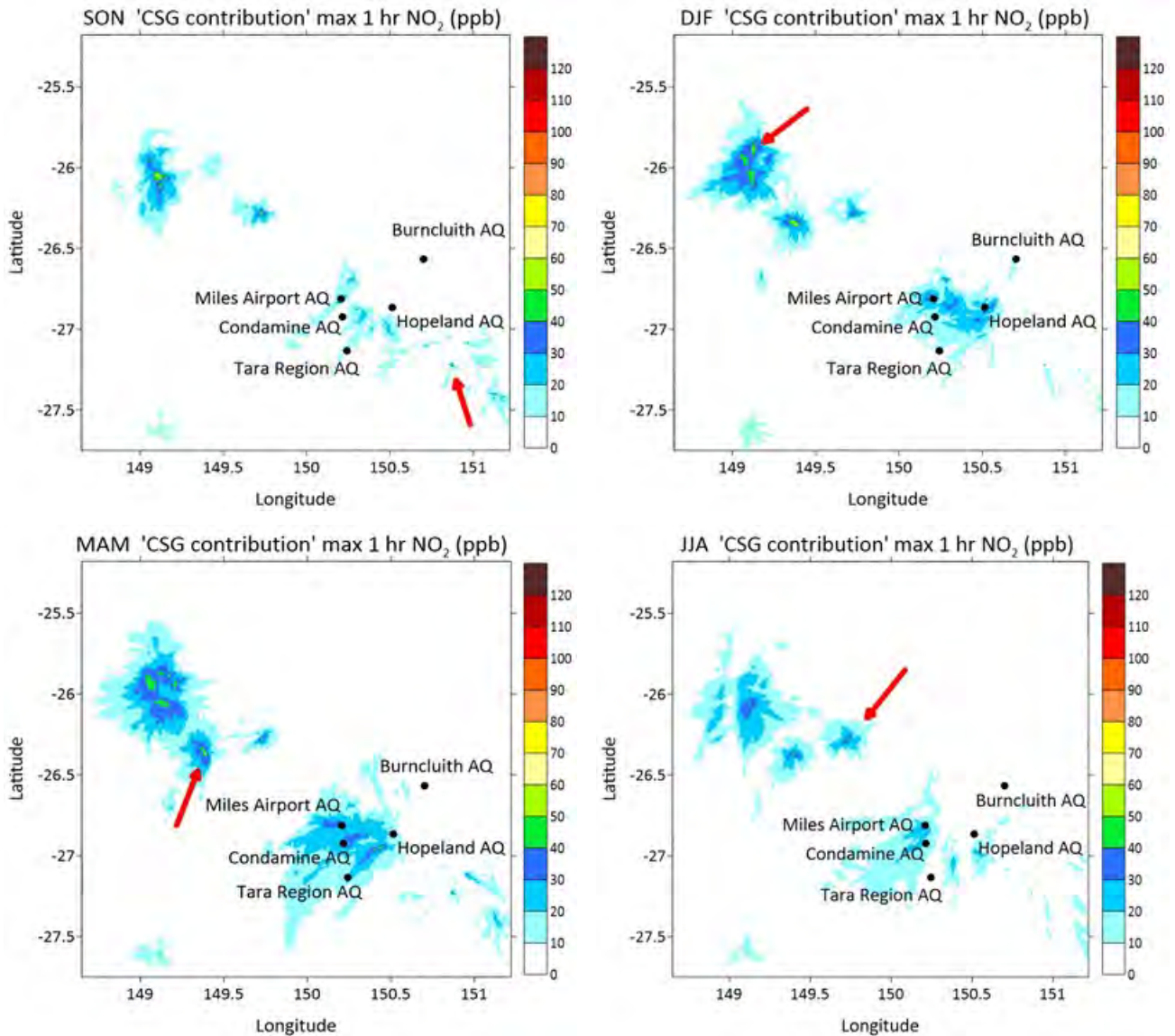


Figure 5.36 The contribution of the CSG-related emissions to the modelled maximum 1-hour average NO₂ concentration (maximum in each grid square from Figure 5.35) during each season (ppb). Note that the concentrations shown in each grid square may be from different time periods. The red arrow indicates the location of the maximum value for the season.

Figure 5.37 shows the maximum contribution of the CSG-related emissions to the 1-hour average modelled NO₂ concentrations in each grid square for the modelled year. Note, this is calculated in each grid square by subtracting, every hour, the 1-hour average NO₂ concentration for the run without CSG sources from that for the run with all sources and then calculating the maximum value for the year from the hourly values. Importantly, in each grid square the two values that are subtracted are from the same day and time in the year. Note this figure is showing the maximum contribution to the NO₂ concentration values whilst Figure 5.37 shows the contribution to the maximum NO₂ concentration values.

Generally the maximum modelled contributions away from the CSG-related emission sources are less than 10 ppb with larger values around the CSG-related emission sources. The largest maximum value is 103 ppb (indicated by the red arrow) which is 86 % of the air quality objective (120 ppb, Table 5.1) and is about 1 km from CSG-related emission sources.

Due to the model overestimating the 1-hour average NO₂ concentrations as discussed in Section 5.3.1 these results are also most likely an overestimate.

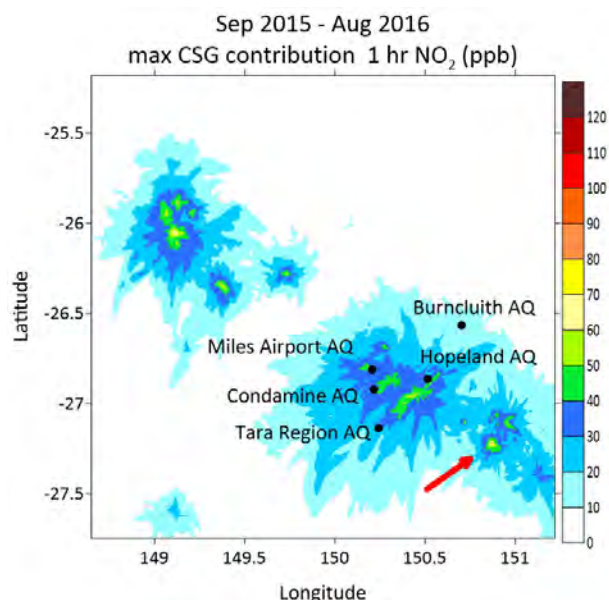


Figure 5.37 The maximum contribution of the CSG-related emissions to the modelled 1-hour average NO₂ concentrations during the modelled year (ppb). Note that the concentrations shown in each grid square may be from different time periods. The red arrow indicates the location of the maximum value for the year.

Over the modelled 1 km grid domain during the modelled year there are no exceedances of the 1-hour average NO₂ air quality objective (120 ppb, Table 5.1) and there are 2 exceedances of 80 % of the air quality objective (96 ppb) and both include a large contribution from the CSG-related emissions. Table 5.7 lists the two 80 % exceedances along with the contribution and the percentage contribution of the CSG-related emissions to the 80 % exceedances. Both 1-hour average modelled NO₂ values are similar and both have contributions due to the CSG-related emissions of greater than 99 %.

Due to the model overestimating the 1-hour average NO₂ concentrations as discussed in Section 5.3.1 these results are also most likely an overestimate.

Table 5.7 The two values of modelled 1-hour average NO₂ concentrations that exceed 80 % of the air quality objective (96 ppb) and the contribution (ppb) and the percentage contribution of the CSG-related emissions to the exceedances.

1-hour NO ₂ 80 % exceedances (ppb)	Contribution of the CSG-related emissions to 80 % exceedances (ppb)	Percentage contribution of the CSG-related emissions to 80 % exceedances
103.9	103.5	99.6
103.4	103.0	99.7

Figure 5.38 shows the location of the modelled 1-hour average NO₂ concentrations that exceed 80 % of the air quality objective (96 ppb). The 2 exceedances occur at the same location on the same day, one hour apart, and they are located about 1 km from CSG-related emission sources. Both predicted exceedances occur at night when the boundary layer height is low and the local winds are calm.

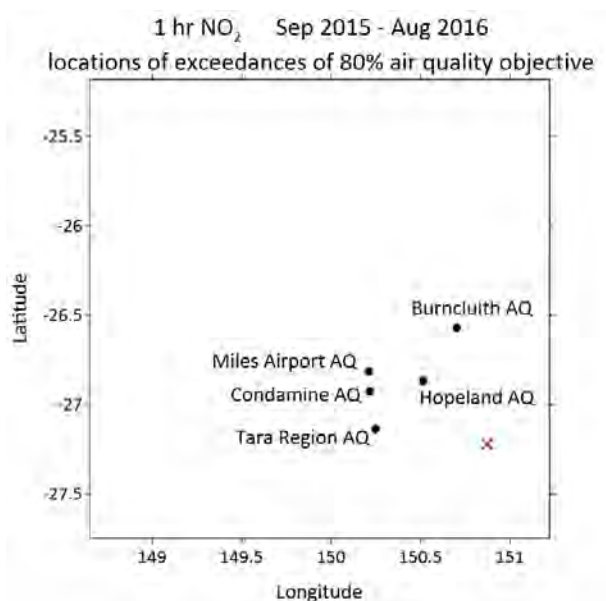


Figure 5.38 The location, marked by a red cross, of the modelled 1-hour average NO₂ concentration that exceeds 80 % of the air quality objective (96 ppb).

5.3.4 Modelled effect of the CSG-related emissions on NO₂ levels at Town sites

Model results are presented at the Town sites to investigate the effects of the CSG-related emissions to NO₂ concentrations over the region.

Table 5.8 presents the annual average concentrations of NO₂ for the model results with all sources and without the CSG sources at the Town sites. All modelled concentrations are well below the

annual average air quality objective for NO₂ (30 ppb, Table 5.1). At the Town sites the modelled annual average 1-hour NO₂ concentrations with all emission sources included are 0.2 -0.6 ppb higher than those for the model run without CSG-related emission sources.

Table 5.8 The modelled annual average concentrations of NO₂ (ppb) at the Town sites.

Annual average (ppb)	Modelled NO ₂ (all sources)	Modelled NO ₂ (without CSG sources)
Chinchilla	1.3	1.0
Miles township	1.6	1.0
Roma	1.1	0.9
Tara township	0.9	0.7
Warra	1.5	1.2

Figure 5.39 shows the maximum 1-hour average NO₂ concentrations for each month of the model simulation at the Town sites. The bar plots show the model results with all sources in red and the model results without the CSG sources in purple. The dashed horizontal red line shows the value of the air quality objective.

The 1-hour average NO₂ air quality objective (120 ppb, Table 5.1) and 80 % of the 1-hour average NO₂ air quality objective (96 ppb, Table 5.1) are not exceeded by the modelled 1-hour average NO₂ concentrations at any Town site in any month.

The largest contributions due to the CSG-related emissions are seen at Miles township with a maximum contribution of 19 ppb which is 16 % of the air quality objective for 1-hour average NO₂ (120 ppb, Table 5.1) and the smallest contributions due to the CSG-related emissions are modelled at Roma.

The maximum modelled 1-hour average NO₂ concentration of 42 ppb occurred at Warra during September with less than a 3 % contribution from the CSG-related emissions and is predominantly due to a modelled fire.

Due to the model overestimating the 1-hour average NO₂ concentrations as discussed in Section 5.3.1 these results are also most likely an overestimate.

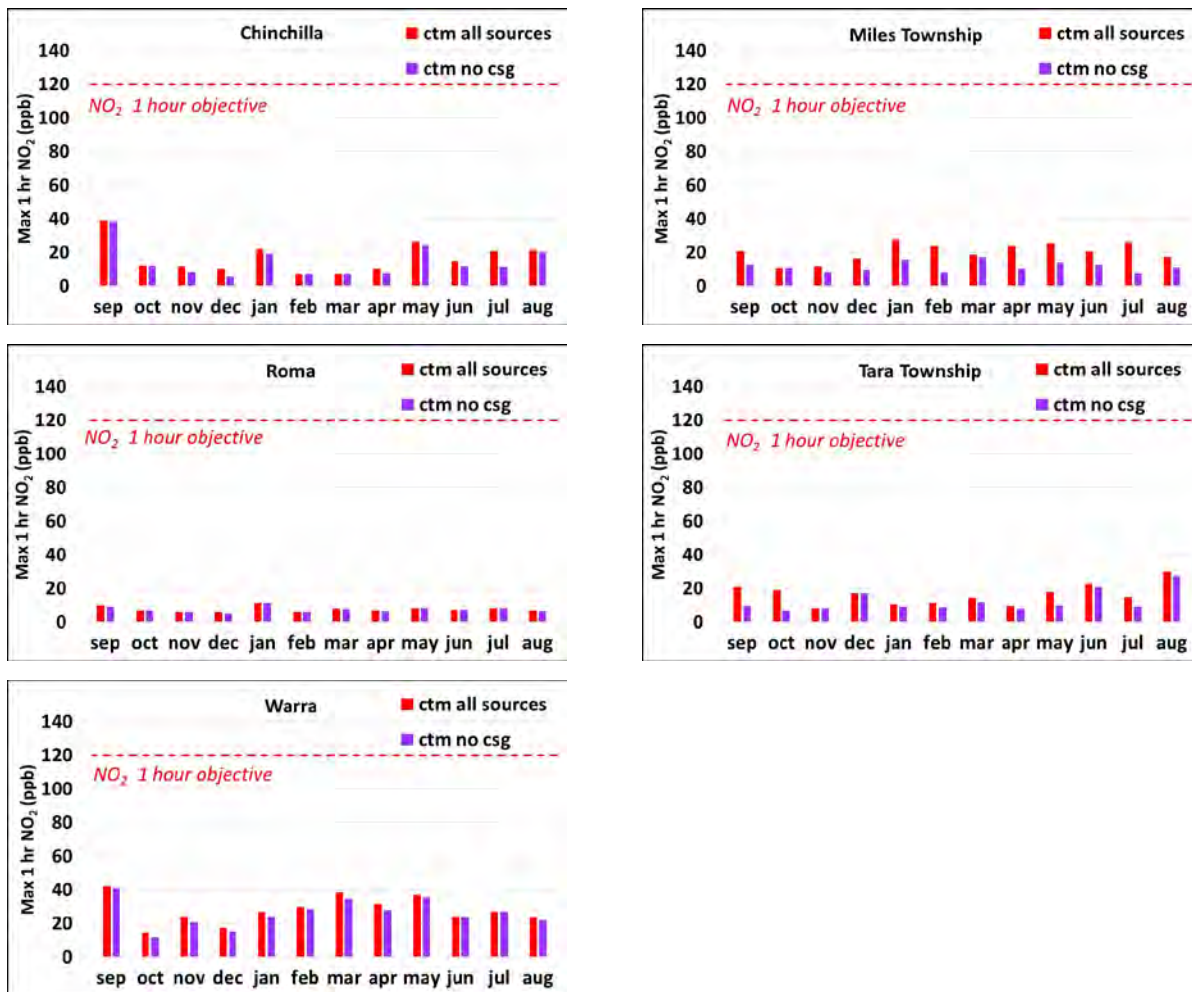


Figure 5.39 The modelled maximum 1-hour average NO₂ concentrations (ppb) for each month of September 2015 – August 2016 at the Town sites: model results with all sources (red) and model results without the CSG sources (purple).

The modelled contribution from the CSG-related emissions to the 1-hour average NO₂ concentrations at each of the Town sites is presented in Figure 5.40. Each plot shows the percentage of model hours within each season for the modelled contribution from the CSG-related emissions to the 1-hour average NO₂ concentrations.

On average 98.6 % of the time the contribution from the CSG-related emissions at the Town sites is less than 5 ppb which is 4 % of the 1-hour average NO₂ air quality objective (120 ppb, Table 5.1). Miles township is predicted to have the largest frequency of change due to the CSG-related emissions during DJF and MAM. The lowest frequency of change due to the CSG-related emissions is modelled at Roma.

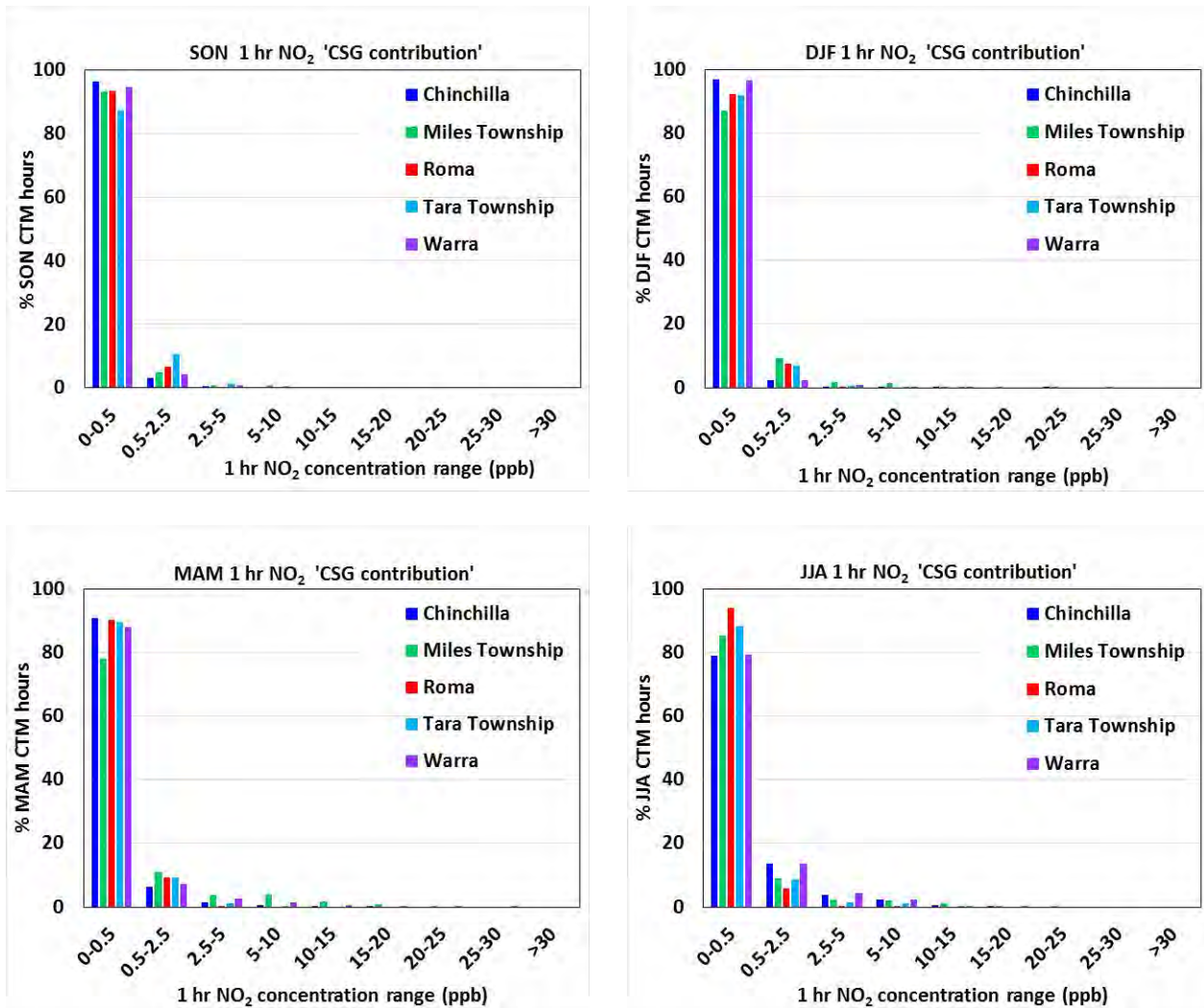


Figure 5.40 The modelled contribution from the CSG-related emissions to the 1-hour average NO₂ concentration (ppb) at the Town sites shown as a frequency distribution for each season. The x-axis shows the concentration ranges of the contribution from the CSG-related emissions and the y-axis shows the percentage of model hours.

Figure 5.41 shows plots of the modelled 1-hour average NO₂ concentrations with all sources against the contribution from the CSG-related emissions to the modelled 1-hour average NO₂ concentrations at Miles township, one of the Town sites. Those for the other Town sites are shown in Appendix E. The plots are seasonal and one point is plotted for each modelled hour.

At Miles township the pattern is similar to that at the Gas field sites; when the modelled contributions are greater than about 10 ppb they account for (mostly) greater than 85 % of the 1-hour average NO₂ concentration value. This is similar at Chinchilla. There is less of a change due to the CSG-related emissions at Roma (< 7 ppb) with the 1-hour average NO₂ concentration values generally less than 10 ppb. Warra shows a different pattern, changes greater than 10 ppb due to the CSG-related emissions account for 30 – 95 % of the NO₂ concentration value.

The largest increases (> 15 ppb) at Miles township occur mostly during JJA and the maximum increase in the 1-hour average NO₂ concentration due to the CSG-related emissions is 26 ppb

which is 22 % of the air quality objective for NO₂ (120 ppb, Table 5.1) and 92 % of the 1-hour modelled NO₂ concentration value.

Due to the model overestimating the 1-hour average NO₂ concentrations as discussed in Section 5.3.1 these results are also most likely an overestimate.

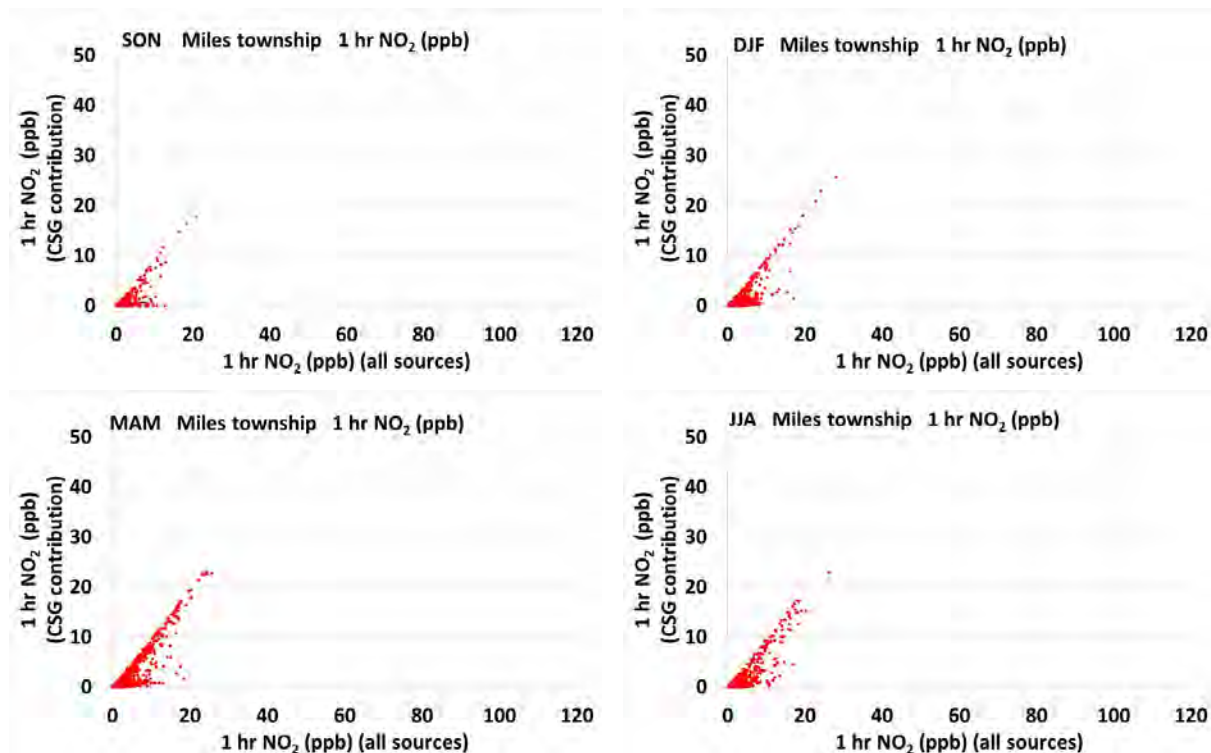


Figure 5.41 The modelled contribution from the CSG-related emissions to the 1-hour average NO₂ concentration (ppb) at Miles township shown as a scatter plot for each season. The x-axis shows the modelled 1-hour average NO₂ concentrations with all sources (ppb) and the y-axis shows the contribution from the CSG-related emissions to the 1-hour average NO₂ concentration (ppb).

5.3.5 Summary

The impacts of CSG activity on the 1-hour average NO₂ concentrations modelled in the Surat Basin are summarised below. Note, due to the model overestimating the 1-hour average NO₂ concentration peaks as discussed in Section 5.3.1 the general 1-hour average NO₂ concentration results are most likely an overestimate, possible reasons are summarised below.

Comparison of the model results with the observations

- Comparison of the observed and modelled time series of 1-hour average NO₂ concentrations at Miles Airport and Condamine shows the background NO₂ concentration is mostly captured by the model, whereas the modelled NO₂ concentration overestimates many of the observed peak values. At Hopeland the observed NO₂ concentration time series has fewer and smaller peaks than at the other Gas field sites and the model overestimates these peak values particularly during JJA. At the Regional sites there are NO₂

concentration observations for most of JJA and the observed and modelled peaks are smaller compared to those at the Gas field sites but the model still overestimates the peaks.

- The overprediction of the NO₂ concentration peaks when all sources are included and the underprediction of NO₂ concentration peaks when no CSG sources are included suggests that the CSG-related emissions generally result in larger NO₂ concentration peaks and that some level of CSG-related emissions is needed in the model to reproduce the observed NO₂ concentration pattern.
- The predicted concentration of NO₂ from the all sources run is mostly larger than observed and there are a number of possible reasons why the model overestimates the CSG-related NO₂ peaks: 1) NO_x emissions may be overestimated at some CSG-related emission sources, 2) the effective height of release of some CSG-related emissions may not be correctly represented in the model, 3) the time pattern of release of some CSG-related emission sources may not be correctly represented in the model and/or 4) the height of the night-time boundary layer may not be correctly represented in the model.
- At the Gas field sites there is good agreement between the modelled annual average NO₂ concentration with all sources and the observed values where available.

Contribution of the CSG-related emissions to the modelled 1-hour average NO₂ concentrations

- On average 95 % of the time at the Gas field and Regional sites and 98.6 % of the time at the Town sites the contribution from the CSG-related emissions is less than 5 ppb which is 4 % of the air quality objective for 1-hour average NO₂.
- The lowest frequency of change due to the CSG-related emissions is modelled at Burncluith and Roma, while the largest frequency of change due to the CSG-related emissions occurs at the Gas field sites particularly during MAM and JJA.
- The largest contributions due to the CSG-related emissions to the 1-hour average NO₂ concentrations occur at Miles Airport and Condamine. The smallest contributions occur at Roma and Burncluith.
- At the Gas field and Regional sites and at Miles township and Chinchilla modelled contributions greater than 10 ppb account for mostly greater than 85 % of the 1-hour average NO₂ concentration value.
- The maximum predicted contribution to the 1-hour average NO₂ concentration due to the CSG-related emissions occurs at Condamine and is 41 ppb which is 34 % of the air quality objective for NO₂ and 97 % of the 1-hour modelled NO₂ concentration value.
- Over the entire model 1 km grid domain during the modelled year the maximum predicted contribution of the CSG-related emissions to the modelled 1-hour average NO₂ concentrations is 103 ppb which is 86 % of the air quality objective and occurs about 1 km from CSG-related emission sources.
- Note that the model cannot resolve near-source impacts of plumes therefore impacts within a few kilometres of a point emission source may be under or overestimated.

Contribution of the CSG-related emissions to exceedances of the air quality objective or 80 % of the air quality objective

- There are no modelled exceedances of the annual average NO₂ air quality objective at any of the Gas field, Regional or Town sites.
- At the Gas Field, Regional or Town sites there are no modelled exceedances of the 1-hour average NO₂ air quality objective or 80 % of the air quality objective during any month.
- Over the entire modelled 1 km grid domain during the modelled year there are no exceedances of the 1-hour average NO₂ air quality objective and there are 2 exceedances of 80 % of the air quality objective and both include a large contribution from the CSG-related emissions (greater than 99 %). Both 1-hour average modelled NO₂ values occur at the same location on the same day, one hour apart, and they are located about 1 km from CSG-related emission sources. Due to the model overestimating the 1-hour average NO₂ concentrations as discussed in Section 5.3.1 these results are also most likely an overestimate.

5.4 Carbon Monoxide

Carbon monoxide (CO) is one of the six key pollutants included in the Ambient Air Quality NEPM (NEPM, 2016). CO is a gas formed from incomplete combustion of carbon-containing fuel. Carbon monoxide was identified as a key pollutant in CSG Industry EIS (QGC 2010, APLNG 2010). CSG-related sources include combustion of gas in flares and engines, and diesel engine emissions.

5.4.1 Modelled effect of the CSG-related emissions at the observation sites

Time series plots of the observed and modelled concentrations of 1-hour average CO at Burncluith are shown in Figure 5.42. The observations are shown in blue, the model results with all emission sources in red and the model results without the CSG-related emission sources in purple. The time series are presented for different seasons. For comparison purposes and completeness time series at Miles Airport, Condamine, Hopeland and Tara Region are shown in Appendix D. In the time series figure it is not always possible to see the two modelled time series, the red (all sources) concentration series is plotted first and then the purple (no CSG sources) series is plotted. Where the values of each series are the same only the last plotted series will be seen, which is the purple one (no CSG sources). Therefore, when red is seen on the plot it is because the two modelled series have different values at that point in time and the difference between the two values is the contribution to the concentration from the CSG-related emissions; this contribution is shown in Figure 5.43 (the contribution for the other sites is shown in Appendix D).

For comparison between the observed and modelled CO concentrations only observations made at Burncluith are relevant due to the sensitivity of the instruments used to measure CO. Observations at the Gas field sites are measured with instruments that have an uncertainty of 1000 ppb and a resolution of 100 ppb, well within requirements for regulatory purposes, but not sufficiently sensitive for comparison with model results due to the low concentrations of CO observed in the region, e.g. the annual average CO concentration observed at Burncluith is 80 ppb.

The observed and modelled CO concentrations at Burncluith plotted in Figure 5.42 show broad agreement, although there are a number of observed CO concentration peaks not captured by the model. Some of these are possibly due to a smoke source(s) not present in the model emissions (e.g. hot spots not in the emission files due to cloud cover or particularly in winter a nearby house with a wood heater not in the emission files). The largest modelled CO concentration peak coincides with the largest observed CO concentration peak in September 2015 and the modelled peak is due to smoke from modelled vegetation fires, confirmed by comparison with the modelled smoke tracer levoglucosan (not shown). The modelled peak is larger than the observed peak - see Section 5.1.1 for a discussion about differences between the observed and modelled data. Tara Region and the Gas field sites show similar modelled CO concentration time series, - small values and a number of larger peaks due to model fires.

At Burncluith the modelled time series for CO concentration with all sources included shows little difference from the time series without the CSG sources (Figure 5.42 and Figure 5.43). At the Gas field sites (see Appendix D) the contributions due to the CSG-related emissions are larger and

more frequent than at Burncluith, while at Tara Region the contributions fall between those at Burncluith and the Gas field sites.

The modelled contribution from the CSG-related emissions to the 8-hour average CO concentrations at each of the observation sites is presented in Figure 5.44. Each plot shows the percentage of model hours within each season for the modelled contribution from the CSG-related emissions to the 8-hour average CO concentrations.

On average 98 % of the time the contribution from the CSG-related emissions at all sites is less than 10 ppb which is 0.1 % of the air quality objective for CO (9000 ppb, Table 5.1). The lowest frequency of change due to the CSG-related emissions is modelled at Burncluith which is furthest from major CSG-related sources, while the largest frequency of change due to the CSG-related emissions occurs at the Gas field sites which are closest to major CSG-related sources. There is little seasonal difference.

Figure 5.45 shows plots of the modelled 8-hour average CO concentrations with all sources against the contribution from the CSG-related emissions to the modelled 8-hour average CO concentrations at Miles Airport. Those for Condamine, Hopeland, Tara Region and Burncluith are shown in Appendix E. The plots are seasonal and one point is plotted for each 8-hour modelled value.

At Miles Airport the largest modelled increases (> 20 ppb) in the 8-hour average CO concentrations due to the CSG-related emissions occur during MAM, with the CSG-related emissions contributing up to 38 % of the value of CO. However, even when this occurs the maximum increase in the 8-hour average CO concentration due to the CSG-related emissions is 28 ppb which is 0.3 % of the 8-hour air quality objective (9000 ppb, Table 5.1). The results for the other sites are similar with a lower contribution from the CSG-related emissions to the 8-hour average CO concentrations at Tara Region and Burncluith, reflecting the greater distance of these sites from major CSG-related sources.

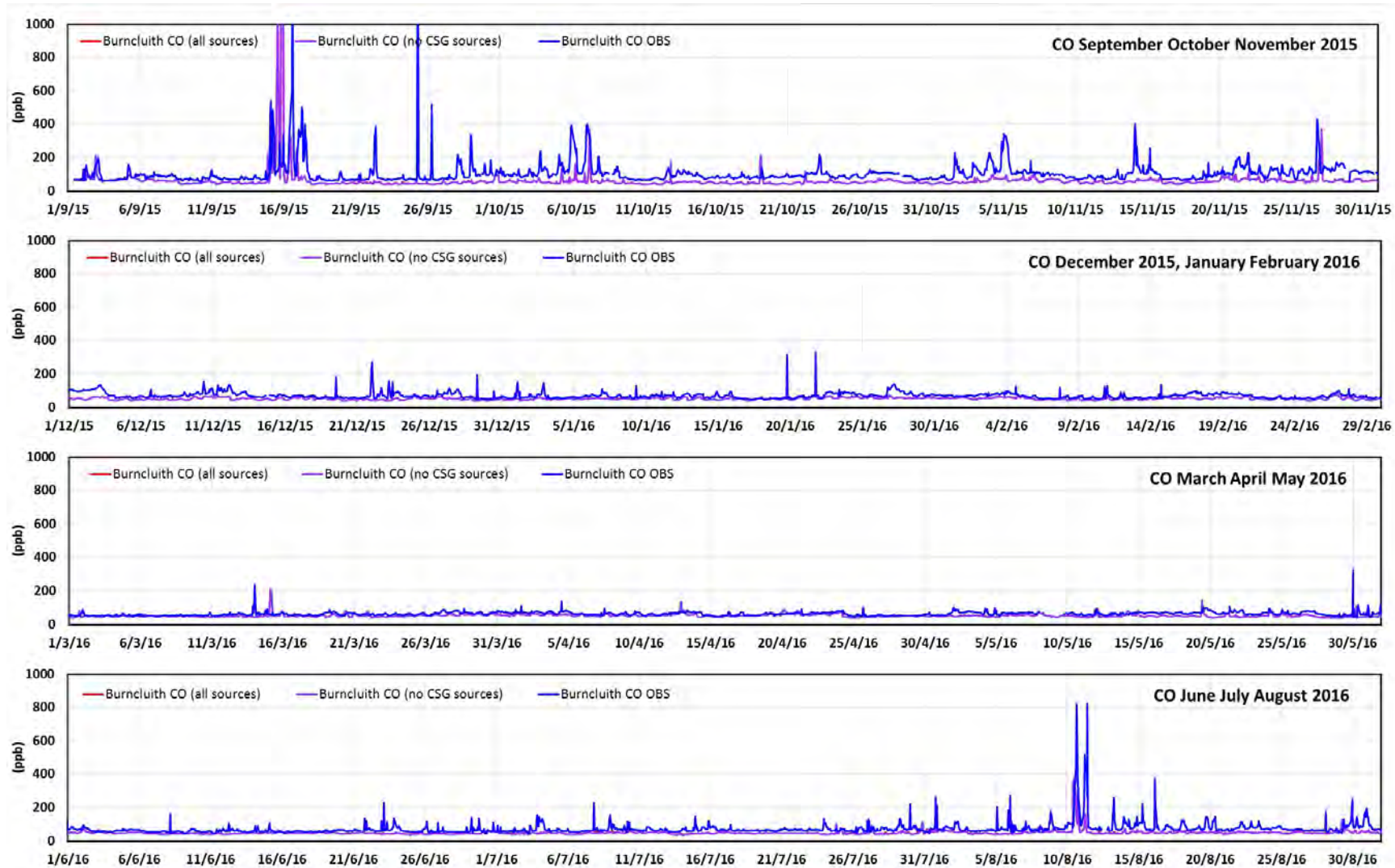


Figure 5.42 The observed and modelled time series of the 1-hour average CO concentrations (ppb) at Burncluith for the modelled year (red = model results with all sources, purple = model results without CSG sources, blue = observations). (peaks off scale: model, 15/9/15 21:00 = 6302 ppb, OBS 16/9/15 15:00 = 1170 ppb, 25/9/15 08:00 1143 ppb)

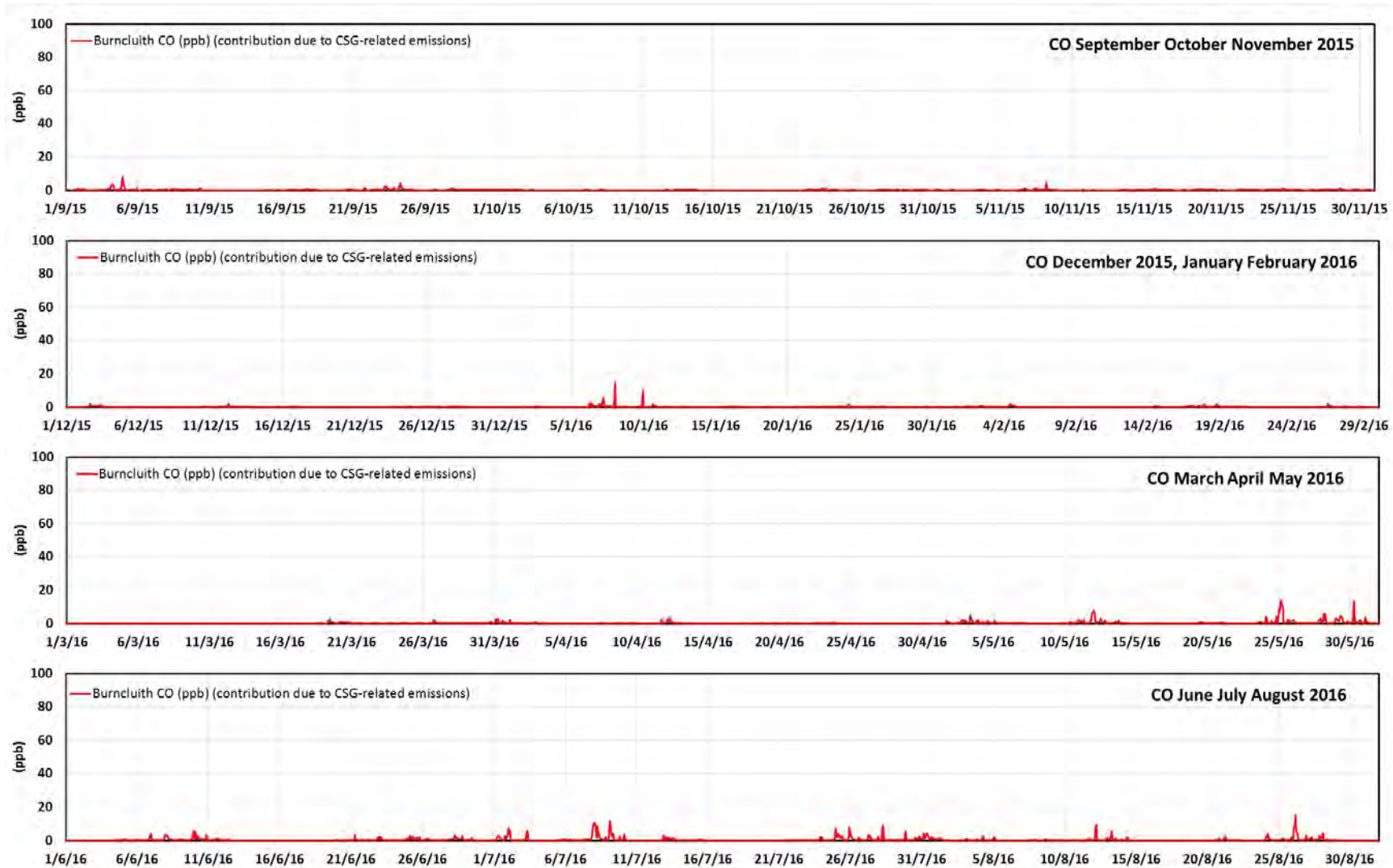


Figure 5.43 The modelled contributions from the CSG-related emissions to the 1-hour average CO concentrations (ppb) at Burncluith for the modelled year.

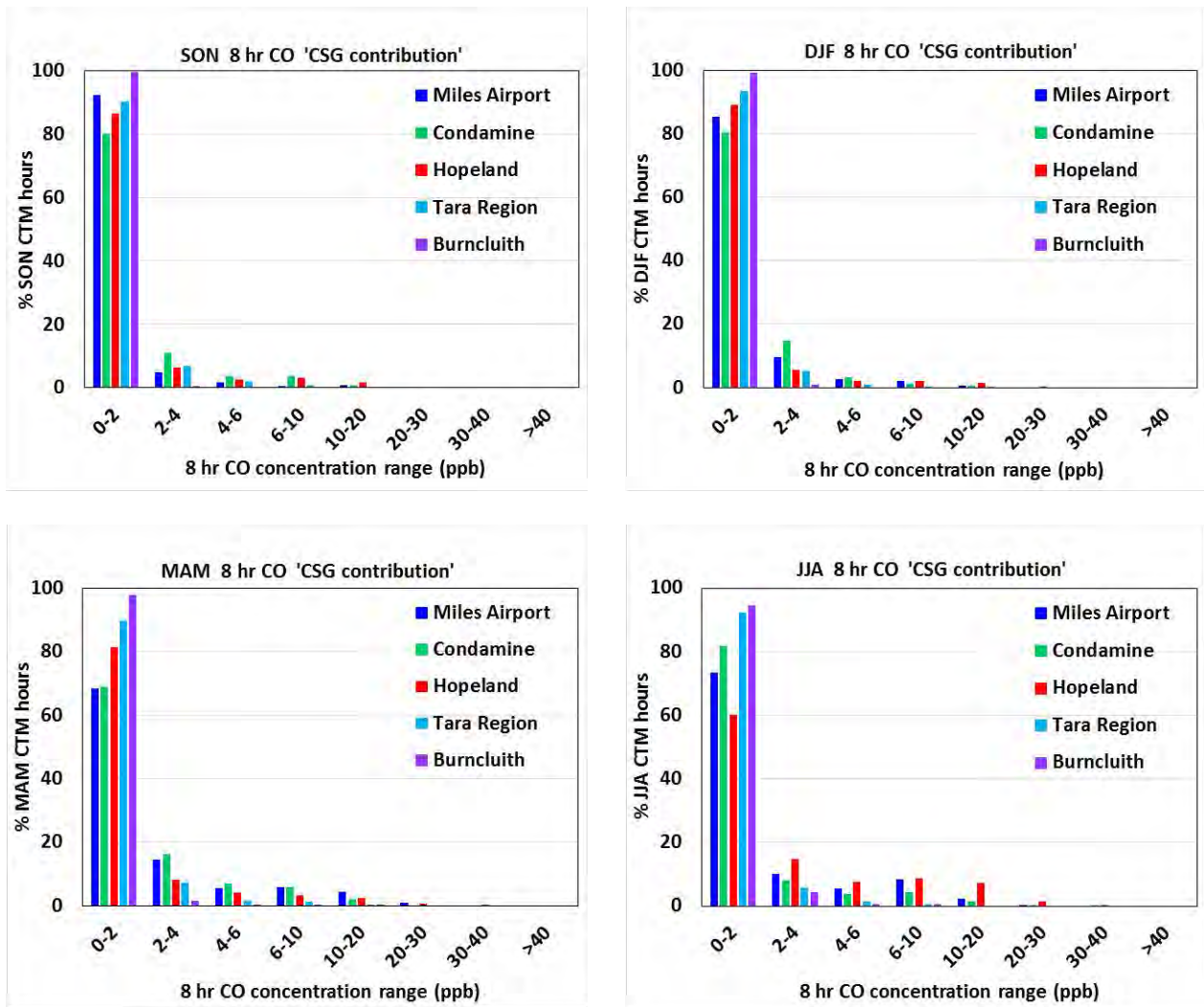


Figure 5.44 The modelled contribution from the CSG-related emissions to the 8-hour average CO concentration (ppb) at the Gas field and Regional sites shown as a frequency distribution for each season. The x-axis shows the concentration ranges of the contribution from the CSG-related emissions and the y-axis shows the percentage of model hours.

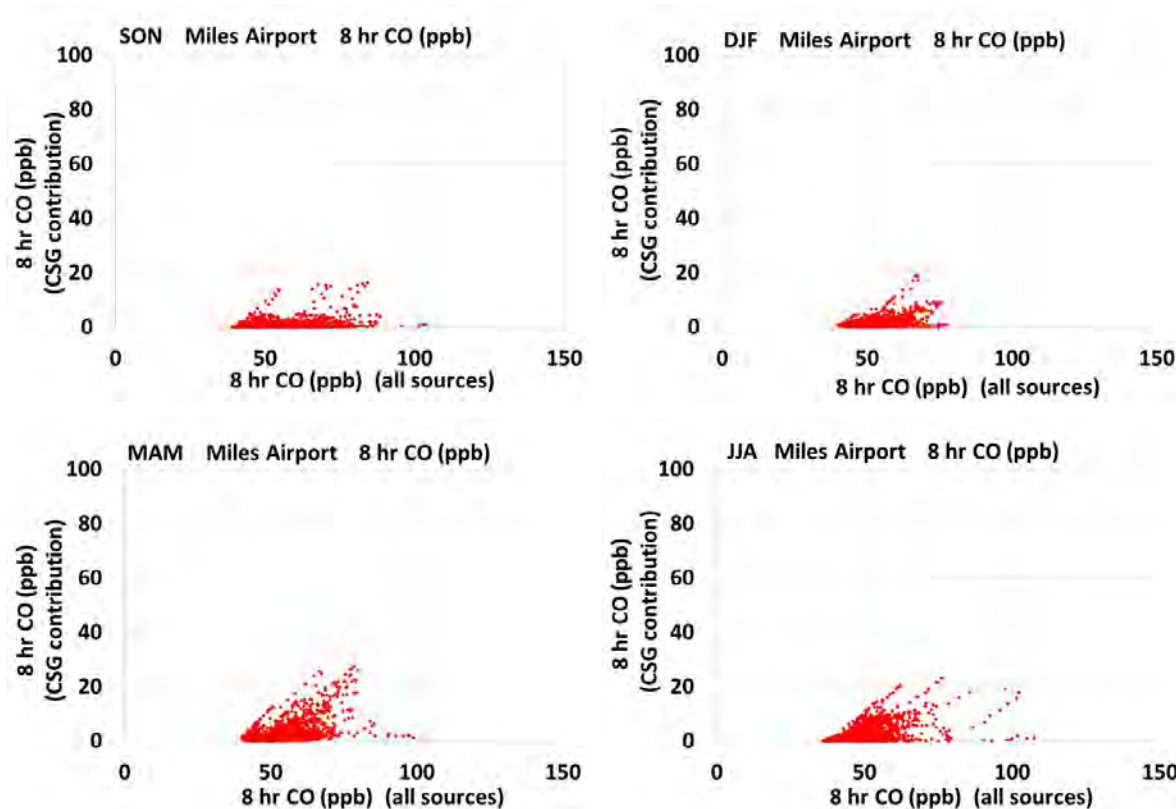


Figure 5.45 The modelled contribution from the CSG-related emissions to the 8-hour average CO concentration (ppb) at Miles Airport shown as a scatter plot for each season. The x-axis shows the modelled 8-hour average CO concentrations with all sources (ppb) and the y-axis shows the contribution from the CSG-related emissions to the 8-hour average CO concentrations (ppb).

5.4.2 Comparison with Air Quality Objectives at Observation Sites

In this section the model results are compared to air quality objectives to assess whether there are any modelled exceedances of CO at the Gas field or Regional sites. The air quality objectives used to assess the pollutant concentrations are presented in Table 5.1.

Figure 5.46 shows the maximum 8-hour average CO concentrations for each month of the model simulation, at the Gas field and Regional sites. The bar plots show the observed values in blue, the model results with all sources in red and the model results without CSG sources in purple. The dashed horizontal red line shows the value of the air quality objective. Observed values are only shown when at least 75 % of observations are available for the month.

The 8-hour average CO air quality objective (9000 ppb, Table 5.1) and 80 % of the 8-hour average CO air quality objective are not exceeded by the observed or modelled 8-hour average CO concentrations at any site in any month.

At all sites the maximum modelled 8-hour average CO concentrations with all sources and without CSG sources are low. At Burncluith the maximum modelled 8-hour average CO concentration for September is larger than the observed due to a modelled fire, see Section 5.1.1. The largest

contributions due to the CSG-related emissions are 7 – 21 ppb at the Gas field sites which are 0.08 – 0.23 % of the air quality objective for CO, and less than 9 ppb at the Regional sites which is 0.1 % of the air quality objective for CO.

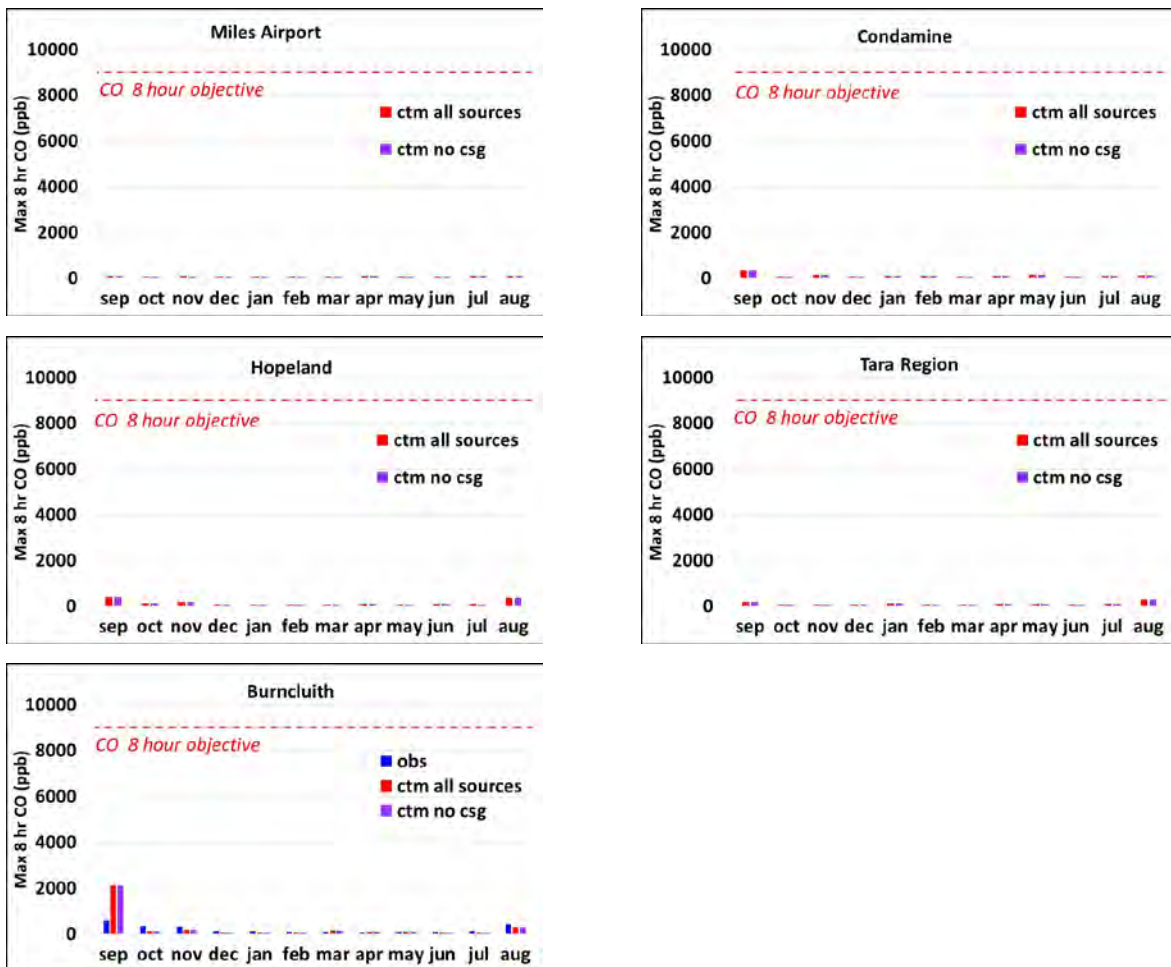


Figure 5.46 The maximum 8-hour average CO concentrations (ppb) for each month of September 2015 – August 2016 at the Gas field and Regional sites: observed (blue), model results with all sources (red) and model results without the CSG sources (purple).

5.4.3 Comparison with Air Quality Objectives for the Region

Figure 5.47 shows spatial plots over the model 1 km grid domain of the modelled maximum 8-hour average CO concentrations with all sources included for each season. Note that each grid square shows the maximum concentration modelled for that grid square *for that entire season*. As such the maximum concentration shown in each grid square may be from different time periods.

The 8-hour average CO air quality objective of 9000 ppb and 80 % of the 8-hour average CO air quality objective of 7200 ppb are not exceeded anywhere in the modelled domain during any season and the areas of largest values in the model domain are predominantly the result of

modelled fires (compare areas of higher concentrations in Figure 5.47 with the higher concentrations of the unique smoke tracer levoglucosan in Figure 5.9)

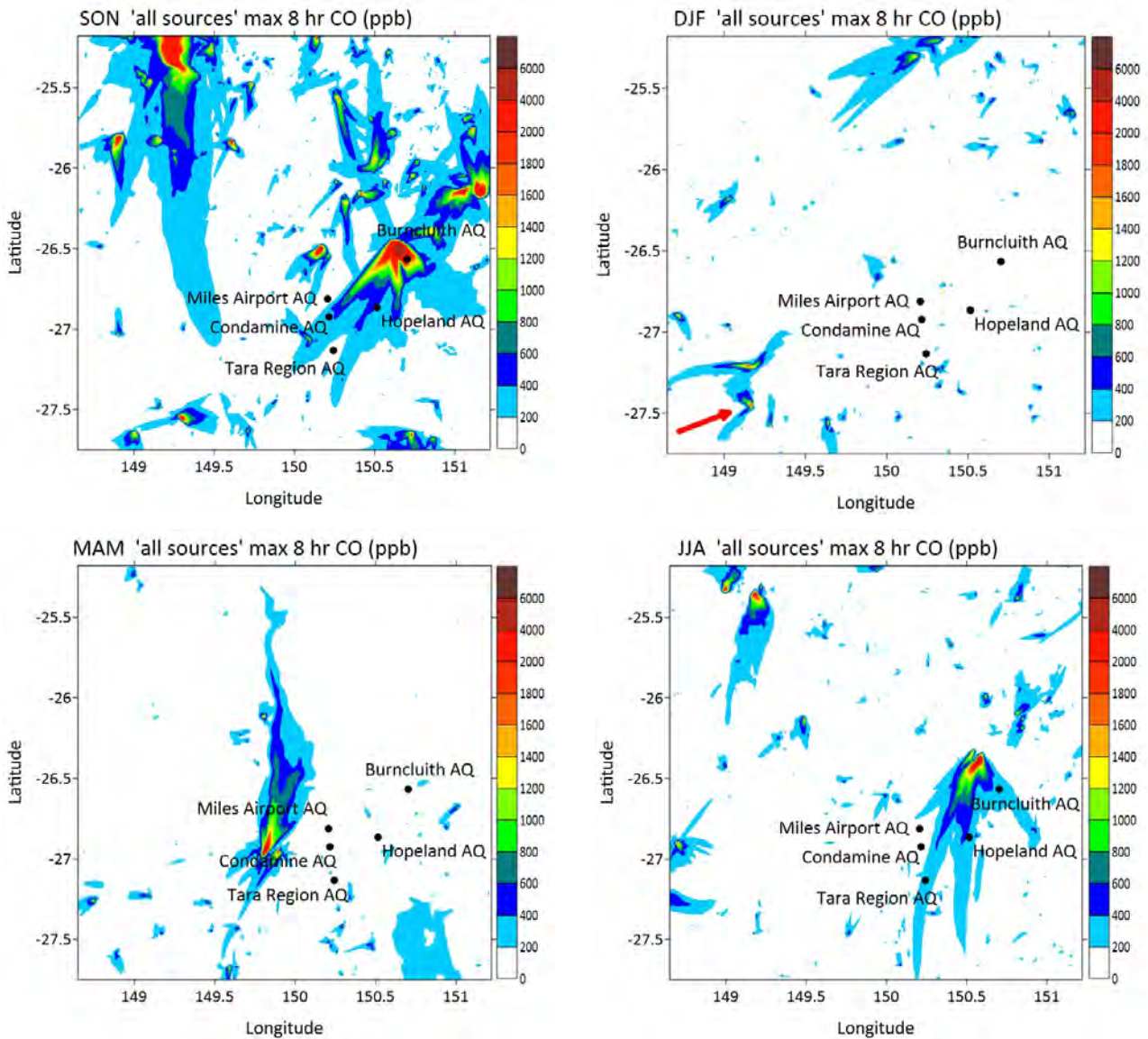


Figure 5.47 The maximum concentration of the 8-hour average CO in each grid square for the model results with all sources during each season (ppb). Note that the maximum concentrations shown in each grid square may be from different time periods. The red arrow indicates the location of the maximum value for the season.

Figure 5.48 shows the contribution, in each grid square for each season, of the CSG-related emissions to the maximum modelled 8-hour average CO concentrations shown in Figure 5.47. Note, this is calculated for each grid square by subtracting the maximum 8-hour average CO concentration for the season in the run without the CSG sources from the maximum 8-hour average CO concentration for the same season in the run with all sources. Importantly, in each grid square the two maximum values that are subtracted may each be from a different day and time during the season.

The contributions due to the CSG-related emissions are small over the region, generally less than 10 ppb. The largest CSG contributions to the maximum 8-hour CO concentrations occur close to CSG-related emission sources with the largest contribution of 94 ppb during SON (indicated by the red arrow).

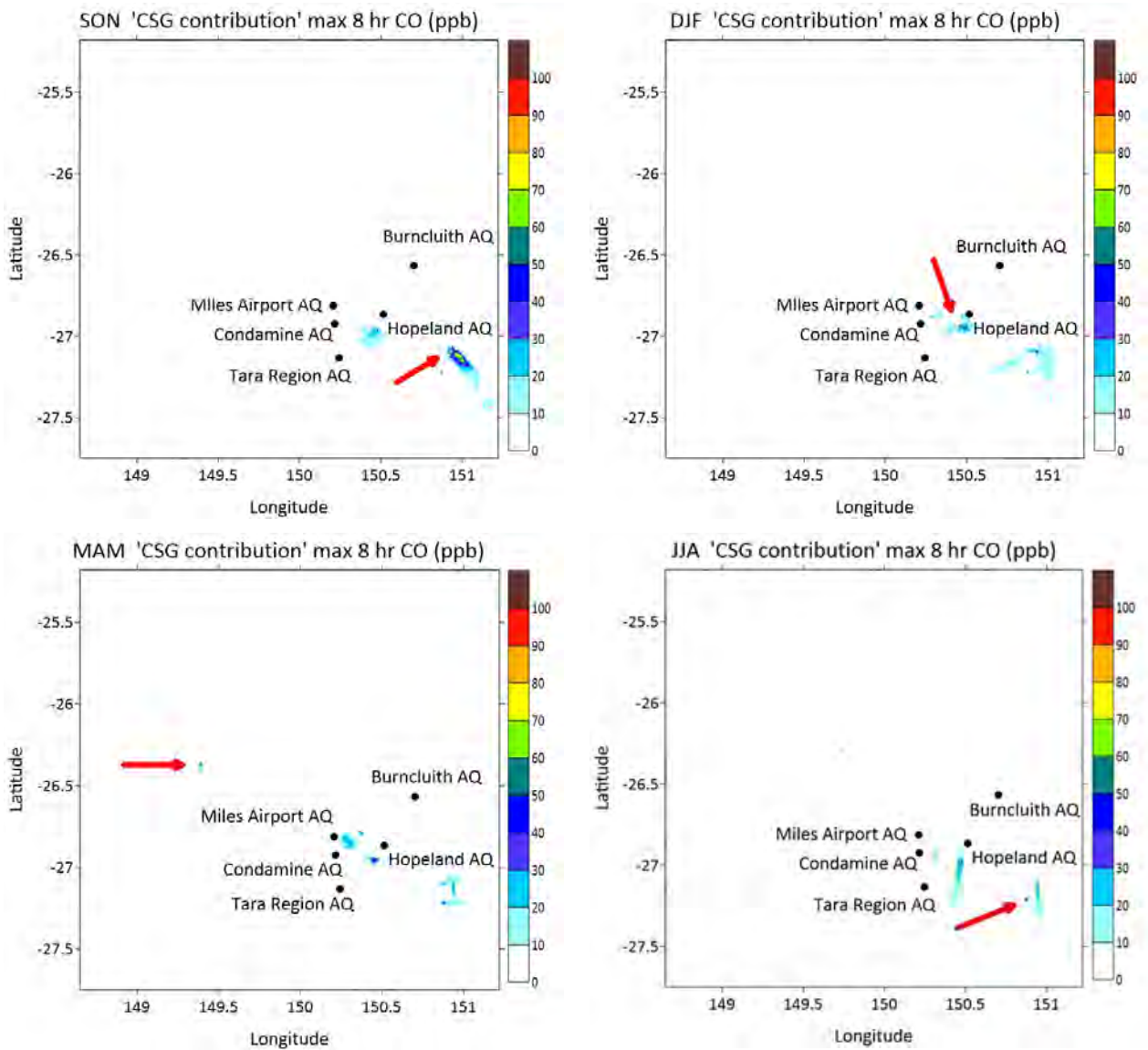


Figure 5.48 The contribution of the CSG-related emissions to the modelled maximum 8-hour average CO concentration (maximum in each grid square from Figure 5.47) during each season (ppb). Note that the concentrations shown in each grid square may be from different time periods. The red arrow indicates the location of the maximum value for the season.

Figure 5.49 shows the maximum contribution of the CSG-related emissions to the 8-hour average modelled CO concentrations in each grid square for the modelled year. Note, this is calculated in each grid square by subtracting, every hour, the 8-hour average CO concentration for the run without CSG sources from that for the run with all sources and then calculating the maximum value for the year from the hourly values. Importantly, in each grid square the two values that are

subtracted are from the same day and time in the year. Note this figure is showing the maximum contribution to the CO concentration values whilst Figure 5.48 shows the contribution to the maximum CO concentration values.

Generally the maximum modelled contributions are less than 10 ppb with larger values close to CSG-related emission sources in the southern part of the domain. The largest maximum value is 122 ppb (indicated by the red arrow) which is 1.4 % of the air quality objective (9000 ppb, Table 5.1) and is about 1.0 km from CSG-related emission sources. Note that the model cannot resolve near-source impacts of plumes therefore impacts within a few kilometres of a point emission source may be under or overestimated.

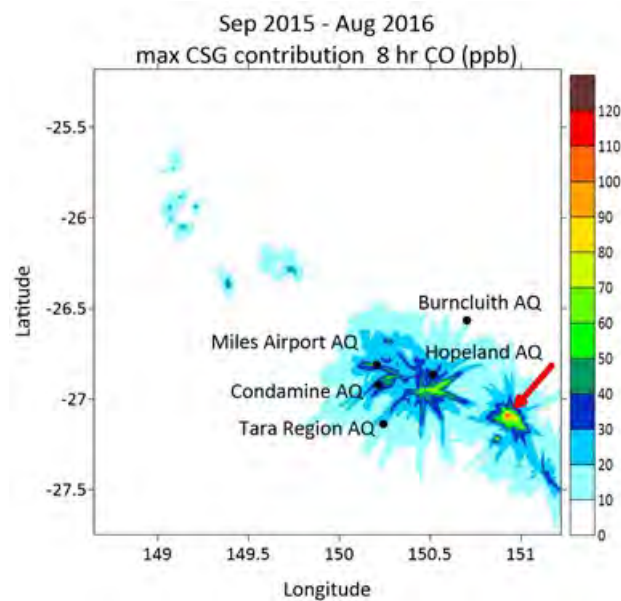


Figure 5.49 The maximum contribution of the CSG-related emissions to the modelled 8-hour average CO concentrations during the modelled year (ppb). Note that the concentrations shown in each grid square may be from different time periods. The red arrow indicates the location of the maximum value for the year.

5.4.4 Modelled effect of the CSG-related emissions on CO levels at Town sites

Model results are presented at the Town sites to investigate the effects of the CSG-related emissions to CO concentrations over the region.

Figure 5.50 shows the maximum 8-hour average CO concentrations for each month of the model simulation at the Town sites. The bar plots show the model results with all sources in red and the model results without the CSG sources in purple. The dashed horizontal red line shows the value of the air quality objective.

The 8-hour average CO air quality objective (9000 ppb, Table 5.1) and 80 % of the 8-hour average CO air quality objective (7200 ppb, Table 5.1) are not exceeded by the modelled 8-hour average CO concentrations at any of the Town sites in any month.

At the Town sites the maximum modelled 8-hour average CO concentrations for each month are low, generally less than 200 ppb, with a few elevated values predominantly due to fires. The largest contributions due to the CSG-related emissions are less than 14 ppb at the Town sites.

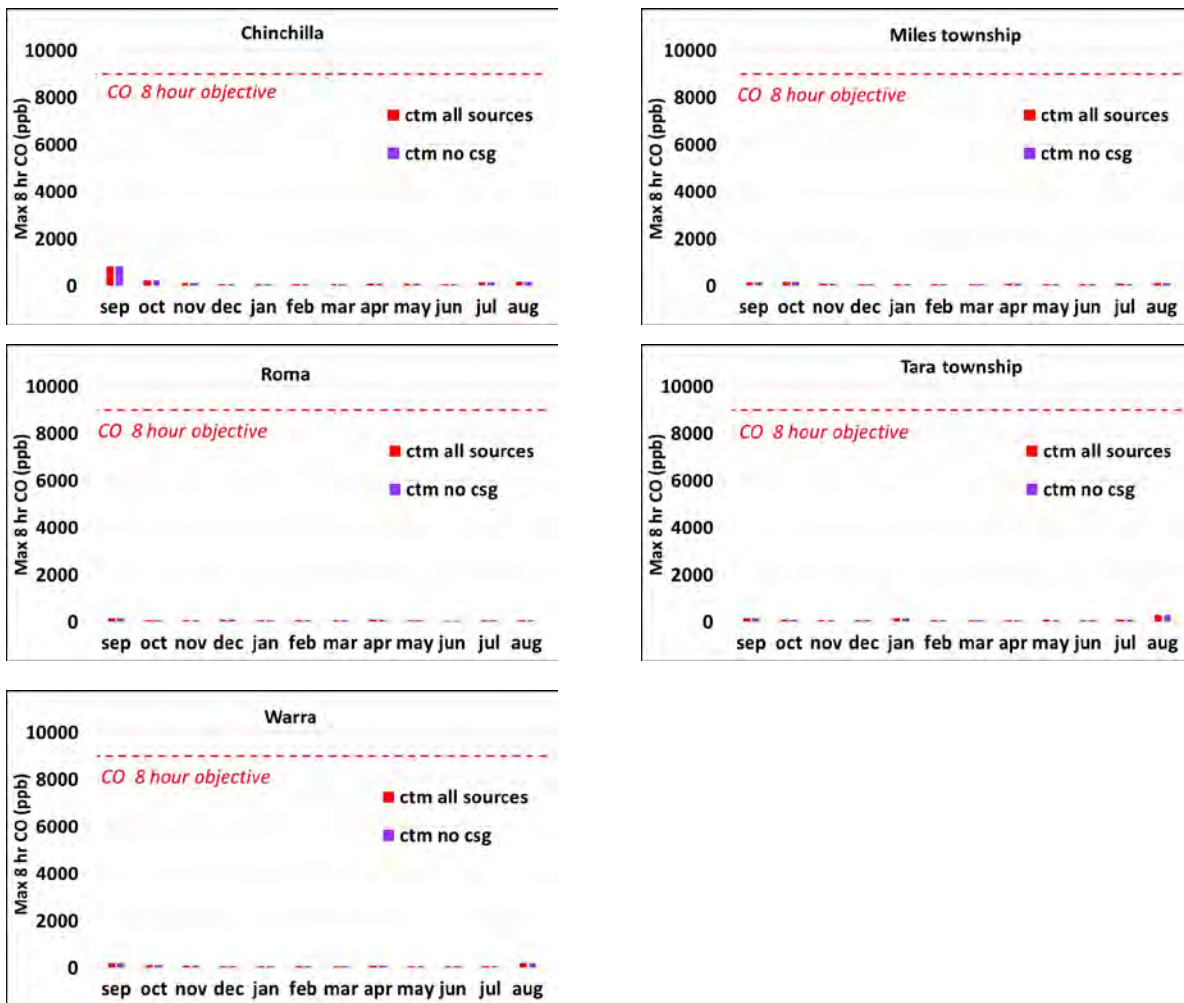


Figure 5.50 The modelled maximum 8-hour average CO concentrations (ppb) for each month of September 2015 – August 2016 at the Town sites: model results with all sources (red) and model results without the CSG sources (purple).

The modelled contribution from the CSG-related emissions to the 8-hour average CO concentrations at each of the Town sites is presented in Figure 5.51. Each plot shows the percentage of model hours within each season for the modelled contribution from the CSG-related emissions to the 8-hour average CO concentrations.

On average 99.7 % of the time the contribution from the CSG-related emissions at the Town sites is less than 10 ppb which is 0.1 % of the 8-hour air quality objective for CO (9000 ppb, Table 5.1) with the largest frequency of changes occurring during MAM and JJA.

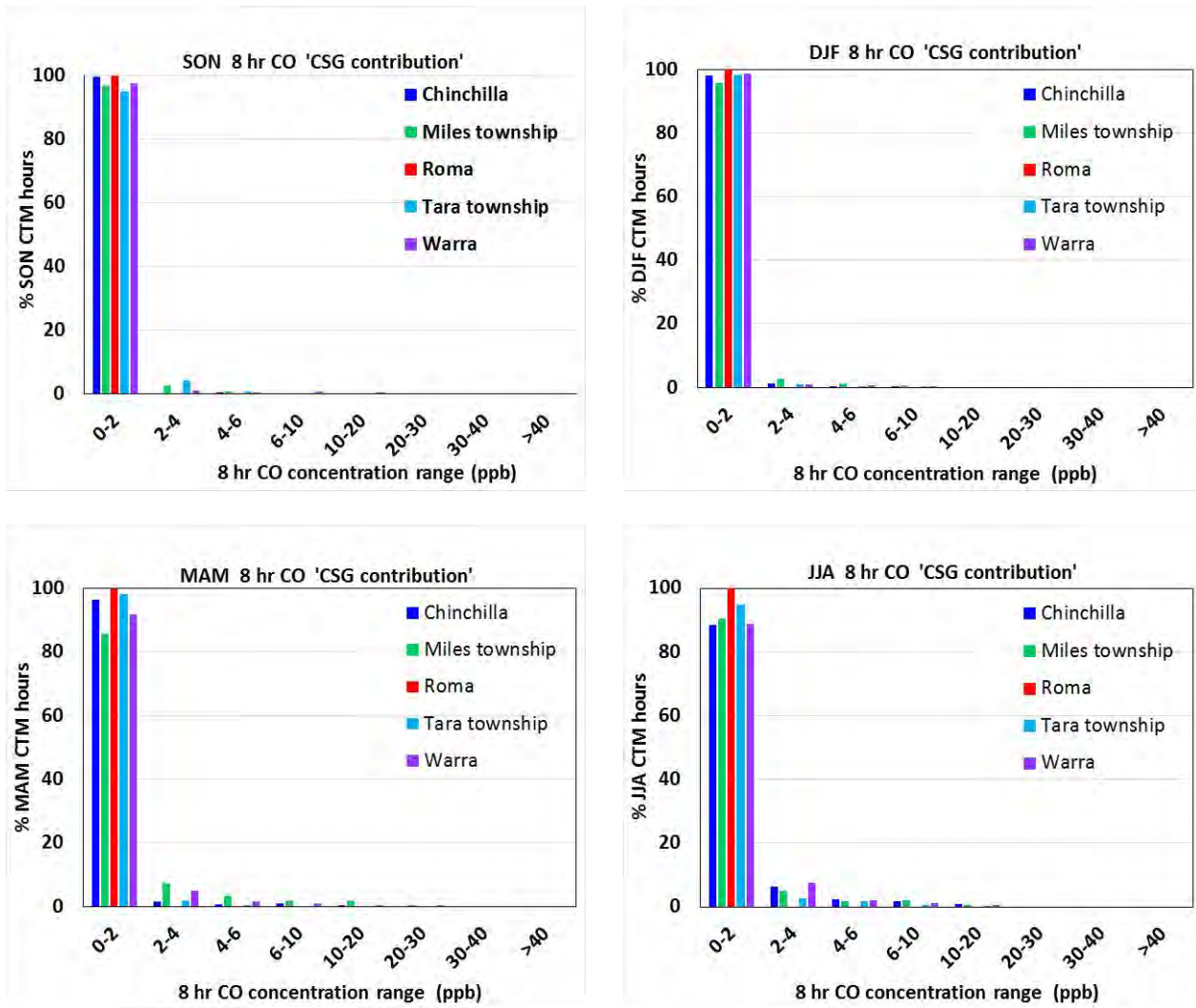


Figure 5.51 The modelled contribution from the CSG-related emissions to the 8-hour average CO concentration (ppb) at the Town sites shown as a frequency distribution for each season. The x-axis shows the concentration ranges of the contribution from the CSG-related emissions and the y-axis shows the percentage of model hours.

Figure 5.52 shows plots of the modelled 8-hour average CO concentrations with all sources against the contribution from the CSG-related emissions to the modelled 8-hour average CO concentrations at Warra, one of the Town sites. The plots are seasonal and one point is plotted for each 8-hour modelled value. Similar plots for the other Town sites are shown in Appendix E.

At Warra the largest increases (> 10 ppb) in the modelled 8-hour average CO due to the CSG-related emissions occur during SON, MAM and JJA, with the CSG-related emissions contributing up to 28 % of the CO concentration value. However, even when this occurs the maximum increase in 8-hour average CO concentration due to the CSG-related emissions is 25 ppb which is 0.3 % of the 8-hour air quality objective (9000 ppb, Table 5.1). The results for the other sites are similar with less of a contribution to 8-hour average CO concentration due to the CSG-related emissions at Roma.

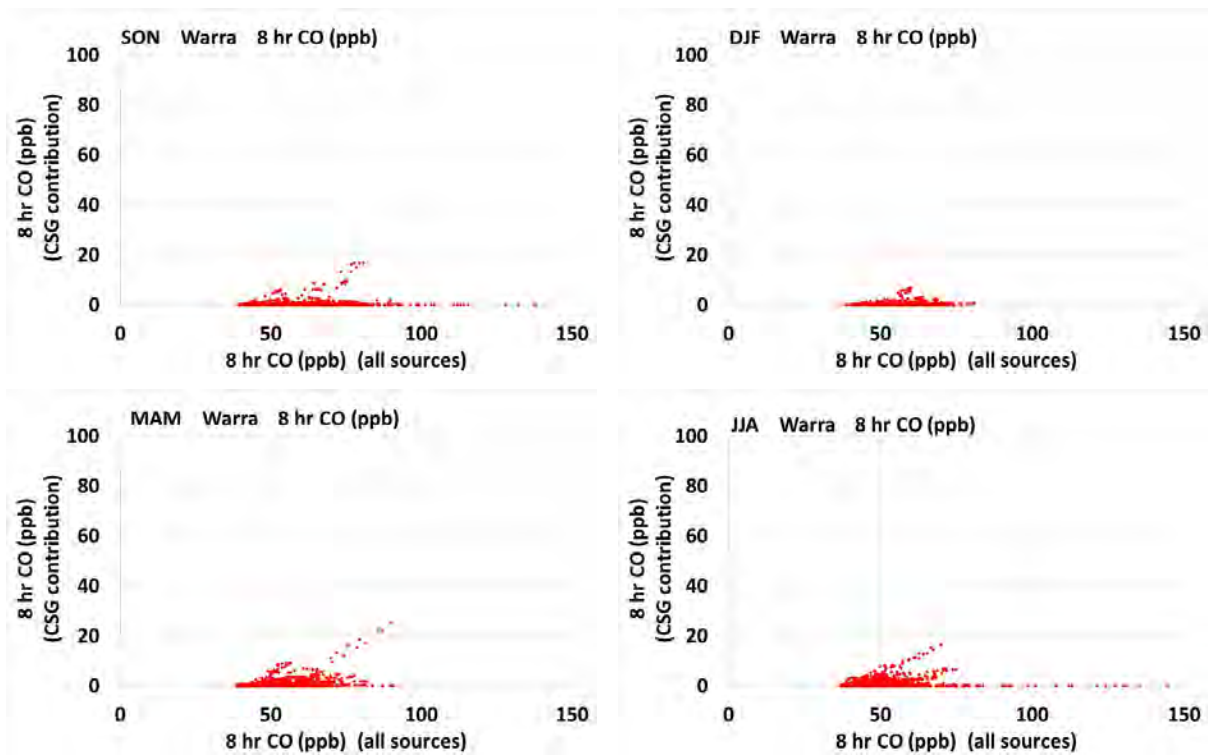


Figure 5.52 The modelled contribution from the CSG-related emissions to the 8-hour average CO concentration (ppb) at Warra shown as a scatter plot for each season. The x-axis shows the modelled 8-hour average CO concentrations with all sources (ppb) and the y-axis shows the contribution from the CSG-related emissions to the 8-hour average CO concentration (ppb).

5.4.5 Summary

The impacts of CSG activity on the 8-hour average CO concentrations modelled in the Surat Basin are summarised below:

Comparison of the model results with the observations

- The observed and modelled times series of the 1-hour average CO concentrations at Burncluith show broad agreement, although there are a number of observed peaks of CO not captured by the model. Some of these are possibly due to a smoke source from vegetation fires or a local residential chimney not present in the model emissions.

Contribution of the CSG-related emissions to the modelled 8-hour average CO concentrations

- On average 98 % of the time at the Gas field and Regional sites and 99.7 % of the time at the Town sites the contribution from the CSG-related emissions is less than 10 ppb which is 0.1 % of the air quality objective.
- The lowest frequency of change due to the CSG-related emissions is modelled at Burncluith which is furthest from major CSG sources, while the largest frequency of change due to the CSG-related emissions occurs at the Gas field sites.
- At Miles Airport and Warra the largest modelled increases (> 20 ppb) due to the CSG-related emissions occur during MAM, with the CSG-related emissions contributing up to 38

% of the value of CO. The resulting concentration is less than 0.3 % of the air quality objective.

- Over the entire model 1 km grid domain during the modelled year the maximum predicted contribution of the CSG-related emissions to the modelled 8-hour average CO concentrations is 122 ppb which is 1.4 % of the air quality objective and occurs about 1 km from CSG-related emission sources.
- Note that the model cannot resolve near-source impacts of plumes therefore impacts within a few kilometres of a point emission source may be under or overestimated.

Contribution of the CSG-related emissions to exceedances of the air quality objective or 80 % of the air quality objective

- At the Gas Field, Regional or Town sites there are no modelled exceedances of the 8-hour average CO air quality objective or 80 % of the air quality objective during any month.
- Over the entire modelled 1 km grid domain during the modelled year there are no exceedances of the 8-hour average CO air quality objective or 80 % of the 8-hour average CO air quality objective.

5.5 Air Toxics

Volatile organic compounds (VOCs) are a group of gases which are relatively short lived and participate in photochemical reactions in the atmosphere. In the study region, CSG-related emissions of VOCs include fuel and gas combustion, and some VOCs such as ethane and propane are present in small quantities in CSG and so are likely to be associated with leaking and venting of CSG (Lawson et al., 2017b). Other sources of VOCs in the study area include vegetation and soils, vegetation fires, agriculture and domestic commercial sources.

In this section model results for the VOCs formaldehyde and benzene are presented as these pollutants are listed in the Air Toxics NEPM (NEPM, 2011). Results for toluene and xylenes which are also listed in the Air Toxics NEPM are presented in Appendix D.

Benzene, along with toluene and xylenes (BTX) is emitted from many man-made sources (e.g. vehicles, industry), as well as some other sources such as wildfires. Benzene, toluene and xylene are often co-emitted from the same sources. A review of emission sources from CSG infrastructure (Lawson et al., 2017b) found that BTX is present in gas combustion emissions, including gas-fired engines and compressors, and is also emitted from motor vehicles and generators. Emissions and venting of CSG was identified as a possible further CSG-related source.

Formaldehyde is an aldehyde, which is a class of VOC. Domestic solid fuel burning and motor vehicles are listed as the main emission sources of formaldehyde Australia wide (NPI 2017). In the study area, combustion of gas in engines, compressors and flares as well as fuel burning is a source of formaldehyde. However unlike BTX, formaldehyde is also produced continuously in the atmosphere as products from photochemical reactions of VOCs (both manmade and natural), and oxidation of methane. As such there is a certain background concentration of formaldehyde present in the atmosphere even if there are no nearby direct emissions – however direct emissions will increase the concentrations above background levels.

Passive Radiello VOC sampling at 10 sites in the monitoring study (Lawson et al., 2018a) provided 2-weekly concentrations of benzene and formaldehyde for comparison with the modelling results (along with a range of other VOCs). The measurement detection frequency of benzene and other VOCs was low at the Gas field sites (Miles Airport, Hopeland and Condamine) (~30 %) whereas benzene was detected in almost all samples at the Chinchilla township site. Therefore in this Section model output for Chinchilla rather than Miles Airport is shown and compared to Chinchilla observations. A comparison for toluene and xylenes is presented in Appendix D. The observations coincide with the model runs from September 2015 until January 2016 and are in the form of two-weekly averages. Observations of TVOC during the modelled period are only available at the Hopeland site for several months, and concentrations are < 1 ppmC (or 1000ppbC) (the lowest reportable concentration) (Lawson et al., 2018a). The modelled TVOC concentrations with all sources are shown in Appendix D. There are no state or federal air quality objectives for TVOCs.

5.5.1 Modelled effect of the CSG-related emissions at the observation sites

Time series plots of the observed and modelled concentrations of formaldehyde and benzene at Chinchilla are shown in Figure 5.53 and Figure 5.55, respectively. The observed values are shown

by the straight sections of the blue line in the figures, based on 2-week sampling periods. The model results are 1-hour average concentrations shown in red for all sources and in purple for the model results without the CSG sources. The time series are presented for different seasons. For comparison purposes and completeness time series at Miles Airport, Condamine, Hopeland, Tara Region and Burncluith are shown in Appendix D. In the time series figure it is not always possible to see the two modelled time series, the red (all sources) concentration series is plotted first and then the purple (no CSG sources) series is plotted. Where the values of each series are the same only the last plotted series will be seen, which is the purple one (no CSG sources). Therefore, when red is seen on the plot it is because the two modelled series have different values at that point in time and the difference between the two values is the contribution to the concentration from the CSG-related emissions; this contribution is shown in Figure 5.54 for formaldehyde and in Figure 5.56 for benzene (those at Tara Region and the Gas field sites are shown in Appendix D).

Comparison of the observations with the modelled output (Figure 5.53 and Figure 5.55) (note different averaging periods and monitoring for only 5 of the 12 months) shows reasonable agreement for both species although the model at times tends to overestimate formaldehyde concentrations by a small amount (1-2 ppb) and underestimate benzene concentrations by a smaller amount (up to 0.1 ppb). This is also true at the Gas field and Regional sites (see Appendix D).

The time series for the modelled 1-hour average formaldehyde concentrations with all sources shows a range of contributions due to the CSG-related emissions at Chinchilla and the Gas field and Regional sites, although the formaldehyde concentration values are relatively small (see Figure 5.53, Figure 5.54 and Appendix D). Mostly contributions due to the CSG-related emissions can be seen as an increased height of some peaks, less so at Burncluith.

The time series for the modelled 1-hour average benzene concentrations with all sources at Chinchilla (Figure 5.55) show almost no contribution due to the CSG-related emissions (Figure 5.56). At the Gas field and Regional sites there are small contributions due to the CSG-related emissions (Figure 5.55Appendix D).

Larger modelled peaks in 1-hour average formaldehyde and benzene concentrations can be seen at various sites coinciding with previously identified model fires around 16/9/15, 7/10/15 and 9-11/8/16 (the modelled fires are discussed in Section 5.1.1)

Results for toluene and xylenes are presented in Appendix D and are similar to those for benzene.

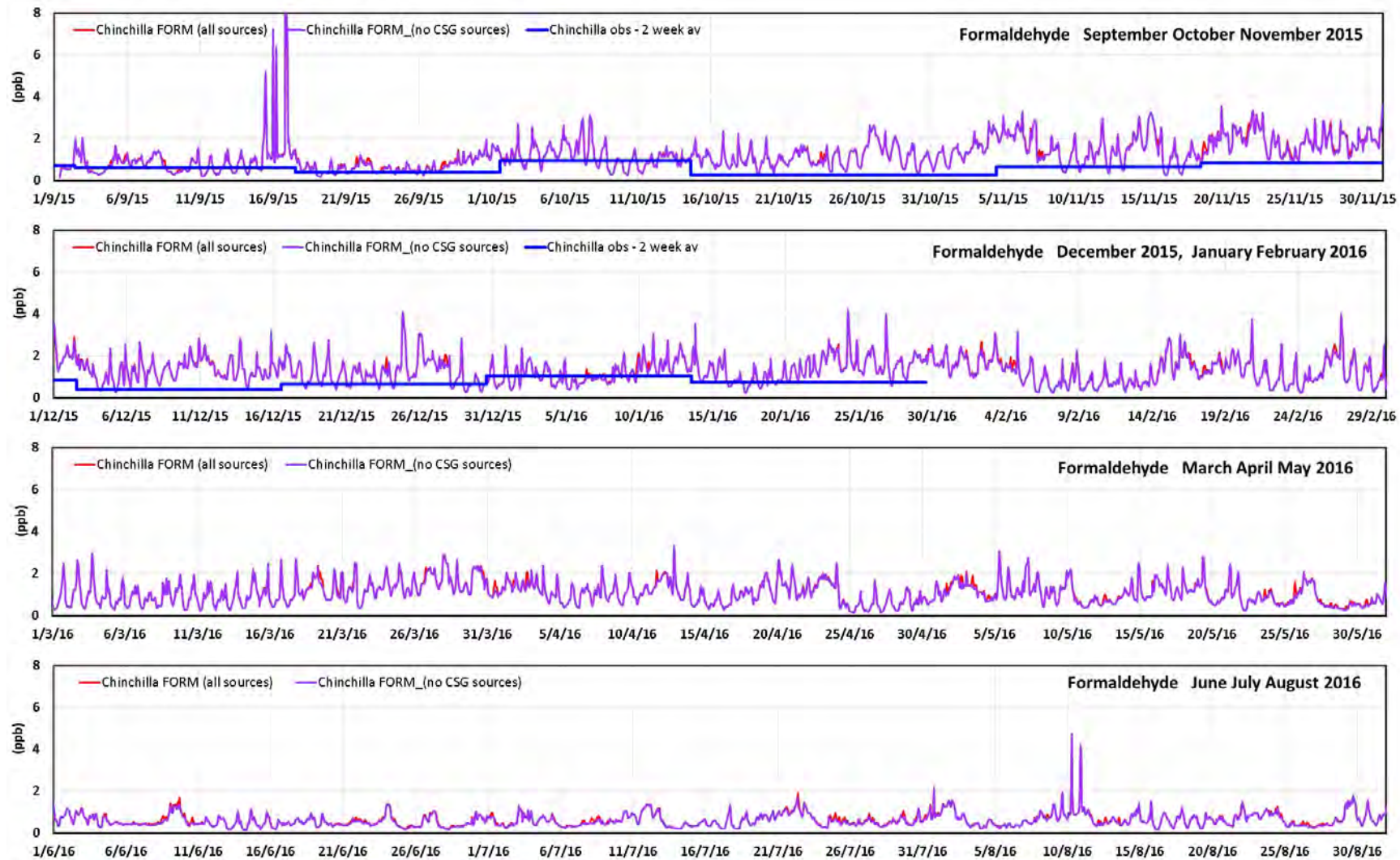


Figure 5.53 The observed (2-week sampling period) and modelled (1-hour average) time series of the formaldehyde concentrations (ppb) at Chinchilla for the modelled year (red = model results with all sources, purple = model results without CSG sources, blue = observations). (peak off scale: model, 16/9/15 21:00 = 15.3 ppb)

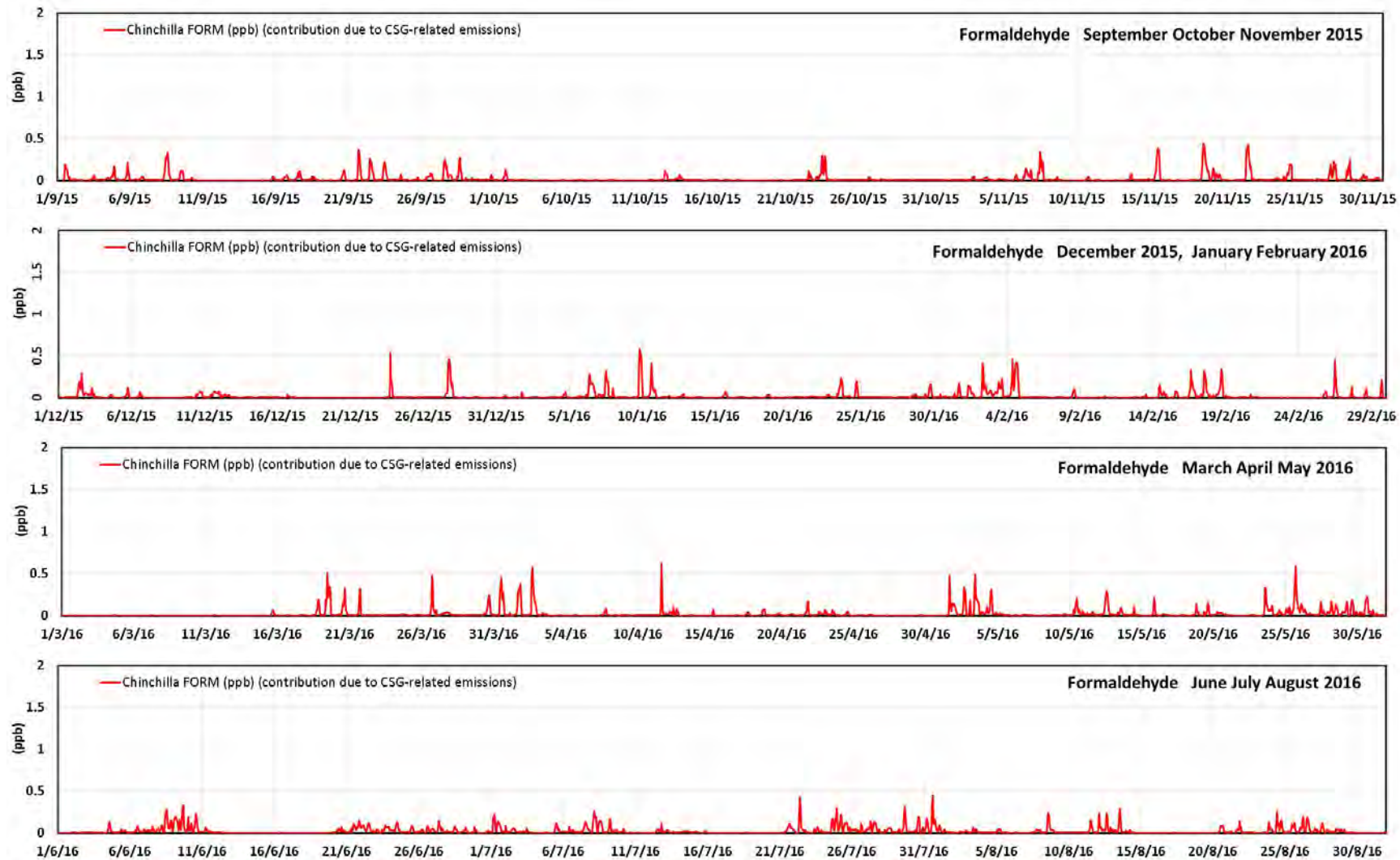


Figure 5.54 The modelled contributions from the CSG-related emissions to the 1-hour average formaldehyde concentrations (ppb) at Chinchilla for the modelled year.

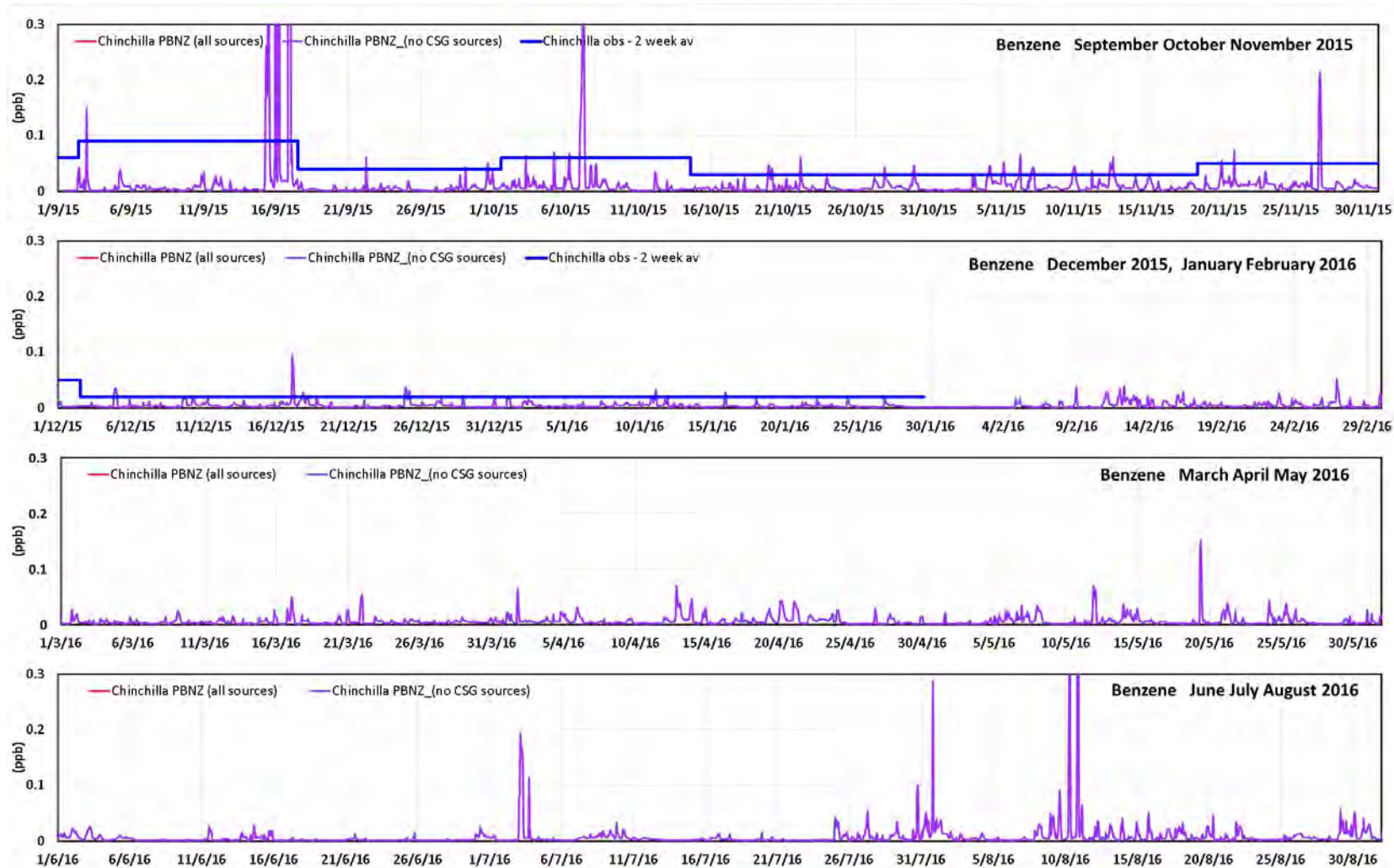


Figure 5.55 The observed (2-week sampling period) and modelled (1-hour average) time series of benzene concentrations (ppb) at Chinchilla for the modelled year (red = model results with all sources, purple = model results without CSG sources, blue = observations). (peaks off scale: model, 15/9/15 12:00 = 0.5 ppb, 16/9/15 00:00, 05:00, 21:00 = 1.2, 1.2, 3.0 ppb, 7/10/15 06:00 = 0.4 ppb, 10/8/16 07:00, 21:00 = 0.82, 0.60 ppb).

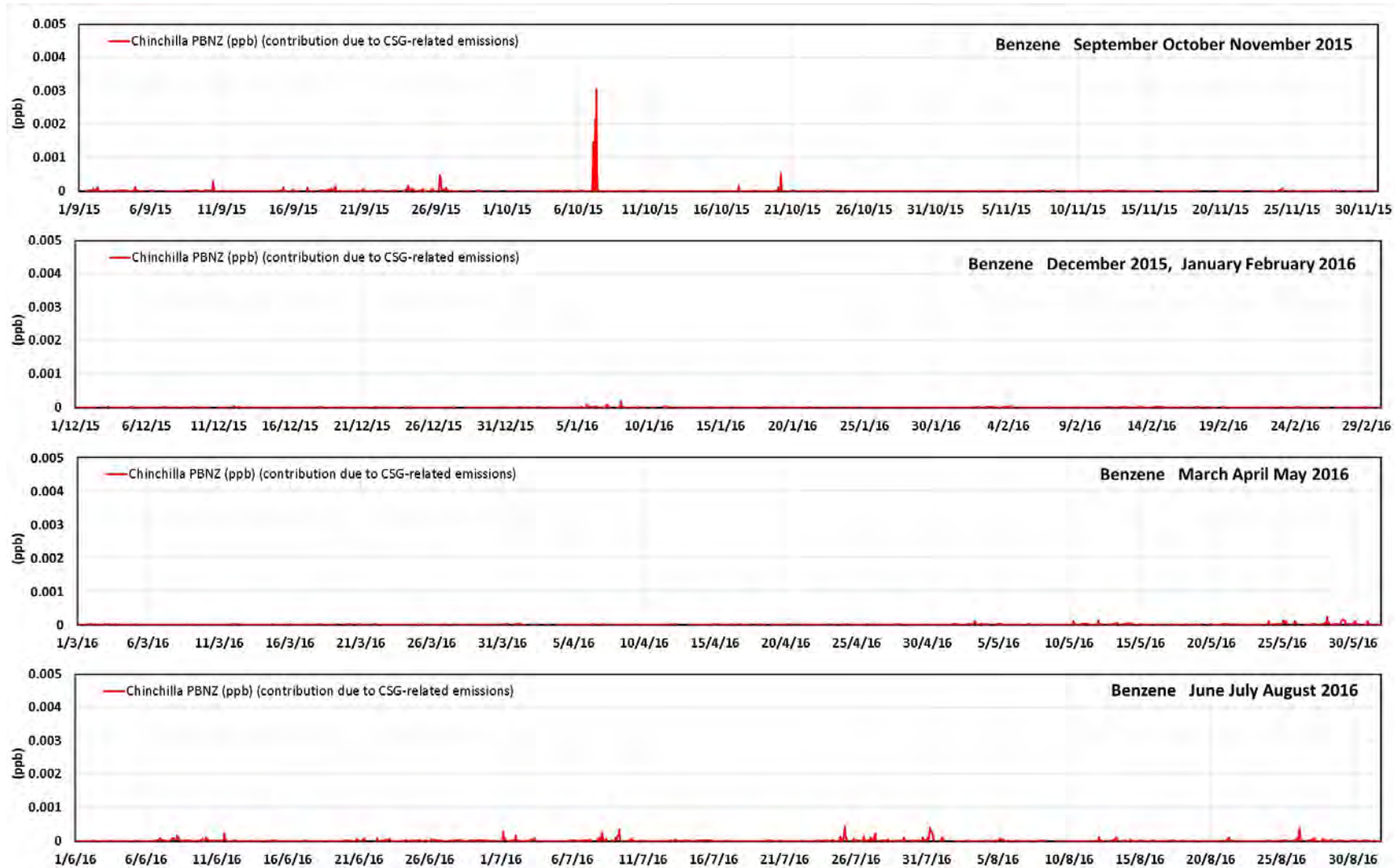


Figure 5.56 The modelled contributions from the CSG-related emissions to the 1-hour average benzene concentrations (ppb) at Chinchilla for the modelled year.

The modelled contribution from the CSG-related emissions to the 24-hour average formaldehyde concentrations at each of the observation sites is presented in Figure 5.57. Each plot shows the percentage of model hours within each season for the modelled contribution from the CSG-related emissions to the 24-hour average formaldehyde concentrations.

On average 99 % of the time the contribution from the CSG-related emissions at all sites is less than 0.2 ppb, which is 0.5 % of the 24-hour air quality objective for formaldehyde (40 ppb, Table 5.1). The smallest frequency of change is seen at Burncluith, while the largest frequency of change occurs at Condamine during SON, DJF and MAM.

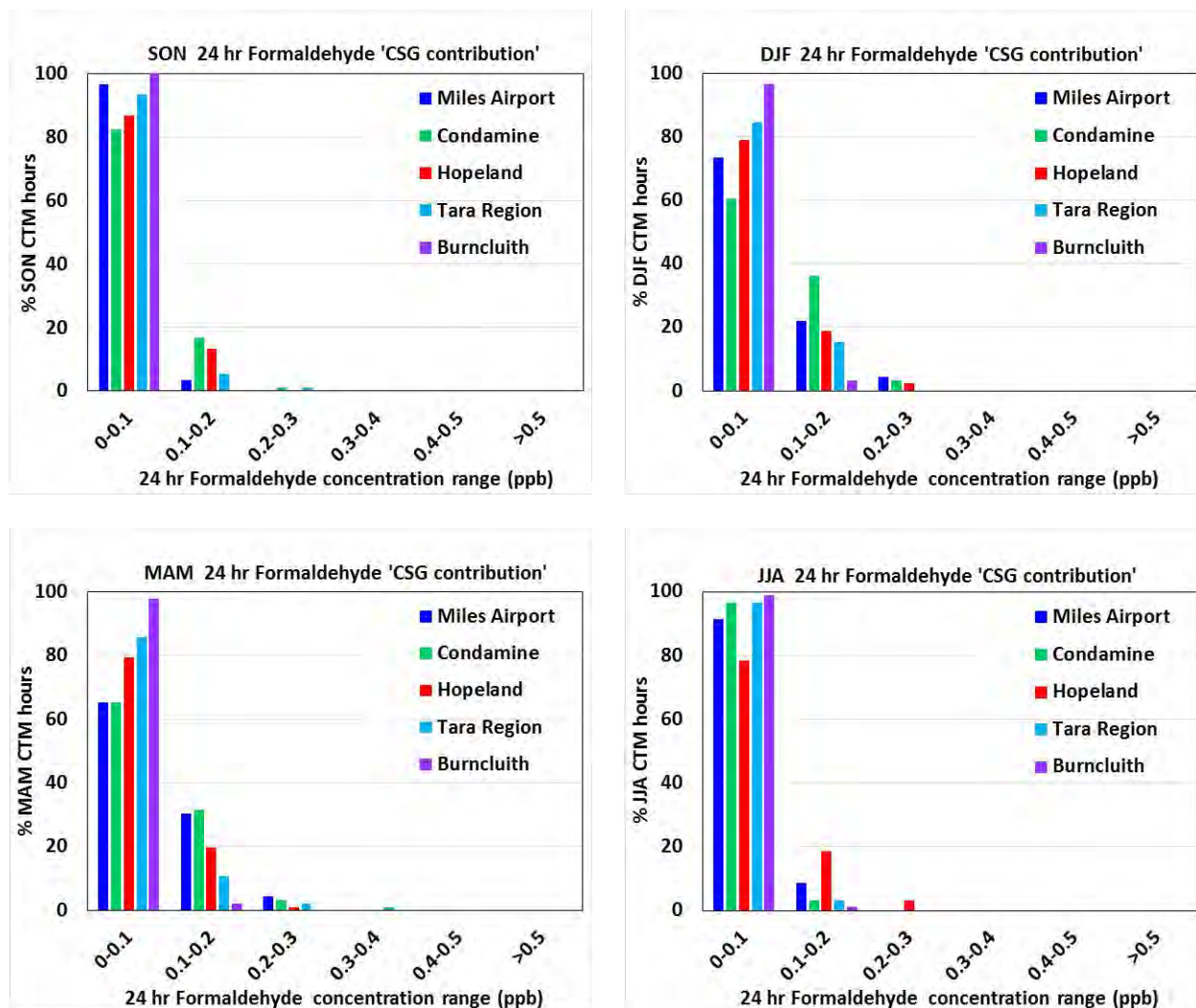


Figure 5.57 The modelled contribution from the CSG-related emissions to the 24-hour average formaldehyde concentration (ppb) at the Gas field and Regional sites shown as a frequency distribution for each season. The x-axis shows the concentration ranges of the contribution from the CSG-related emissions and the y-axis shows the percentage of model hours.

The modelled contribution from the CSG-related emissions to the 24-hour average benzene concentrations at each of the observation sites is presented in Figure 5.58. Each plot shows the

percentage of model hours within each season for the modelled contribution from the CSG-related emissions to the 24-hour average benzene concentrations.

The contribution to 24-hour average benzene concentrations from the CSG-related emissions at all sites is less than 0.01 ppb 100 % of the time. There is no 24-hour air quality objective for benzene but to put this concentration in context, benzene concentration measured in terrestrially influenced air at Cape Grim, a rural site in north-west Tasmania is 0.01 ppb (approximately a 2-week average) and the measured benzene concentration at a rural town in Victoria is 0.07 ppb (the average is based on weekly integrated measurements - for a summary of benzene measurements see Lawson et al., 2018a). The annual average air quality objective for benzene is 3 ppb (Table 5.1). As such, changes in the 24-hour average benzene concentration due to the CSG-related emissions are well below air quality objectives.

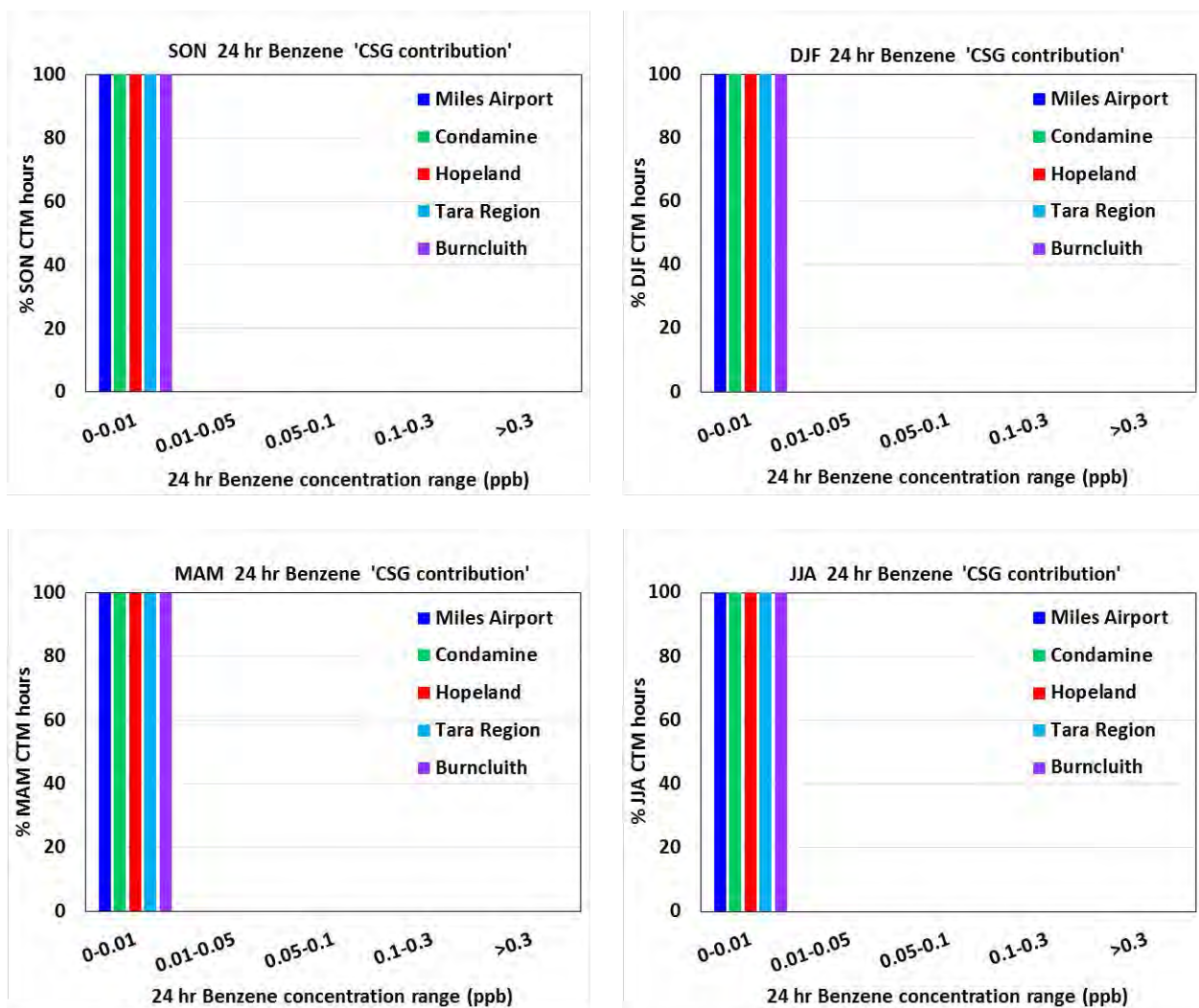


Figure 5.58 The modelled contribution from the CSG-related emissions to the 24-hour average benzene concentration (ppb) at the Gas field and Regional sites shown as a frequency distribution for each season. The x-axis shows the concentration ranges of the contribution from the CSG-related emissions and the y-axis shows the percentage of model hours.

Figure 5.59 shows plots of the modelled 24-hour average formaldehyde concentrations with all sources against the contribution from the CSG-related emissions to the modelled 24-hour average formaldehyde concentrations at Miles Airport. Those for Condamine, Hopeland, Tara Region and Burncluith are shown in Appendix E and Chinchilla is shown in Section 5.5.3. The plots are seasonal and one point is plotted for each modelled day.

At Miles Airport the largest modelled increases (> 0.2 ppb) in the 24-hour average formaldehyde concentrations due to the CSG-related emissions occur during DJF and MAM, with the CSG-related emissions contributing up to 15 % of the total formaldehyde concentration. When this occurs the maximum increase in 24-hour average formaldehyde concentration due to the CSG-related emissions is 0.27 ppb which is 0.7 % of the 24-hour air quality objective (40 ppb, Table 5.1). The largest contribution due to the CSG-related emissions occurs at Tara Region and is 0.3 ppb which is 0.75 % of the air quality objective. The results for the Gas field sites are similar with the CSG-related emissions contributing up to 29 % for the largest modelled increases. Burncluith has a smaller contribution to the 24-hour average formaldehyde concentration, reflecting the greater distance from major CSG-related sources. At all sites the modelled 24-hour average formaldehyde concentrations are smallest during JJA.

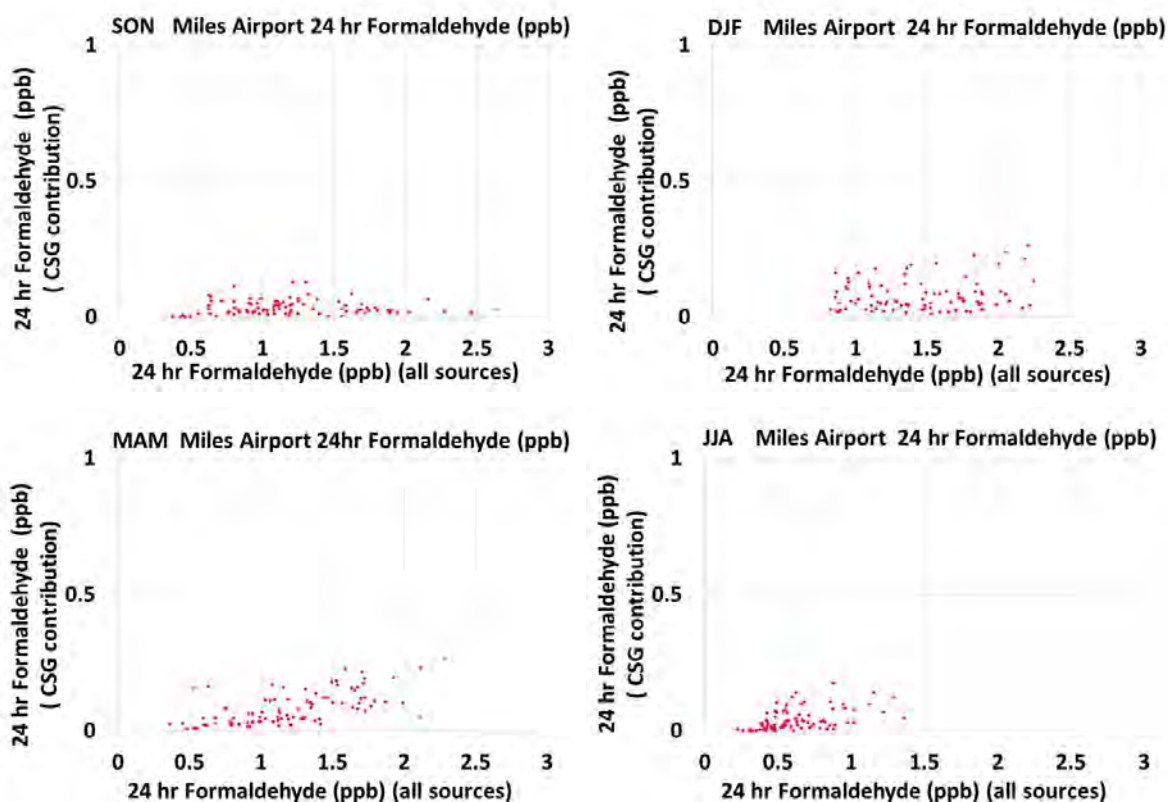


Figure 5.59 The modelled contribution from the CSG related emissions to the 24-hour average formaldehyde concentration (ppb) at Miles Airport shown as a scatter plot for each season. The x-axis shows the modelled 24-hour average formaldehyde concentrations with all sources (ppb) and the y-axis shows the contribution from the CSG-related emissions to the 24-hour average formaldehyde concentration (ppb).

Figure 5.60 shows plots of the modelled 24-hour average benzene concentrations with all sources against the contribution from the CSG-related emissions to the modelled 24-hour average benzene concentrations at Miles Airport. Those for Condamine, Hopeland, Tara Region and Burncluith are shown in Appendix E and Chinchilla is shown in Section 5.5.3. The plots are seasonal and one point is plotted for each modelled day.

At Miles Airport and the other Gas field sites and the Regional sites there is almost no change in the modelled 24-hour average benzene due to the CSG-related emissions, as can also be seen in Figure 5.58.

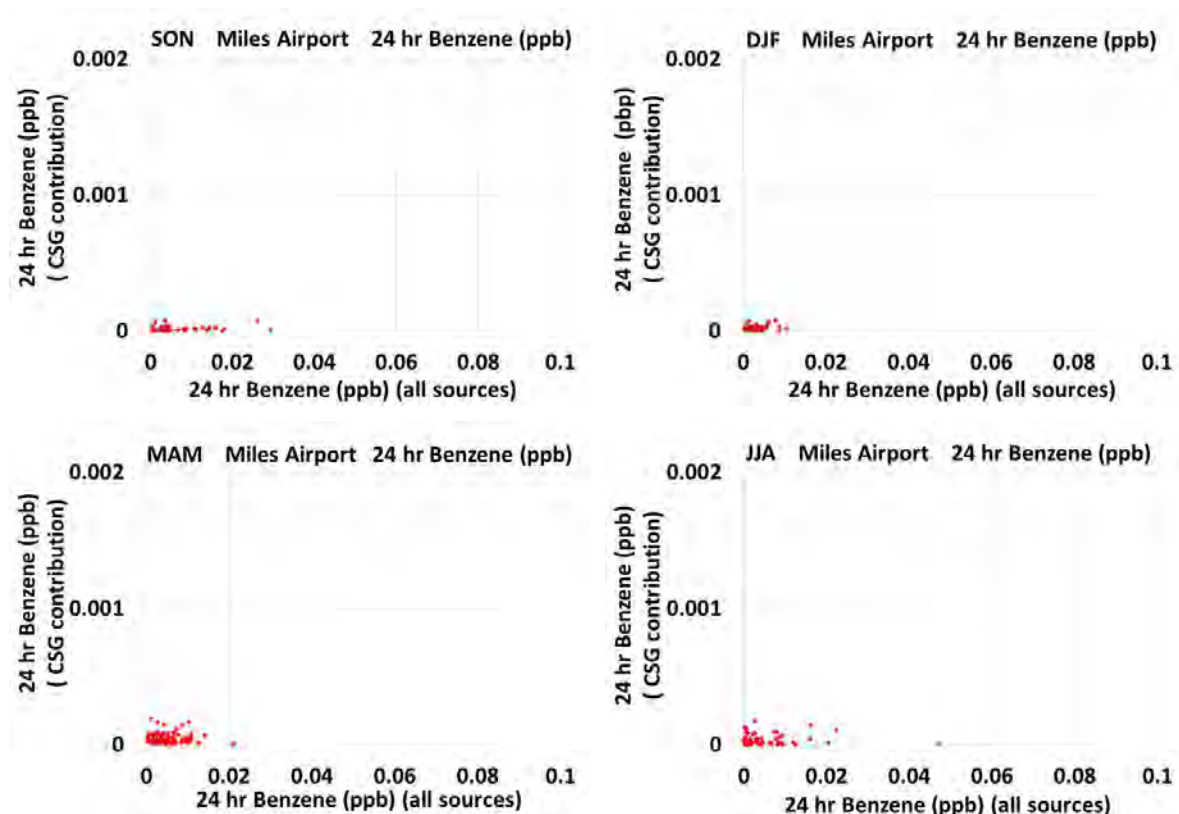


Figure 5.60 The modelled contribution from the CSG related emissions to the 24-hour average benzene concentration (ppb) at Miles Airport shown as a scatter plot for each season. The x-axis shows the modelled 24-hour average benzene concentrations with all sources (ppb) and the y-axis shows the contribution from the CSG-related emissions to the 24-hour average benzene concentration (ppb).

5.5.2 Comparison with Air Quality Objectives at Observation Sites

In this section the model results are compared to air quality objectives to assess whether there are any modelled exceedances of formaldehyde or benzene at the Gas field or Regional sites. The air quality objectives used to assess the pollutant concentrations are presented in Table 5.1.

Table 5.9 presents the observed annual average concentrations of formaldehyde and benzene. The formaldehyde observations are from 22-23/7/15 to 27-29/1/16 except at Hopeland where observations began on 24/6/15. The formaldehyde averages are therefore 6-monthly except at

Hopeland where they are seven monthly. The benzene observations are annual from 20-22/1/15 to 27-29/1/16. Table 5.9 also presents the annual average concentrations of modelled formaldehyde and benzene with all sources and without the CSG-related sources included. The averages are for Chinchilla and the Gas field and Regional sites.

The annual average air quality objectives (8.9 ppb for formaldehyde and 3 ppb for benzene, Table 5.1) are not exceeded by the observed or modelled annual average formaldehyde or benzene concentrations. In addition, the modelled annual average formaldehyde concentrations with all sources and without the CSG sources are similar, model runs with the CSG sources included have annual average concentrations between 0.02 and 0.06 ppb higher than the model runs without the CSG sources.

For benzene the modelled annual average concentrations with all sources included and without CSG sources are essentially the same – the maximum contribution due to the CSG-related emissions is 0.00002 ppb at Miles Airport.

The modelled annual average formaldehyde values are slightly higher than observed, while those for benzene are slightly lower than observed. Note however that the time periods for the observations and model results are different, the modelled average values are from 1/9/15 - 31/8/16 and the observed annual average values are for different time periods as listed above.

Table 5.9 The annual average modelled concentrations of formaldehyde and benzene (ppb). The six-month-average observations of formaldehyde except at Hopeland where they are 7-month average observations. The annual average observations of benzene (ppb) from 20-22/1/15 to 27-29/1/16 (see Lawson et al., 2018a for discussion of observations).

Annual average (ppb)	Observed Formaldehyde	Modelled Formaldehyde (all sources)	Modelled Formaldehyde (without CSG sources)	Observed Benzene	Modelled Benzene (all sources)	Modelled Benzene (without CSG sources)
Miles Airport	0.747	1.116	1.058	0.025	0.006	0.006
Condamine	0.694	1.129	1.067	0.023	0.007	0.007
Hopeland	0.606	1.078	1.026	0.023	0.008	0.008
Tara Region	0.814	1.082	1.039	0.023	0.006	0.006
Burncluith	0.516	1.103	1.087	0.026	0.010	0.010
Chinchilla	0.652	1.058	1.038	0.062	0.008	0.008

Figure 5.61 shows the maximum 24-hour average formaldehyde concentrations for each month of the model simulation, at each observation site, while Figure 5.62 shows those for 24-hour average benzene concentrations. The bar plots show the model results with all sources in red and the model results without CSG sources in purple. The dashed horizontal red line shows the value of

the air quality objective for formaldehyde. Observations are not included as they are two-weekly averaged values.

The 24-hour average formaldehyde air quality objective (40 ppb Table 5.1) and 80 % of the 24-hour average formaldehyde air quality objective (32 ppb Table 5.1) are not exceeded by the modelled 24-hour average formaldehyde concentrations at any site in any month.

At all sites the maximum modelled 24-hour average formaldehyde concentrations with all sources and without the CSG sources are small and similar, the largest contribution due to the CSG-related emissions occurs at Tara Region and is 0.3 ppb which is 0.75 % of the air quality objective.

Somewhat elevated values are modelled in September 2015 at Burncluith as a result of a modelled fire.

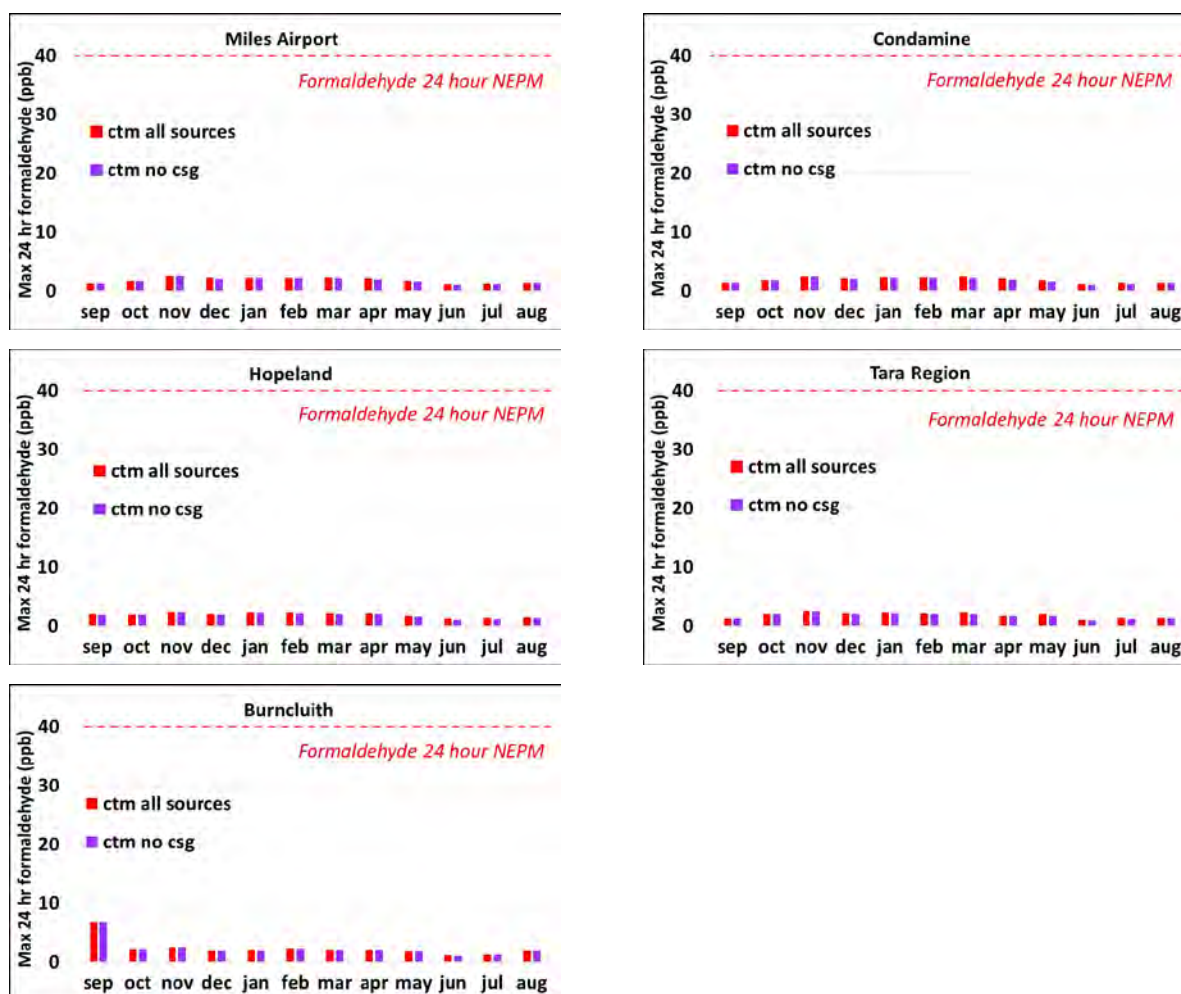


Figure 5.61 The maximum 24-hour average formaldehyde concentrations (ppb) for each month of September 2015 – August 2016 at the Gas field and Regional sites: model results with all sources (red) and model results without the CSG sources (purple).

There is no 24-hour air quality objective for benzene but Figure 5.62 shows the maximum values are small, generally well below 10 % of the annual average objective. At all sites the maximum modelled 24-hour average benzene concentrations with all sources and without CSG sources are

similar, the largest contribution due to the CSG-related emissions is 0.0005 ppb at Hopeland. Somewhat elevated values are modelled in September 2015 at Condamine, Hopeland and Burncluith as a result of a modelled fire.

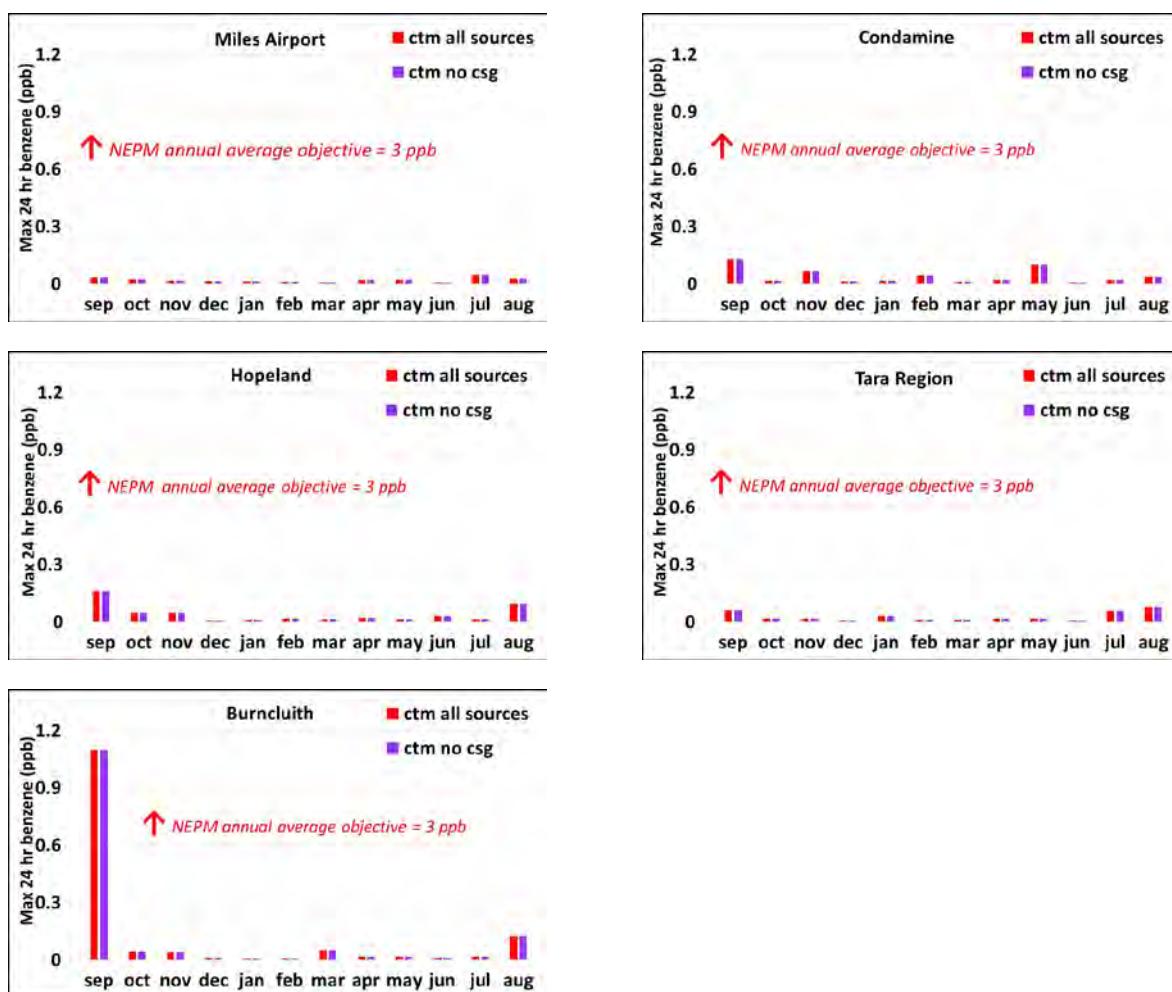


Figure 5.62 The maximum 24-hour average benzene concentrations (ppb) for each month of September 2015 – August 2016 at the Gas field and Regional sites: model results with all sources (red) and model results without the CSG sources (purple).

5.5.3 Comparison with Air Quality Objectives for the Region

Figure 5.63 shows spatial plots over the model 1 km grid domain of the modelled maximum 24-hour average formaldehyde concentrations with all sources included for each season and Figure 5.65 is the equivalent figure for the modelled maximum 24-hour average benzene concentrations. Note that each grid square shows the maximum concentration modelled for that grid square *for that entire season*. As such the maximum concentration shown in each grid square may be from different days during the season.

The 24-hour average formaldehyde air quality objective of 40 ppb (Table 5.1) and 80 % of the 24-hour average formaldehyde air quality objective of 32 ppb are not exceeded anywhere in the

modelled domain during any season. The maximum grid values are 17.3 ppb for SON, 7.4 ppb for DJF (indicated by the red arrow), 18.8 ppb for MAM and 14.7 ppb for JJA for both the model with all sources and the model without the CSG sources.

There is no 24-hour air quality objective for benzene but the maximum grid values (Figure 5.65) are 3.35 ppb for SON, 1.12 ppb for DJF (indicated by the red arrow), 3.87 ppb for MAM and 2.9 ppb for JJA for both the model with all sources and the model without the CSG sources. The largest values of the 24-hour average formaldehyde and benzene in the model domain are a result of modelled fires (compare the areas of the higher concentrations in Figure 5.63 and Figure 5.65 with the higher concentrations of the unique smoke tracer levoglucosan in Figure 5.9).

Figure 5.64 shows the contribution, in each grid square for each season, of the CSG-related emissions to the modelled maximum 24-hour average formaldehyde concentrations shown in Figure 5.63. Note, this is calculated for each grid square by subtracting the maximum 24-hour average formaldehyde concentration for the season in the run without CSG sources from the maximum 24-hour average formaldehyde concentration for the same season in the run with all sources. Importantly, in each grid square the two maximum values that are subtracted may each be from a different day during the season. Figure 5.66 shows the equivalent figure for the modelled maximum 24-hour average benzene concentrations.

The contributions due to the CSG-related emissions to the maximum 24-hour average formaldehyde are small over the region and do not exceed 0.7 ppb which is 1.8 % of the 24-hour air quality objective (40 ppb, Table 5.1) (maximum value is 0.64 ppb for MAM - indicated by the red arrow).

The contributions due to the CSG-related emissions to the maximum 24-hour average benzene are very small over the region and do not exceed 0.011 ppb (maximum value is 0.011 ppb for SON - indicated by the red arrow).

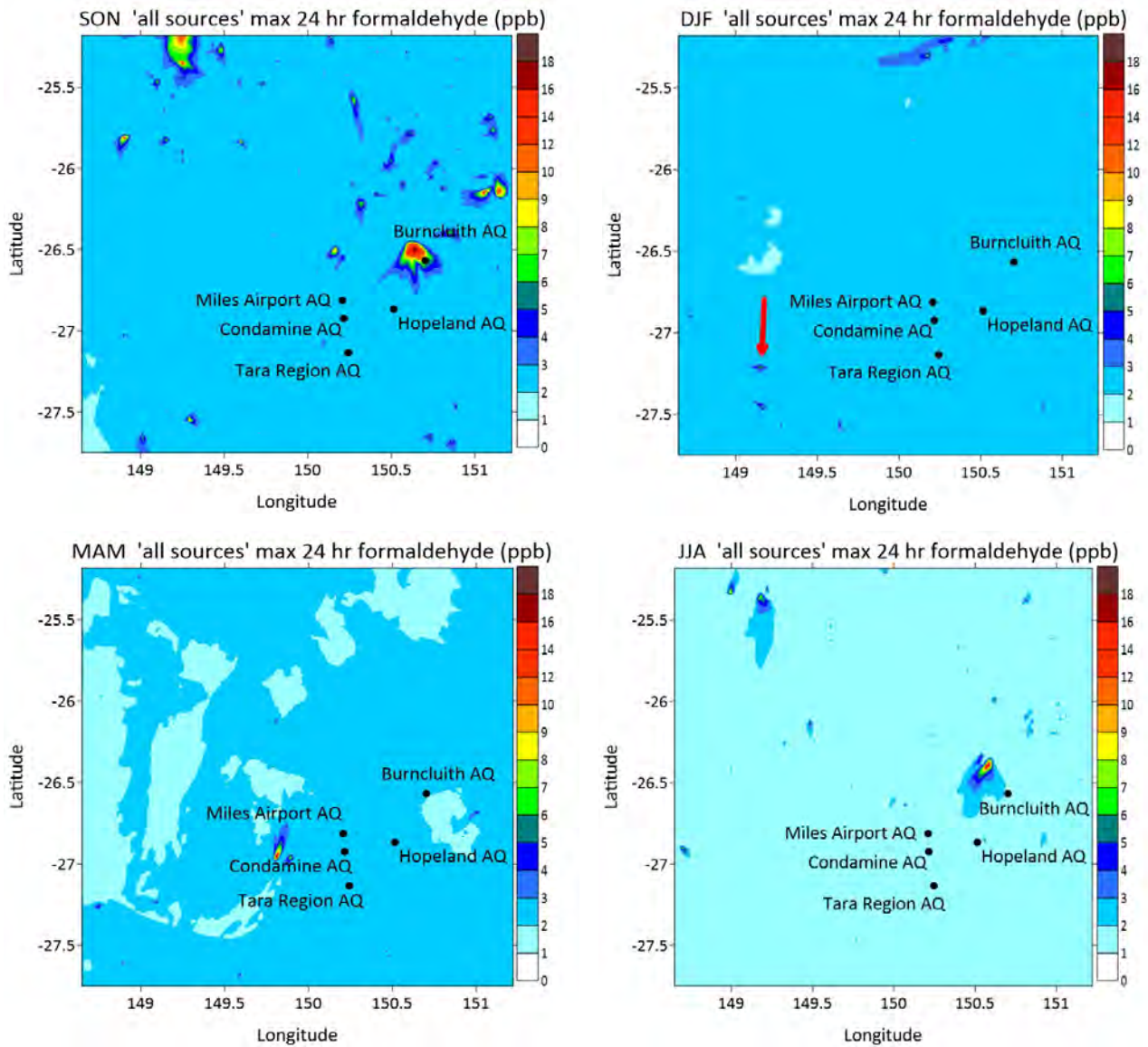


Figure 5.63 The maximum concentration of the 24-hour average formaldehyde in each grid square for the model results with all sources during each season (ppb). Note that the maximum concentrations shown in each grid square may be from different days during the season. The red arrow indicates the location of the maximum value for the season.

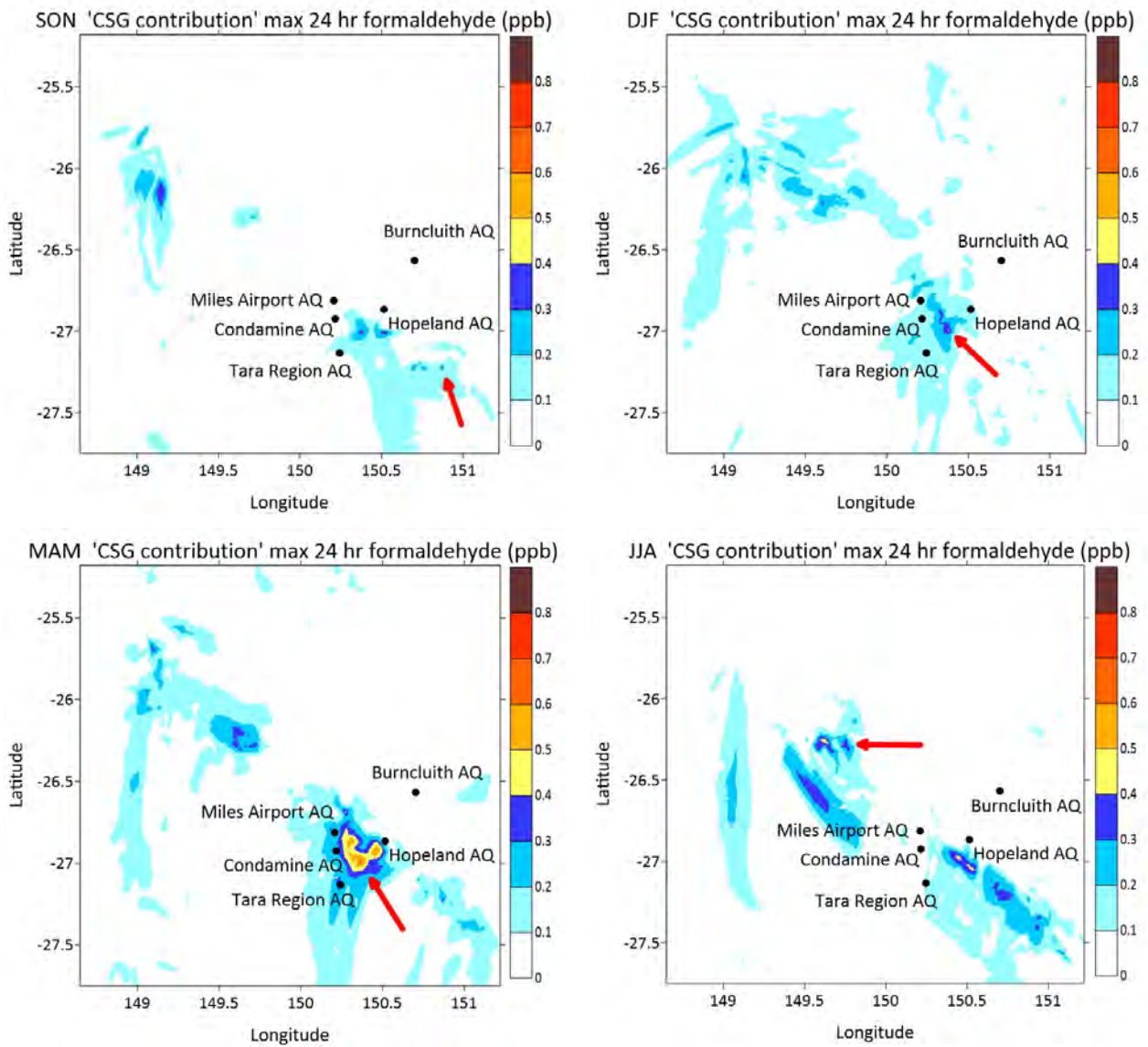


Figure 5.64 The contribution of the CSG-related emissions to the modelled maximum 24-hour average formaldehyde concentration (maximum in each grid square from Figure 5.63) during each season (ppb). Note that the concentrations shown in each grid square may be from different days during the season. The red arrow indicates the location of the maximum value for the season.

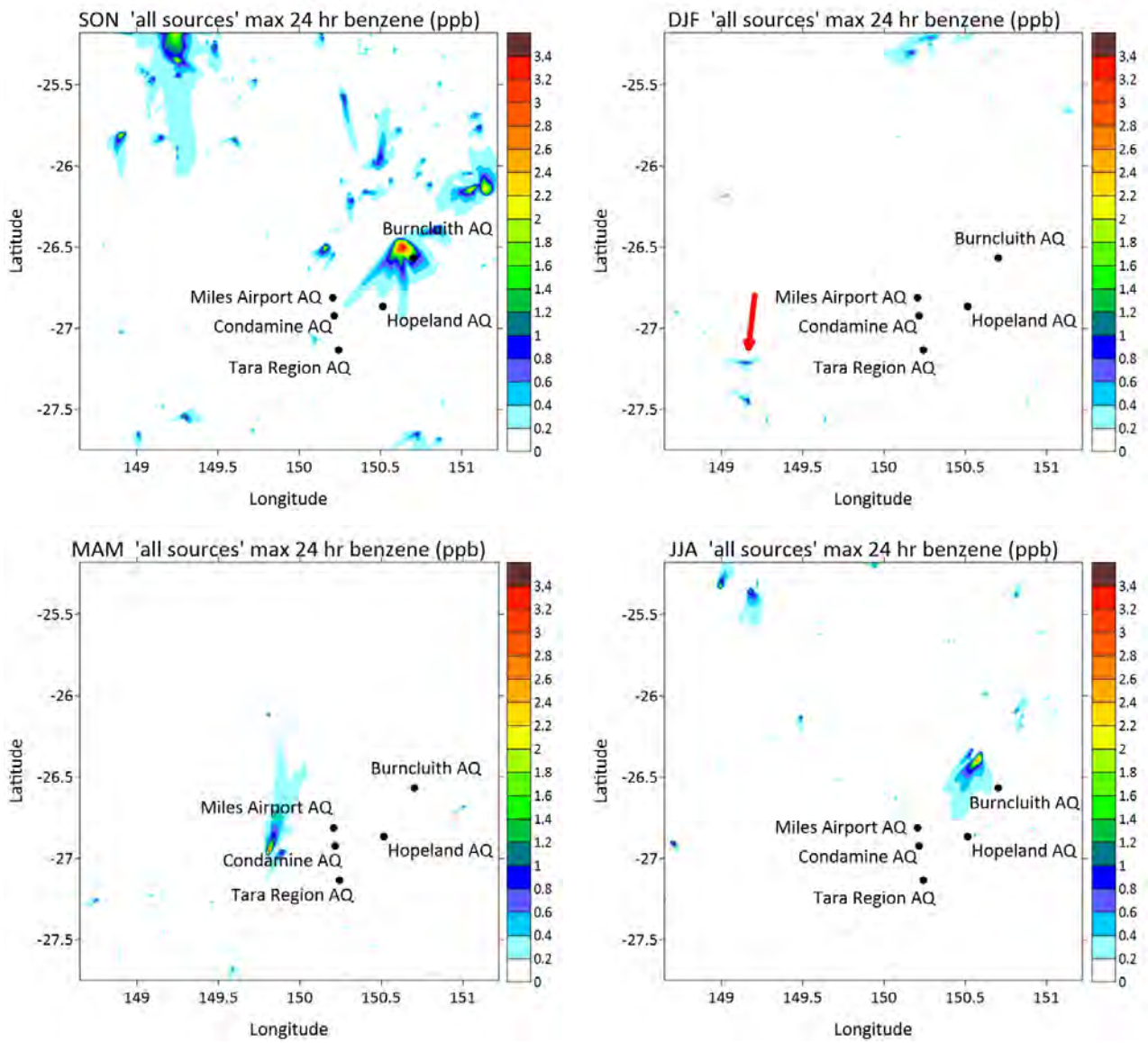


Figure 5.65 The maximum concentration of the 24-hour average benzene in each grid square in the model results with all sources during each season (ppb). Note that the maximum concentrations shown in each grid square may be from different days during the season. The red arrow indicates the location of the maximum value for the season.

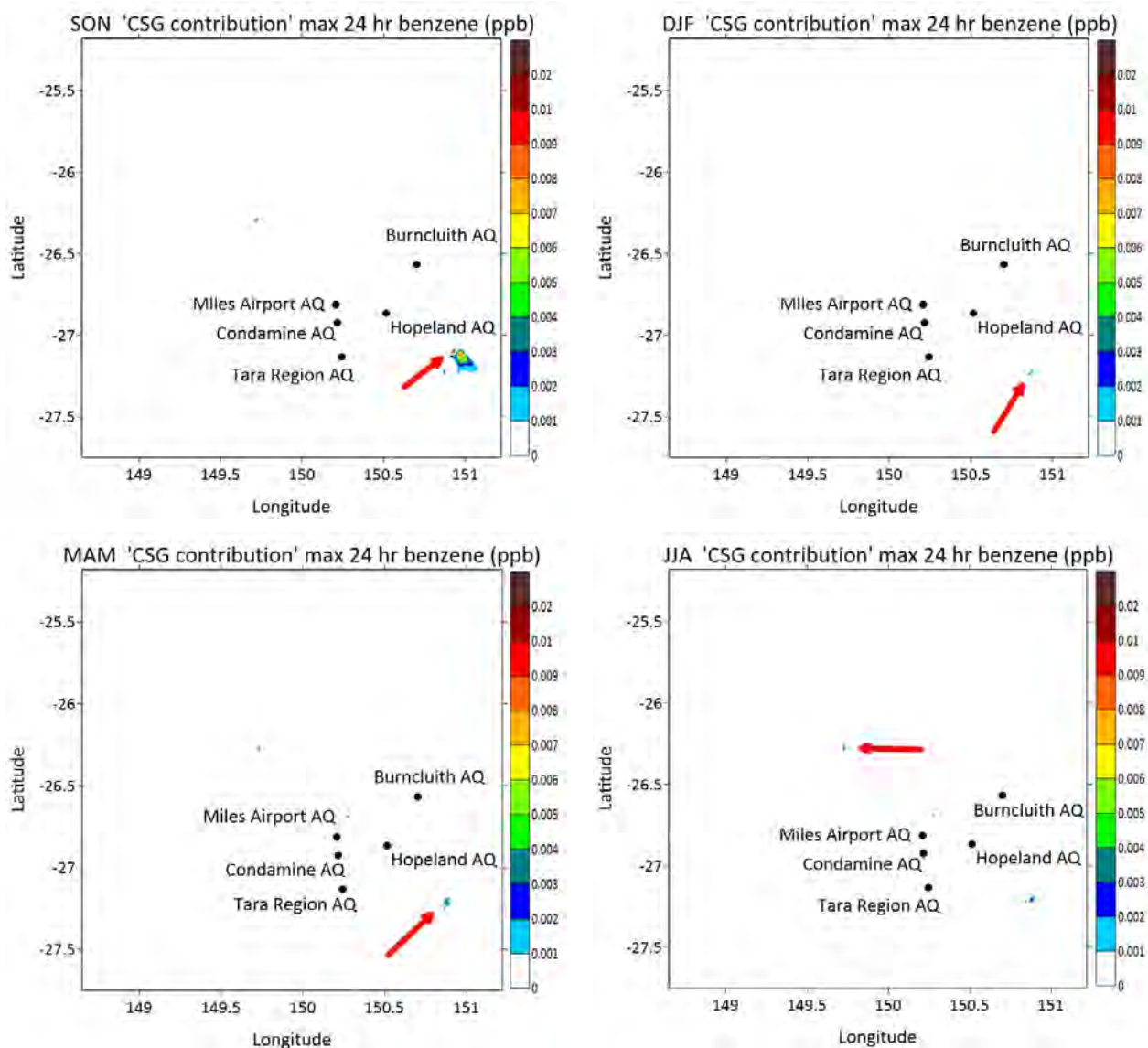


Figure 5.66 The contribution of the CSG-related emissions to the modelled maximum 24-hour average benzene concentration (maximum in each grid square from Figure 5.65) during each season (ppb). Note that the concentrations shown in each grid square may be from different days during the season. The red arrow indicates the location of the maximum value for the season.

Figure 5.67 shows the maximum contribution of the CSG-related emissions to the 24-hour average modelled formaldehyde concentrations in each grid square for the modelled year. Note, this is calculated in each grid square by subtracting, every day, the 24-hour average formaldehyde concentration for the run without CSG sources from that for the run with all sources and then calculating the maximum value for the year from the daily values. Importantly, in each grid square the two values that are subtracted are from the same day in the season. Note this figure is showing the maximum contribution to the formaldehyde concentration values whilst Figure 5.66 shows the contribution to the maximum formaldehyde concentration values.

Generally the maximum contributions are less than 0.2 ppb with larger values close to CSG sources. The largest maximum contribution is 0.7 ppb (indicated by the red arrow) which is 1.8 % of the air quality objective (40 ppb, Table 5.1) and occurs about 1 km from CSG-related emission

sources. Note that the model cannot resolve near-source impacts of plumes therefore impacts within a few kilometres of a point emission source may be under or overestimated.

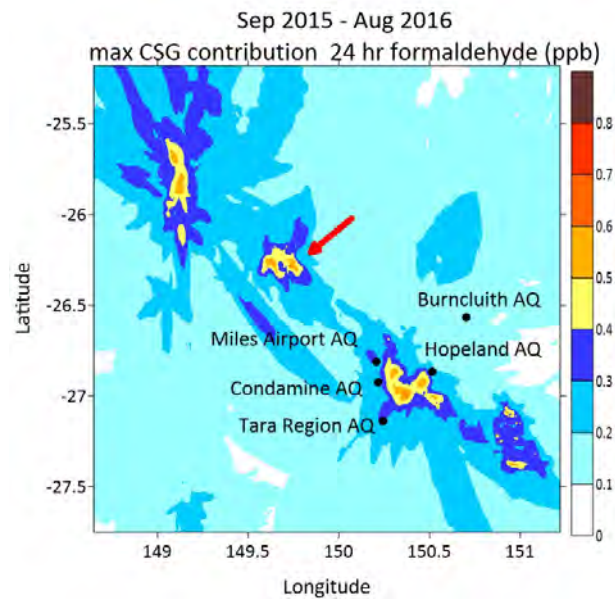


Figure 5.67 The maximum contribution of the CSG-related emissions to the modelled 24-hour average formaldehyde concentrations during the modelled year (ppb). Note that the concentrations shown in each grid square may be from different days during the year. The red arrow indicates the location of the maximum value for the year.

Figure 5.68 shows the maximum contribution of the CSG-related emissions to the 24-hour average modelled benzene concentrations in each grid square for the modelled year. Note, this is calculated as for formaldehyde.

Generally the maximum contributions are less than 0.01 ppb with a very small area of slightly larger values close to CSG-related emission sources. The largest maximum contribution is 0.017 ppb (indicated by the red arrow) and occurs about 1 km from CSG-related emission sources.

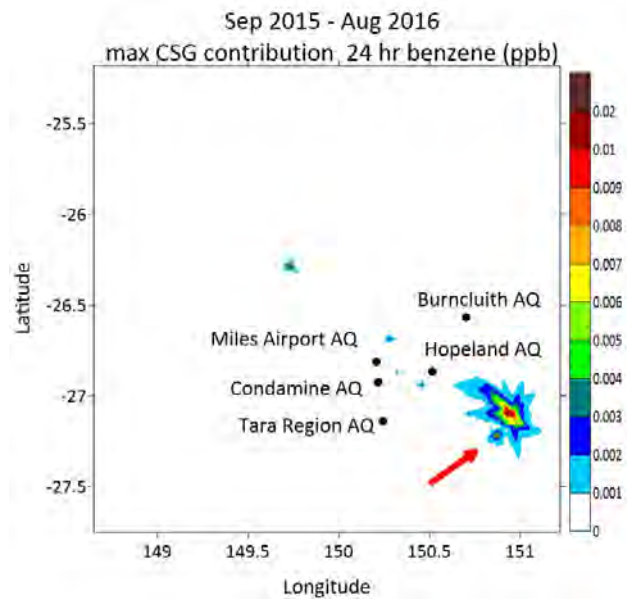


Figure 5.68 The maximum contribution of the CSG-related emissions to the modelled 24-hour average benzene concentrations during the modelled year (ppb). Note that the concentrations shown in each grid square may be from different days during the year. The red arrow indicates the location of the maximum value for the year.

5.5.4 Modelled effect of the CSG-related emissions on air pollutant levels at Town sites.

Model results are presented at the Town sites to investigate the effects of the CSG-related emissions to formaldehyde and benzene concentrations over the region.

Table 5.10 presents the annual average concentrations of formaldehyde and benzene for the model results with all sources and without the CSG sources at the Town sites. All the modelled concentrations are well below the annual average air quality objective for formaldehyde and benzene (8.9 ppb for formaldehyde and 3 ppb for benzene, Table 5.1). At the Town sites the modelled annual average formaldehyde concentrations with all sources included and without the CSG sources are similar, the model runs with the CSG sources included have annual average concentrations between 0.02 and 0.04 ppb higher than the model runs without the CSG sources.

For benzene the modelled annual average concentrations with all sources included and without the CSG sources are essentially the same – the maximum contribution due to the CSG-related emissions is 0.000006 ppb at Miles township.

Table 5.10 The modelled annual average concentrations of formaldehyde and benzene (ppb) at the Town sites.

Annual average (ppb)	Modelled Formaldehyde (all sources)	Modelled Formaldehyde (without CSG sources)	Modelled Benzene (all sources)	Modelled Benzene (without CSG sources)
Chinchilla	1.058	1.038	0.008	0.008
Miles township	1.115	1.084	0.006	0.006
Roma	1.067	1.045	0.004	0.004
Tara township	1.081	1.045	0.006	0.006
Warra	0.999	0.982	0.007	0.007

Figure 5.69 and Figure 5.70 show the maximum 24-hour average formaldehyde and benzene concentrations, respectively for each month of the model simulation, at the Town sites. The bar plots show the model results with all sources in red and the model results without the CSG sources in purple. The dashed horizontal red line shows the value of the air quality objective for formaldehyde.

The 24-hour average formaldehyde air quality objective (40 ppb Table 5.1) and 80 % of the 24-hour average formaldehyde air quality objective (32 ppb Table 5.1) are not exceeded by the modelled 24-hour average formaldehyde concentrations at any Town site in any month.

At the Town sites the maximum modelled 24-hour average formaldehyde concentrations with all sources and without CSG sources are similar and well below the air quality objective. The largest contribution due to the CSG-related emissions occurs at Miles township and is 0.2 ppb which is 0.5 % of the air quality objective.

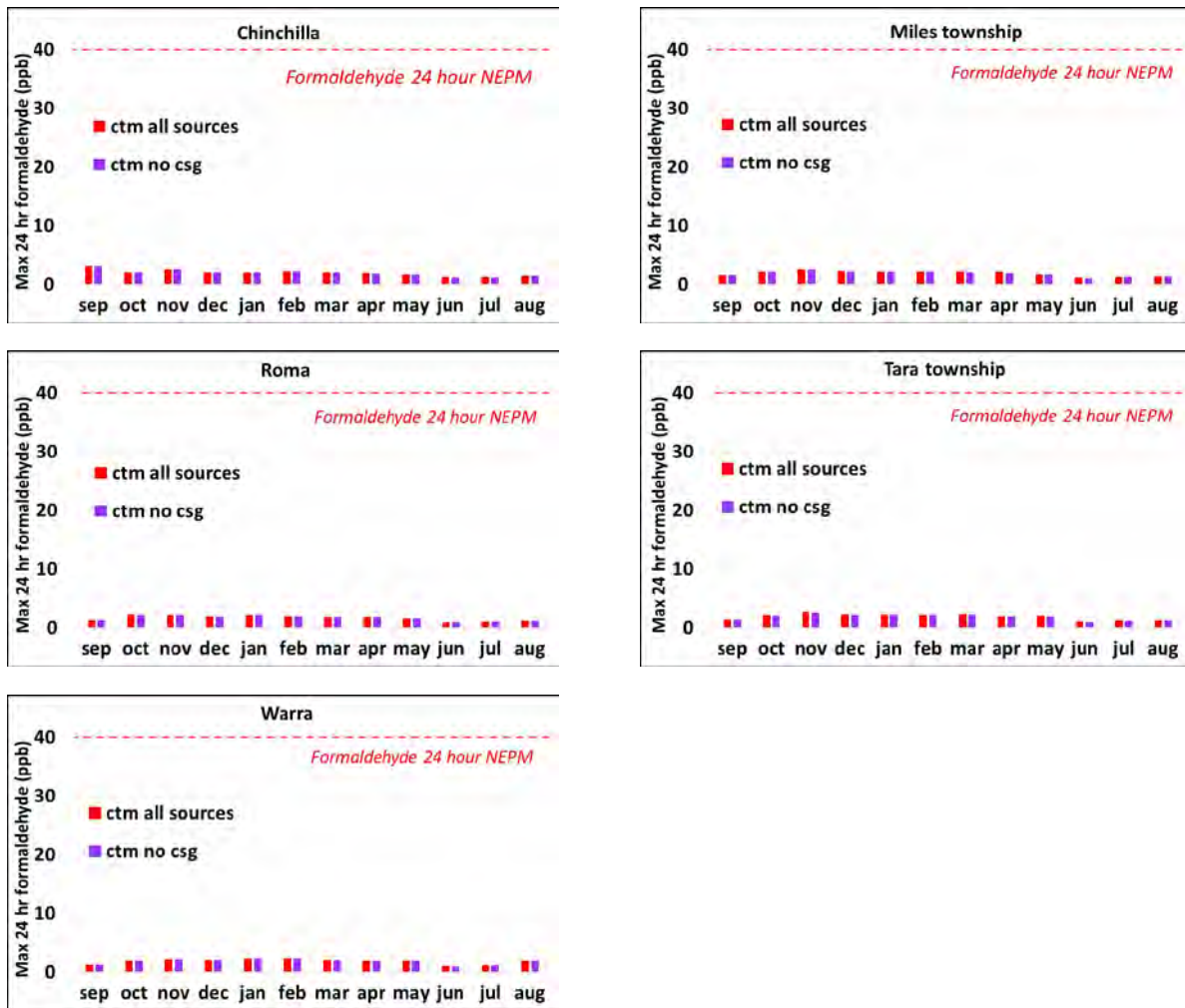


Figure 5.69 The modelled maximum 24-hour average formaldehyde concentrations (ppb) for each month of September 2015 – August 2016 at the Town sites: model results with all sources (red) and model results without the CSG sources (purple).

There is no 24-hour air quality objective for benzene but Figure 5.70 shows the maximum values are generally well below 10 % of the annual average objective (3 ppb, Table 5.1). At the Town sites the maximum modelled 24-hour average benzene concentrations with all sources and without the CSG sources are almost the same, the largest contribution due to the CSG-related emissions is 0.001 ppb at Warra. Somewhat elevated values are modelled in September 2015 at Chinchilla as a result of a modelled fire.

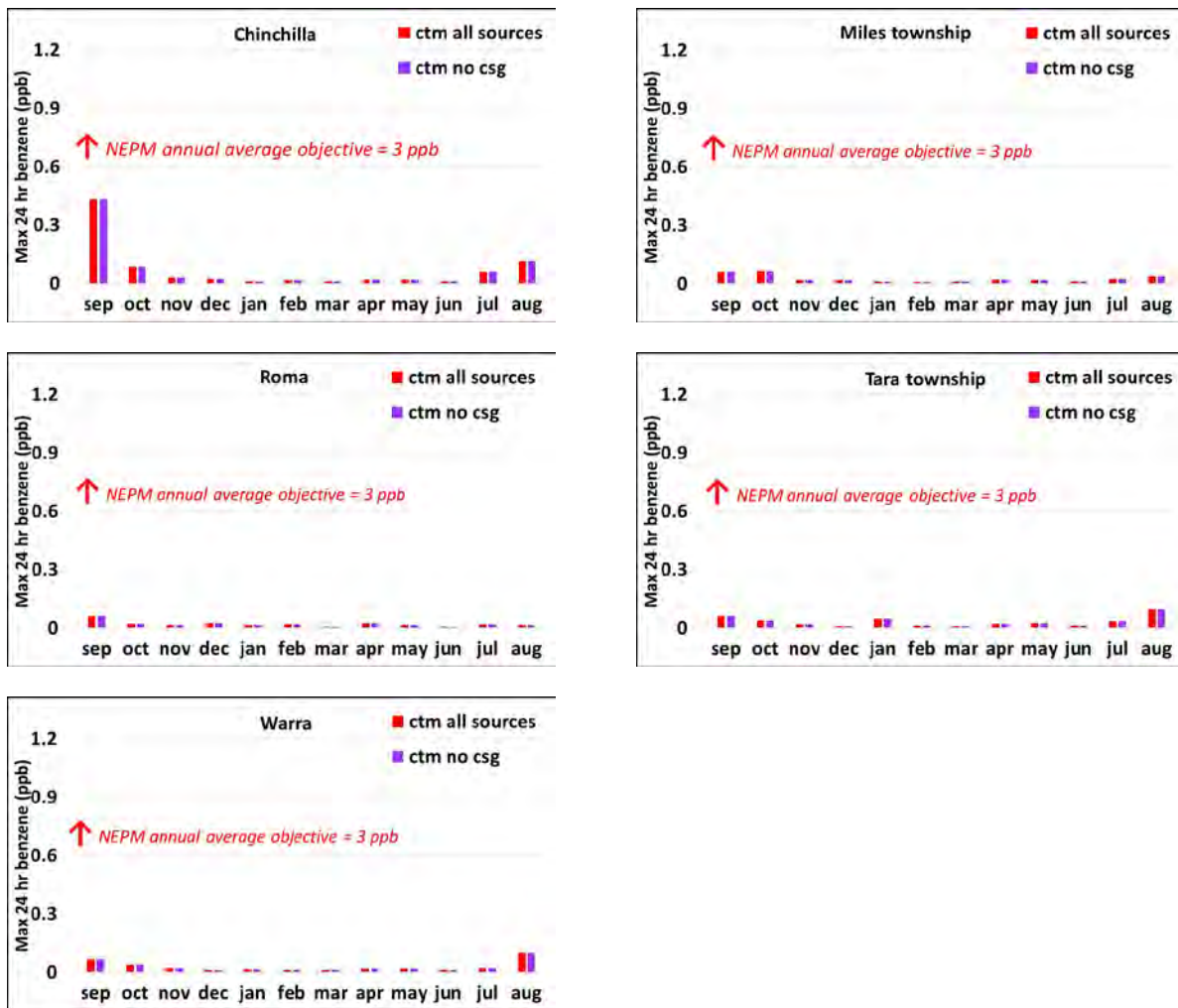


Figure 5.70 The modelled maximum 24-hour average benzene concentrations (ppb) for each month of September 2015 – August 2016 at the Town sites: model results with all sources (red) and model results without the CSG sources (purple).

The modelled contribution from the CSG-related emissions to the 24-hour average formaldehyde concentrations at each of the Town sites is presented in Figure 5.71 and for the 24-hour average benzene concentrations in Figure 5.72. Each plot shows the percentage of model hours within each season for the modelled contribution from the CSG-related emissions to the 24-hour average formaldehyde or benzene contributions.

On average 99.9 % of the time the contribution to the 24-hour average formaldehyde concentrations (see Figure 5.71) from the CSG-related emissions at the Town sites is less than 0.2 ppb which is 0.5 % of the 24-hour air quality objective for formaldehyde (40 ppb, Table 5.1). The largest frequency of changes is modelled at Miles township and Tara township for the 24-hour formaldehyde.

The contribution to the 24-hour average benzene concentrations (see Figure 5.72) from the CSG-related emissions at the Town sites is less than 0.01 ppb 100 % of the time.

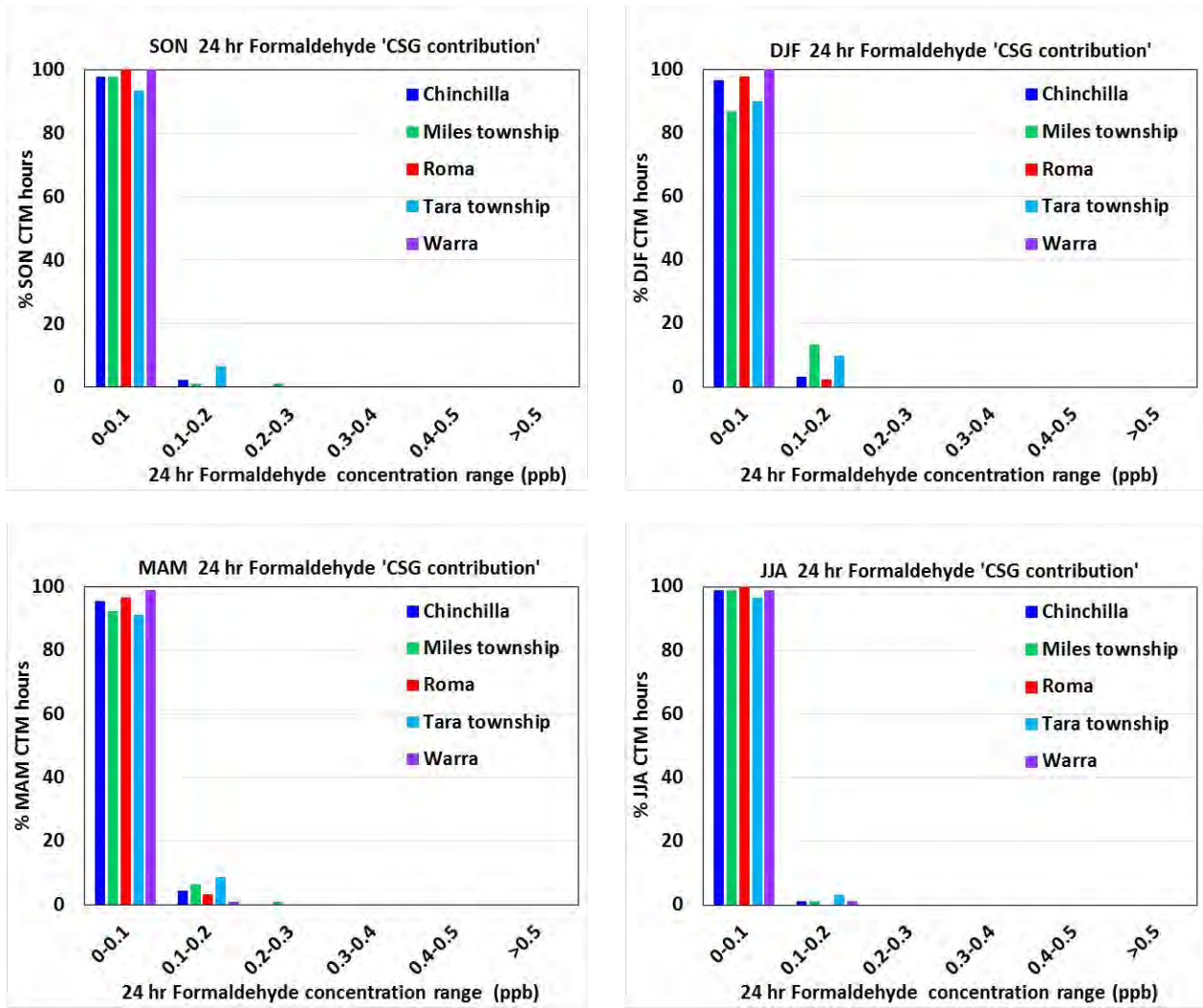


Figure 5.71 The modelled contribution from the CSG-related emissions to the 24-hour average formaldehyde concentration (ppb) at the Town sites shown as a frequency distribution for each season. The x-axis shows the concentration ranges of the contribution from the CSG-related emissions and the y-axis shows the percentage of model hours.

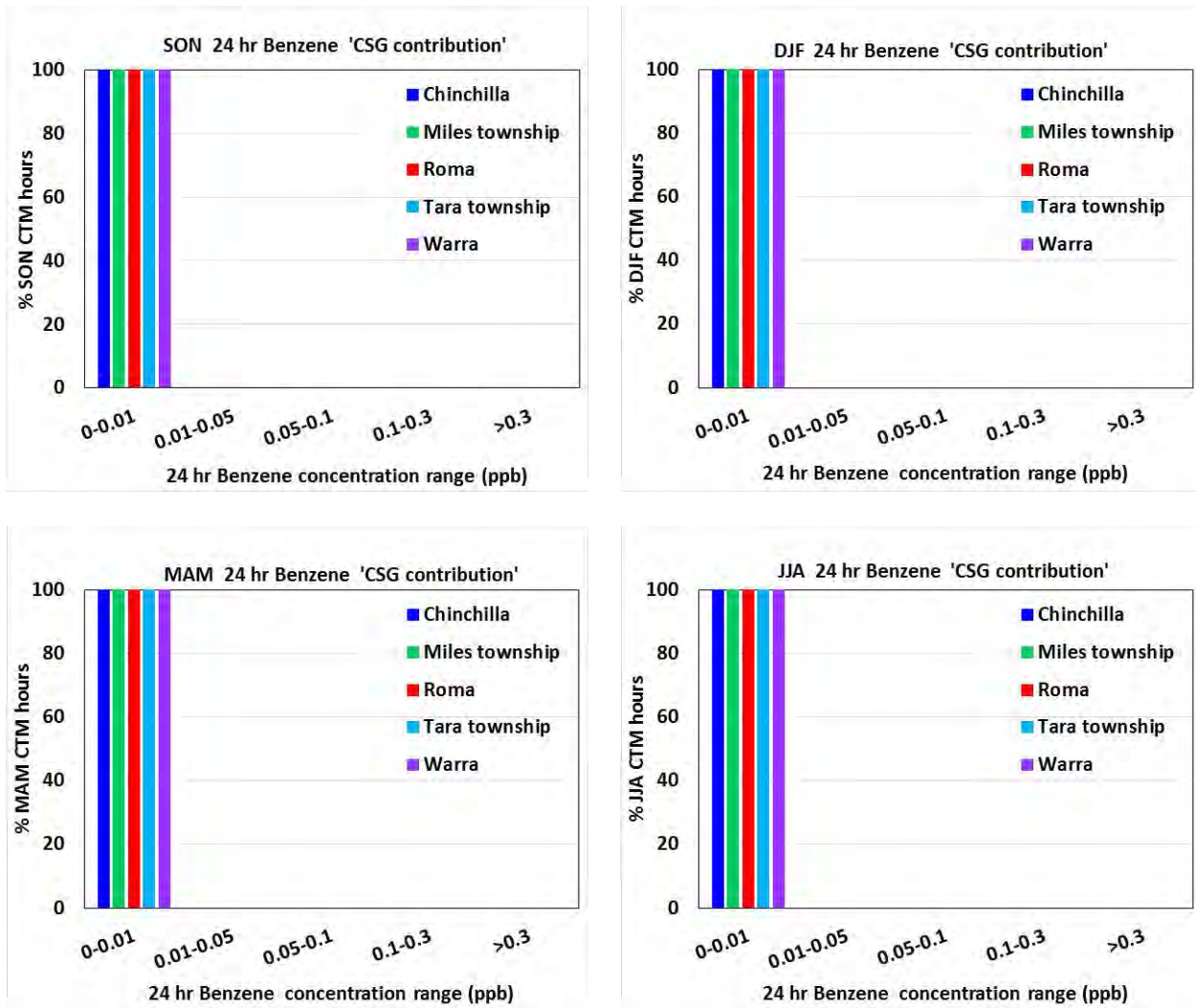


Figure 5.72 The modelled contribution from the CSG-related emissions to the 24-hour average benzene concentration (ppb) at the Town sites shown as a frequency distribution for each season. The x-axis shows the concentration ranges of the contribution from the CSG-related emissions and the y-axis shows the percentage of model hours.

Figure 5.73 shows plots of the modelled 24-hour average formaldehyde concentrations with all sources against the contribution from the CSG-related emissions to the modelled 24-hour average formaldehyde concentrations at Chinchilla, one of the Town sites. Those for the other Town sites are shown in Appendix E. The plots are seasonal and one point is plotted for each modelled day.

At Chinchilla the largest modelled increases (> 0.1 ppb) in 24-hour average formaldehyde concentrations due to the CSG-related emissions occur throughout the year, with the CSG-related emissions contributing up to 15 % of the total formaldehyde concentration. When this occurs the maximum increase in the 24-hour average formaldehyde concentration due to the CSG-related emissions is 0.15 ppb which is 0.4 % of the 24-hour air quality objective (40 ppb, Table 5.1). The results for the other Town sites show a similar pattern.

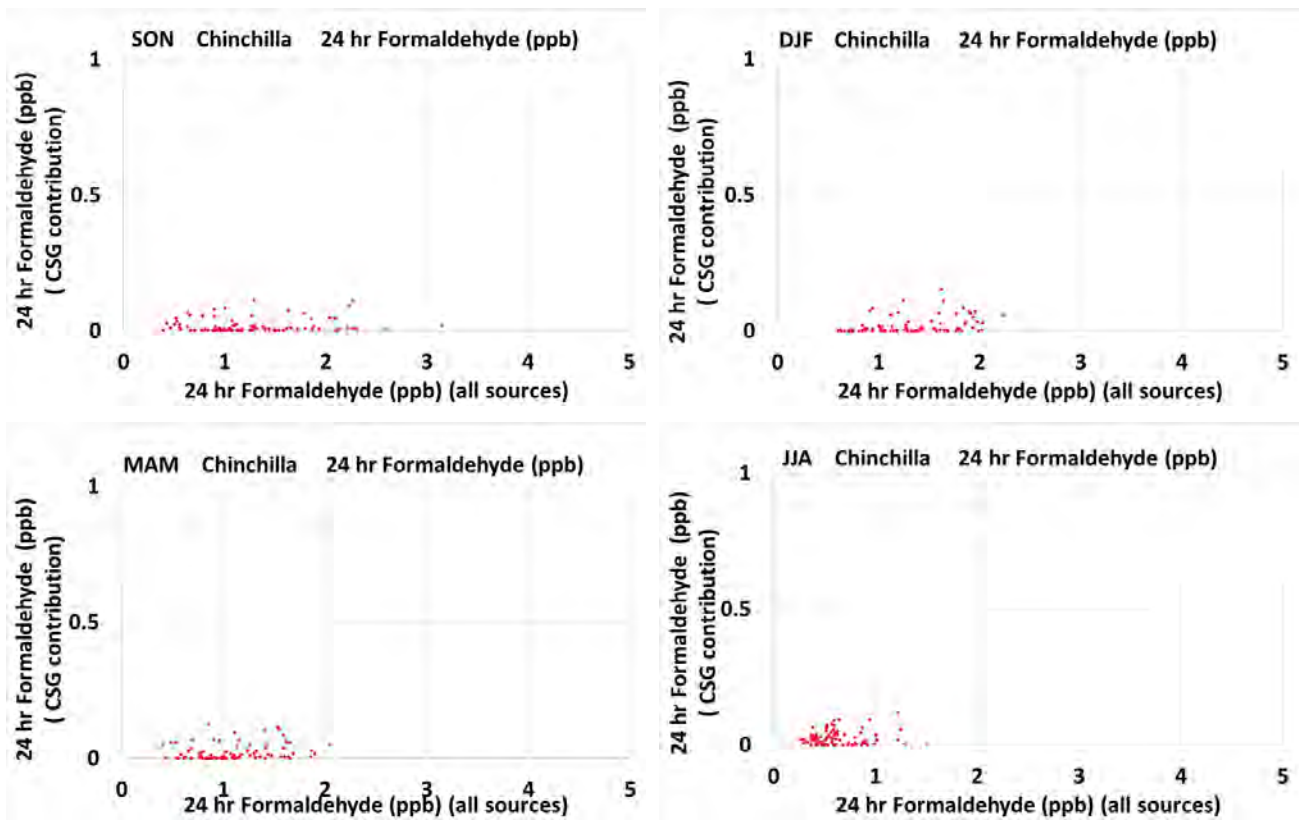


Figure 5.73 The modelled contribution from the CSG-related emissions to the 24-hour average formaldehyde concentration (ppb) at Chinchilla shown as a scatter plot for each season. The x-axis shows the modelled 24-hour average formaldehyde concentrations with all sources (ppb) and the y-axis shows the contribution from the CSG-related emissions to the 24-hour average formaldehyde concentration (ppb).

Figure 5.74 shows plots of the modelled 24-hour average benzene concentrations with all sources against the contribution from the CSG-related emissions to the modelled 24-hour average benzene concentrations at Warra, one of the Town sites. Those for the other Town sites are shown in Appendix E. The plots are seasonal and one point is plotted for each modelled day.

The results for Warra are shown here as the results for the other Town sites show almost no contribution from the CSG-related emissions to the modelled 24-hour average benzene (see Appendix E). At Warra the maximum contribution from the CSG-related emissions to the total 24-hour benzene concentration is 0.001 ppb on one day during SON, with CSG-related emissions contributing 7 % of the total value of benzene (0.001 ppb).

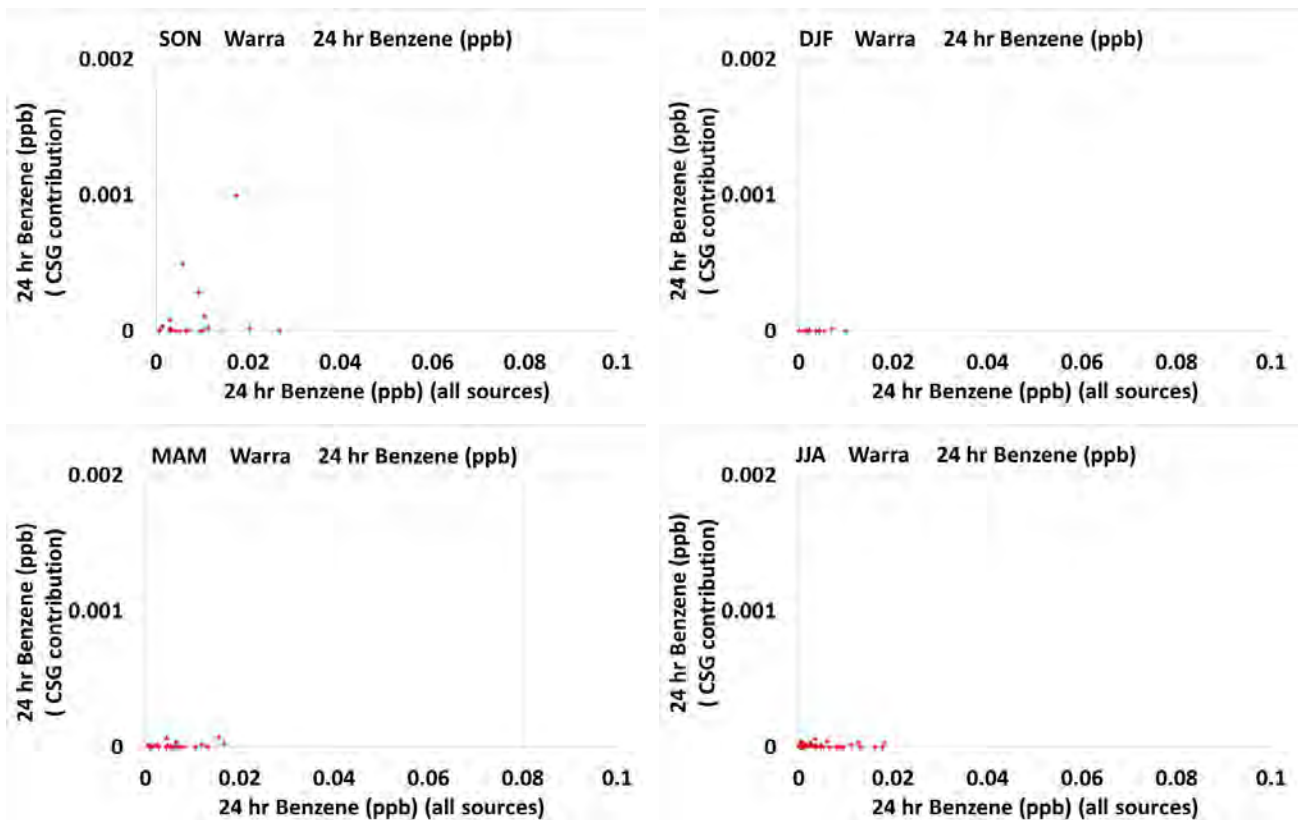


Figure 5.74 The modelled contribution from the CSG-related emissions to the 24-hour average benzene concentration (ppb) at Warra shown as a scatter plot for each season. The x-axis shows the modelled 24-hour average benzene concentrations with all sources (ppb) and the y-axis shows the contribution from the CSG-related emissions to the 24-hour average benzene concentration (ppb).

5.5.5 Summary

The impacts of CSG activity on the 24-hour formaldehyde concentrations modelled in the Surat Basin are summarised below:

Comparison of the model results with the observations

- The observed and modelled time series of formaldehyde concentrations show reasonable agreement although the model at times tends to overestimate formaldehyde by a small amount (1-2 ppb) at Chinchilla and at the Gas field and Regional sites. Note there are different averaging periods, the observations are sampled at 2-week periods while the model results are 1-hour averages.

Contribution of the CSG-related emissions to the modelled 24-hour average formaldehyde concentrations

- On average 99 % of the time at the Gas field and Regional sites and 99.9 % of the time at the Town sites the contribution from the CSG-related emissions is less than 0.2 ppb which is 0.5 % of the air quality objective.

- At the Gas field sites the largest modelled increases (> 0.2 ppb) in the 24-hour average formaldehyde concentrations contribute up to 29 % of the total formaldehyde concentration. When this occurs the maximum increase in 24-hour average formaldehyde concentration due to the CSG-related emissions is 0.27 ppb which is 0.7 % of the 24-hour air quality objective.
- The largest contribution due to the CSG-related emissions occurs at Tara Region and is 0.3 ppb which is 0.75 % of the air quality objective.
- Over the entire model 1 km grid domain during the modelled year the maximum predicted contributions are less than 0.2 ppb with larger values close to CSG sources. The largest maximum contribution is 0.7 ppb which is 1.8 % of the air quality objective and occurs about 1 km from CSG-related emission sources.
- Note that the model cannot resolve near-source impacts of plumes therefore impacts within a few kilometres of a point emission source may be under or overestimated.

Contribution of the CSG-related emissions to exceedances of the air quality objective or 80 % of the air quality objective

- At the Gas field, Regional or Town sites there are no modelled exceedances of the annual average formaldehyde air quality objective.
- At the Gas Field, Regional or Town sites there are no modelled exceedances of the 24-hour average formaldehyde air quality objective or 80 % of the air quality objective during any month.
- Over the entire modelled 1 km grid domain during the modelled year there are no exceedances of the 24-hour average formaldehyde air quality objective or 80 % of the 24-hour average formaldehyde air quality objective.

The impacts of CSG activity on the 24-hour benzene concentrations modelled in the Surat Basin are summarised below:

Comparison of the model results with the observations

- The observed and modelled time series of benzene concentrations show reasonable agreement although the model at times tends to underestimate benzene by a small amount (up to 0.1 ppb) at Chinchilla and at the Gas field and Regional sites. Note there are different averaging periods, the observations are sampled at 2-week periods while the model results are 1-hour averages.

Contribution of the CSG-related emissions to the modelled 24-hour average benzene concentrations

- At the Gas field, Regional and Town sites the contribution from the CSG-related emissions is less than 0.01 ppb 100 % of the time.

- At the Gas field, Regional and Town sites there are almost no changes in modelled 24-hour average benzene concentrations due to the CSG-related emissions.
- Over the entire model 1 km grid domain during the modelled year the maximum predicted contributions are less than 0.01 ppb with a very small area of slightly larger values close to CSG-related emission sources. The largest maximum contribution is 0.017 ppb and occurs about 1 km from CSG-related emission sources.

Contribution of the CSG-related emissions to exceedances of the air quality objective or 80 % of the air quality objective

- At the Gas field, Regional or Town sites there are no modelled exceedances of the annual average benzene air quality objective.
- There is no 24-hour air quality objective for benzene but to put the concentrations in context, benzene concentration measured in terrestrially influenced air at Cape Grim, a rural site in north-west Tasmania is 0.01 ppb (approximately a 2-week average) and the measured benzene concentration at a rural town in Victoria is 0.07 ppb (the average is based on weekly integrated measurements - for a summary of benzene measurements see Lawson et al., 2018a). The annual average air quality objective for benzene is 3 ppb and in this study the maximum observed annual average benzene concentration is 0.062 ppb at Chinchilla and the maximum modelled is 0.01 ppb at Burncluith.

5.6 Representativeness of observation sites to wider region

To assess whether air pollution levels at the Gas field air monitoring sites are representative of wider regional air quality, the modelled concentration of pollutants at a further six towns are briefly investigated. These towns are chosen to add to the locations already investigated to help provide good coverage over the region of modelled air quality data. The additional towns are Drillham, Glenmorgan, Surat, Taroom, Wandoan and Yuleba and their locations are shown in Figure 5.75, they will be referred to collectively as 'Extra Town sites'. Shown also in Figure 5.75 are the Gas field, Regional and Town sites as well as the locations of modelled CSG-related emission sources.

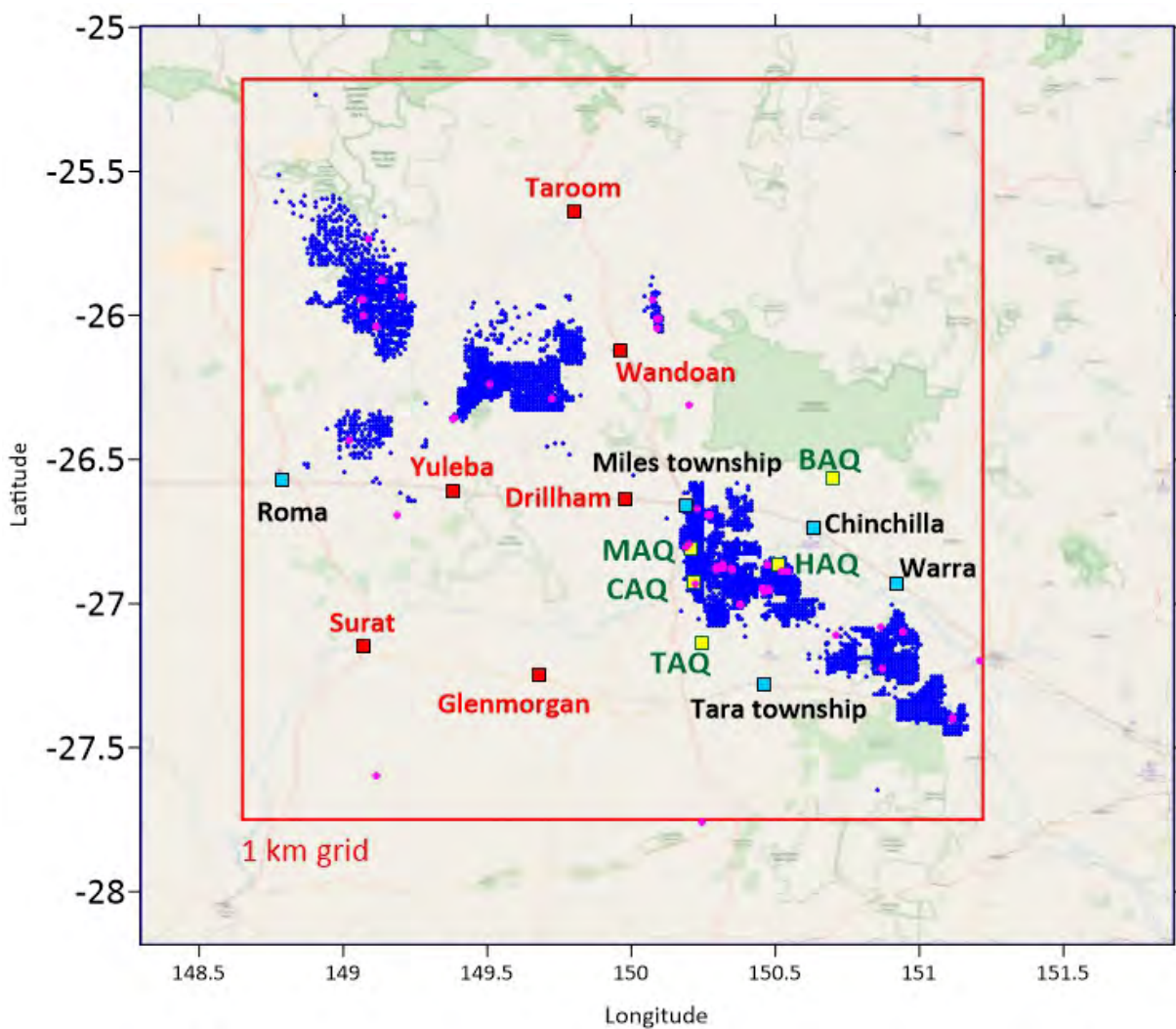


Figure 5.75 Locations of the air quality monitoring sites (green and yellow squares), 'Town sites' (blue) and 'Extra Town sites' (red) on the 1 km modelling grid. Locations of the modelled CSG-related emission sources are also shown, blue = well areas, high point vent areas, other area sources, pink = stacks, flares, other point sources.

Appendix G shows the modelled change in the 24-hour average PM_{2.5}, 1 and 4-hour average O₃, 1-hour average NO₂, 8-hour average CO and 24-hour average formaldehyde concentrations, respectively, due to the CSG-related emissions at each of the Extra town sites. Each plot shows the contribution or change in pollutant concentrations from the CSG-related emissions as a frequency distribution for each season. These results for the Extra town sites together with the results for the Gas field, Regional and Town sites are collated and presented in the figures below.

Figure 5.76 shows the percentage of the modelled hours for the year where the change in the 24-hour average PM_{2.5} concentration due to the CSG-related emissions is greater than 0.25 µg m⁻³ (1 % of the 24-hour PM_{2.5} air quality objective) (red bar) or greater than 0.5 µg m⁻³ (2 % of the 24-hour PM_{2.5} air quality objective) (blue bar). The Gas field (Miles Airport, Condamine and Hopeland) and Miles township sites show the largest frequency of change due to the CSG-related emissions for PM_{2.5} changes greater than 0.25 µg m⁻³. For changes greater than 0.5 µg m⁻³ (blue bar) Miles Airport has the largest frequency of change, 12 % of the time, Miles township is next with 1.4 % of the time, while all other sites have changes greater than 0.5 µg m⁻³ less than 1 % of the time. Note that the maximum change due to the CSG-related emissions in the 24-hour average PM_{2.5} at any of the sites is 4.6 µg m⁻³ at Miles Airport, which is 18.4 % of the air quality objective.

For PM_{2.5} the Gas field and Regional observation sites were well placed to capture the range of contributions due to the CSG-related emissions. The highest and most frequent contributions occur in the Gas field site area and the smallest and least frequent contributions occur at Burncluith.

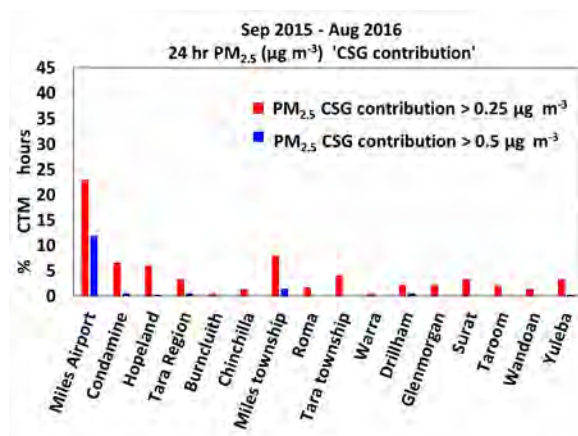


Figure 5.76 Percentage of model hours in the year where the contribution to the 24-hour average PM_{2.5} concentration due to the CSG-related emission is greater than 0.25 µg m⁻³ (red) or greater than 0.5 µg m⁻³ ppb (blue). Note that 0.25 and 0.5 µg m⁻³ are 1 and 2 % respectively of the 24-hour PM_{2.5} air quality objective.

Figure 5.77 shows the percentage of the modelled hours for the year where the change in the 1-hour average O₃ concentration due to the CSG-related emissions is greater than 2 ppb (or < -2 ppb) (2 % of the 1-hour O₃ air quality objective) (red bar) or greater than 5 ppb (or < -5 ppb) (5 % of the 1-hour O₃ air quality objective) (blue bar). The Gas field, Tara Region, Miles township and Tara township sites show the largest frequency of change due to the CSG-related emissions for O₃ changes greater than 2 ppb (or < -2 ppb). For changes greater than 5 ppb (or < -5 ppb) (blue bar)

the Gas field sites show the largest frequency of change; 7 % of the time on average, while all other sites show changes greater than 5 ppb (or < - 5 ppb) less than 3 % of the time. Note that the maximum change due to the CSG-related emissions in the 1-hour average O₃ at any of the sites is 11 ppb at Hopeland, which is 11 % of the air quality objective.

For O₃ the Gas field and Regional observation sites were well placed to capture the range of contributions due to the CSG-related emissions. The highest and most frequent contributions occur in the Gas field site area and the smallest and least frequent contributions occur at Burncluith.

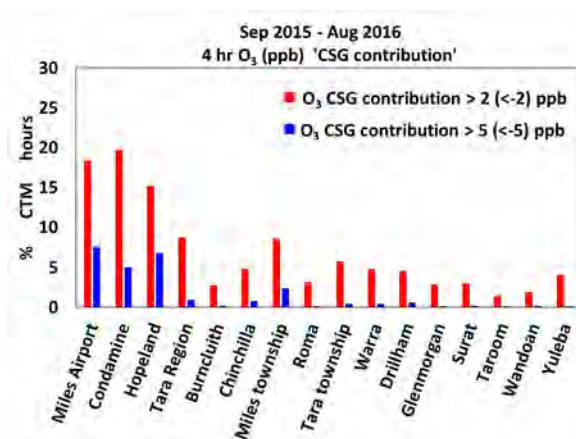


Figure 5.77 Percentage of model hours in the year where the contribution to the 4-hour average O₃ concentration due to the CSG-related emissions is greater than 2 (or less than -2) ppb (red) or greater than 5 (or less than -5) ppb (blue). Note that 2 and 5 ppb are 2.5 and 6.25 % respectively of the 4-hour O₃ air quality objective.

Figure 5.78 shows the percentage of the modelled hours for the year where the change in the 1-hour average NO₂ concentration due to the CSG-related emissions is greater than 2.5 ppb (2 % of the 1-hour NO₂ air quality objective) (red bar) or greater than 5 ppb (5 % of the 1-hour NO₂ air quality objective) (blue bar). The Gas field, Tara Region and Miles township sites show the largest frequency of change due to the CSG-related emissions for NO₂ changes greater than 2.5 ppb. For changes greater than 5 ppb (blue bar) the Gas field sites show the largest frequency of change, 7 % of the time on average, while all other sites have changes greater than 5 ppb less than 3.5 % of the time. Note that the maximum change due to the CSG-related emissions in 1-hour average NO₂ at any of the sites is 41 ppb at Hopeland, which is 34 % of the air quality objective.

For NO₂ the Gas field and Regional observation sites were well placed to capture the range of contributions due to the CSG-related emissions. The highest and most frequent contributions occur in the Gas field site area and the smallest and least frequent contributions occur at Burncluith.

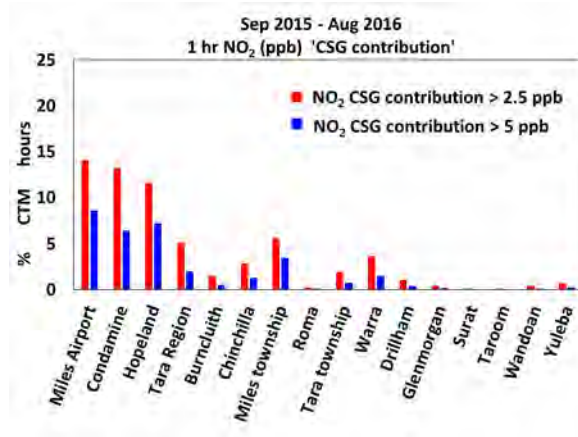


Figure 5.78 Percentage of model hours in the year where the contribution to the 1-hour average NO₂ concentration due to the CSG-related emissions is greater than 2.5 ppb (red) or greater than 5 ppb (blue). Note that 2.5 and 5 ppb are 2 and 4 % respectively of the 1-hour NO₂ air quality objective.

Figure 5.79 shows the percentage of the modelled hours within each season where the change in the 8-hour average CO concentration due to the CSG-related emissions is greater than 6 ppb (0.07 % of the 8-hour CO air quality objective) (red bar) or greater than 10 ppb (0.1 % of the 8-hour CO air quality objective) (blue bar). The Gas field sites show the largest frequency of change due to the CSG-related emissions for CO changes greater than 6 ppb. For changes greater than 10 ppb (blue bar) the Gas field sites show the largest frequency of change, 2.5 % of the time on average, while all other sites have changes greater than 10 ppb less than 1 % of the time on average. Note that the maximum change due to the CSG-related emissions in the 8-hour average CO at any of the sites is 51 ppb at Condamine, which is 0.6 % of the air quality objective.

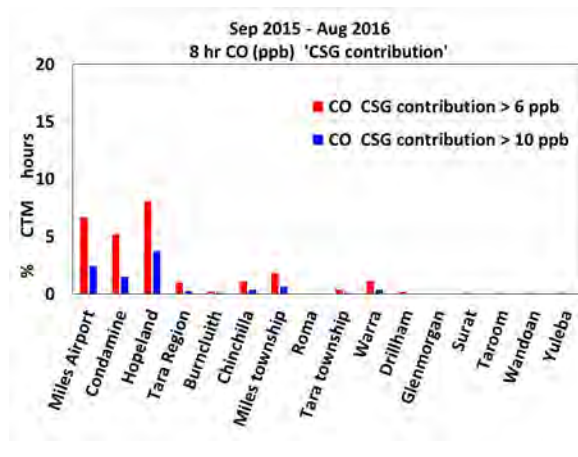


Figure 5.79 Percentage of model hours in the year where the contribution to the 8-hour average CO concentration due to the CSG-related emissions is greater than 6 ppb (red) or greater than 10 ppb (blue). Note that 6 and 10 ppb are 0.07 and 0.1 % respectively of the 8-hour CO air quality objective.

For CO the Gas field and Regional observation sites were well placed to capture the range of contributions due to the CSG-related emissions. The highest and most frequent contributions occur in the Gas field site area and the smallest and least frequent contributions occur at Burncluith.

Figure 5.80 shows the percentage of the modelled hours within each season where the change in the 24-hour average formaldehyde concentration due to the CSG-related emissions is greater than 0.1 ppb (0.25 % of the 24-hour formaldehyde air quality objective) (red bar) or greater than 0.2 ppb (0.5 % of the 24-hour formaldehyde air quality objective) (blue bar). The Gas field, Tara Region, Miles township and Tara township sites show the largest frequency of change due to the CSG-related emissions for formaldehyde changes greater than 0.1 ppb. For changes greater than 0.2 ppb the Gas field (Miles Airport, Condamine and Hopeland) and Tara Region sites show the largest frequency of change, 2 % of the time on average. Note that the maximum change due to the CSG-related emissions in the 24-hour average formaldehyde concentration at any of the sites is 0.3 ppb at Tara Region, which is 0.75 % of the air quality objective.

For formaldehyde the Gas field and Regional observation sites were well placed to capture the range of contributions due to the CSG-related emissions. The highest and most frequent contributions occur in the Gas field site area and the smallest and least frequent contributions occur at Burncluith.

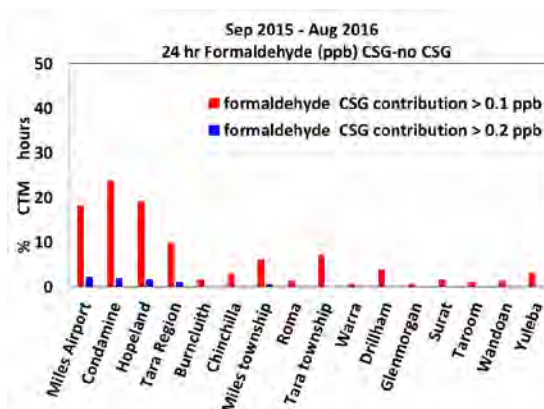


Figure 5.80 Percentage of model hours in the year where the contribution to the 24-hour average formaldehyde concentration due to the CSG-related emissions is greater than 0.1 (red) or greater than 0.2 (blue) ppb. Note that 0.1 and 0.2 ppb are 0.25 and 0.5 % respectively of the 24-hour formaldehyde air quality objective.

The maximum modelled contribution from the CSG-related emissions to the modelled 24-hour average benzene concentrations at all of the sites is 0.001 ppb at Warra. A benzene concentration difference of 0.001 ppb is extremely small and would be challenging to detect in the atmosphere even with very sensitive instrumentation; and as such the change in benzene concentration due to the CSG-related emissions at all sites can be considered negligible.

In summary, the modelling shows that in most cases the Gas field monitoring sites (Miles Airport, Condamine and Hopeland) experience the greatest change in pollutant concentrations due to the CSG-related emissions, albeit these changes are very small. In general, Burncluith monitoring site

shows relatively little change in pollutant concentrations due to the CSG-related emissions while the Tara Region site shows changes smaller than the Gas field sites but larger than Burncluith. The level of impact of the CSG-related emissions generally corresponds with the distance of monitoring sites from CSG infrastructure.

As such, this modelling indicates that the location of the Gas field sites was appropriate for the three-year monitoring study, because these sites are likely to have experienced the largest impact of CSG-related emissions in the region, with smaller impacts at other sites.

5.7 Implications of model assumptions, uncertainties and exclusions

The findings of this modelling study need to take into account the possible impact of the inventory and model assumptions, uncertainties and exclusions discussed in Section 3.3.

While an assessment of uncertainty in the emission inventory is outside the scope of this project, the assumptions in the inventory listed in Section 3.3 may have the following impacts on the model outputs:

- The exclusion of transient emissions from CSG development activities and other transient sources is likely to lead to modelled atmospheric concentrations of pollutants which are underestimated. The degree of underestimation will depend on both the duration, magnitude and frequency of the missing sources. Note that air quality modelling studies at regional scales do not typically include transient emissions.
- The representation of emissions as time-invariant, when in fact they vary over hours to days to weeks may lead to modelled concentrations that at times underestimate or overestimate the pollutant levels in the atmosphere. As such the maximum modelled concentrations and relative contribution from the CSG industry will include uncertainties due to simplifying assumptions in the emissions inventory. However, utilising the model output over a longer time period (e.g. data averaged to months to a year) will minimise the impact of the missing temporal variability on findings.
- The model cannot resolve near-source impacts of plumes, therefore impacts within a few kilometres of a point emission source may be under or overestimated. As such to accurately resolve concentrations of pollutants emitted from a nearby source which are approaching air quality objectives (e.g. some NO₂ events in this study) a different model would need to be employed.
- The use of emission data from previous years/months other than the modelled period may lead to an underestimation or overestimation of pollutant levels, if the emission rates are significantly different to the modelled time period.
- The reported CSG-related emissions used in this study may not be representative of years other than 2015/16 due to changes in production rates of CSG in the Surat Basin over time (DNRME 2019), in particular increases in CSG production of about 30% from June 2016-June 2018 (DNMRE 2019).

As such, conclusions drawn from this modelling study must consider the possible impacts of the above assumptions.

One way to explore the impact of assumptions that may lead to an underestimate of CSG predicted contribution is to examine a simple scenario where the contribution of pollutants due to CSG-related emissions is increased in each model grid square (1 x 1 km) by an approximate value of 30%. This allows for a possible underestimate of the CSG-related contribution to pollutant levels by 30%. We can examine how many 'near exceedance' events (> 80 % of the air quality objective) would become exceedance events if the concentration in each grid cell due to CSG-related emissions is 30 % higher. PM_{2.5} and NO₂ are explored here as both are emitted from the CSG

industry. It is important to note that an increase in pollutant concentrations by 30 % cannot be directly related to an increase in CSG-related emissions by 30 %, because the concentrations of pollutants are all dependant to different degrees on chemical transformations and reactions in the atmosphere. Note also that an increase in production of CSG in the region by 30% may not translate to an increase of 30% in CSG-related emissions.

For PM_{2.5} there are 8 modelled exceedances of the 24-hour air quality objective (Table 5.3) and 15 further exceedances of 80 % of the air quality objective (Section 5.1.3) with a contribution from CSG-related emissions greater than 1 µg m⁻³. Of the >80 % events, CSG-related emissions contribute between 5– 92 % of the 24-hour average concentration. If the contribution of 24-hour average PM_{2.5} concentration due to CSG-related emissions is increased by 30%, the PM_{2.5} concentration during 4 of the > 80 % events exceeds the air quality objective, making a total of 12 24-hour modelled exceedance events rather than 8. A further 4 of the >80 % events would be within 2 µg m⁻³ of exceeding the air quality objective.

As described in Section 5.3, the model in this study tends to over predict NO₂ concentrations. However the model predicts no exceedances of the air quality objective (120 ppb, Table 5.1) and 2 exceedances of 80 % of the air quality objective with CSG-related emissions contributing > 99 % of the concentration during these events which are within 1 km of a CSG-related emission source (See Section 5.3.3 and Table 5.7). If the contribution of CSG-related emissions to the concentration is increased by 30 % both of these > 80 % events would become 1-hour exceedances, and it is possible that some modelled NO₂ exceedances may also occur elsewhere near to CSG-related emission sources.

It is not appropriate to do this simple calculation for O₃ as it is a secondary pollutant that forms from reactions of its precursors (NO_x and VOCs) in sunlight. As such, the concentrations of modelled O₃ are dependent on concentrations of precursors from both CSG and non-CSG sources as well as meteorology, and so an increase in CSG-related precursor emissions is unlikely to have a linear effect on the resulting predicted O₃ concentration.

In summary, increasing the modelled contribution of CSG-related emissions to PM_{2.5} and NO₂ concentrations in each grid square by 30 % (noting that this is not equivalent to increasing CSG-related emissions by 30 % for reasons described above) results in

- An increase in the number of modelled PM_{2.5} 24-hour exceedance events from 8 to 11, with 4 more events within 2 µg m⁻³ of exceeding the objective
- Increases the number of modelled 1-hour NO₂ exceedances from 0 to at least 2, within 1 km of CSG-related emissions sources.

Increasing concentrations due to CSG-related emissions by 30 % does lead to small increases in the number of exceedance events for PM_{2.5} and NO₂. However it is important to note that this small number of additional exceedances occurs in only a few grid cells of 66,000 total grid cells in the model which is run for an entire year. As such, this is a relatively minor increase in the number of exceedances when considering the total time and area modelled. Given this, even if the CSG contribution to pollutant concentrations in each grid cell is 30% higher, the overall findings of this study would be unlikely to change significantly.

5.8 Relationship of the model findings to the monitoring study

This section provides a brief discussion of how the findings of the modelling study presented here relate to the previous findings from the 3-year monitoring study (Lawson et al., 2018c).

Model data show that levels of air pollutants are generally well below air quality objectives at 5 monitoring sites, in agreement with observations from these same sites (Lawson et al., 2018c). Modelling data also shows low levels of formaldehyde and benzene at Chinchilla and the Gas field and Regional sites, in agreement with observations (Lawson et al., 2018a).

In terms of exceedance of air quality objectives, the monitoring study showed 7 PM_{2.5} exceedances of the 24-hour air quality objective occurred at the gas field sites during 2015-2018 and these were mostly attributed to smoke from vegetation fires. While the model was challenged to accurately predict the timing of these PM_{2.5} smoke events due to differences in the location of modelled and observed PM_{2.5} plumes, the model did show that largest PM_{2.5} values and PM_{2.5} 24-hour exceedances in the model domain were all the result of smoke from vegetation fires. In agreement with the observations at the Gas Field and Regional sites, the model predicted no exceedances of other pollutants (NO₂, CO, O₃, benzene, formaldehyde) in the wider Surat Basin, except for a few small areas within the model 1 km grid domain during spring when the model did predict exceedances of the 4-hour O₃ air quality objective due to vegetation fires.

The monitoring study also measured 3 PM₁₀ exceedances and 18 TSP exceedances of 24-hour average air quality objectives at the Gas field sites. In most cases the PM₁₀ and TSP was likely composed of soil or dust which had become airborne due to activities such as vehicles driving on unsealed roads, CSG development or operational activities, cattle farming and other agricultural activities. TSP and PM₁₀ are dominated by large particles that undergo rapid deposition or removal from air, and this was the case for many of the observed TSP and PM₁₀ exceedances events, where peaks in particles were sharp and short-lived indicating a nearby source.

As discussed in Section 3.3, the modelling system utilised in this study is not suitable for capturing the types of short lived, localised PM₁₀ and TSP particle events that were occasionally observed at the monitoring sites. This is in part because the emission inventory does not include localised and one-off or unpredictable events such as an individual vehicle travelling past on an unsealed road, sudden livestock movement, dust from a seasonal cropping activity (e.g. harvesting) and CSG development or transient operational activities involving earthworks. Even if highly irregular, short-lived and one-off emissions could be reliably captured in the emissions inventory, accurately resolving the concentrations of PM₁₀ and TSP from very nearby (i.e. within a kilometre) short lived (i.e. less than a few hours in duration) sources would be very challenging for a chemical transport model such as used in this study.

Finally this modelling indicates that the contribution of CSG-related emissions was likely highest at the Gas Field sites during the monitoring study when compared to the two Regional monitoring sites and 11 town sites in the region. As such data from these monitoring sites is likely to provide a 'worst case' regional impact from CSG-related emissions during 2015 - 2016.

6 Summary and next steps

6.1 Summary of the study findings

This modelling study examines the impact of CSG-related emissions from a wide range of operational activities (both processing and production) associated with the CSG industry in the Surat basin in 2015-2016. The model does not include emissions associated with the development of CSG-related infrastructure or infrequent/incidental CSG operational activities.

An overall summary of findings is as follows. These results are for the entire 258 km x 258 km modelling domain, unless otherwise specified.

- The modelled pollutant concentrations agreed reasonably well with the monitoring data from the observation sites. The model was able to broadly reproduce background concentrations, diurnal behaviours, periods of general concentration increase and frequency of peaks. The model was challenged in some cases to reproduce peaks from local fire events (PM_{2.5}), and overestimated the magnitude of local, CSG-related NO₂ events. As such, the modelled contribution of CSG-related sources to NO₂ concentrations in this study are likely to be overestimates.
- Modelled ambient concentrations were in general well below air quality objectives. There were some modelled exceedances of the 24-hour average PM_{2.5} objective and some modelled near exceedances (>80 % of air quality objective) for 1-hour NO₂ and 4-hour O₃ concentrations (Air NEPM (2016), QLD EPP (2008)).

Smoke from vegetation fires resulted in the largest modelled air quality impacts over the region, particularly for PM_{2.5}, CO and O₃. Smoke from vegetation fires was the main contributor to the modelled exceedances of the 24-hour PM_{2.5} air quality objective.

- Where CSG-related emissions contributed to an exceedance of the 24-hour air quality objective for PM_{2.5} (8 occasions in total), CSG emissions contributed at most 4-37 % of the total 24-hour PM_{2.5} concentration. Over the modelled 1 km domain during the modelled year CSG-related emissions contributed to 0.06 % of all the PM_{2.5} exceedances. The predominant source of PM_{2.5} exceedances in the region is from vegetation fires. When CSG-related emissions contributed to values of PM_{2.5}, O₃ and NO₂ which were >80 % of the relative air quality objective (Air NEPM (2016) and Qld EPP (2008)), CSG-related emissions contributed at most 15 – 92 %, 4 % and 99 % to the total concentration respectively.
- The maximum impact of the modelled CSG-related emissions on air pollutant levels tended to be localised and occurred within a few kilometres of emission sources (for example GPFs) particularly for NO₂ and PM_{2.5}. For O₃ the maximum impact of CSG-related emissions was generally to decrease the O₃ concentration near combustion sources (due to reaction of O₃ with NO_x). CSG-related emissions sometimes contributed to higher O₃ concentrations downwind from CSG-related emission sources.

- At the Gas field, Regional and at 11 town sites in the region the largest modelled contributions of CSG-related emissions to the 4-hour O₃ concentrations occur most frequently in the summer months. Generally the largest modelled contributions from CSG-related emissions occur for larger O₃ values (i.e. increased peak concentrations). However when the modelled concentrations of O₃ in the region were highest (> 80 % of the air quality objective), CSG-related emissions made a minor (4 ppb) contribution to the total concentration (3 – 7 % of the total 4-hour O₃ concentration).
- The modelled concentrations of air toxics benzene and formaldehyde were very low and well below air quality objectives (Air Toxics NEPM (2011), Texas AMCV (2016a)). The modelled contribution of CSG-related emissions to ambient concentrations of these air toxics was very low to negligible.
- The modelling indicates that the contribution of CSG-related emissions to air pollutant levels was highest at the Gas field sites when compared to the two Regional sites and 11 town sites in the region. As such, air quality data from the Gas field monitoring sites (Lawson et al 2018c) were well-located to experience CSG-related air pollution impacts. These sites are likely to provide a ‘worst case’ regional impact from CSG-related emissions for the period 2015 - 2016.
- Combustion of gas and/or diesel in CSG infrastructure/sources was the likely major source of CSG-related emissions of PM_{2.5}, CO, NO₂, and precursors leading to O₃, rather than fugitive emissions of CSG itself.

6.2 Significance of this study and next steps

This air quality modelling study provides the first detailed assessment of the influence of CSG-related emissions on ambient air quality in an unconventional gas region in Australia. A major component of this work was the development of a comprehensive and detailed emissions inventory to represent the release of a range of air pollutants from a wide variety of sources, including CSG-related sources, at high spatial resolution in the Surat Basin. Findings from this study could be used by government agencies to better understand the contribution that CSG operational activities made to air pollutant levels in the Surat Basin during 2015-2016. This work also provides an understanding of the spatial distribution of pollutant levels over the wider Surat Basin over the course of a year; information that cannot easily be collected through an observation network of only a few sites.

The findings from this study could be used to inform future policy development in the region. CSG production volumes have increased in the Surat Basin region by about 30 % between 2016 and 2018 (DNRME 2019), and during this time there are likely to have been changes to the number and types of CSG-related emission sources, as well as other potential changes to non-CSG-related emissions sources in the region. As such, the modelling system developed in this work could be used to assess CSG impacts in subsequent years (2017 onwards), pending an appropriate update to the emissions inventory. The modelling system could also be used to explore potential CSG impacts on additional air pollutants, if required

Further work to investigate the reason/s for the modelled over-prediction of NO₂ in this study could also be undertaken.

7 References

- ABS (2015) Australian Bureau of Statistics Motor Vehicle Census - 2015. Available at <http://www.abs.gov.au/AUSSTATS/abs@.nsf/Lookup/9309.0Main+Features131%20Jan%202015?OpenDocument>.
- AEMO (2015) Australia Energy Market Operator. Web Archive Public_DISPATCHSCADA 2010-2015. Purchased December 2015.
- APLNG (2010) Environmental Impact Statement, Volume 2, Gas fields <https://www.aplng.com.au/about-us/compliance/eis.html>
- ASGS (2011) Australian Statistical Geography Standard (ASGS) Volume 1 - Main Structure and Greater Capital City Statistical Areas (cat no. 1270.0.55.001). Available at [http://www.ausstats.abs.gov.au/ausstats/subscriber.nsf/0/D3DC26F35A8AF579CA257801000DCD7D/\\$File/1270055001_july%202011.pdf](http://www.ausstats.abs.gov.au/ausstats/subscriber.nsf/0/D3DC26F35A8AF579CA257801000DCD7D/$File/1270055001_july%202011.pdf).
- Azzi, M., Cope, M., and M. Rae (2012) Sustainable Energy Deployment within the Greater Metropolitan Region, NSW-Environmental Trust, CSIRO, North Ryde, Australia, 2012.
- Azzi, M., Angove, D., Campbell, I., Cope, M., Emmerson, K., Feron, P., Patterson, M., Tibbett, A., and S. White (2014) Assessing Atmospheric Emissions from Amine based CO₂ PCC Process and their Impacts on the Environment – A Case Study. Volume 2: Atmospheric chemistry of MEA and 3D air quality modelling of emissions from the Loy Yang PCC plant. CSIRO, Australia. <https://scholar.google.com.au/scholar?oi=bibs&cluster=15081745420128950887&btnI=1&hl=en>
- Broome, R. A., Cope, M. E., Goldsworthy, B., Goldsworthy, L., Emmerson, K., Jegasothy, E., and G. G. Morgan (2016) The mortality effect of ship-related fine particulate matter in the Sydney greater metropolitan region of NSW, Australia, *Environ. Int.*, 87, 85–93, <https://doi.org/10.1016/j.envint.2015.11.012>.
- Cardno (2014) Traffic and Transport Assessment Technical Report: Gas Field Development Project – Environmental Impact Statement
- Cope, M.E., Hess, G.D., Lee, S., Tory, K., Azzi, M., Carras, J., Lilley, W., Manins, P.C., Nelson, P., Ng, L., Puri, K., Wong, N., Walsh, S. and M. Young (2004) The Australian Air Quality Forecasting System. Part I: Project description and early outcomes. *J Appl Meteorol* 43, 649-662, <https://doi.org/10.1175/2093.1>
- Cope, Martin, Sunhee Lee, Mick Meyer, Fabienne Reisen, Camilla Trindade, Andrew Sullivan and Nic Surawski, Alan Wain, David Smith, Beth Ebert, Christopher Weston, Luba Volkova, Kevin Tolhurst, Thomas Duff, Sean Walsh, Nigel Tapper, Sarah Harris, Chris Rudiger, Alex Holmes, Musa Kilinc, Clare Paton-Walsh, Elise-Andree Guerette, Maximilien Desservettaz, Grant Edwards, Katrina Macsween and Dean Howard (2019) Smoke Emission and Transport Modelling. Research Report 102, The State of Victoria Department of Environment, Land,

Water and Planning. https://www.ffm.vic.gov.au/__data/assets/pdf_file/0027/420759/No-102_Cope-et.al_2019.pdf

- Cope, Martin, Sunhee Lee, Julie Noonan, Bill Lilley, Dale Hess and Merched Azzi (2009) Chemical Transport Model – Technical Description. CAWCR Technical Report No. 015, October 2009, Series: Technical report (Centre for Australian Weather and Climate Research)
- Cope, M., Keywood, M., Emmerson, K., Galbally, I., Boast K., Chambers, S., Cheng, M., Crumeyrolle, S., Dunne, E., Fedele, R., Gillett, R., Griffiths, A., Harnwell, J., Katzfey, J., Hess, D., Lawson, S., Miljevic, B., Molloy, S., Powell, J., Reisen, F., Ristovski, Z., Selleck, P., Ward, J., Zhang, C., and J. Zeng (2014) The Sydney Particle Study – Stage II. CSIRO, <http://www.environment.nsw.gov.au/aqms/sydparticlestudy.htm>, p. 151.
- Cope, Martin; Lee, Sunhee; Meyer, Mick; Reisen, Fabienne; Trindade, Camila; Sullivan, Andrew; Surawski, Nic; Wain, Alan; Smith, David; Ebert, Beth; Weston, Christopher; Volkova, Luba; Tolhurst, Kevin; Duff, Thomas; Walsh, Sean; Tapper, Nigel; Harris, Sarah; Rudiger, Chris; Holmes, Alex; Kilinc, Musa; Paton-Walsh, Clare; Guerette, Elise-Andree; Desservettaz, Max; Edwards, Grant; Macsween, Katrina and Dean Howard (2016) Smoke Emission and Transport Modelling. Final Report. Pages: 199. Publisher: DELWP, Place of Publication: CSIRO
- Cope, Martin and Kathryn Emmerson (2016) Operational evaluation of CCAM-CTM_cb05_aer2, Research Note, September 2016, CSIRO, Climate Research Centre.
- Cope, Martin; Powell, Jenny; Broome, Richard and Geoff Morgan (2017) Wood heater simulations: July 2010 – June 2011. Appendix 2 – Wood heaters and power stations in the Greater Metropolitan region of NSW. CSIRO Climate Research Centre.
- Day, Stuart, Mark Dell’Amico, Robyn Fryand and Hoda Javanmard Tousi (2014) Field Measurements of Fugitive Emissions from Equipment and Well Casings in Australian Coal Seam Gas Production Facilities. CSIRO Energy Technology Report to the Department of the Environment, CSIRO Australia. <https://www.environment.gov.au/system/files/resources/57e4a9fd-56ea-428b-b995-f27c25822643/files/csg-fugitive-emissions-2014.pdf>
- DAF (2014a) Department of Agriculture and Fisheries, 2014. *Agricultural land audit - current cattle feedlots – Queensland*. State of Queensland (Department of Agriculture and Fisheries). Published 31 January 2014. Available at <http://qldspatial.information.qld.gov.au/catalogue/>
- DAF (2014b) Department of Agriculture and Fisheries, 2014. *Agricultural land audit - current poultry farms – Queensland*. State of Queensland (Department of Agriculture and Fisheries). Published 31 January 2014. Available at <http://qldspatial.information.qld.gov.au/catalogue/>
- DAF (2014c) Department of Agriculture and Fisheries, 2014. *Agricultural land audit - current piggeries – Queensland*. State of Queensland (Department of Agriculture and Fisheries). Published 31 January 2014. Available at <http://qldspatial.information.qld.gov.au/catalogue/>
- Delaney, W. and A. G. Marshall (2011) Victorian Air Emissions Inventory for 2006, Proceedings of the 20th International Clean Air and Environment Conference, 5-8 July 2011, Clean Air Society of Australia and New Zealand, Eastwood, NSW, Australia.
- DNRME (2010) Attributes and Locations of Queensland Roads

- DNRME (2015a) Department of Natural Resources and Mines 2015a. *Mining lease surface areas – Queensland*. State of Queensland (Department of Natural Resources and Mines). Published 13 October 2015. Available at: <http://qldspatial.information.qld.gov.au/catalogue/>
- DNRME (2015b) Department of Natural Resources and Mines, 2015b, *Coal seam gas well locations – Queensland*. Available at <http://qldspatial.information.qld.gov.au/catalogue/custom/detail.page?fid={C45038EB-BB83-4B16-9231-1905ED753D77}>
- DNRME (2015c) Department of Natural Resources and Mines, 2015c, *Exploration and production permits - Queensland*. Available at <http://qldspatial.information.qld.gov.au/catalogue/custom/detail.page?fid=%7BB0D192C5-4076-43E8-9A2C-94A0FA928AF9%7D>
- DNRME (2019) Queensland petroleum and gas production statistics (June 2018). Available at: <https://data.qld.gov.au/dataset/petroleum-gas-production-and-reserve-statistics/resource/9746212a-e0c6-484d-95ad-b2be1c46027d>
- DTMR (2015) Department of Transport and Main Roads 2015. *Traffic census 2014 - Queensland*. State of Queensland (Department of Transport and Main Roads). Published 14 May 2015. Available at <http://qldspatial.information.qld.gov.au/catalogue/>
- ECMWF CAMS Global Fire Assimilation System data - <https://apps.ecmwf.int/datasets/data/cams-gfas/>
- ECMWF ERA-interim <https://www.ecmwf.int/en/forecasts/datasets/reanalysis-datasets/era-interim>
- Emissions – Population-based emissions inventory <http://www.nepc.gov.au/system/files/resources/9947318f-af8c-0b24-d928-04e4d3a4b25c/files/aaqprcrttapmphase2200105final.pdf>
- Emissions – SEQR, EPA and BBC (2004). *Air Emissions Inventory: South East Queensland Region*. http://www.epa.qld.gov.au/environmental_management/air/air_quality_monitoring/air_quality_reports/air_emissions_inventory/
- Emmerson, K. M., Galbally, I. E., Guenther, A. B., Paton-Walsh, C., Guerette, E.-A., Cope, M. E., Keywood, M. D., Lawson, S. J., Molloy, S. B., Dunne, E., Thatcher, M., Karl, T., and S. D. Maleknia (2016) Current estimates of biogenic emissions from eucalypts uncertain for southeast Australia, *Atmos. Chem. Phys.*, 16, 6997–7011, <https://doi.org/10.5194/acp-16-6997-2016>.
- Galbally, I. E., Cope, M., Lawson, S. J., Bentley, S. T., Cheng, M., Gillet, R. W., Selleck, P., Petraitis, B., Dunne, E., and S. Lee (2008) Sources of Ozone Precursors and Atmospheric Chemistry in a Typical Australian City, available at: <http://pandora.nla.gov.au/pan/97227/20090326-1709/www.environment.gov.au/atmosphere/airquality/publications/ozone-precursors.html> (last access: 28 September 2017).
- Goldsworthy, B. (2017) Spatial and temporal allocation of ship exhaust emissions in Australian coastal waters using AIS data: Analysis and treatment of data gaps. *Atmospheric Environment* 163, 77-86.

- Hurley, P.J., Physick, W.L., Luhar, A.K. and M. Edwards (2005) The air pollution model (TAPM) version 3. Part 2, Summary of some verification studies. CSIRO, CSIRO Atmospheric Research, Aspendale, Victoria 3195 Australia.
- Katestone (2010) Australia Pacific LNG Gas Fields Project Area – Air Quality Impact Assessment. Prepared for Worley Parsons on behalf of APLNG.
- Katestone (2017) Surat Basin Air Emissions Inventory Summary Report, prepared for CSIRO by Katestone Environmental Pty Ltd, December 2017, 84p
- Keywood, M., Cope, M., Meyer, C. P. M., Iinuma, Y., and K. Emmerson (2015) When smoke comes to town: the impact of biomass burning smoke on air quality, *Atmos. Environ.*, 121, 13–21, <https://doi.org/10.1016/j.atmosenv.2015.03.050>, 2015.
- Lawson, S. J., Cope, M., Lee, S., Galbally, I. E., Ristovski, Z., and M. D. Keywood (2017a) Biomass burning at Cape Grim: exploring photochemistry using multi-scale modelling, *Atmos. Chem. Phys.*, 17, 11707–11726, <https://doi.org/10.5194/acp-17-11707-2017>.
- Lawson S.J., Hibberd M.F. and M. D. Keywood (2017b) Ambient Air Quality in the Surat Basin- Overview of Study Design, Report for the Gas Industry Social and Environmental Research Alliance (GISERA), Project No G.3, Available: <https://gisera.csiro.au/wp-content/uploads/2018/03/GHG-3-Study-Design.pdf>
- Lawson, S.J., Powell, J.C., Noonan J., Dunne, E., Cheng, M., Selleck, P.W., Harnwell, J. and D. Etheridge (2018a) An assessment of ambient air quality in the Surat Basin Queensland: Interim data summary, September 2014 – December 2016, CSIRO, Australia. Available <https://gisera.csiro.au/wp-content/uploads/2016/02/GHG-3-Milestone-2-report.pdf>
- Lawson, S.J., Powell, J.C., Noonan J., Selleck, P.W and D. Etheridge (2018b) Ambient air quality in the Surat Basin, Queensland. Final data summary: January 2017 - February 2018, CSIRO, Australia. Available <https://gisera.csiro.au/wp-content/uploads/2018/09/G3-2017-18-data-summary-report.pdf>
- Lawson, S.J., Powell, J.C., Noonan J., Dunne, E., and D Etheridge (2018c) Ambient air quality in the Surat Basin, Queensland. Overall assessment of air quality in region from 2014-2018, CSIRO, Australia. Available: <https://gisera.csiro.au/wp-content/uploads/2018/09/G3-final-AQ-assessment-report.pdf>
- Lu, H. and Y. P. Shao (1999) A new model for dust emission by saltation bombardment, *J. Geophys. Res.-Atmos.*, 104, 16827–16841, <https://doi.org/10.1029/1999jd900169>.
- Luhar, A., Etheridge, D., Loh, Z., Noonan, J., Spencer, D. and S. Day (2018) Characterisation of regional fluxes of methane in the Surat Basin, Queensland, CSIRO, Australia. Available <https://gisera.csiro.au/wp-content/uploads/2018/10/GHG-1-Final-Report.pdf>
- Luhar, A.K. and P.J. Hurley (2003) Evaluation of TAPM, a prognostic meteorological and air pollution model, using urban and rural point-source data. *Atmospheric Environment* 37, 2795-2810.
- Luhar, A. K., Mitchell, R. M., Meyer, C. P., Qin, Y., Campbell, S., Gras, J. L., and D. Parry (2008) Biomass burning emissions over northern Australia constrained by aerosol measurements: II

– Model validation, and impacts on air quality and radiative forcing, *Atmos. Environ.*, 42, 1647–1664, <https://doi.org/10.1016/j.atmosenv.2007.12.040>.

McGregor, J.L. (2015) Recent developments in variable-resolution global climate modelling, *Climatic Change*, 129, 369–380, <https://doi.org/10.1007/s10584-013-0866-5>

Meyer, C.P., Luhar, A.K. and R. M. Mitchell (2008) Biomass burning emissions over northern Australia constrained by aerosol measurements: I—Modelling the distribution of hourly emissions. *Atmospheric Environment* 42, 1629–1646.

NEPM (2011) National Environment Protection (Air Toxics) Measure (NEPM) (2011) <https://www.legislation.gov.au/Details/F2011C00855>

NEPM (2016) National Environment Protection (Ambient Air Quality) Measure (NEPM) (2016) <https://www.legislation.gov.au/Details/F2016C00215>

NPI (2007) National Pollutant Inventory (NPI), 2007. Emission estimation technique manual for Intensive livestock - beef cattle, v3.1. National Pollutant Inventory, Commonwealth Department of the Environment. <http://www.npi.gov.au/resource/emission-estimation-technique-manual-intensive-livestock-beef-cattle-version-31>

NPI (2008) National Pollutant Inventory (NPI), 2008. Emission estimation technique manual for Combustion Engines Version 3.0 <http://www.npi.gov.au/resource/emission-estimation-technique-manual-combustion-engines-version-30>

NPI (2012) National Pollutant Inventory (NPI), 2012. Emission estimation technique manual for Fossil Fuel Electric Power Generation Version 3.0 <http://www.npi.gov.au/resource/emission-estimation-technique-manual-fossil-fuel-electric-power-generation>

NPI (2013a) National Pollutant Inventory (NPI) 2013a. Emission estimation technique manual for Oil and Gas Extraction and Production. Version 2.0 <http://www.npi.gov.au/resource/emission-estimation-technique-manual-oil-and-gas-extraction-and-production-version-20>

NPI (2013b) National Pollutant Inventory (NPI) 2013b. Emission estimation technique manual for Intensive Livestock - Poultry Raising, v3.0. National Pollutant Inventory, Commonwealth Department of the Environment. <http://www.npi.gov.au/resource/emission-estimation-technique-manual-intensive-livestock-poultry-raising-version-30>

NPI (2017) National Pollutant Inventory (NPI) 2017 <http://www.npi.gov.au/npi-data/latest-data>

NSW EPA (2008) New South Wales Environment Protection Authority, 2008. Air Emissions Inventory for the Greater Metropolitan Region in New South Wales. <https://www.epa.nsw.gov.au/your-environment/air/air-emissions-inventory/air-emissions-inventory-2008>

NSW EPA (2012a) New South Wales Environment Protection Authority, 2012a. Air Emissions Inventory for the Greater Metropolitan Region in New South Wales, Technical Report No. 3: 2008 Calendar Year Commercial Emissions, Environment Protection Authority, 59–61 Goulburn Street, Sydney South 1232, Australia

- NSW EPA (2012b) New South Wales Environment Protection Authority, 2012b. Air Emissions Inventory for the Greater Metropolitan Region in New South Wales, Technical Report No. 7: 2008 Calendar Year On-Road Mobile Emissions, Environment Protection Authority, 59–61 Goulburn Street, Sydney South 1232, Australia
- QLD EPP (2008) Environment Protection (Air) Policy (2008)
<https://www.legislation.qld.gov.au/LEGISLTN/CURRENT/E/EnvProtAirPo08.pdf>
- Queensland Globe (2015) Queensland Government <https://www.business.qld.gov.au/running-business/support-assistance/mapping-data-imagery/queensland-globe>
- Queensland Government (2013) Animal Care and Protection Amendment Regulation (No. 2) 2013, Explanatory Notes for SL 2013 No. 103. Available at
https://www.legislation.qld.gov.au/LEGISLTN/SLS/RIS_EN/2013/13SL103E.pdf.
- Sarwar, G., Luecken, D., Yarwood, G., Whitten, G. Z., and W. P. L. Carter (2008) Impact of an updated carbon bond mechanism on predictions from the CMAQ modeling system: preliminary assessment, *J. Appl. Meteorol.*, 47, 3–14,
<https://doi.org/10.1175/2007jamc1393.1>.
- Simon, H., Baker, K.R. and S. Phillips (2012) Compilation and interpretation of photochemical model performance statistics published between 2006 and 2012. *Atmospheric Environment* 61, 124-139. <https://doi.org/10.1016/j.atmosenv.2012.07.012>
- Simon, H., Beck, L., Bhave, P. V., Divita Jr., F., Hsu, Y., Luecken, D., Mobley, J. D., Pouliot, G. A., Reff, A., Sarwar, G. and M. Strum (2010) The Development and Uses of EPA's SPECIATE Database, *Atmospheric Pollution Research*, 1: 196-206, 2010.
- Sustainable Table (2015) Free Range Egg and Chicken Guide. Available at
<http://www.sustainabletable.org.au/Hungryforinfo/Free-range-egg-and-chicken-guide/tabid/113/Default.aspx>.
- Texas Commission on Environmental Quality (2016a) Air Monitoring Comparison Values, Available: <https://www.tceq.texas.gov/toxicology/amcv/about>, Accessed 2/3/2017.
- Texas Commission on Environmental Quality (2016b) Effects Screening Levels, Available: https://www.tceq.texas.gov/toxicology/esl/list_main.html/#esl_1, Accessed: 2/3/2017.
- Thatcher, Marcus (2016) Evaluation of simulated meteorology for Surat Basin. CSIRO Report VIIRS hotspot data (<https://earthdata.nasa.gov/earth-observation-data/near-real-time/firms/viirs-i-band-active-fire-data>).

Appendix A CCAM meteorological performance

Key for the tables:

- TEMP = near surface dry bulb temperature (° C)
- WS10 = 10 m wind speed (m s⁻¹)
- U10 = east-west component of the wind vector (m s⁻¹)
- V10 = north-south component of the wind vector (m s⁻¹)
- obs = Observations
- mod = Model Predictions
- num_obs = Number of hourly-averaged values used for the statistics
- mea = Arithmetic mean
- std = Standard Deviation
- RMSE = Root Mean Square Error
- RMSE_S = Systematic Root Mean Square Error
- RMSE_U = Unsystematic Root Mean Square Error
- corr = Pearson Correlation Coefficient (0 = no correlation, 1 = exact correlation)
- IOA = Index of Agreement (0 = no agreement, 1 = perfect agreement)
- SKILL_E < 1 shows skill
- SKILL_V near to 1 shows skill
- SKILL_R < 1 shows skill
- Total possible no of obs - SON = 2184, DJF = 2184, MAM = 2208, JJA = 2208

Statistics used are from Hurley et al. (2005) and the formulas are given below:

O is the observed value, P is the predicted value, N is the number of observations/predictions and

$\hat{P}_i = a + bO_i$ is the linear regression fitted formula with intercept (a) and slope (b)

$$P_{mean} = \frac{1}{N} \sum_{i=1}^N P_i$$

$$O_{mean} = \frac{1}{N} \sum_{i=1}^N O_i$$

$$P_{std} = \sqrt{\frac{1}{N-1} \sum_{i=1}^N (P_i - P_{mean})^2}$$

$$O_{std} = \sqrt{\frac{1}{N-1} \sum_{i=1}^N (O_i - O_{mean})^2}$$

$$RMSE = \sqrt{\frac{1}{N} \sum_{i=1}^N (P_i - O_i)^2}$$

$$RMSE_S = \sqrt{\frac{1}{N} \sum_{i=1}^N (\hat{P}_i - O_i)^2}$$

$$RMSE_U = \sqrt{\frac{1}{N} \sum_{i=1}^N (\hat{P}_i - P_i)^2}$$

$$corr = \frac{N(\sum_{i=1}^N O_i P_i) - (\sum_{i=1}^N O_i)(\sum_{i=1}^N P_i)}{\sqrt{[N(\sum_{i=1}^N O_i^2) - (\sum_{i=1}^N O_i)^2][N(\sum_{i=1}^N P_i^2) - (\sum_{i=1}^N P_i)^2]}}$$

$$IOA = 1 - \frac{\sum_{i=1}^N (P_i - O_i)^2}{\sum_{i=1}^N (|P_i - O_{mean}| + |O_i - O_{mean}|)^2}$$

$$SKILL_E = \frac{RMSE_U}{O_{std}}$$

$$SKILL_V = \frac{P_{std}}{O_{std}}$$

$$SKILL_R = \frac{RMSE}{O_{std}}$$

The performance of CCAM is evaluated following Hurley et al. (2005), Cope and Emmerson (2016) and Cope et al. (2017). Validation of the simulated meteorology in the model is performed by comparing the model predictions with the meteorological observations at Miles Airport, Condamine, Hopeland, Tara Region and Burncluith. The observations are at a height of 10 m while the model values are at about 20 m.

Table A.1 shows performance statistics at Miles Airport for wind speed, wind direction and temperature from CCAM. For comparison purposes tables for the other sites follow. Each season is presented starting with SON at the top followed by DJF, MAM and JJA. Following Cope and Emmerson (2016) there are a number of criteria that need to be met to judge a model as performing well:

- Comparable observed and model means
- Comparable observed and model standard deviations - SKILL_V close to one
- Root Mean Square Error (RMSE) < the observed standard deviation – SKILL_E and SKILL_R < 1
- Index of Agreement (IOA) >> 0 (=1 for perfect agreement)

Miles Airport has less than 20 % difference between most observed and model means (for temperature and wind), while the standard deviations are comparable except for wind speed during DJF. The IOA is greater than 0.7 for all variables except for wind speed which registers the smallest IOA value during each season. Wind speed also has the smallest correlation coefficient, 0.5 – 0.6, while other variables have correlations greater than 0.7.

At the other sites there are similar results, the observed and model means have some values different by greater than 20 % but the values are small. The IOA tends to be good, roughly greater than 0.8 except for wind speed. In general the smallest correlation is seen for wind speed. Burncluith, a Regional site, while showing similar results for temperature, overestimates the wind speed by about 2 m s⁻¹.

Figure A.1 shows the probability density functions (pdf) for the wind speed, wind direction and temperature for Miles Airport. Those for the other sites follow in Figure A.2, Figure A.3, Figure A.4 and Figure A.5. The wind speed pdf at Miles Airport shows a good comparison for most of the year, although during JJA the frequency of light winds (< 3 m s⁻¹) is underpredicted and winds of 4-5 m s⁻¹ are overpredicted. The wind direction pdf comparison is good except that the frequency of north-easterlies is underpredicted. The model temperature pdf predicts two peaks so slightly overpredicts the frequency of higher temperatures 30 – 35° C.

Comparing all the sites generally temperature pdfs compare well, except for slight underpredictions of lower temperatures and slight overpredictions of higher temperatures. The

wind speed pdfs show, in general, a slight underprediction of lower wind speeds ($< 3 \text{ m s}^{-1}$) and a slight overprediction of higher wind speeds. Wind direction pdfs at Miles Airport and Condamine underpredict north easterlies while the other sites show a good comparison, also reproducing the reduction in north easterlies during winter. Burncluith shows the poorest comparison of all the sites for wind speed where low wind speeds are underpredicted particularly during MAM and JJA, and high wind speeds are overpredicted all year.

The results indicate that CCAM is showing skill for each of these variables, perhaps slightly less so for the wind speed particularly at Burncluith although the IOA values are generally good for all variables. This gives confidence in using CCAM meteorology to drive the CTM. A previous study in the Surat Basin evaluated the simulated CCAM meteorology during 2014 – 2015 and found similar results (Thatcher, 2016).

Time series of the observed and modelled temperature (Figure A.6), wind speed (Figure A.7) and wind direction (Figure A.8) at Miles Airport are shown for interest.

Table A.1 CCAM performance statistics for Miles Airport from top to bottom: SON, DJF, MAM, JJA.

Miles Airport	num_obs	mea_obs	mea_mod	std_obs	std_mod	RMSE	RMSE_S	RMSE_U	CORR	IOA	SKILL_E	SKILL_V	SKILL_R
TEMP – SON	1995	21.8	23.1	6.5	5.9	2.14	1.50	1.52	0.97	0.97	0.23	0.91	0.33
WS10 – SON	1995	3.7	3.8	1.6	1.6	1.56	0.77	1.35	0.52	0.72	0.85	1.00	0.98
U10 – SON	1995	-0.8	-0.6	2.7	2.6	2.03	0.84	1.85	0.71	0.84	0.69	0.98	0.76
V10 – SON	1995	-0.9	-0.9	2.8	3.0	2.16	0.57	2.08	0.72	0.85	0.76	1.10	0.78

Miles Airport	num_obs	mea_obs	mea_mod	std_obs	std_mod	RMSE	RMSE_S	RMSE_U	CORR	IOA	SKILL_E	SKILL_V	SKILL_R
TEMP – DJF	1294	26.2	27.7	5.1	4.9	2.35	1.60	1.72	0.94	0.94	0.34	0.96	0.46
WS10 – DJF	1293	3.8	4.0	1.4	1.7	1.64	0.61	1.52	0.47	0.68	1.09	1.23	1.17
U10 – DJF	1293	-1.0	-0.9	2.6	2.7	2.08	0.78	1.93	0.70	0.83	0.73	1.02	0.79
V10 - DJF	1293	-1.1	-1.1	2.7	3.1	2.14	0.44	2.09	0.74	0.86	0.76	1.13	0.78

Miles Airport	num_obs	mea_obs	mea_mod	std_obs	std_mod	RMSE	RMSE_S	RMSE_U	CORR	IOA	SKILL_E	SKILL_V	SKILL_R
TEMP – MAM	1718	21.3	22.4	6.3	5.4	2.12	1.53	1.47	0.96	0.97	0.23	0.87	0.34
WS10 – MAM	1719	3.1	3.3	1.4	1.5	1.27	0.47	1.17	0.64	0.79	0.86	1.11	0.92
U10 – MAM	1719	-0.7	-0.6	2.1	2.2	1.64	0.56	1.54	0.70	0.84	0.75	1.05	0.80
V10 - MAM	1719	-1.0	-1.0	2.3	2.7	1.74	0.27	1.72	0.77	0.87	0.73	1.15	0.74

Miles Airport	num_obs	mea_obs	mea_mod	std_obs	std_mod	RMSE	RMSE_S	RMSE_U	CORR	IOA	SKILL_E	SKILL_V	SKILL_R
TEMP – JJA	2204	13.8	14.9	5.1	4.7	1.92	1.27	1.44	0.95	0.96	0.28	0.93	0.38
WS10 – JJA	2206	3.1	3.7	1.4	1.5	1.37	0.75	1.14	0.64	0.77	0.81	1.05	0.96
U10 – JJA	2206	-0.6	-0.5	2.4	2.7	1.81	0.42	1.76	0.75	0.87	0.73	1.10	0.75
V10 - JJA	2206	-0.3	-0.4	2.3	2.9	1.98	0.19	1.97	0.73	0.84	0.86	1.26	0.86

Table A.2 CCAM performance statistics for Condamine from top to bottom: SON, DJF, MAM, JJA.

Condamine	num_obs	mea_obs	mea_mod	std_obs	std_mod	RMSE	RMSE_S	RMSE_U	CORR	IOA	SKILL_E	SKILL_V	SKILL_R
TEMP – SON													
WS10 – SON													
U10 – SON													
V10 – SON													

Condamine	num_obs	mea_obs	mea_mod	std_obs	std_mod	RMSE	RMSE_S	RMSE_U	CORR	IOA	SKILL_E	SKILL_V	SKILL_R
TEMP – DJF													
WS10 – DJF													
U10 – DJF													
V10 - DJF													

Condamine	num_obs	mea_obs	mea_mod	std_obs	std_mod	RMSE	RMSE_S	RMSE_U	CORR	IOA	SKILL_E	SKILL_V	SKILL_R
TEMP – MAM	2065	21.7	23.2	6.6	5.3	2.87	2.27	1.76	0.94	0.94	0.27	0.79	0.43
WS10 – MAM	2057	2.2	2.2	1.1	0.9	1.13	0.76	0.84	0.39	0.63	0.75	0.81	1.01
U10 – MAM	2057	-1.3	-1.1	1.7	1.5	1.19	0.61	1.03	0.73	0.85	0.61	0.90	0.71
V10 - MAM	2057	-0.4	0.0	1.1	1.5	1.16	0.40	1.08	0.70	0.78	1.00	1.40	1.07

Condamine	num_obs	mea_obs	mea_mod	std_obs	std_mod	RMSE	RMSE_S	RMSE_U	CORR	IOA	SKILL_E	SKILL_V	SKILL_R
TEMP – JJA	2208	13.4	15.1	5.4	4.5	2.77	2.13	1.76	0.92	0.92	0.33	0.84	0.51
WS10 – JJA	2208	2.6	2.5	1.4	0.9	1.31	1.04	0.80	0.43	0.62	0.57	0.63	0.93
U10 – JJA	2208	-0.4	0.0	2.3	1.9	1.40	0.86	1.10	0.81	0.88	0.48	0.82	0.61
V10 - JJA	2208	-0.2	0.2	1.8	1.8	1.30	0.58	1.16	0.76	0.86	0.64	0.99	0.72

Table A.3 CCAM performance statistics for Hopeland from top to bottom: SON, DJF, MAM, JJA.

Hopeland	num_obs	mea_obs	mea_mod	std_obs	std_mod	RMSE	RMSE_S	RMSE_U	CORR	IOA	SKILL_E	SKILL_V	SKILL_R
TEMP – SON	2156	21.1	23.0	6.6	5.7	2.94	2.27	1.87	0.94	0.94	0.28	0.86	0.45
WS10 – SON	2155	3.4	3.1	1.7	1.3	1.57	1.09	1.14	0.51	0.70	0.66	0.77	0.91
U10 – SON	2155	-1.3	-1.0	2.6	2.4	1.69	0.80	1.48	0.78	0.88	0.58	0.92	0.66
V10 – SON	2155	-0.9	-0.7	2.4	2.2	1.91	0.99	1.63	0.66	0.81	0.68	0.90	0.80

Hopeland	num_obs	mea_obs	mea_mod	std_obs	std_mod	RMSE	RMSE_S	RMSE_U	CORR	IOA	SKILL_E	SKILL_V	SKILL_R
TEMP – DJF	1779	25.3	27.1	4.8	4.9	2.76	1.91	1.98	0.91	0.92	0.41	1.01	0.57
WS10 – DJF	1779	3.8	3.4	1.5	1.5	1.58	0.90	1.30	0.47	0.68	0.86	0.97	1.05
U10 – DJF	1779	-2.1	-1.6	2.5	2.5	1.67	0.70	1.52	0.79	0.88	0.60	0.99	0.66
V10 - DJF	1779	-0.7	-0.4	2.3	2.1	1.82	0.90	1.58	0.67	0.81	0.69	0.93	0.80

Hopeland	num_obs	mea_obs	mea_mod	std_obs	std_mod	RMSE	RMSE_S	RMSE_U	CORR	IOA	SKILL_E	SKILL_V	SKILL_R
TEMP – MAM	2206	21.2	23.1	6.3	5.3	2.85	2.29	1.71	0.95	0.94	0.27	0.84	0.45
WS10 – MAM	2206	2.9	2.8	1.6	1.3	1.34	0.82	1.06	0.59	0.76	0.66	0.83	0.84
U10 – MAM	2206	-1.6	-1.4	2.3	2.1	1.31	0.54	1.19	0.83	0.91	0.52	0.93	0.57
V10 - MAM	2206	0.1	0.2	1.8	1.8	1.58	0.69	1.42	0.62	0.79	0.79	1.00	0.87

Hopeland	num_obs	mea_obs	mea_mod	std_obs	std_mod	RMSE	RMSE_S	RMSE_U	CORR	IOA	SKILL_E	SKILL_V	SKILL_R
TEMP – JJA	2207	13.5	15.1	5.2	4.6	2.55	1.85	1.75	0.92	0.93	0.33	0.87	0.49
WS10 – JJA	1992	3.0	3.1	1.7	1.3	1.30	0.89	0.95	0.66	0.79	0.56	0.74	0.76
U10 – JJA	1992	-0.1	-0.1	2.8	2.6	1.37	0.51	1.27	0.87	0.93	0.46	0.94	0.49
V10 - JJA	1992	0.4	0.4	2.0	2.1	1.58	0.51	1.50	0.71	0.84	0.74	1.05	0.78

Table A.4 CCAM performance statistics for Tara Region from top to bottom: SON, DJF, MAM, JJA.

Tara Region	num_obs	mea_obs	mea_mod	std_obs	std_mod	RMSE	RMSE_S	RMSE_U	CORR	IOA	SKILL_E	SKILL_V	SKILL_R
TEMP – SON	2184	22.1	23.2	6.1	5.7	1.98	1.29	1.50	0.96	0.97	0.25	0.94	0.33
WS10 – SON	2184	3.7	4.0	1.7	1.6	1.70	0.94	1.41	0.51	0.71	0.82	0.95	0.98
U10 – SON	2184	-1.0	-1.0	2.4	2.8	1.78	0.27	1.76	0.78	0.87	0.72	1.15	0.73
V10 – SON	2184	-1.3	-1.0	2.8	2.9	2.01	0.66	1.89	0.76	0.87	0.68	1.05	0.72

Tara Region	num_obs	mea_obs	mea_mod	std_obs	std_mod	RMSE	RMSE_S	RMSE_U	CORR	IOA	SKILL_E	SKILL_V	SKILL_R
TEMP – DJF	2174	25.7	27.2	4.7	4.9	2.47	1.47	1.98	0.91	0.93	0.42	1.03	0.52
WS10 – DJF	2174	3.4	4.0	1.5	1.8	1.80	0.87	1.57	0.47	0.66	1.05	1.19	1.20
U10 – DJF	2174	-1.5	-1.7	2.2	2.8	1.88	0.25	1.86	0.75	0.85	0.84	1.26	0.84
V10 - DJF	2174	-1.0	-0.7	2.4	2.8	2.06	0.57	1.98	0.70	0.83	0.83	1.17	0.86

Tara Region	num_obs	mea_obs	mea_mod	std_obs	std_mod	RMSE	RMSE_S	RMSE_U	CORR	IOA	SKILL_E	SKILL_V	SKILL_R
TEMP – MAM	2206	22.0	23.3	5.8	5.2	2.12	1.53	1.46	0.96	0.96	0.25	0.90	0.36
WS10 – MAM	2206	2.7	3.5	1.4	1.5	1.59	0.94	1.28	0.56	0.70	0.90	1.08	1.12
U10 – MAM	2206	-1.3	-1.5	1.9	2.4	1.47	0.26	1.45	0.80	0.88	0.77	1.30	0.78
V10 - MAM	2206	-0.4	-0.1	2.0	2.5	1.75	0.42	1.70	0.72	0.83	0.85	1.22	0.87

Tara Region	num_obs	mea_obs	mea_mod	std_obs	std_mod	RMSE	RMSE_S	RMSE_U	CORR	IOA	SKILL_E	SKILL_V	SKILL_R
TEMP – JJA	2208	13.8	15.0	4.8	4.5	1.92	1.30	1.42	0.95	0.96	0.29	0.94	0.40
WS10 – JJA	2208	2.8	3.8	1.6	1.5	1.60	1.14	1.12	0.65	0.74	0.70	0.92	1.00
U10 – JJA	2208	-0.1	0.1	2.3	2.9	1.52	0.30	1.49	0.86	0.91	0.65	1.28	0.66
V10 - JJA	2208	0.0	0.3	2.3	2.8	1.69	0.29	1.67	0.80	0.88	0.72	1.21	0.73

Table A.5 CCAM performance statistics for Burncluith from top to bottom: SON, DJF, MAM, JJA.

Burncluith	num_obs	mea_obs	mea_mod	std_obs	std_mod	RMSE	RMSE_S	RMSE_U	CORR	IOA	SKILL_E	SKILL_V	SKILL_R
TEMP – SON	2184	20.9	22.6	6.3	5.7	2.63	1.91	1.81	0.95	0.95	0.29	0.90	0.42
WS10 – SON	2184	2.0	3.6	1.2	1.5	2.07	1.63	1.26	0.52	0.58	1.01	1.18	1.65
U10 – SON	2184	-0.6	-1.1	1.7	2.7	1.85	0.59	1.75	0.76	0.81	1.04	1.61	1.10
V10 – SON	2184	-0.4	-0.7	1.5	2.5	1.81	0.36	1.78	0.70	0.78	1.16	1.62	1.19

Burncluith	num_obs	mea_obs	mea_mod	std_obs	std_mod	RMSE	RMSE_S	RMSE_U	CORR	IOA	SKILL_E	SKILL_V	SKILL_R
TEMP – DJF	2174	24.8	26.5	4.6	5.0	2.55	1.72	1.88	0.93	0.93	0.40	1.08	0.55
WS10 – DJF	2174	2.0	3.8	1.1	1.6	2.30	1.80	1.43	0.49	0.50	1.35	1.55	2.17
U10 – DJF	2174	-1.1	-1.9	1.5	2.7	2.03	0.96	1.79	0.75	0.76	1.17	1.77	1.32
V10 - DJF	2174	-0.3	-0.2	1.3	2.5	1.93	0.40	1.88	0.67	0.72	1.44	1.93	1.47

Burncluith	num_obs	mea_obs	mea_mod	std_obs	std_mod	RMSE	RMSE_S	RMSE_U	CORR	IOA	SKILL_E	SKILL_V	SKILL_R
TEMP – MAM	2208	21.0	22.8	6.1	5.3	2.63	2.07	1.62	0.95	0.95	0.26	0.86	0.43
WS10 – MAM	2208	1.7	3.4	1.2	1.5	2.07	1.70	1.19	0.59	0.59	1.01	1.26	1.77
U10 – MAM	2208	-0.8	-1.6	1.5	2.4	1.78	0.97	1.49	0.79	0.80	1.00	1.64	1.19
V10 - MAM	2208	0.0	0.2	1.2	2.2	1.67	0.30	1.64	0.66	0.73	1.38	1.85	1.41

Burncluith	num_obs	mea_obs	mea_mod	std_obs	std_mod	RMSE	RMSE_S	RMSE_U	CORR	IOA	SKILL_E	SKILL_V	SKILL_R
TEMP – JJA	2208	13.6	15.2	5.4	4.5	2.64	2.01	1.71	0.92	0.93	0.32	0.83	0.49
WS10 – JJA	2208	2.0	3.6	1.5	1.4	2.02	1.70	1.09	0.65	0.65	0.74	0.98	1.37
U10 – JJA	2208	0.3	0.3	1.8	2.9	1.65	0.66	1.51	0.85	0.87	0.83	1.59	0.91
V10 - JJA	2208	0.4	0.5	1.6	2.6	1.75	0.27	1.73	0.74	0.81	1.07	1.57	1.08

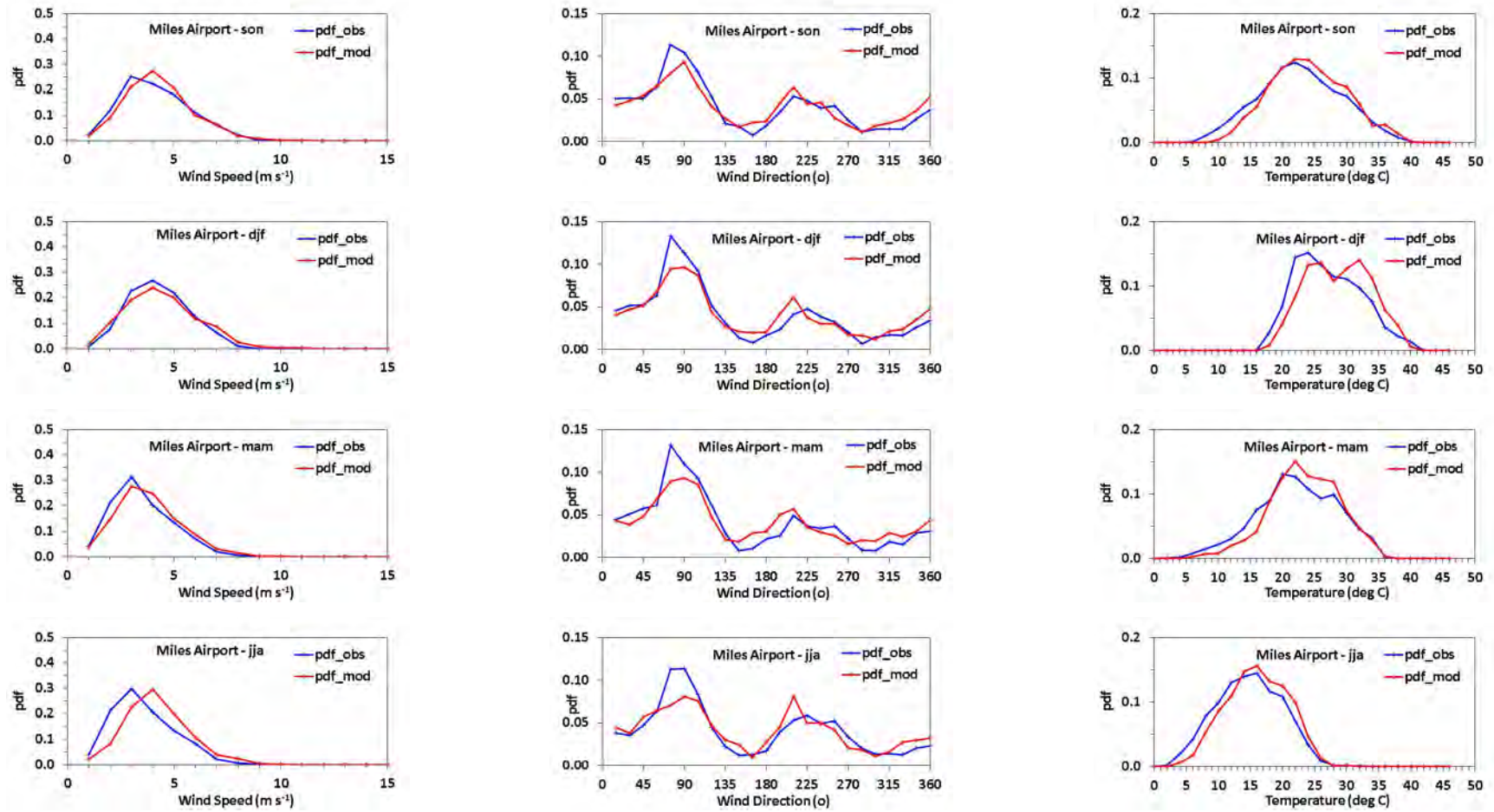


Figure A.1 The observed and modelled probability density functions for (left) wind speed ($m s^{-1}$), (middle) wind direction (degrees) and (right) temperature ($^{\circ} C$) (right) at Miles Airport for all seasons.

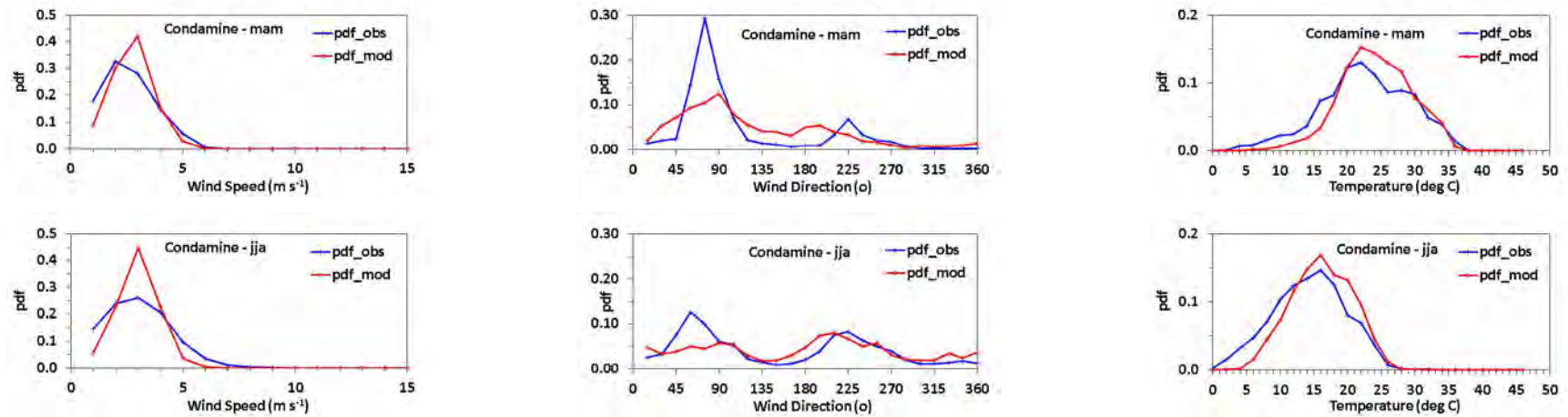


Figure A.2 The observed and modelled probability density functions for (left) wind speed (m s^{-1}), (middle) wind direction (degrees) and (right) temperature ($^{\circ}\text{C}$) (right) at Condamine for all seasons.

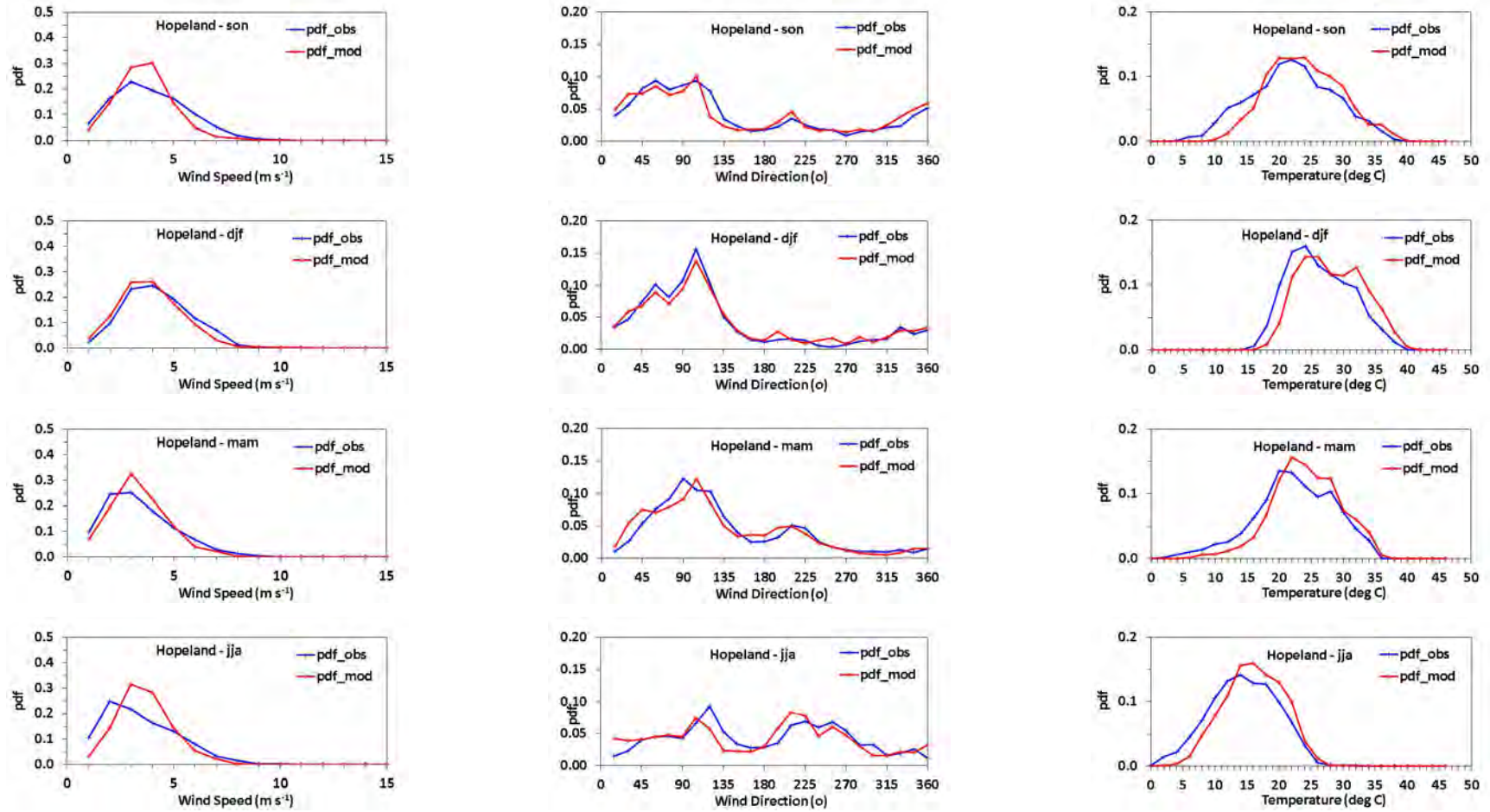


Figure A.3 The observed and modelled probability density functions for (left) wind speed (m s^{-1}), (middle) wind direction (degrees) and (right) temperature ($^{\circ}\text{C}$) (right) at Hopeland for all seasons.

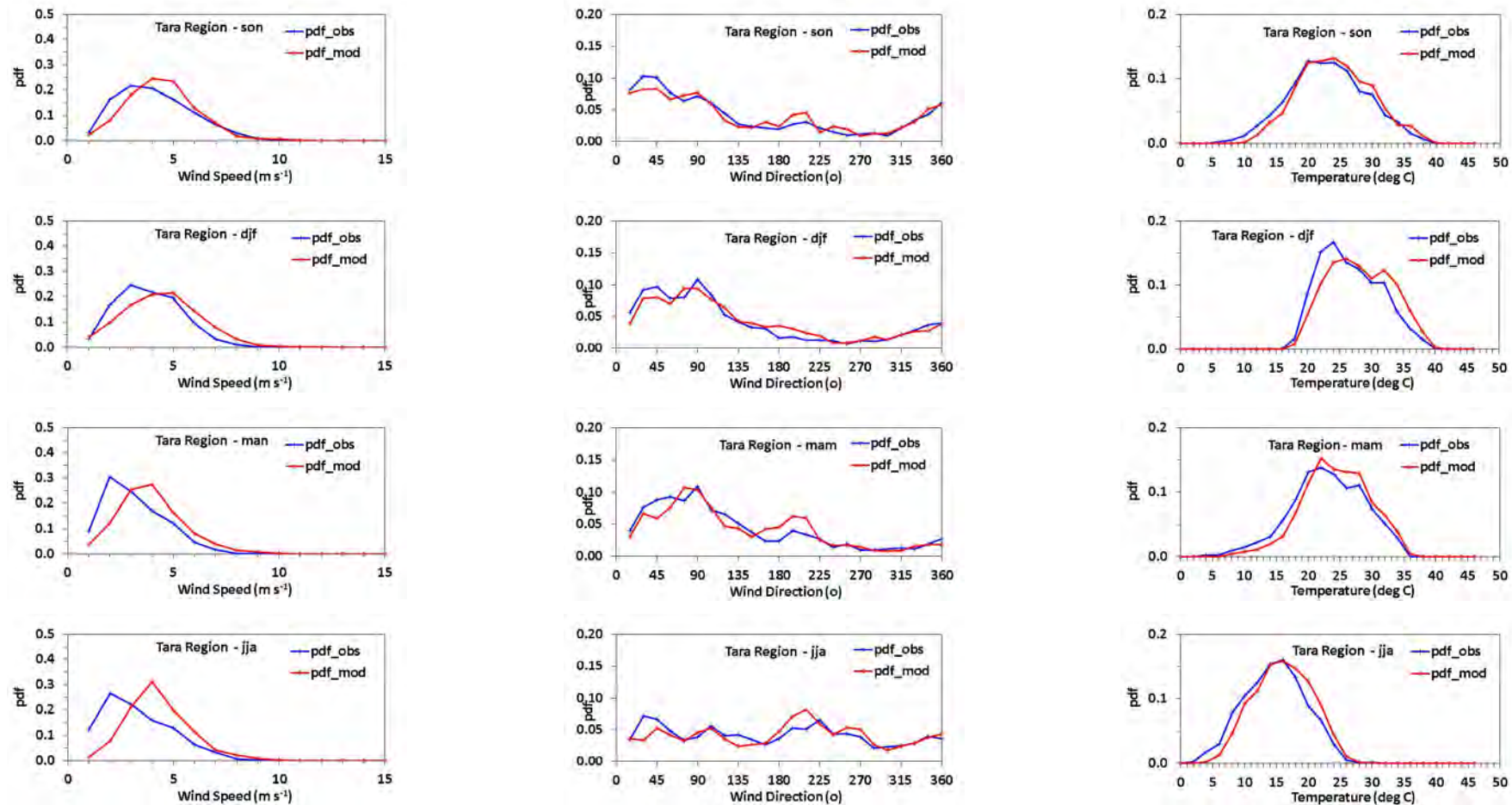


Figure A.4 The observed and modelled probability density functions for (left) wind speed (m s^{-1}), (middle) wind direction (degrees) and (right) temperature ($^{\circ}\text{C}$) (right) at Tara Region for all seasons.

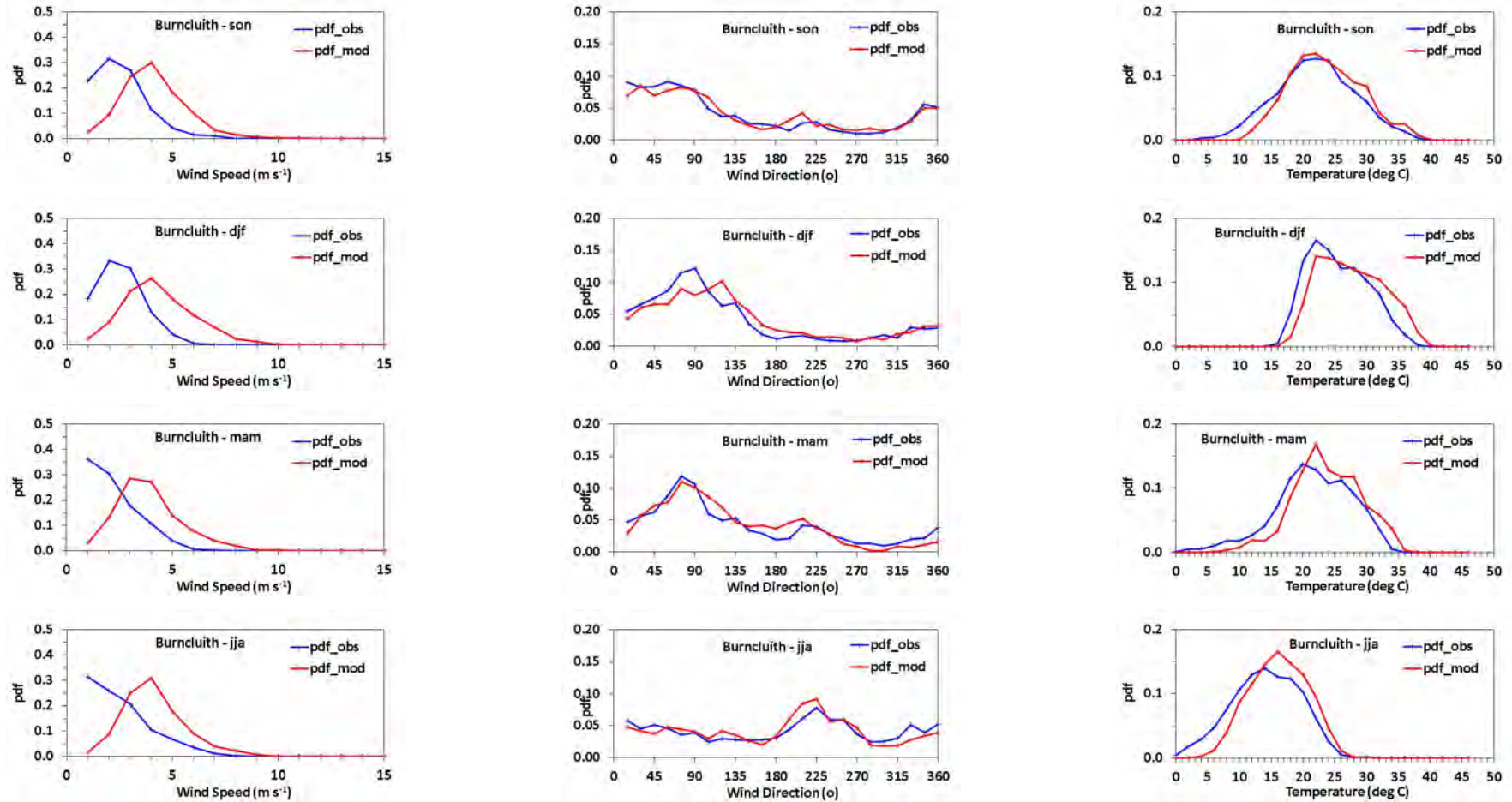


Figure A.5 The observed and modelled probability density functions for (left) wind speed (m s^{-1}), (middle) wind direction (degrees) and (right) temperature ($^{\circ}\text{C}$) (right) at Burncluith for all seasons.

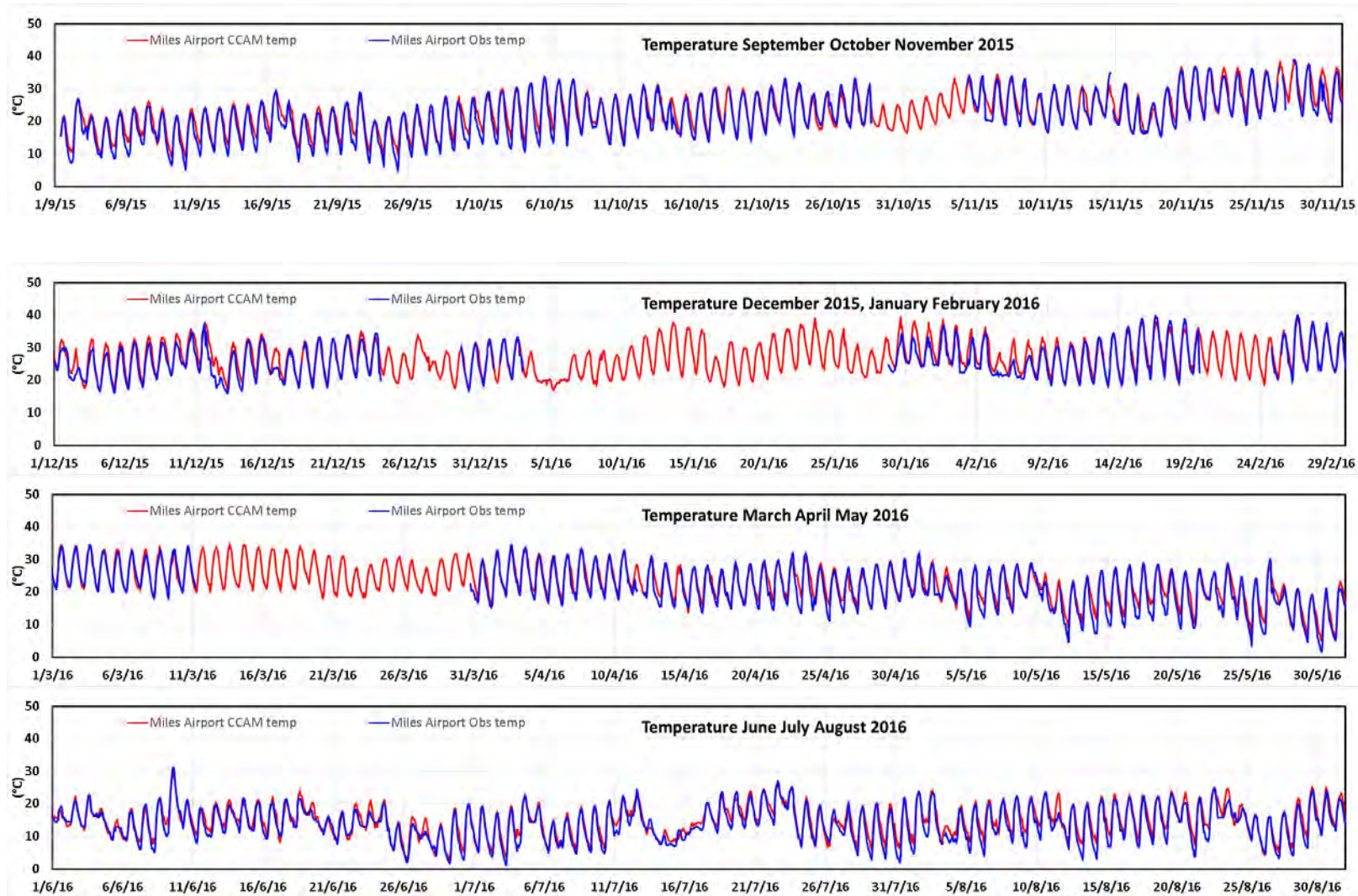


Figure A.6 The observed and modelled time series for temperature (° C) at Miles Airport for the modelled year (blue=observations, red=model).

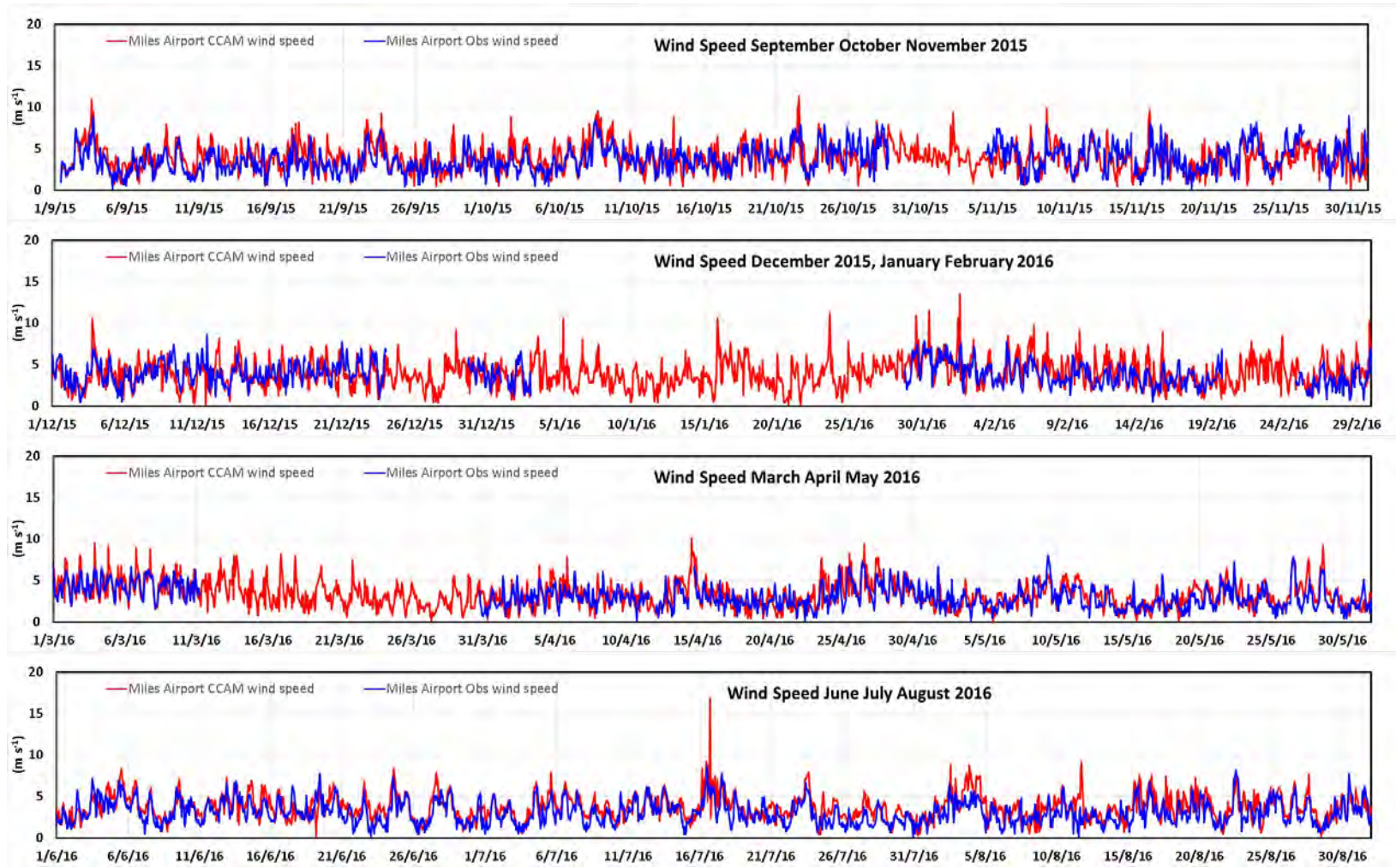


Figure A.7 The observed and modelled time series for wind speed (m s^{-1}) at Miles Airport for the modelled year (blue=observations, red=model).

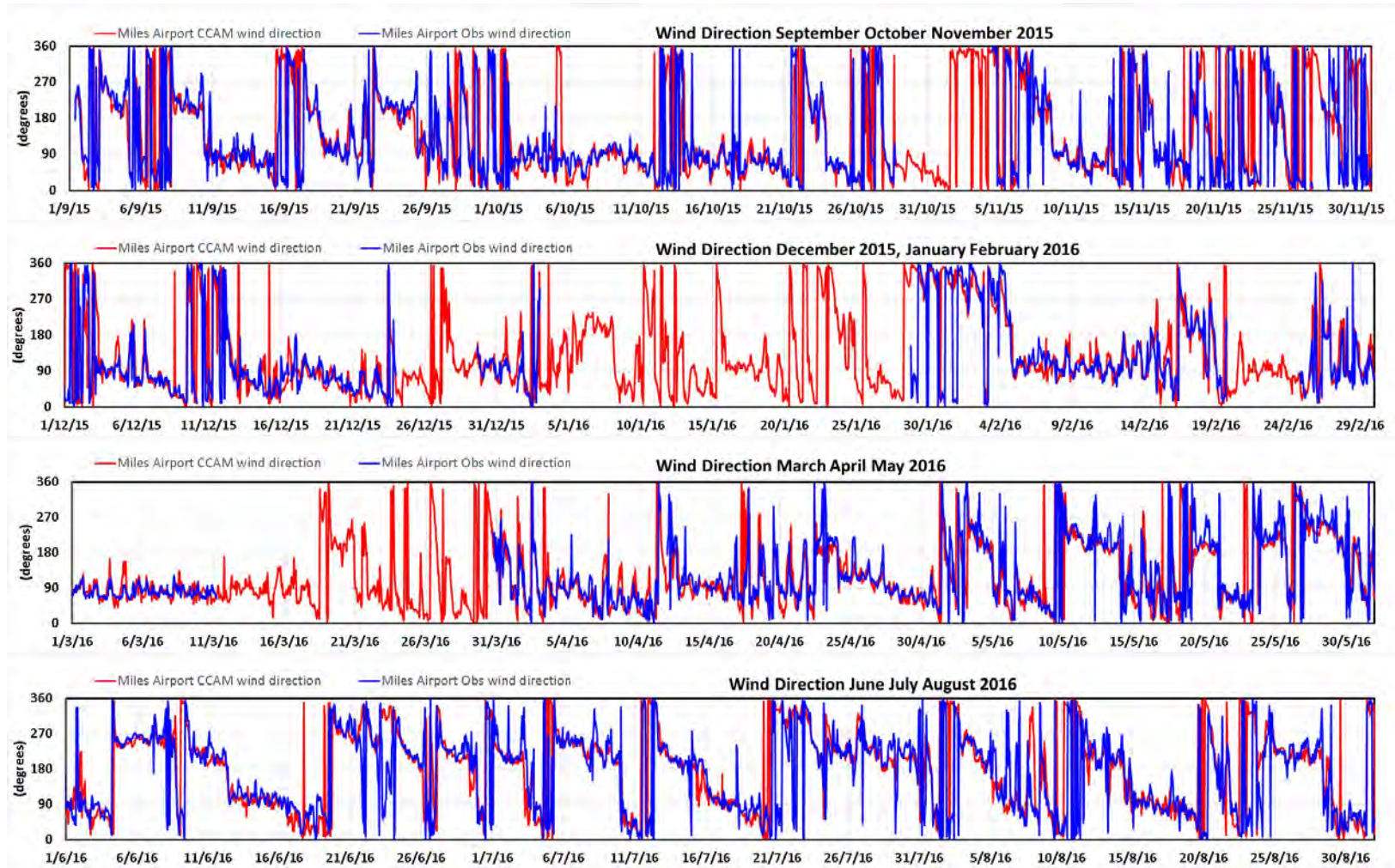


Figure A.8 The observed and modelled time series for wind direction (degrees) at Miles Airport for the modelled year (blue=observations, red=model).

Appendix B CTM Performance Information

The performance of the CTM is evaluated following Cope and Emmerson (2016) and Cope et al. (2017). Cope and Emmerson (2016) point out that because the CTM is an ensemble mean and volume averaged model (like most regional models) and observations are collected at point locations differences between paired observations and model results may be expected before the many other reasons for differences are considered (e.g. meteorology, emissions, resolution).

To properly evaluate the CTM a range of statistical approaches should be used. They note that for a study over a 12-month period robust metrics such as mean bias, mean error, fraction bias and error, and qualitative measures such as time series plots should be used (Simon et al., 2012). Other metrics such as Index of Agreement (IOA), and the correlation coefficient may still be used but since they provide a measure of the relationship between observations and model results that have been paired in time and space the inherent difficulty of the test needs to be considered.

The following performance information for PM_{2.5}, O₃ and NO₂ includes:

- time series – the observed and modelled comparisons are presented in the main report (Section 5 and Appendix D)
- statistical summary based on the paired observed and modelled data (Hurley et al., 2005), statistical definitions are presented in Appendix A
 - the observed and modelled mean concentrations
 - the observed and modelled standard deviation
 - root mean square errors (RMSE), unsystematic (RMSEu) and systematic (RMSEs)
 - Pearson correlation coefficient (=0 no correlation, =1 exact correlation)
 - IOA 0 no agreement, IOA = 1 perfect agreement
 - SKILL_e = RMSE_u / OBS_{std} (< 1 shows skill)
 - SKILL_v = CTM_{std} / OBS_{std} (near to 1 shows skill)
 - SKILL_r = RMSE / OBS_{std} (< 1 shows skill)
- Quantile-quantile plots (q-q plots) – compare the unpaired observed and modelled concentrations and are used commonly in air quality model evaluation studies (e.g. Luhar and Hurley, 2003, Luhar et al., 2018). It is a plot of the sorted observed concentrations against the sorted modelled concentrations. If all the points are on the 1:1 line then the observed and modelled data come from a population with the same distribution.

For a model to perform well the following are considered (note: According to Simon et al., (2012) perfect agreement for any one metric is not by itself indicative of good model performance, multiple metrics need to be considered.):

- Comparable observed and model means

- Comparable observed and model standard deviations - SKILLv close to one
- Root Mean Square Error (RMSE) < the observed standard deviation - SKILLe and SKILLr < 1
- Systematic Root Mean Square Error (RMSEs) and the Unsystematic Root Mean Square Error (RMSEu) < the observed standard deviation
- Index of Agreement (IOA) >> 0 (=1 for perfect agreement)
- q-q plots – observed and modelled data are close to the 1:1 line.

PM_{2.5}

Time series plots of the observed and modelled concentrations of 1-hour average PM_{2.5} (Figure 5.1 and Appendix D) at the Gas field sites show broad agreement with the model capturing the background values of PM_{2.5} and periods of slightly elevated PM_{2.5}. There are a number of observed peaks of PM_{2.5} that do not appear in the modelled Gas field sites PM_{2.5} data. Many of the larger and broader observed peaks are due to fires which the model has simulated reasonably well but does not produce exact matches in time and space with the observations (see Section 5.1.1).

Figure B.1 shows the 24-hour PM_{2.5} statistical analysis results for each season for the Gas field sites (there are no PM_{2.5} observations at the Regional sites). There is generally agreement between the 24-hour PM_{2.5} observed and modelled mean values with the difference between them 2 – 16 % of the observed mean, with the largest difference during SON when vegetation fires occurred.

The standard deviations for the observations and the model are small during DJF and MAM with differences between the modelled and observed values of 21 % and 32 %, respectively. During SON and JJA the observed standard deviation is larger than modelled by 35 % and 47 %, respectively.

The RMSE, RMSEs and RMSEu are all less than the observed standard deviation (SKILLe and SKILLr < 1) for SON and JJA while during DJF and MAM only the RMSEs is less than the observed standard deviation.

The correlation coefficients are 0.09 – 0.71 which range from the lowest end to the higher end of similar studies (Simon et al., 2012). The IOA ranges from 0.41 – 0.75 and since values above 0.5 are considered to be a good result (Hurley et al., 2005) all seasons except for MAM are doing well for this statistic. For these measures the model PM_{2.5} performs better during SON and JJA.

Figure B. shows q-q plots of the observed and modelled 24-hour average PM_{2.5} for the Gas field sites for all seasons. Most of the q-q plots show that the model is doing very well for PM_{2.5} concentration values below about 10 µg m⁻³. For PM_{2.5} concentration values greater than 10 µg m⁻³ the model tends to underpredict during all seasons except for Condamine during MAM. For Hopeland during JJA the model underpredicts PM_{2.5} concentrations greater than about 30 µg m⁻³.

As discussed in Section 5.1.1 the model does not predict the larger PM_{2.5} concentration peaks associated with fires. The model predicts the fires but does not model them at the concentration, time and location as observed. As Cope et al. (2017) found the model is challenged to capture the most extreme observed PM_{2.5} events.

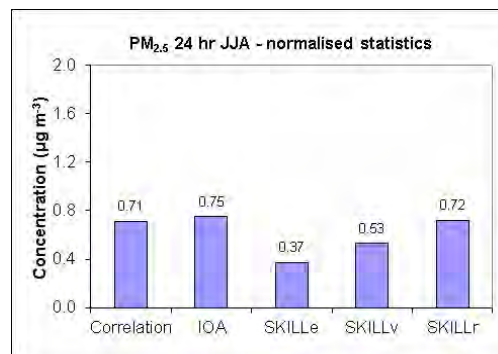
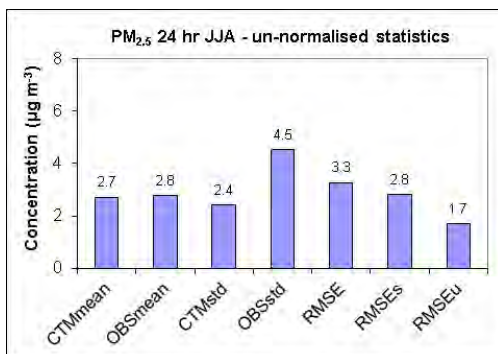
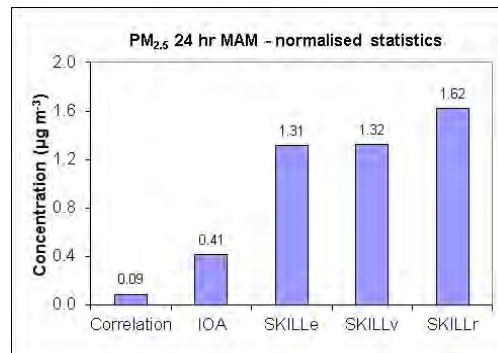
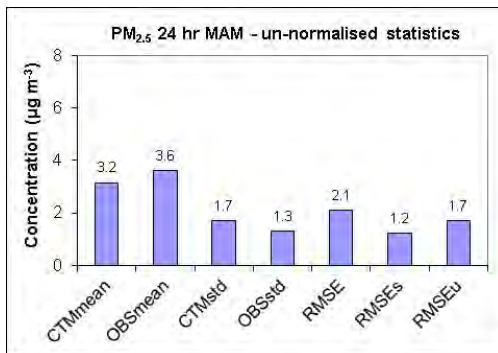
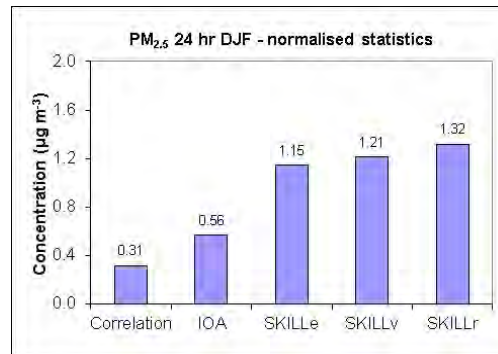
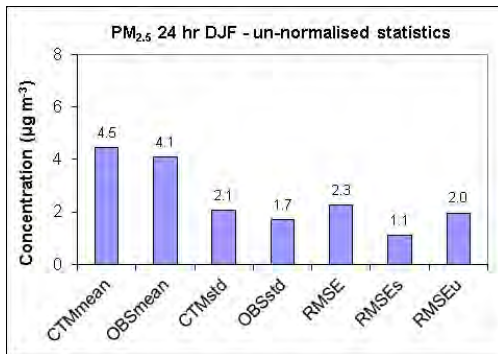
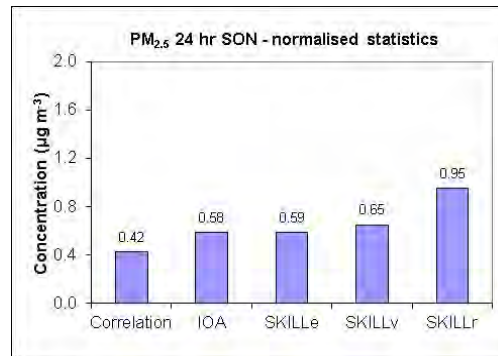
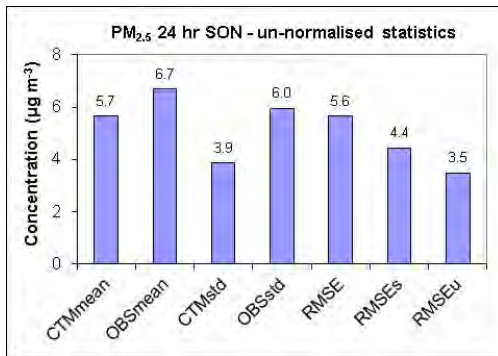


Figure B.1 The CTM performance for the 24-hour averaged PM_{2.5} concentration (µg m⁻³) at the Gas field sites during the given season. Key: OBS = Observations; CTM = Model Predictions; mean = Arithmetic mean; std = Standard Deviation; RMSE = Root Mean Square Error; RMSEs = Systematic Root Mean Square Error; RMSEu = Unsystematic Root Mean Square Error; correlation = Pearson Correlation Coefficient (0 = no correlation, 1 = exact correlation); IOA = Index of Agreement (0 = no agreement, 1 = perfect agreement); SKILL_E=(RMSE_U)/(STD_{OBS}) (<1 shows skill); SKILL_V=(STD_{MOD})/(STD_{OBS}) (near to 1 shows skill); SKILL_R=(RMSE)/(STD_{OBS}) (<1 shows skill).

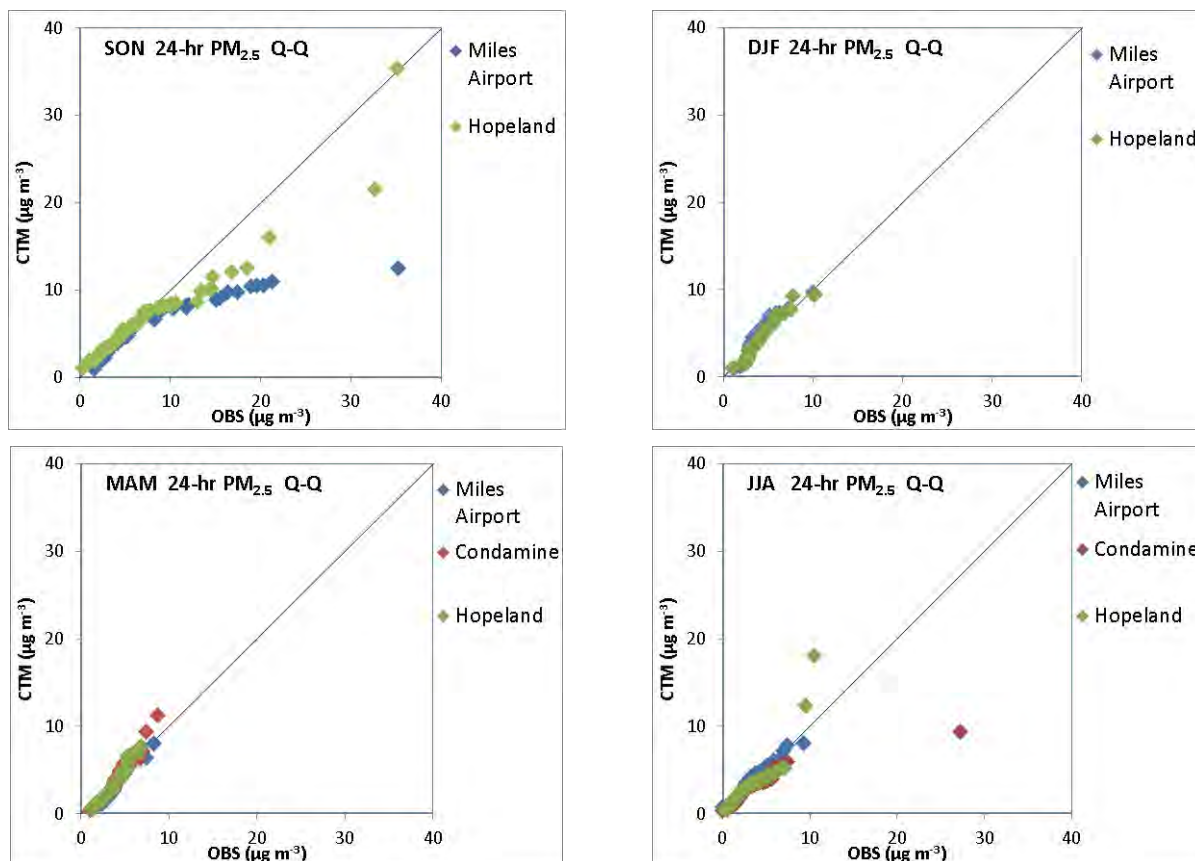


Figure B.2 Quantile-quantile plots of the observed and modelled 24-hour averaged $PM_{2.5}$ ($\mu g m^{-3}$) at the Gas field sites.

O₃

Time series plots of the observed and modelled concentrations of O₃ show reasonable agreement in the diurnal pattern of maximum concentrations during the middle of the day (or later in the afternoon) and minimum concentrations during the night-time and early-morning hours. The CTM also reproduced well the observed time periods with reduced amplitude in the diurnal pattern. There was some underprediction and overprediction of maxima and minima at various sites (see Section 5.2.1).

Figure B. and Figure B.4 show the 1-hour and 4-hour O₃ statistical analysis results for each season for the Gas field and Regional sites (when data was available). There is generally agreement between the observed and modelled O₃ means (1-hour and 4-hour) with the difference between them 3 – 22 % of the observed mean, with the largest difference during DJF.

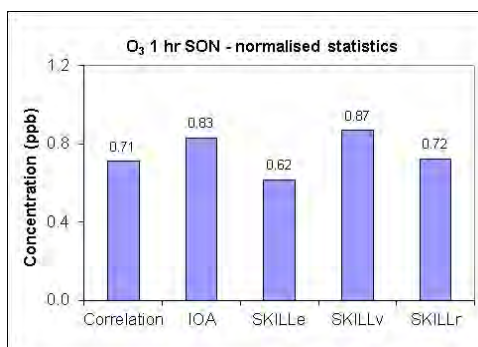
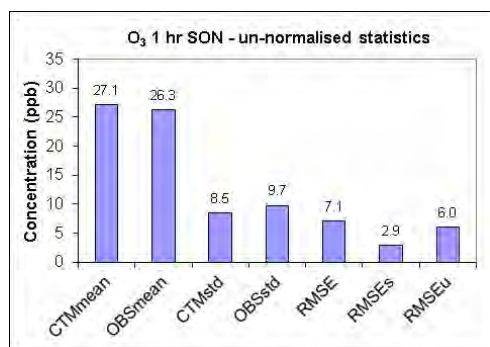
The standard deviations are comparable as shown by SKILL_v being 5 – 13 % less than one and the RMSE, RMSE_s and RMSE_u are all less than the OBS_{std} (SKILL_e and SKILL_r < 1) which indicates that the model is performing well.

The correlation coefficients are 0.59 – 0.74 which are similar to other studies (Simon et al., 2012) and the IOA ranges from 0.77 – 0.84. These all indicate model skill.

Figure B. and Figure B. show q-q plots of the observed and modelled 1-hour and 4-hour averaged O₃ concentrations respectively for the Gas field and Regional sites for all seasons. Most of the q-q

plots show that the model is doing reasonably well, although there tends to be a consistent small overestimation or underestimation at most sites during particular seasons. For example at Miles Airport 1-hour O₃ concentrations are slightly underestimated during SON and slightly overestimated during DJF, while at Hopeland 1-hour O₃ concentrations are slightly overestimated during SON and DJF and slightly underestimated during JJA. During DJF and MAM the model tends to overpredict some of the larger O₃ values. At Burncluth 4-hour O₃ concentrations during JJA are overestimated more than at other sites and more so for smaller and larger O₃ values (at Burncluth low wind speed frequencies were underpredicted and high wind speed frequencies were overpredicted during JJA).

Overall the statistical analysis suggests satisfactory model performance on the whole, with generally some underprediction of larger O₃ concentration values and some small seasonal bias in O₃ concentrations. The statistical analysis has similar results to other studies (Cope and Emmerson, 2016).



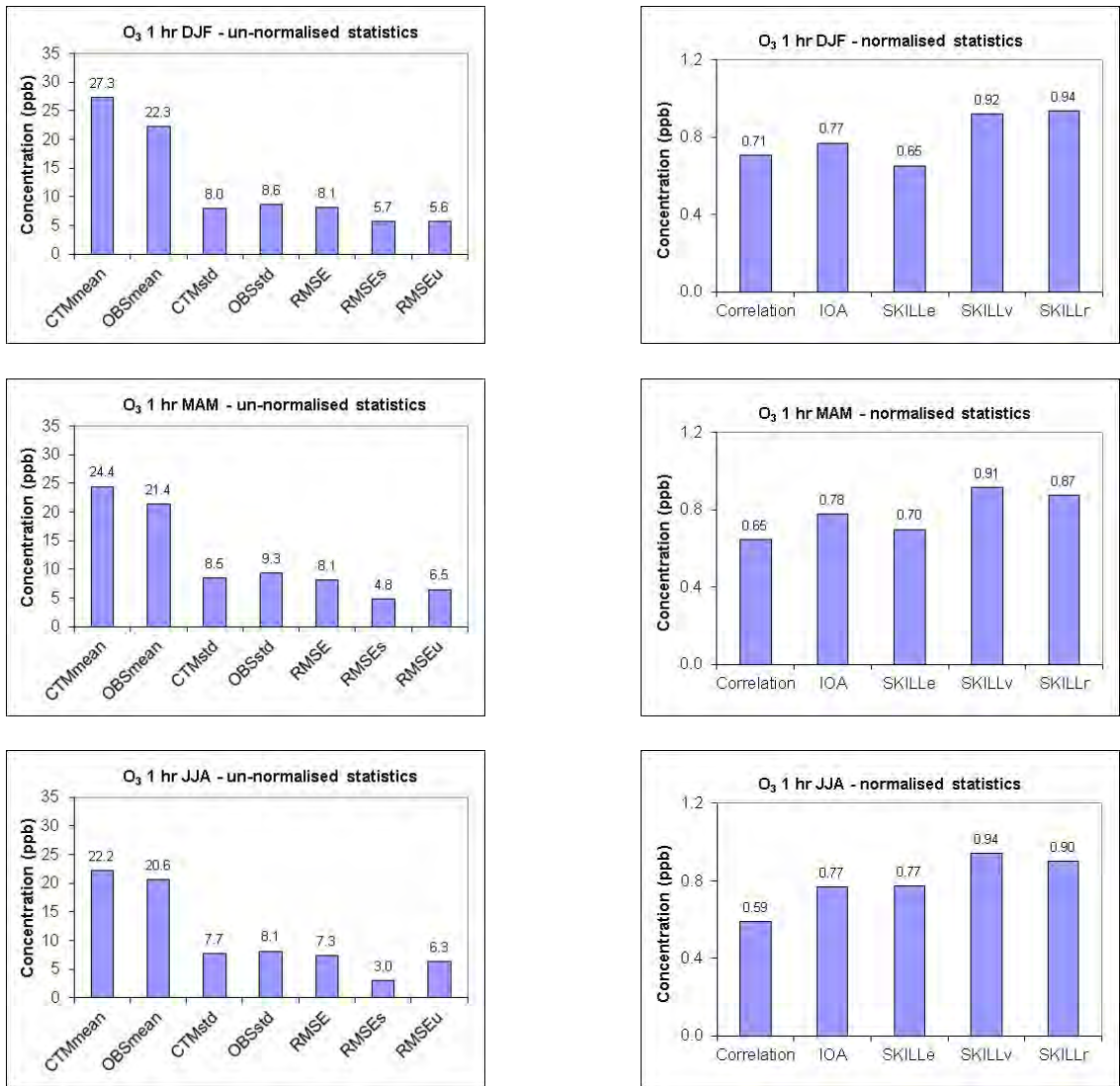


Figure B.3 The CTM performance for the 1-hour averaged O₃ concentration (ppb) at the Gas field and Regional sites during the given season. Key: OBS = Observations; CTM = Model Predictions; mean = Arithmetic mean; std = Standard Deviation; RMSE = Root Mean Square Error; RMSEs = Systematic Root Mean Square Error; RMSEu = Unsystematic Root Mean Square Error; correlation = Pearson Correlation Coefficient (0 = no correlation, 1 = exact correlation); IOA = Index of Agreement (0 = no agreement, 1 = perfect agreement); SKILL_E=(RMSE_U)/(STD_{OBS}) (<1 shows skill); SKILL_V=(STD_{MOD})/(STD_{OBS}) (near to 1 shows skill); SKILL_R=(RMSE)/(STD_{OBS}) (<1 shows skill).

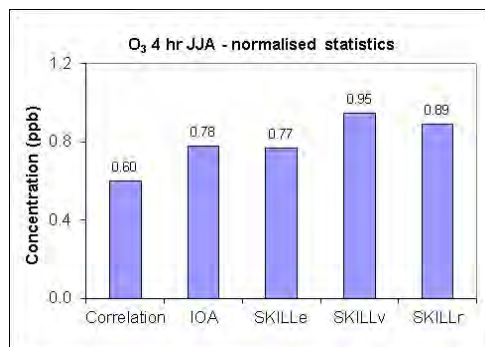
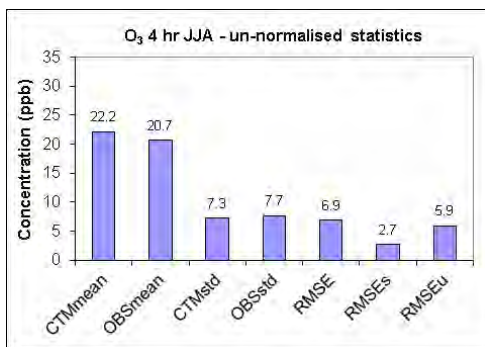
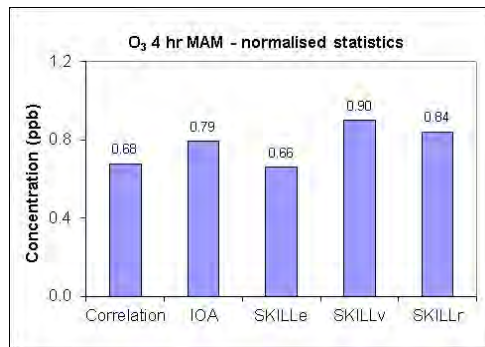
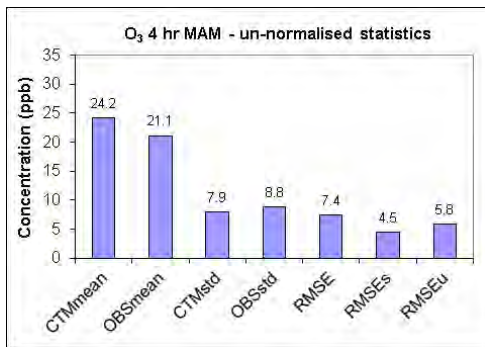
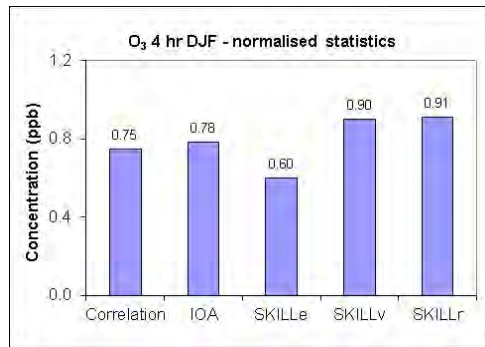
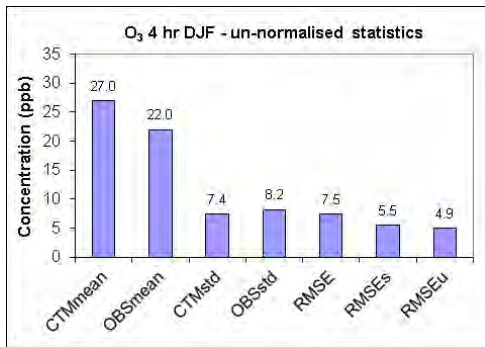
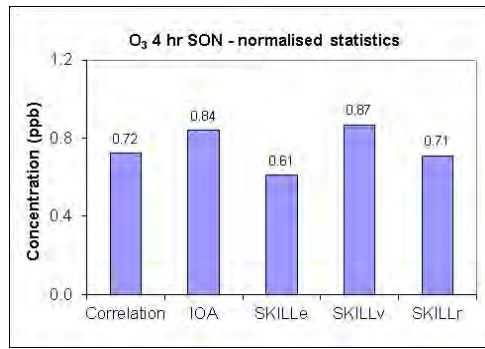
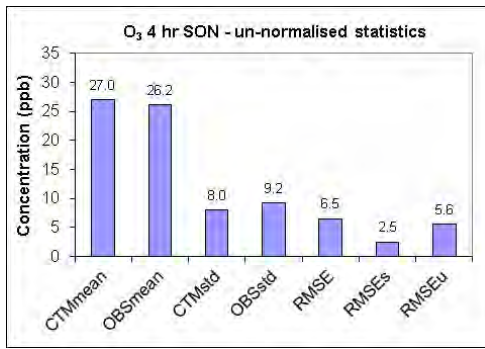


Figure B.4 The CTM performance for the 4-hour averaged O₃ concentration (ppb) at the Gas field and Regional sites during the given season. Key: OBS = Observations; CTM = Model Predictions; mean = Arithmetic mean; std = Standard Deviation; RMSE = Root Mean Square Error; RMSEs = Systematic Root Mean Square Error; RMSEu = Unsystematic Root Mean Square Error; correlation = Pearson Correlation Coefficient (0 = no correlation, 1 = exact correlation); IOA = Index of Agreement (0 = no agreement, 1 = perfect agreement); SKILL_E=(RMSE_U)/(STD_{OBS}) (<1 shows skill); SKILL_V=(STD_{MOD})/(STD_{OBS}) (near to 1 shows skill); SKILL_R=(RMSE)/(STD_{OBS}) (<1 shows skill).

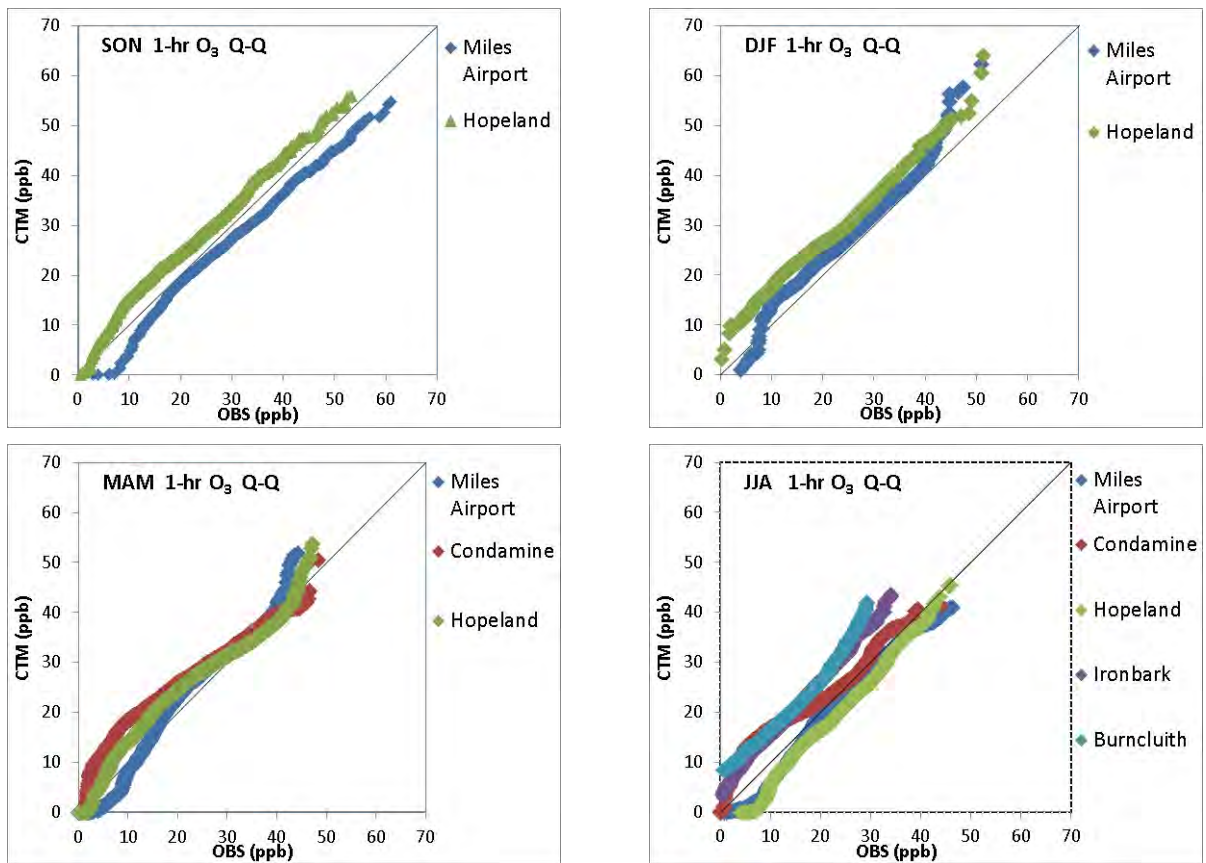


Figure B.5 Quantile-quantile plots of the observed and modelled 1-hour averaged O₃ (ppb) at the Gas field and Regional sites.

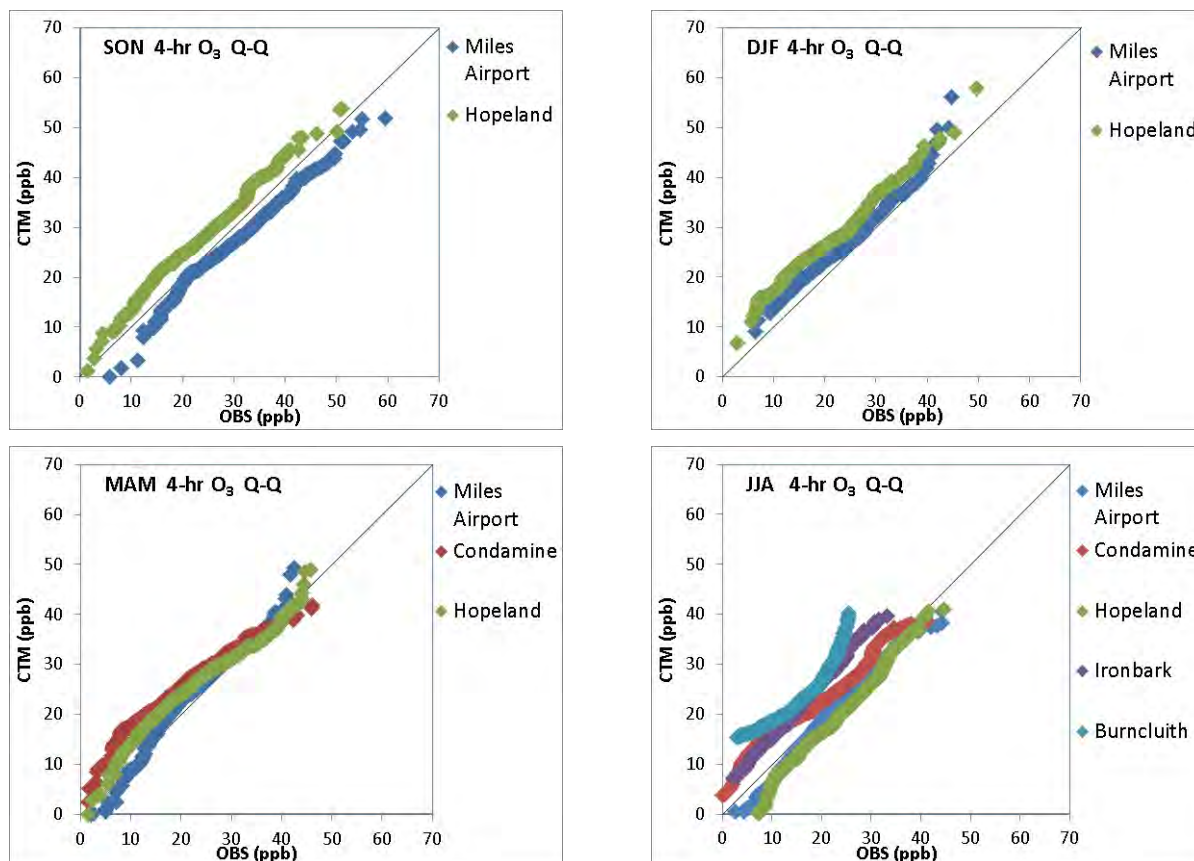


Figure B.6 Quantile-quantile plots of the observed and modelled 4-hour averaged O₃ (ppb) at the Gas field and Regional sites.

NO₂

Time series plots of observed and modelled 1-hour average NO₂ concentrations at Miles Airport (Figure 5.26) shows the background NO₂ is mostly captured by the model (except during SON), whereas the modelled NO₂ overestimates many of the observed peak values. Importantly even though the magnitude of the peaks is overestimated the frequency and timing of a number of the peaks are captured by the model. Comparing the time series during SON with that during MAM shows the model reproduces the increased frequency of peaks as observed but less so in the other seasons. The comparison at Condamine (see Appendix D) is similar to that at Miles Airport. At Hopeland, the observed NO₂ time series has fewer and smaller peaks than at the other Gas field sites and the model overestimates the magnitude of these peak values particularly during JJA. At the Regional sites there are NO₂ observations for most of JJA and the observed and modelled peaks are smaller compared to those at the Gas field sites. However the model still overestimates the magnitude of the peaks.

Figure B.1 shows the 1-hour NO₂ concentration statistical analysis results for each season for the Gas field and Regional sites (when data was available). Except during SON there is generally agreement between the 1-hour NO₂ observed and modelled means with differences between 0 – 14 % of the observed mean. During SON there is a 46 % difference between the observed and modelled means.

The standard deviations for the modelled 1-hour NO₂ concentrations are generally twice the observed, highlighting the much larger variation within the modelled results compared to the observed. SKILLv a measure of how close the standard deviations are between observed and modelled is well over one for all seasons, showing very low skill.

The other statistical measures all show very little skill, SKILLe and SKILLr are well above one and the correlation and the IOA are all low.

Figure B.8 shows q-q plots of the observed and modelled 1-hour average NO₂ concentrations for the Gas field and Regional sites for all seasons. Most of the q-q plots show that the model is doing reasonably well for only the small NO₂ concentration values below about 5 ppb. For NO₂ concentration values greater than about 5 ppb the model overpredicts during all seasons, as is seen in the overprediction of peaks in the time series comparison.

The modelled concentration of the 1-hour average NO₂ is mostly larger than the observed and there are a number of possible reasons why the model overestimates the CSG-related NO₂ peaks: 1) NO_x emissions may be overestimated at some CSG-related emission sources, 2) the effective height of release of some CSG-related emissions may not be correctly represented in the model, 3) the time pattern of release of some CSG-related emission sources may not be correctly represented in the model and/or 4) the height of the night-time boundary layer may not be correctly represented in the model.

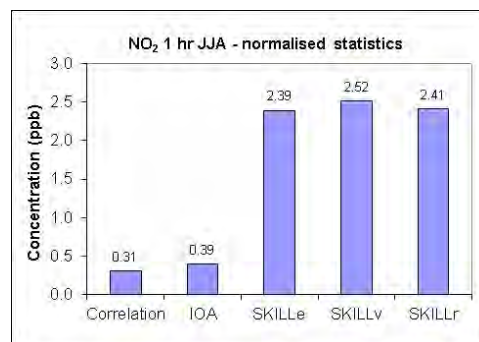
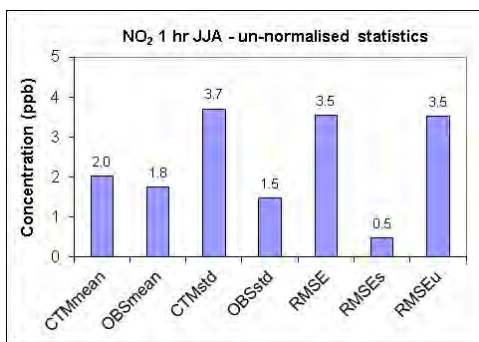
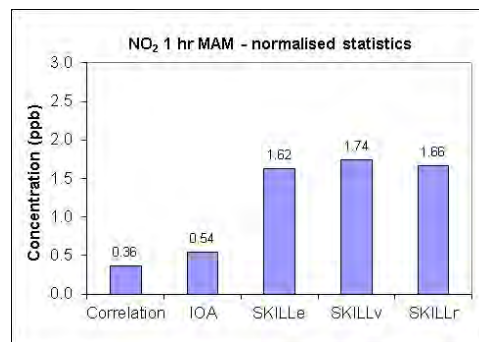
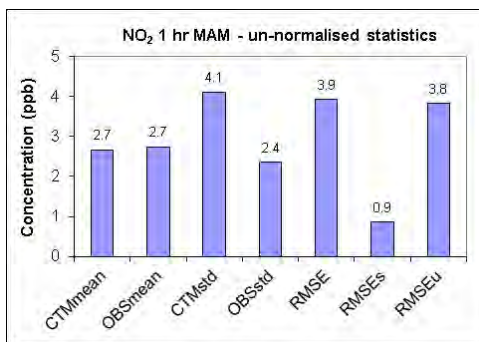
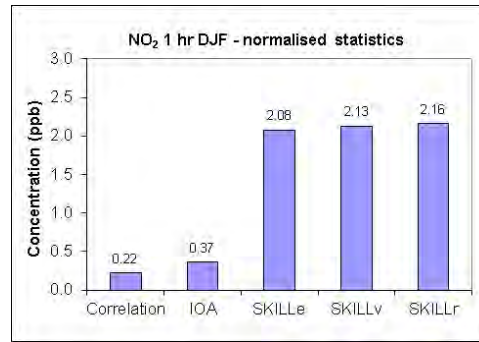
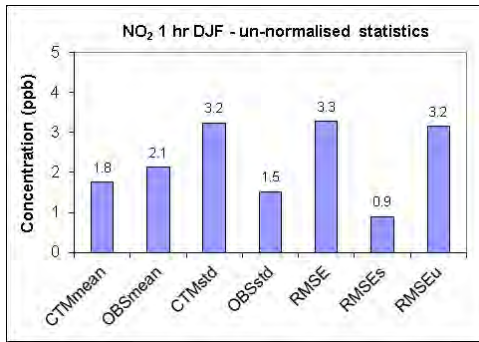
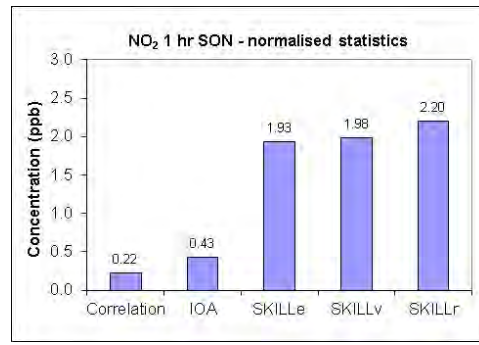
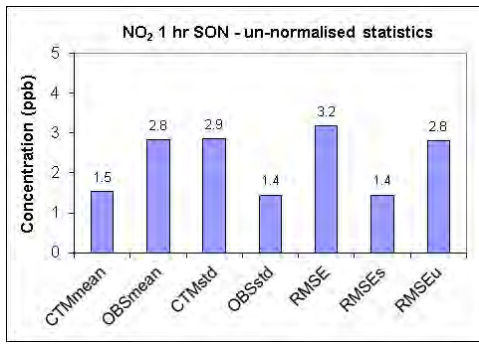


Figure B.7 The CTM performance for the 1-hour averaged NO₂ concentration (ppb) at the Gas field sites during the given season. Key: OBS = Observations; CTM = Model Predictions; mean = Arithmetic mean; std = Standard Deviation; RMSE = Root Mean Square Error; RMSEs = Systematic Root Mean Square Error; RMSEu = Unsystematic Root Mean Square Error; correlation = Pearson Correlation Coefficient (0 = no correlation, 1 = exact correlation); IOA = Index of Agreement (0 = no agreement, 1 = perfect agreement); SKILL_E=(RMSE_U)/(STD_{OBS}) (<1 shows skill); SKILL_V=(STD_{MOD})/(STD_{OBS}) (near to 1 shows skill); SKILL_R=(RMSE)/(STD_{OBS}) (<1 shows skill).

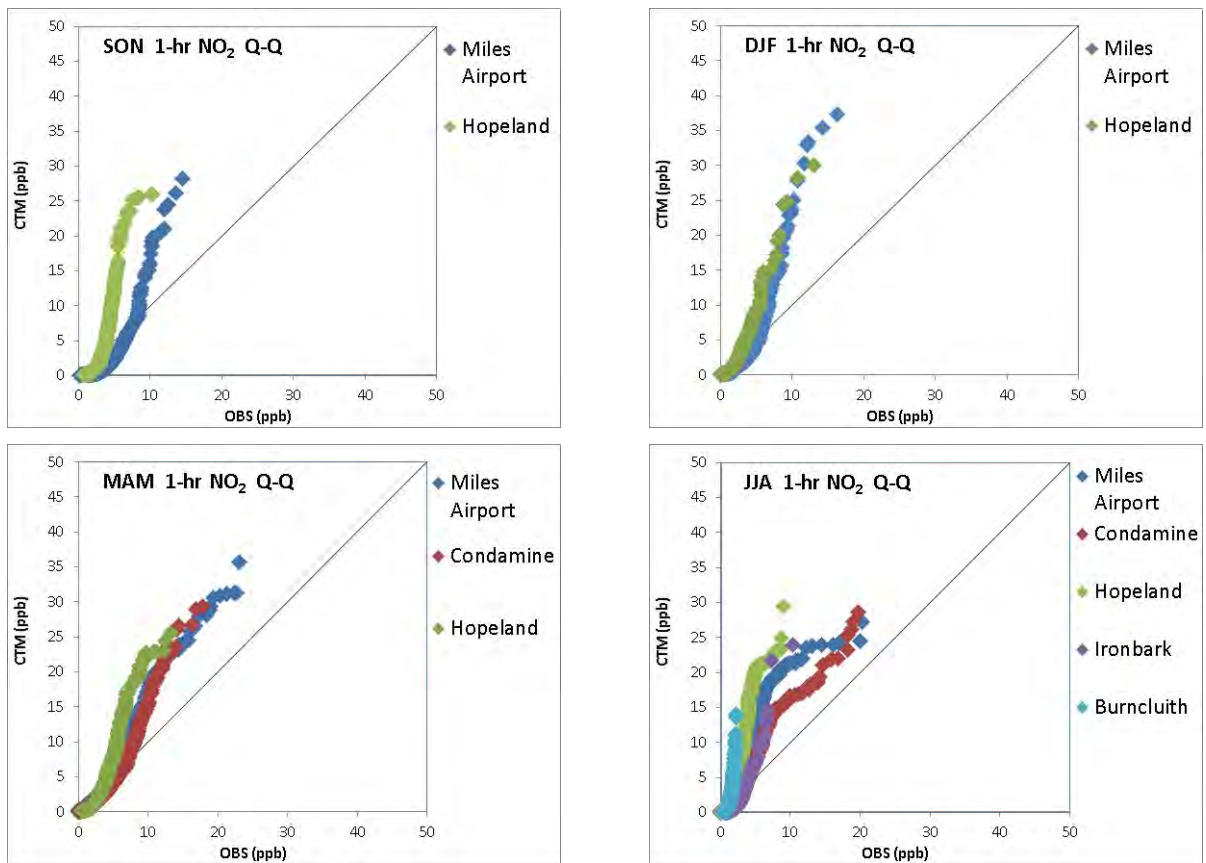


Figure B.8 Quantile-quantile plots of the observed and modelled 1-hour averaged NO₂ (ppb) at the Gas field sites.

Appendix C Sources and methodologies for local anthropogenic emission inventory

- An overview of how emissions were calculated for the following sources is provided below.
CSG-related sources
- Power generation
- Mines and Quarries
- Agriculture
- Domestic Wood heating
- Motor vehicles

This emission inventory was generated by Katestone Environmental and text below is summarised and in some cases reproduced from Katestone 2017.

C.1 CSG related emissions

C.1.1 Origin emissions

Origin provided detailed information on the sources and activity rates for Origin's infrastructure in the Surat Basin for each month of 2015. The inventory included processing and production emissions from the following petroleum leases: Talinga/Orana, Spring Gully, Peat, Condabri and Combabula/Reedy Creek.

The following information was used to generate the Origin Inventory:

- Description of petroleum lease assets (e.g. wells, transmission network, gas processing facility infrastructure, water treatment plant infrastructure).
- Description of pipeline assets.
- Monthly activity data from all Origin's Surat Basin assets from January 2015 to December 2015, including:
 - CSG produced from wells
 - Water produced from wells
 - Sales quality CSG to pipeline
 - CSG consumption in assets, such as:
 - Compressors
 - Engines
 - Generators
 - Microturbines

- Flares – gas production and processing amounts
- Diesel consumption for transport (mobile sources)
- Diesel consumption in stationary engines
- Queensland Globe dataset, published by the State of Queensland (DNRME 2015a-c):
 - Coal seam gas well locations.

The following sections describe the approach that was taken to assign Origin emissions spatially.

Production emissions

Production emissions were assigned as fugitive emissions within each 1 km by 1 km grid cell of the Surat Basin modelling area. Production emissions include:

- Well leaks and pneumatic valve releases
- High point vent releases
- CSG combustion emissions in wellhead microturbines
- Diesel combustion in vehicles.

Production emissions within each 1 km by 1 km grid cell of the Surat Basin modelling area were calculated as follows:

Well leaks and pneumatic valve releases

- Origin's active gas wells in 2015 in each petroleum lease were identified from Queensland Globe (DNRME 2015a-c).
- A fugitive emission rate has been applied to each well across each of the gas fields based on measurements made by CSIRO (Day et al., 2014).

High point vents

- High point vents were assumed to occur every 500 metres of water gathering network.
- A fugitive emission rate based on measurements made by CSIRO (Day et al., 2014) was applied to each high point vent

Wellhead emissions

- A proportion of the wells located in Talinga and Spring Gully petroleum leases use CSG microturbines to provide power for pumps and ancillary infrastructure.
- Air emissions from these sources were calculated from the volume of gas consumed by the microturbines and NPI emission factor for the combustion of natural gas in microturbines (NPI, 2008).
- Emissions were then spread evenly across each well within the relevant petroleum lease.

Mobile sources

- Emissions from mobile sources within each gas field were calculated based on the volume of diesel consumed and the NPI emission factor for the combustion of diesel in light vehicles (NPI, 2008).

- Emissions were then spread evenly across each petroleum lease based on the number of wells in each petroleum lease.

Processing emissions

Processing emissions were assigned as point sources within the Surat Basin modelling grid.

Processing emissions include:

- Fuel consumption in gas processing assets (represented as stack sources)
- CSG consumption in flares.

Processing emissions were calculated as follows:

Stack Sources:

- Stack sources in each petroleum lease were identified from the data received from Origin.
- For each stack source the following information was identified:
 - Source location (latitude and longitude)
 - Source type (compressor, generator, boiler etc.)
 - Fuel type
 - Source characteristics (height, diameter, velocity, temperature)
 - Air emission controls (such as low NO_x burners or selective non-catalytic reduction).
- The emission rate of air pollutants from each stack source was calculated using the amount of fuel consumed and NPI emission factors that reflect the source type, fuel type and any air emission control.
- For stack sources of the same type, fuel consumption was evenly distributed across each source unless source specific information was provided on fuel consumption rate.

Flare sources:

- Flare sources were identified from the data received from Origin.
- For each flare source the following information was identified:
 - Source location (latitude and longitude)
 - Amount of gas flared per month.
- Annual emission rate from each flare source was calculated using the amount of gas sent to each flare and flaring emission factors from the NPI Oil and Gas Extraction and Production Handbook (NPI 2013a).
- A site specific TVOC emission factor from flaring was used, based on the methodology in NPI (2013a) and information provided by Origin.

C.1.2 QGC emissions

QGC provided detailed information on the sources and activity rates for QGC's infrastructure in the Surat Basin for each month of 2015.

The following information was used to generate the QGC Inventory:

- Description of QGC's coal seam gas Authority to Prospects (ATPs) in the Surat Basin including:
 - ATP 610
 - ATP 620
 - ATP 632
 - ATP 648
 - ATP 651
 - ATP 676
 - ATP 768
 - ATP 852.
- Description and location of assets within each ATP (e.g. wells, high point vents, field compressor stations, central processing plants and water treatment plants).
- CSG production data from all QGC's Surat Basin ATPs from January 2015 to December 2015.
- Monthly CSG flaring and venting data from all QGC's Surat Basin ATPs from January 2015 to December 2015.
- 2015 diesel consumption rate of stationary and mobile sources within each ATP.
- 2015 QGC vehicle kilometres travelled on unpaved roads in Surat Basin (QGC Upstream operations).

The following sections describe the approach that was taken to assign QGC emissions spatially.

Production emissions

Production emissions were assigned as fugitive emissions within each 1 km by 1 km grid cell of the Surat Basin modelling area. Production emissions include:

- Well leaks and pneumatic valve releases
- High point vent releases
- CSG combustion emissions in gas engines at well heads
- CSG combustion emissions in flares at well heads
- Diesel combustion in vehicles
- Wheel generated dust from vehicle movements.

Production emissions within each 1 km by 1 km grid cell of the Surat Basin modelling area were calculated as follows:

Well leaks and pneumatic valve releases

- QGC's active gas wells in 2015 in each ATP were identified from the dataset of well locations provided by QGC.
- A fugitive emission rate was applied to each well across each of the gas fields based on measurements made by CSIRO (Day et al., 2014).

High point vents

- QGC high point vents were identified from the dataset provided by QGC.

- A fugitive emission rate based on measurements made by CSIRO (Day et al., 2014) was applied to each high point vent

Wellhead gas engines emissions

- A proportion of the wells located in QGC's ATPs use gas engines to provide power for wellhead pumps and ancillary infrastructure.
- Air emissions from these sources were calculated from the volume of gas consumed by the wellhead engines (provided by QGC) and NPI emission factors (NPI, 2008).

Wellhead flare emissions

- A proportion of the wells located in QGC's ATPs included flaring.
- Air emissions from these sources were calculated from the volume of gas flared at wells in each ATP and the NPI flaring emission factors (NPI 2013a)
- A site specific TVOC emission factor from flaring was used based on the methodology in NPI (2013a) and information provided by QGC.

Diesel combustion in engines

- Emissions from mobile sources within each ATP were calculated based on the volume of diesel consumed and NPI emission factor (NPI 2008)
- Emissions were then spread evenly across each ATP based on the number of wells in each ATP.

Wheel generated dust from vehicle movements

- Emissions of dust from vehicle movements within each ATP were calculated based on information provided by QGC that included the total number of vehicle kilometres travelled in all QGC ATPs and the NPI emission factor for wheel generated dust from unpaved roads at industrial sites (NPI, 2013a).
- Emissions were then spread evenly across each ATP based on the number of wells in each ATP.

Processing emissions

Processing emissions were assigned as point sources within the Surat Basin modelling grid. Processing emissions include:

- Fuel consumption (CSG or diesel) in gas processing assets (represented as stack sources)
- CSG consumption in flares
- Diesel consumption at ATP processing facilities.

Processing emissions were calculated as follows:

Stack Sources:

- Stack sources in each ATP were identified from the data received from QGC.
- For each stack source the following information was identified:
 - Source location (latitude and longitude)
 - Source type (compressor, engines, generator, boiler etc.)

- Fuel consumption rate per hour.
- The emission rate of air pollutants from each stack source was calculated using the amount of fuel consumption rate and NPI emission factors that reflect the source type and fuel type.

Flare sources:

- Flare sources at QGC’s processing operations were identified by ATP from the data received from QGC and included:
 - field compressor station flares
 - central processing plant flares.
- Air emissions from these sources were calculated from the volume of gas flared at each facility in each ATP (as provided by QGC) and NPI flaring emission factors (NPI 2013a)
- A site specific TVOC emission factor from flaring was used, rather than the default, based on the methodology in NPI (2013a) and information provided by QGC.

Diesel combustion at ATP facilities

- Emissions from diesel consumption at ATP processing facilities were calculated based on the volume of diesel consumed and NPI emission factor (NPI 2008)
- Emissions were then assigned to each ATP processing facility based on the location provided by QGC.

C.1.3 Arrow emissions

Air emissions data for the year 2015 were provided by Arrow using methods consistent with NPI reporting requirements. Major sources of gas field emissions were Daandine and Tipton operations and Kogan Gas field.

The following information was used to generate the Arrow CSG Inventory:

- National Pollutant Inventory (NPI) data for the 2015/16 reporting year – (<http://www.npi.gov.au/>)
- Annual emissions data provided by Arrow for Daandine and Tipton operations for 2015/16. Both Daandine and Tipton are classified as ‘facilities’ for NPI purposes. Each of these ‘facilities’ includes CSG wells, gathering system infrastructure and CSG processing facilities. Arrow provided a breakdown of emissions data that enabled emissions from production (wells and gathering system) and processing (gas processing plant) to be considered separately. Arrow has advised that the underlying emissions estimation methodologies are consistent with NPI requirements

The major sources of emissions by gas field are:

- Daandine Operations:
 - Production – gas engines (well head) and flaring
 - Processing – gas engines (compression) and flaring.
- Tipton Operations:

- Production – gas engines (well head) and flaring
- Processing – gas engines (compression).
- Kogan Gas Field
 - Production – gas engines (well head) and flaring.
- Approximately half of Arrow’s wells require pumps for water removal, well head water pumps are electrically driven by gas engines located in close proximity to the well head.
- Queensland Globe dataset (DNRME 2015a-c):
 - Coal seam gas well locations
 - Exploration and production permits – Queensland.

The following approach was taken to assign emissions spatially:

Production

- Fugitive emission sources from Arrow activities in the Surat Basin were identified from the NPI 2015/16 NPI database as reported by Arrow.
- The fugitive emissions were applied to Arrow’s gas field areas based on the number and location of wells identified in the Queensland Globe dataset (DNRME 2015a-c).
- These emissions have been evenly apportioned to the active wells within each gas field (Daandine, Tipton and Kogan).

Processing

- Emission sources at Arrow’s gas processing plants were identified from NPI emissions data together with more detailed emissions data provided by Arrow for the 2015/16 reporting period.
- The processing related emissions provided by Arrow were assumed to apply uniformly across each plant.

C.1.4 Santos emissions

Emissions from Santos operations relied on publicly available emissions data only. Emission sources associated with the Roma, Scotia, Fairview gas fields as well as the Moonie processing facility were included.

The following information was used to generate the Santos Inventory:

- National Pollutant Inventory (NPI) data for Santos operations in the Surat Basin for the 2013/14 and 2015/16 reporting years – (<http://www.npi.gov.au/>).
- Queensland Globe dataset (DNRME 2015a-c):
 - Coal seam gas well locations
 - Exploration and production permits – Queensland

The calculation methodology was as follows:

Production emissions

Production emissions were assigned as fugitive emissions within each 1 km by 1 km grid cell of the Surat Basin modelling area. Production emissions within each 1 km by 1 km grid cell of the Surat Basin modelling area were calculated as follows:

Fugitive releases

- Fugitive emissions from Santos activities in the Surat Basin was identified from the fugitive emissions reported by Santos for NPI 2015/16.
- The fugitive emissions were applied to Santos gas field areas based on the number and location of wells identified in the Queensland globe dataset (DNRME 2015a-c).

Processing emissions

Processing emissions were assigned as point sources within the Surat Basin modelling area. Processing emissions include:

- Fuel consumption in gas processing assets at Roma, Scotia, Fairview and Moonie gas processing plants

Processing emissions were calculated as follows:

Point sources:

- A point source that represents each Santos processing plant was identified from the NPI data and Queensland Globe mapping (DNRME 2015a-c).
- The emission rate of air pollutants from each point source was derived from Santos' 2015/16 NPI reported emissions.

C.1.5 Other Producer emissions

Emissions from Other Producers was taken from publicly available data. Processing sources in this category included Silver Springs gas processing plant, Wallumbilla Gas Processing Terminal, Kogan North Gas Plant and Dalby Compressor station.

The following information was used to generate the Other Producers Inventory:

- National Pollutant Inventory (NPI) data for CSG operations by APT Petroleum Pipelines, APT Management Services, AGL Gas Storage in the 2015/16 reporting year – (<http://www.npi.gov.au/>)
- Queensland Globe dataset (DNRME 2015a-c):
 - coal seam gas well locations
 - Exploration and production permits – Queensland.

Processing emissions

Processing emissions were assigned as point sources within the Surat Basin modelling area. Processing emissions include:

- Fuel consumption in gas processing assets

Processing emissions were calculated as follows:

Point sources:

- A point source that represents each processing plant was identified from the NPI data and Queensland Globe mapping (DNRME 2015a-c).
- A kilogram per annum (kg/annum) emission rate of air pollutants from each point source was derived from the 2015/16 NPI reported emissions.

C.2 Power Generation

Emissions were characterised for the following 8 power stations in the Surat Basin:

- Braemar 1 Power Station (gas, open cycle turbines)
- Braemar 2 Power Station (gas, open cycle turbines)
- Condamine Power Station (gas, combined cycle turbines)
- Daandine Power Station (gas, reciprocating engines)
- Darling Downs Power Station (gas, combined cycle turbines)
- Roma Power Station (gas, open cycle turbines)
- Kogan Power Station (coal)
- Millmerran Power Station (coal)

Air emissions from power stations are related to the combustion of coal or natural gas and fugitive emissions such as dust from coal storage.

The following information was used to generate the Power Generation Inventory:

- NPI for the 2013/14 reporting year
- Actual electricity generation for each power station from the Australian Energy Market Operator (AEMO, 2015) for 2013 to 2015, inclusive
- Stack characteristics sourced from Australia Pacific LNG Project Volume 5: Attachments Attachment 28: Air Quality Impact Assessment – Gas Fields (Katestone, 2010).

Power station specific emission factors (kg/MWh) were developed using the NPI reported emissions for 2013/14 and actual annual electricity generation from AEMO (2015) for the 2013/14 reporting year for each pollutant. Where specific air pollutants were not available from the NPI, the emissions were calculated using the NPI emission factor handbooks (NPI, 2008, 2012).

Fugitive emissions were based on the emissions for the NPI 2013/14 reporting year for all power stations.

C.3 Mines and Quarries

Emissions from 6 coal mines, 2 gold mines and 5 quarries have been included in the Surat Basin emissions inventory.

- Coal mines

- Cameby Downs
- Kogan Creek
- New Acland
- Wilkie Creek
- Commodore
- Meandu
- Gold mines
 - Cracow
 - Mt Rawdon
- Quarries
 - Toowoomba
 - Boral Wondai
 - Boral Malu
 - Boral Wellcamp Downs
 - Boral Warriars

Air emissions from mines and quarries are related to the combustion of fuel and fugitive emissions associated with the activity, such as dust from haul roads.

The following information was used to generate the Mines and Quarries Emissions Inventory:

- NPI for the 2013/14 reporting year (<http://www.npi.gov.au/>)
- Queensland Globe (2015)
 - Key resource areas - resource processing area
 - Mining lease surface areas

The following approach was taken to assign emissions spatially:

- NPI emissions were assumed to apply uniformly across each source area (mine surface rights)
- An annual mass emission rate was calculated assuming constant emissions throughout the year.

C.4 Agriculture

Emissions from 264 feedlots, 145 piggeries and 16 poultry farms have been included in the Surat Basin emissions inventory.

Feedlots

The following information was used to generate the inventory for feedlots:

- NPI for the 2013/14 reporting year for facilities in the study area with the ANZSIC (Australian and New Zealand Standard Industrial Classification) description *Beef Cattle Feedlots (Specialised)*.
- DNRME and DAF (2014a) (Department of Agriculture and Fisheries) Queensland Globe datasets:

- Lot and plan boundaries contained in the *Property boundaries Queensland* cadastral dataset and locations and head of cattle numbers
- Emission factors from NPI, (2007)
- The inventory was populated using emission rates reported to the NPI for the 2013/14 reporting year, where possible. Emissions from facilities that did not report to the NPI were calculated from the head of cattle numbers in the DAF dataset and NPI emission factors.

Poultry Farms

The following information was used to generate the inventory for poultry farms:

- NPI for the 2013/14 reporting year for facilities in the study area with the ANZSIC description *Poultry farming (Eggs)*
- DNRME and DAF (2014b) Queensland Globe datasets
 - Lot and plan boundaries and locations and bird numbers
- Approvals documentation, Google Earth imagery to determine approximate floor areas for some poultry farm sheds
- Stocking densities based on industry literature (Sustainable Table, 2015; Queensland Government, 2013) and industry experience.
- Emission factors for ammonia from the Emission estimation technique manual for Intensive Livestock - Poultry Raising (NPI, 2013b) and derived PM₁₀ emission factor (NSW EPA, 2012a),
- Where possible the inventory was populated using emission rates reported to the NPI (2013/14 reporting year), otherwise where no NPI reported emissions were available, emissions were calculated using NPI emission factors corresponding to the type of farm and number of birds at each poultry farm.

Piggeries

The following information was used to generate the inventory for piggeries:

- Emissions of ammonia reported to the NPI for the 2013/14 reporting year for facilities in the study area with the ANZSIC description *Pig Farming*
- DNRME and DAF (2014c) Queensland Globe datasets
 - Lot and plan boundaries and locations of piggeries
- The NPI reporting threshold of 10,000 kg/annum of ammonia emissions.
- The inventory was populated using ammonia emission rates reported to the NPI for the 2013/14 reporting year, where possible. Where no NPI reported emissions were available, emissions were assumed to be 70% of the reporting threshold of 10,000 kg/annum.

Checks were undertaken to avoid double counting feedlots, poultry farms and piggeries listed in both the NPI and DAF datasets.

C.5 Domestic Wood Heating

The following information was used to generate the Domestic Wood Heating Inventory for slow combustion heaters (with/without compliance plates), open fireplaces and pot belly stoves.

- NSW EPA GMR Inventory 2008 (NSW EPA, 2012a):
 - Emission factors for domestic wood heating
 - diurnal, weekly and monthly profiles for domestic wood heating.
- Number of dwellings in a given area based on the 2011 census (ASGS, 2011).

The following approach was taken to assign emissions spatially:

- The average ownership of solid fuel heaters and the average consumption of fuel per heater were taken from NSW EPA (2012a) and used to determine a consumption factor for each heater type per dwelling
- The consumption factor was then applied to estimate the total annual consumption of fuel within a given area

Diurnal, weekly and monthly profiles were constructed from information presented in the NSW EPA GMR Inventory (NSW EPA 2012a).

C.6 Motor Vehicles

The estimation of emissions attributed to motor vehicles was based on the approach adopted in the NSW EPA GMR Inventory 2008 (NSW EPA, 2012b). The following information was used to generate the motor vehicle inventory:

- Attributes and Locations of Queensland Roads (DNRME, 2010).
- DTMR's (Department of Transport and Main Roads) Queensland Globe dataset (DTMR 2015)
 - Annual average daily traffic data (AADT)
- Australian Bureau of Statistics:
 - Population and land use data (ASGS, 2011)
 - Vehicle fleet by age and fuel type from the Motor Vehicle Census (ABS, 2015)
- NSW EPA GMR Inventory 2008 (NSW EPA, 2012b):
 - Hourly vehicle kilometres travelled (VKT) distribution for average weekday/weekend by vehicle type
 - Hourly average speeds by road type
 - Fleet composite splitting factors by vehicle type and road type
 - Twenty-four hour VKT weighted average speeds
 - Estimated number of axles for heavy duty fleet
 - Base exhaust hot running emissions by vehicle and fuel type
 - Base tyre wear, brake wear and road wear emission factors

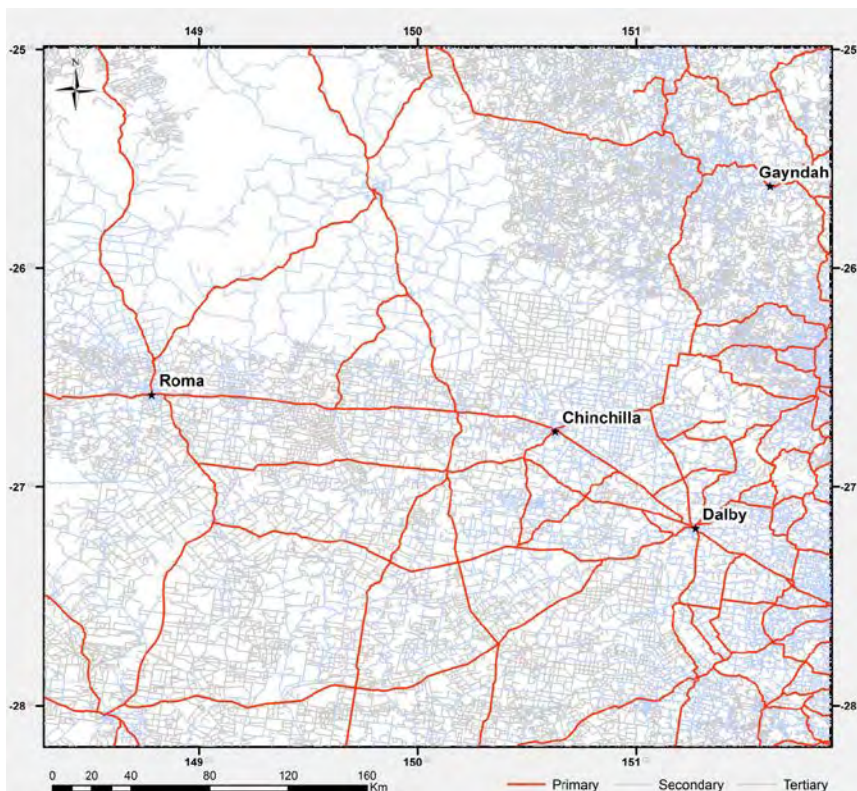


Figure C.1 Primary, secondary and tertiary roads used in the motor vehicle emission inventory. Source: Katestone 2017

Roads

Emissions from motor vehicles travelling on primary, secondary and tertiary roads were considered (Figure C.1).

Attributes and the locations of the roads in GIS format were sourced from DNRME (2010). The road categories in DNRME (e.g. highway, local road, vehicular track etc) were categorised into primary, secondary or tertiary roads to be compatible with the NSW EPA GMR Inventory 2008 (NSW EPA, 2012b).

Vehicles

In this study, vehicles were classified as light, heavy or diesel light duty vehicles. The motor vehicle census for Queensland was used to determine vehicle fleet by age as well as breakdown of vehicle by fuel type for Australia (ABS, 2015).

Traffic flows

Annual average daily traffic data (AADT) for most of the primary roads were based on actual data (DTMR, 2015). For secondary roads, traffic flows were interpolated depending on population density (Cardno, 2014) derived from the Australian Statistical Geography Standard (ASGS, 2011). For tertiary roads, two vehicles were assumed to be travelling per day. It was also assumed that only diesel light duty vehicles travel on tertiary roads

Diurnal profile

The diurnal profile by day type was determined by using the information provided in the NSW EPA GMR Inventory 2008 (NSW EPA, 2012b) regarding the distance travelled by each type of vehicle for each hour and for each day type.

Emission factors

Base hot running exhaust emissions were based on emission factors used in the NSW EPA GMR Inventory 2008 (NSW EPA, 2012b). Speed correction factors were also used. Non-exhaust particulate emission factors for petrol and diesel vehicles including tyre wear, brake wear, and road wear are consistent with assumptions and methods used in the NSW EPA GMR Inventory 2008 (NSW EPA, 2012b).

Appendix D CTM-CCAM Time Series Plots

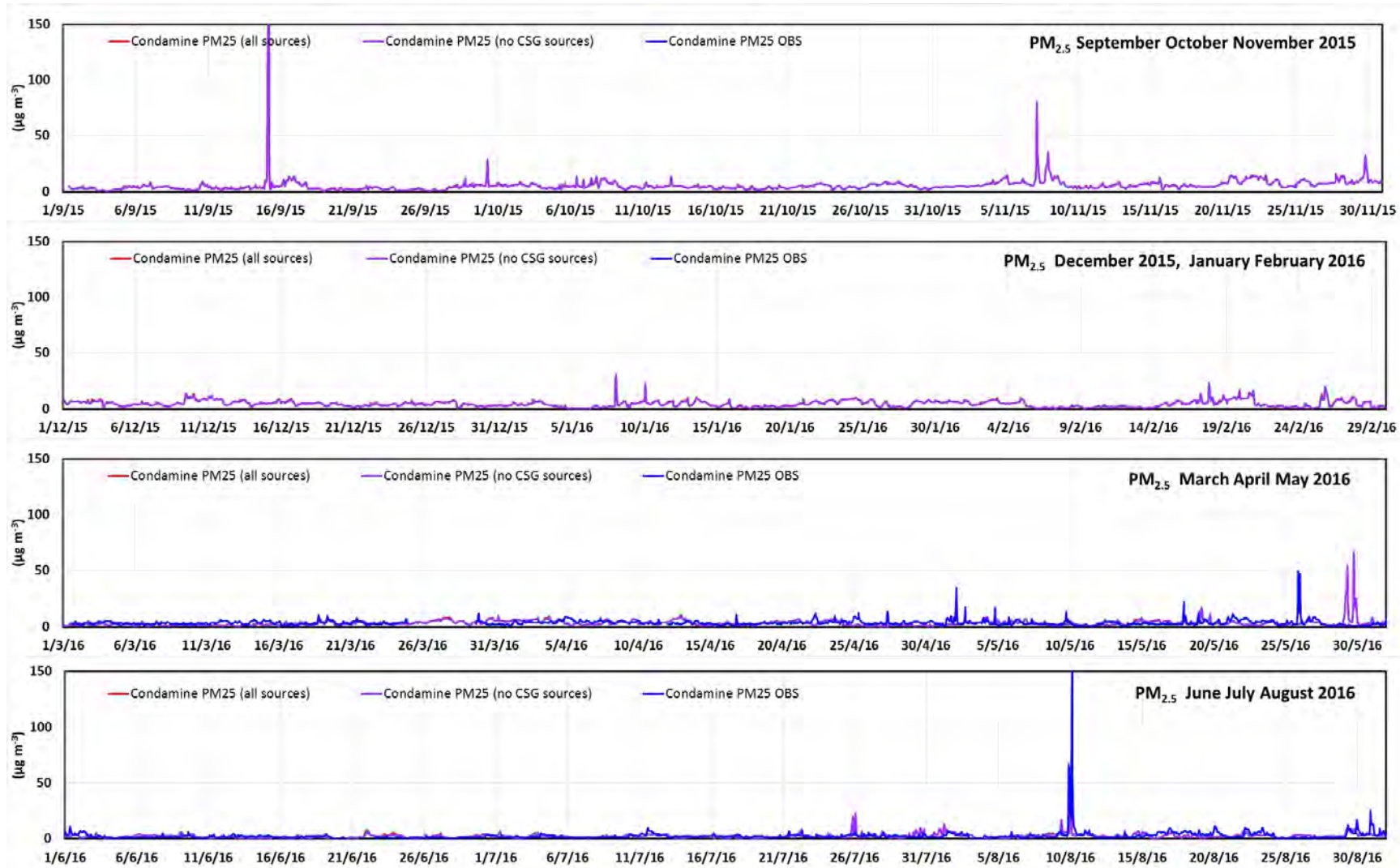


Figure D.1 The observed and modelled time series of the 1-hour average PM_{2.5} concentrations ($\mu\text{g m}^{-3}$) at Condamine for the modelled year (red = model results with all sources, purple = model results without CSG sources, blue = observations). (peaks off scale: model, 15/9/15 04:00 = 246 $\mu\text{g m}^{-3}$, OBS 10/8/16 03:00 = 177 $\mu\text{g m}^{-3}$)

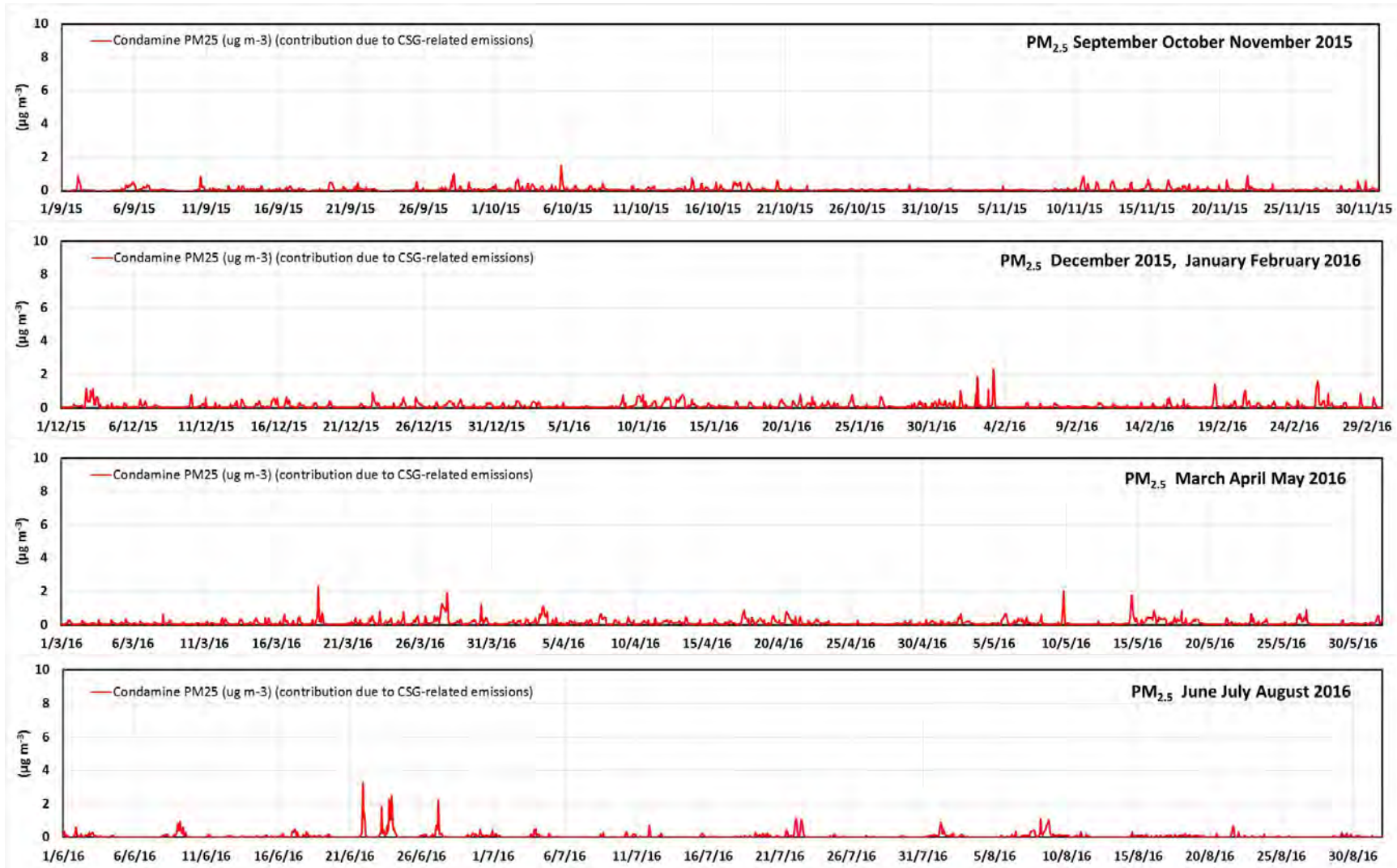


Figure D.2 The modelled contributions from the CSG-related emissions to the 1-hour average PM_{2.5} concentrations (µg m⁻³) at Condamine for the modelled year.

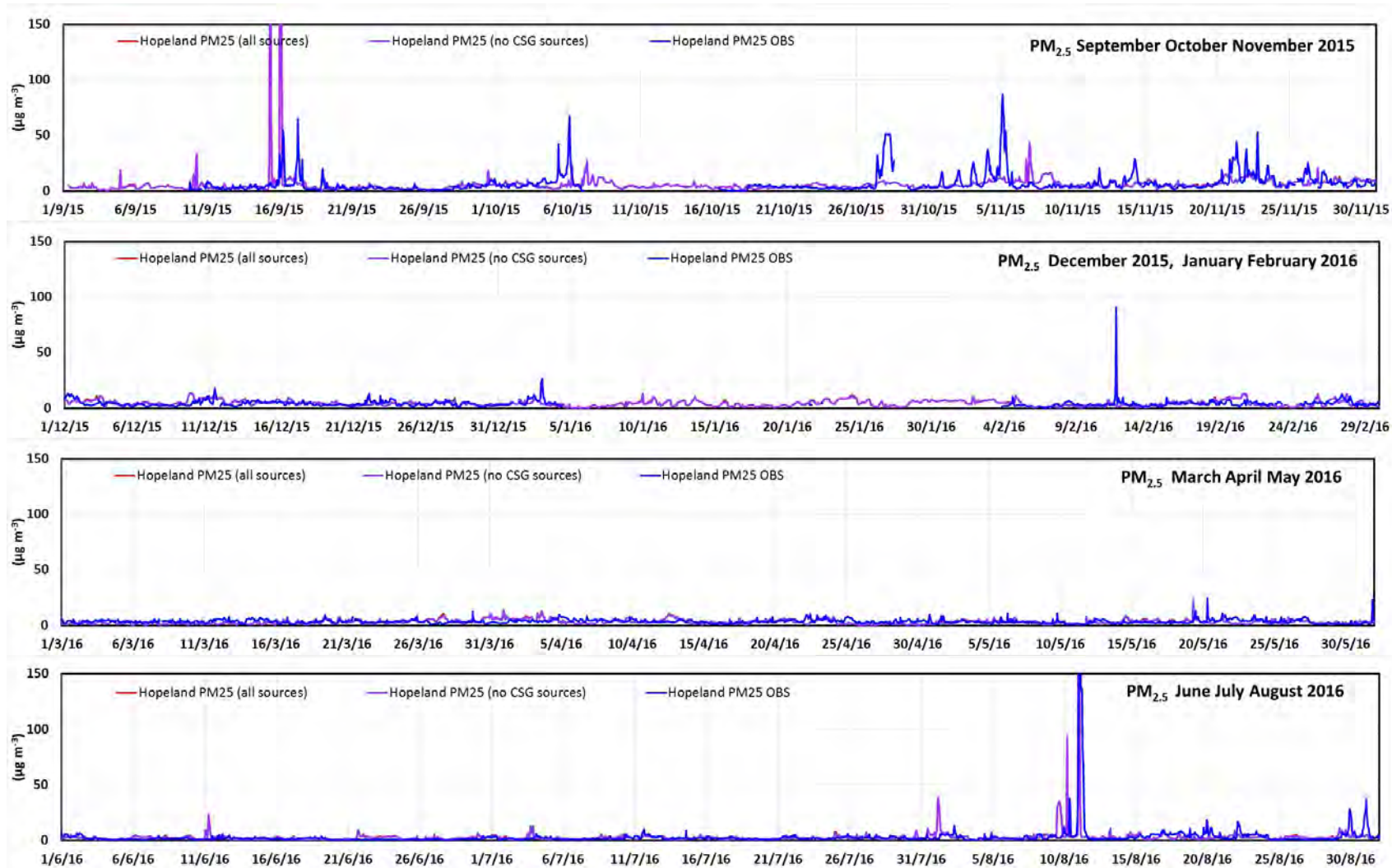


Figure D.3 The observed and modelled time series of the 1-hour average PM_{2.5} concentrations ($\mu\text{g m}^{-3}$) at Hopeland for the modelled year (red = model results with all sources, purple = model results without CSG sources, blue = observations). (peaks off scale: model, 15/9/15 09:00 = 222 $\mu\text{g m}^{-3}$, 16/9/15 01:00 = 254 $\mu\text{g m}^{-3}$, OBS 11/8/16 01:00 = 249 $\mu\text{g m}^{-3}$)

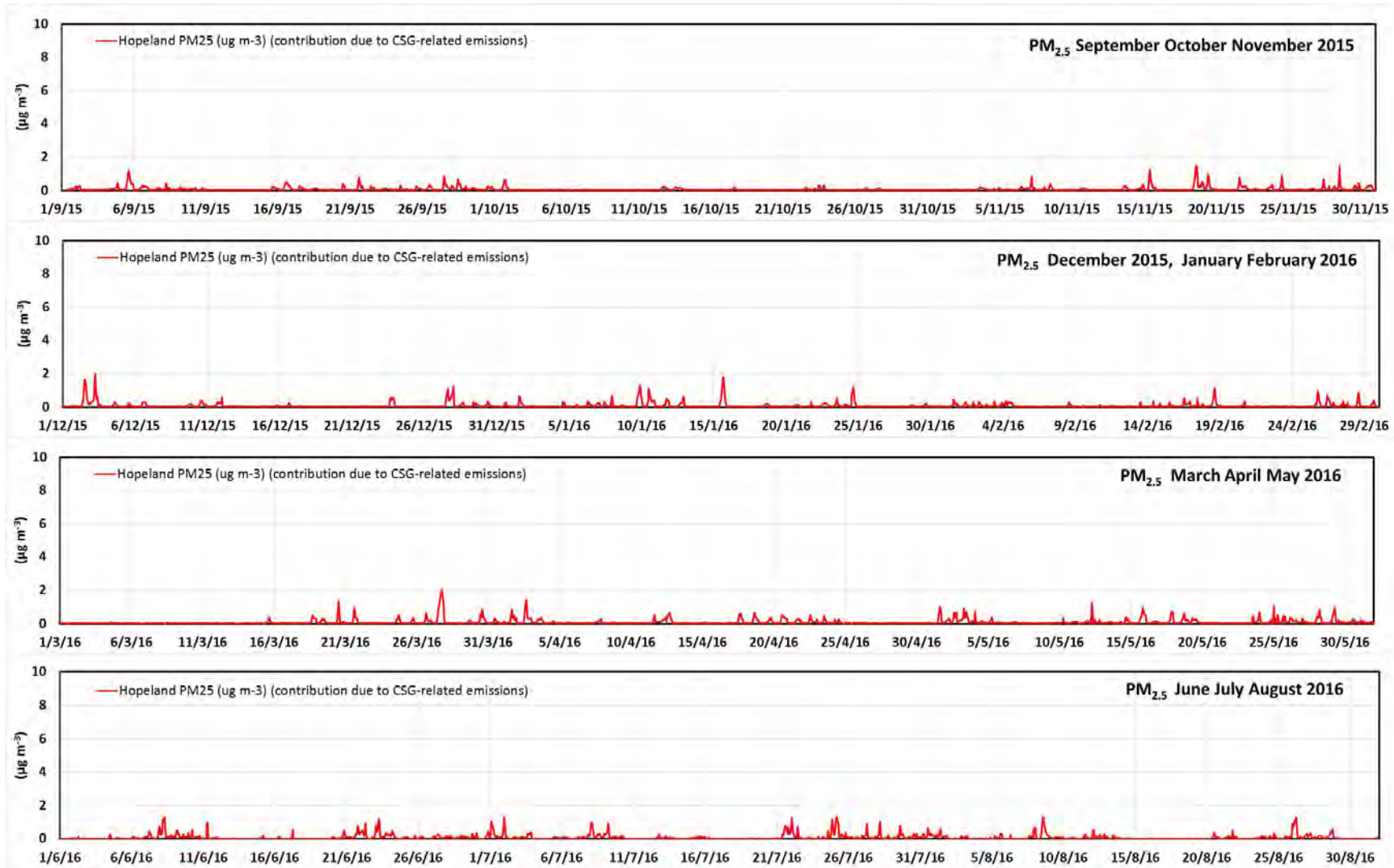


Figure D.4 The modelled contributions from the CSG-related emissions to the 1-hour average PM_{2.5} concentrations ($\mu\text{g m}^{-3}$) at Hopeland for the modelled year.

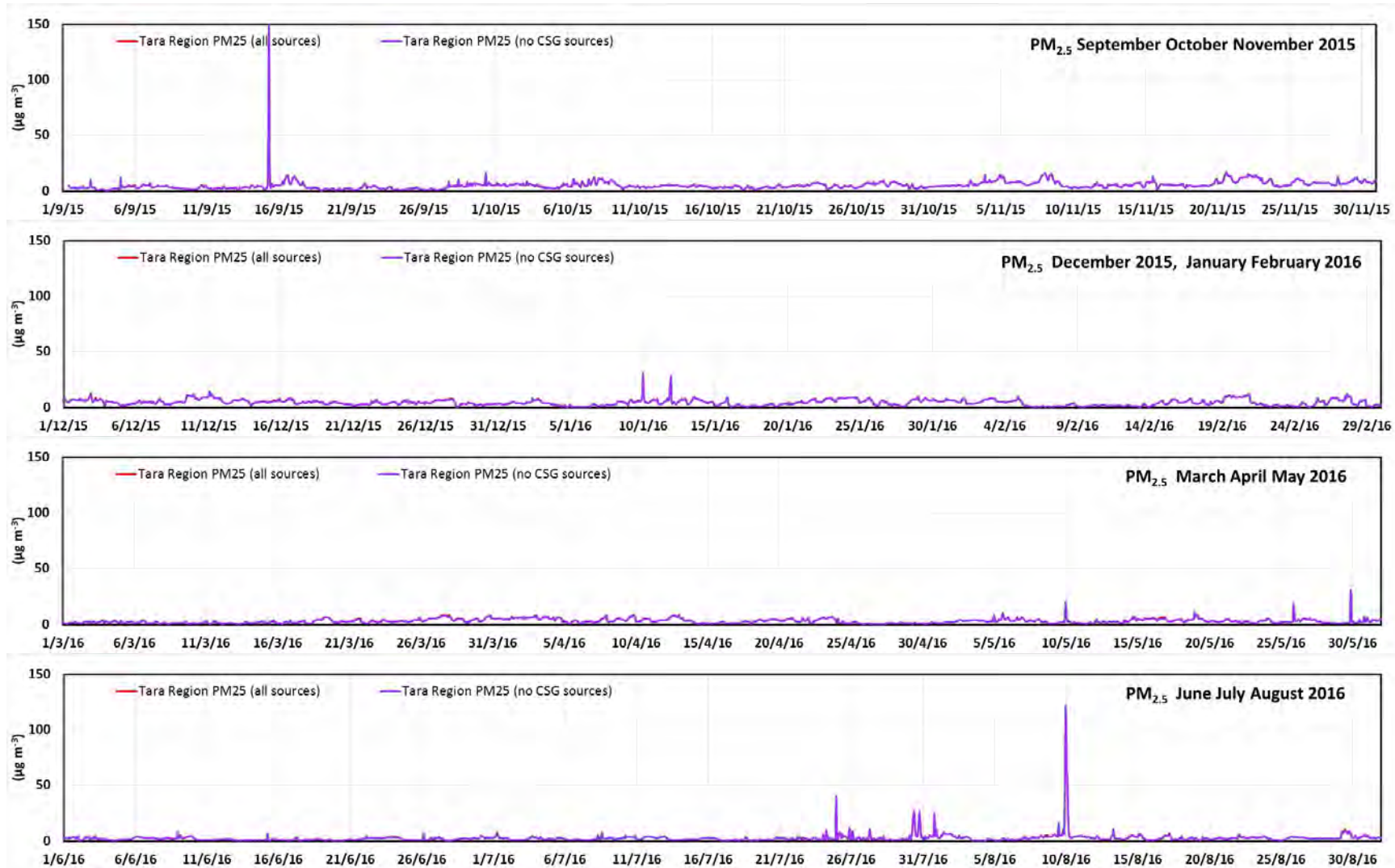


Figure D.5 The modelled time series of the 1-hour average PM_{2.5} concentrations ($\mu\text{g m}^{-3}$) at Tara Region for the modelled year (red = model results with all sources, purple = model results without CSG sources, blue = observations). (peaks off scale: model, 15/9/15 07:00 = 159 $\mu\text{g m}^{-3}$)



Figure D.6 The modelled contributions from the CSG-related emissions to the 1-hour average PM_{2.5} concentrations (µg m⁻³) at Tara Region for the modelled year.

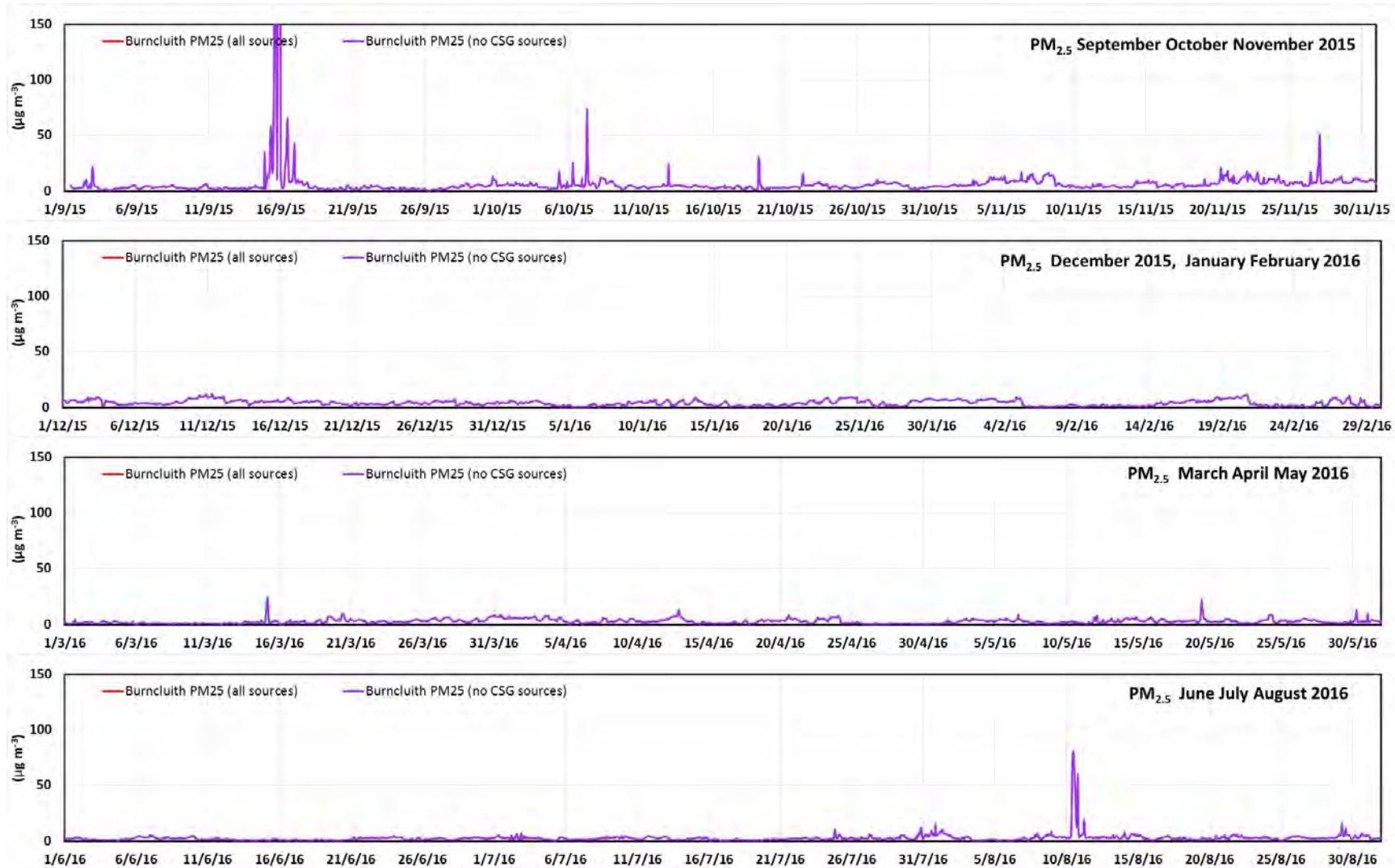


Figure D.7 The modelled time series of the 1-hour average PM_{2.5} concentrations ($\mu\text{g m}^{-3}$) at Burncluith for the modelled year (red = model results with all sources, purple = model results without CSG sources, blue = observations). (peaks off scale: model, 15/9/15 21:00 = 2036 $\mu\text{g m}^{-3}$)

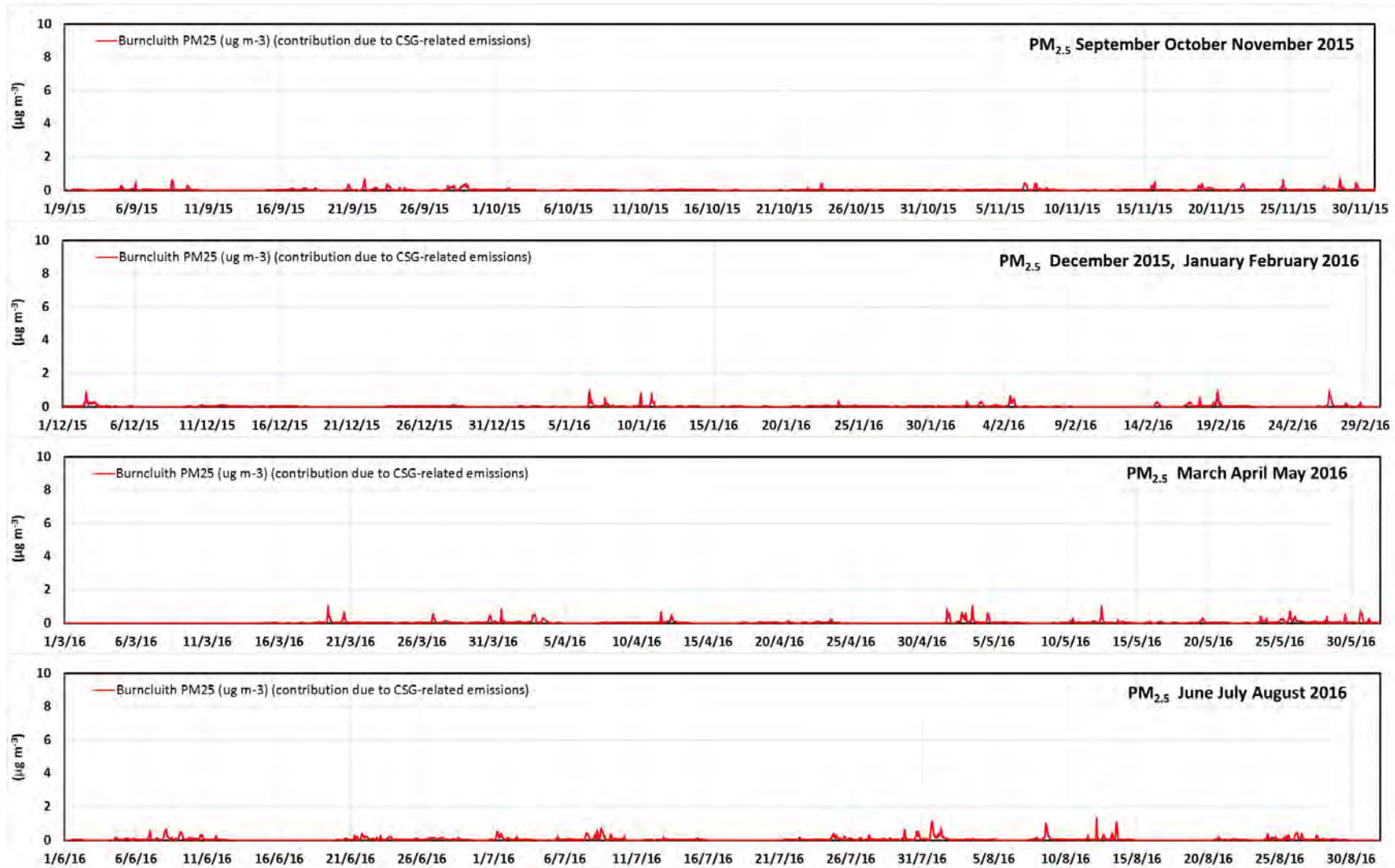


Figure D.8 The modelled contributions from the CSG-related emissions to the 1-hour average PM_{2.5} concentrations (µg m⁻³) at Burncluith for the modelled year.

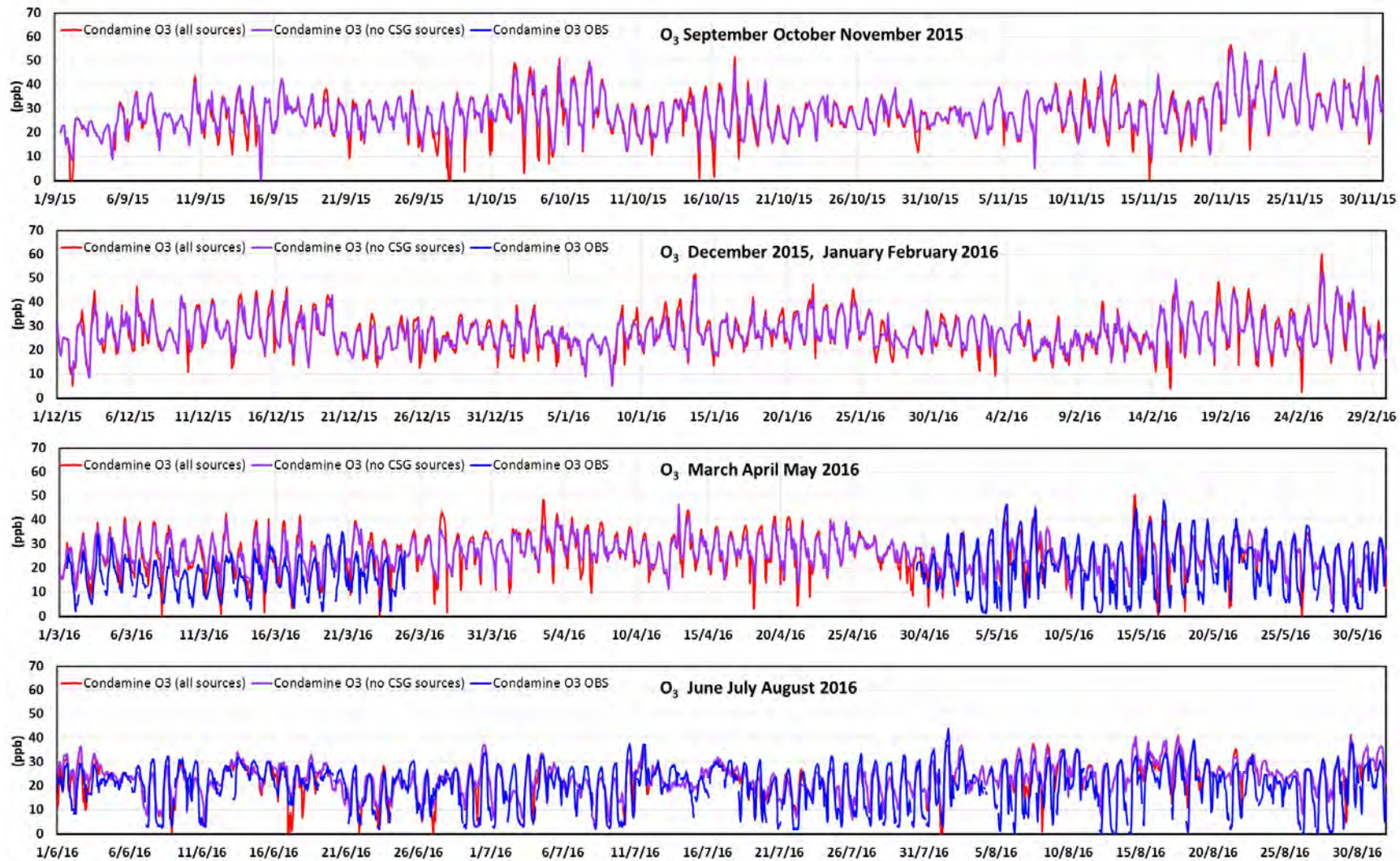


Figure D.9 The observed and modelled time series of the 1-hour average O₃ concentrations (ppb) at Condamine for the modelled year (red = model results with all sources, purple = model results without CSG sources, blue = observations).

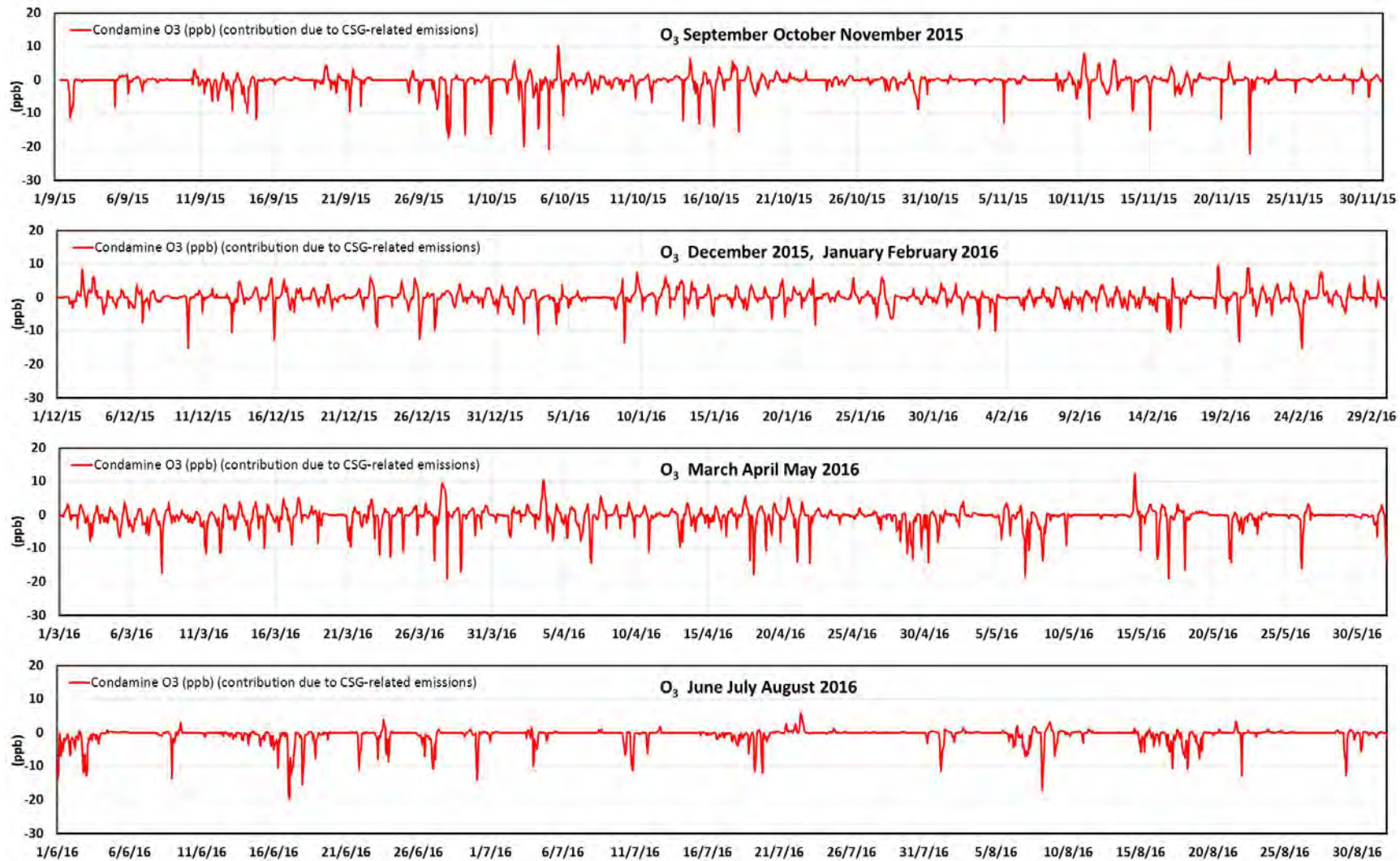


Figure D.10 The modelled contributions from the CSG-related emissions to the 1-hour average O₃ concentrations (ppb) at Condamine for the modelled year.

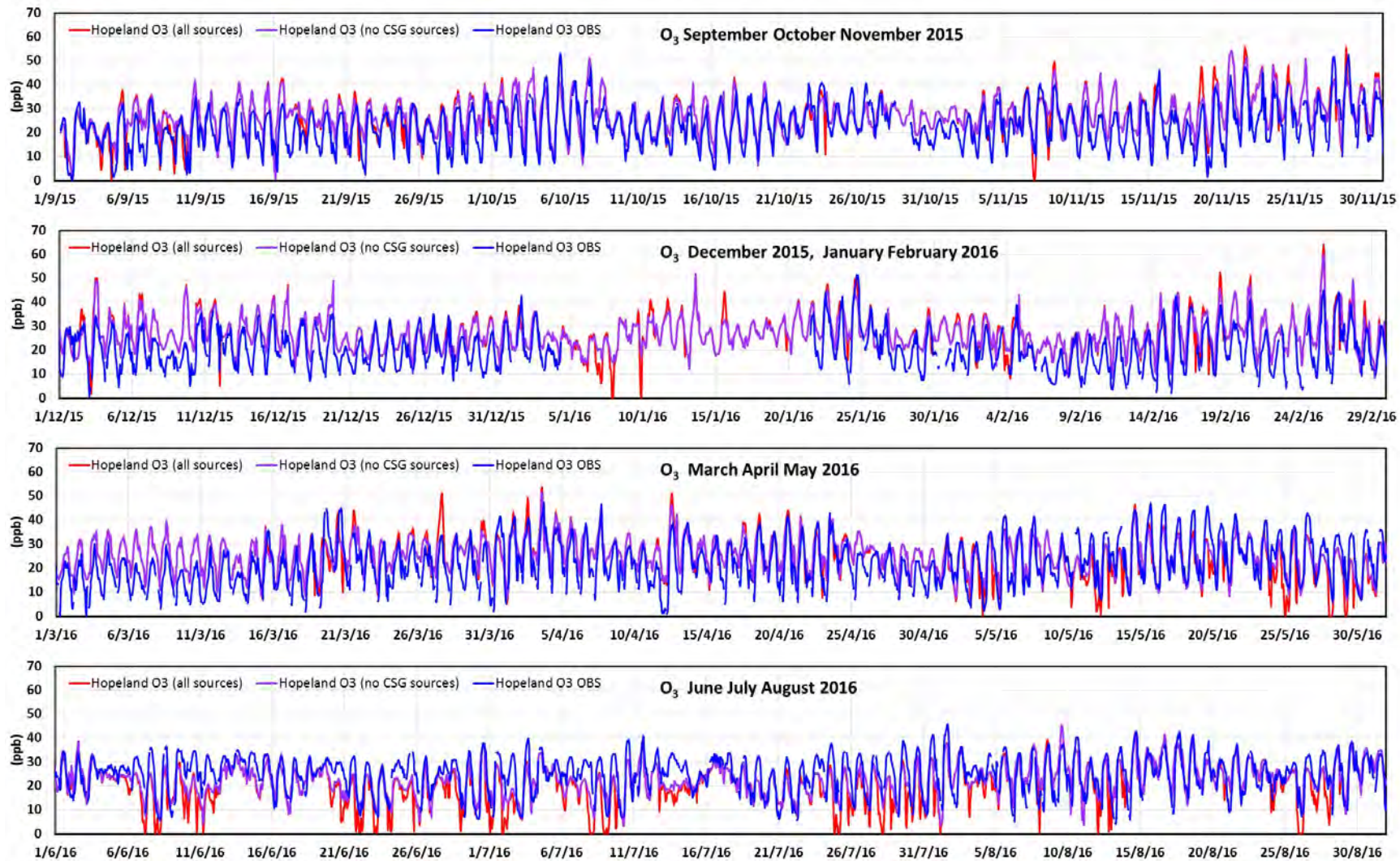


Figure D.11 The observed and modelled time series of the 1-hour average O₃ concentrations (ppb) at Hopeland for the modelled year (red = model results with all sources, purple = model results without CSG sources, blue = observations).

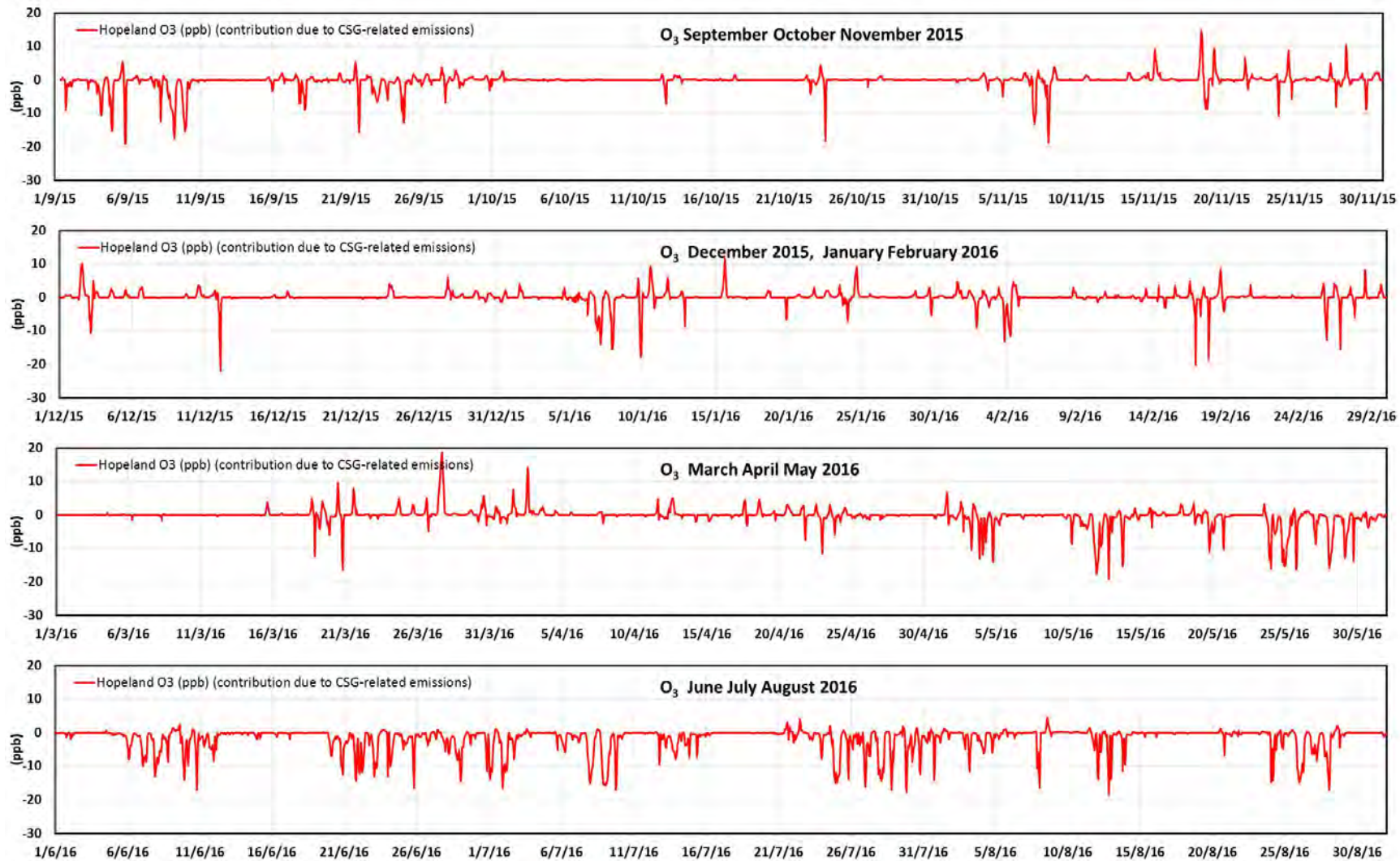


Figure D.12 The modelled contributions from the CSG-related emissions to the 1-hour average O₃ concentrations (ppb) at Hopeland for the modelled year.

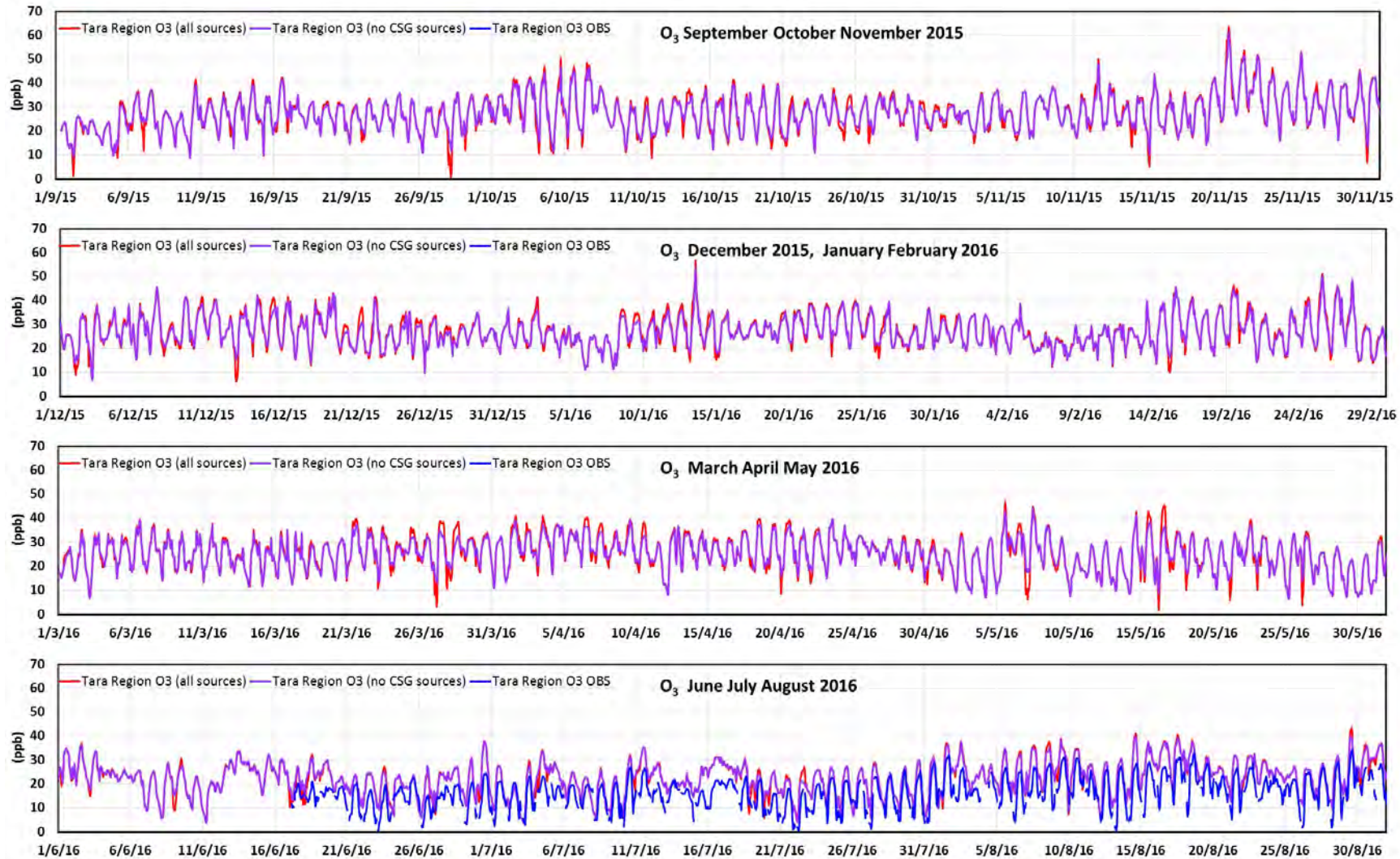


Figure D.13 The observed and modelled time series of the 1-hour average O₃ concentrations (ppb) at Tara Region for the modelled year (red = model results with all sources, purple = model results without CSG sources, blue = observations).

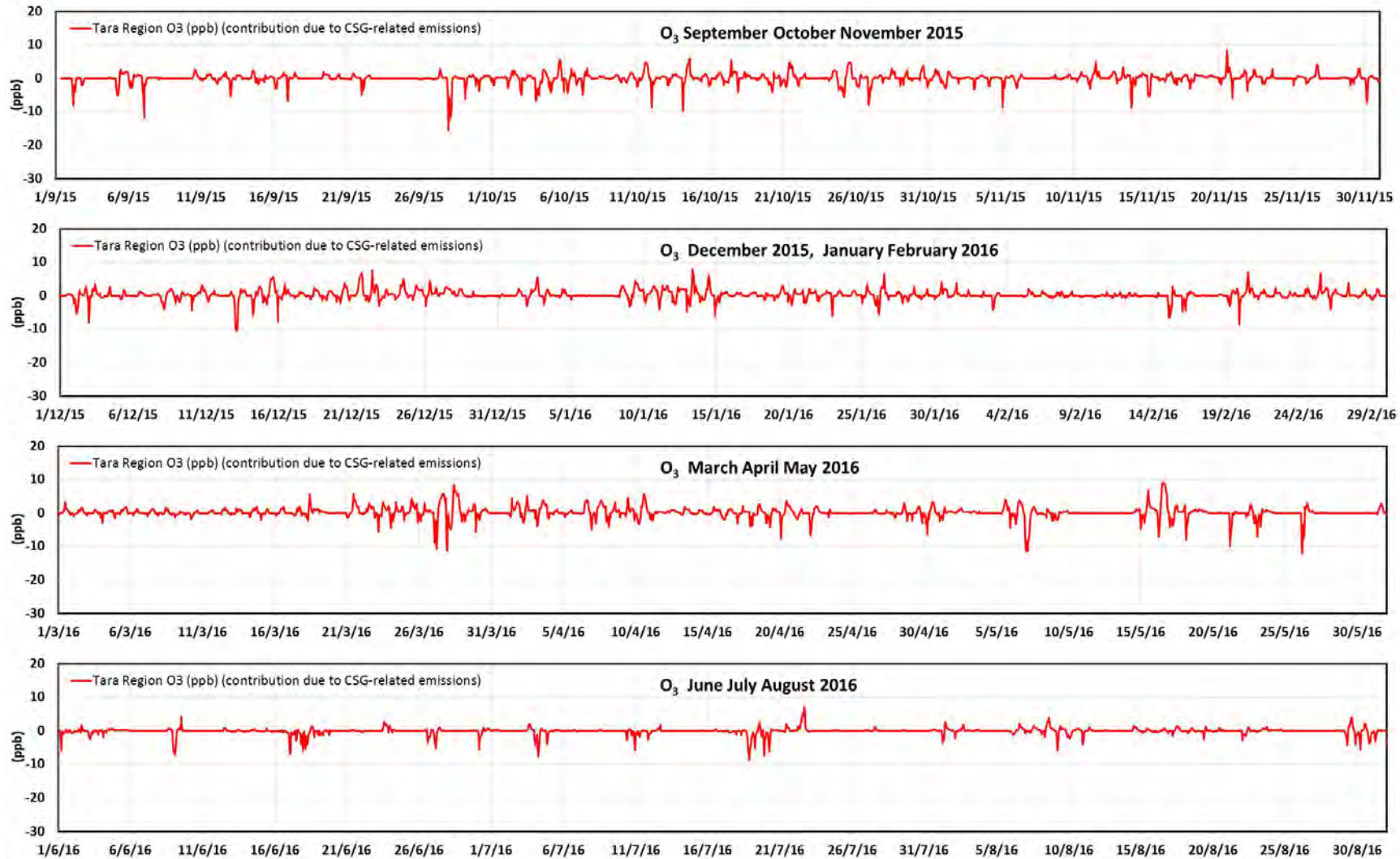


Figure D.14 The modelled contributions from the CSG-related emissions to the 1-hour average O₃ concentrations (ppb) at Tara Region for the modelled year.

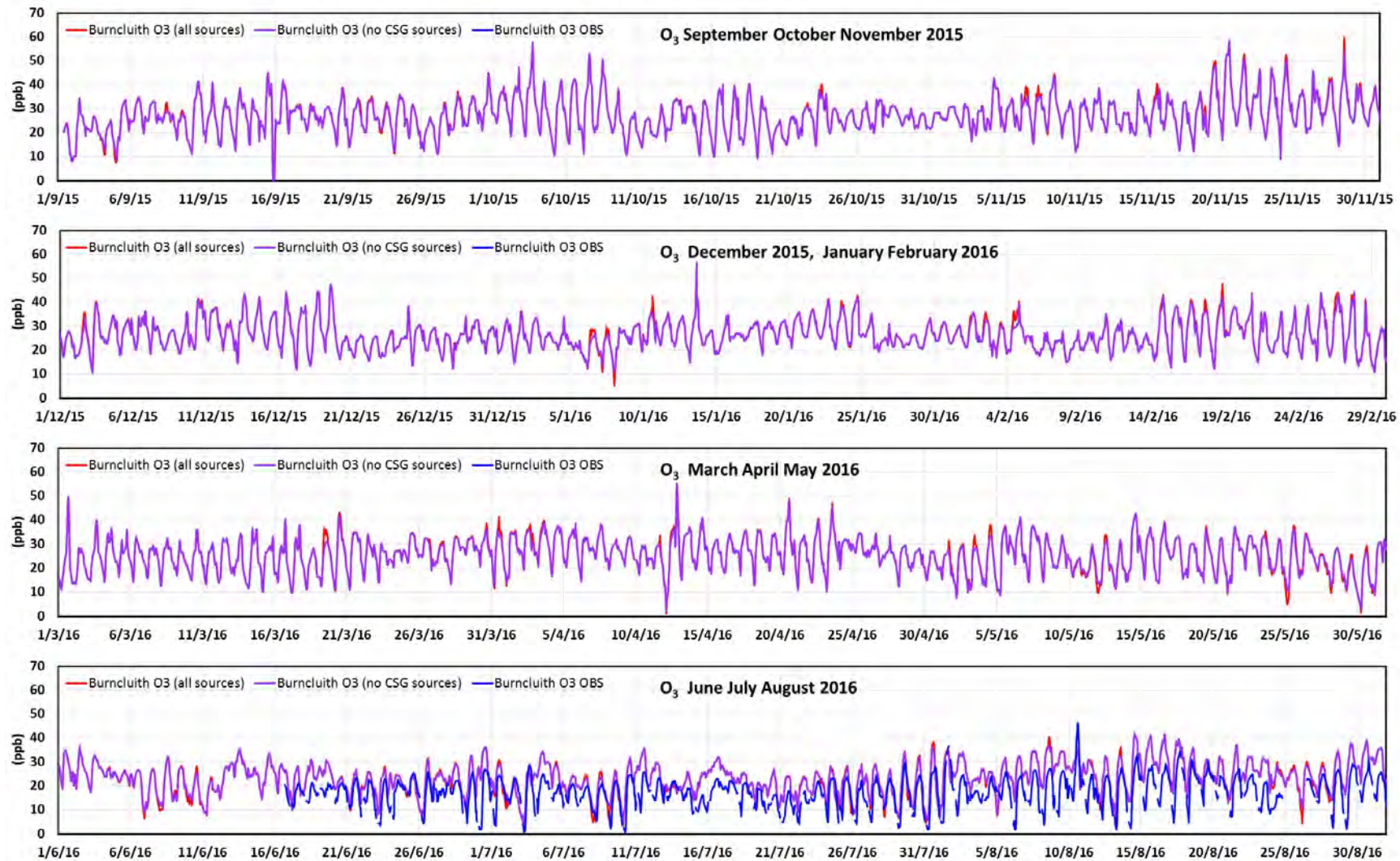


Figure D.15 The observed and modelled time series of the 1-hour average O₃ concentrations (ppb) at Burncluith for the modelled year (red = model results with all sources, purple = model results without CSG sources, blue = observations).

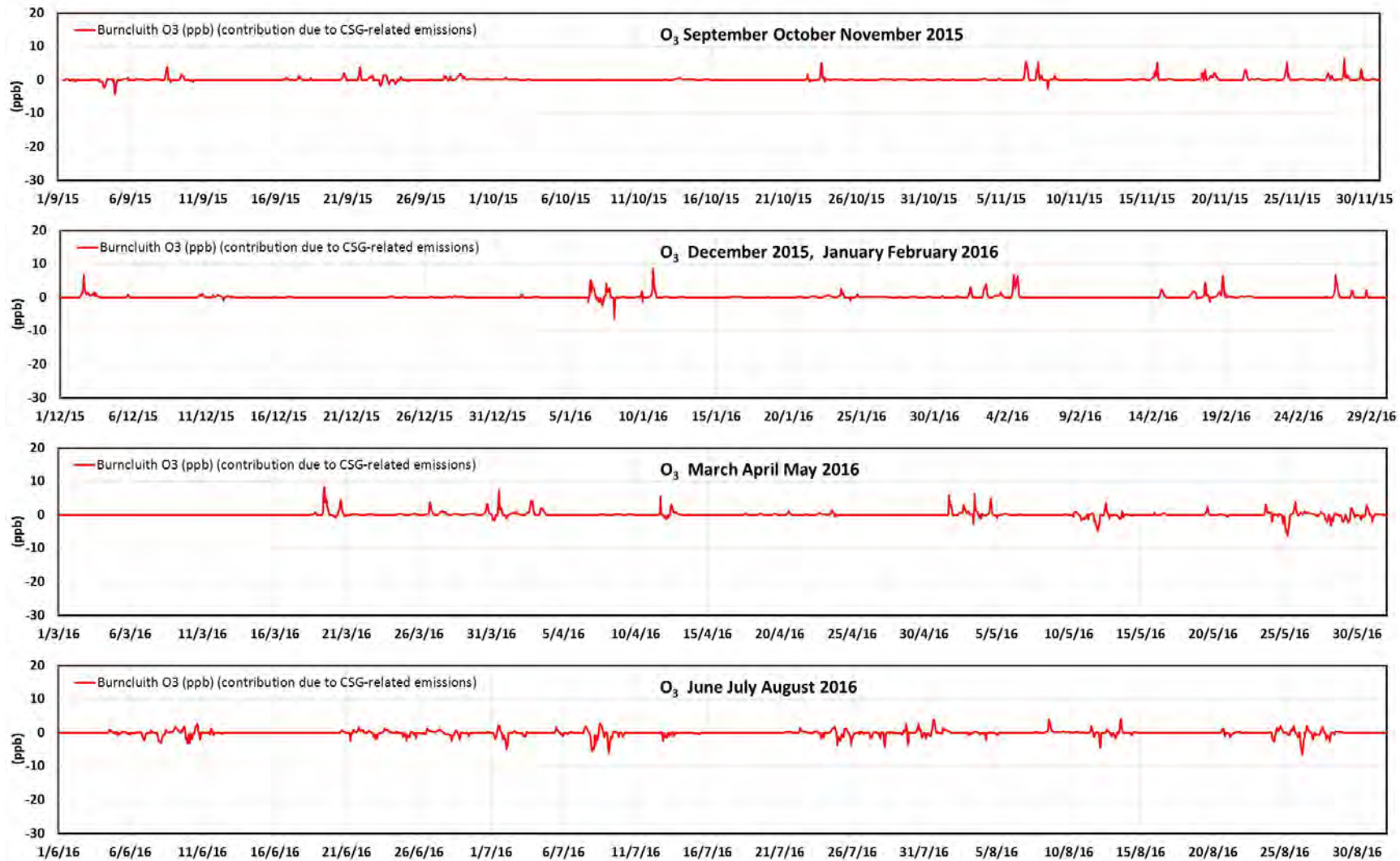


Figure D.16 The modelled contributions from the CSG-related emissions to the 1-hour average O₃ concentrations (ppb) at Burncluith for the modelled year.

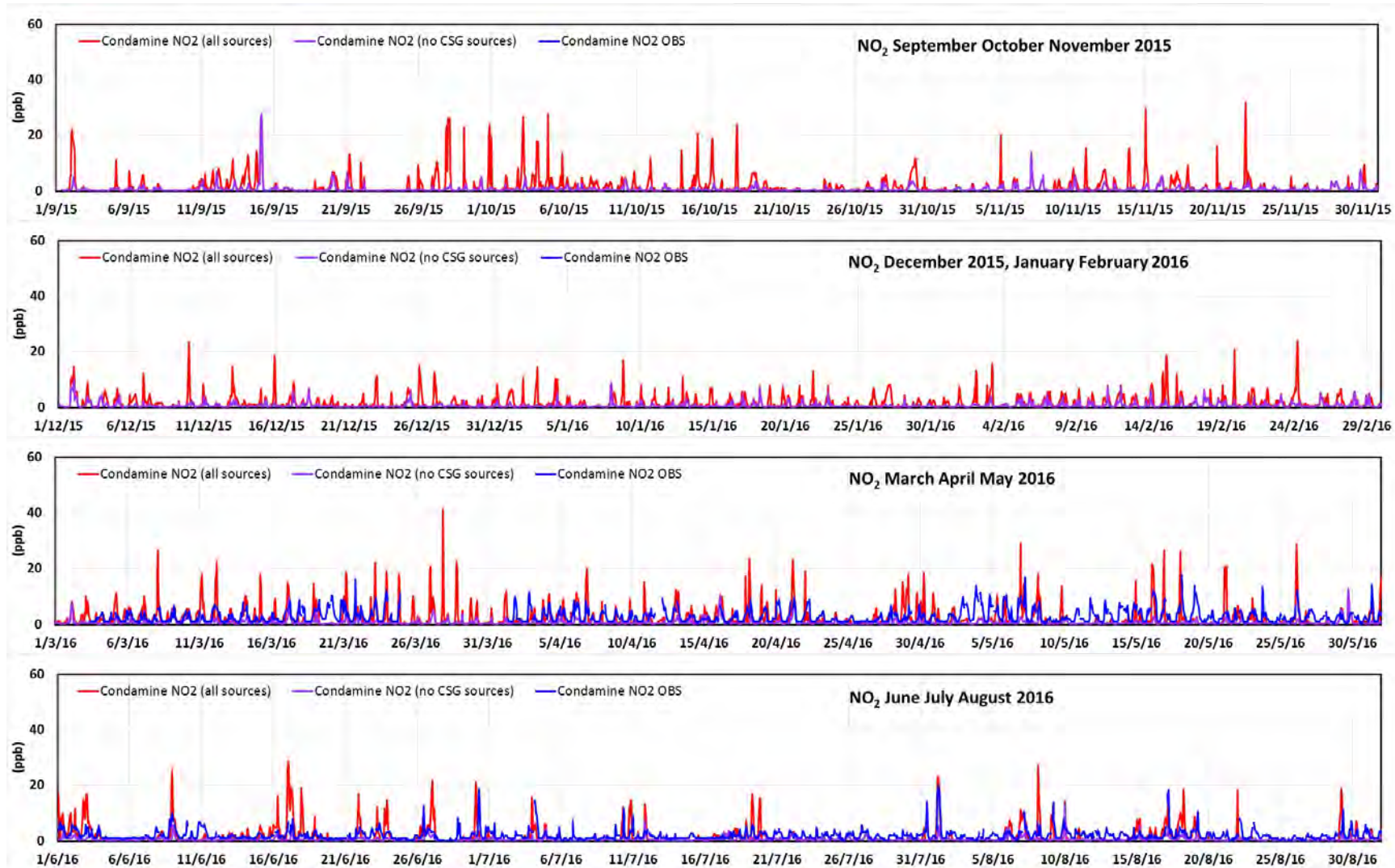


Figure D.17 The observed and modelled time series of the 1-hour average NO₂ concentrations (ppb) at Condamine for the modelled year (red = model results with all sources, purple = model results without CSG sources, blue = observations).

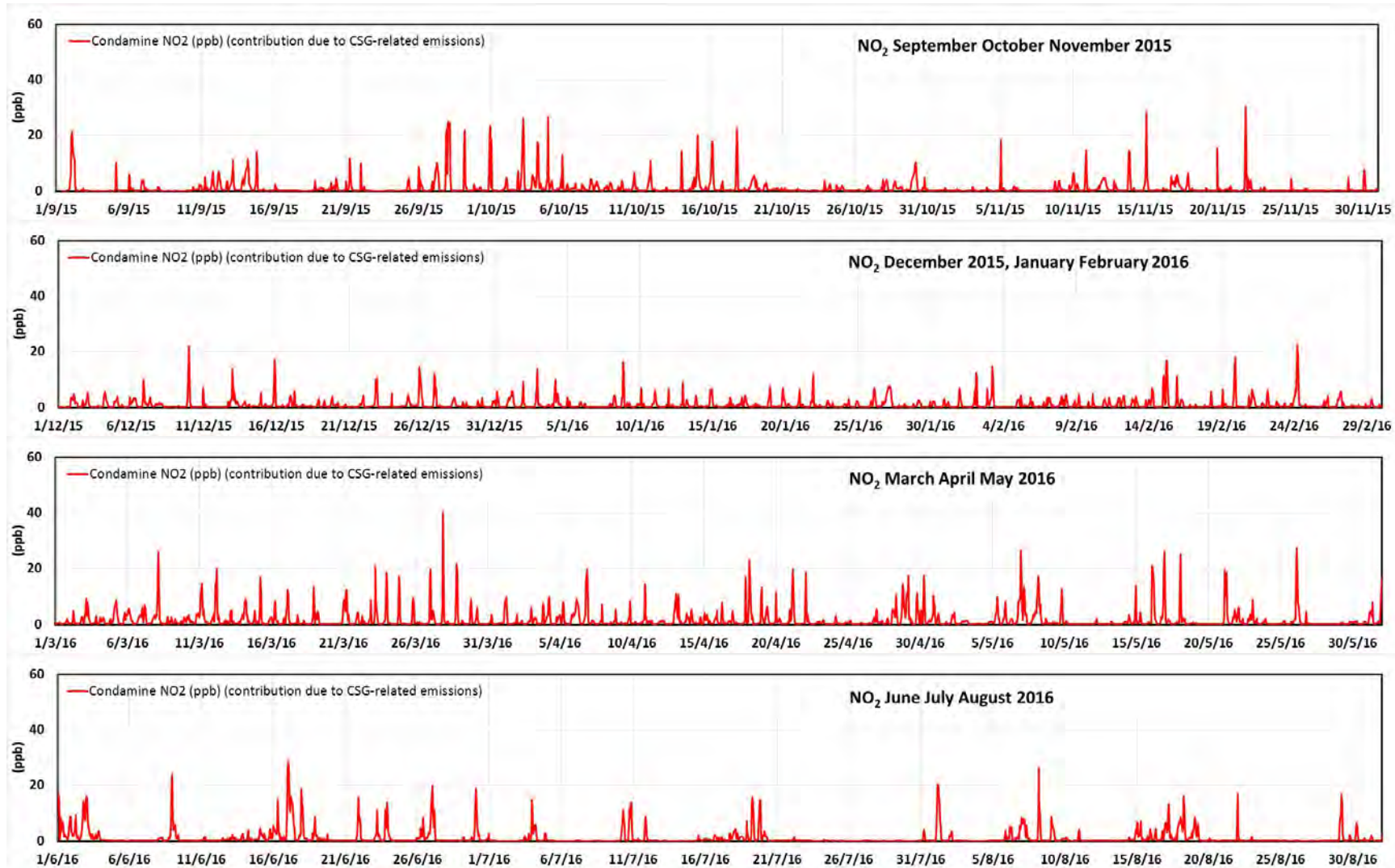


Figure D.18 The modelled contributions from the CSG-related emissions to the 1-hour average NO₂ concentrations (ppb) at Condamine for the modelled year.

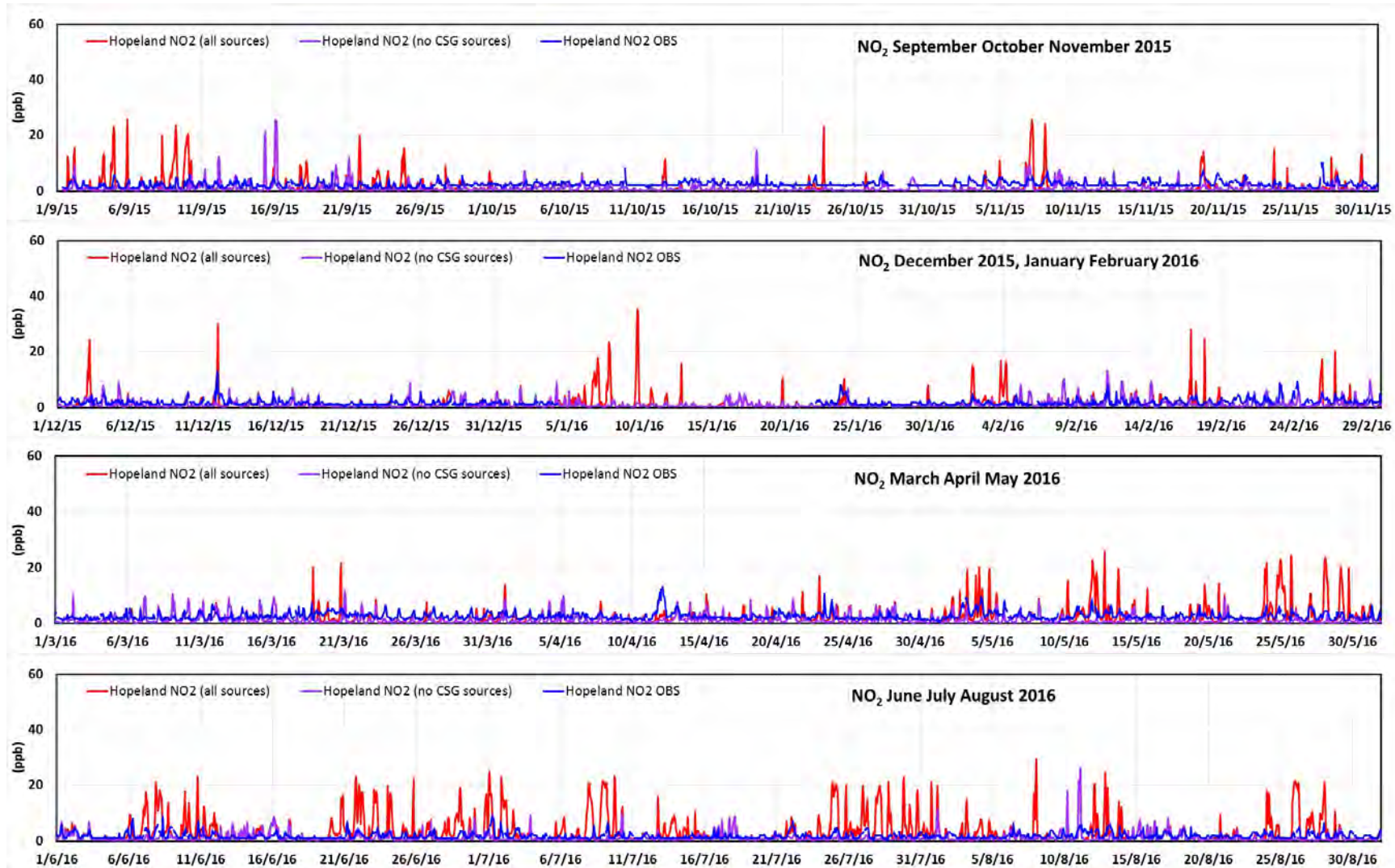


Figure D.29 The observed and modelled time series of the 1-hour average NO₂ concentrations (ppb) at Hopeland for the modelled year (red = model results with all sources, purple = model results without CSG sources, blue = observations).

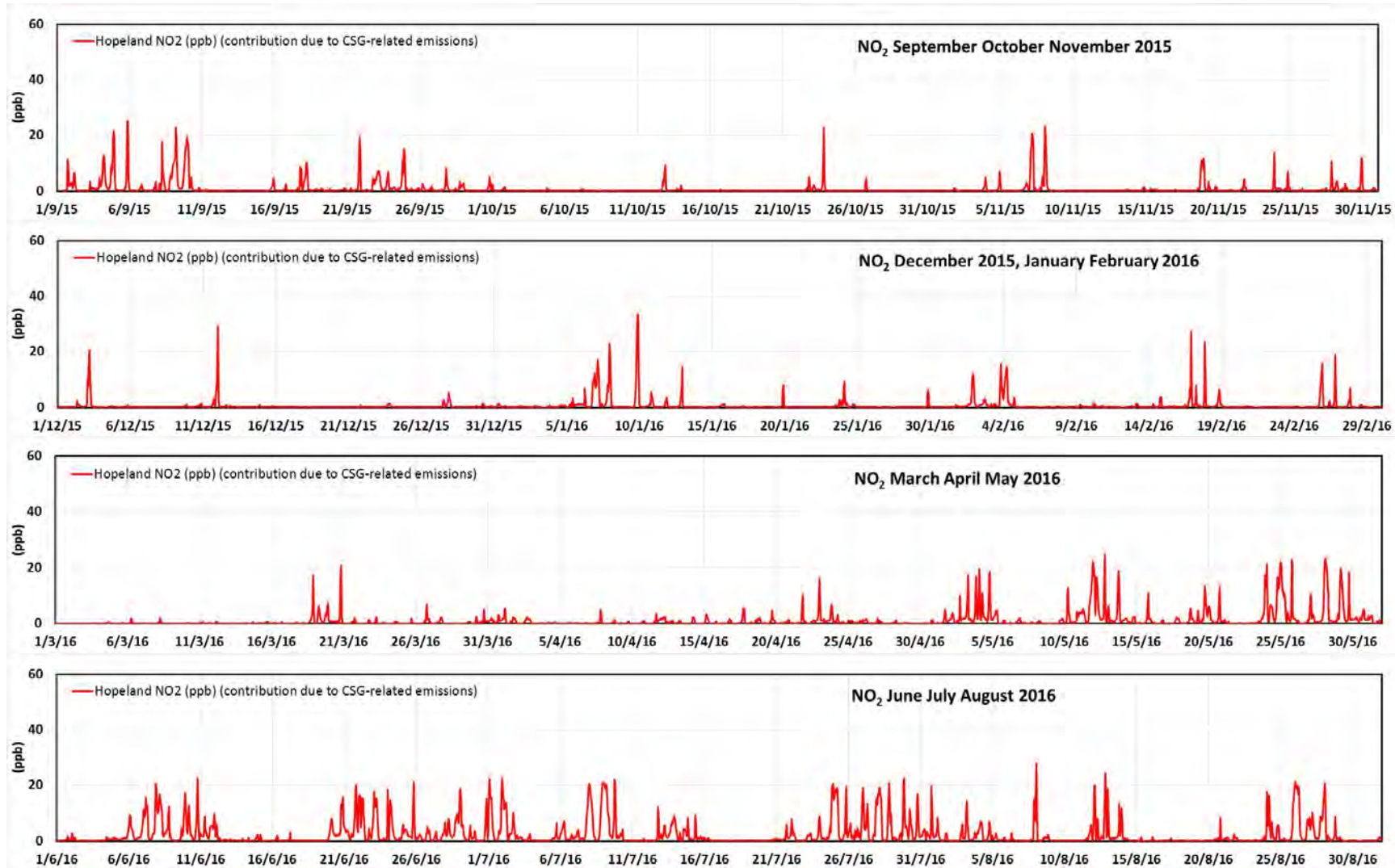


Figure D.20 The modelled contributions from the CSG-related emissions to the 1-hour average NO₂ concentrations (ppb) at Hopeland for the modelled year.

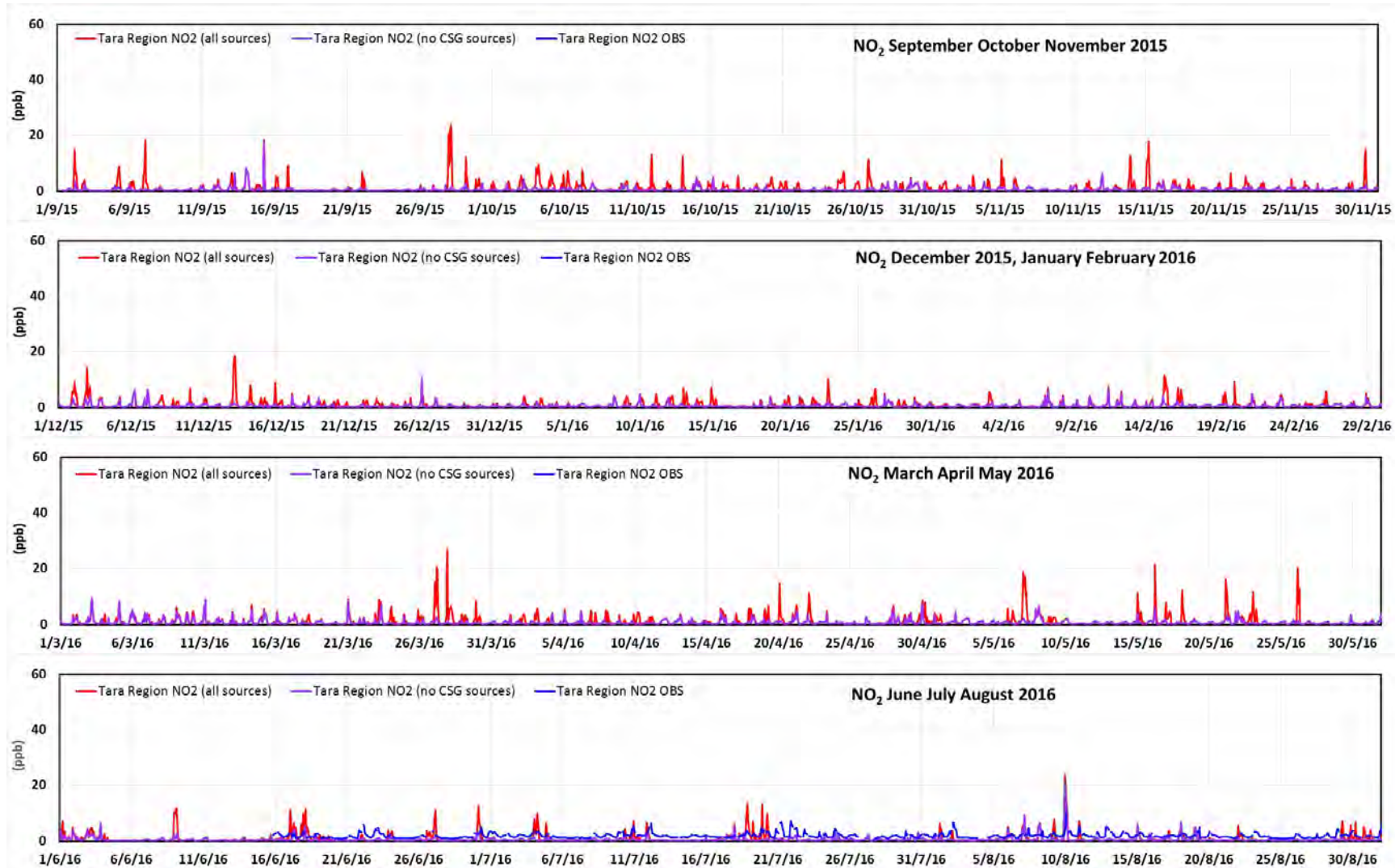


Figure D.3 The observed and modelled time series of the 1-hour average NO₂ concentrations (ppb) at Tara Region for the modelled year (red = model results with all sources, purple = model results without CSG sources, blue = observations).

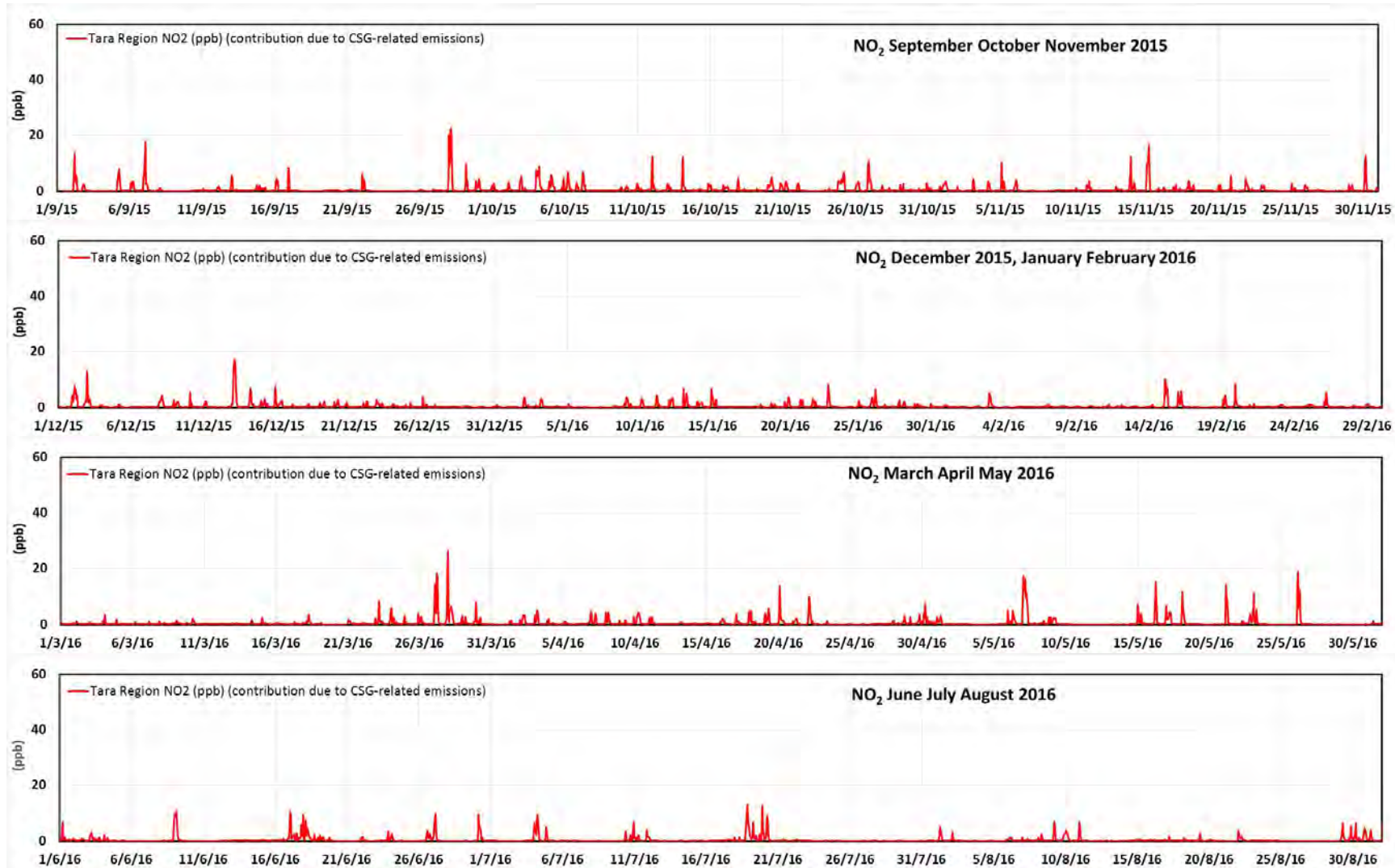


Figure D.22 The modelled contributions from the CSG-related emissions to the 1-hour average NO₂ concentrations (ppb) at Tara Region for the modelled year.

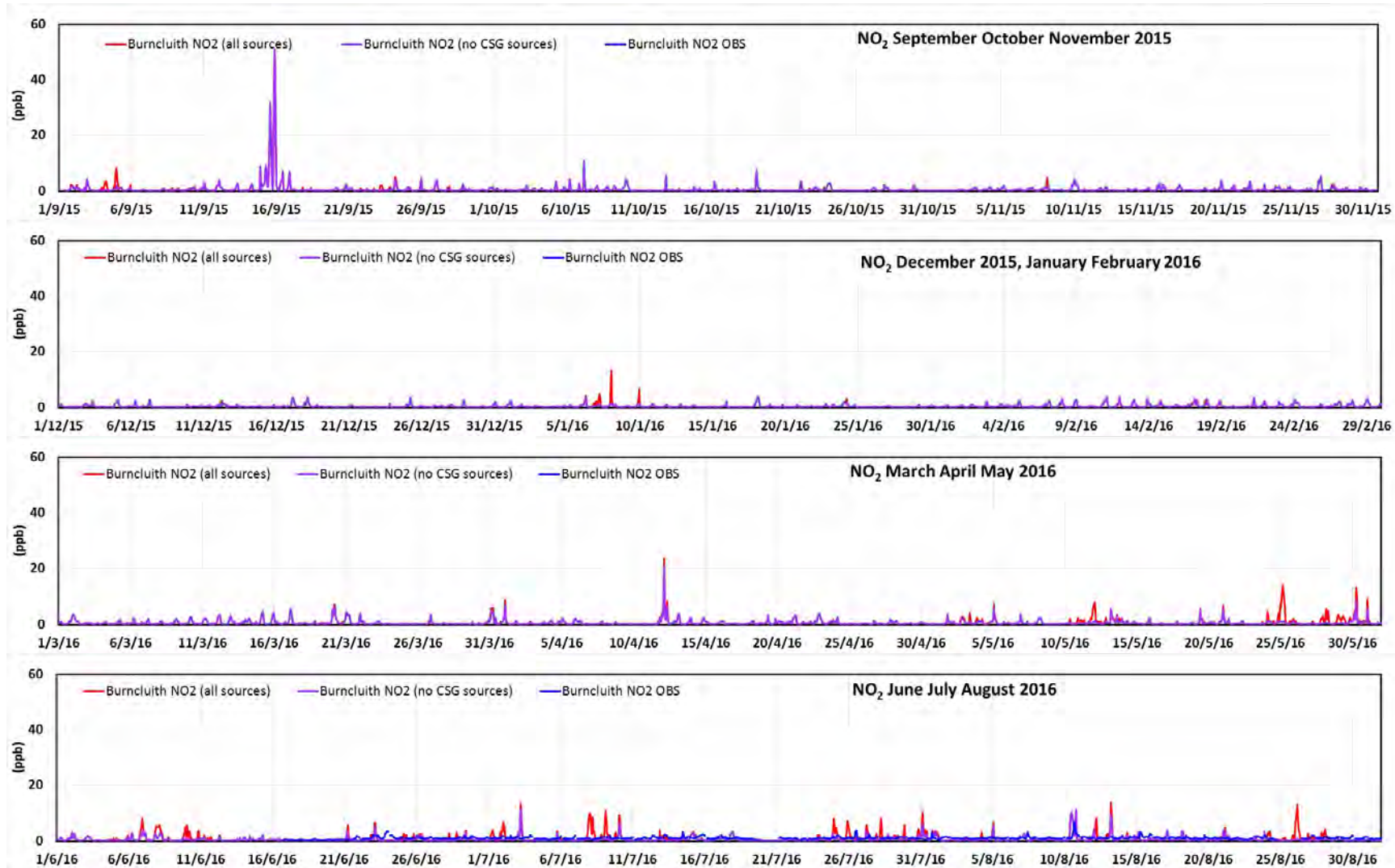


Figure D.234 The observed and modelled time series of the 1-hour average NO₂ concentrations (ppb) at Burncluith for the modelled year (red = model results with all sources, purple = model results without CSG sources, blue = observations).

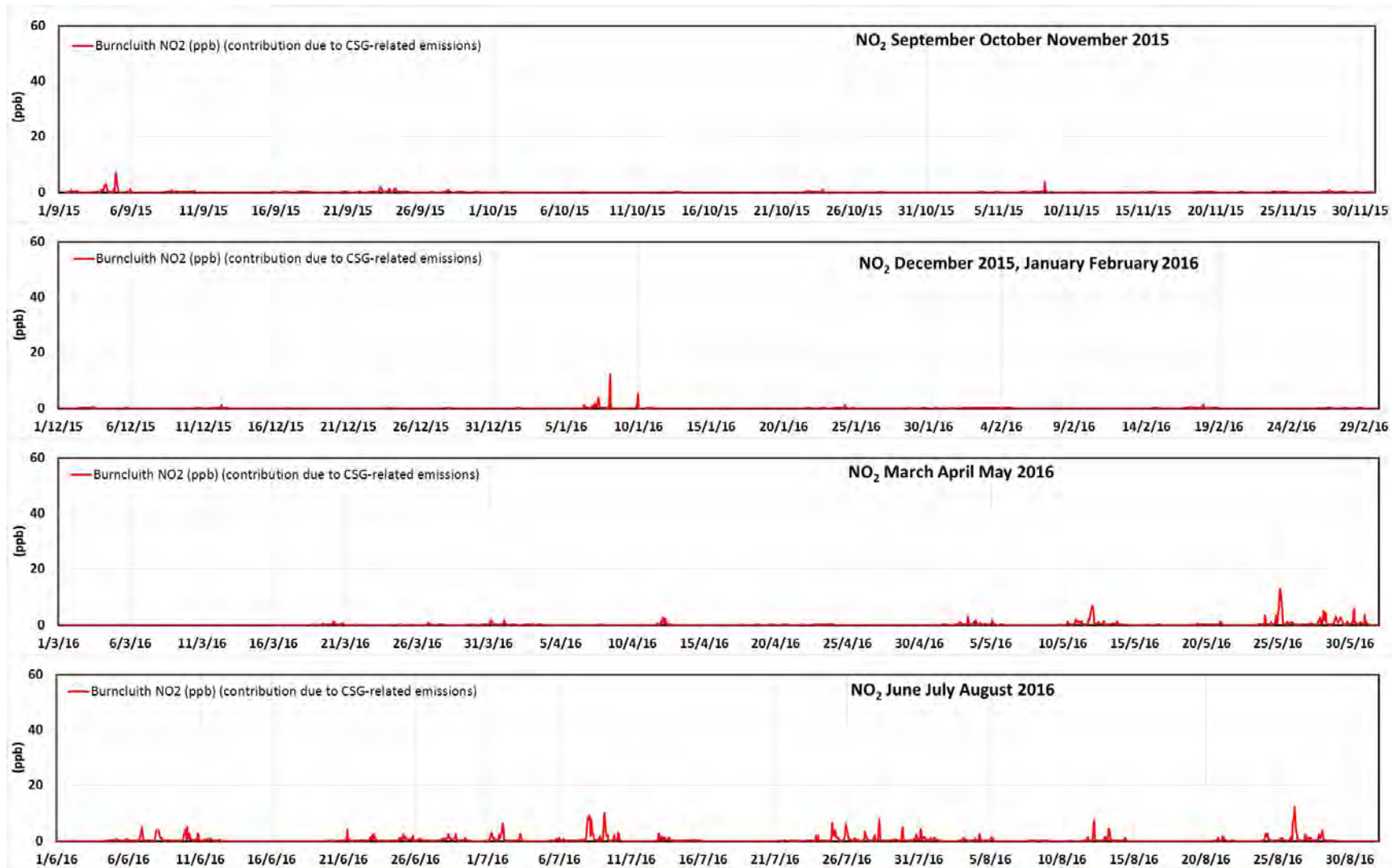


Figure D.24 The modelled contributions from the CSG-related emissions to the 1-hour average NO₂ concentrations (ppb) at Burncluith for the modelled year.

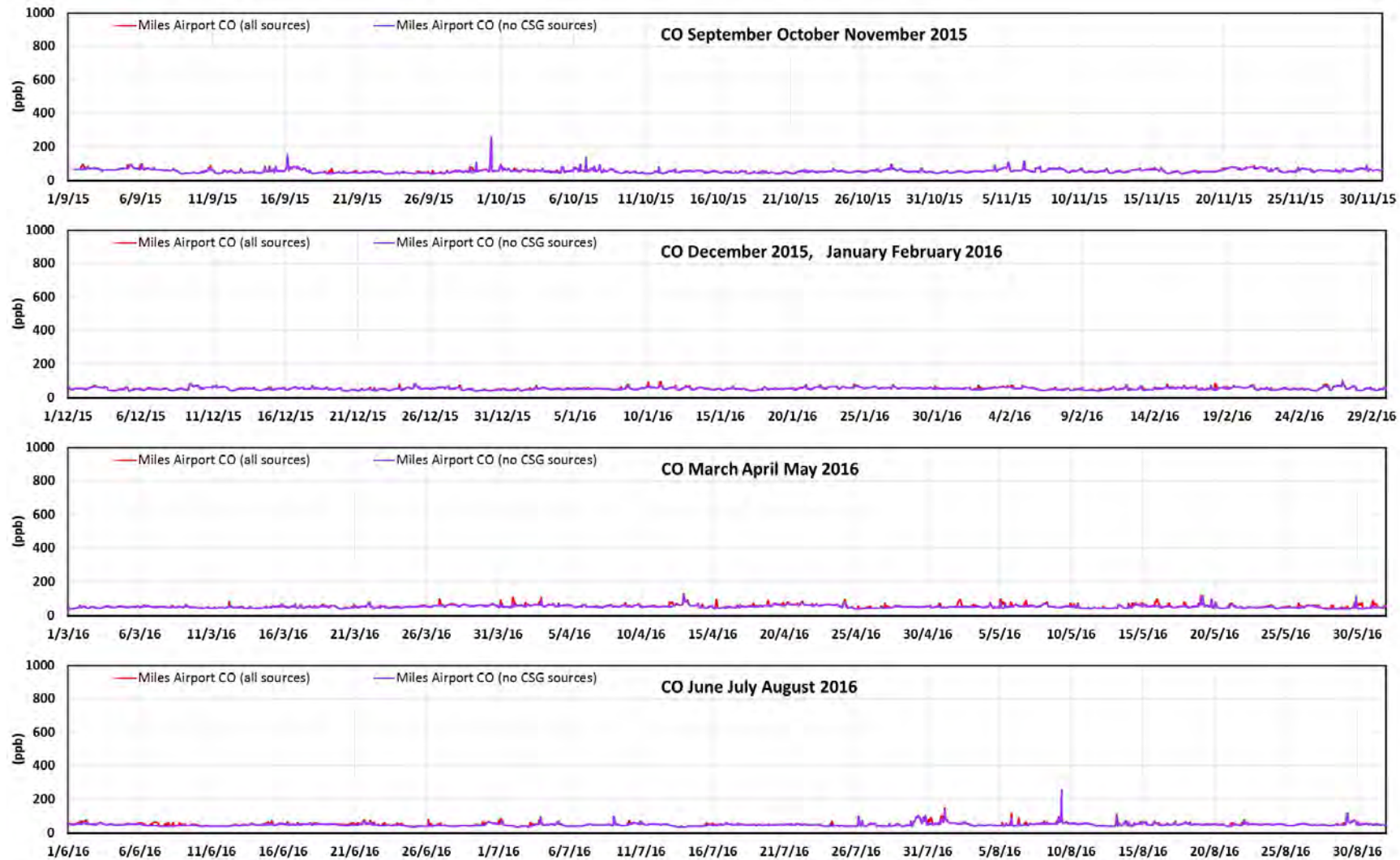


Figure D.25 The modelled time series of the 1-hour average CO concentrations (ppb) at Miles Airport for the modelled year (red = model results with all sources, purple = model results without CSG sources).

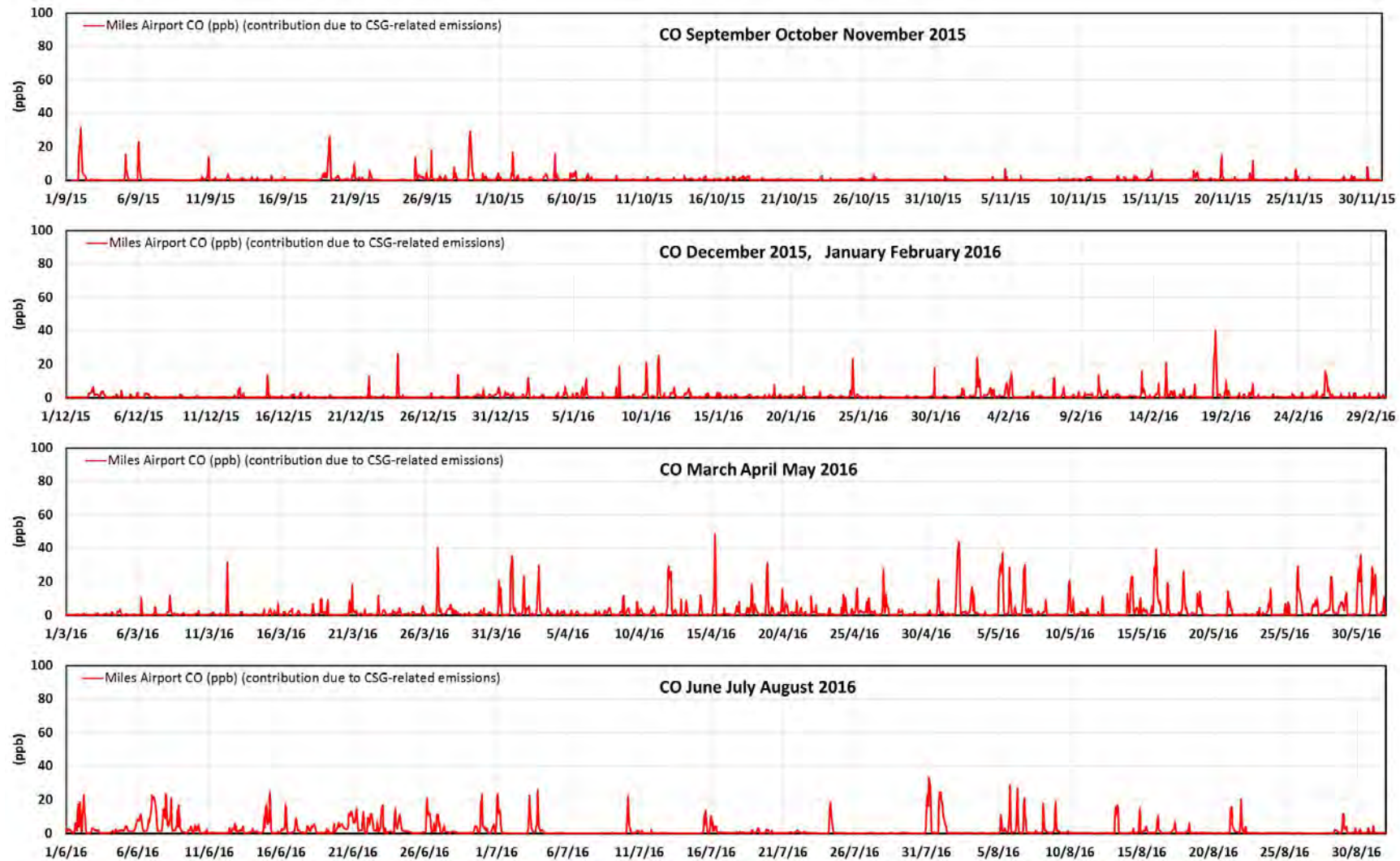


Figure D.26 The modelled contributions from the CSG-related emissions to the 1-hour average CO concentrations (ppb) at Miles Airport for the modelled year.

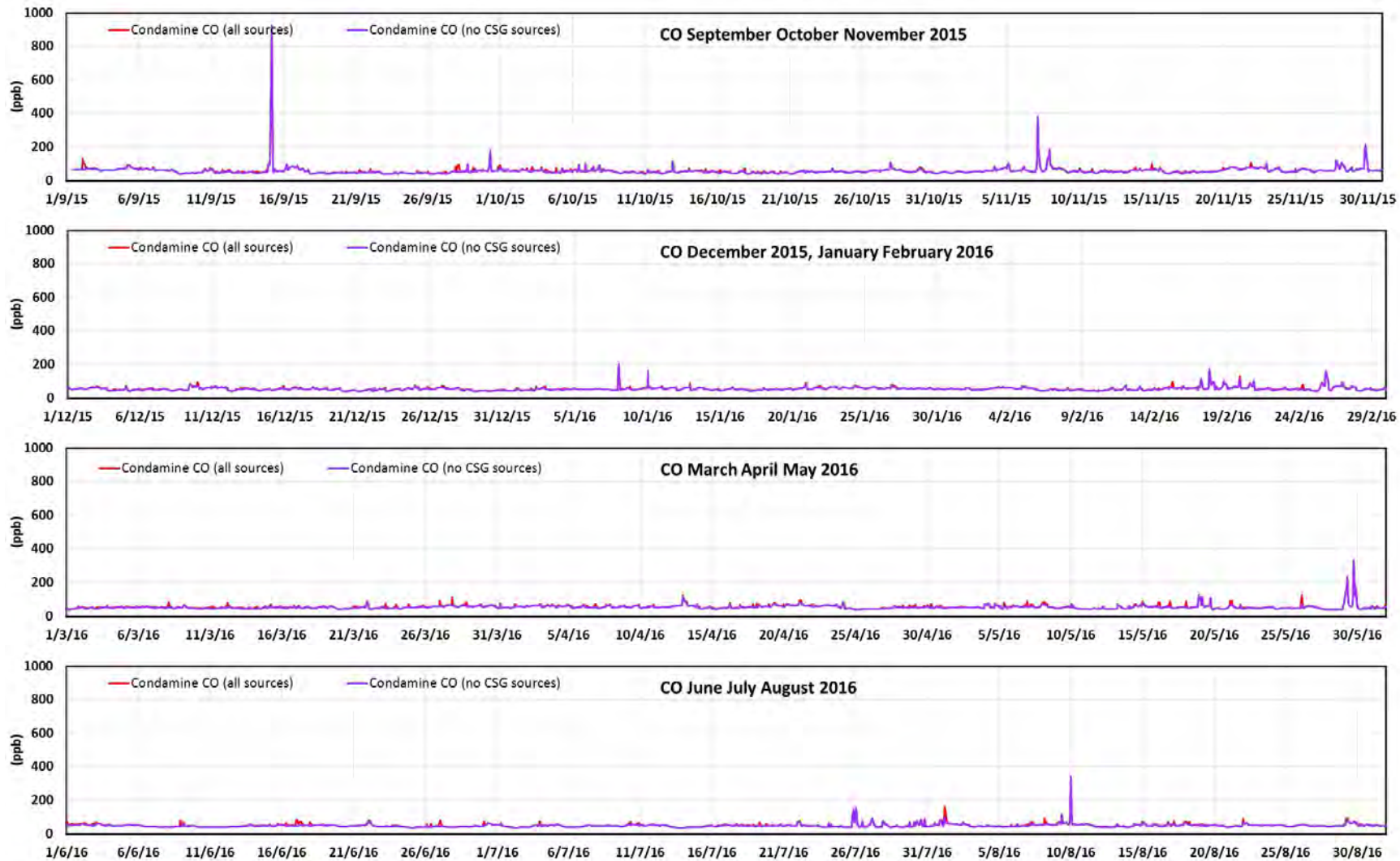


Figure D.275 The modelled time series of the 1-hour average CO concentrations (ppb) at Condamine for the modelled year (red = model results with all sources, purple = model results without CSG sources).

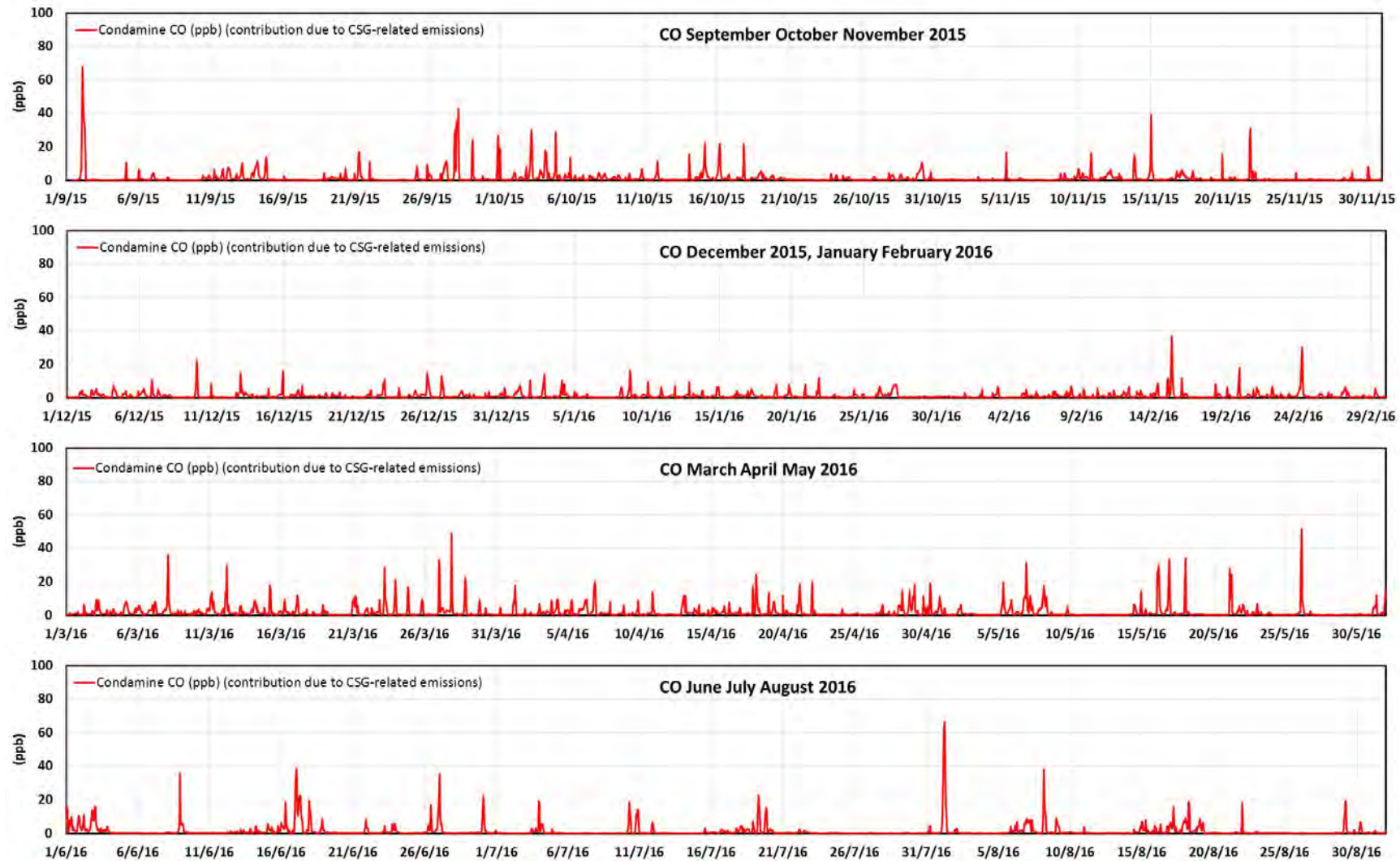


Figure D.28 The modelled contributions from the CSG-related emissions to the 1-hour average CO concentrations (ppb) at Condamine for the modelled year.

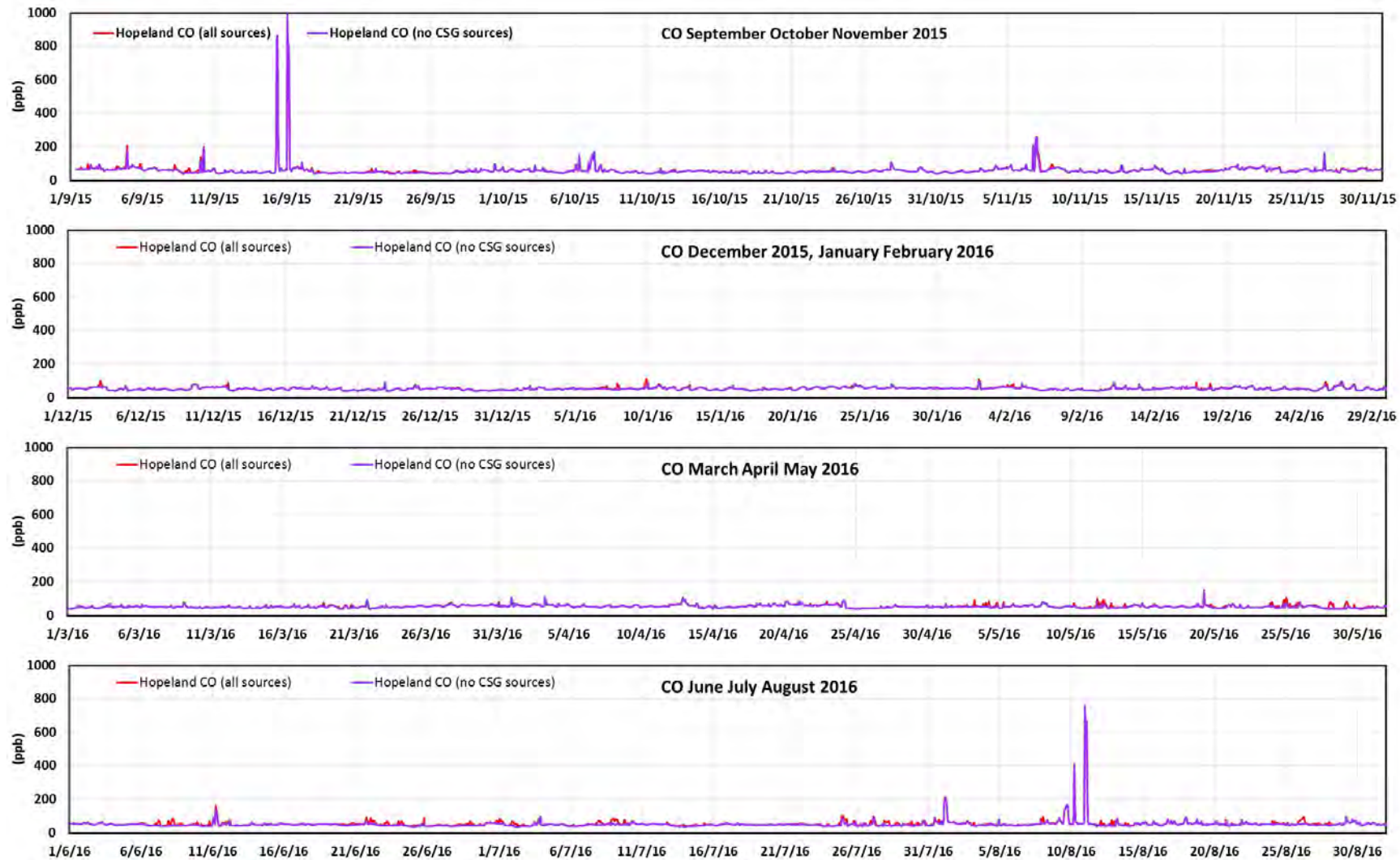


Figure D.29 The modelled time series of the 1-hour average CO concentrations (ppb) at Hopeland for the modelled year (red = model results with all sources, purple = model results without CSG sources).

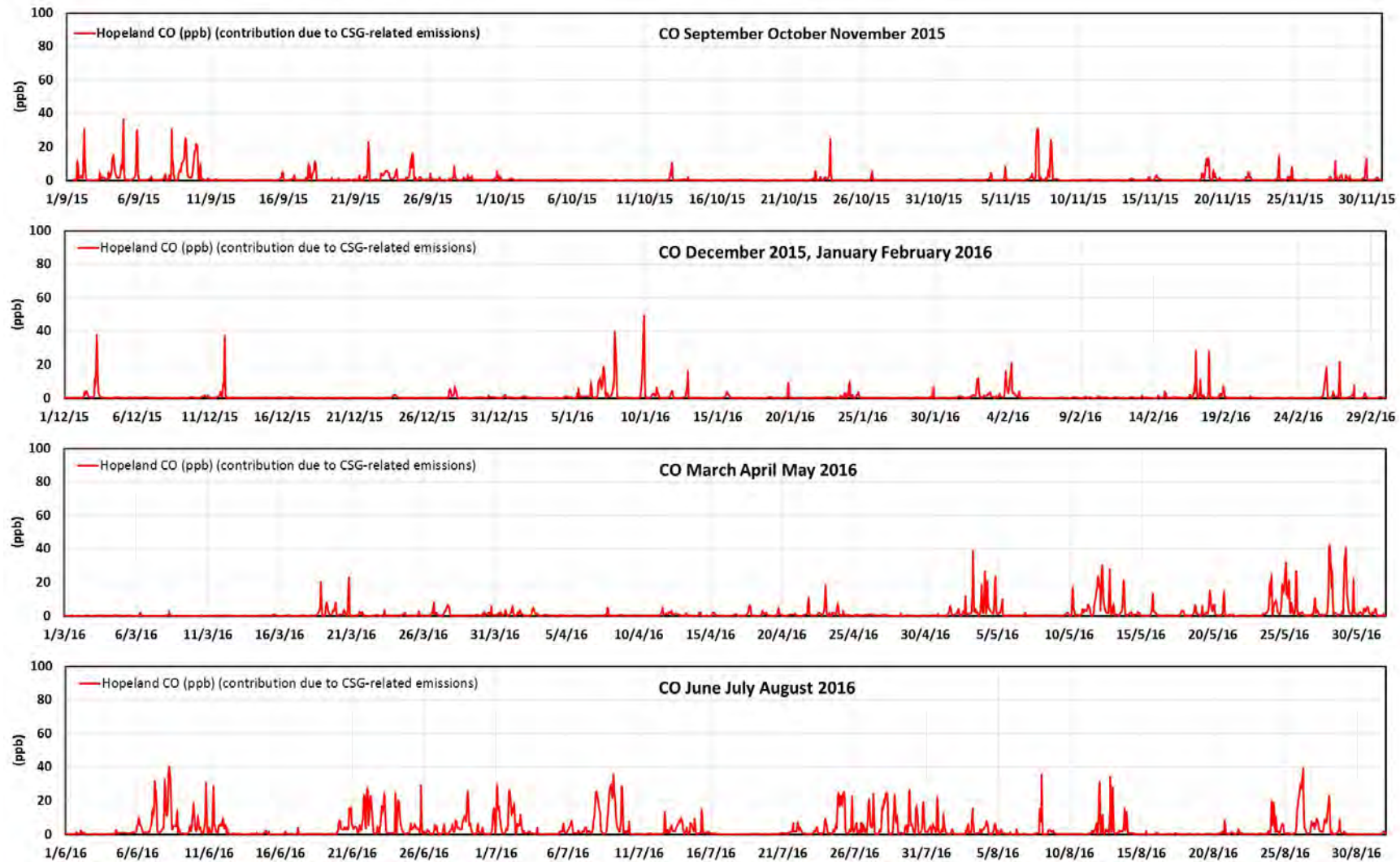


Figure D.30 The modelled contributions from the CSG-related emissions to the 1-hour average CO concentrations (ppb) at Hopeland for the modelled year.

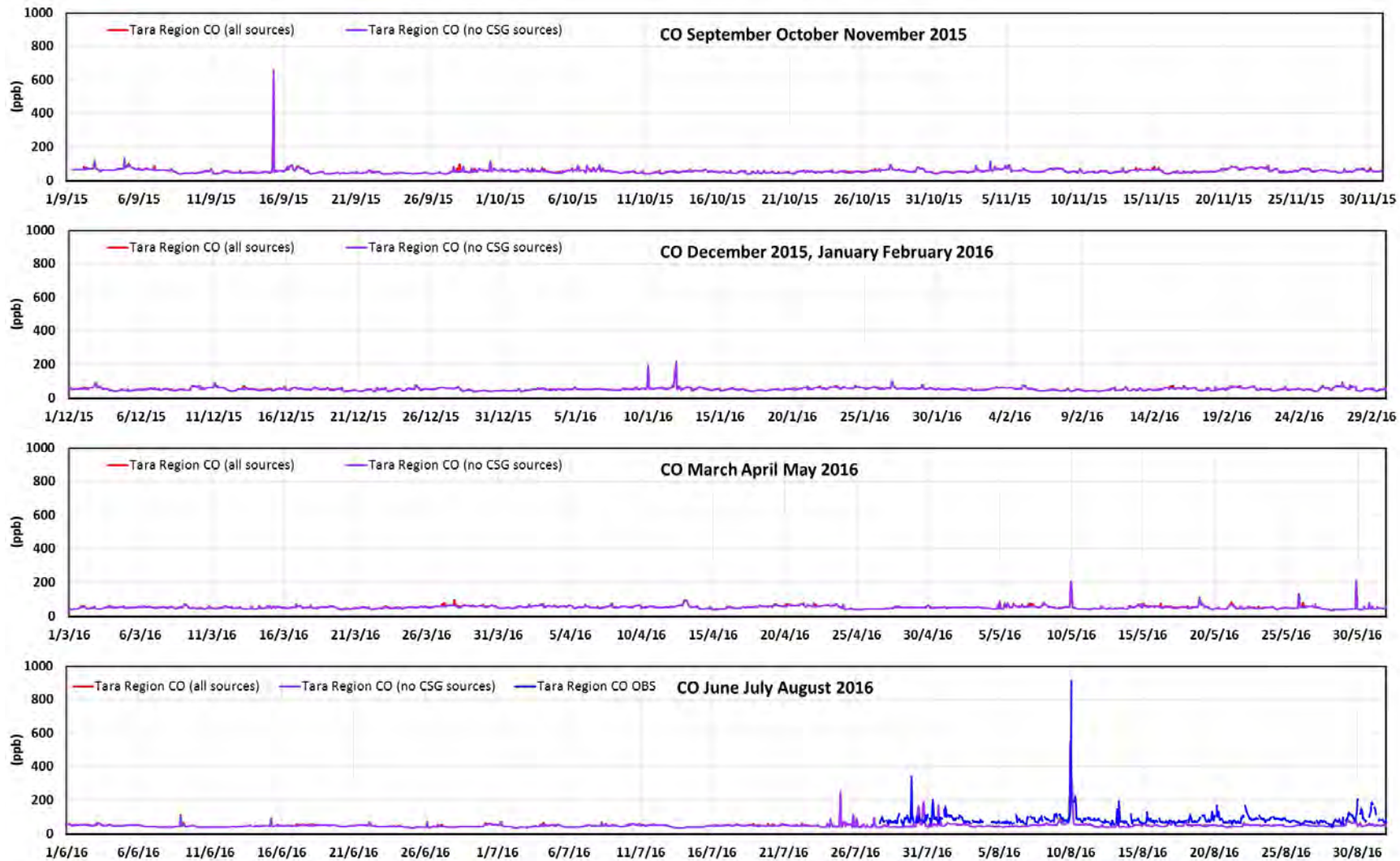


Figure D.316 The observed and modelled time series of the 1-hour average CO concentrations (ppb) at Tara Region for the modelled year (red = model results with all sources, purple = model results without CSG sources, blue = observations).

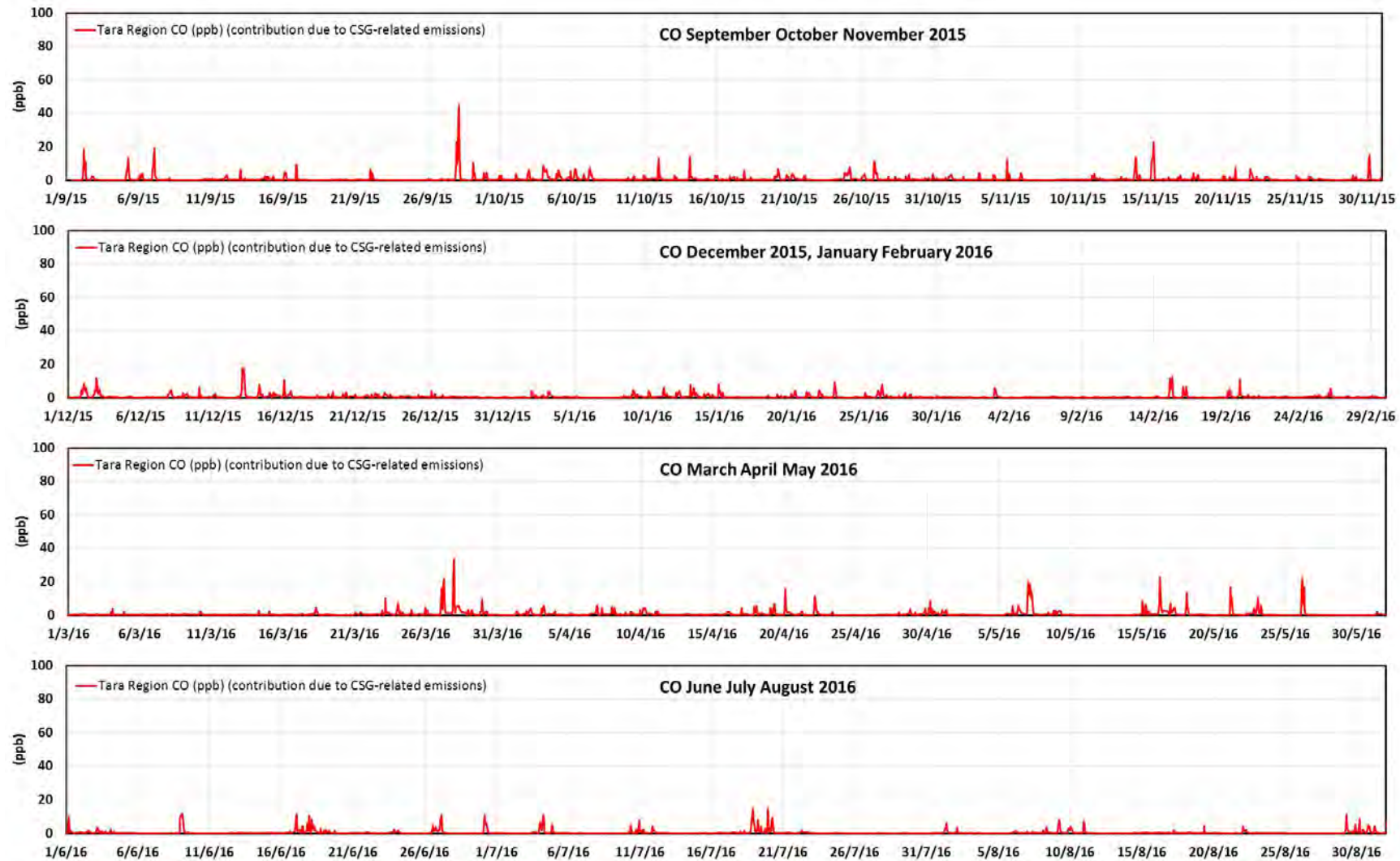


Figure D.32 The modelled contributions from the CSG-related emissions to the 1-hour average CO concentrations (ppb) at Tara Region for the modelled year.

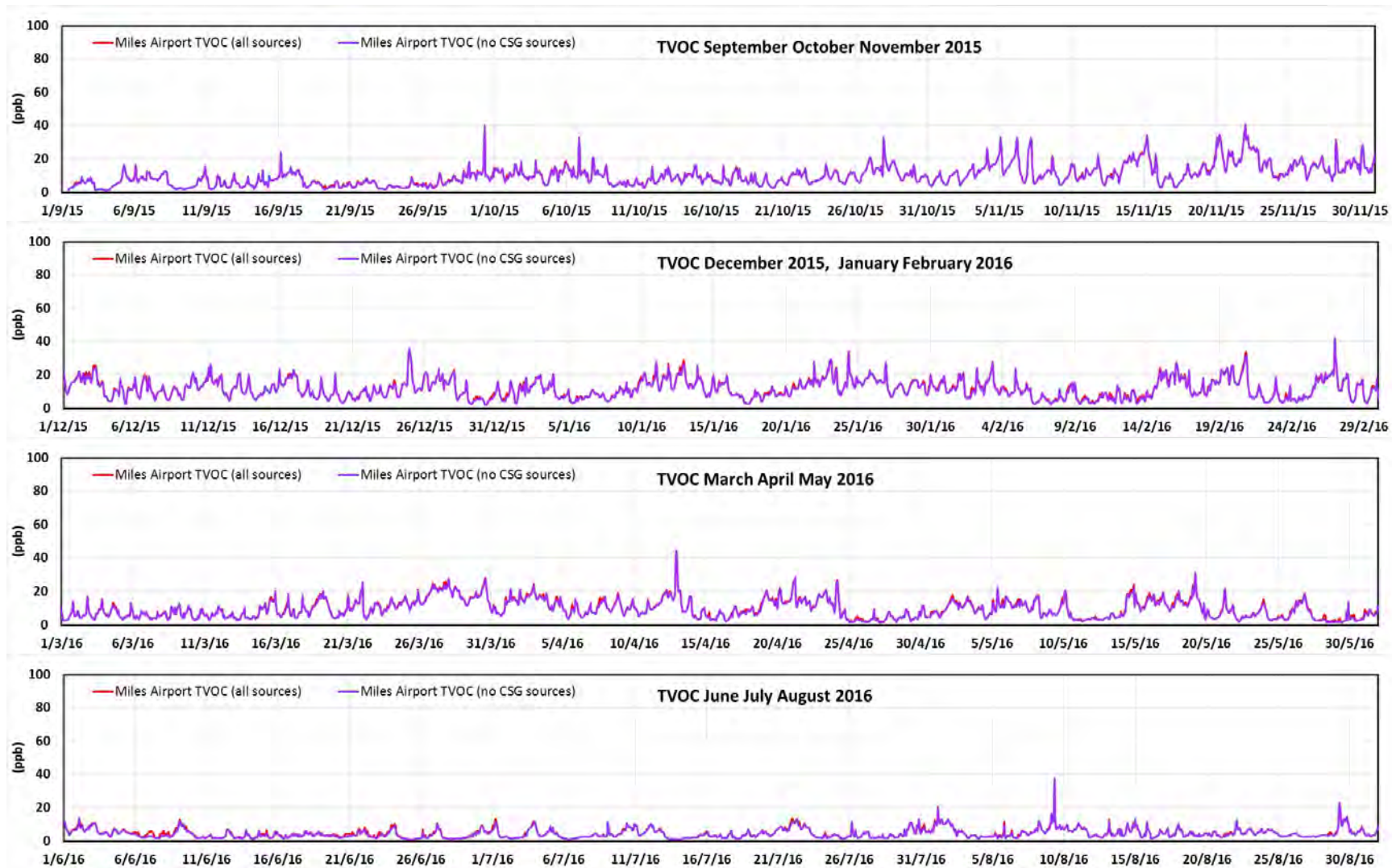


Figure D.33 The modelled time series of the 1-hour average TVOC concentrations (ppb) at Miles Airport for the modelled year (red = model results with all sources, purple = model results without CSG sources).

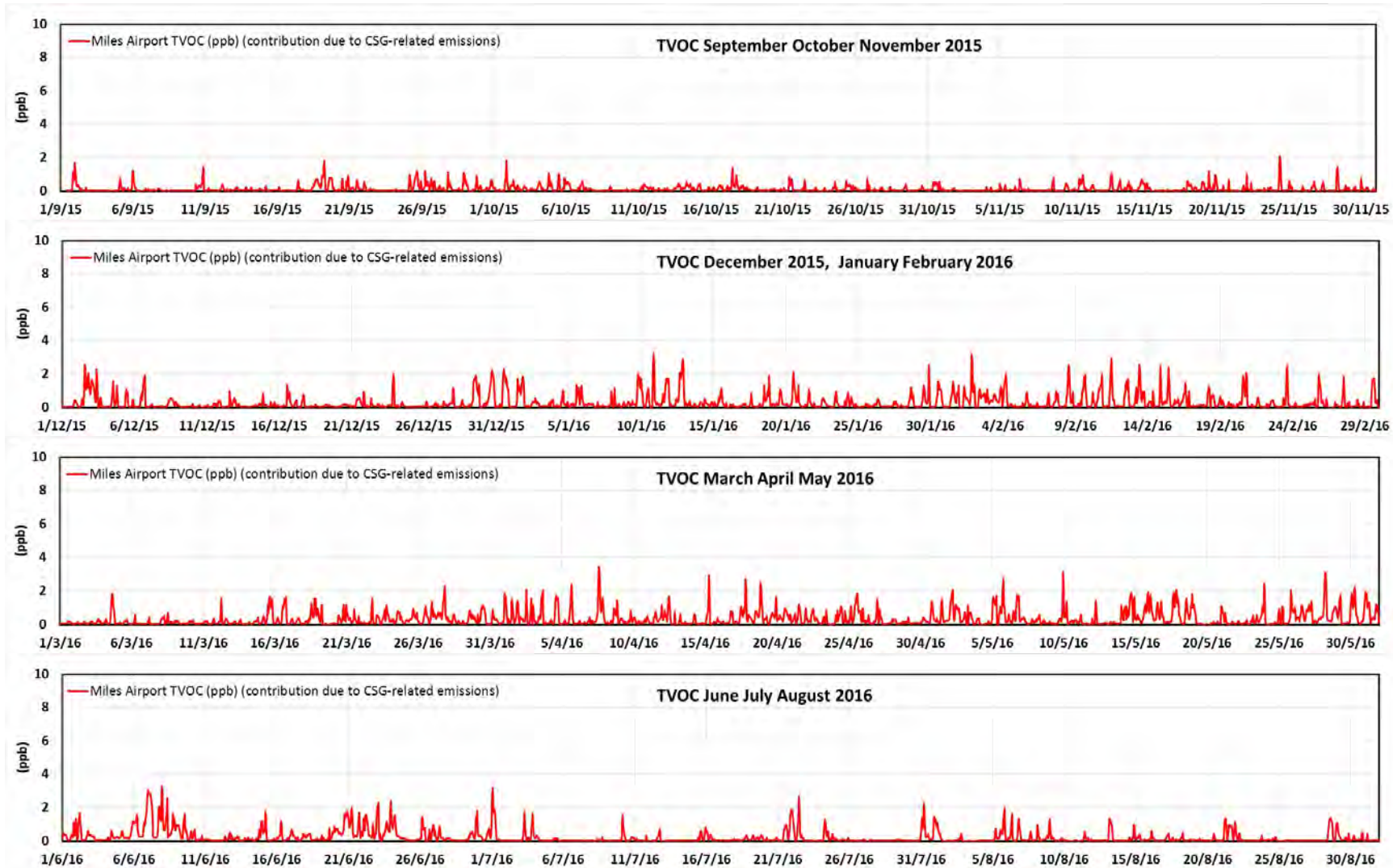


Figure D.34 The modelled contributions from the CSG-related emissions to the to 1-hour average TVOC concentrations (ppb) at Miles Airport for the modelled year.



Figure D.35 The modelled time series of the 1-hour average TVOC concentrations (ppb) at Condamine for the modelled year (red = model results with all sources, purple = model results without CSG sources). (peaks off scale: model, 15/9/15 04:00 = 135 ppb)

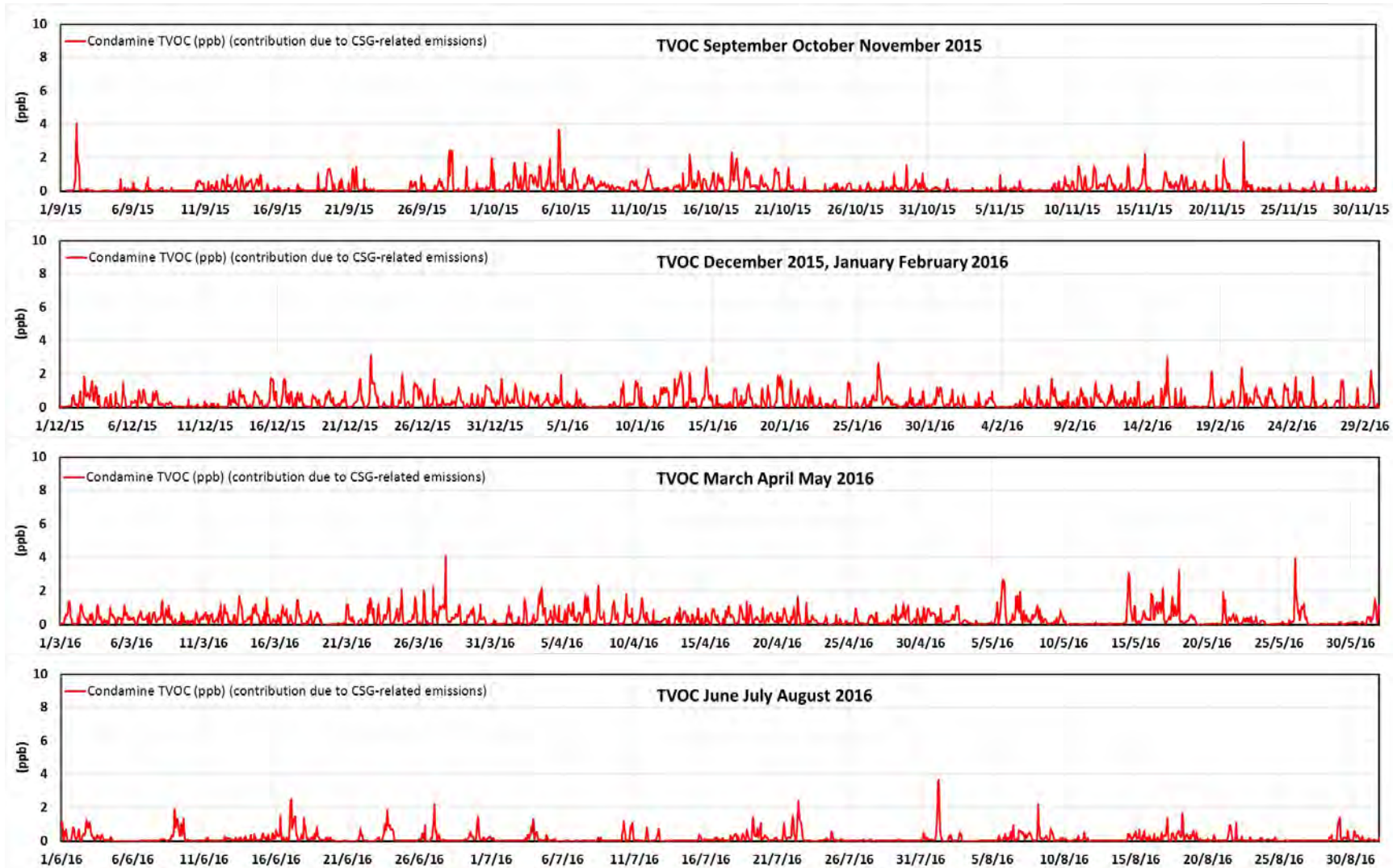


Figure D.36 The modelled contributions from the CSG-related emissions to the 1-hour average TVOC concentrations (ppb) at Condamine for the modelled year.

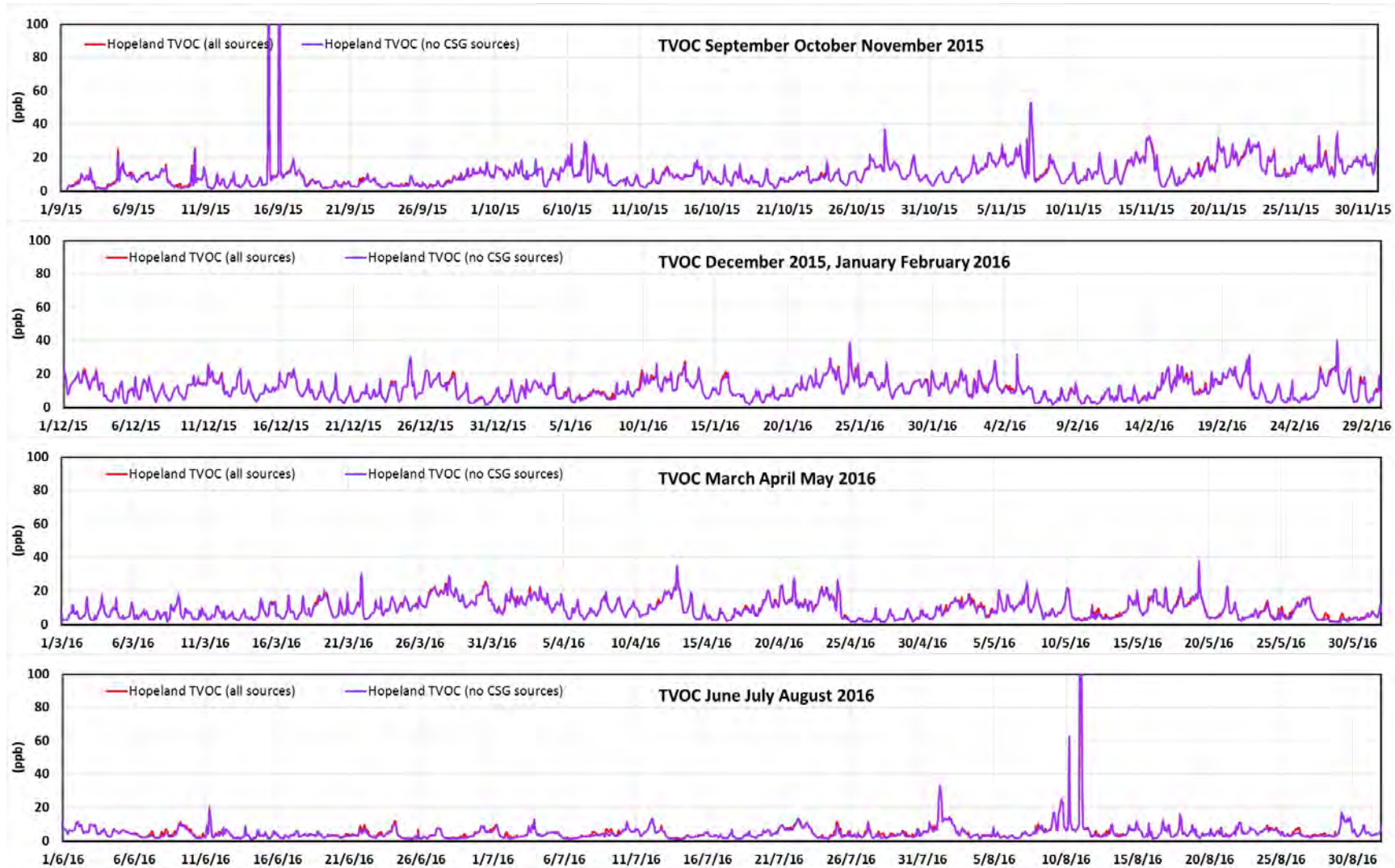


Figure D.37 The modelled time series of the 1-hour average TVOC concentrations (ppb) at Hopeland for the modelled year (red = model results with all sources, purple = model results without CSG sources). (peaks off scale: model, 15/9/15 09:00 = 123 ppb, 16/9/15 01:00 = 155 ppb, 10/8/16 23:00 = 115 ppb)

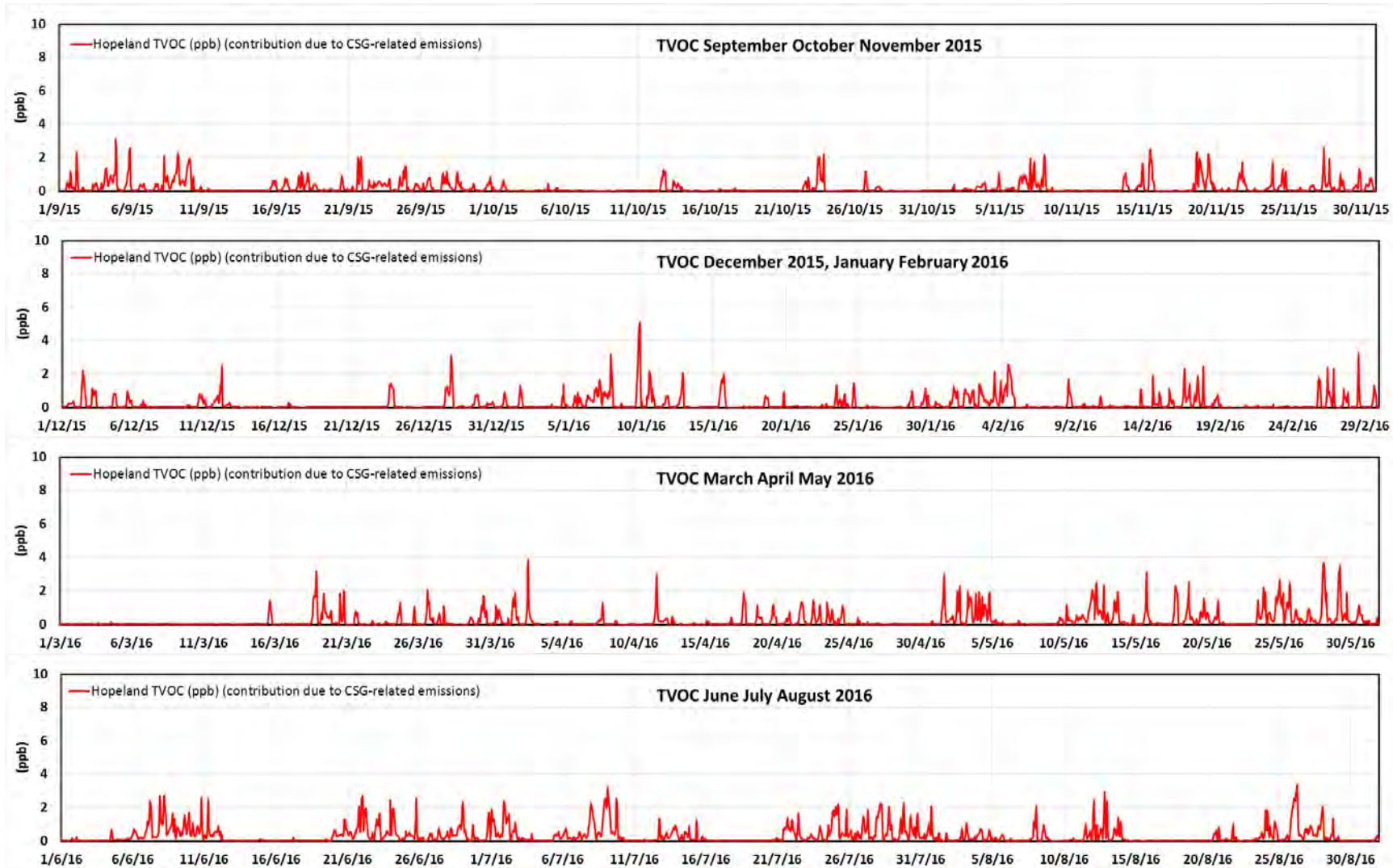


Figure D.38 The modelled contributions from the CSG-related emissions to the 1-hour average TVOC concentrations (ppb) at Hopeland for the modelled year.

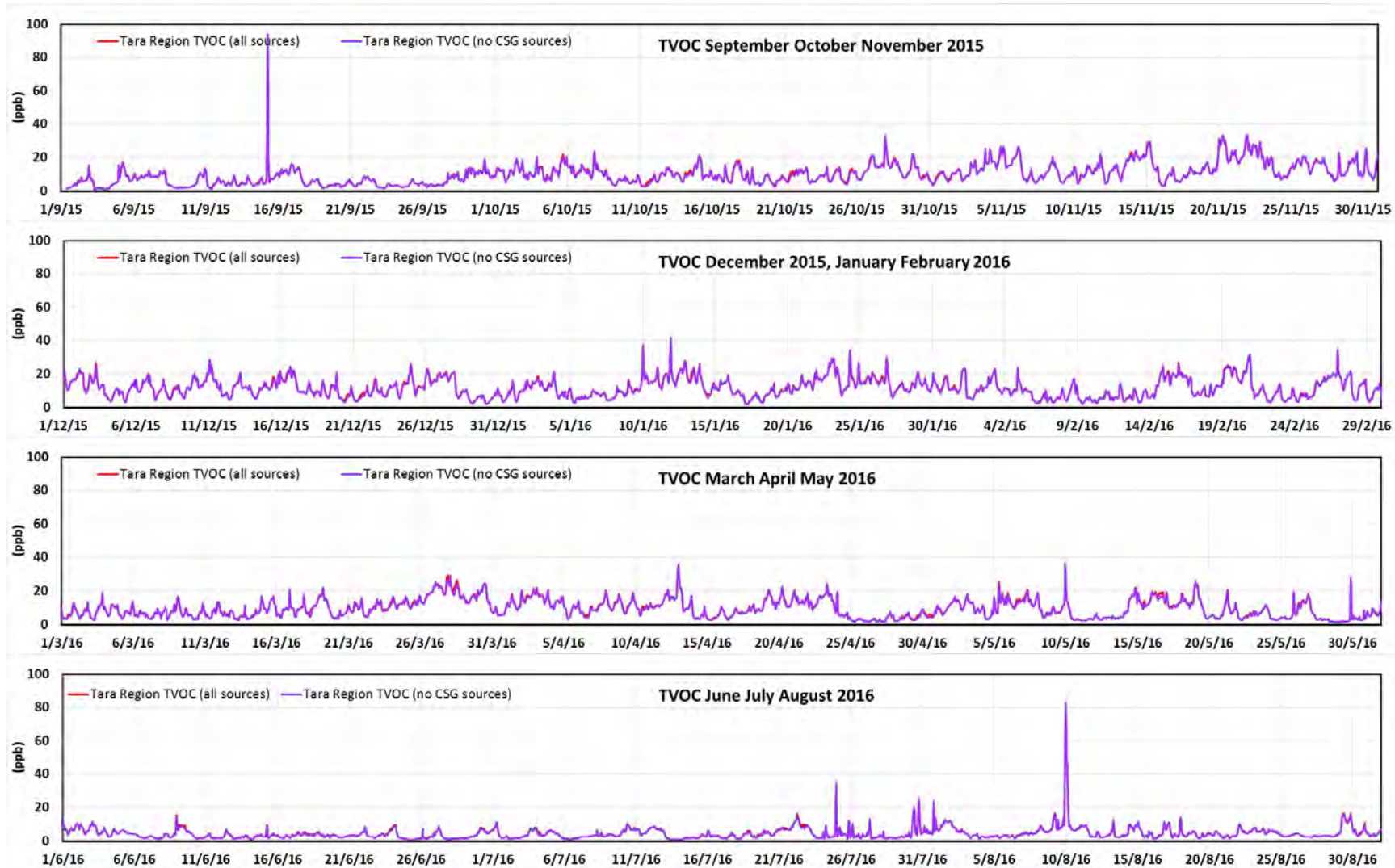


Figure D.39 The modelled time series of the 1-hour average TVOC concentrations (ppb) at Tara Region for the modelled year (red = model results with all sources, purple = model results without CSG sources).

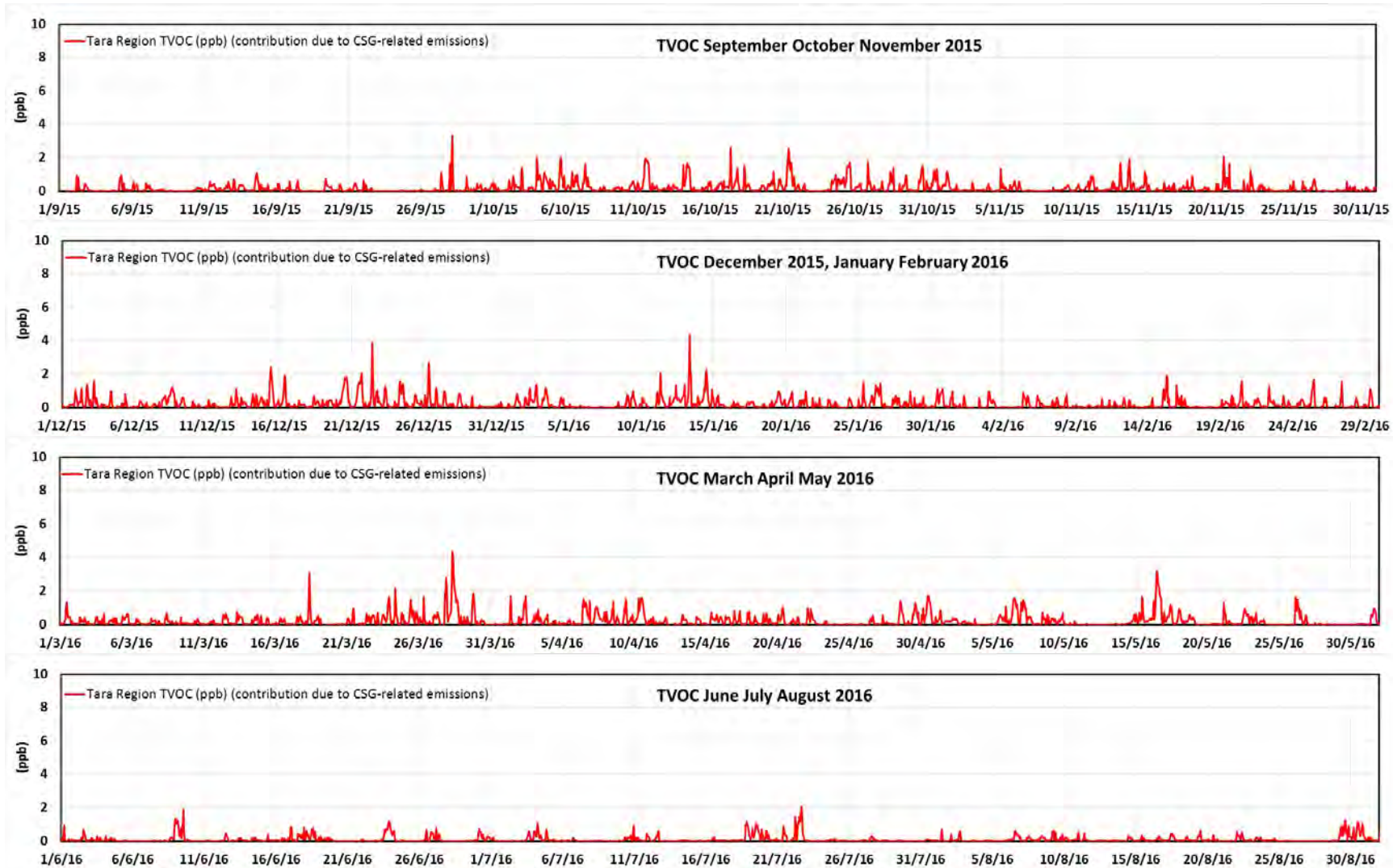


Figure D.40 The modelled contributions from the CSG-related emissions to the 1-hour average TVOC concentrations (ppb) at Tara Region for the modelled year.

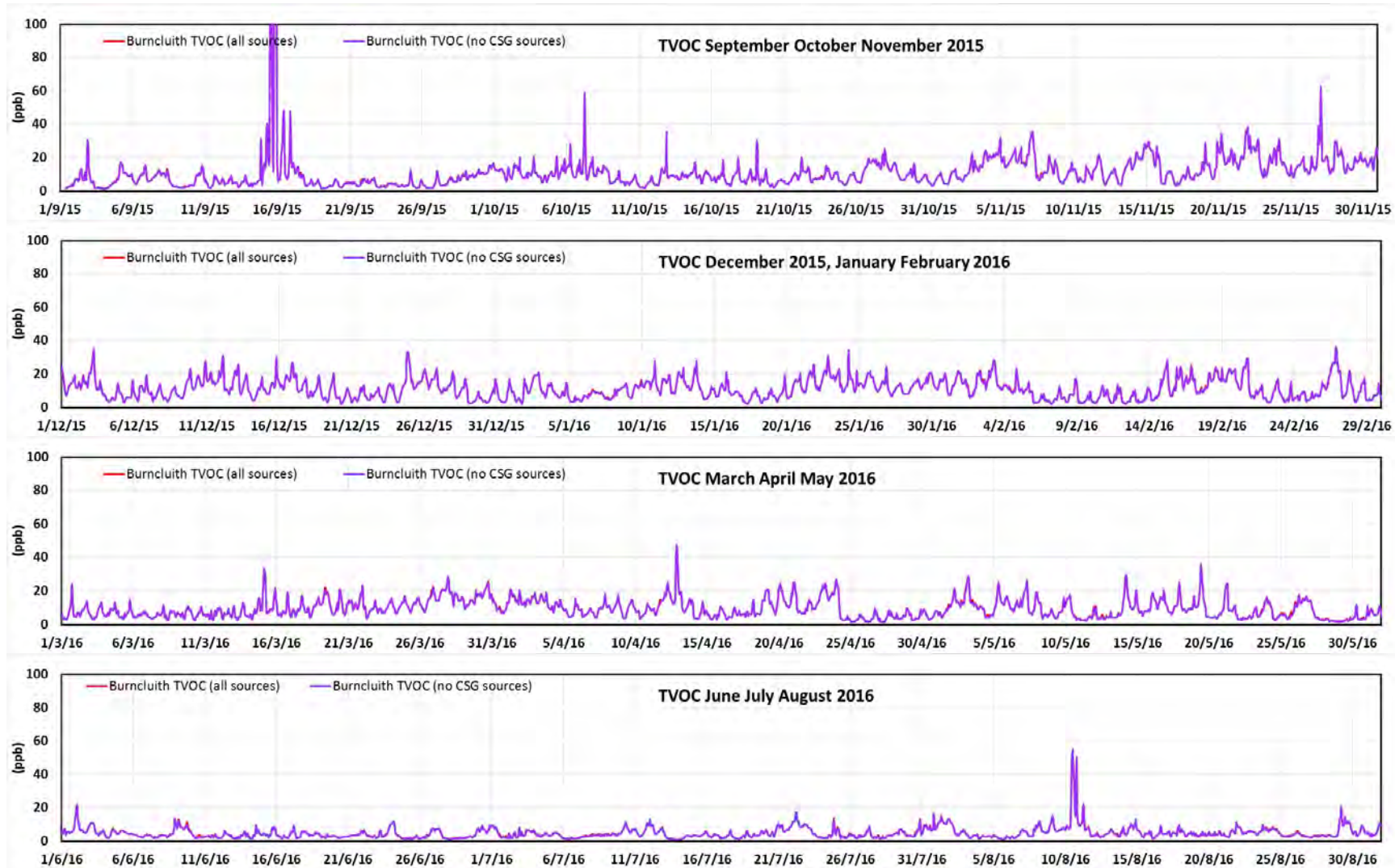


Figure D.41 The modelled time series of the 1-hour average TVOC concentrations (ppb) at Burncluthi for the modelled year (red = model results with all sources, purple = model results without CSG sources). (peaks off scale: model, 15/9/15 21:00 = 945 ppb)

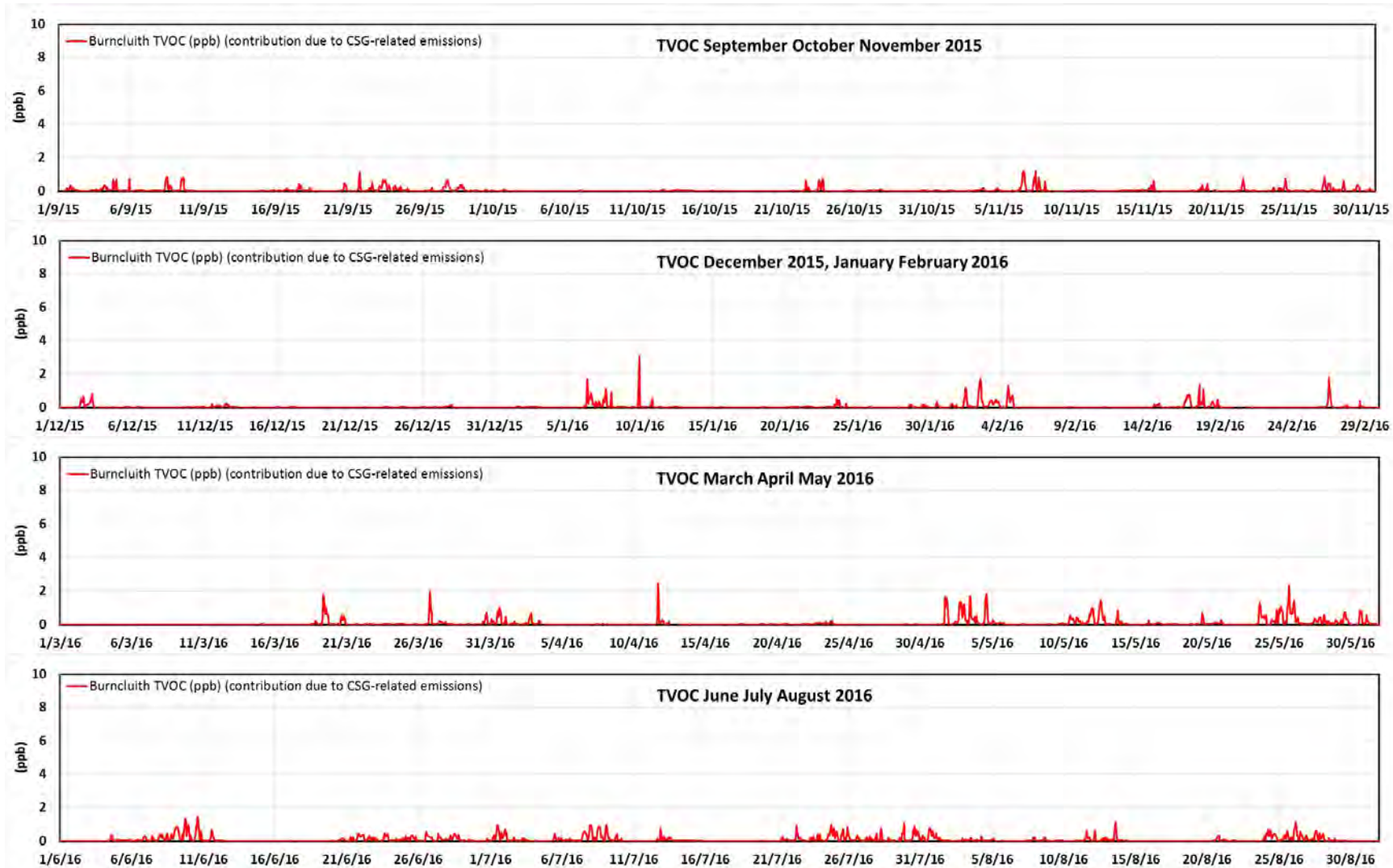


Figure D.42 The modelled contributions from the CSG-related emissions to the 1-hour average TVOC concentrations (ppb) at Burncluith for the modelled year.

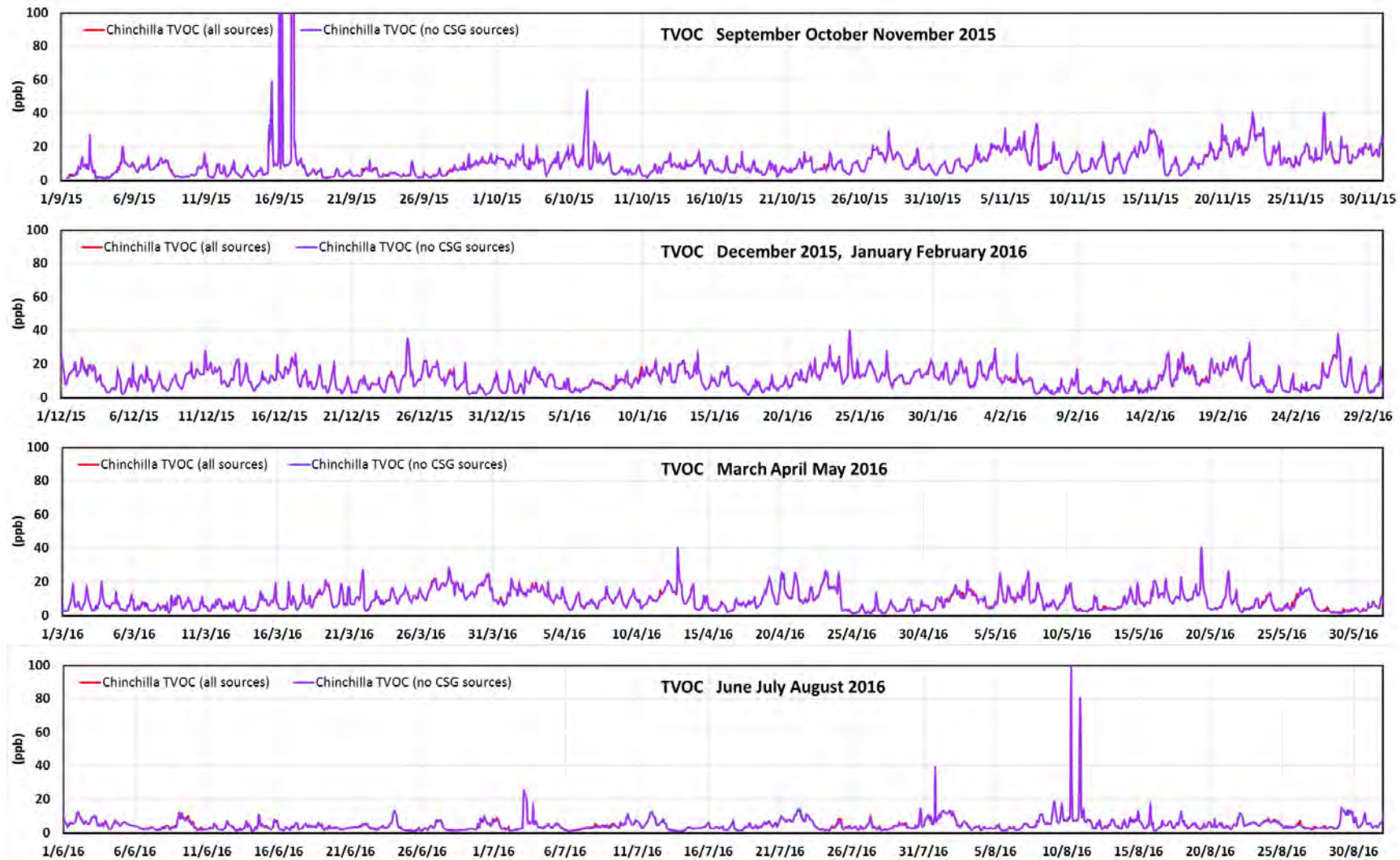


Figure D.43 The modelled time series of the 1-hour average TVOC concentrations (ppb) at Chinchilla for the modelled year (red = model results with all sources, purple = model results without CSG sources). (peaks off scale: model, 16/9/15 00:00, 05:00, 21:00 = 158, 143, 361 ppb, 10/8/16 07:00 = 103 ppb)

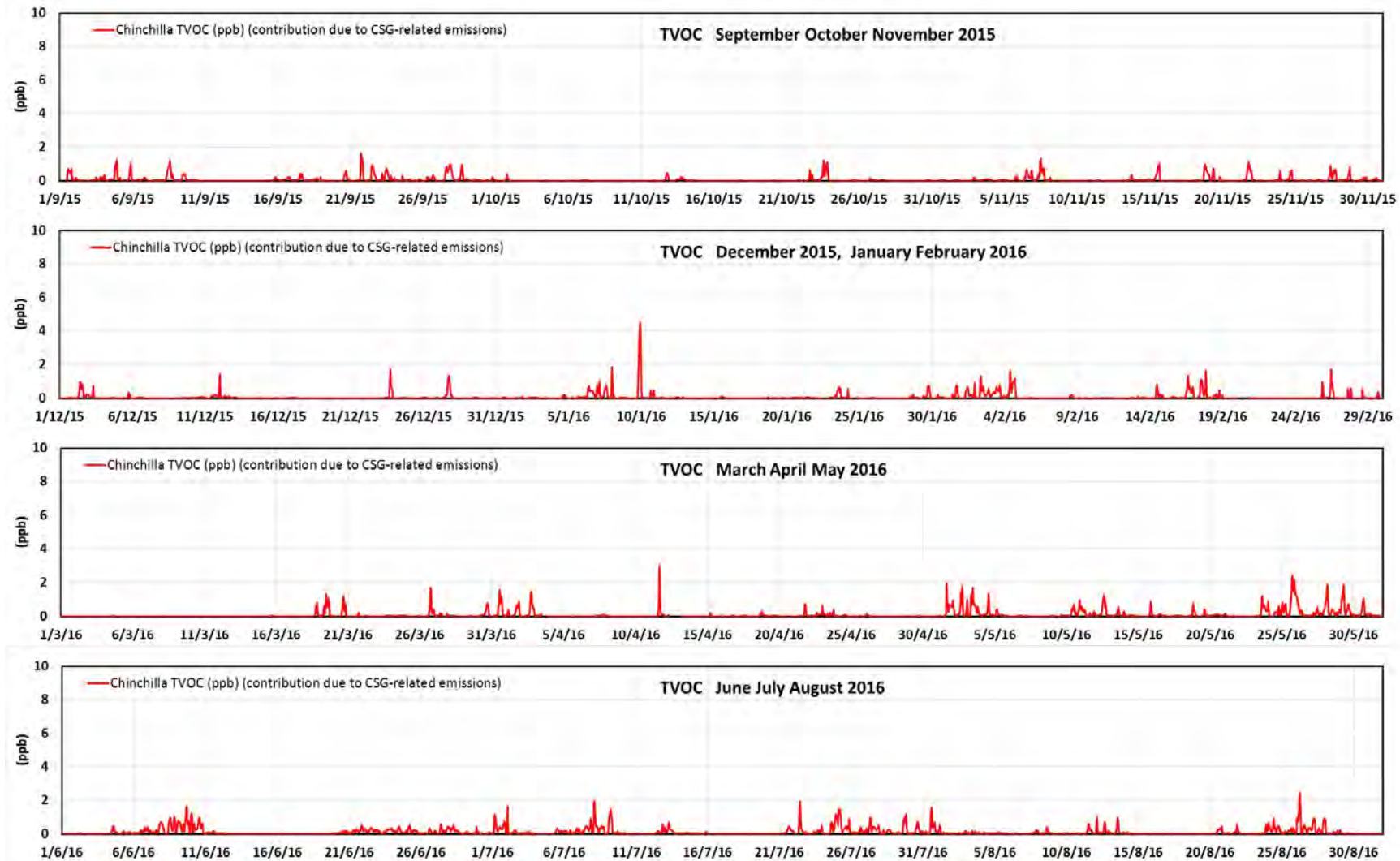


Figure D.44 The modelled contributions from the CSG-related emissions to the 1-hour average TVOC concentrations (ppb) at Chinchilla for the modelled year.

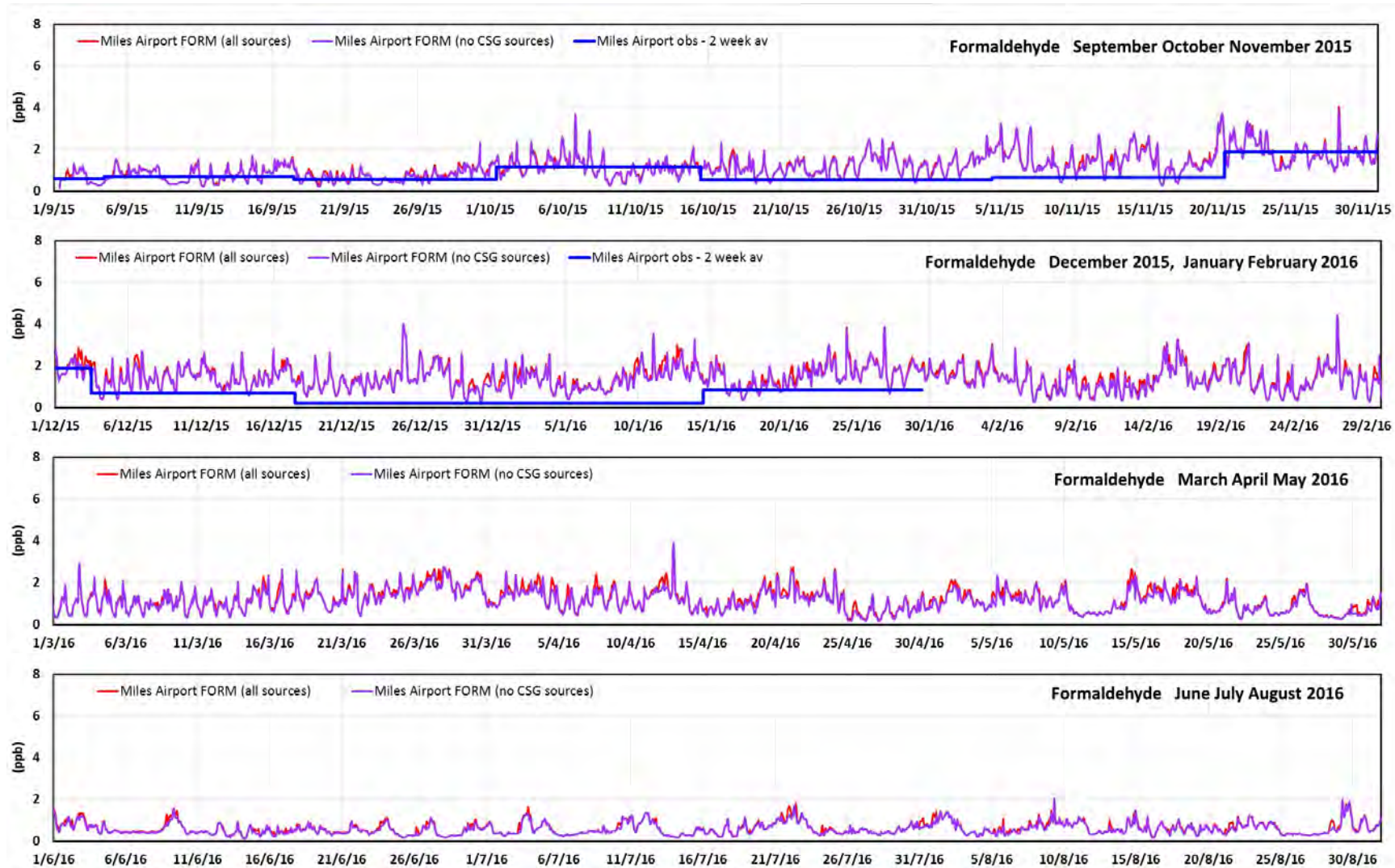


Figure D.45 The observed (2-week sampling period) and modelled (1-hour average) time series of the formaldehyde concentrations (ppb) at Miles Airport for the modelled year (red = model results with all sources, purple = model results without CSG sources, blue = observations).

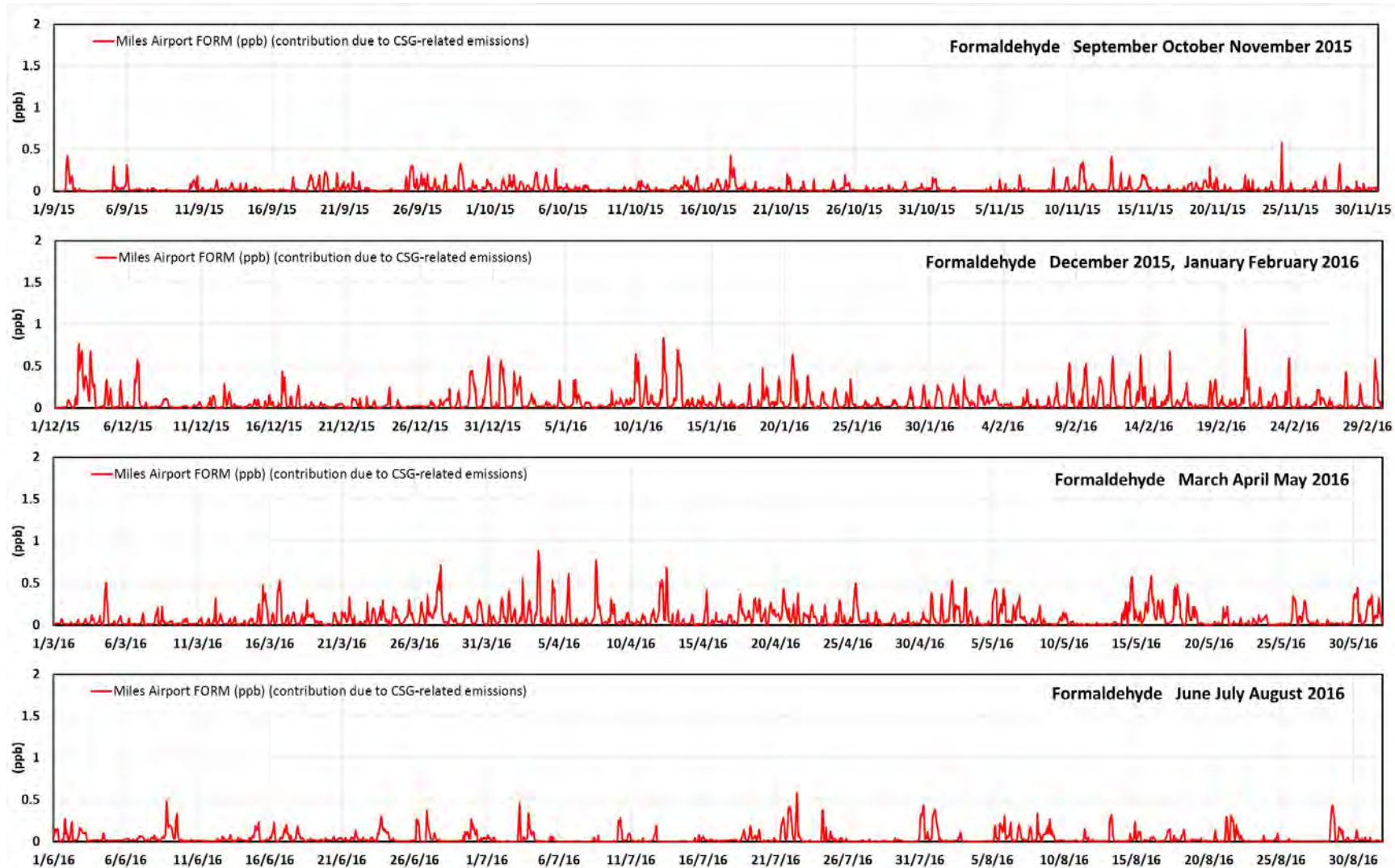


Figure D.46 The modelled contributions from the CSG-related emissions to the 1-hour average formaldehyde concentrations (ppb) at Miles airport for the modelled year.

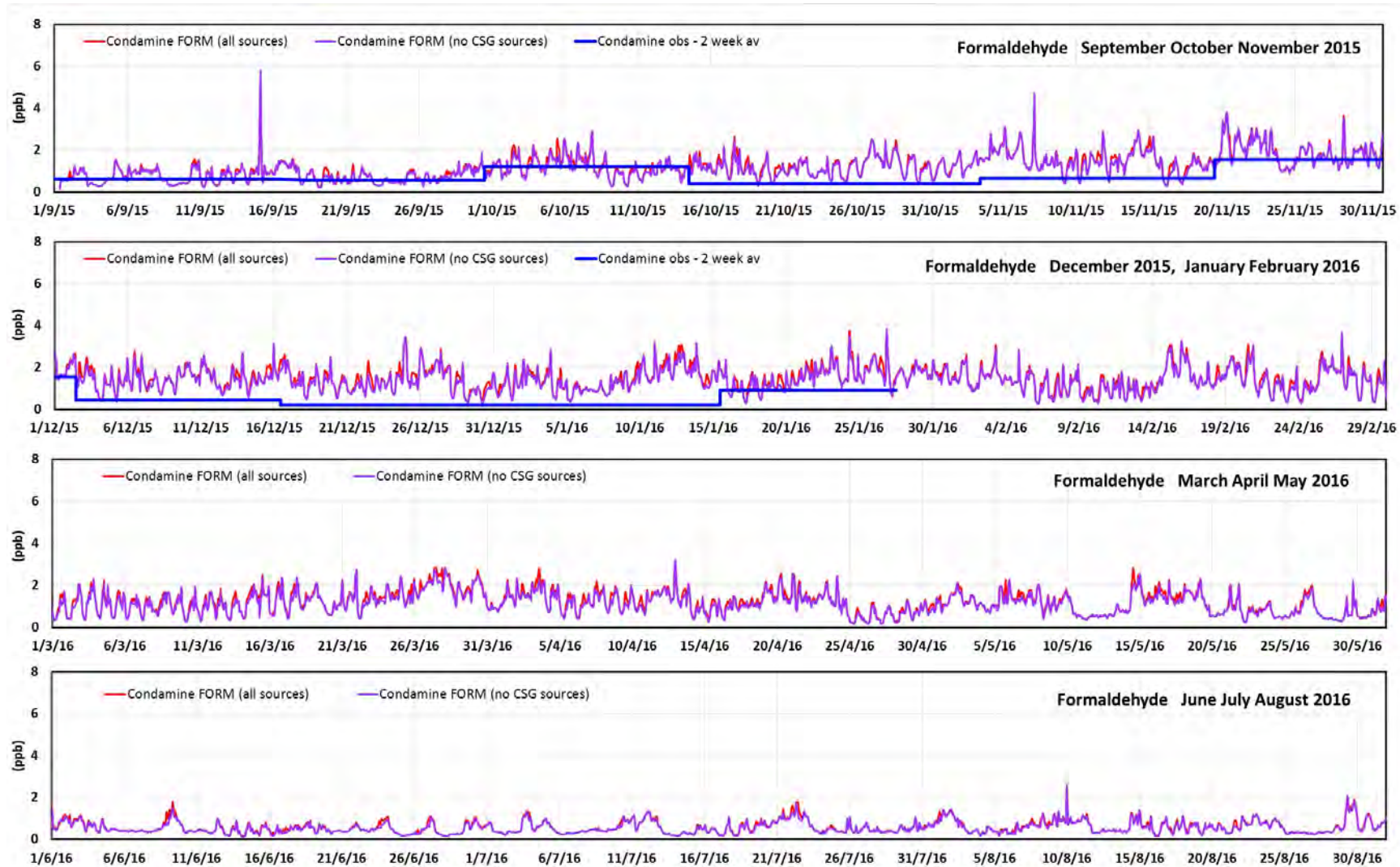


Figure D.47 The observed (2-week sampling period) and modelled (1-hour average) time series of the formaldehyde concentrations (ppb) at Condamine for the modelled year (red = model results with all sources, purple = model results without CSG sources, blue = observations).

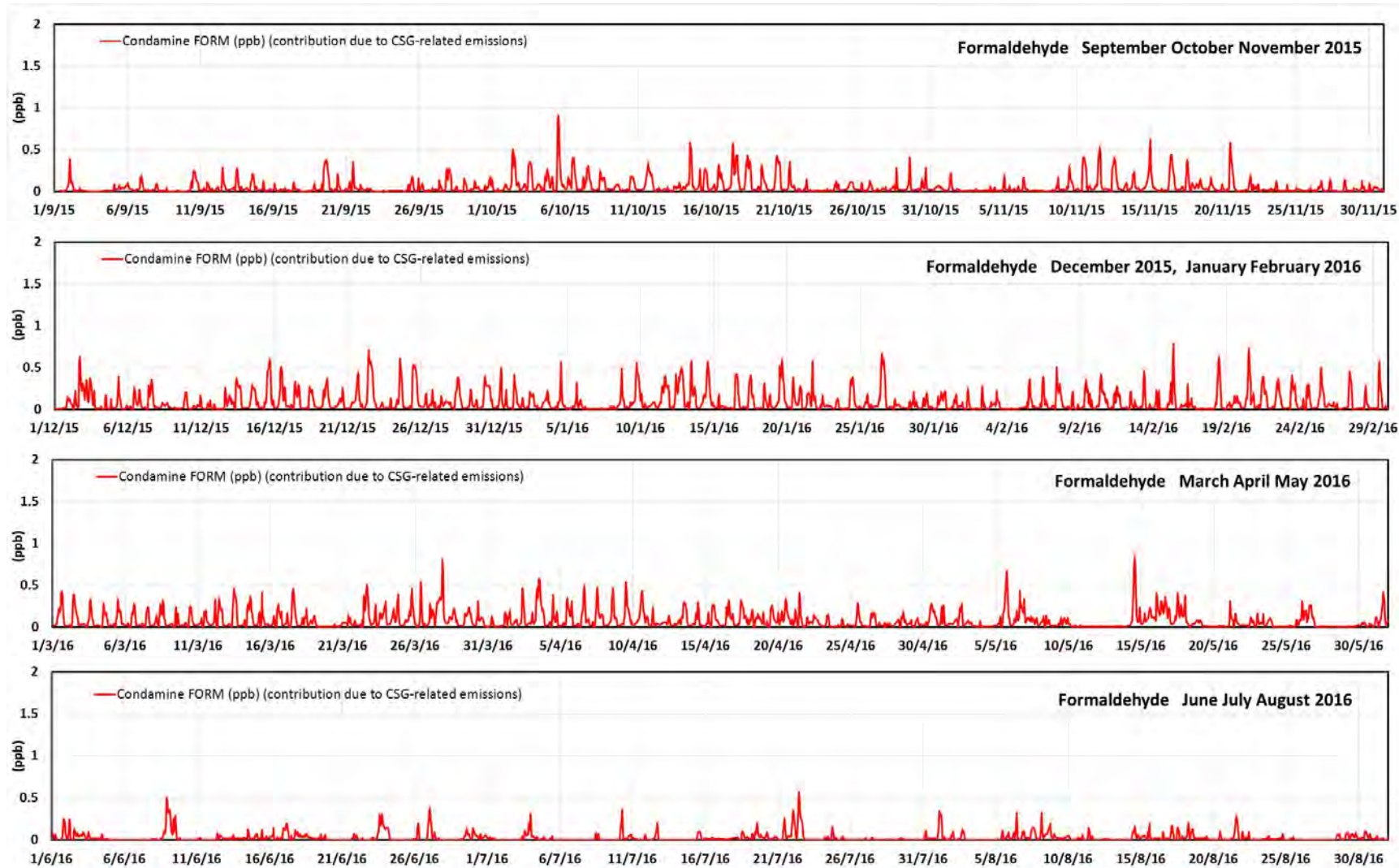


Figure D.48 The modelled contributions from the CSG-related emissions to the 1-hour average formaldehyde concentrations (ppb) at Condamine for the modelled year.

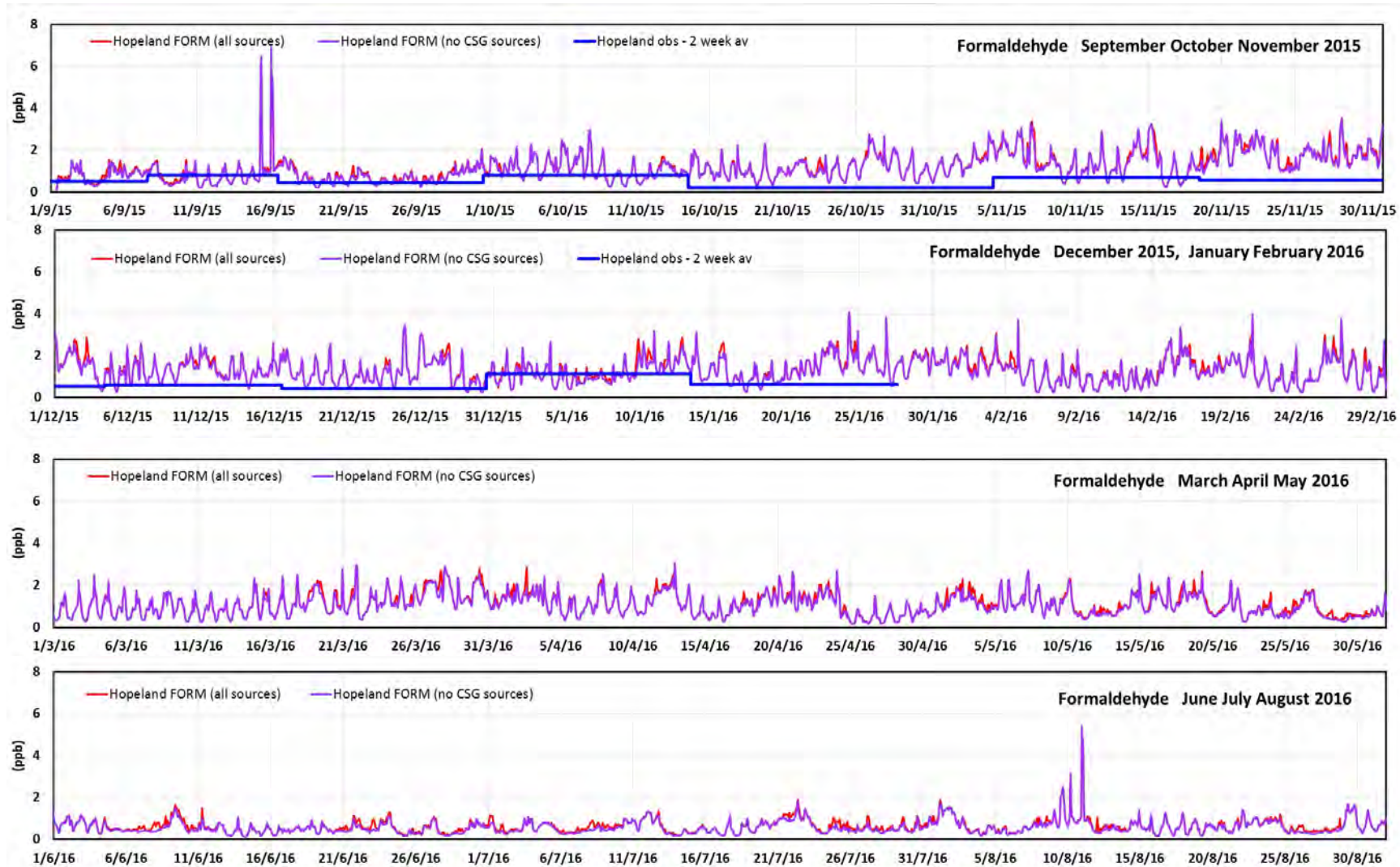


Figure D.49 The observed (2-week sampling period) and modelled (1-hour average) time series of the formaldehyde concentrations (ppb) at Hopeland for the modelled year (red = model results with all sources, purple = model results without CSG sources, blue = observations).

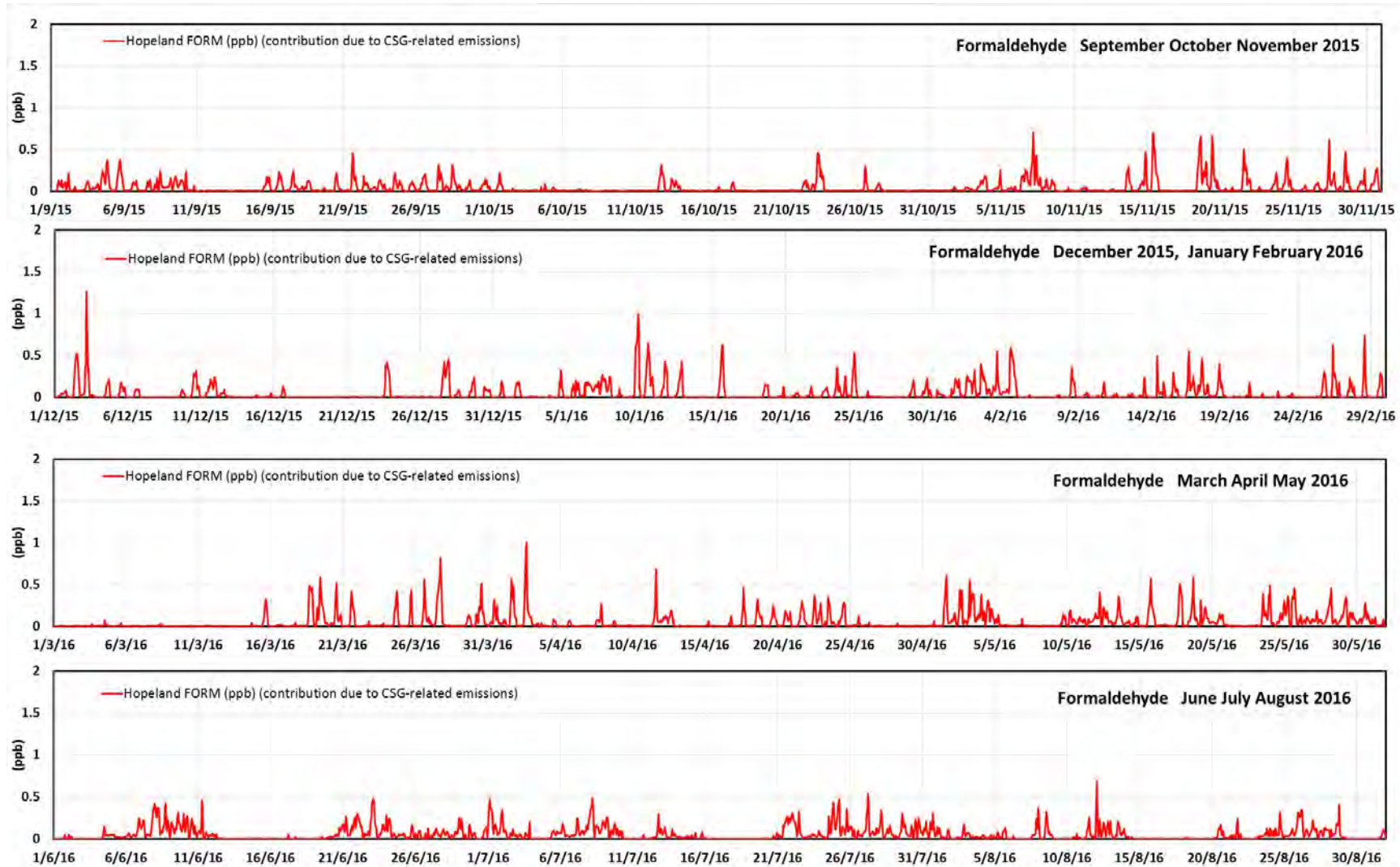


Figure D.50 The modelled contributions from the CSG-related emissions to the 1-hour average formaldehyde concentrations (ppb) at Hopeland for the modelled year.

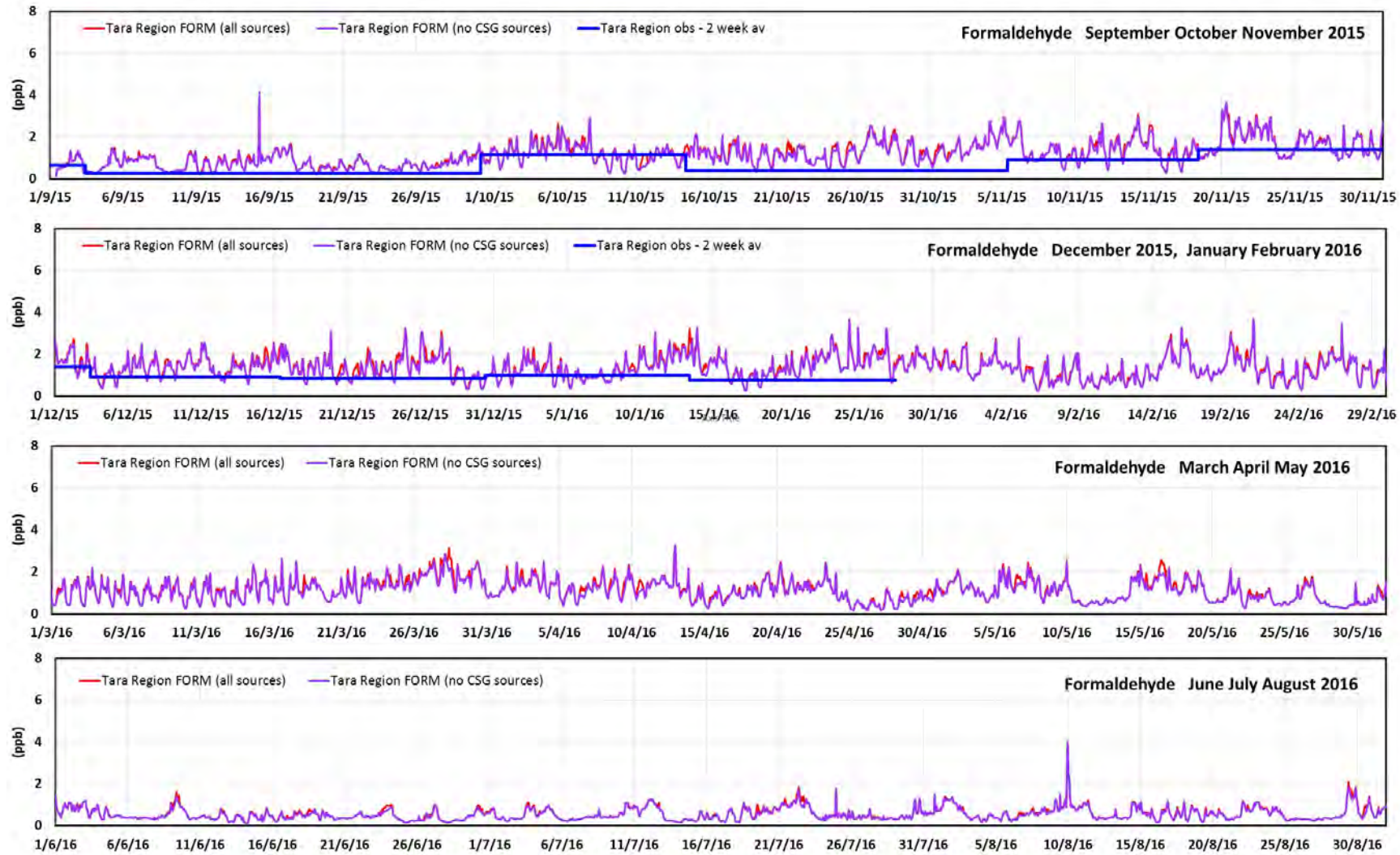


Figure D.51 The observed (2-week sampling period) and modelled (1-hour average) time series of the formaldehyde concentrations (ppb) at Tara Region for the modelled year (red = model results with all sources, purple = model results without CSG sources, blue = observations).

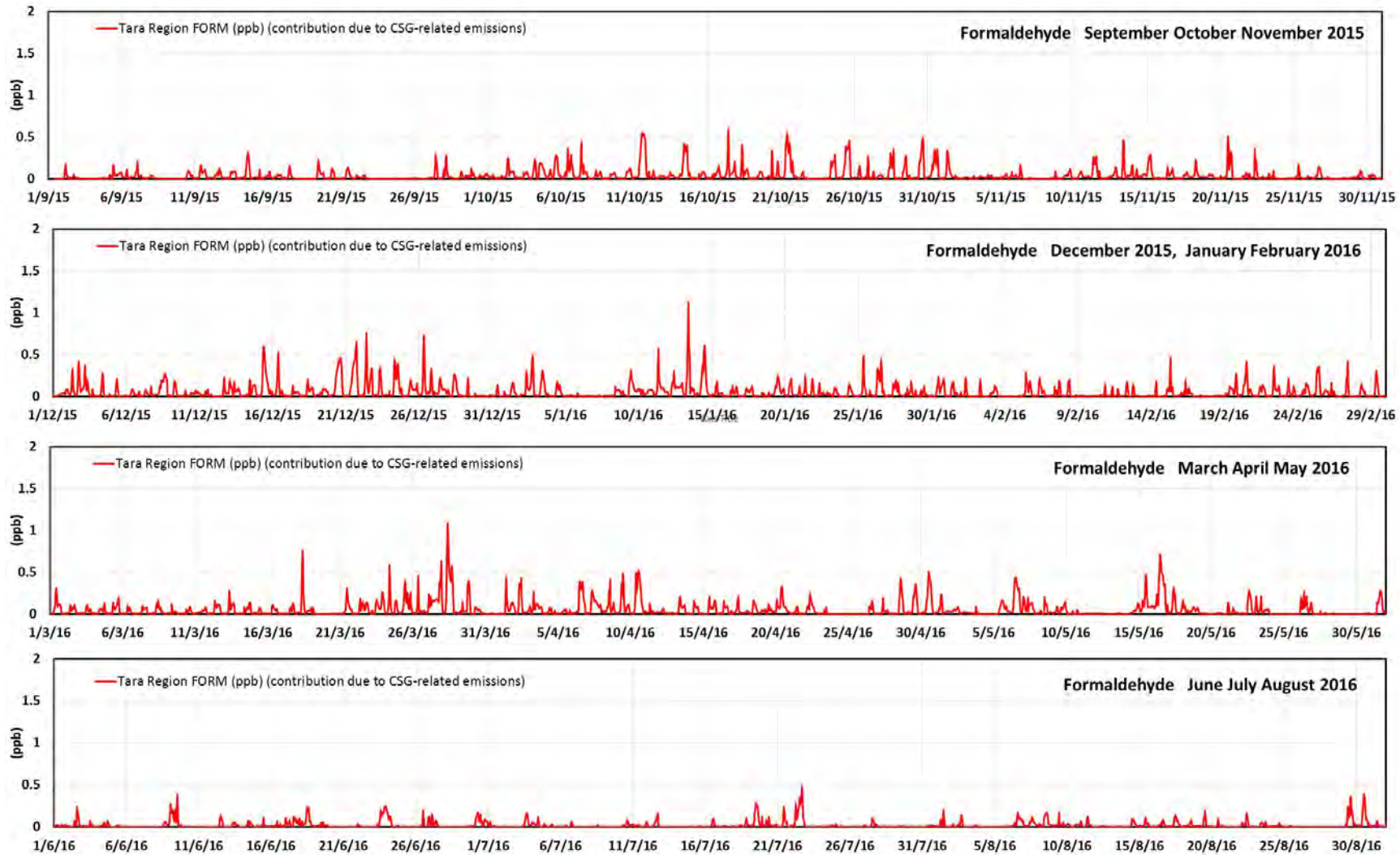


Figure D.52 The modelled contributions from the CSG-related emissions to the 1-hour average formaldehyde concentrations (ppb) at Tara Region for the modelled year.

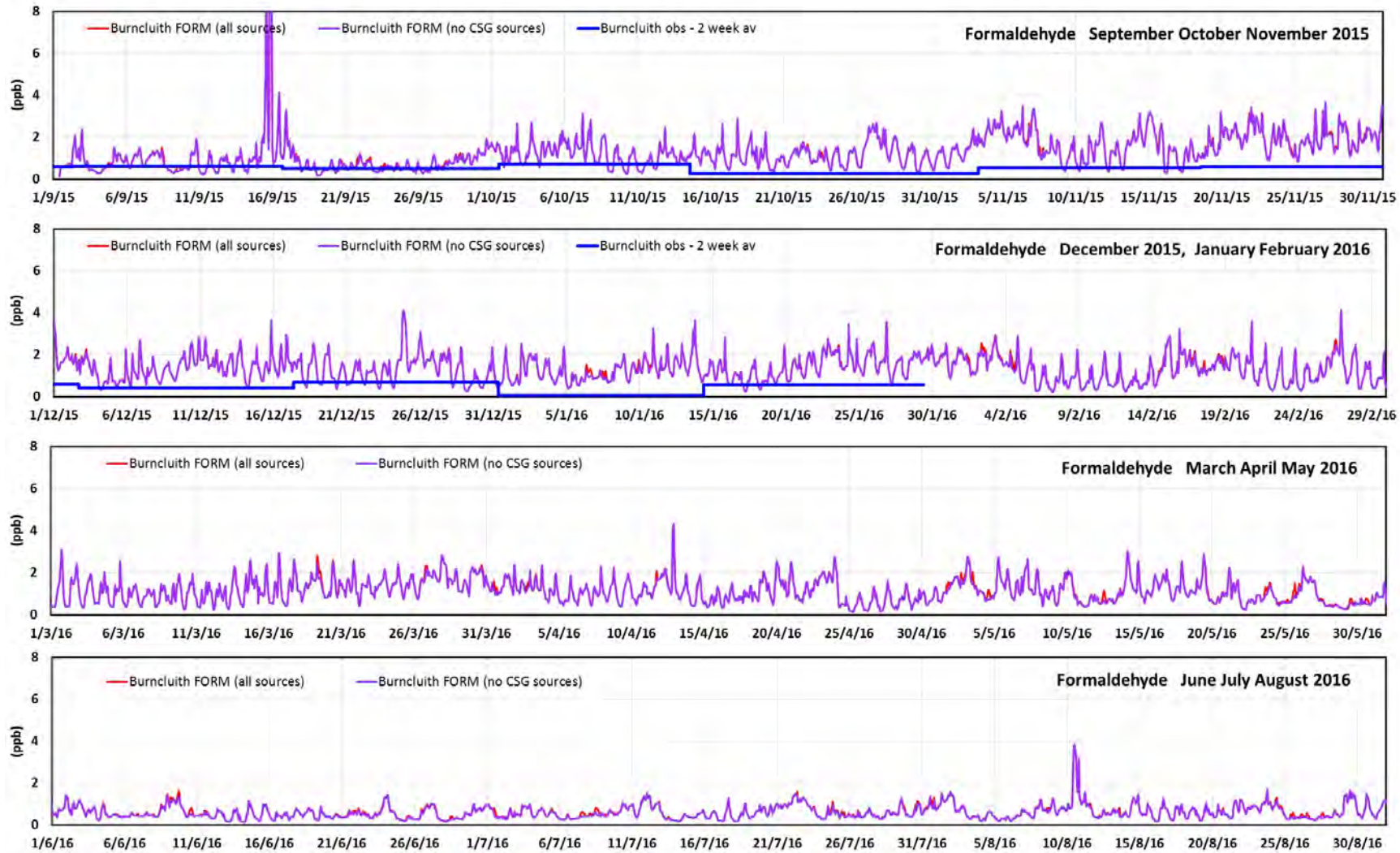


Figure D.53 The observed (2-week sampling period) and modelled (1-hour average) time series of the formaldehyde concentrations (ppb) at Burncluith for the modelled year (red = model results with all sources, purple = model results without CSG sources, blue = observations). (peaks off scale: model, 15/9/15 21:00 = 39 ppb)

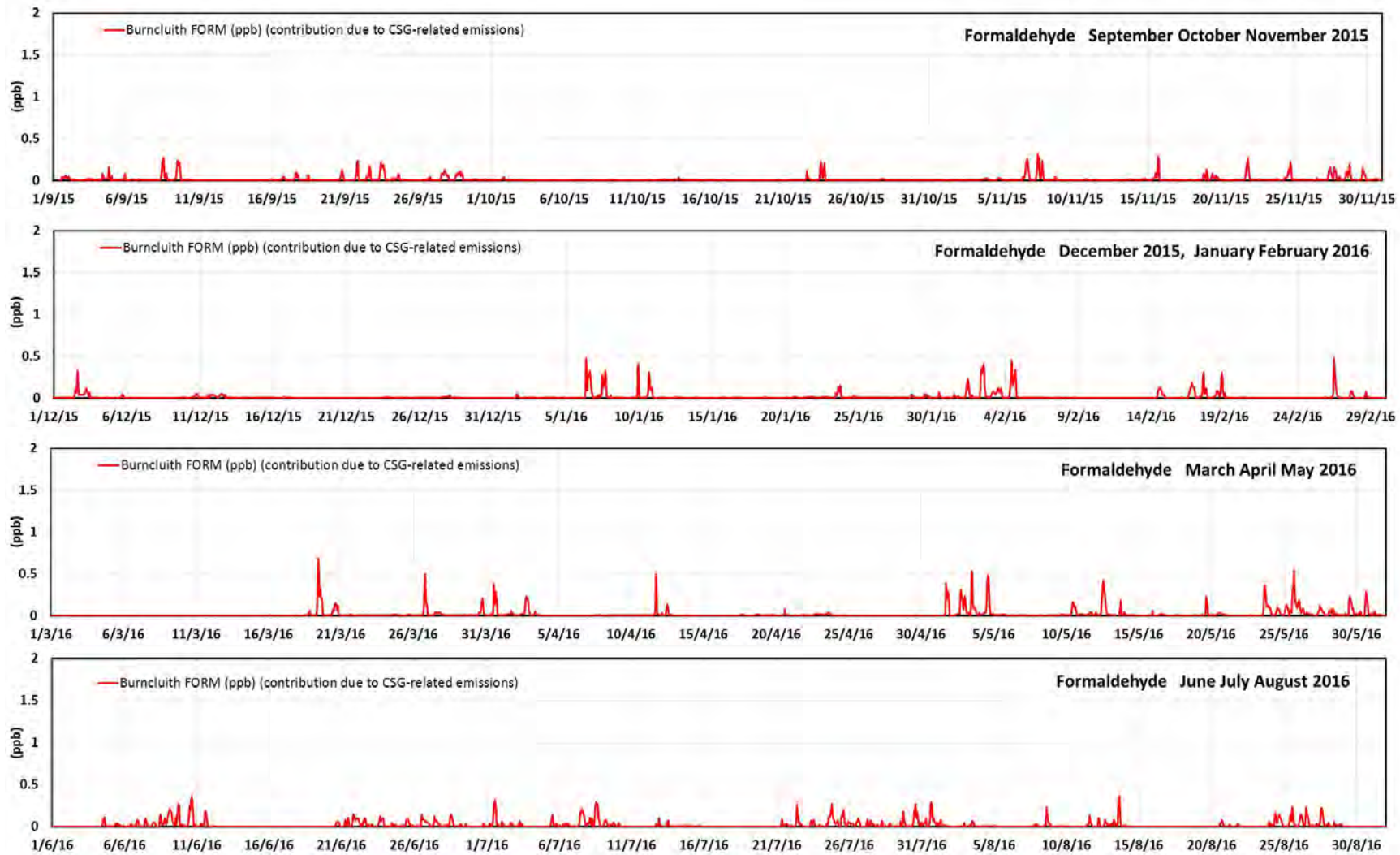


Figure D.54 The modelled contributions from the CSG-related emissions to the 1-hour average formaldehyde concentrations (ppb) at Burncluith for the modelled year.

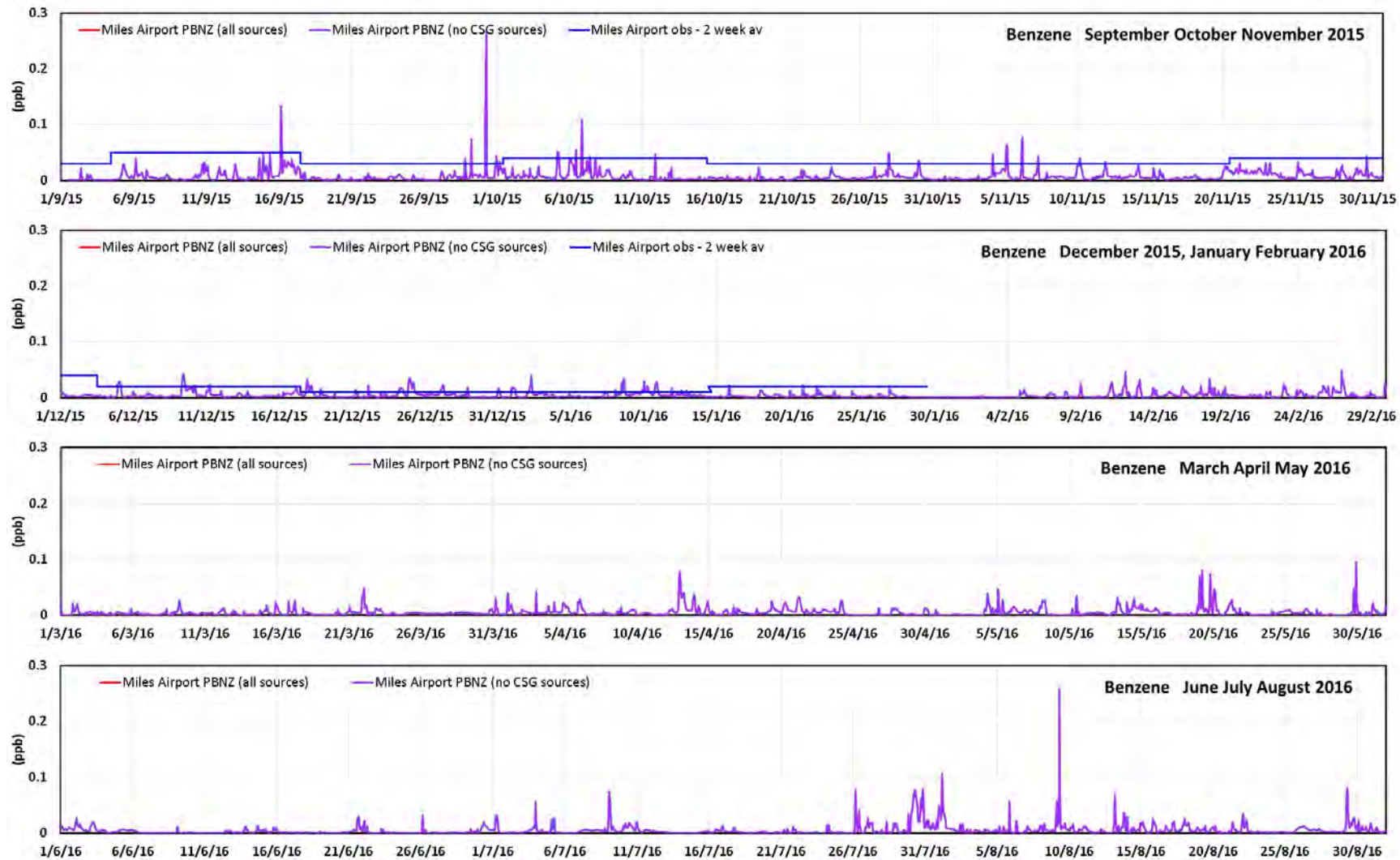


Figure D.55 The observed (2-week sampling period) and modelled (1-hour average) time series of the benzene concentrations (ppb) at Miles Airport for the modelled year (red = model results with all sources, purple = model results without CSG sources, blue = observations).

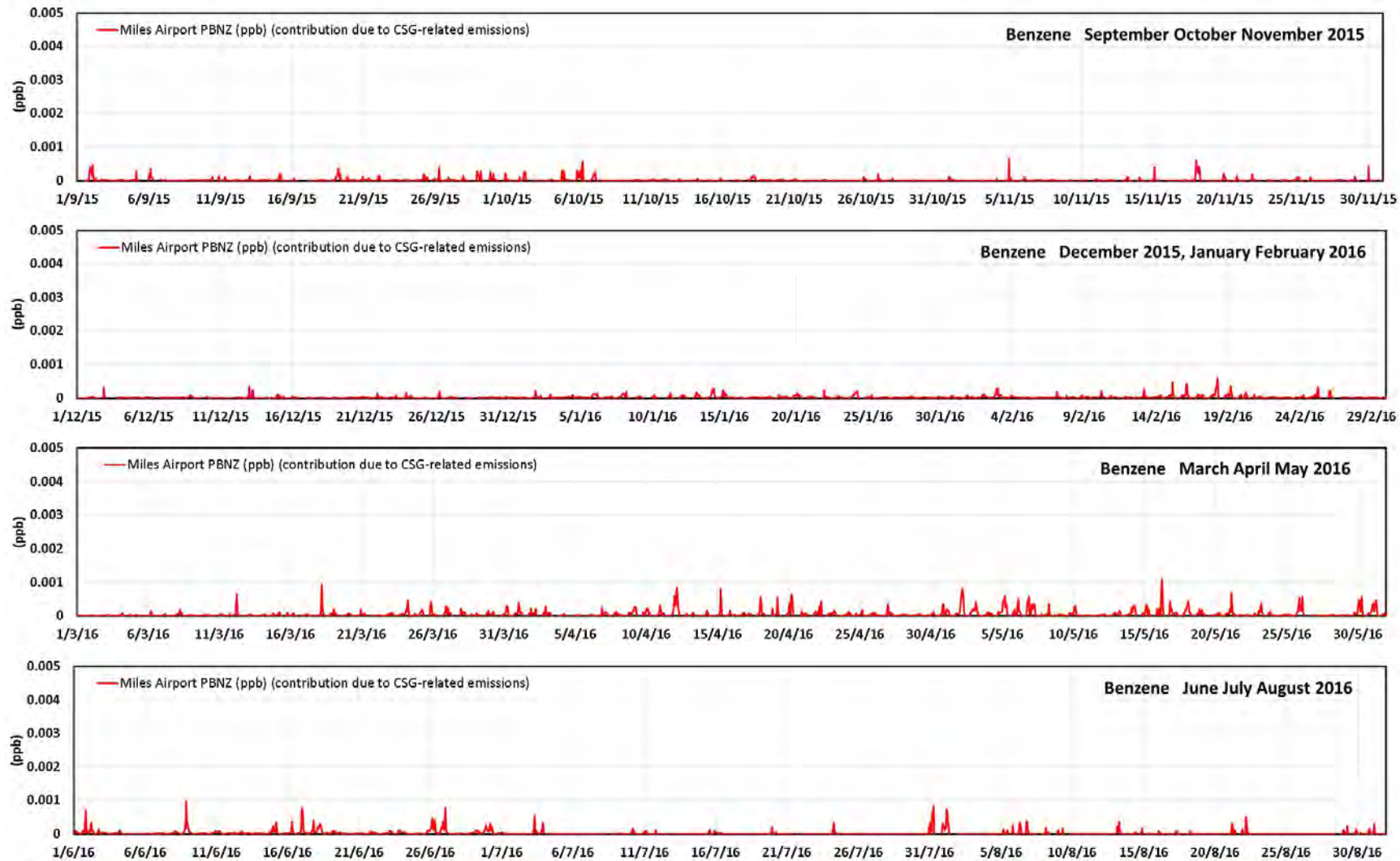


Figure D.56 The modelled contributions from the CSG-related emissions to the 1-hour average benzene concentrations (ppb) at Miles airport for the modelled year.

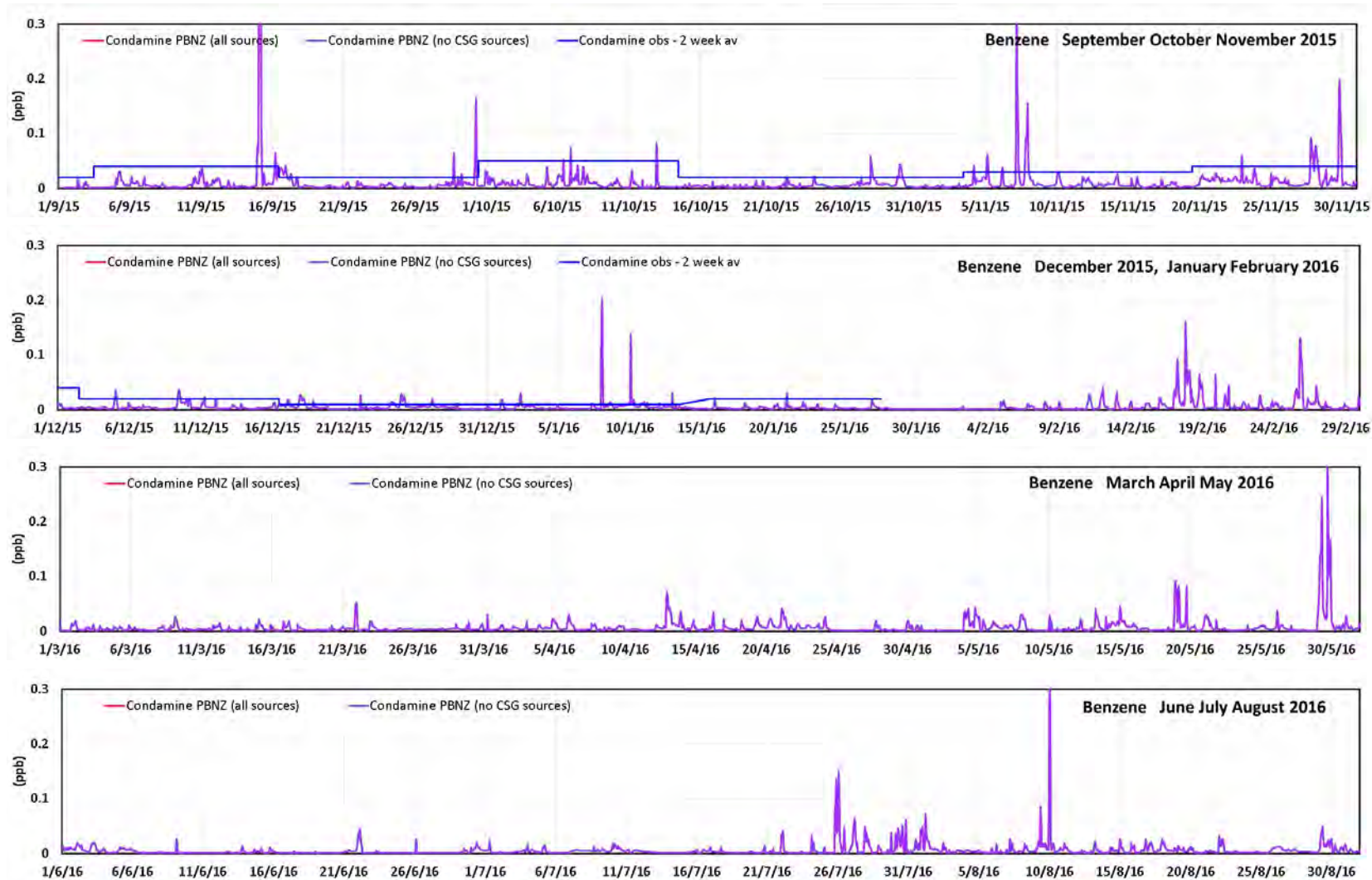


Figure D.57 The observed (2-week sampling period) and modelled (1-hour average) time series of the benzene concentrations (ppb) at Condamine for the modelled year (red = model results with all sources, purple = model results without CSG sources, blue = observations). (peaks off scale: model, 15/9/15 04:00 = 1.12 ppb, 7/11/15 04:00 = 0.40, 29/5/16 17:00 = 0.37 ppb, 10/8/16 00:00 = 0.37 ppb)



Figure D.58 The modelled contributions from the CSG-related emissions to the 1-hour average benzene concentrations (ppb) at Condamine for the modelled year.

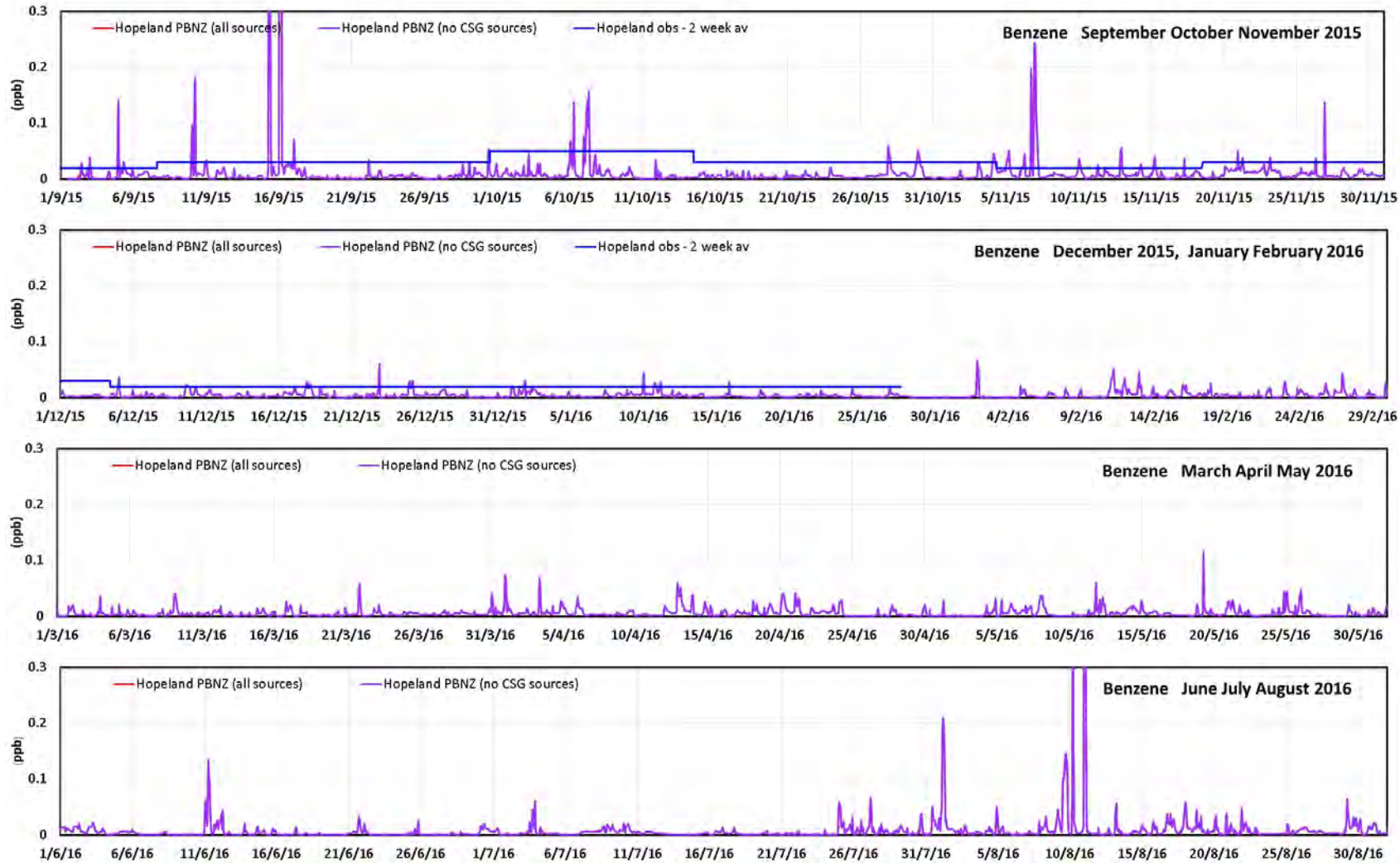


Figure D.59 The observed (2-week sampling period) and modelled (1-hour average) time series of the benzene concentrations (ppb) at Hopeland for the modelled year (red = model results with all sources, purple = model results without CSG sources, blue = observations). (peaks off scale: model, 15/9/15 09:00 = 1.03 ppb, 16/9/15 01:00 = 1.23 ppb, 10/8/16 05:00, 23:00 = 0.47, 0.90 ppb)

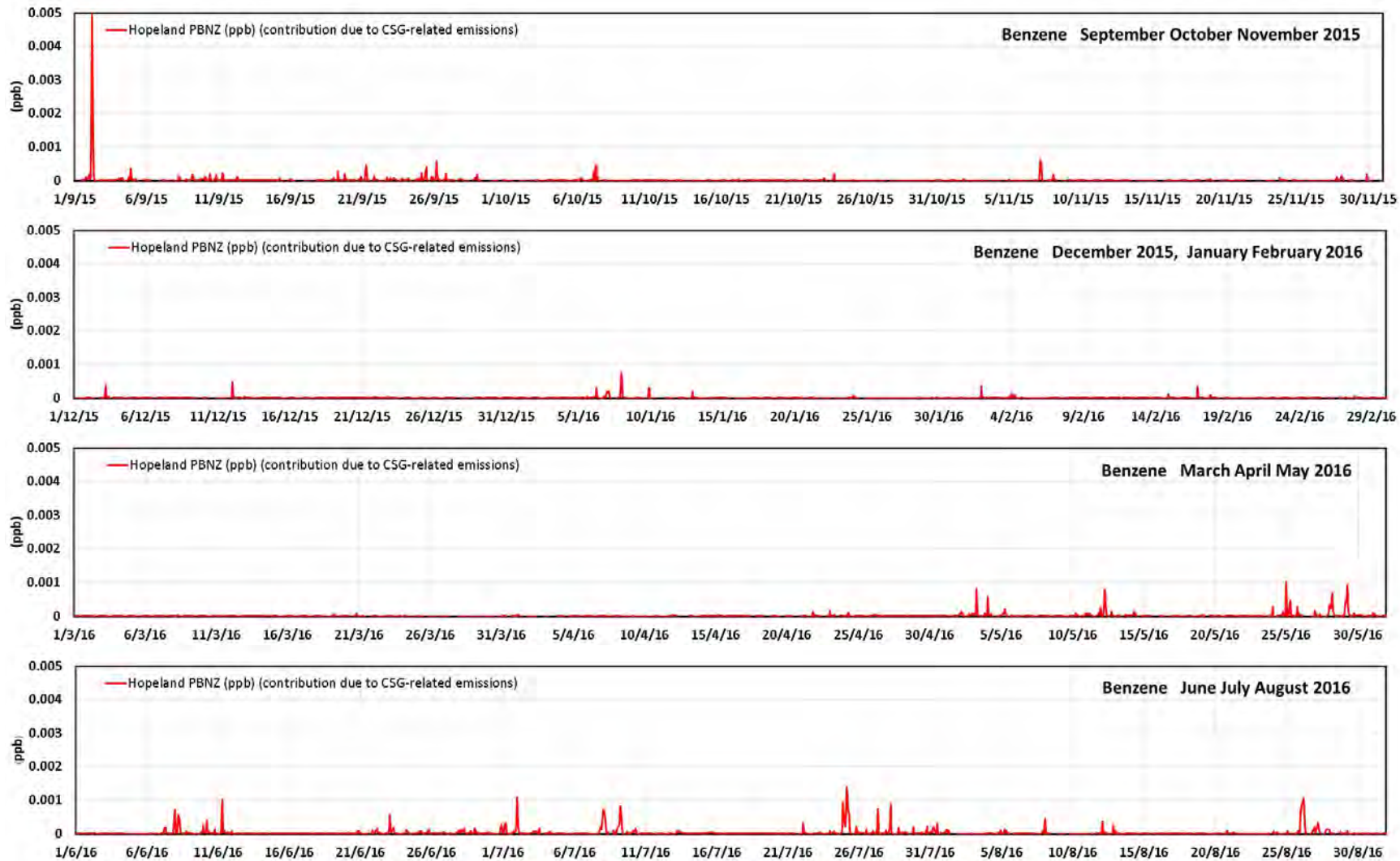


Figure D.60 The modelled contributions from the CSG-related emissions to the 1-hour average benzene concentrations (ppb) at Hopeland for the modelled year.

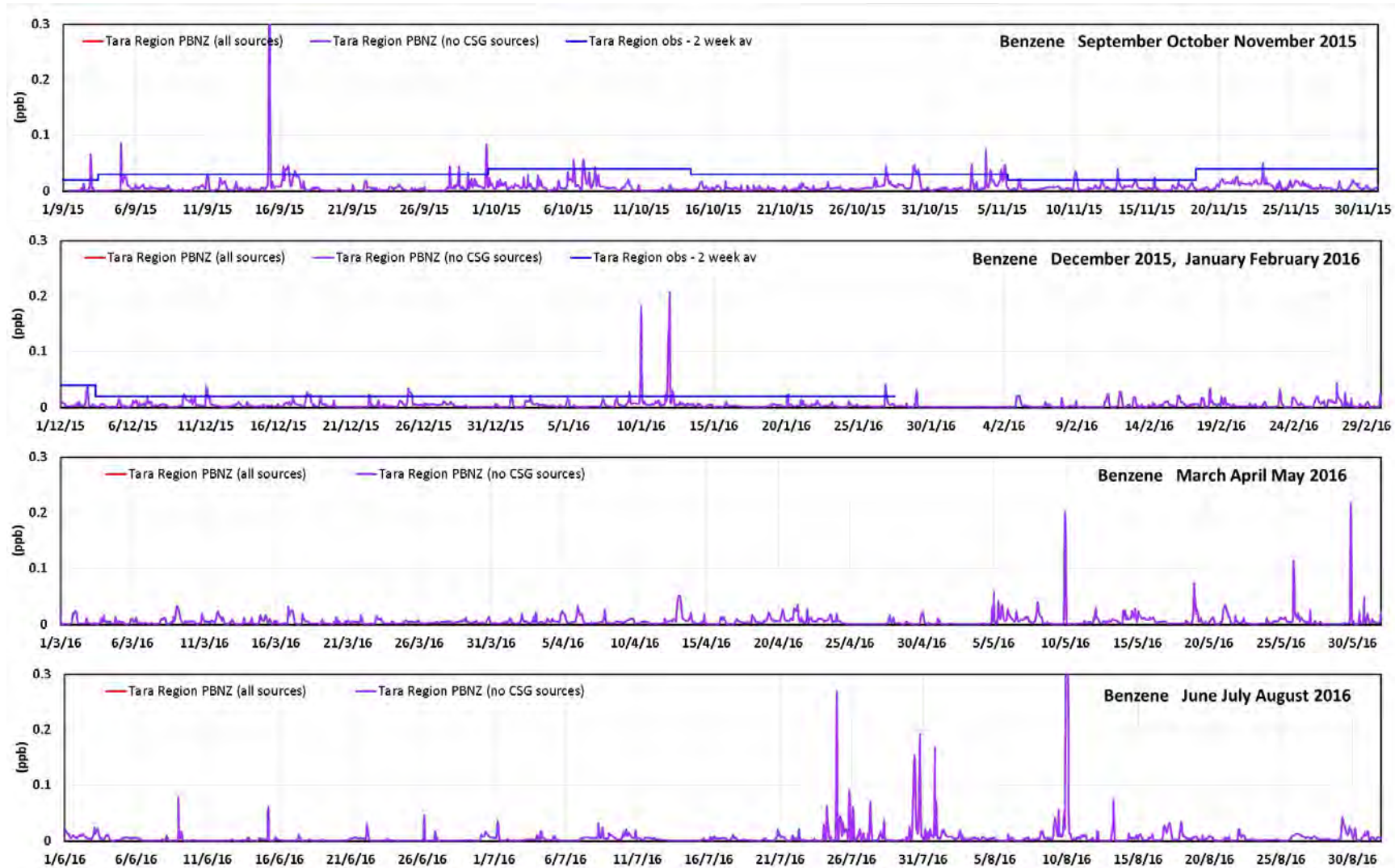


Figure D.61 The observed (2-week sampling period) and modelled (1-hour average) time series of the benzene concentrations (ppb) at Tara Region for the modelled year (red = model results with all sources, purple = model results without CSG sources, blue = observations). (peaks off scale: model, 15/9/15 07:00 = 0.77 ppb, 9/8/16 23:00 = 0.63 ppb)



Figure D.62 The modelled contributions from the CSG-related emissions to the 1-hour average benzene concentrations (ppb) at Tara Region for the modelled year.

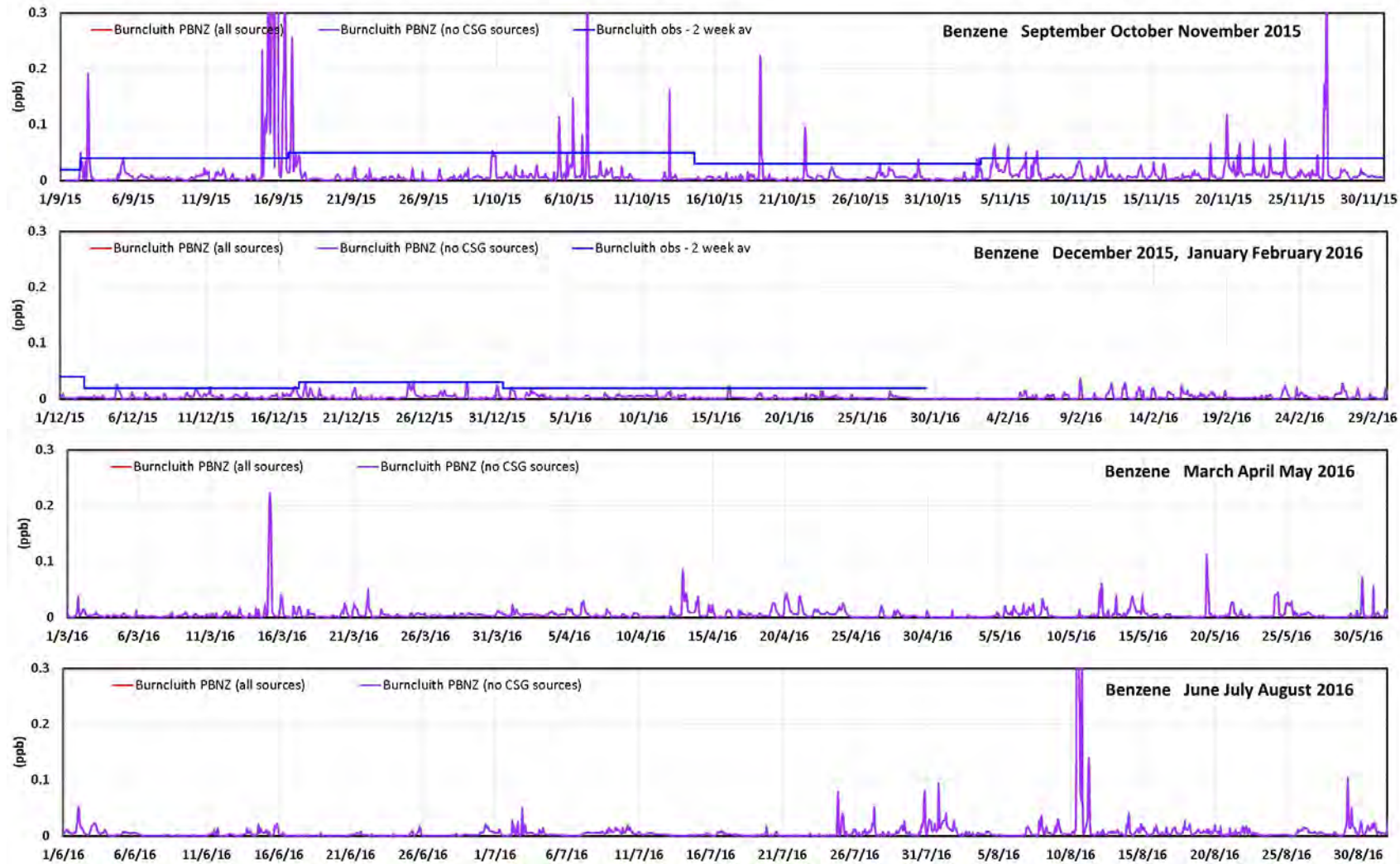


Figure D.63 The observed (2-week sampling period) and modelled (1-hour average) time series of the benzene concentrations (ppb) at Burncluith for the modelled year (red = model results with all sources, purple = model results without CSG sources, blue = observations). (peaks off scale: model, 15/9/15 21:00 = 7.94 ppb, 7/10/15 06:00 = 0.41 ppb, 27/11/15 02:00 = 0.40 ppb, 10/8/16 12:00 = 0.41 ppb)



Figure D.64 The modelled contributions from the CSG-related emissions to the 1-hour average benzene concentrations (ppb) at Burncluith for the modelled year.

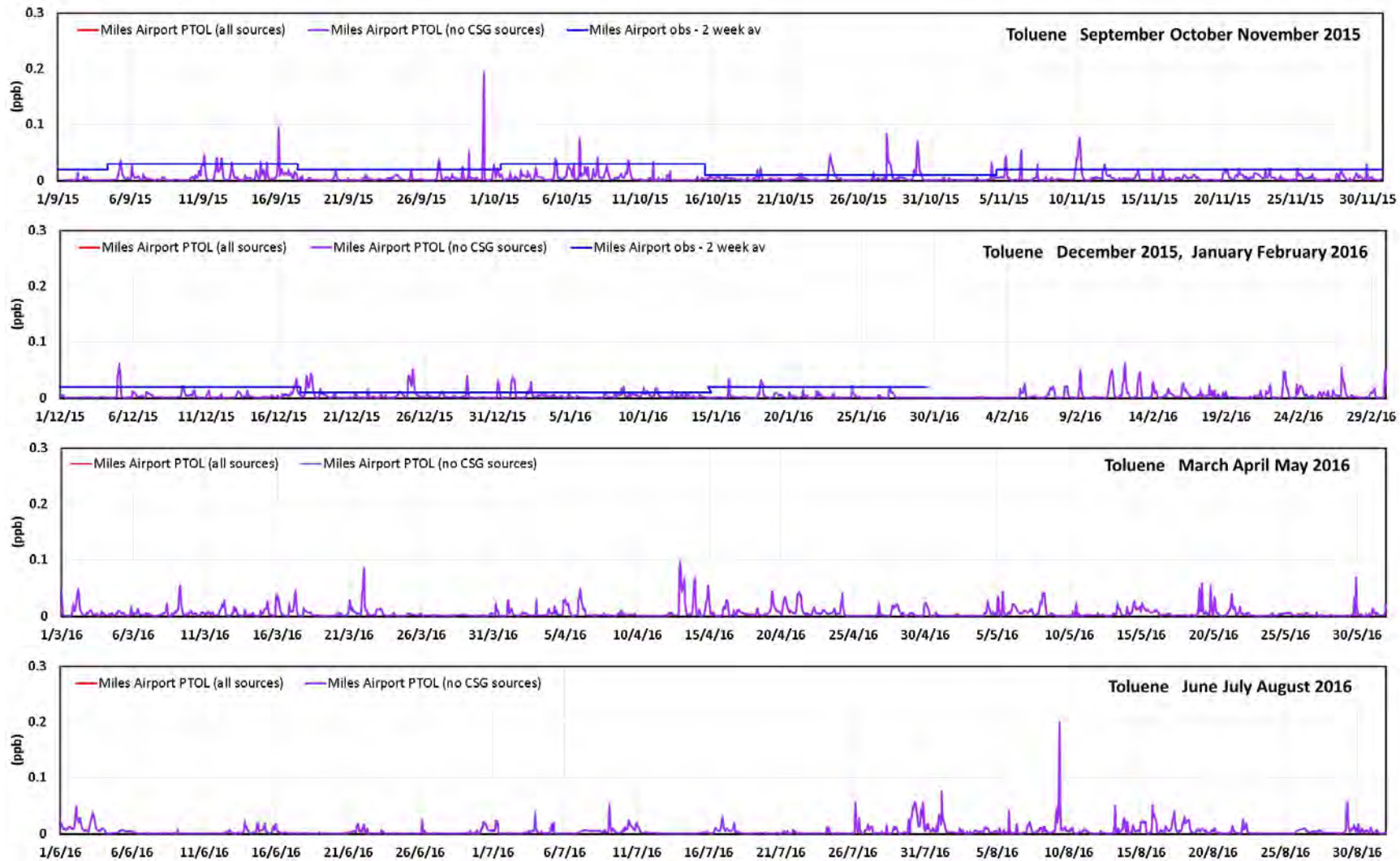


Figure D.65 The observed (2-week sampling period) and modelled (1-hour average) time series of the toluene concentrations (ppb) at Miles Airport for the modelled year (red = model results with all sources, purple = model results without CSG sources, blue = observations).

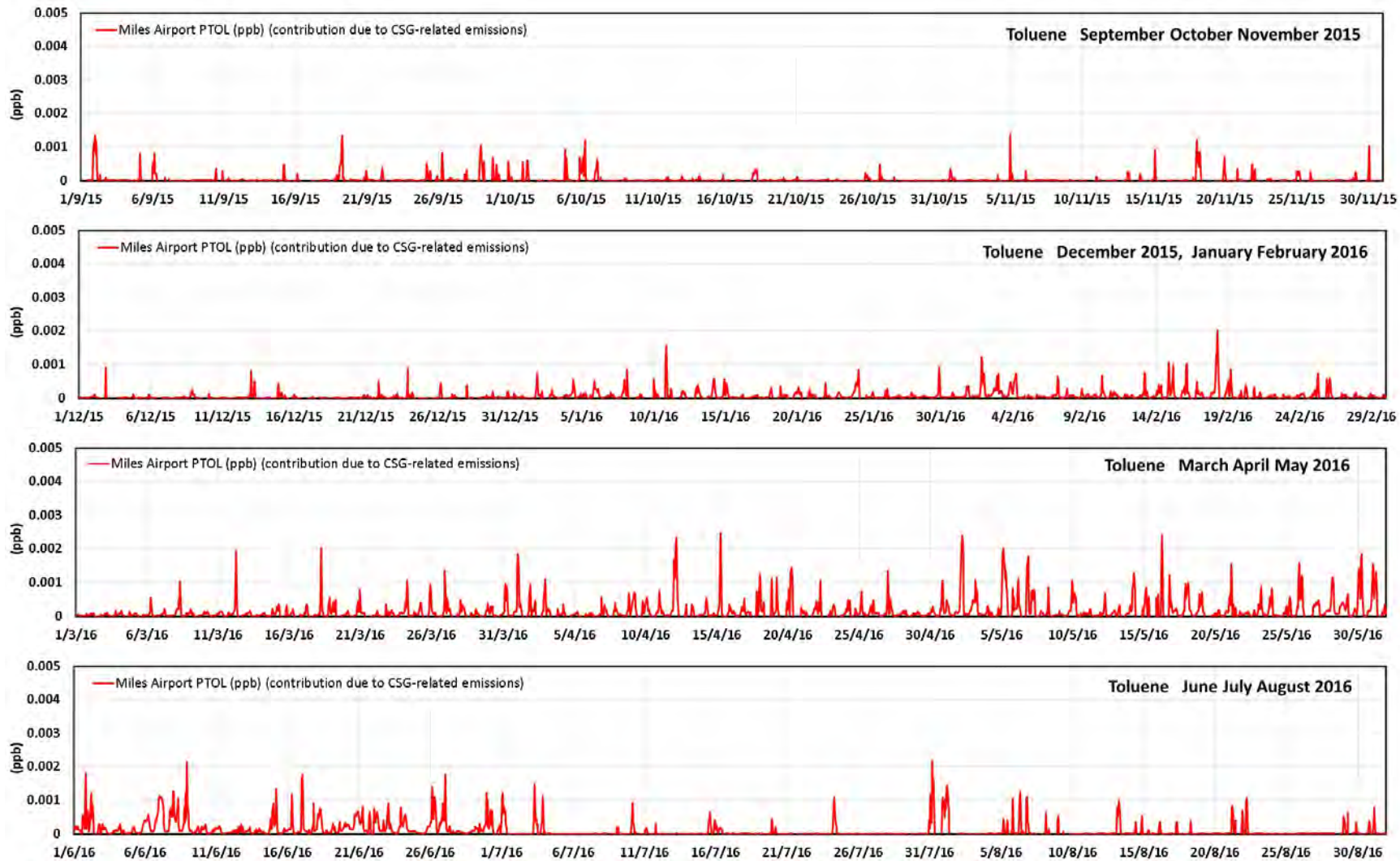


Figure D.66 The modelled contributions from the CSG-related emissions to the 1-hour average toluene concentrations (ppb) at Miles Airport for the modelled year.

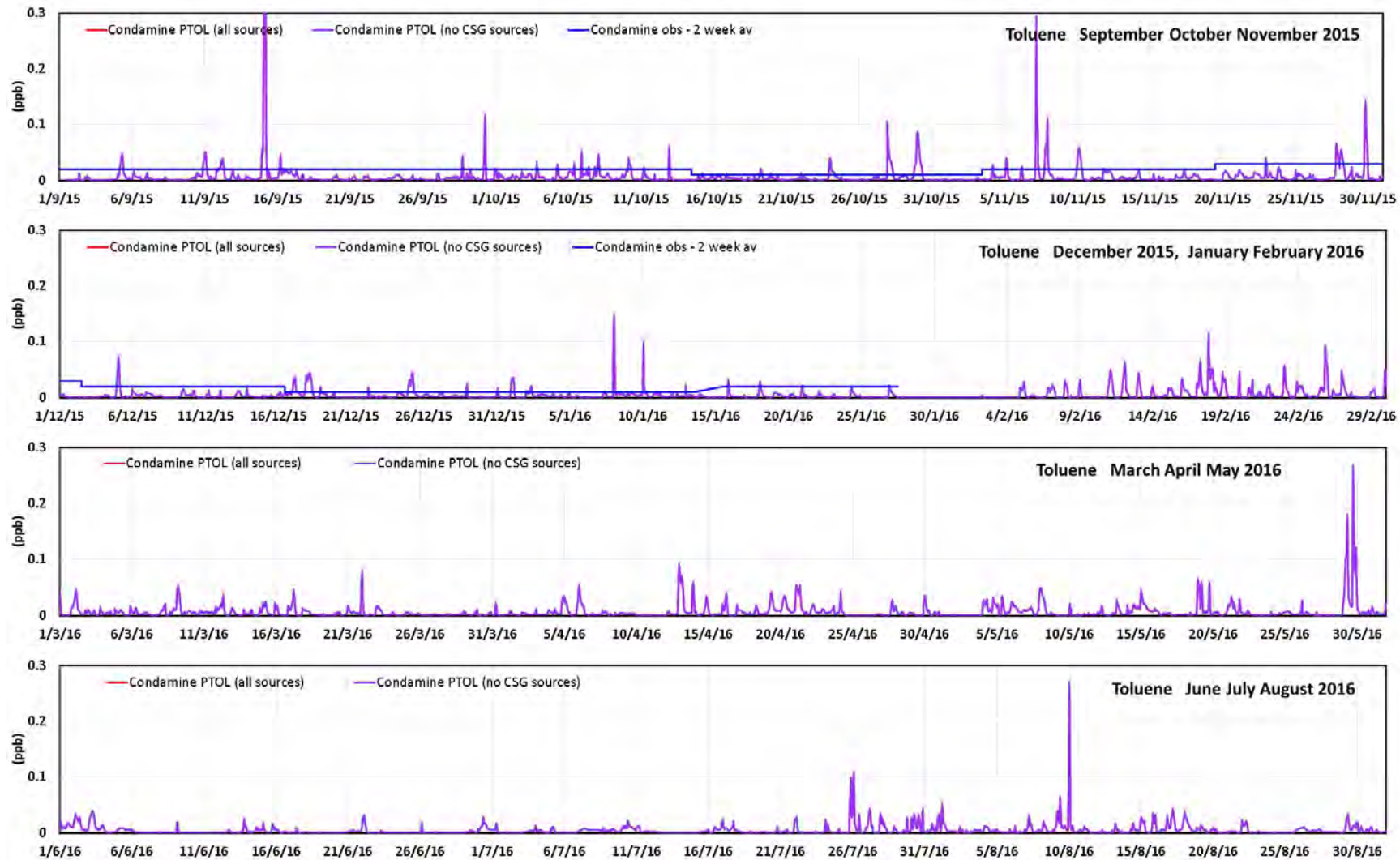


Figure D.67 The observed (2-week sampling period) and modelled (1-hour average) time series of the toluene concentrations (ppb) at Condamine for the modelled year (red = model results with all sources, purple = model results without CSG sources, blue = observations). (peaks off scale: model, 15/9/15 04:00 = 0.82 ppb, 7/11/15 04:00 0.29 ppb)

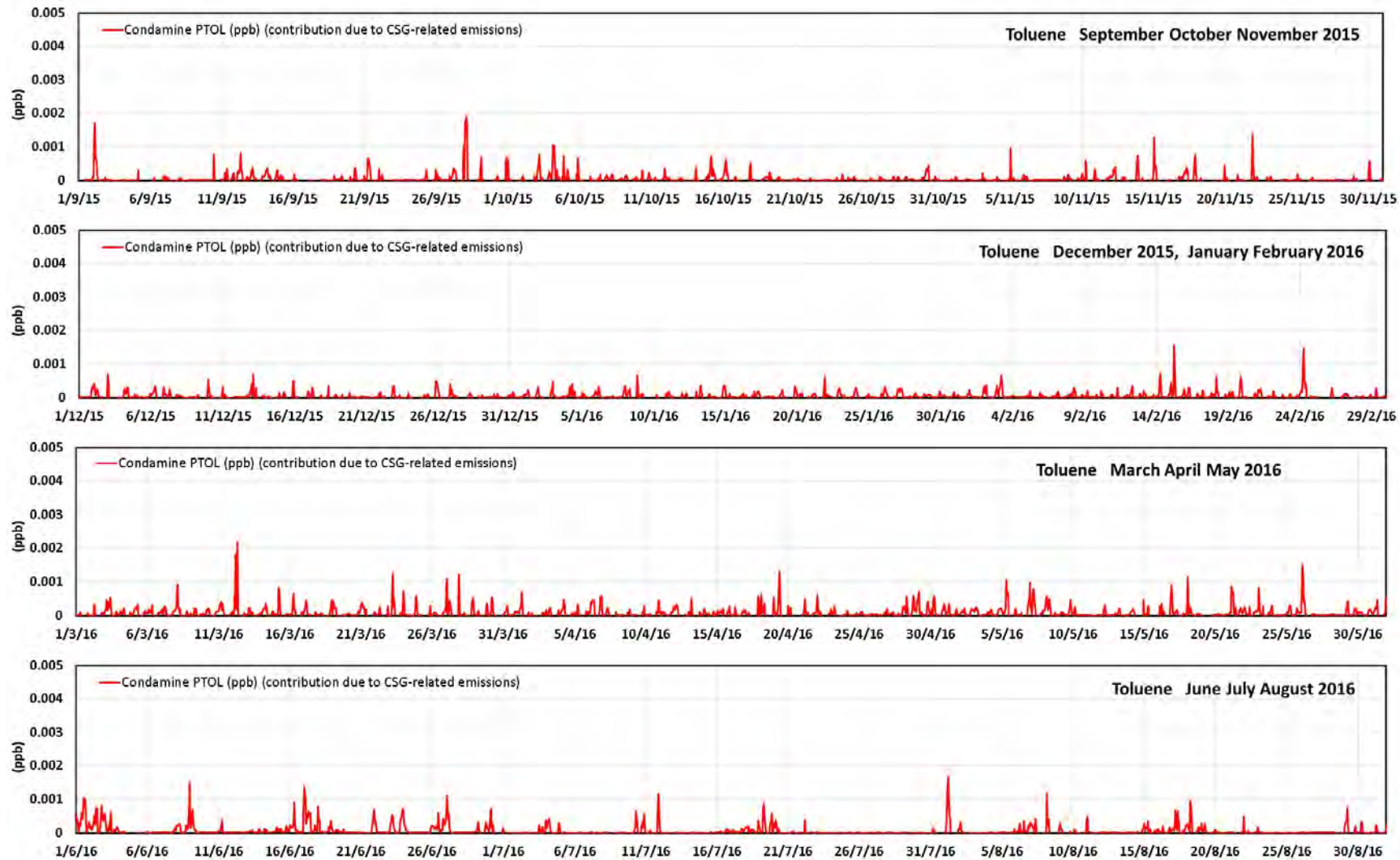


Figure D.68 The modelled contributions from the CSG-related emissions to the 1-hour average toluene concentrations (ppb) at Condamine for the modelled year.

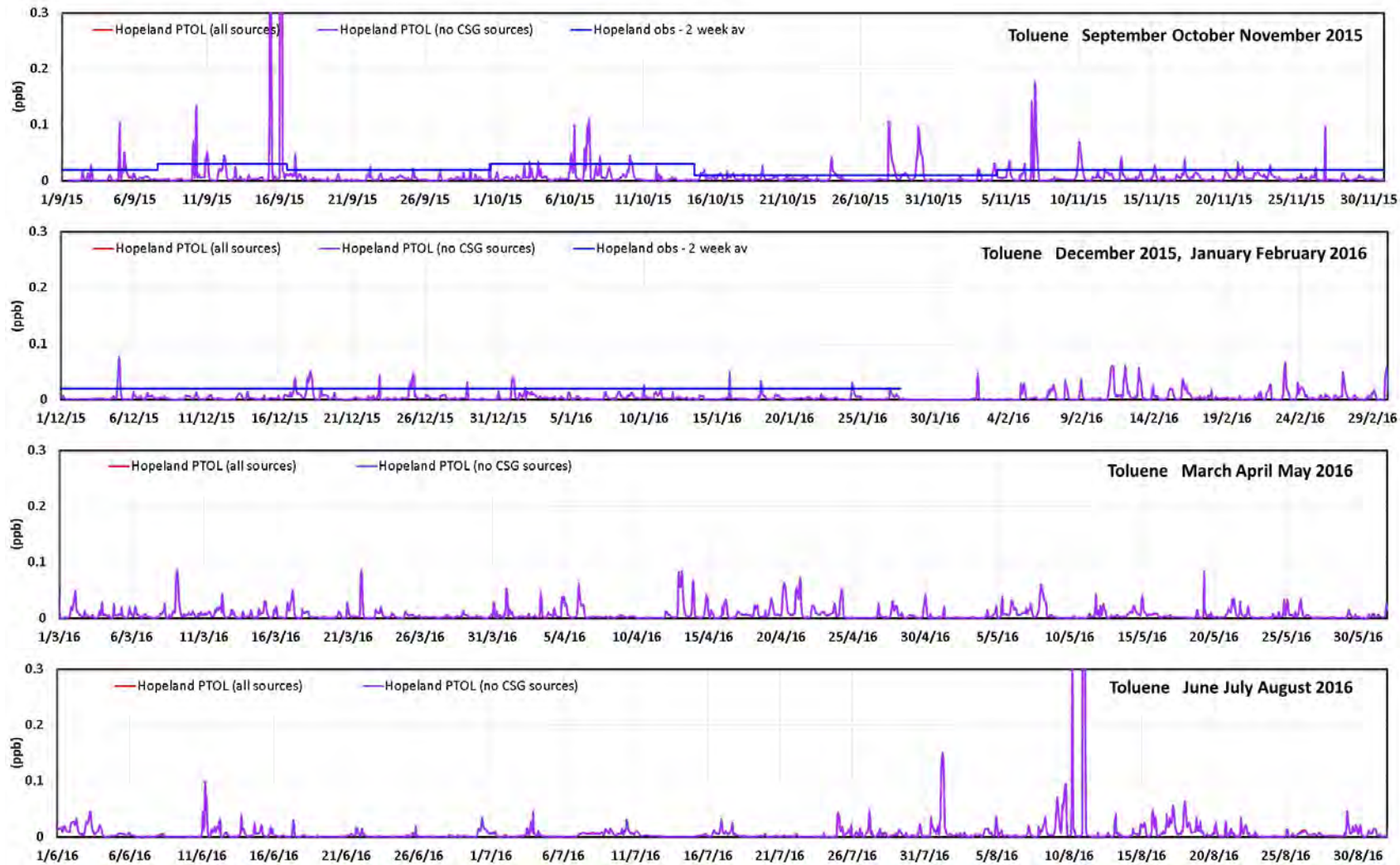


Figure D.69 The observed (2-week sampling period) and modelled (1-hour average) time series of the toluene concentrations (ppb) at Hopeland for the modelled year (red = model results with all sources, purple = model results without CSG sources, blue = observations). (peaks off scale: model, 15/9/15 09:00 = 0.73 ppb, 16/9/15 01:00 = 0.90 ppb, 10/8/16 05:00, 23:00 = 0.34, 0.66 ppb)

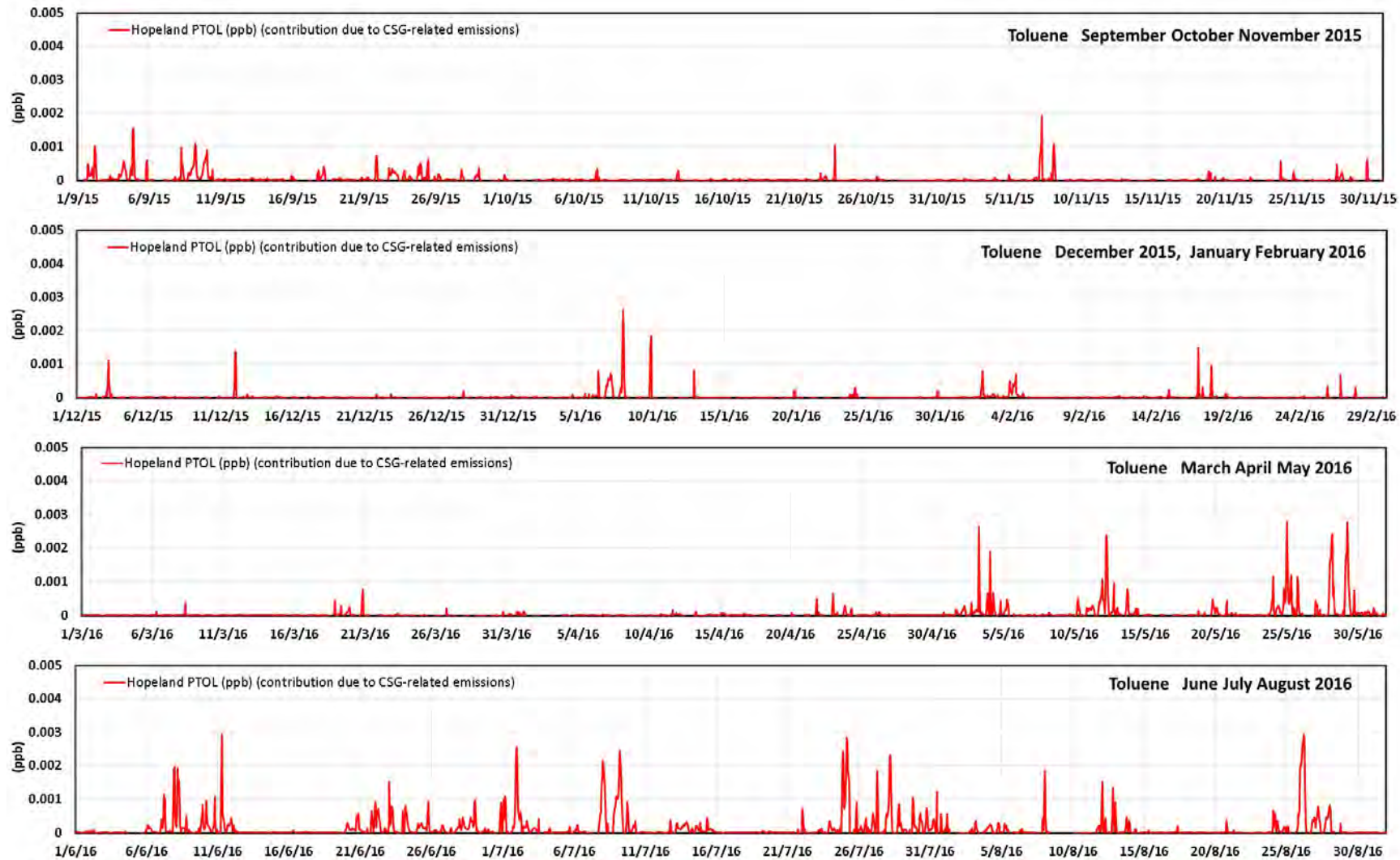


Figure D.70 The modelled contributions from the CSG-related emissions to the 1-hour average toluene concentrations (ppb) at Hopeland for the modelled year.

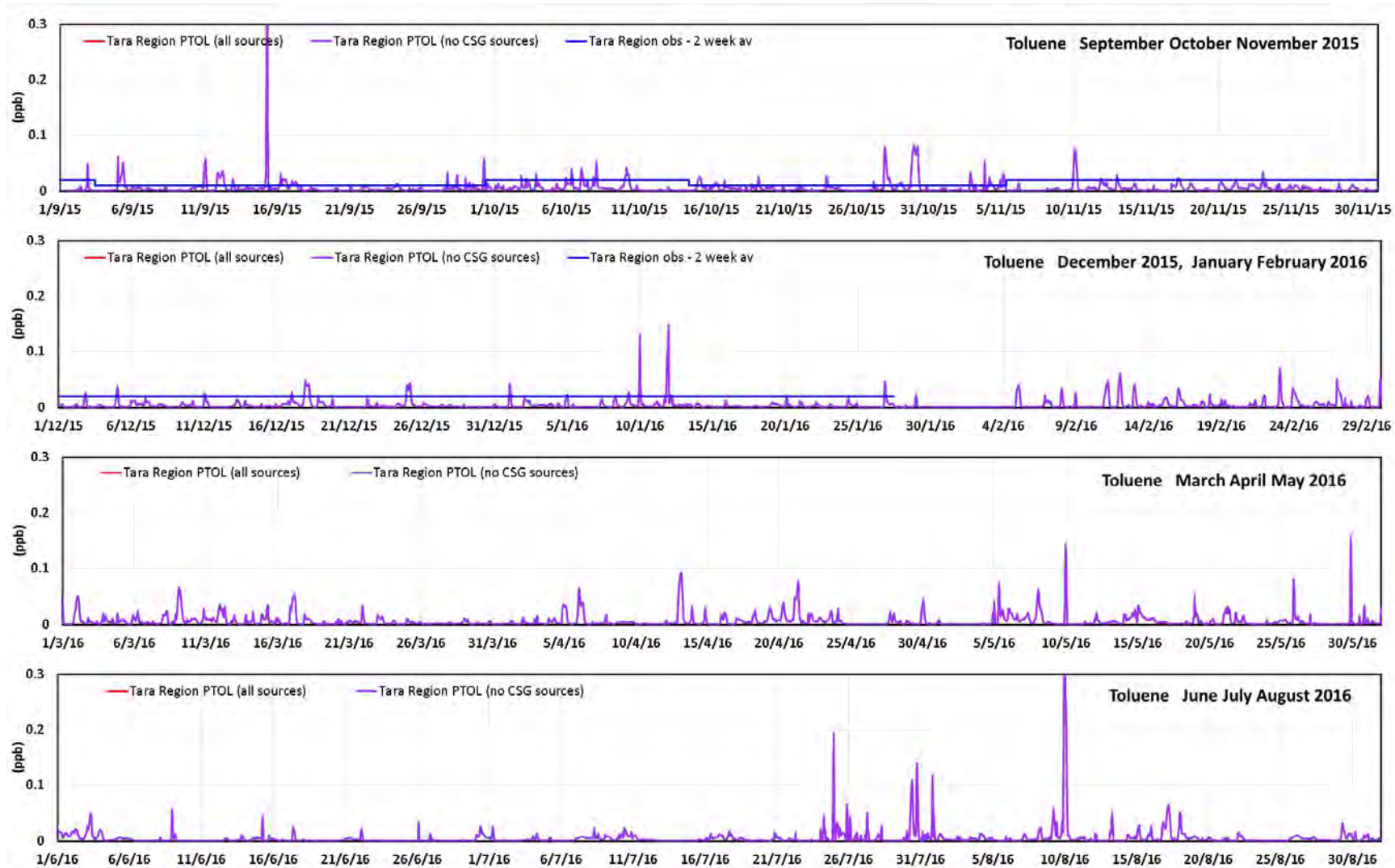


Figure D.71 The observed (2-week sampling period) and modelled (1-hour average) time series of the toluene concentrations (ppb) at Tara Region for the modelled year (red = model results with all sources, purple = model results without CSG sources, blue = observations). (peaks off scale: model, 15/9/15 07:00 = 0.57 ppb, 9/8/16 23:00 = 0.46 ppb)

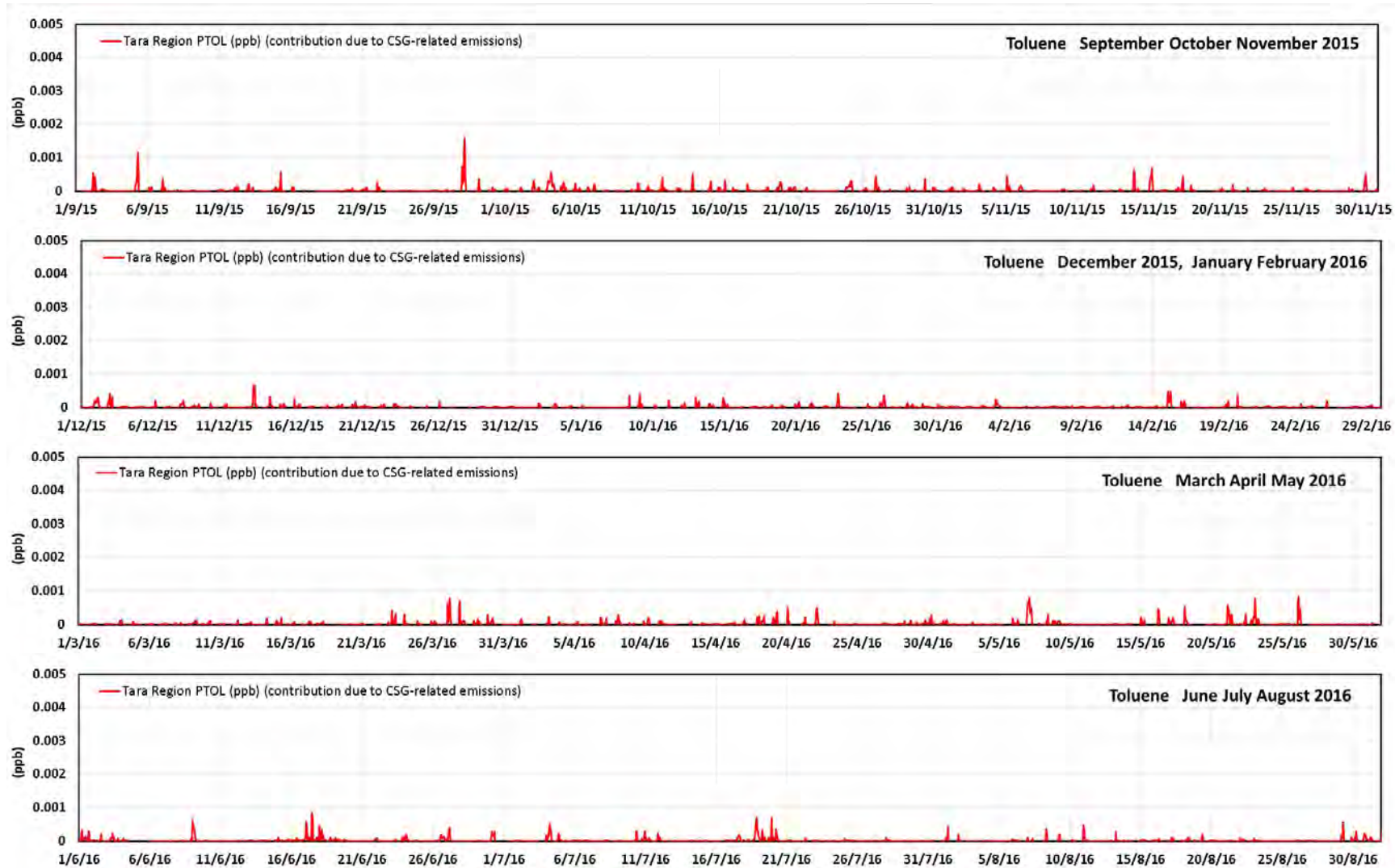


Figure D.72 The modelled contributions from the CSG-related emissions to the 1-hour average toluene concentrations (ppb) at Tara Region for the modelled year.

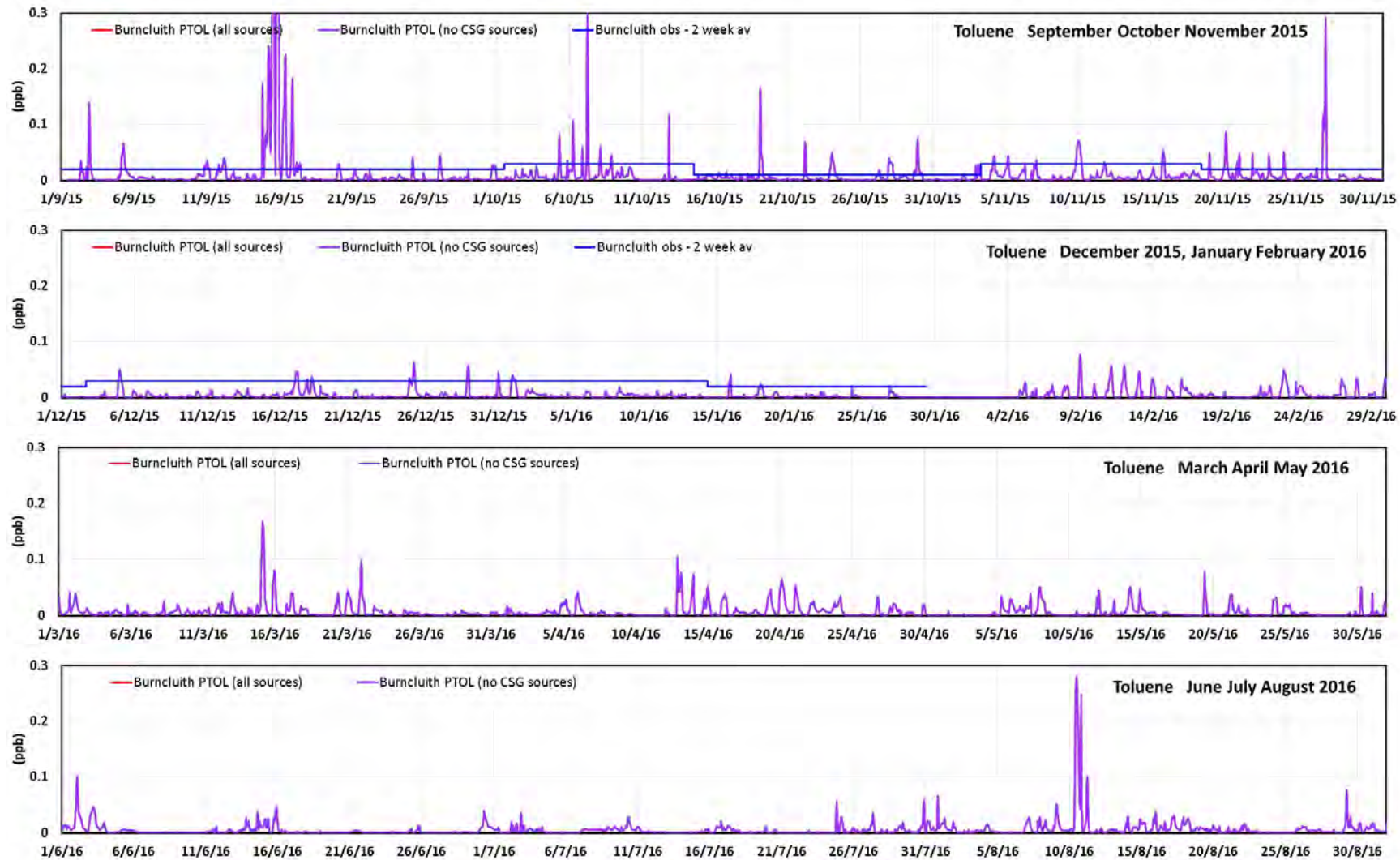


Figure D.73 The observed (2-week sampling period) and modelled (1-hour average) time series of the toluene concentrations (ppb) at Burncluith for the modelled year (red = model results with all sources, purple = model results without CSG sources, blue = observations). (peaks off scale: model, 15/9/15 21:00 = 5.82 ppb, 7/10/15 06:00 = 0.30 ppb)

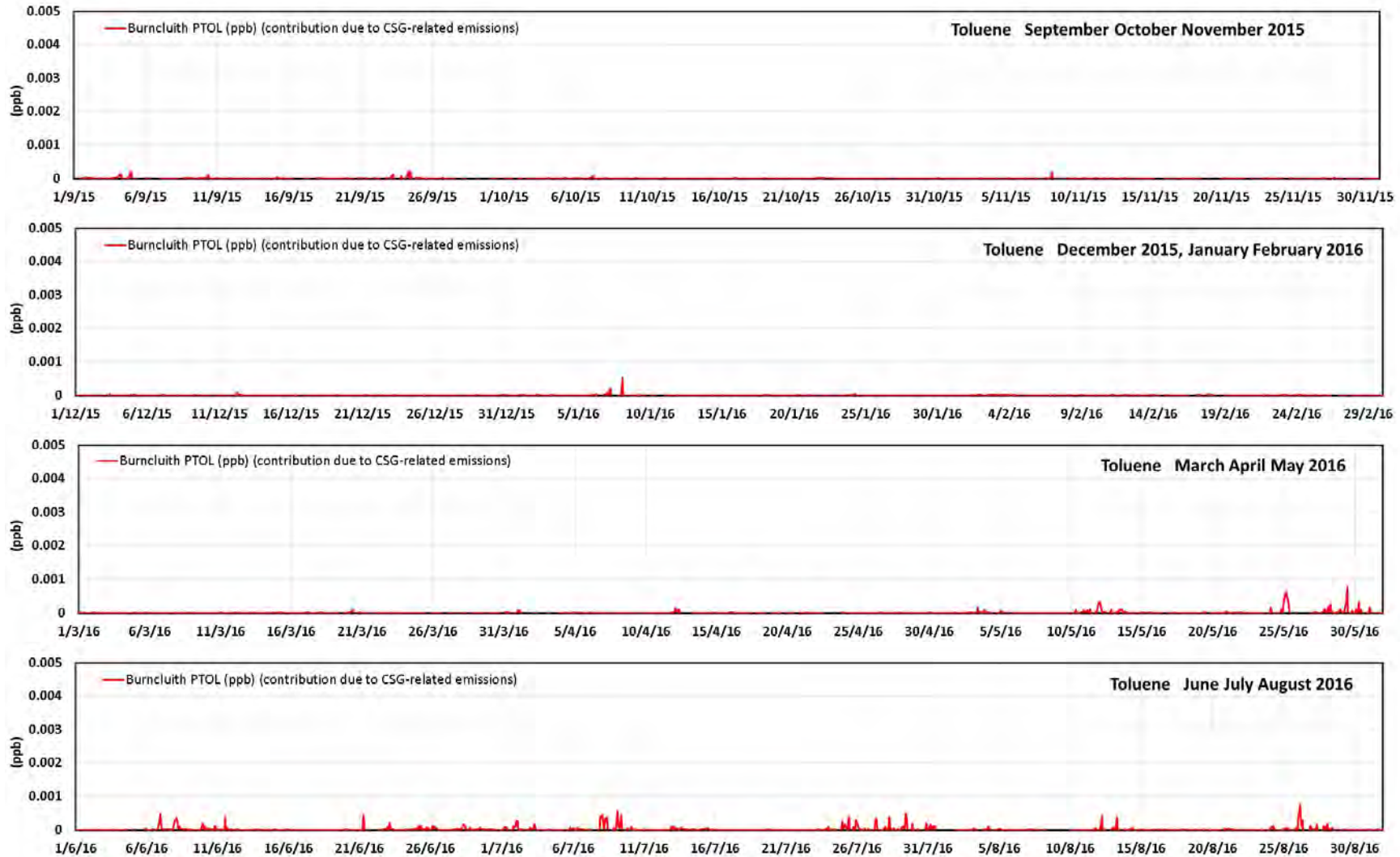


Figure D.74 The modelled contributions from the CSG-related emissions to the 1-hour average toluene concentrations (ppb) at Burncluith for the modelled year.

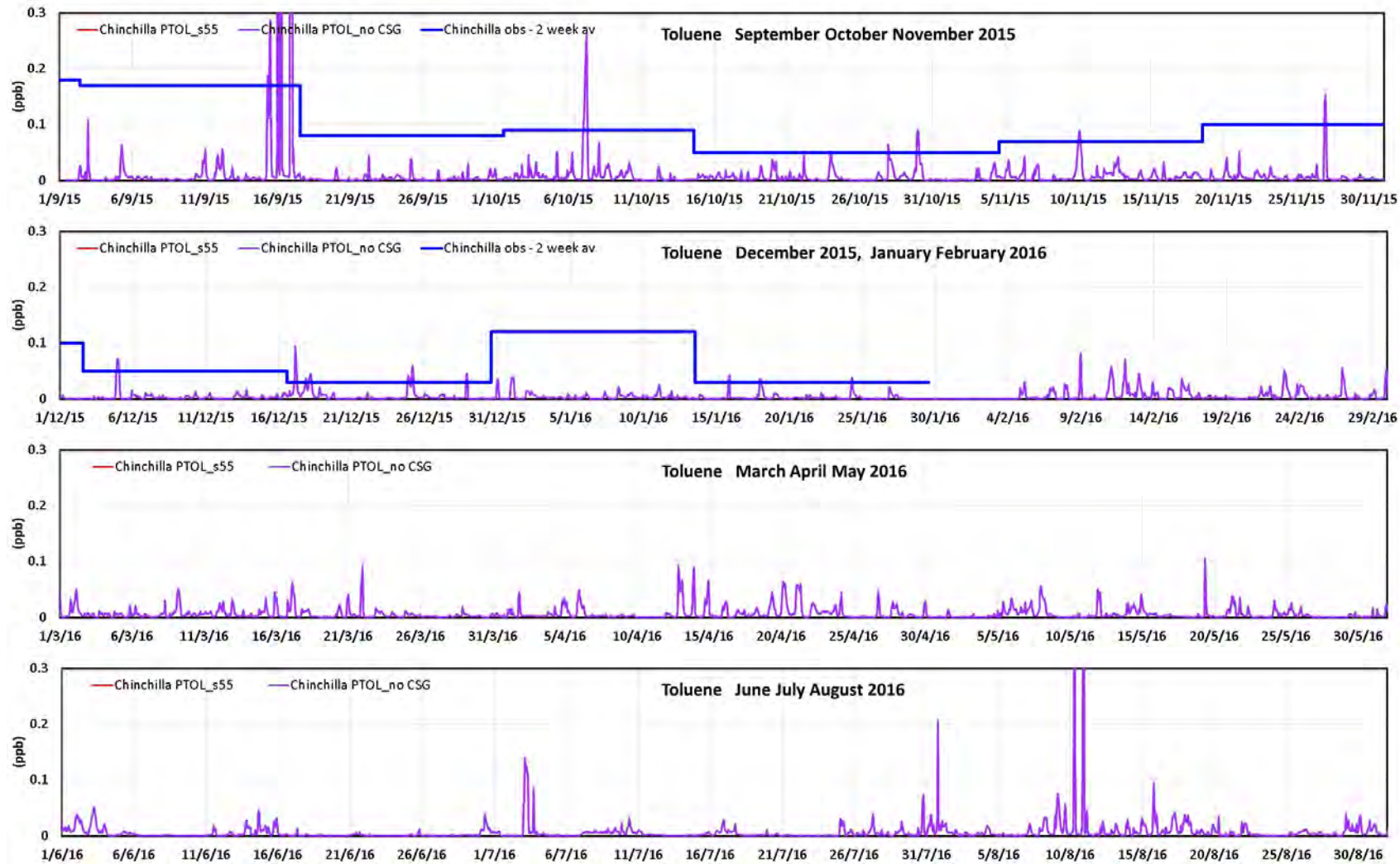


Figure D.75 The observed (2-week sampling period) and modelled (1-hour average) time series of the toluene concentrations (ppb) at Chinchilla for the modelled year (red = model results with all sources, purple = model results without CSG sources, blue = observations). (peaks off scale: model, 16/9/15 00:00, 05:00, 21:00 = 0.91, 0.85, 2.2 ppb, 10/8/16 07:00, 21:00 = 0.60, 0.43 ppb)

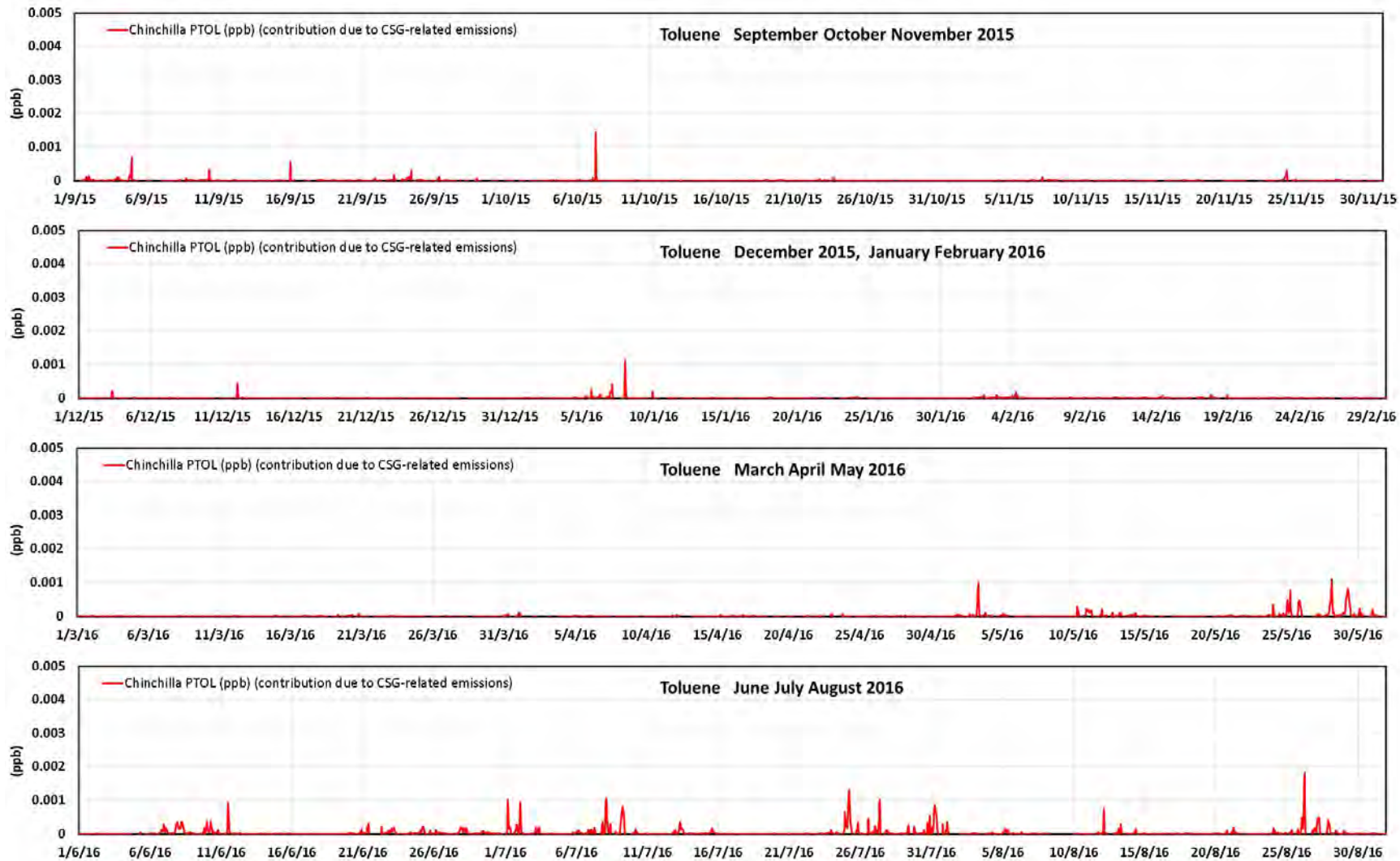


Figure D.76 The modelled contributions from the CSG-related emissions to the 1-hour average toluene concentrations (ppb) at Chinchilla for the modelled year.

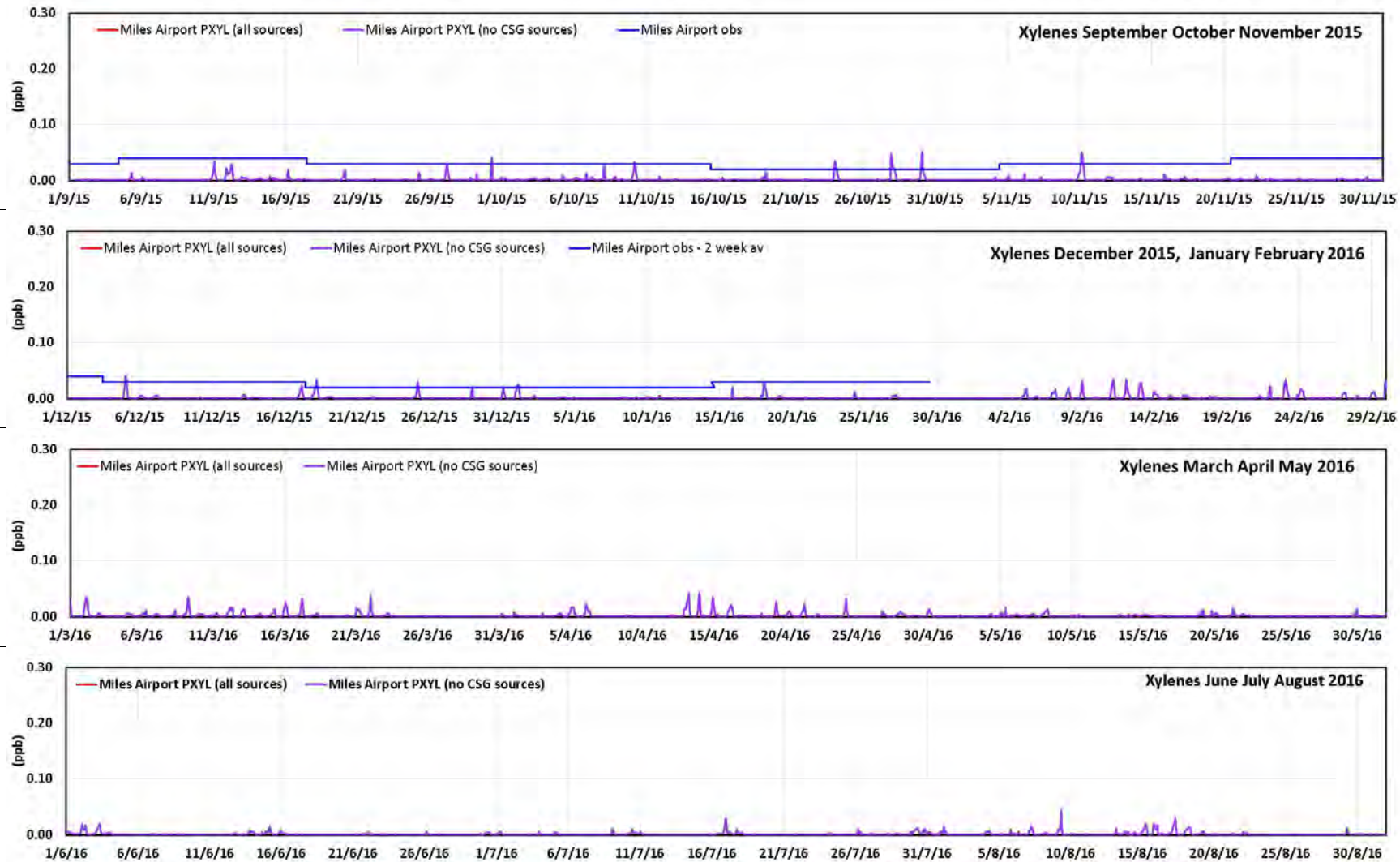


Figure D.77 The observed (2-week sampling period) and modelled (1-hour average) time series of the xylene concentrations (ppb) at Miles Airport for the modelled year (red = model results with all sources, purple = model results without CSG sources, blue = observations).

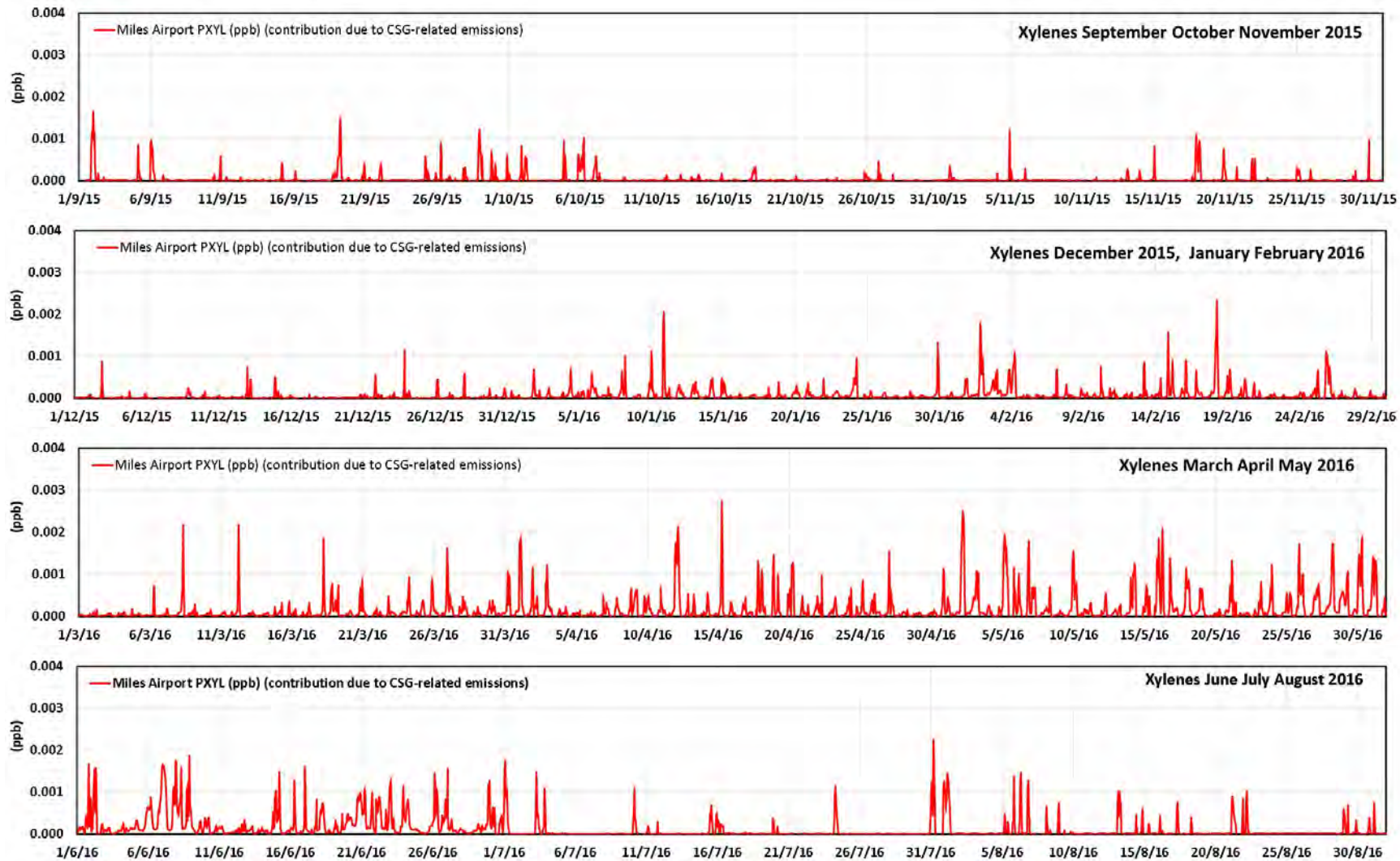


Figure D.78 The modelled contributions from the CSG-related emissions to the 1-hour average xylene concentrations (ppb) at Miles Airport for the modelled year.

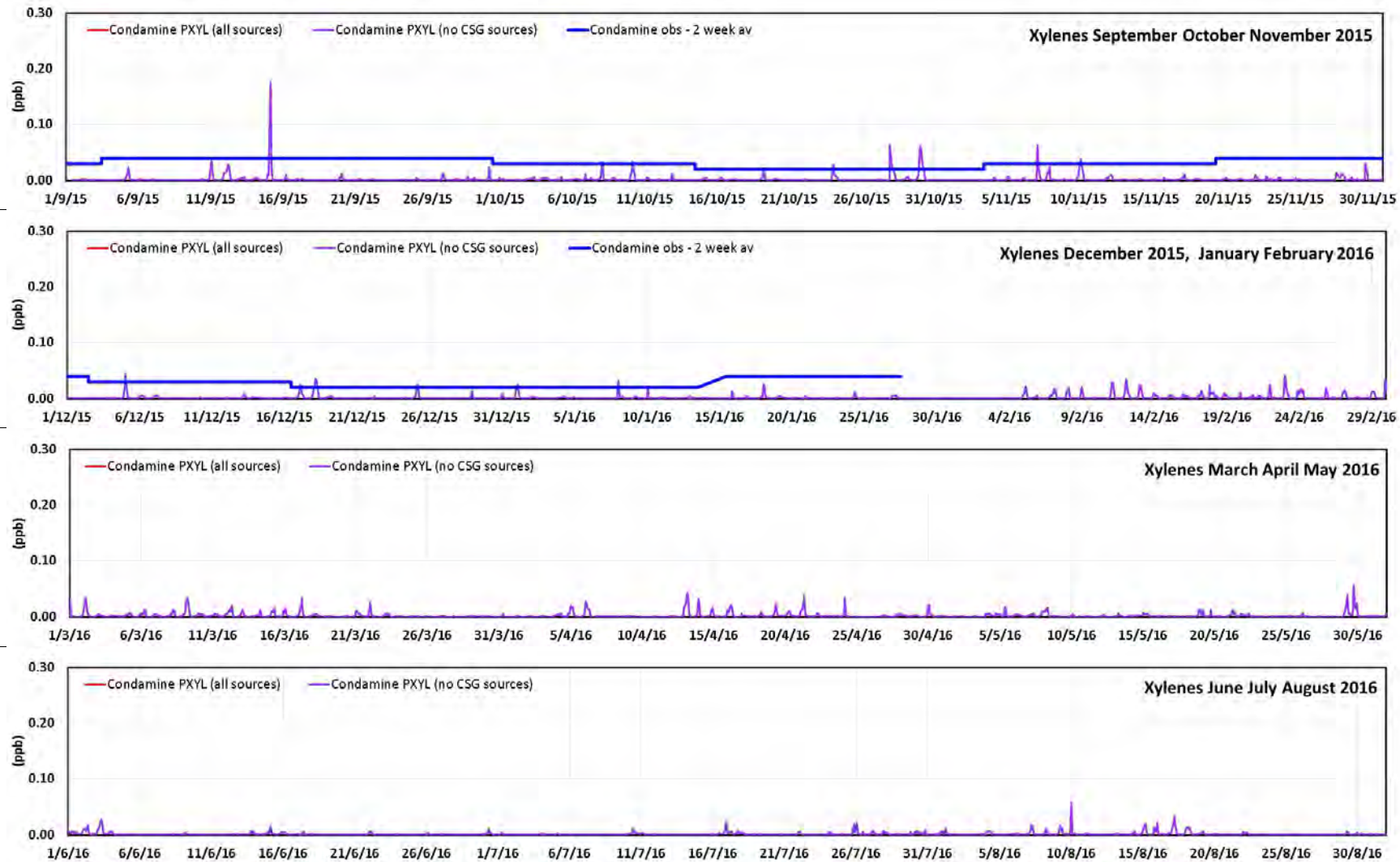


Figure D.79 The observed (2-week sampling period) and modelled (1-hour average) time series of the xylene concentrations (ppb) at Condamine for the modelled year (red = model results with all sources, purple = model results without CSG sources, blue = observations).

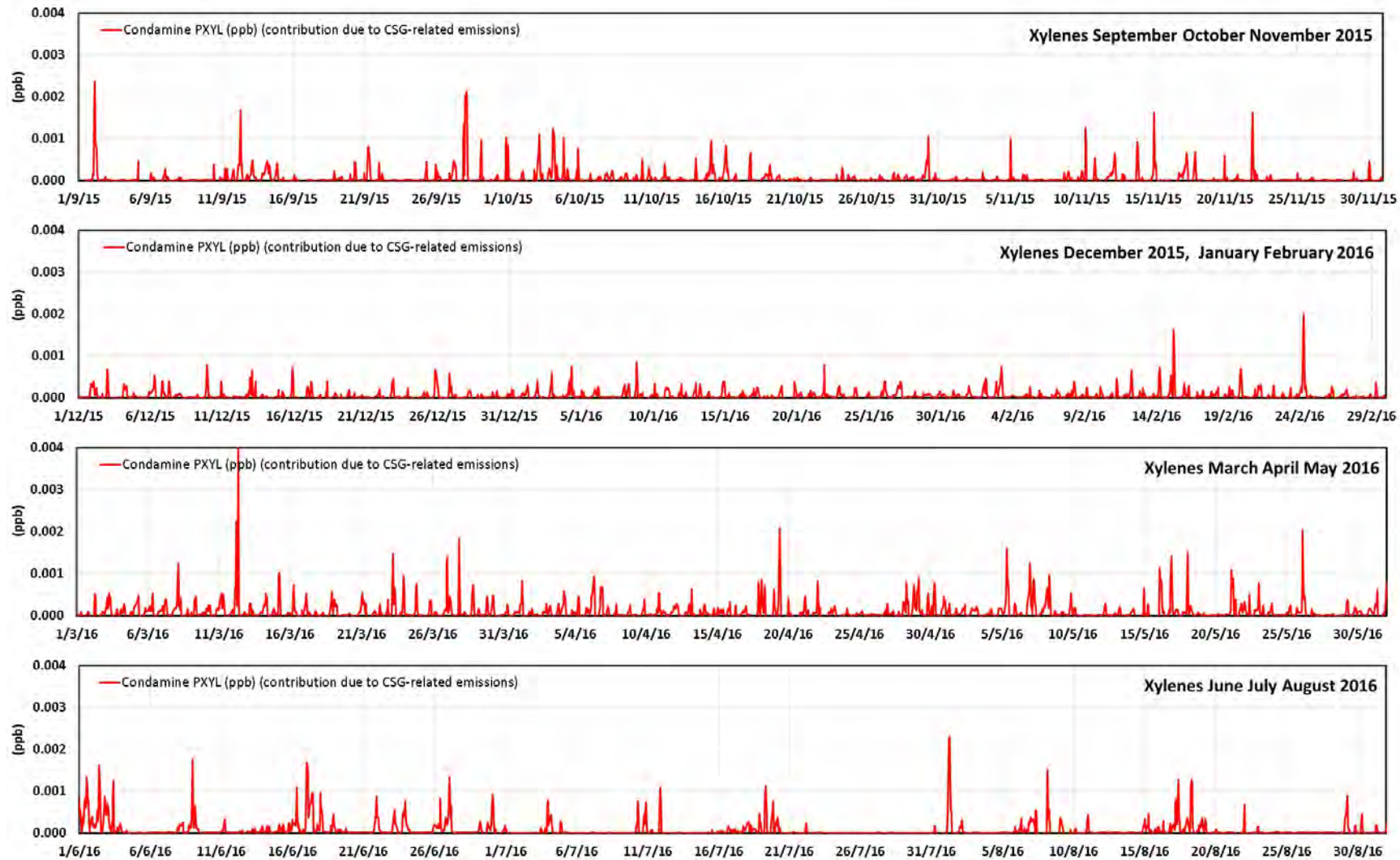


Figure D.80 The modelled contributions from the CSG-related emissions to the 1-hour average xylene concentrations (ppb) at Condamine for the modelled year.

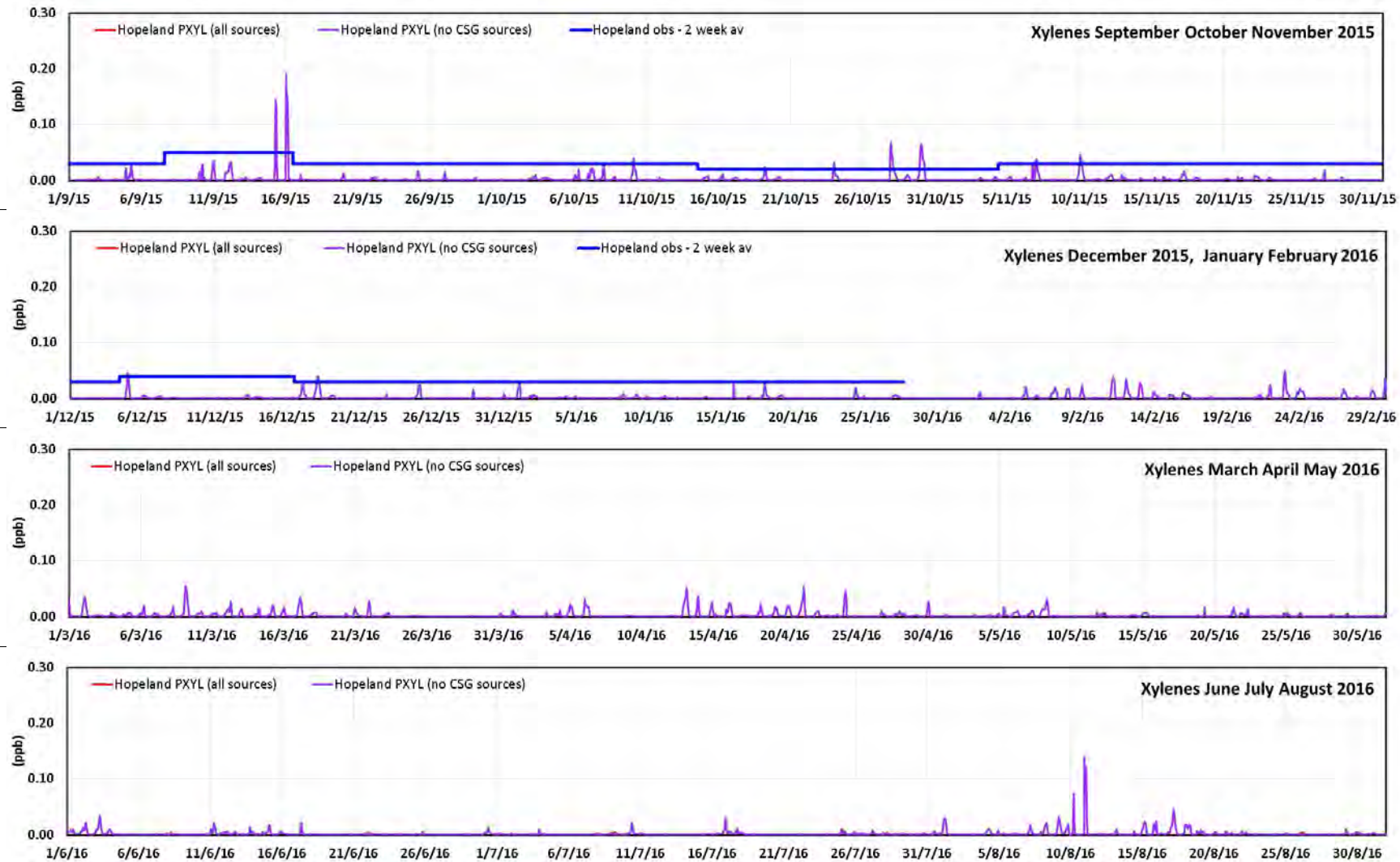


Figure D.81 The observed (2-week sampling period) and modelled (1-hour average) time series of the xylene concentrations (ppb) at Hopeland for the modelled year (red = model results with all sources, purple = model results without CSG sources, blue = observations).

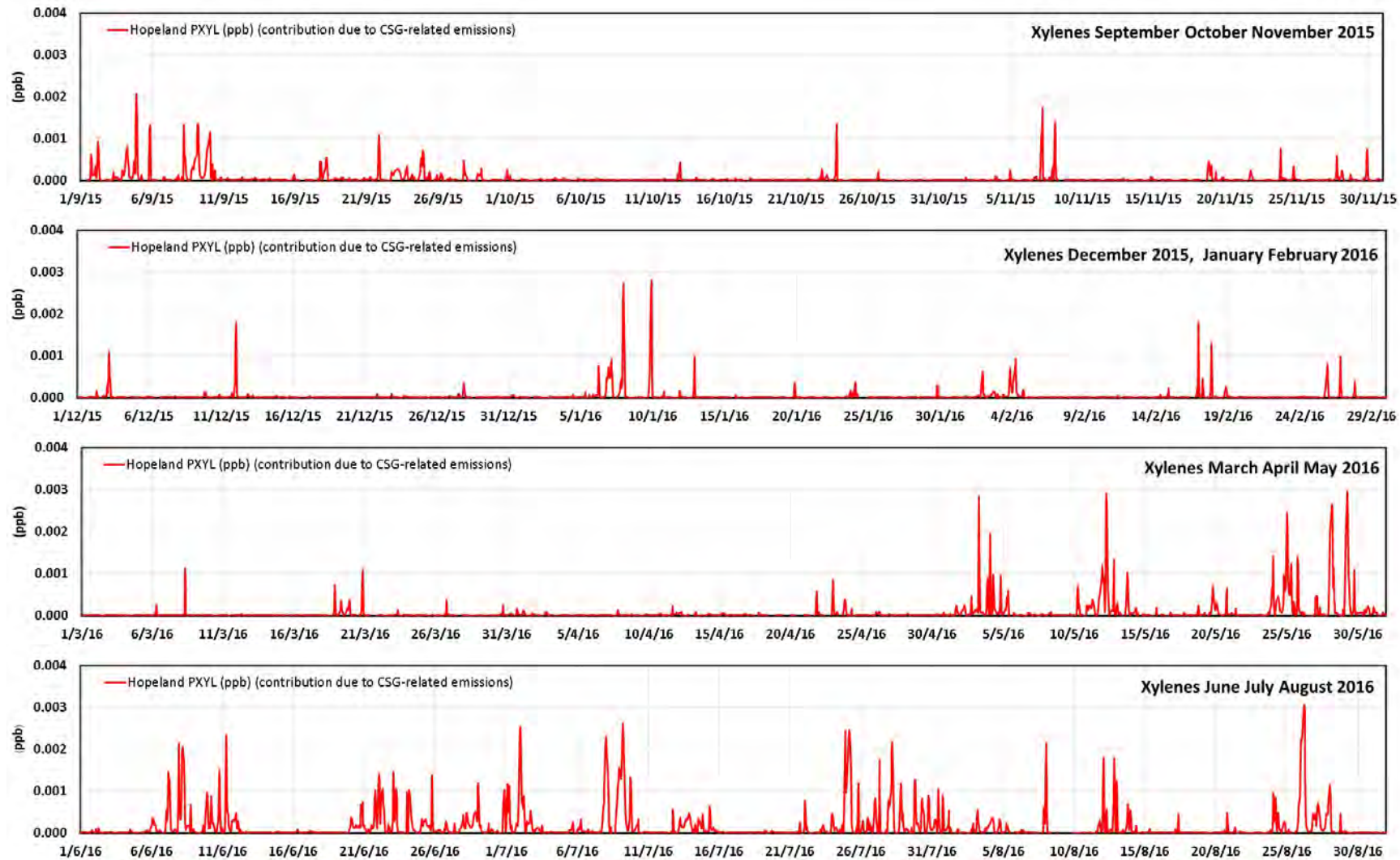


Figure D.82 The modelled contributions from the CSG-related emissions to the 1-hour average xylene concentrations (ppb) at Hopeland for the modelled year.

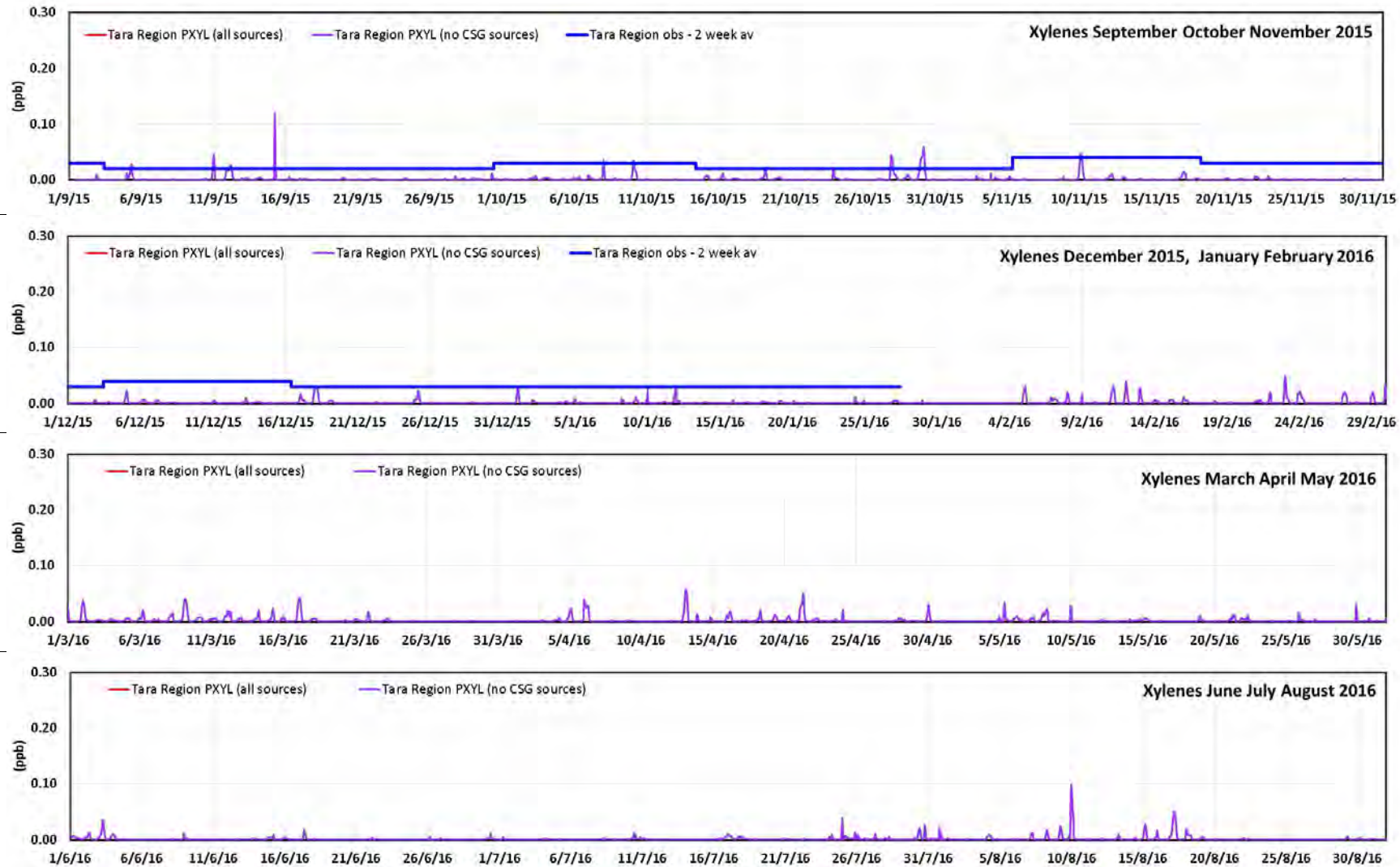


Figure D.83 The observed (2-week sampling period) and modelled (1-hour average) time series of the xylene concentrations (ppb) at Tara Region for the modelled year (red = model results with all sources, purple = model results without CSG sources, blue = observations).

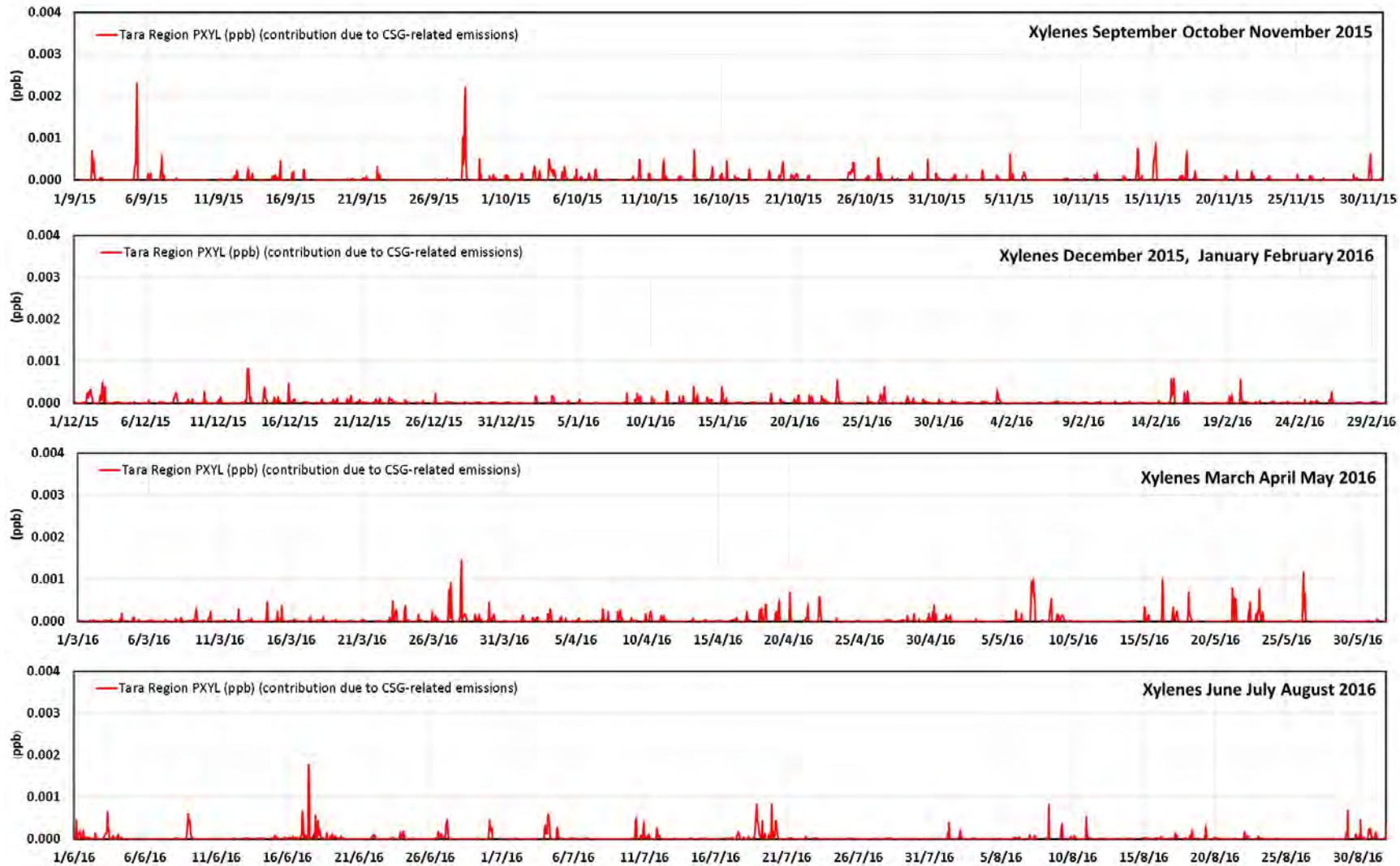


Figure D.84 The modelled contributions from the CSG-related emissions to the 1-hour average xylene concentrations (ppb) at Tara Region for the modelled year.

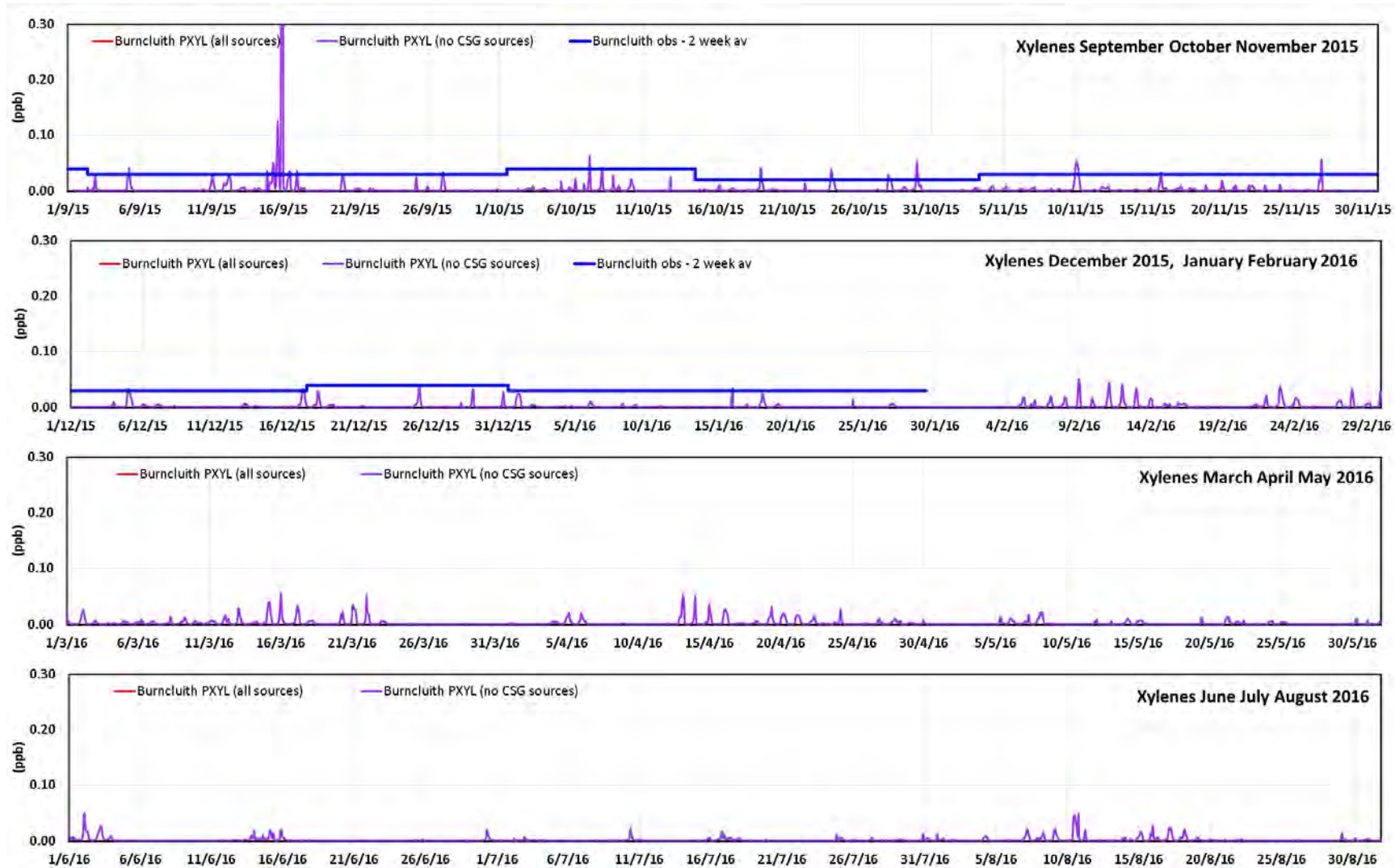


Figure D.85 The observed (2-week sampling period) and modelled (1-hour average) time series of the xylene concentrations (ppb) at Burncluith for the modelled year (red = model results with all sources, purple = model results without CSG sources, blue = observations). (peaks off scale: model, 15/9/15 21:00 = 1.24 ppb)

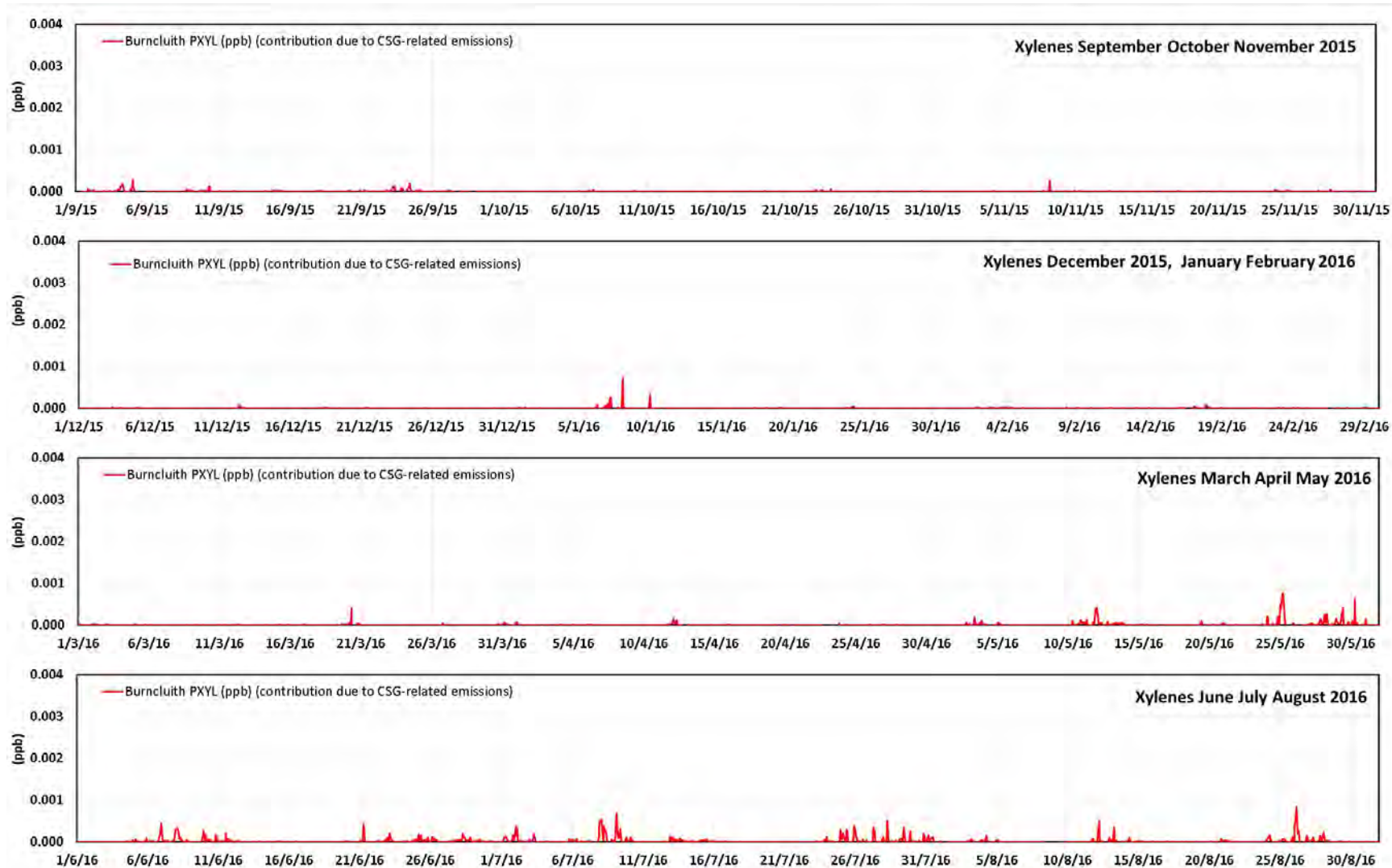


Figure D.86 The modelled contributions from the CSG-related emissions to the 1-hour average xylene concentrations (ppb) at Burncluth for the modelled year.

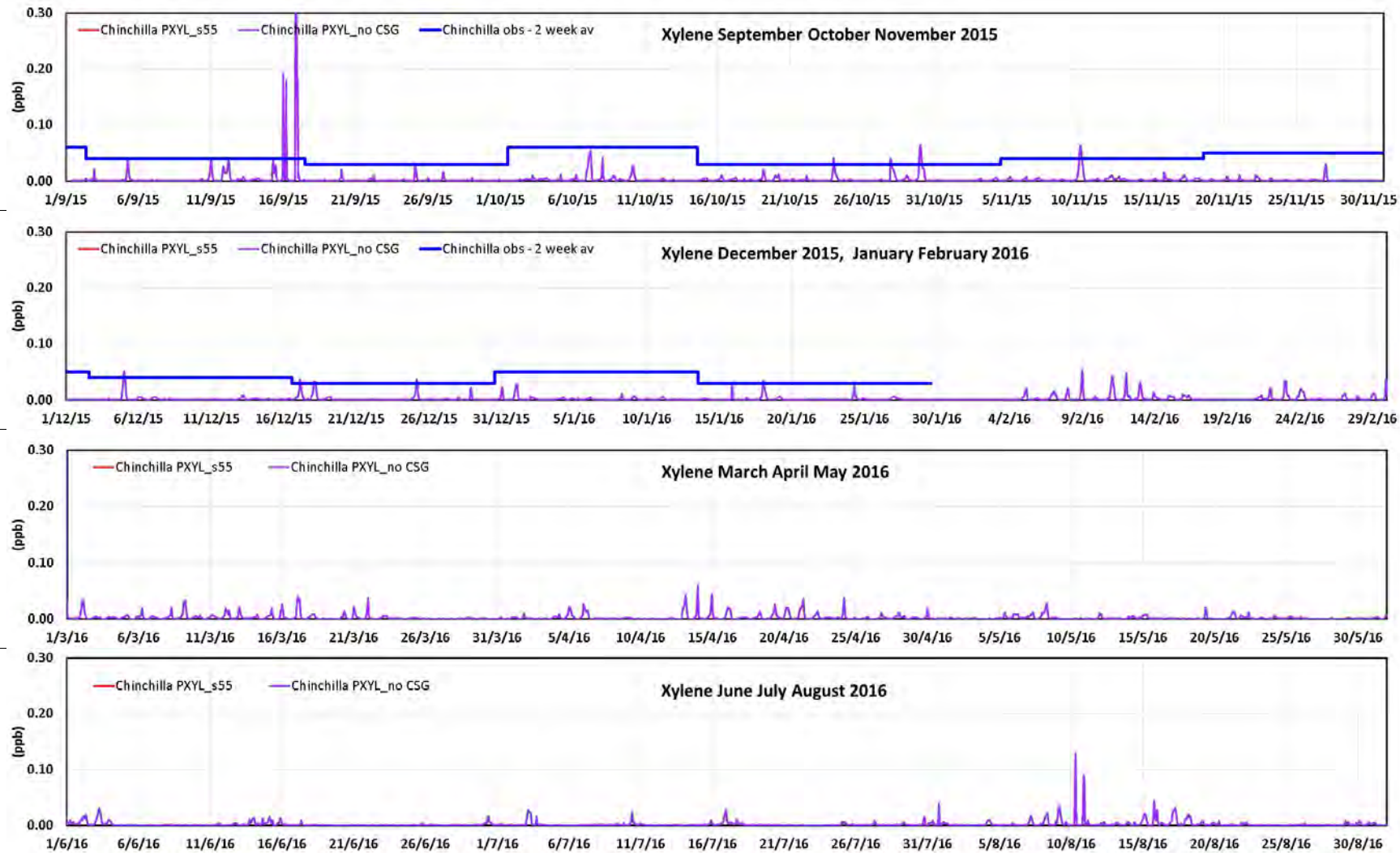


Figure D.87 The observed (2-week sampling period) and modelled (1-hour average) time series of the xylene concentrations (ppb) at Chinchilla for the modelled year (red = model results with all sources, purple = model results without CSG sources, blue = observations). (peaks off scale: model, 16/9/15 21:00 = 0.46 ppb)

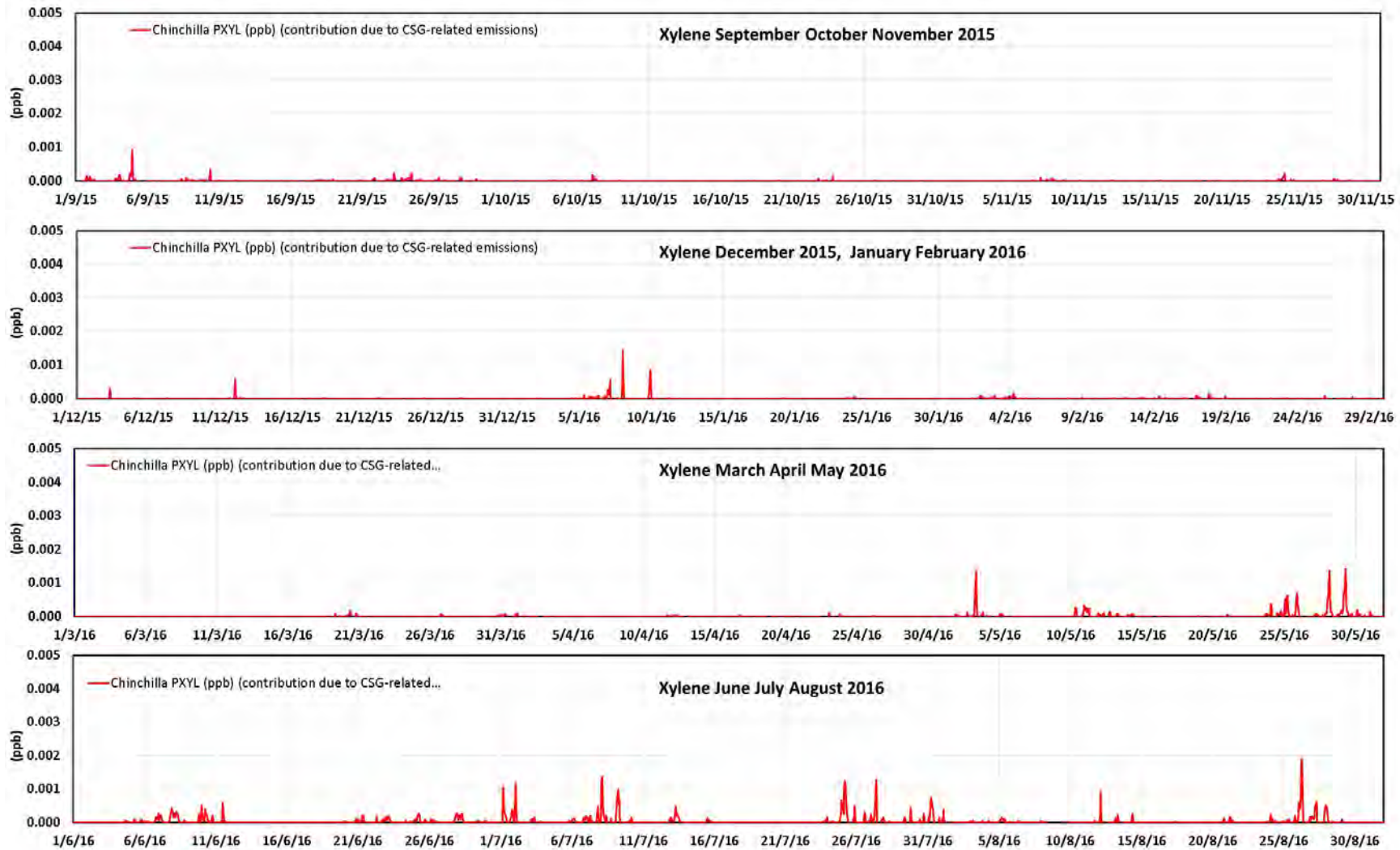


Figure D.88 The modelled contributions from the CSG-related emissions to the 1-hour average xylene concentrations (ppb) at Chinchilla for the modelled year.

Appendix E Extra plots: Modelled effect of CSG at various sites

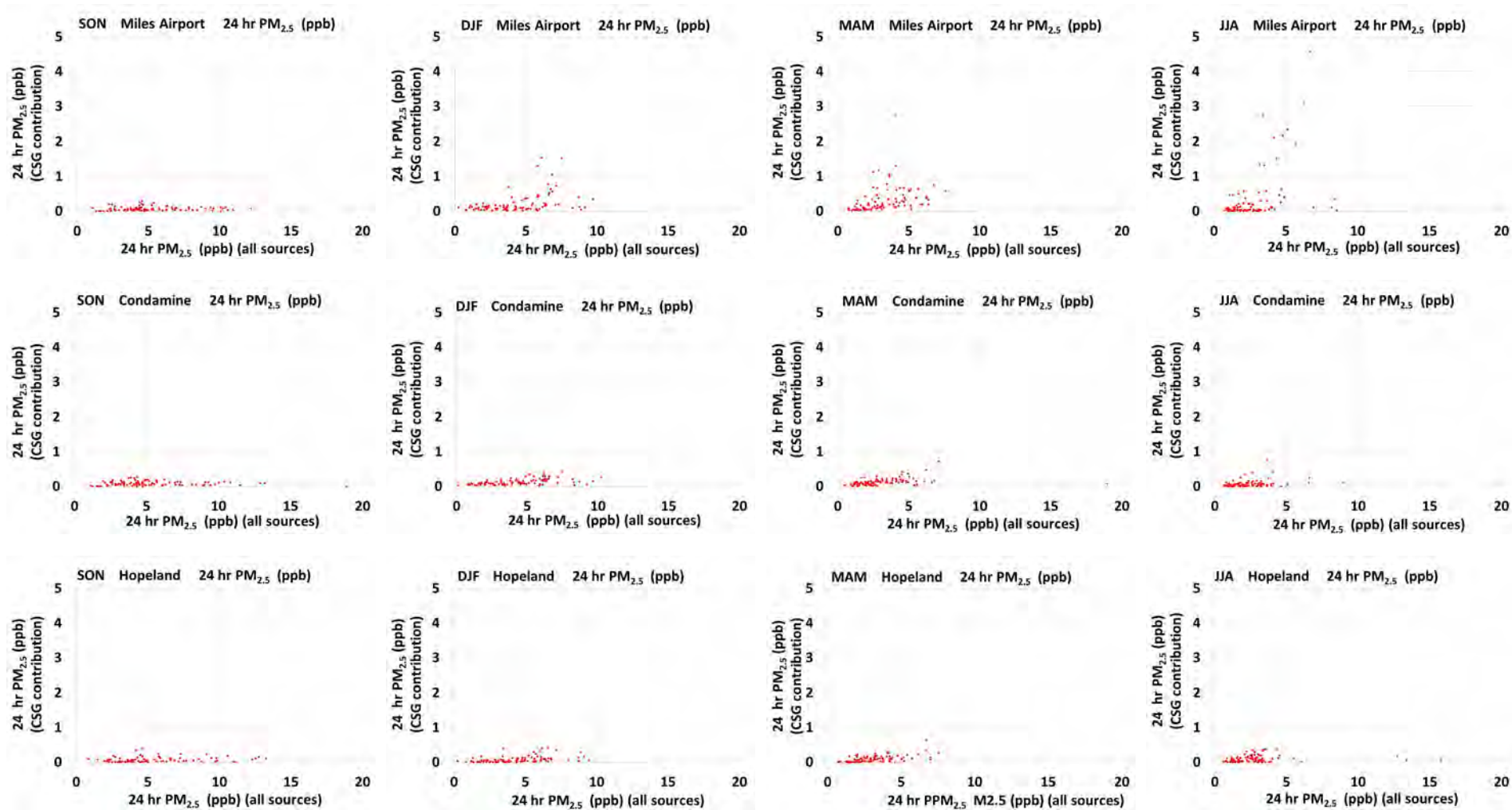


Figure E.1 The modelled contribution from the CSG-related emissions to the 24-hour average PM_{2.5} concentration ($\mu\text{g m}^{-3}$) shown as a scatter plot for each season. The x-axis shows the modelled 24-hour average PM_{2.5} concentrations with all sources ($\mu\text{g m}^{-3}$) and the y-axis shows the contribution from the CSG-related emissions to the 24-hour average PM_{2.5} concentration ($\mu\text{g m}^{-3}$) - top row: Miles Airport, middle row: Condamine, bottom row: Hopeland.

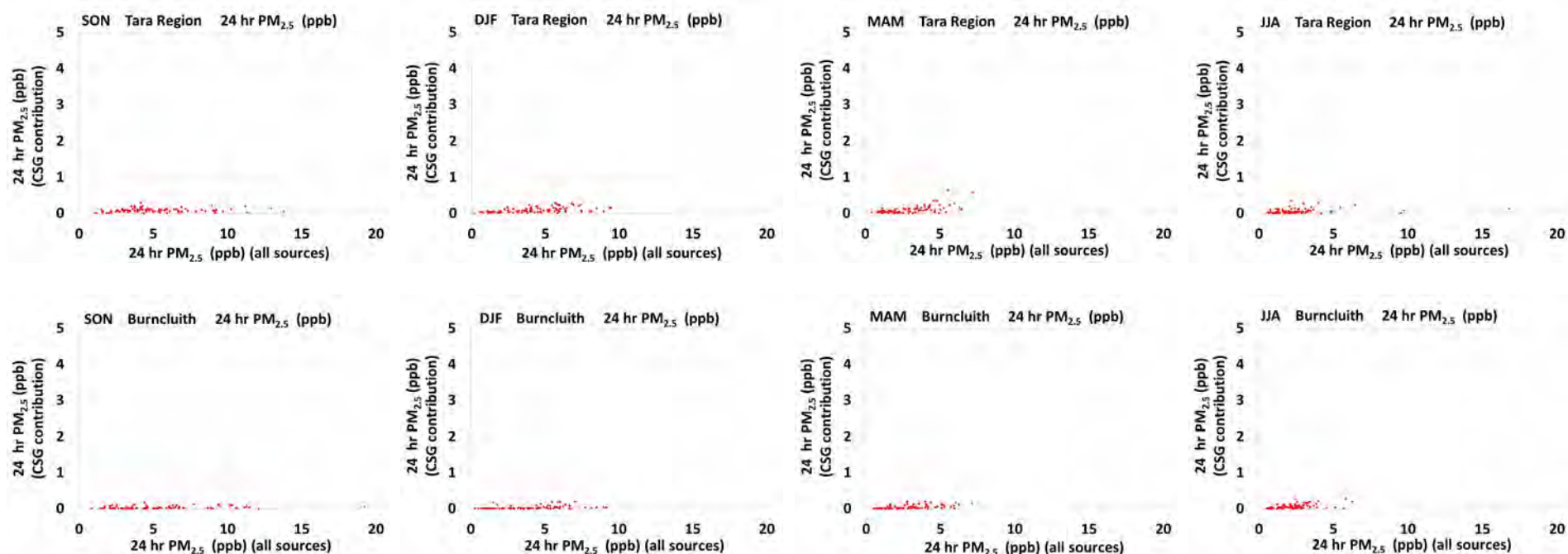


Figure E.2 The modelled contribution from the CSG-related emissions to the 24-hour average PM_{2.5} concentration ($\mu\text{g m}^{-3}$) shown as a scatter plot for each season. The x-axis shows the modelled 24-hour average PM_{2.5} concentrations with all sources ($\mu\text{g m}^{-3}$) and the y-axis shows the contribution from the CSG-related emissions to the 24-hour average PM_{2.5} concentration ($\mu\text{g m}^{-3}$) - top row: Tara Region, bottom row: Burncluith. During the given Season.

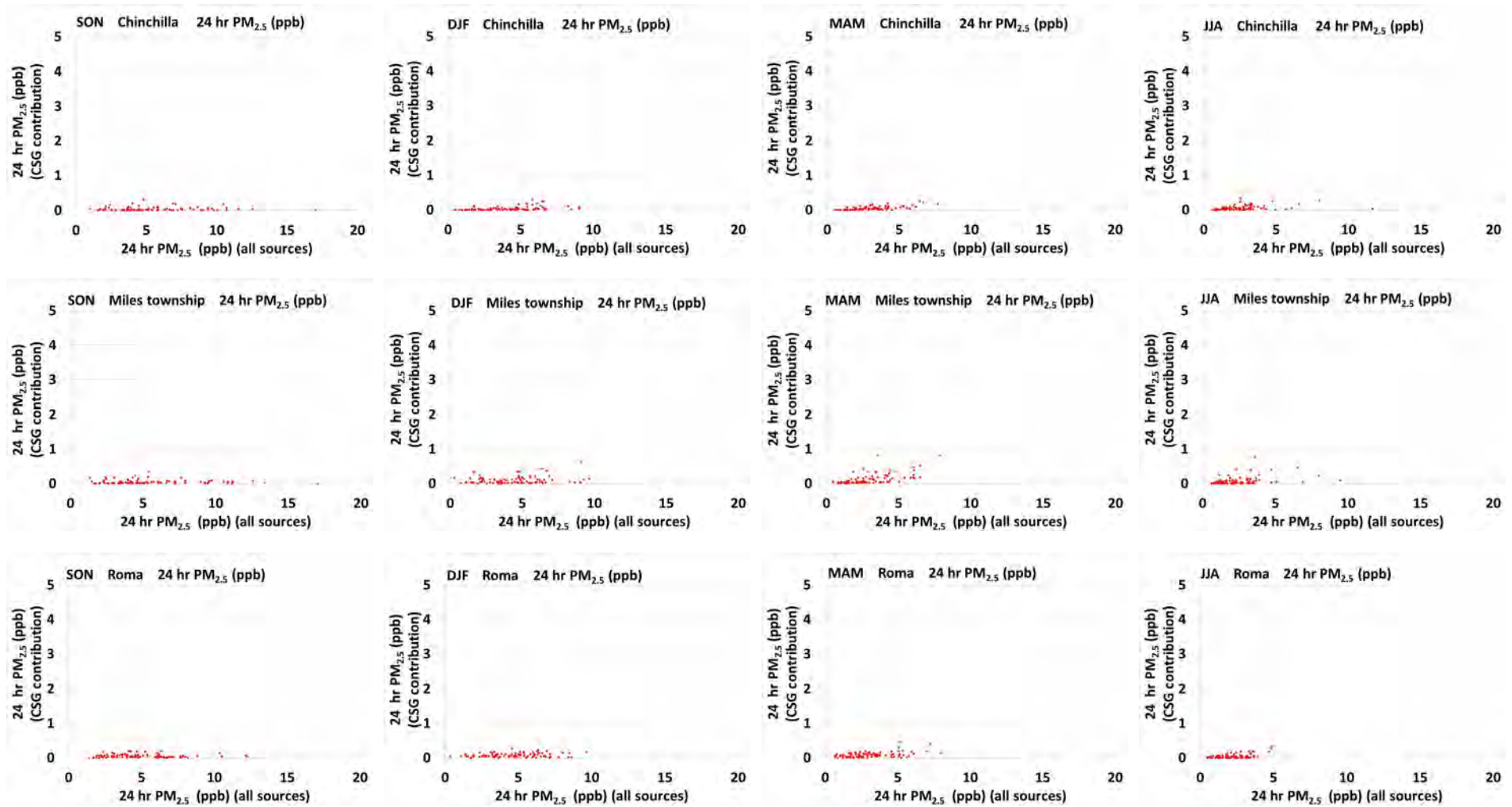


Figure E.3 The modelled contribution from the CSG-related emissions to the 24-hour average PM_{2.5} concentration ($\mu\text{g m}^{-3}$) shown as a scatter plot for each season. The x-axis shows the modelled 24-hour average PM_{2.5} concentrations with all sources ($\mu\text{g m}^{-3}$) and the y-axis shows the contribution from the CSG-related emissions to the 24-hour average PM_{2.5} concentration ($\mu\text{g m}^{-3}$) - top row: Chinchilla, middle row: Miles township, bottom row: Roma.

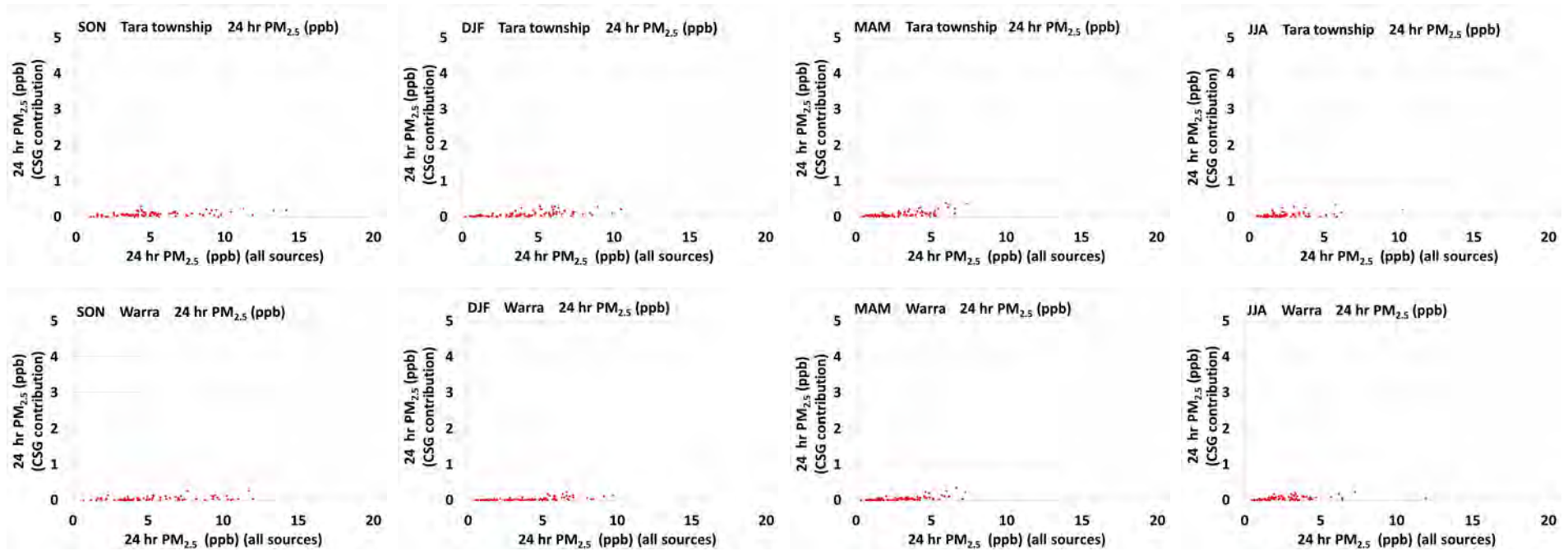


Figure E.4 The modelled contribution from the CSG-related emissions to the 24-hour average PM_{2.5} concentration ($\mu\text{g m}^{-3}$) shown as a scatter plot for each season. The x-axis shows the modelled 24-hour average PM_{2.5} concentrations with all sources ($\mu\text{g m}^{-3}$) and the y-axis shows the contribution from the CSG-related emissions to the 24-hour average PM_{2.5} concentration ($\mu\text{g m}^{-3}$) - top row: Tara township, bottom row: Warra.

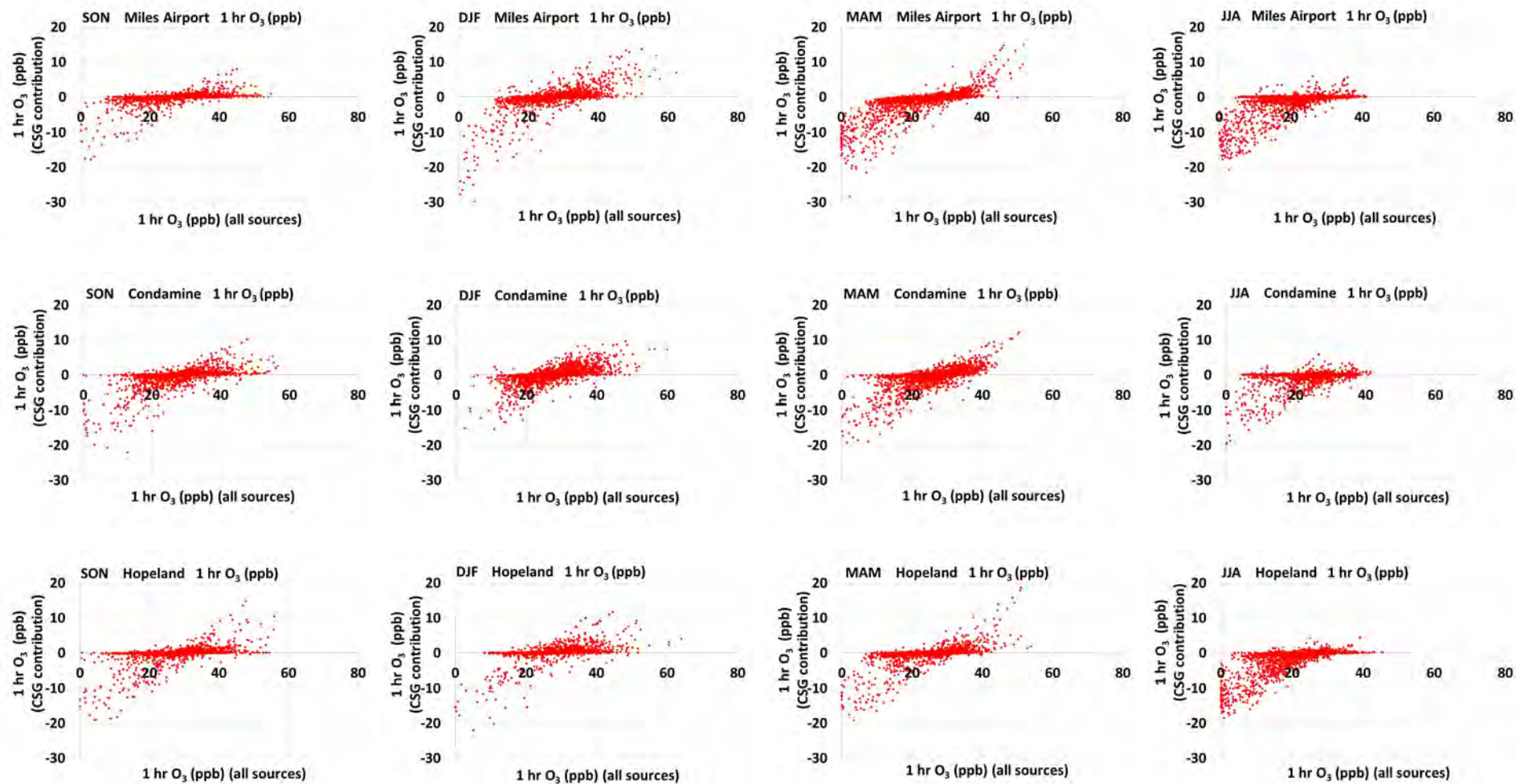


Figure E.5 The modelled contribution from the CSG-related emissions to the 1-hour average O₃ concentration (ppb) shown as a scatter plot for each season. The x-axis shows the modelled 1-hour average O₃ concentrations with all sources (ppb) and the y-axis shows the contribution from the CSG-related emissions to the 1-hour average O₃ concentration (ppb) - top row: Miles Airport, middle row: Condamine, bottom row: Hopeland.

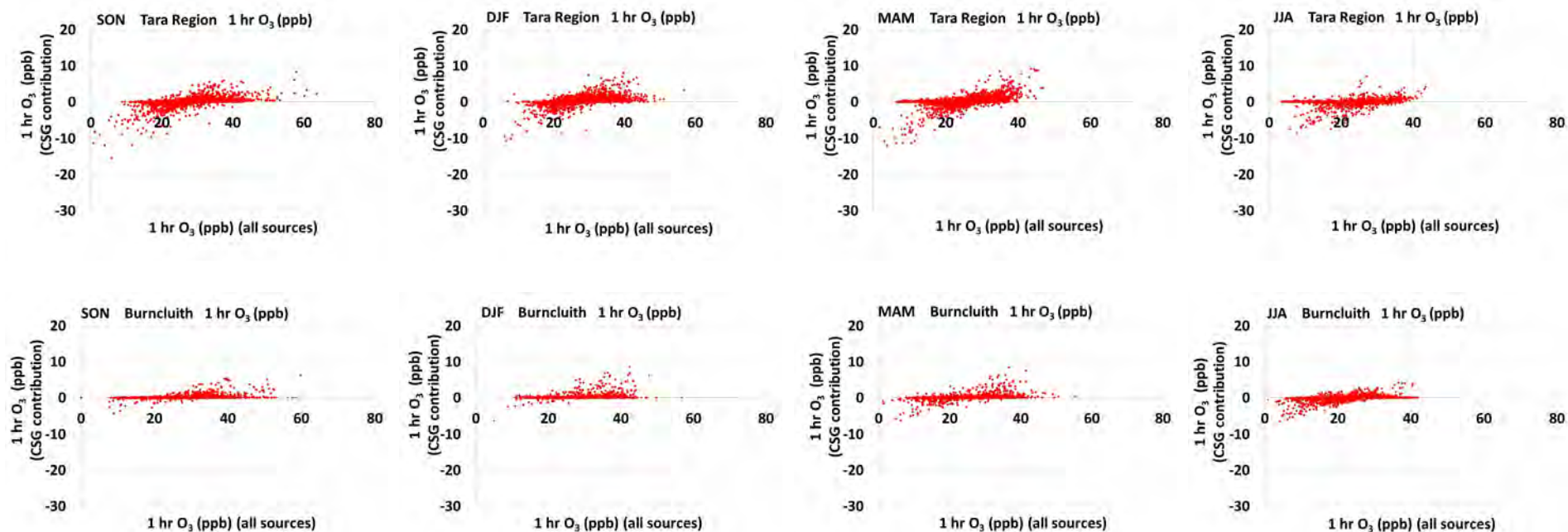


Figure E.6 The modelled contribution from the CSG-related emissions to the 1-hour average O₃ concentration (ppb) shown as a scatter plot for each season. The x-axis shows the modelled 1-hour average O₃ concentrations with all sources (ppb) and the y-axis shows the contribution from the CSG-related emissions to the 1-hour average O₃ concentration (ppb) - top row: Tara Region, bottom row: Burncluith.

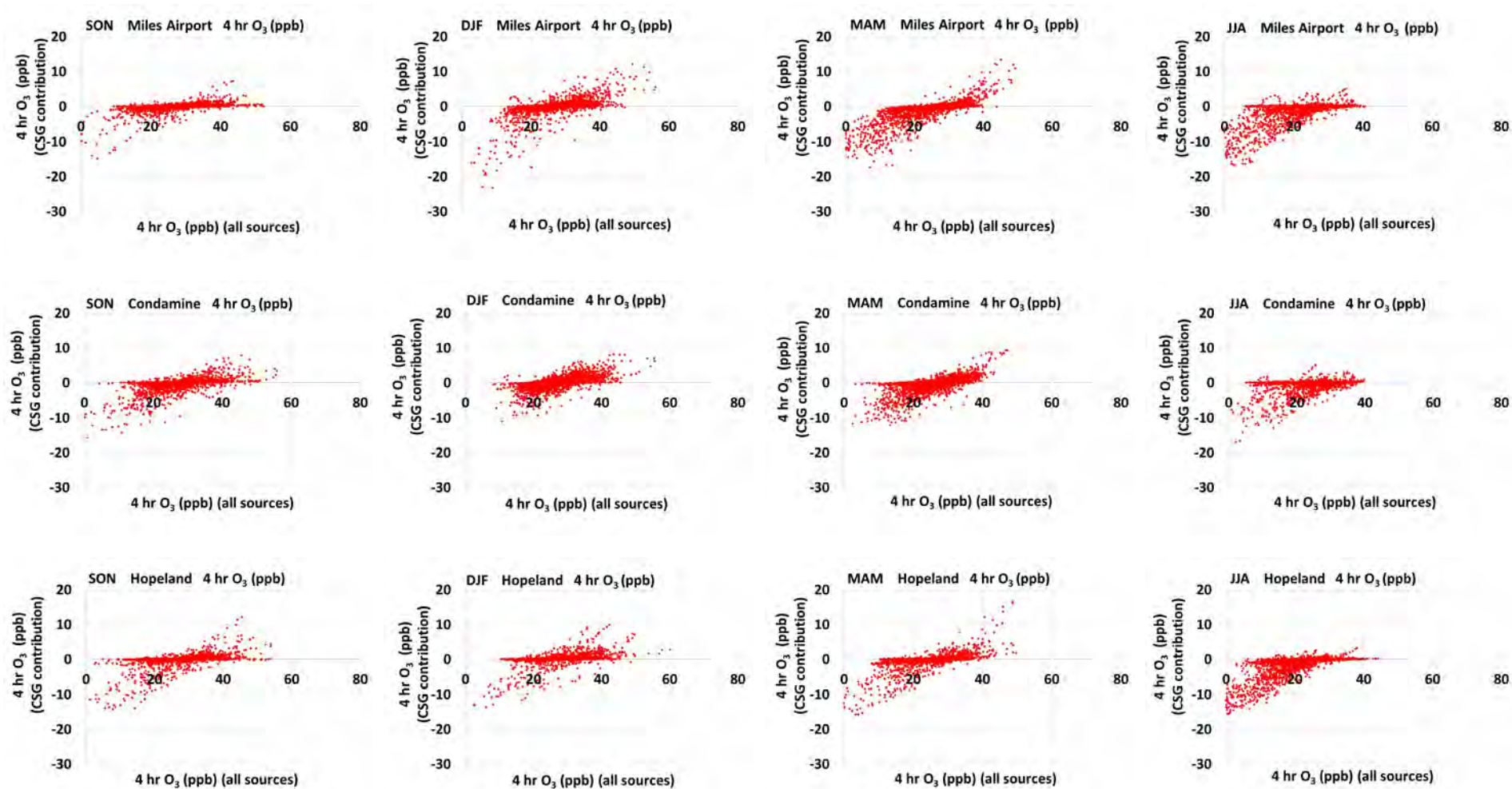


Figure E.7 The modelled contribution from the CSG-related emissions to the 4-hour average O₃ concentration (ppb) shown as a scatter plot for each season. The x-axis shows the modelled 4-hour average O₃ concentrations with all sources (ppb) and the y-axis shows the contribution from the CSG-related emissions to the 4-hour average O₃ concentration (ppb) - top row: Miles Airport, middle row: Condamine, bottom row: Hopeland.

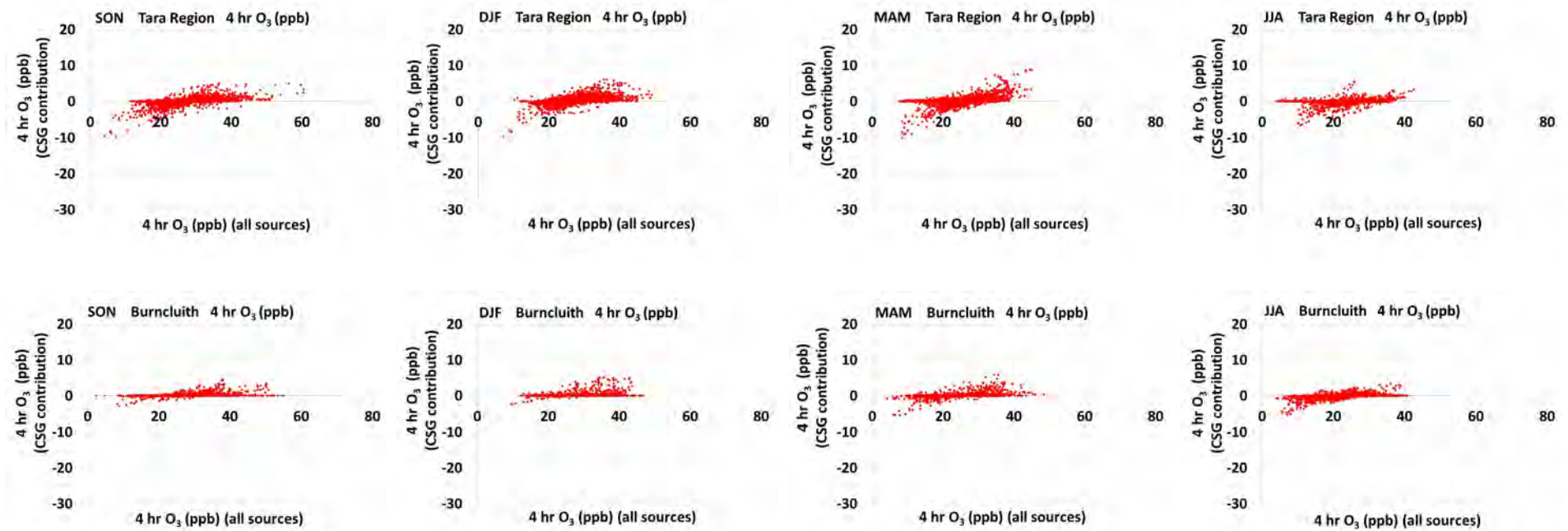


Figure E.8 The modelled contribution from the CSG-related emissions to the 4-hour average O₃ concentration (ppb) shown as a scatter plot for each season. The x-axis shows the modelled 4-hour average O₃ concentrations with all sources (ppb) and the y-axis shows the contribution from the CSG-related emissions to the 4-hour average O₃ concentration (ppb) - top row: Tara Region, bottom row: Burncluith.

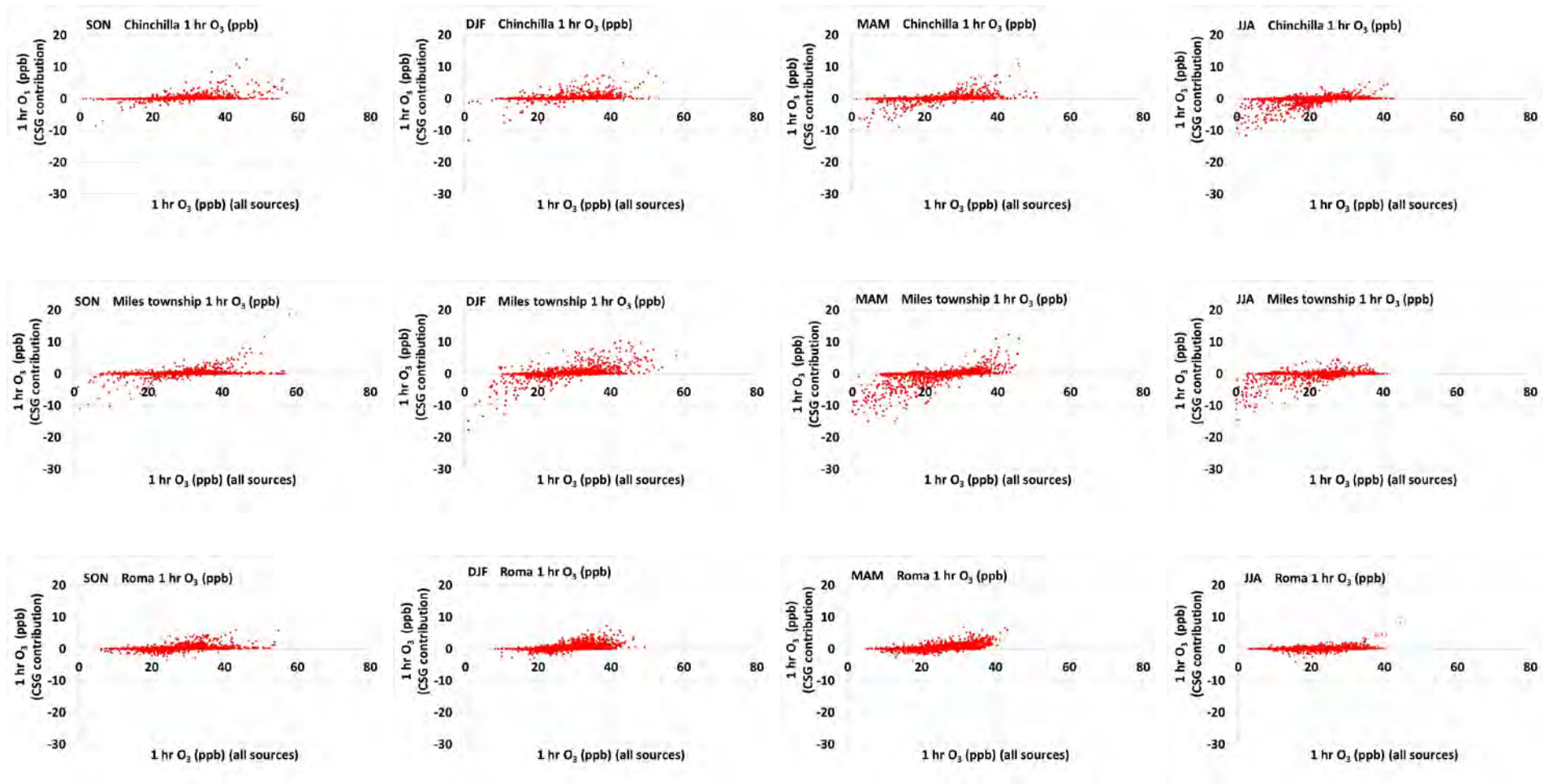


Figure E.9 The modelled contribution from the CSG-related emissions to the 1-hour average O₃ concentration (ppb) shown as a scatter plot for each season. The x-axis shows the modelled 1-hour average O₃ concentrations with all sources (ppb) and the y-axis shows the contribution from the CSG-related emissions to the 1-hour average O₃ concentration (ppb) - top row: Chinchilla, middle row: Miles township, bottom row: Roma.

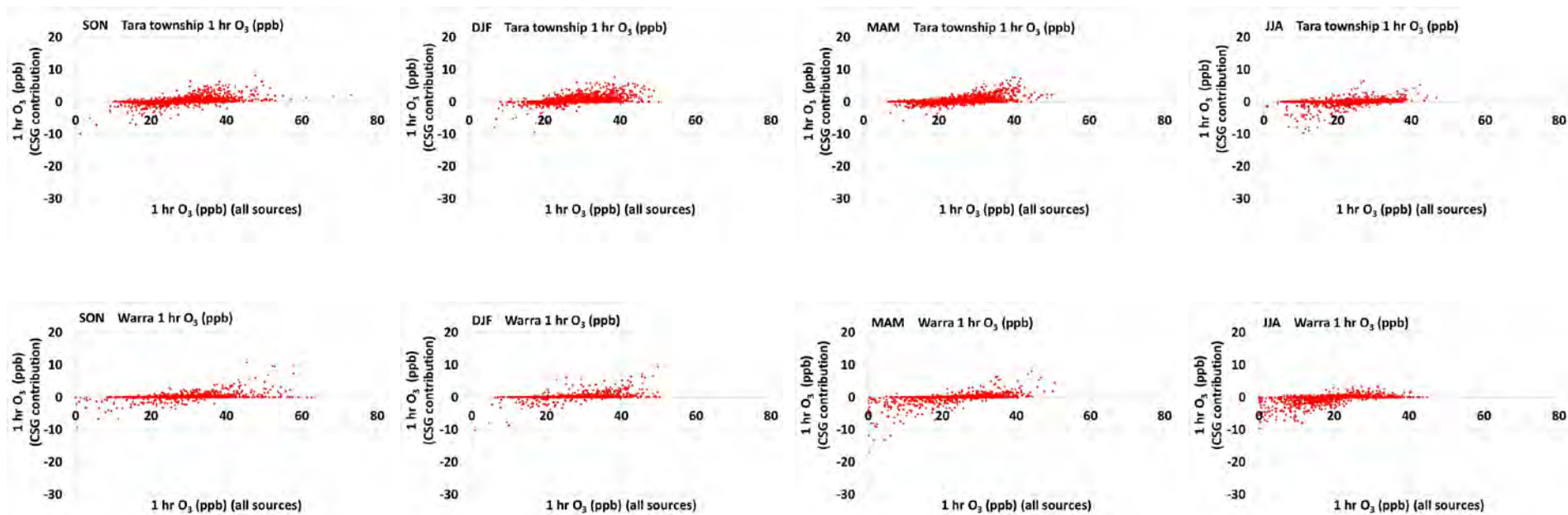


Figure E.10 The modelled contribution from the CSG-related emissions to the 1-hour average O₃ concentration (ppb) shown as a scatter plot for each season. The x-axis shows the modelled 1-hour average O₃ concentrations with all sources (ppb) and the y-axis shows the contribution from the CSG-related emissions to the 1-hour average O₃ concentration (ppb) - top row: Tara township, bottom row: Warra.

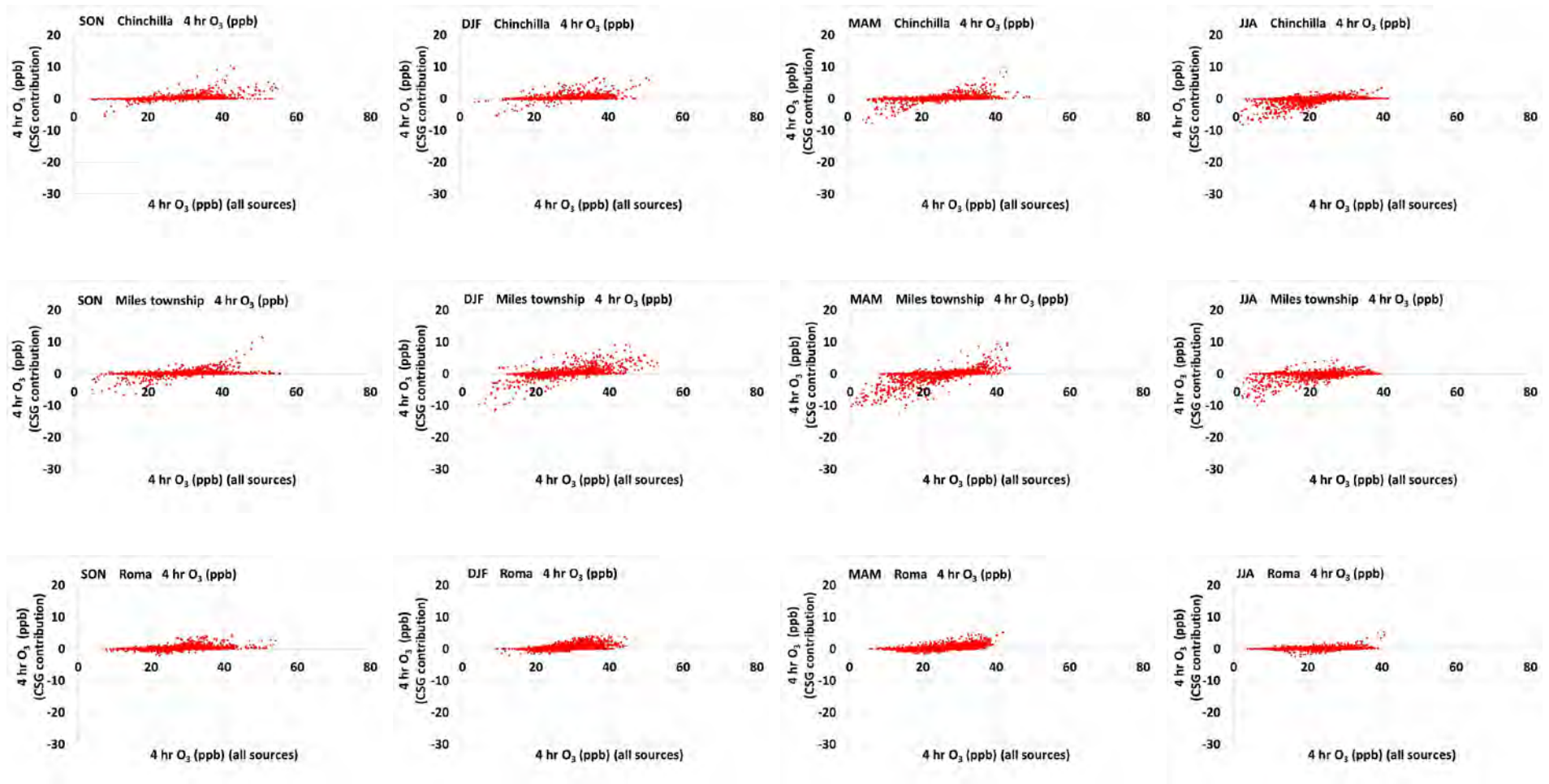


Figure E.11 The modelled contribution from the CSG-related emissions to the 4-hour average O₃ concentration (ppb) shown as a scatter plot for each season. The x-axis shows the modelled 4-hour average O₃ concentrations with all sources (ppb) and the y-axis shows the contribution from the CSG-related emissions to the 4-hour average O₃ concentration (ppb) - top row: Chinchilla, middle row: Miles township, bottom row: Roma.

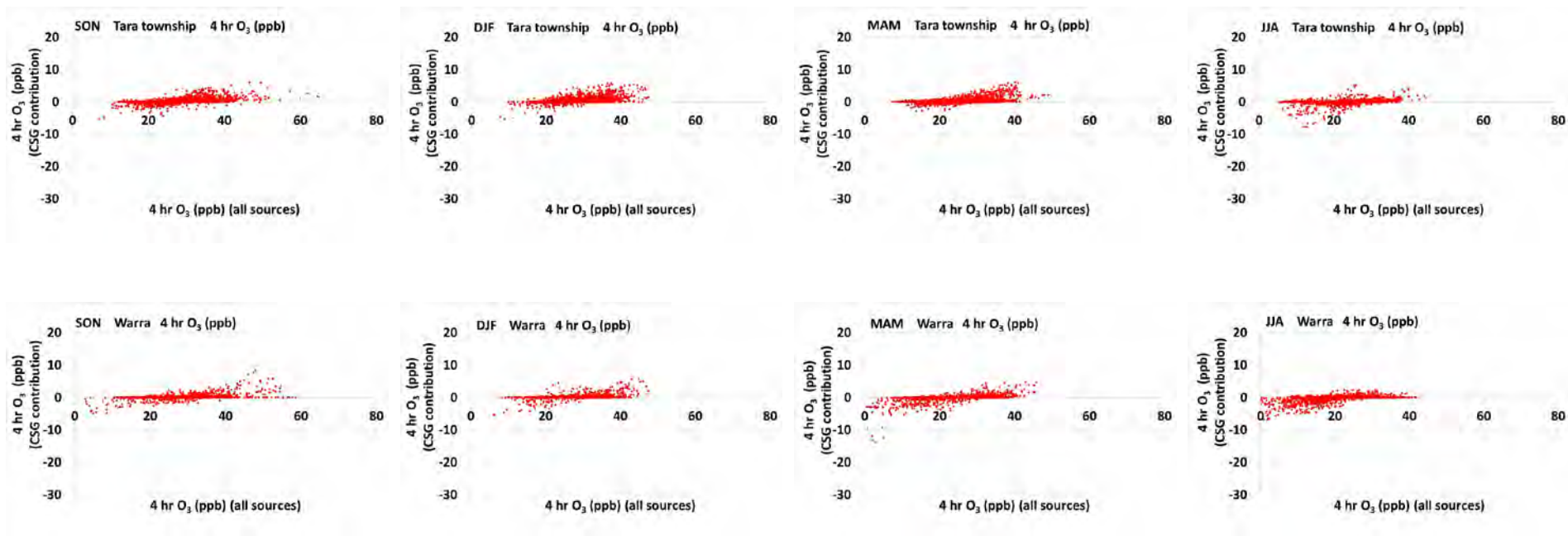


Figure E.12 The modelled contribution from the CSG-related emissions to the 4-hour average O₃ concentration (ppb) shown as a scatter plot for each season. The x-axis shows the modelled 4-hour average O₃ concentrations with all sources (ppb) and the y-axis shows the contribution from the CSG-related emissions to the 4-hour average O₃ concentration (ppb) - top row: Tara township, bottom row: Warra.

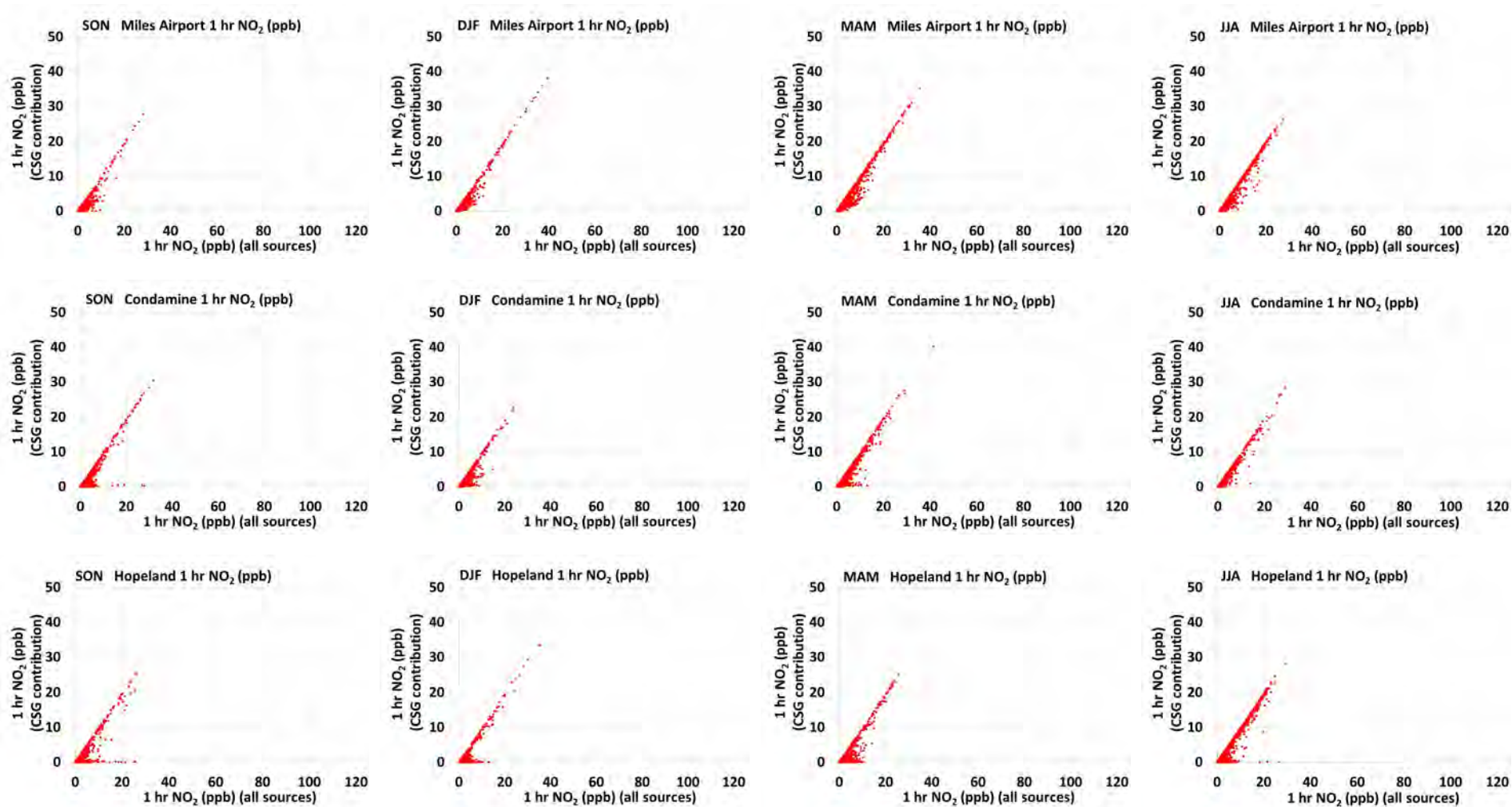


Figure E.13 The modelled contribution from the CSG-related emissions to the 1-hour average NO₂ concentration (ppb) shown as a scatter plot for each season. The x-axis shows the modelled 1-hour average NO₂ concentrations with all sources (ppb) and the y-axis shows the contribution from the CSG-related emissions to the 1-hour average NO₂ concentrations (ppb) - top row: Miles Airport, middle row: Condamine, bottom row: Hopeland.

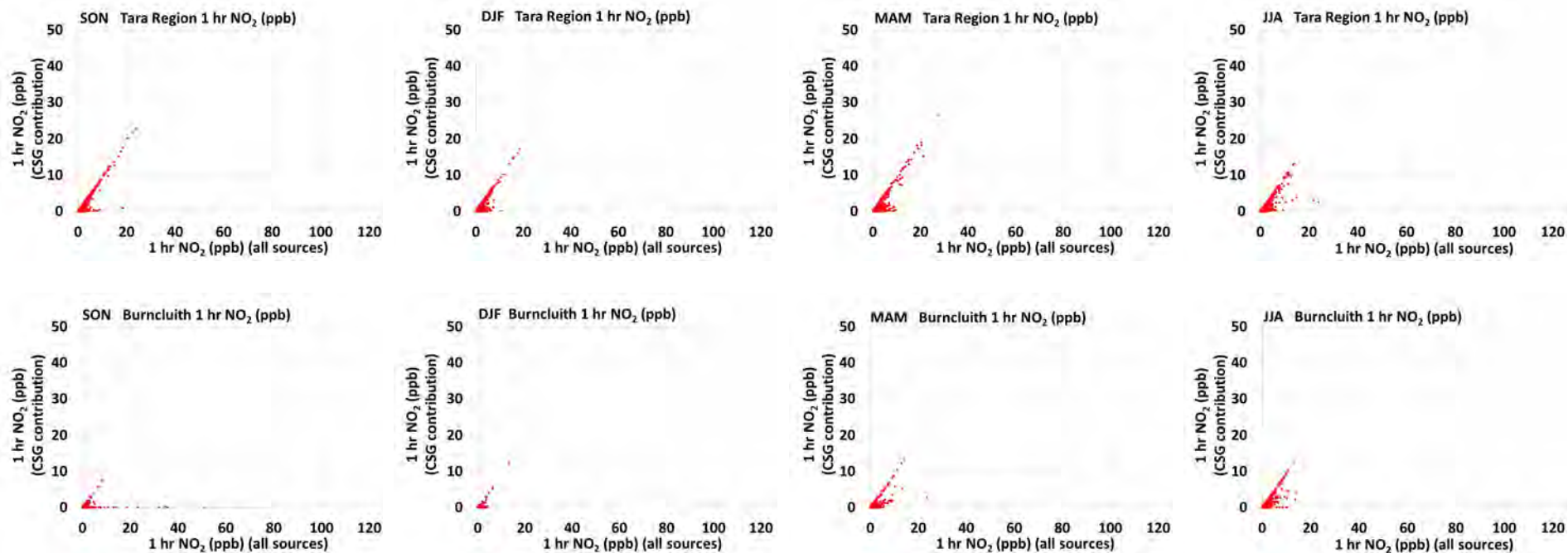


Figure E.14 The modelled contribution from the CSG-related emissions to the 1-hour average NO₂ concentration (ppb) shown as a scatter plot for each season. The x-axis shows the modelled 1-hour average NO₂ concentrations with all sources (ppb) and the y-axis shows the contribution from the CSG-related emissions to the 1-hour average NO₂ concentrations (ppb) - top row: Tara Region, bottom row: Burncluith.

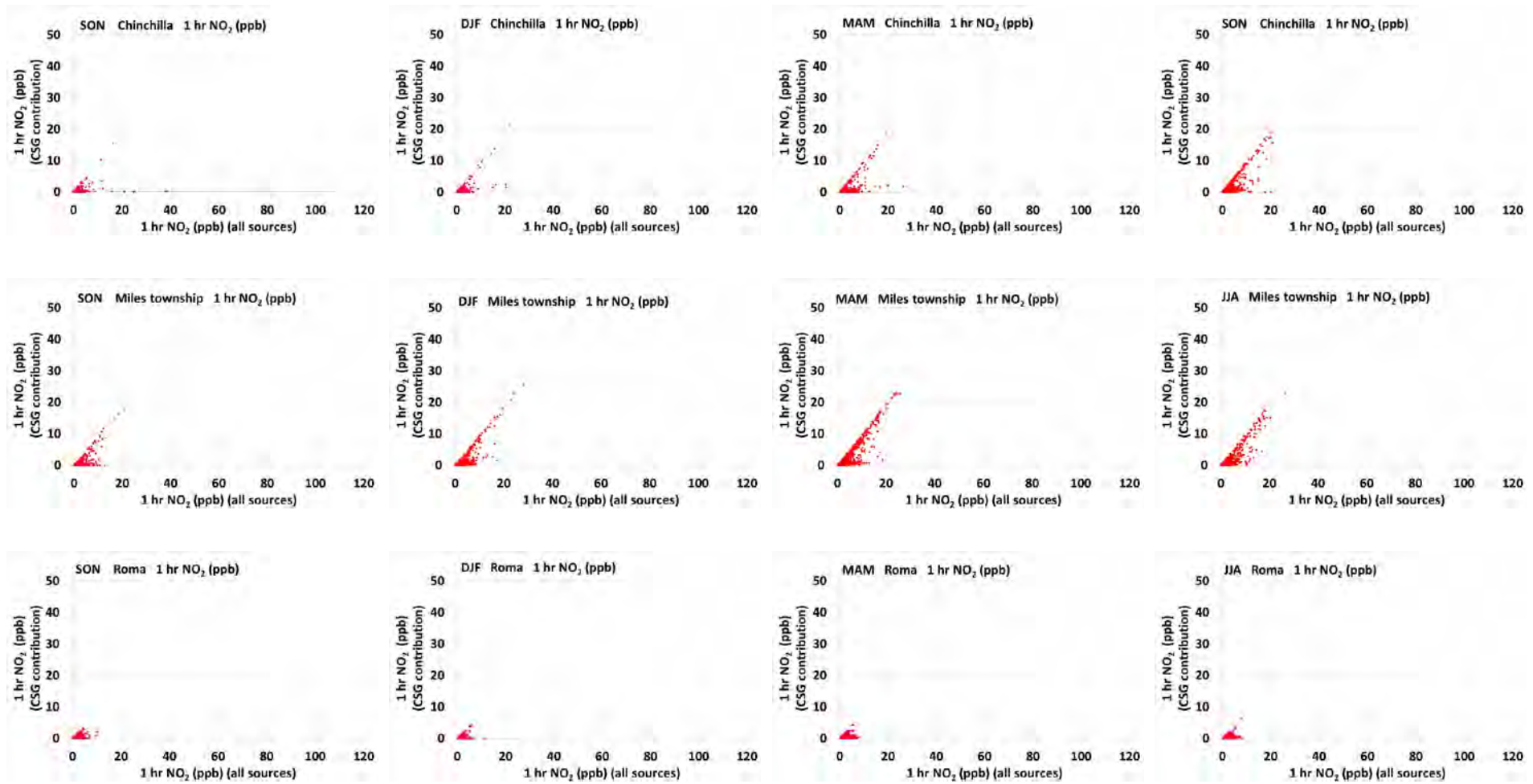


Figure E.15 The modelled contribution from the CSG-related emissions to the 1-hour average NO₂ concentration (ppb) shown as a scatter plot for each season. The x-axis shows the modelled 1-hour average NO₂ concentrations with all sources (ppb) and the y-axis shows the contribution from the CSG-related emissions to the 1-hour average NO₂ concentrations (ppb) - top row: Chinchilla, middle row: Miles township, bottom row: Roma.

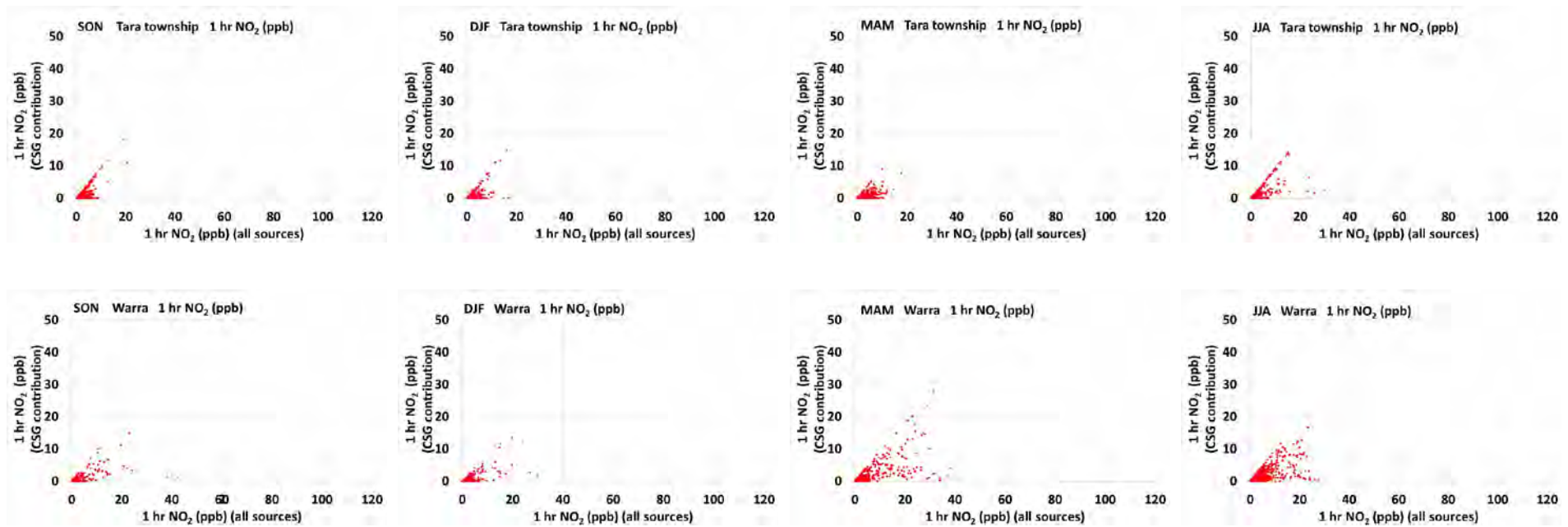


Figure E.16 The modelled contribution from the CSG-related emissions to the 1-hour average NO₂ concentration (ppb) shown as a scatter plot for each season. The x-axis shows the modelled 1-hour average NO₂ concentrations with all sources (ppb) and the y-axis shows the contribution from the CSG-related emissions to the 1-hour average NO₂ concentrations (ppb) - top row: Tara township, bottom row: Warra.

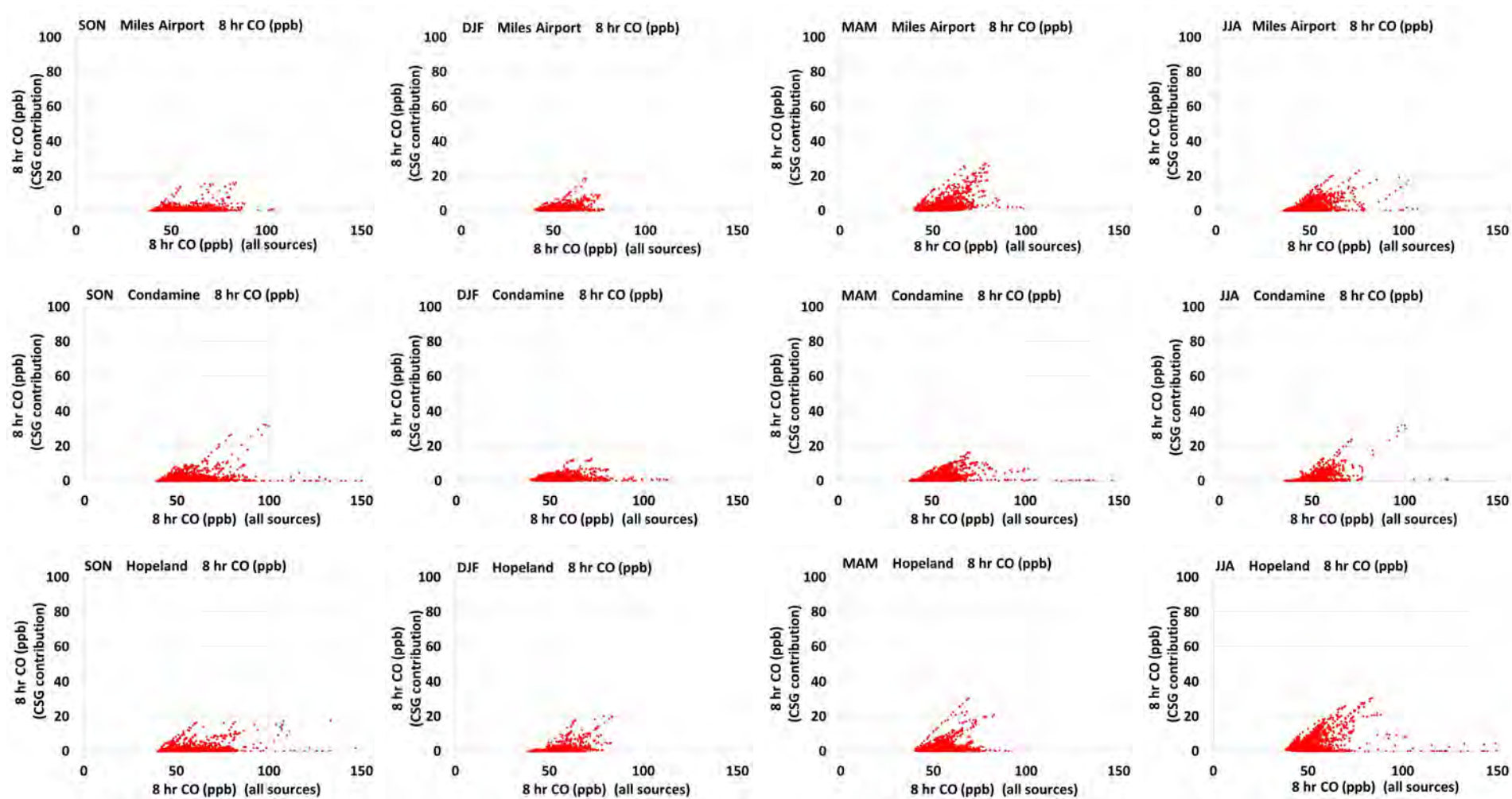


Figure E.177 The modelled contribution from the CSG-related emissions to the 8-hour average CO concentration (ppb) shown as a scatter plot for each season. The x-axis shows the modelled 8-hour average CO concentrations with all sources (ppb) and the y-axis shows the contribution from the CSG-related emissions to the 8-hour average CO concentrations (ppb) - top row: Miles Airport, middle row: Condamine, bottom row: Hopeland.

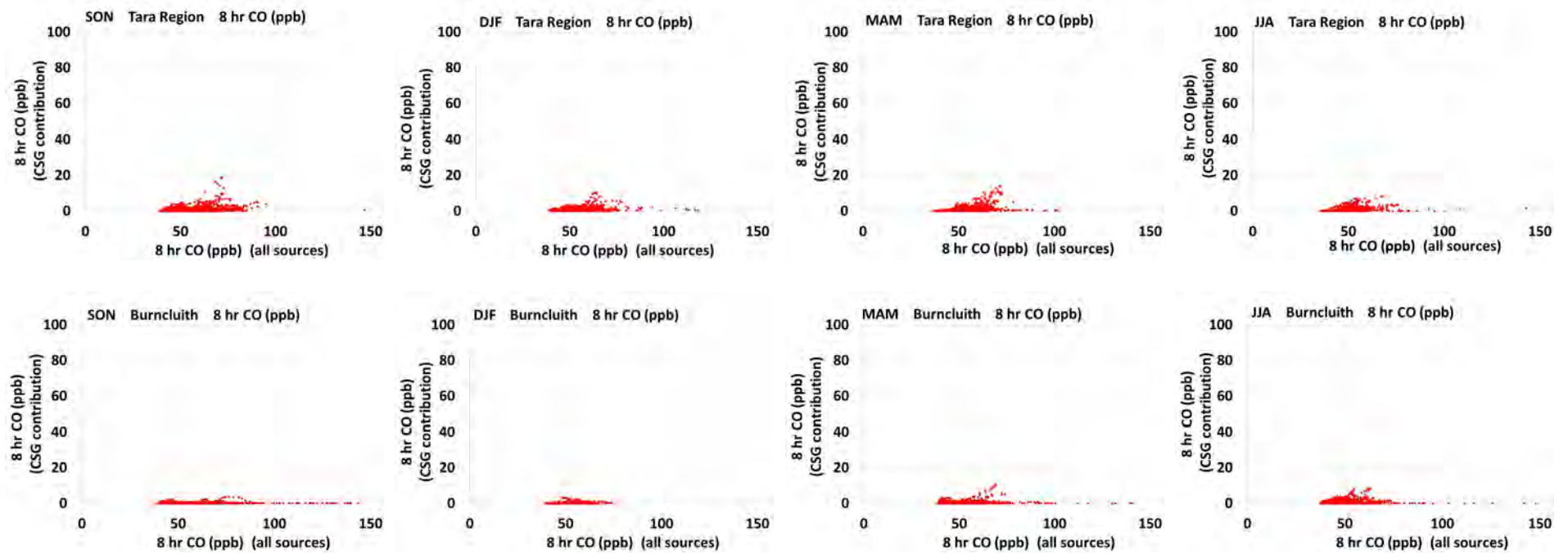


Figure E.188 The modelled contribution from the CSG-related emissions to the 8-hour average CO concentration (ppb) shown as a scatter plot for each season. The x-axis shows the modelled 8-hour average CO concentrations with all sources (ppb) and the y-axis shows the contribution from the CSG-related emissions to the 8-hour average CO concentrations (ppb) - top row: Tara Region, bottom row: Burncluth.

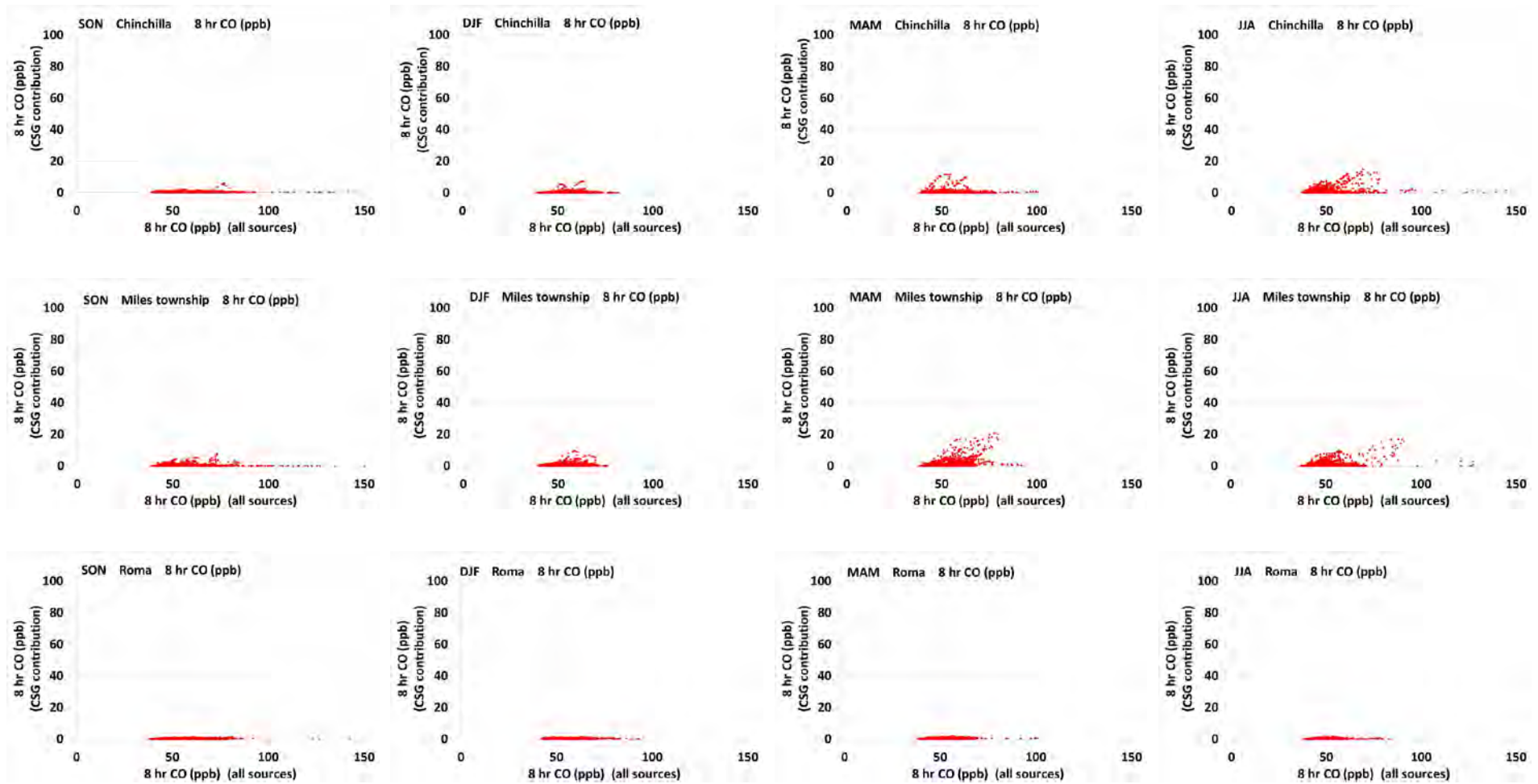


Figure E.19 The modelled contribution from the CSG-related emissions to the 8-hour average CO concentration (ppb) shown as a scatter plot for each season. The x-axis shows the modelled 8-hour average CO concentrations with all sources (ppb) and the y-axis shows the contribution from the CSG-related emissions to the 8-hour average CO concentrations (ppb) - top row: Chinchilla, middle row: Miles township, bottom row: Roma.

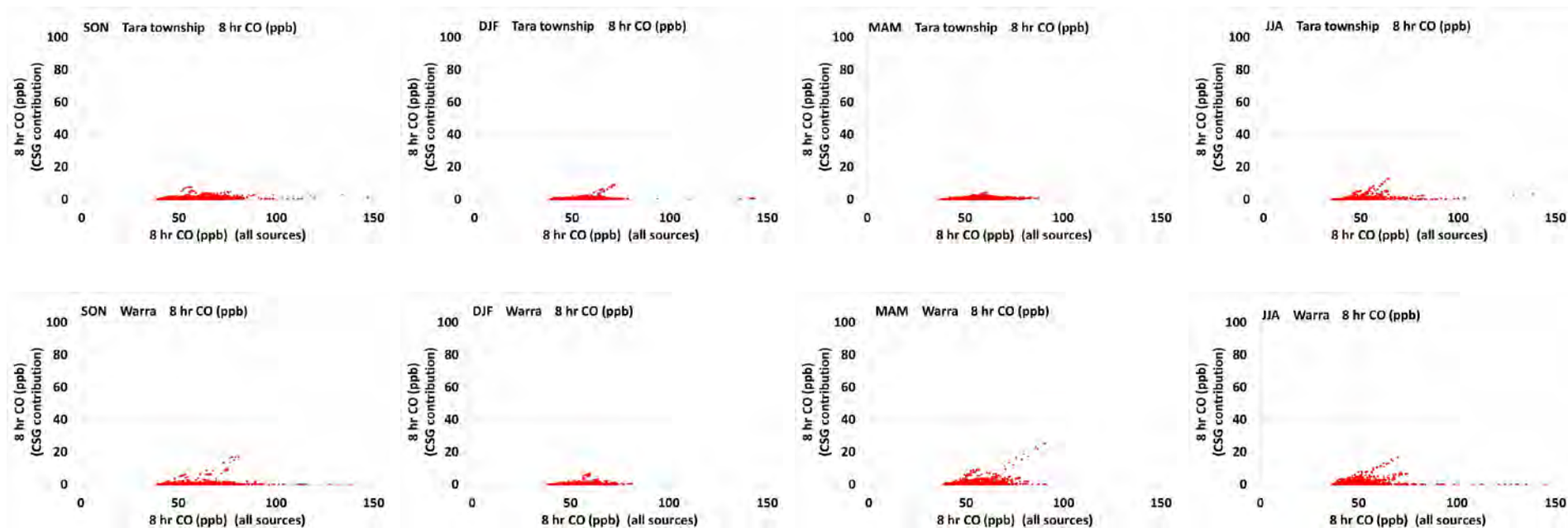


Figure E.20 The modelled contribution from the CSG-related emissions to the 8-hour average CO concentration (ppb) shown as a scatter plot for each season. The x-axis shows the modelled 8-hour average CO concentrations with all sources (ppb) and the y-axis shows the contribution from the CSG-related emissions to the 8-hour average CO concentrations (ppb) - top row: Tara township, bottom row: Warra.

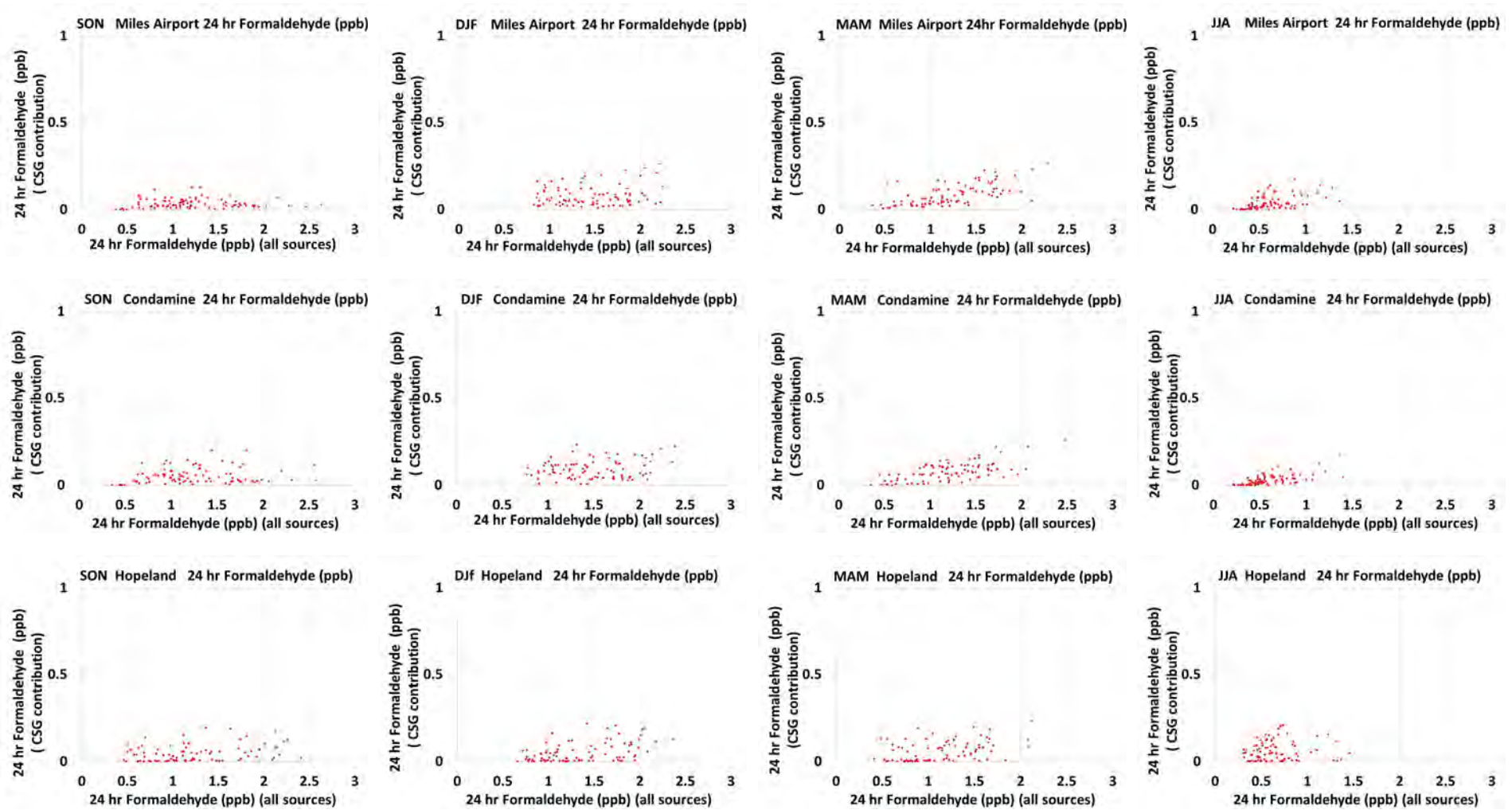


Figure E.21 The modelled contribution from the CSG-related emissions to the 24-hour average formaldehyde concentration (ppb) shown as a scatter plot for each season. The x-axis shows the modelled 24-hour average formaldehyde concentrations with all sources (ppb) and the y-axis shows the contribution from the CSG-related emissions to the 24-hour average formaldehyde concentration (ppb) - top row: Miles Airport, middle row: Condamine, bottom row: Hopeland.

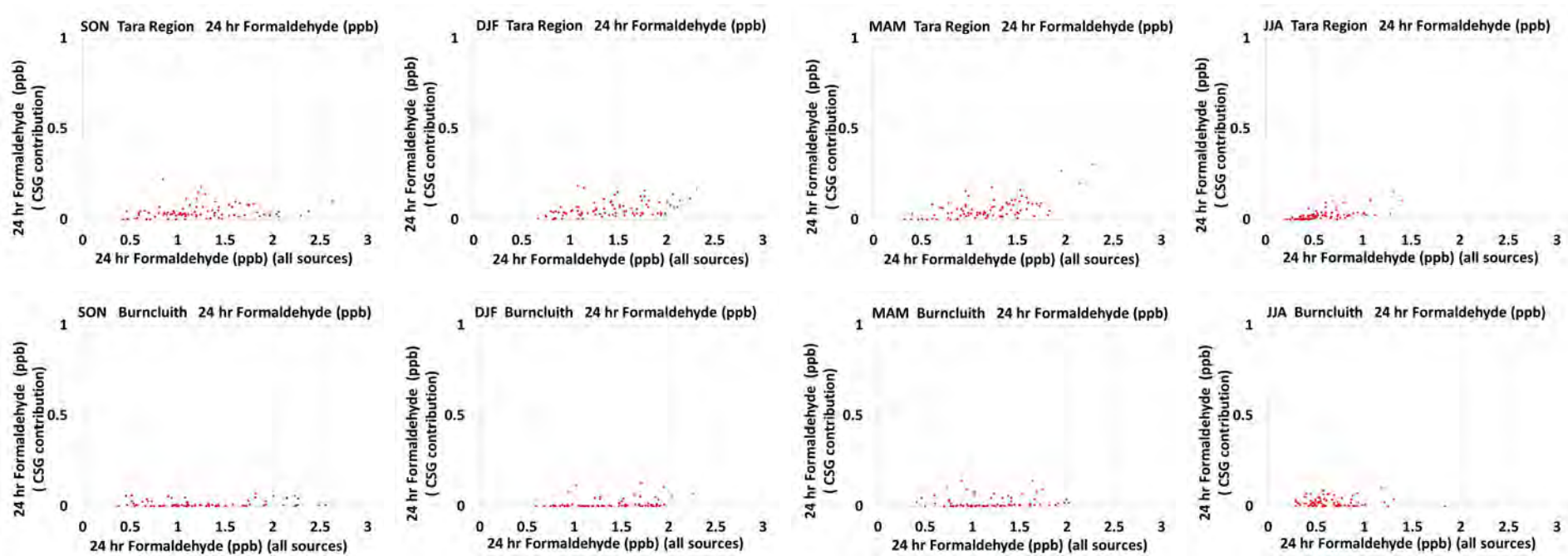


Figure E.22 The modelled contribution from the CSG-related emissions to the 24-hour average formaldehyde concentration (ppb) shown as a scatter plot for each season. The x-axis shows the modelled 24-hour average formaldehyde concentrations with all sources (ppb) and the y-axis shows the contribution from the CSG-related emissions to the 24-hour average formaldehyde concentration (ppb) - top row: Tara Region, bottom row: Burncluith.

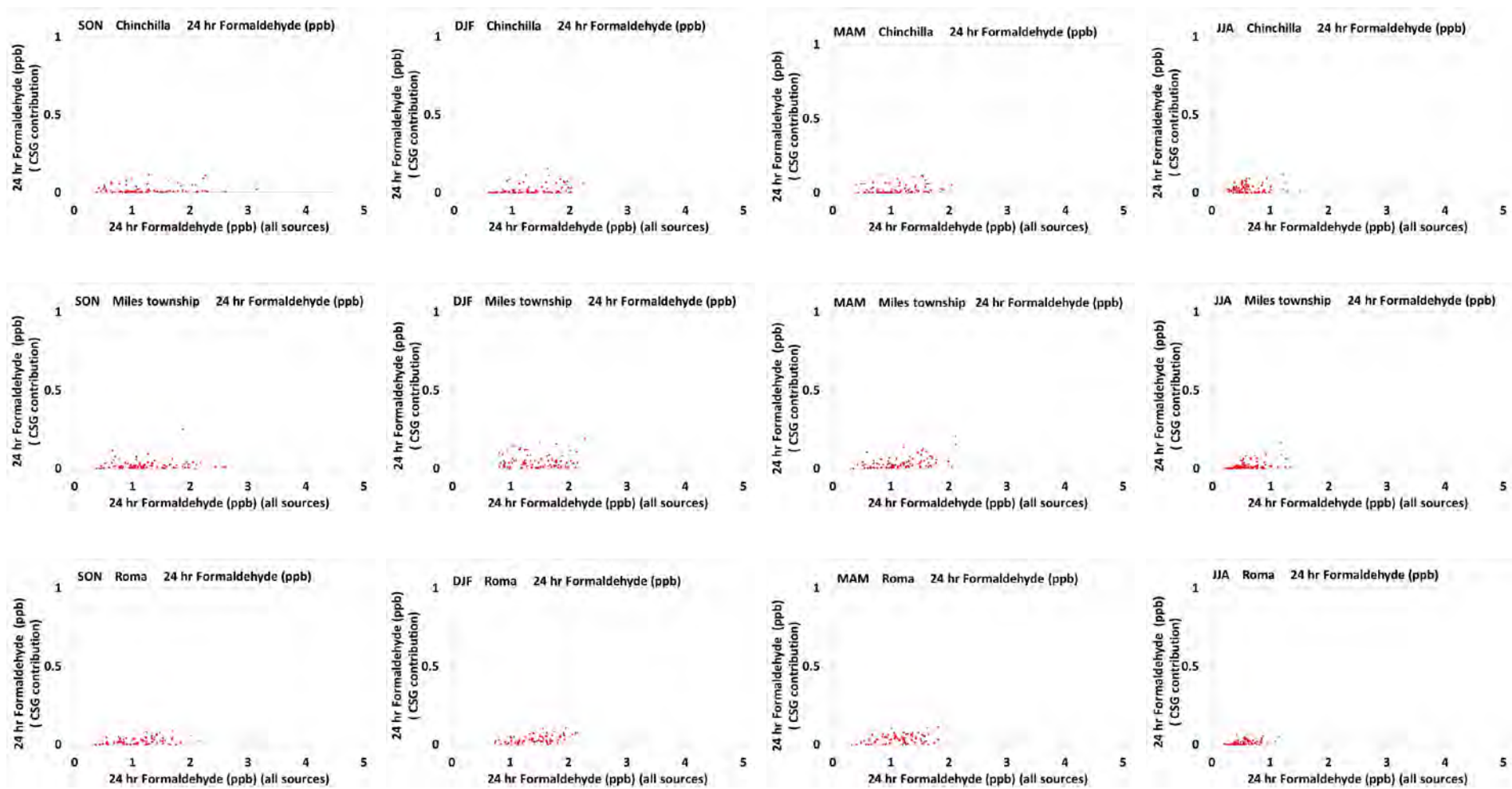


Figure E.23 The modelled contribution from the CSG-related emissions to the 24-hour average formaldehyde concentration (ppb) shown as a scatter plot for each season. The x-axis shows the modelled 24-hour average formaldehyde concentrations with all sources (ppb) and the y-axis shows the contribution from the CSG-related emissions to the 24-hour average formaldehyde concentration (ppb) - top row: Chinchilla, middle row: Miles township, bottom row: Roma

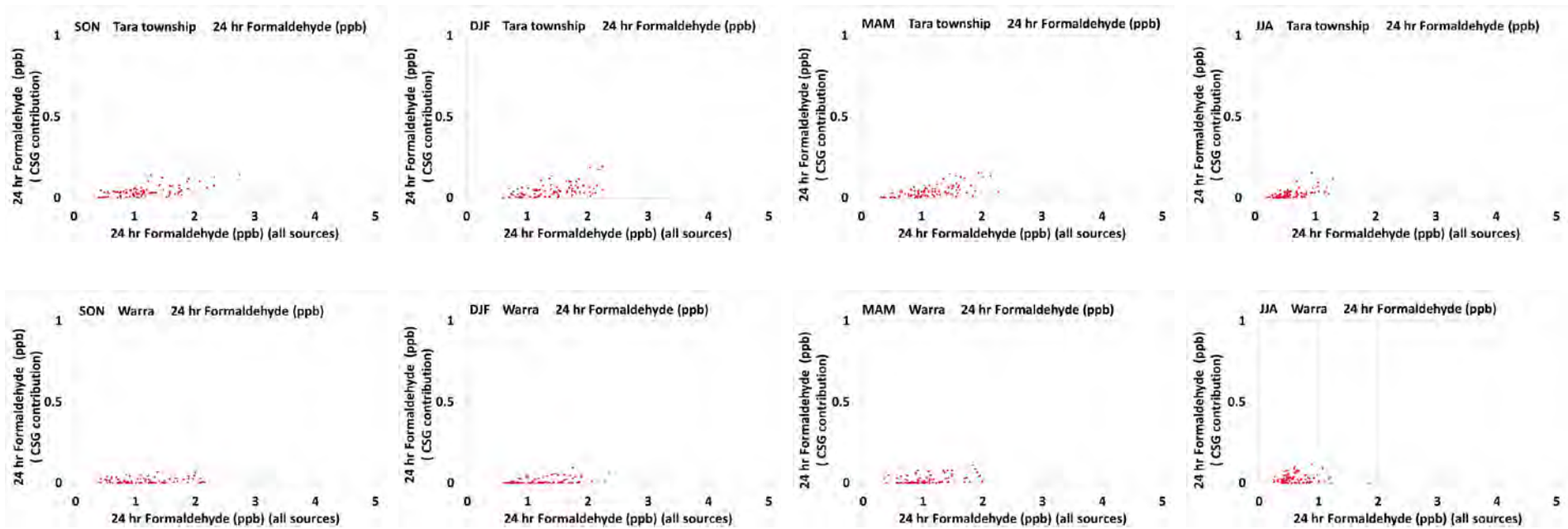


Figure E.24 The modelled contribution from the CSG-related emissions to the 24-hour average formaldehyde concentration (ppb) shown as a scatter plot for each season. The x-axis shows the modelled 24-hour average formaldehyde concentrations with all sources (ppb) and the y-axis shows the contribution from the CSG-related emissions to the 24-hour average formaldehyde concentration (ppb) - top row: Tara township, bottom row: Warra.

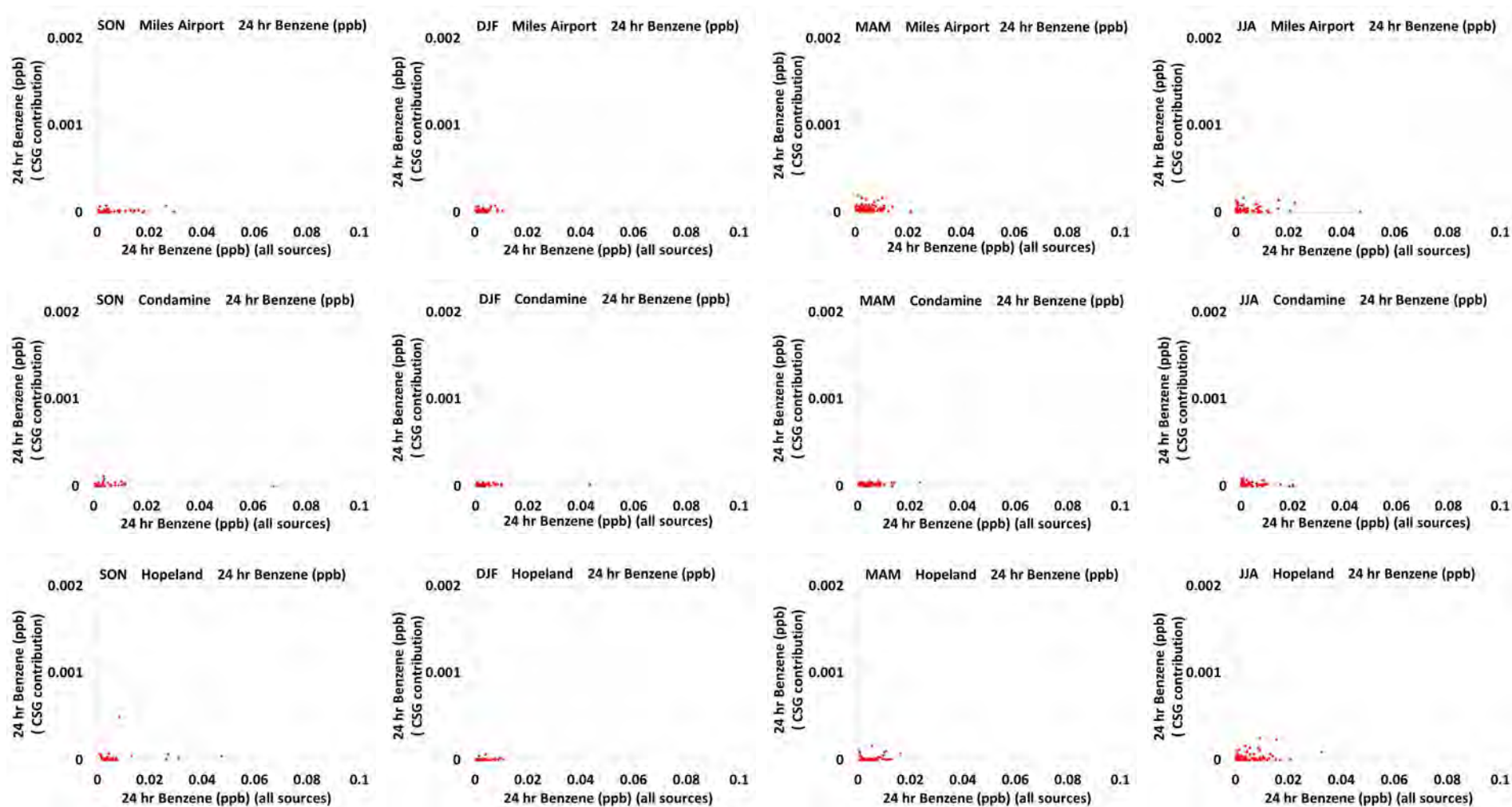


Figure E.195 The modelled contribution from the CSG-related emissions to the 24-hour average benzene concentration (ppb) shown as a scatter plot for each season. The x-axis shows the modelled 24-hour average benzene concentrations with all sources (ppb) and the y-axis shows the contribution from the CSG-related emissions to the 24-hour average benzene concentration (ppb) - top row: Miles Airport, middle row: Condamine, bottom row: Hopeland.

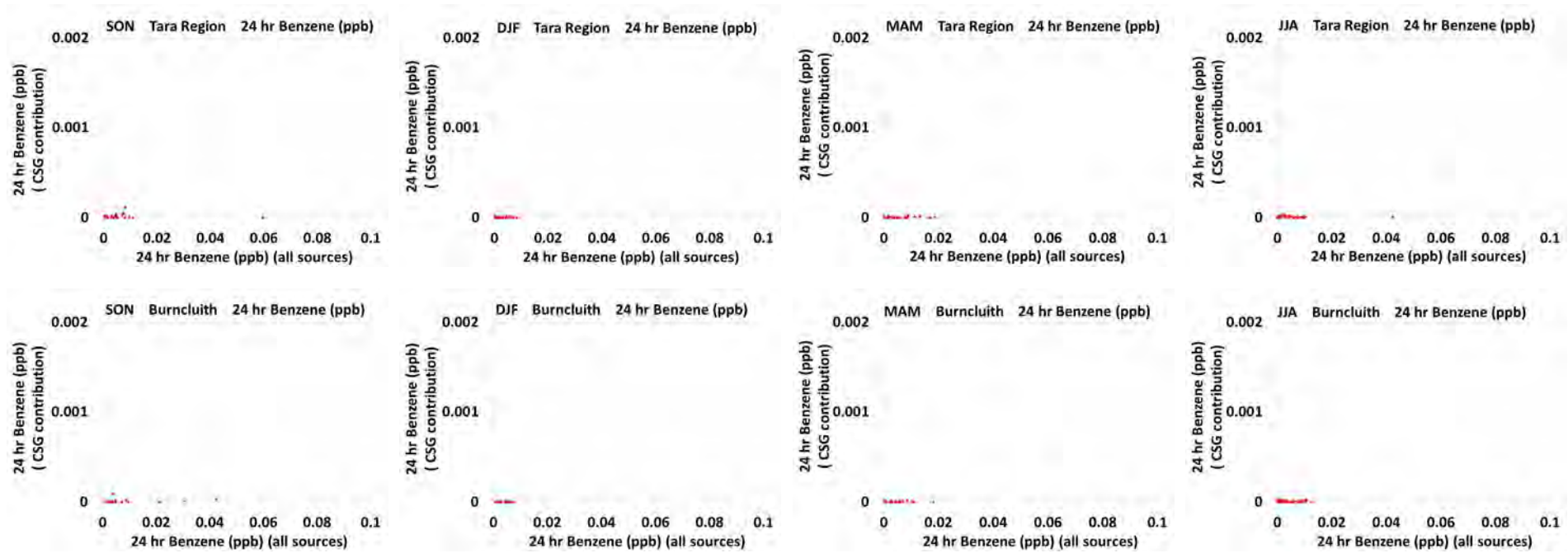


Figure E.206 The modelled contribution from the CSG-related emissions to the 24-hour average benzene concentration (ppb) shown as a scatter plot for each season. The x-axis shows the modelled 24-hour average benzene concentrations with all sources (ppb) and the y-axis shows the contribution from the CSG-related emissions to the 24-hour average benzene concentration (ppb) - top row: Tara Region, bottom row: Burncluith.

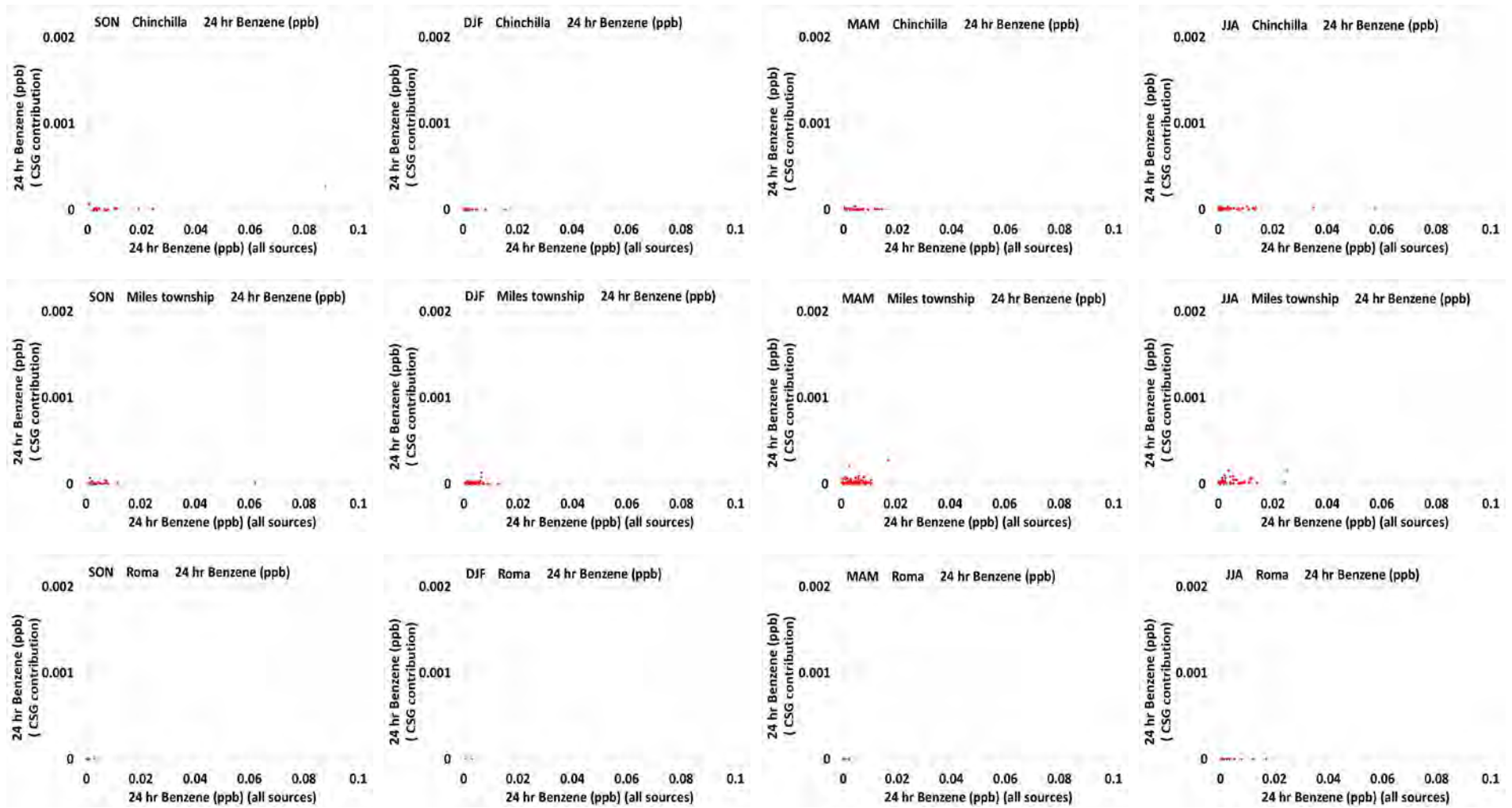


Figure E.27 The modelled contribution from the CSG-related emissions to the 24-hour average benzene concentration (ppb) shown as a scatter plot for each season. The x-axis shows the modelled 24-hour average benzene concentrations with all sources (ppb) and the y-axis shows the contribution from the CSG-related emissions to the 24-hour average benzene concentration (ppb) - top row: Chinchilla, middle row: Miles township, bottom row: Roma

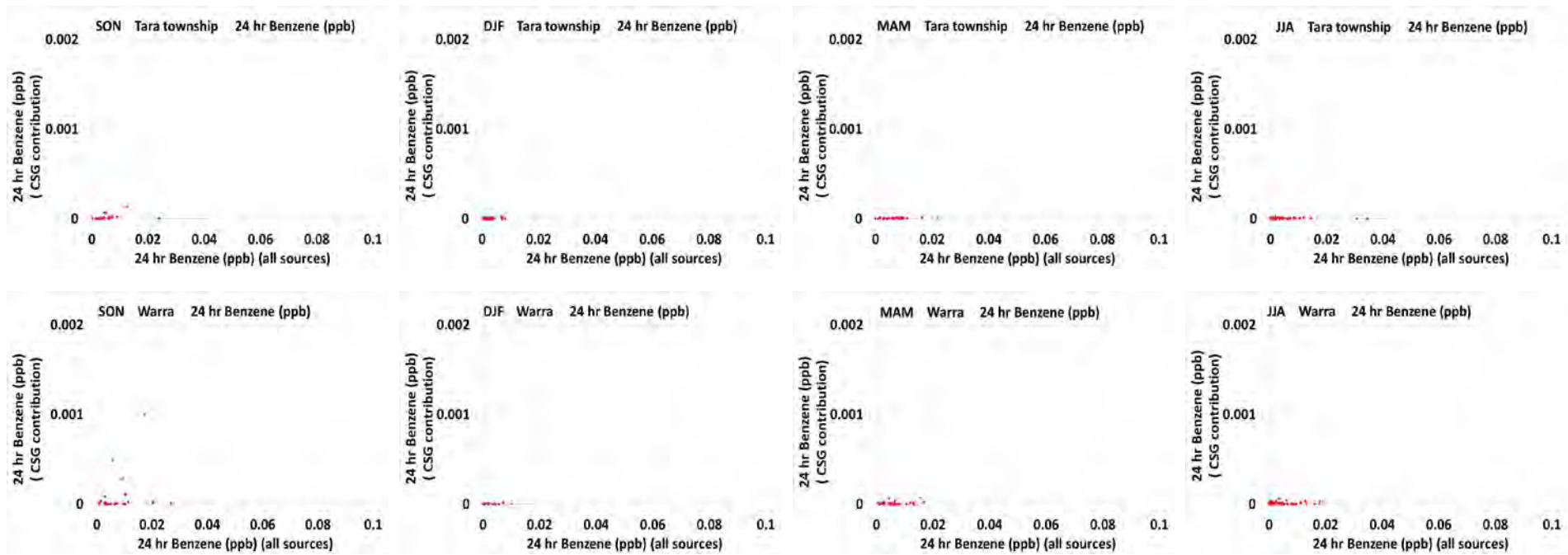


Figure E.28. The modelled contribution from the CSG-related emissions to the 24-hour average benzene concentration (ppb) shown as a scatter plot for each season. The x-axis shows the modelled 24-hour average benzene concentrations with all sources (ppb) and the y-axis shows the contribution from the CSG-related emissions to the 24-hour average benzene concentration (ppb) - top row: Tara township, bottom row: Warra.

Appendix F Extra plots: O₃ 1-hour averages

The modelled contribution from the CSG-related emissions to the 1-hour average O₃ concentrations at each of the observations sites is presented in Figure F.1. Each plot shows the percentage of model hours within each season for the modelled contribution from the CSG-related emissions to the 1-hour average O₃ concentrations. Note the change in O₃ can be negative or positive.

On average 95 % of the time the contribution from the CSG-related emissions at all sites is within ± 5 ppb which is 5 % of the 1-hour O₃ air quality objective (100 ppb, Table 5.1). The smallest frequency of change due to the CSG-related emissions is modelled at Burncluith, while the largest frequency of change due to the CSG-related emissions occurs at Condamine except during JJA.

During SON and DJF the effect of the CSG-related emissions is generally to increase O₃ while during MAM and JJA it is generally to decrease O₃.

Figure F.2 shows plots of the modelled 1-hour average O₃ concentrations with all sources against the contribution from the CSG-related emissions to the modelled 4-hour average O₃ concentrations at Miles Airport. The plots are seasonal and one point is plotted for each hourly modelled value.

At Miles Airport the largest modelled increases (> 5 ppb) in the 1-hour average O₃ concentrations due to the CSG-related emissions occur mostly for larger O₃ values (i.e. increased peak concentrations) during DJF and MAM, with these increases accounting for up to 32 % of the O₃ value. However the maximum increase due to the CSG-related emissions is 15 ppb which is 15 % of the 1-hour O₃ air quality objective (100 ppb, Table 5.1).

The largest decreases (< -10 ppb) are modelled to occur mostly for smaller values of the 1-hour average O₃ concentrations (i.e. deepening the minima) during all seasons but more frequently during MAM and JJA as shown also in Figure 5.18. These decreases account for up to 100 % of the 1-hour average O₃ value – e.g. emissions from the CSG-related sources reduced O₃ to zero probably through removal due to reaction with NO_x. The maximum decrease due to the CSG-related emissions is 30 ppb.

Similar patterns of higher maximums and deeper minima are modelled for Condamine and Hopeland. Hopeland had the largest increase in the 1-hour average O₃ concentrations due to the CSG-related emissions, 18.6 ppb, which equates to 18.6 % of the 1-hour O₃ air quality objective. Tara Region shows a smaller effect on maximum and minimum values of O₃ and the effect at Burncluith due to the CSG-related emissions is smaller again, reflecting the greater distance from the major CSG sources.

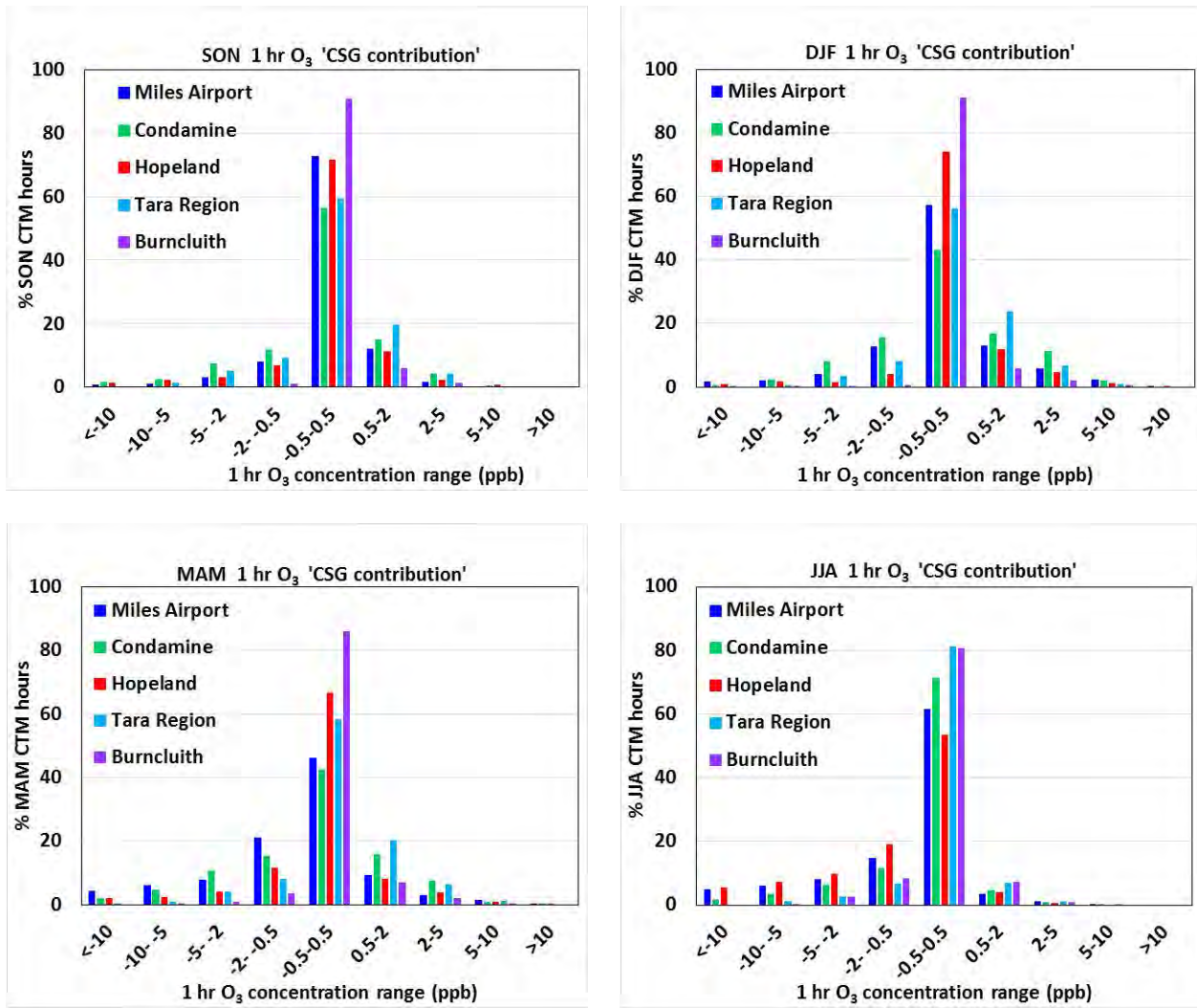


Figure F.1 The modelled contribution from the CSG related emissions to the 1-hour average O₃ concentration (ppb) at the Gas field and Regional sites shown as a frequency distribution for each season. The x-axis shows the concentration ranges of the contribution from the CSG-related emissions and the y-axis shows the percentage of model hours.

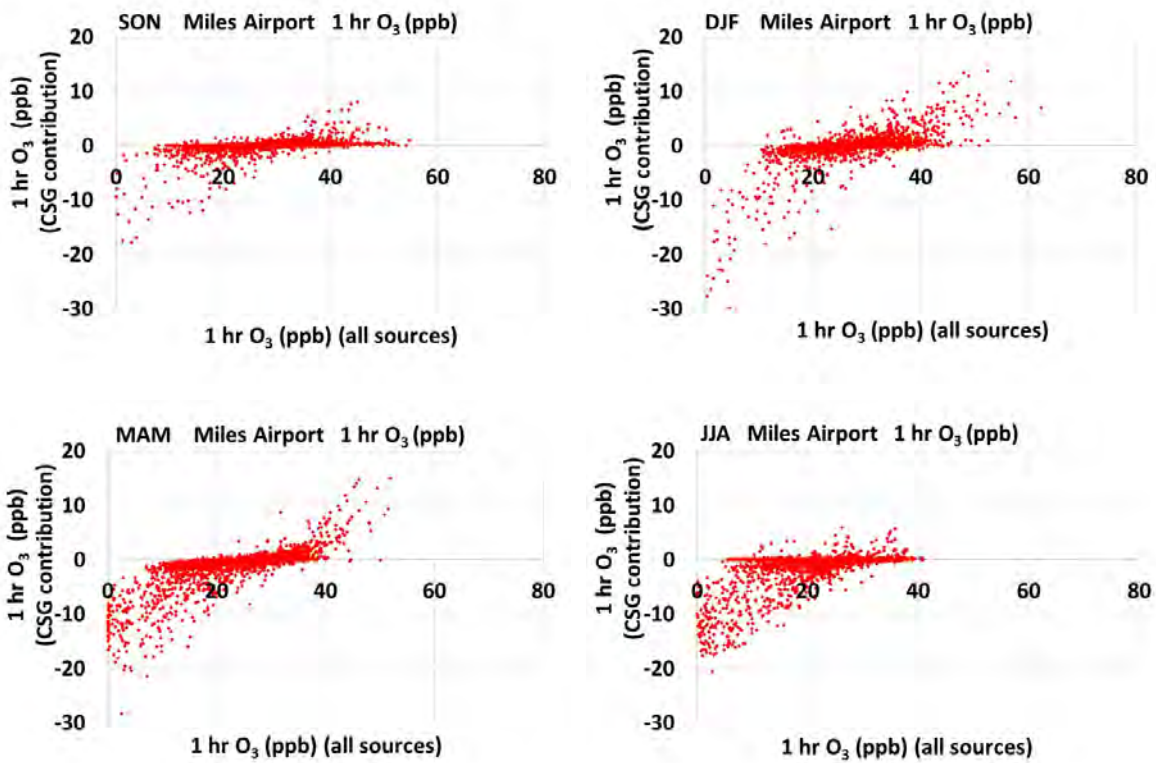


Figure F.2 The modelled contribution from the CSG-related emissions to the 1-hour average O₃ concentration (ppb) at Miles Airport shown as a scatter plot for each season. The x-axis shows the modelled 1-hour average O₃ concentrations with all sources (ppb) and the y-axis shows the contribution from the CSG-related emissions to the 1-hour average O₃ concentration (ppb).

Figure F.3 shows the maximum 1-hour average O₃ concentrations for each month of the model simulation, at the Gas field and Regional sites. The bar plots show the observed values in blue, the model results with all sources in red and the model results without the CSG sources in purple. The dashed horizontal red line shows the value of the air quality objective.

The 1-hour average O₃ air quality objective (100 ppb, Table 5.1) and 80 % of the 1-hour average O₃ air quality objective are not exceeded by the observed or modelled 1-hour average O₃ concentrations at any site in any month.

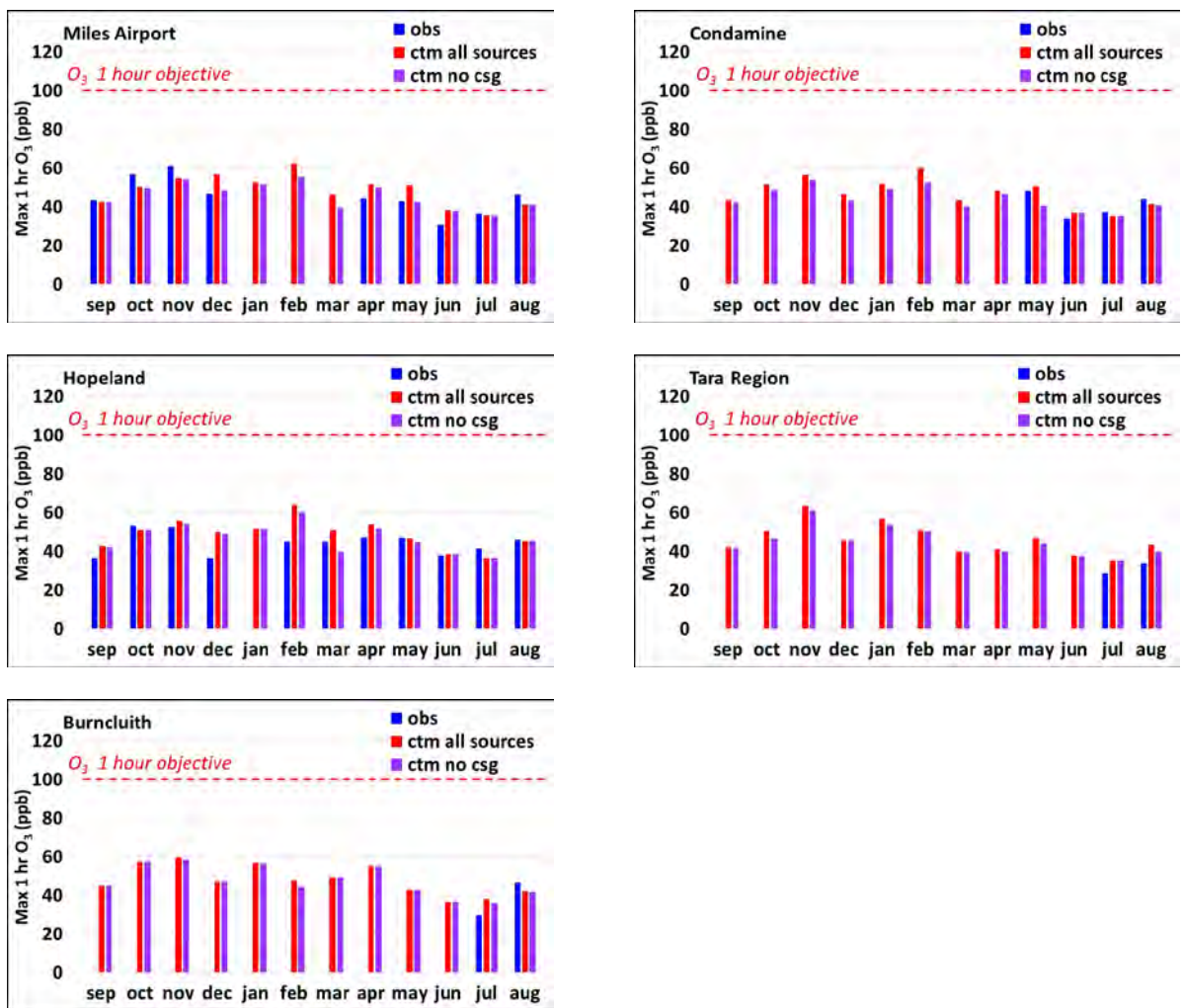


Figure F.3 The maximum 1-hour average O₃ concentrations (ppb) for each month of September 2015 – August 2016 at the Gas field and Regional sites: observed (blue), model results with all sources (red) and model results without the CSG sources (purple).

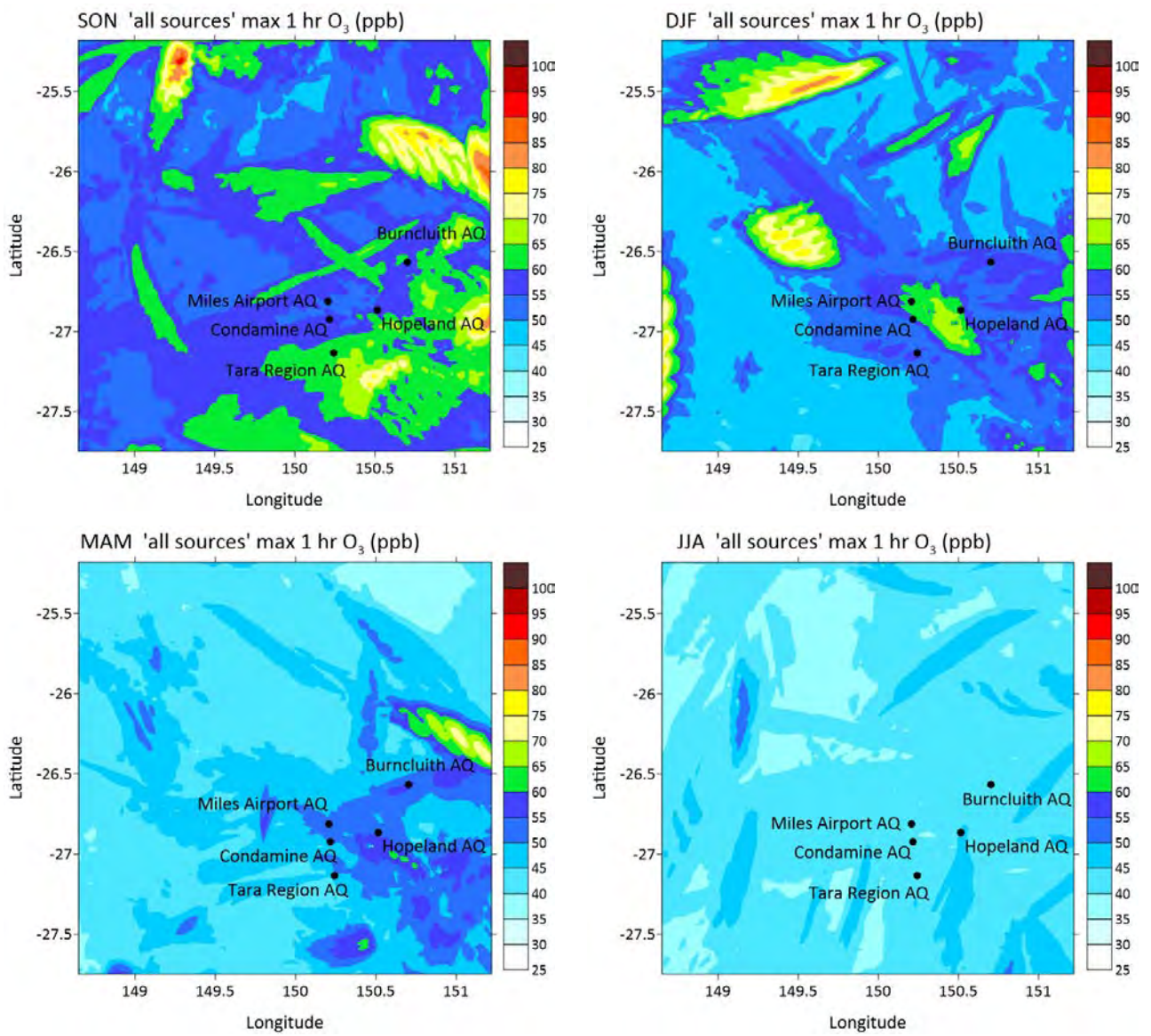


Figure F.4 The maximum concentration of the 1-hour average O₃ in each grid square for the model results with all sources during each season (ppb). Note that the maximum concentrations shown in each grid square may be from different time periods.

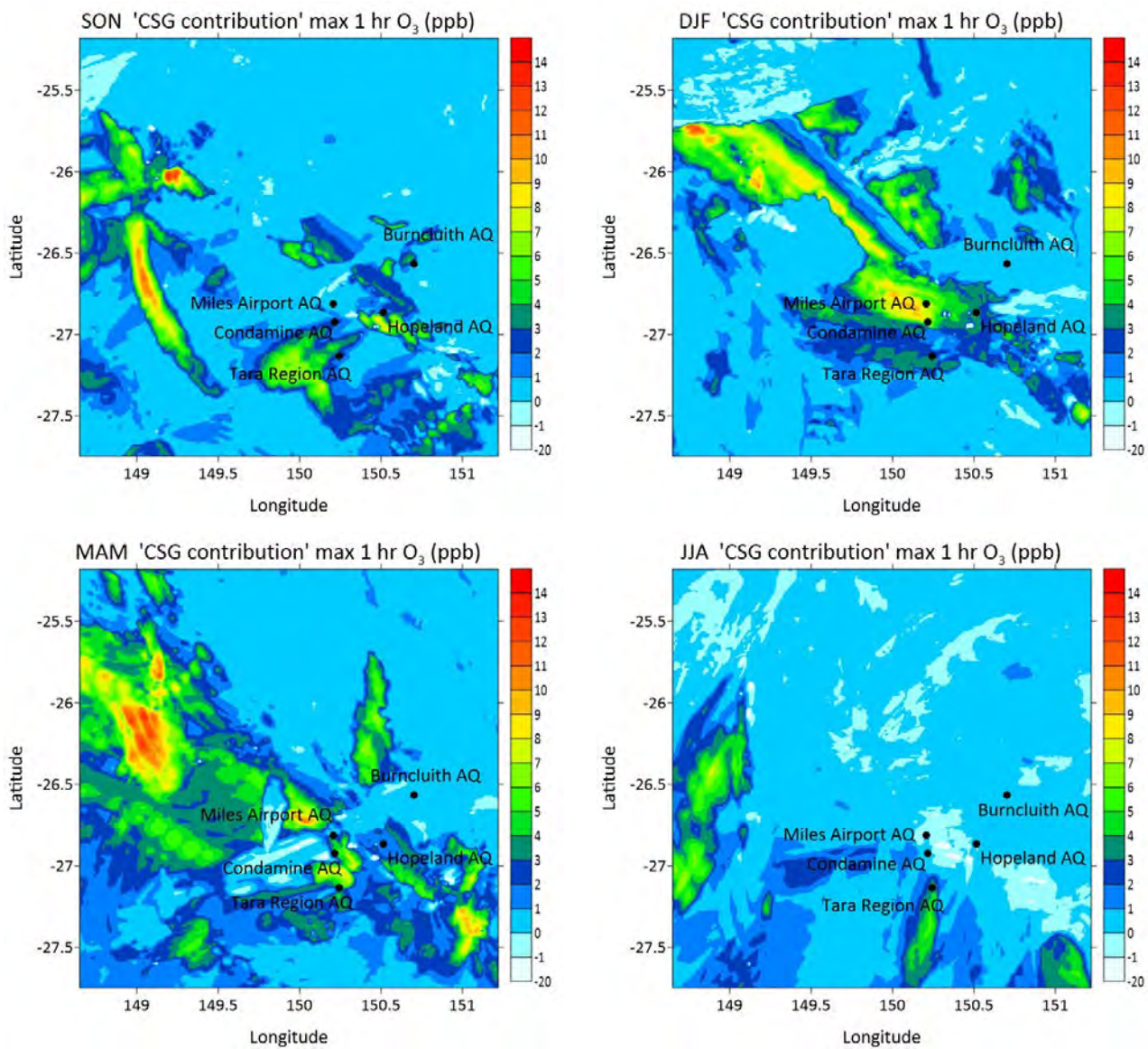


Figure F.5 The contribution of the CSG-related emissions to the modelled maximum 1-hour average O₃ concentration (maximum in each grid square from Figure 5.21F.4) during each season (ppb). Note that the concentrations shown in each grid square may be from different time periods.

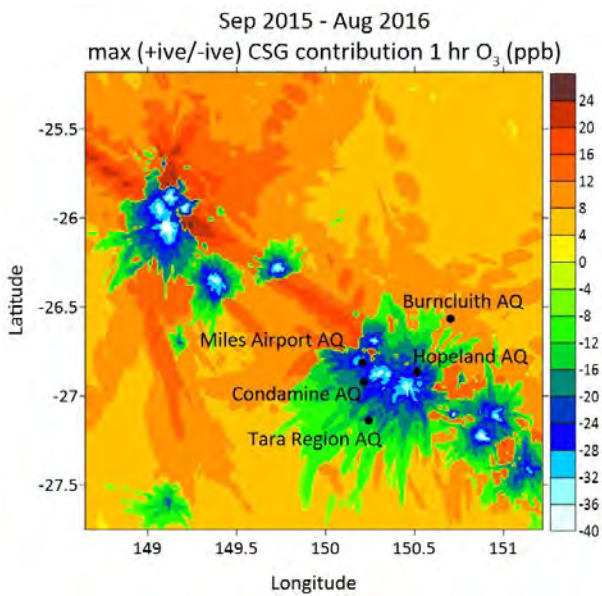
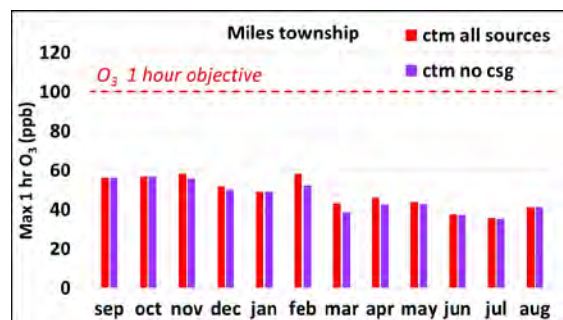
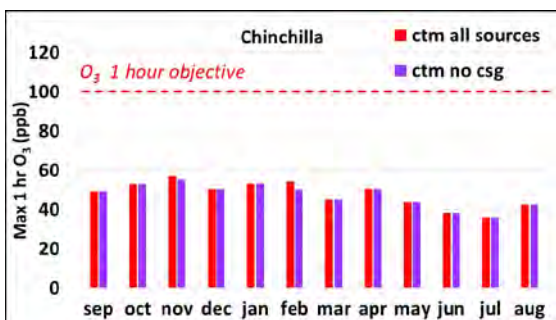


Figure F.6 The maximum contribution of the CSG-related emissions to the modelled 1-hour average O₃ concentrations during the modelled year (ppb). Note that the concentrations shown in each grid square may be from different time periods.

Figure F.7 shows the maximum values of the 1-hour average O₃ concentrations for each month of the model simulation at the Town sites. The bar plots show the model results with all sources in red and the model results without the CSG sources in purple. The dashed horizontal red line shows the value of the air quality objective.

The air quality objectives are not exceeded by the modelled 1-hour average O₃ concentrations at any of the Town sites. The difference between the O₃ maximum monthly values from the model results with all sources and the model results without CSG sources is less than 6 ppb at the Town sites.



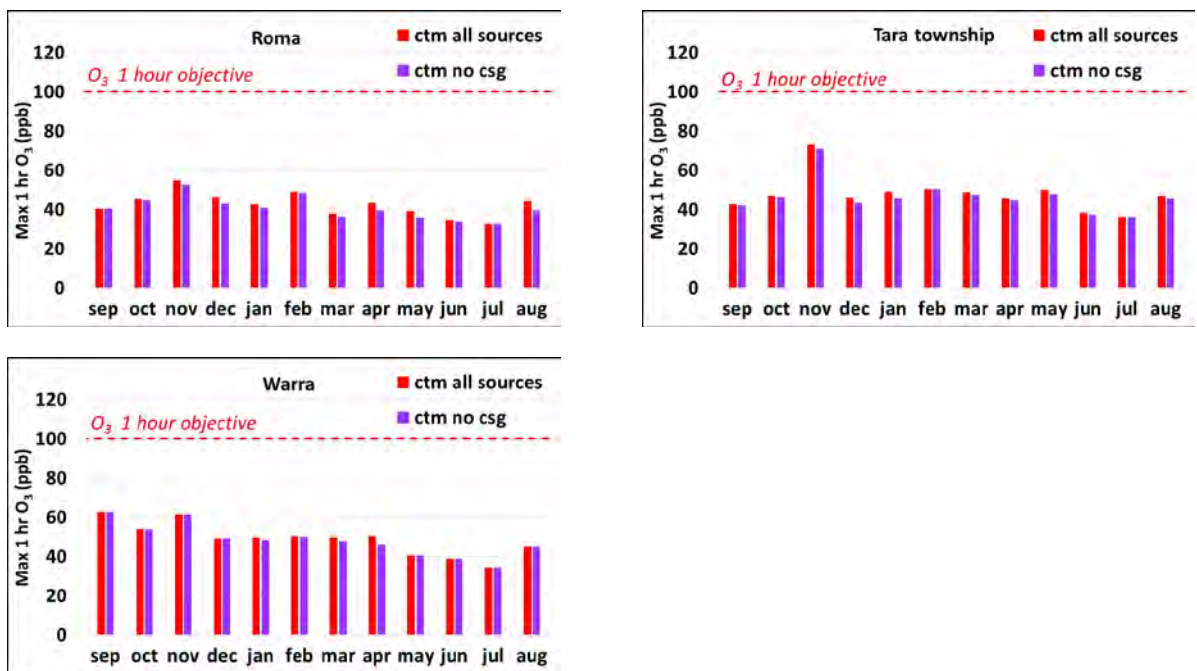
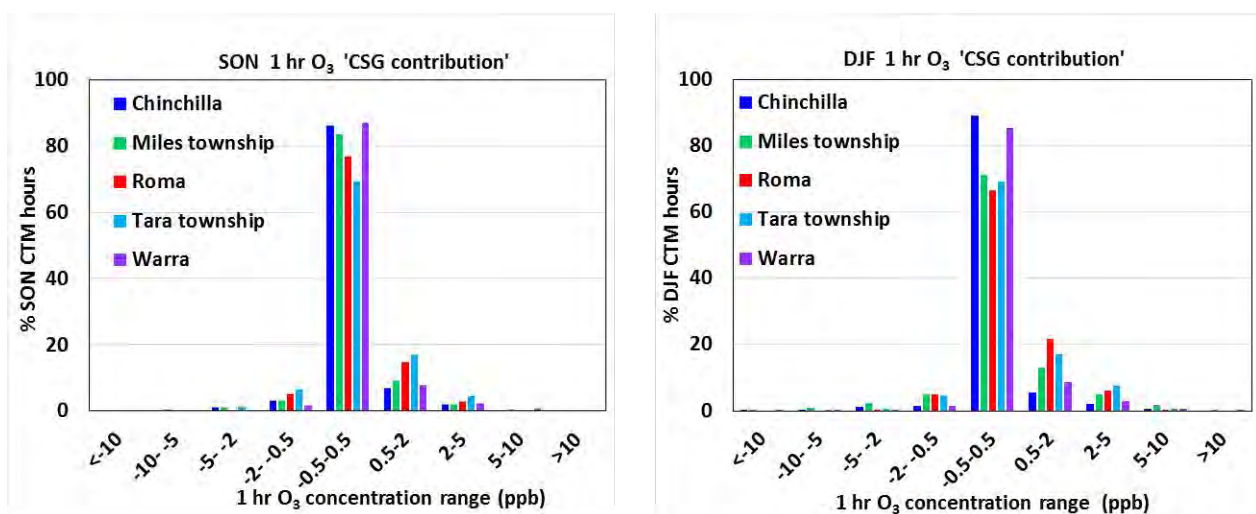


Figure F.7 The modelled maximum 1-hour average O₃ concentrations (ppb) for each month of September 2015 – August 2016 at the Town sites: model results with all sources (red) and model results without CSG sources (purple).

The modelled contribution from the CSG-related emissions to the 1-hour average O₃ concentrations at each of the Town sites is presented in Figure 5.26 F.8. Each plot shows the percentage of model hours within each season for the modelled contribution from the CSG-related emissions to the 1-hour average O₃ concentrations.

On average 99 % of the time the contribution from the CSG-related emissions at the Town sites is within ± 5 ppb which is 5 % of the 1-hour O₃ air quality objective (100 ppb, Table 5.1). The lowest frequency of change is at Chinchilla and Warra except during JJA. The largest frequency of changes is modelled at Roma in DJF and MAM.



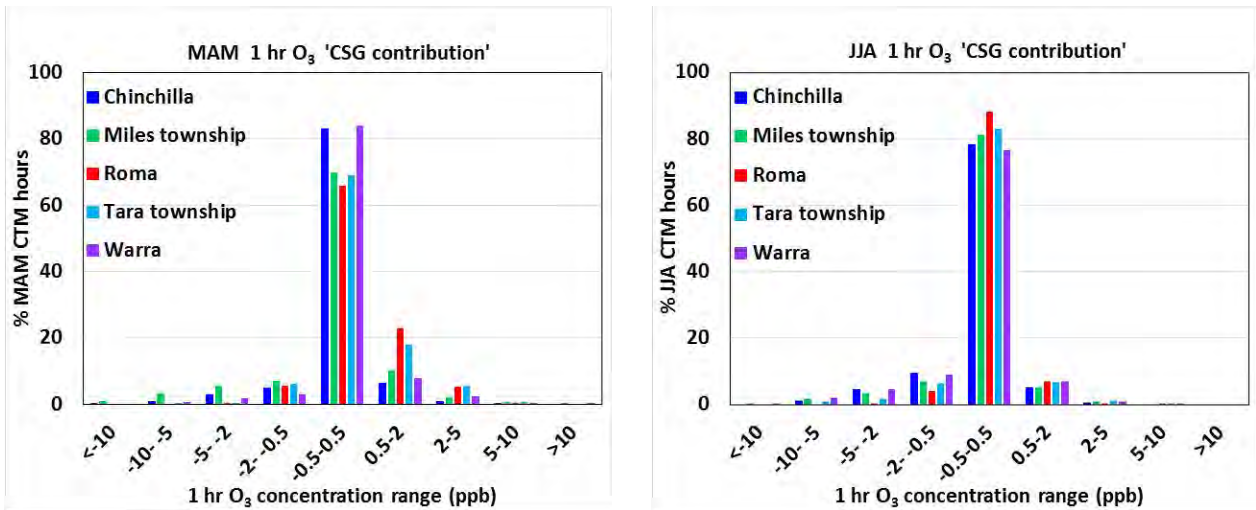
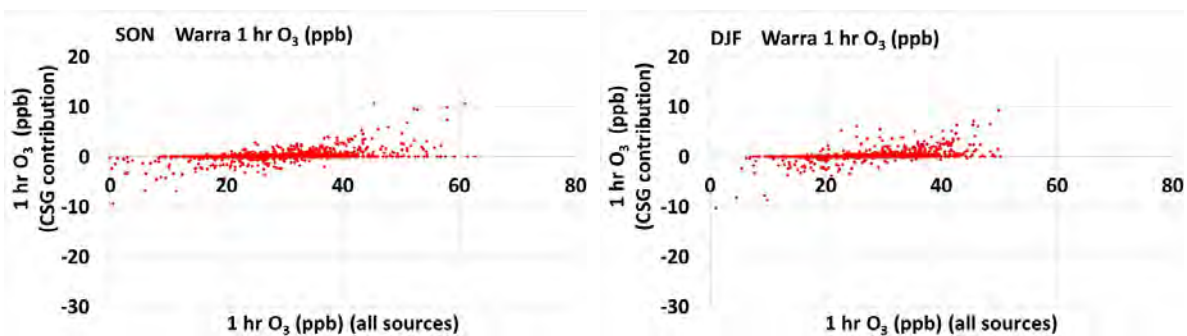


Figure F.8 The modelled contribution from the CSG related emissions to the 1-hour average O_3 concentration (ppb) at the Town sites shown as a frequency distribution for each season. The x-axis shows the concentration ranges of the contribution from the CSG-related emissions and the y-axis shows the percentage of model hours.

Figure F.9 shows plots of the modelled 1-hour average O_3 concentrations with all sources against the contribution from the CSG-related emissions to the modelled 1-hour average O_3 concentrations at Warra, one of the Town sites. The plots are seasonal and one point is plotted for each modelled hour. Results at Warra are representative of those at the other Town sites and those for the 4-hour average O_3 . The results from Warra are also similar to those at the Gas field and Regional sites. The largest changes in the 1-hour O_3 concentrations due to the CSG-related emissions occur at the maximum or minimum values of O_3 concentrations. Of the Town sites Roma shows the smallest changes due to CSG.



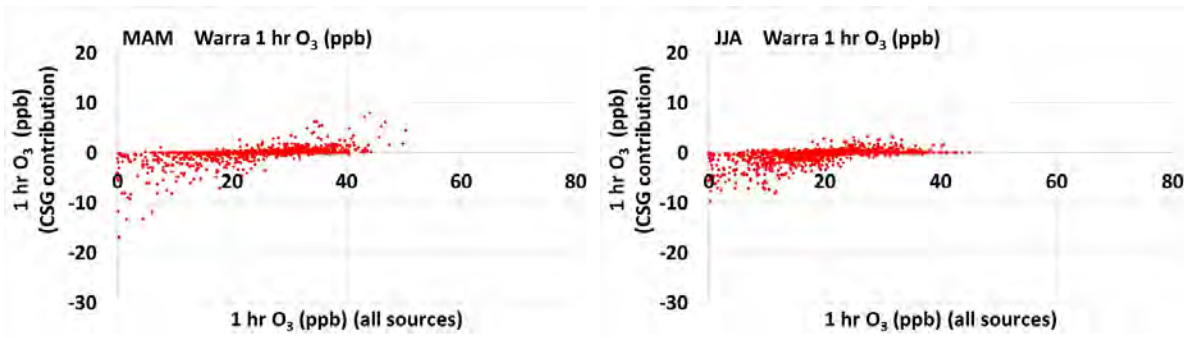


Figure F.9 The modelled contribution from the CSG related emissions to the 1-hour average O₃ concentration (ppb) at Warra shown as a scatter plot for each season. The x-axis shows the modelled 1-hour average O₃ concentrations with all sources (ppb) and the y-axis shows the contribution from the CSG-related emissions to the 1-hour average O₃ concentration (ppb).

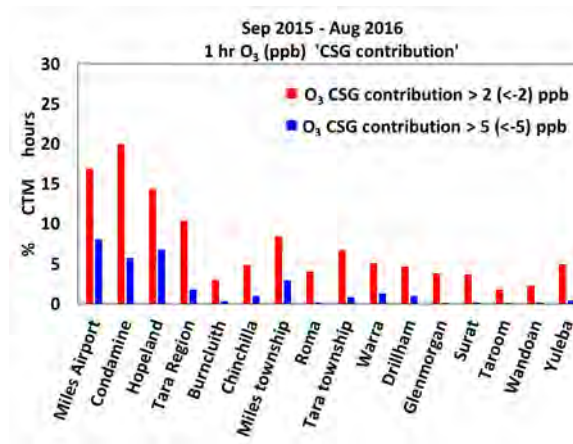


Figure F.10 Percentage of model hours in the year where the contribution to the 1-hour average O₃ concentration due to the CSG-related emissions is greater than 2 (or less than -2) ppb (red) or greater than 5 (or less than -5) ppb (blue). Note that 2 and 5 ppb are 2 and 5 % respectively of the 1-hour O₃ air quality objective.

Appendix G Extra Town sites frequency plots

Appendix G show the modelled contribution from the CSG-related emissions to the 24-hour average PM_{2.5}, 1 and 4-hour average O₃, 1-hour average NO₂, 8-hour average CO and 24-hour average formaldehyde concentrations, respectively, at each of the Extra town sites. Each plot shows the contribution due to the CSG-related emissions as a frequency distribution for each season. At the Extra Town sites the contribution due to the CSG-related emissions:

- For the 24-hour average PM_{2.5} concentrations on average 99.9 % of the time the contribution is less than 0.5 µg m⁻³ which is 1 % of the air quality objective.
- For the 1-hour average O₃ concentrations on average 99.8 % of the time the contribution is within ± 5 ppb which is 5 % of the 1-hour O₃ air quality objective.
- For the 4-hour average O₃ concentrations on average 99.6 % of the time the contribution is within ± 5 ppb which is 6.25 % of the 4-hour O₃ air quality objective.
- For the 1-hour average NO₂ concentrations on average 99.9 % of the time the contribution is less than 5 ppb which is 4 % of the 1-hour NO₂ air quality objective.
- For the 8-hour average CO concentrations on average 99.9 % of the time the contribution is less than 10 ppb which is 0.1 % of the 8-hour CO air quality objective.
- For the 24-hour average formaldehyde concentrations on average 100 % of the time the contribution is less than 0.2 ppb which is 0.5 % of the 24-hour formaldehyde air quality objective.

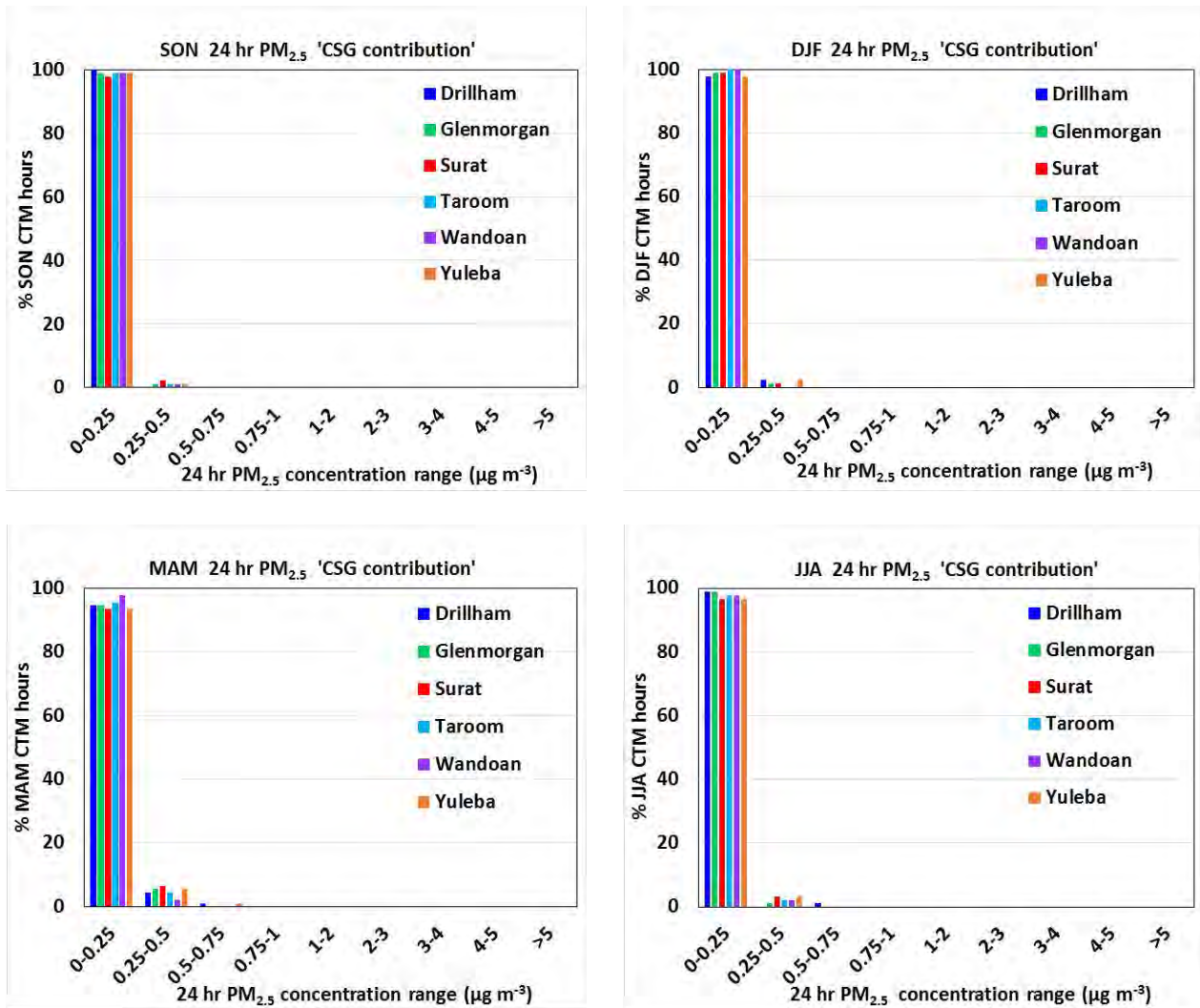


Figure G.1 The modelled contribution from the CSG-related emissions to the 24-hour average PM_{2.5} concentration (µg m⁻³) at the Extra town sites shown as a frequency distribution for each season. The x-axis shows the concentration ranges of the contribution from the CSG-related emissions and the y-axis shows the percentage of model hours.

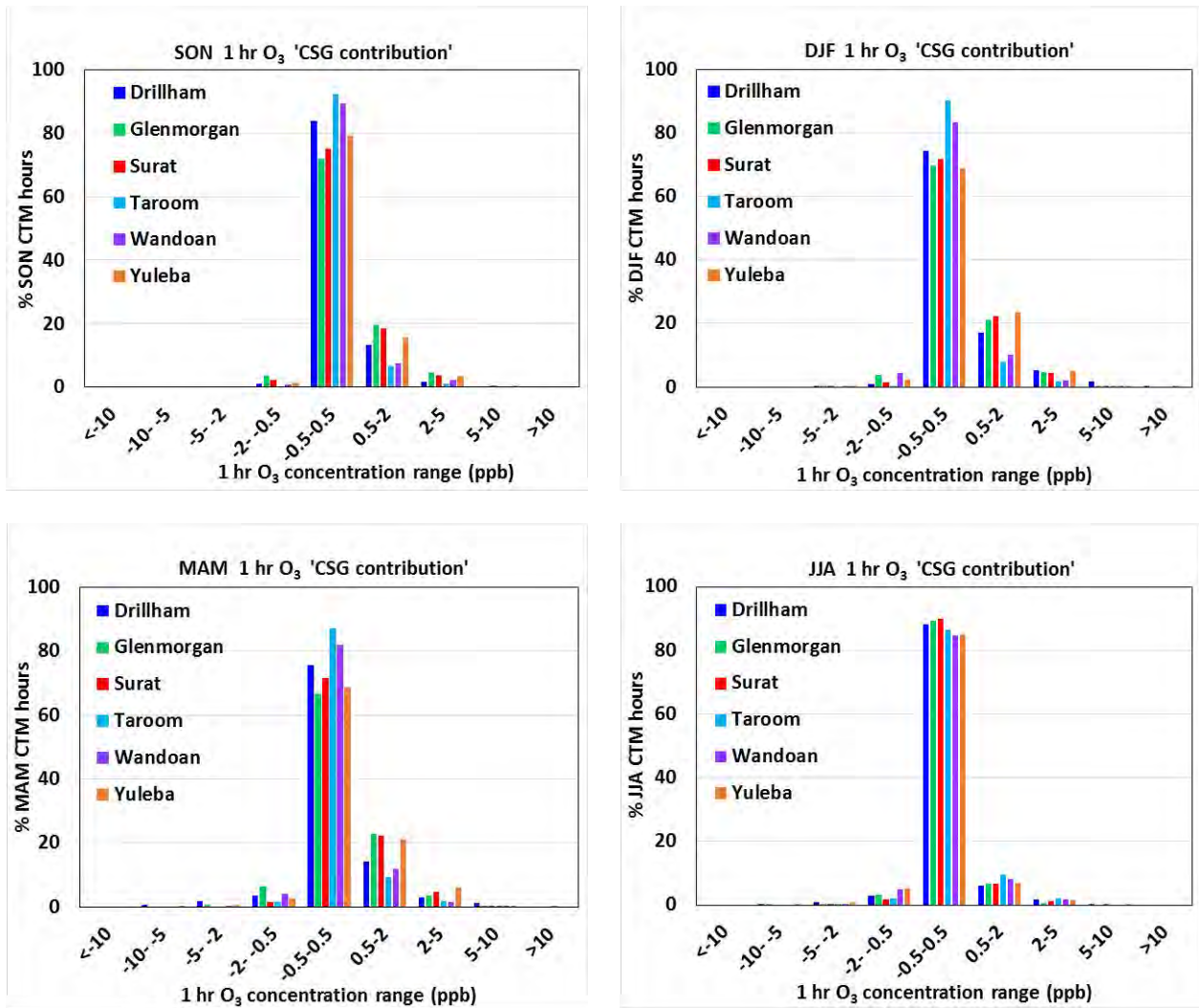


Figure G.2 The modelled contribution from the CSG-related emissions to the 1-hour average O₃ concentration (ppb) at the Extra town sites shown as a frequency distribution for each season. The x-axis shows the concentration ranges of the contribution from the CSG-related emissions and the y-axis shows the percentage of model hours.

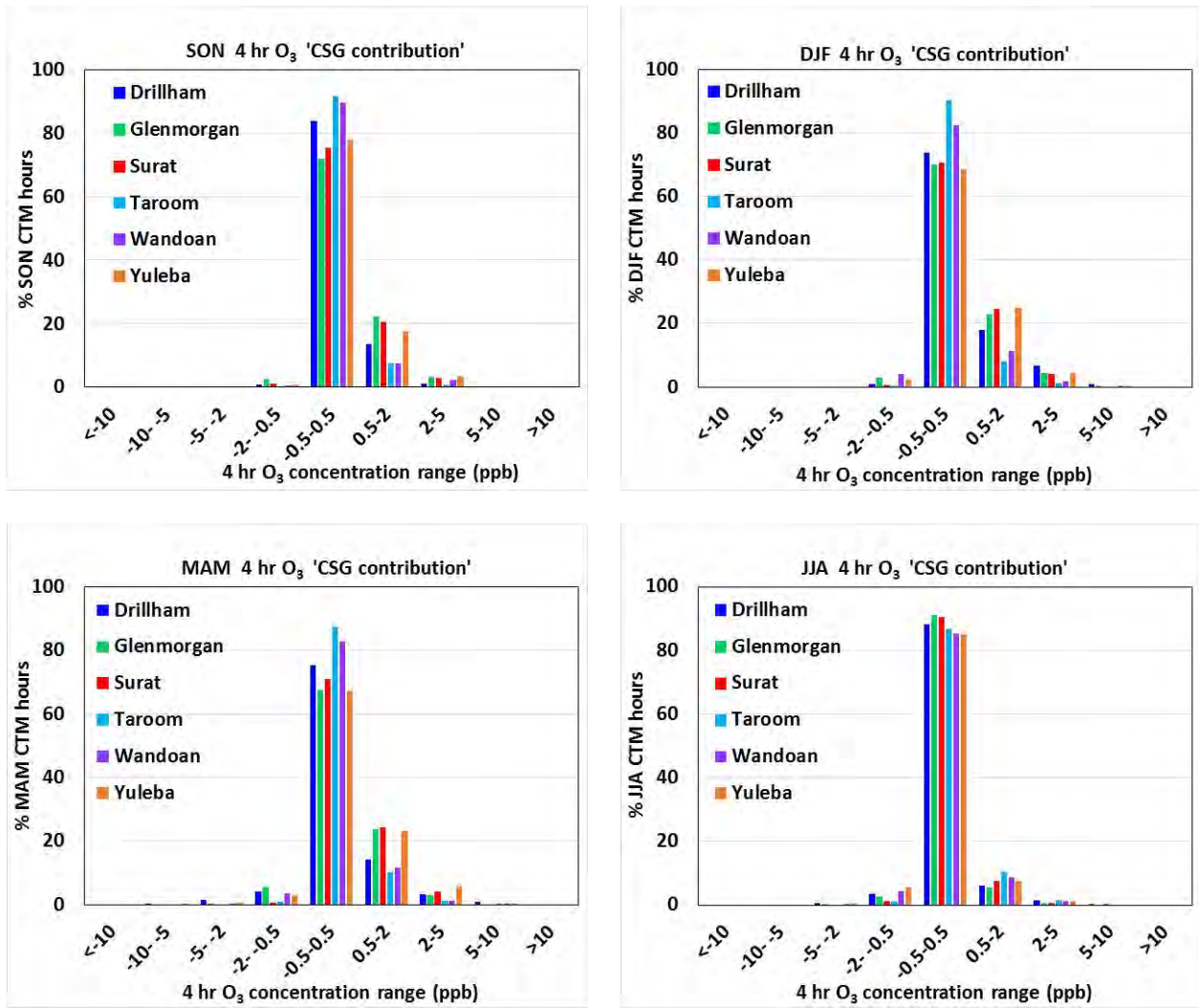


Figure G.3 The modelled contribution from the CSG-related emissions to the 4-hour average O₃ concentration (ppb) at the Extra town sites shown as a frequency distribution for each season. The x-axis shows the concentration ranges of the contribution from the CSG-related emissions and the y-axis shows the percentage of model hours.

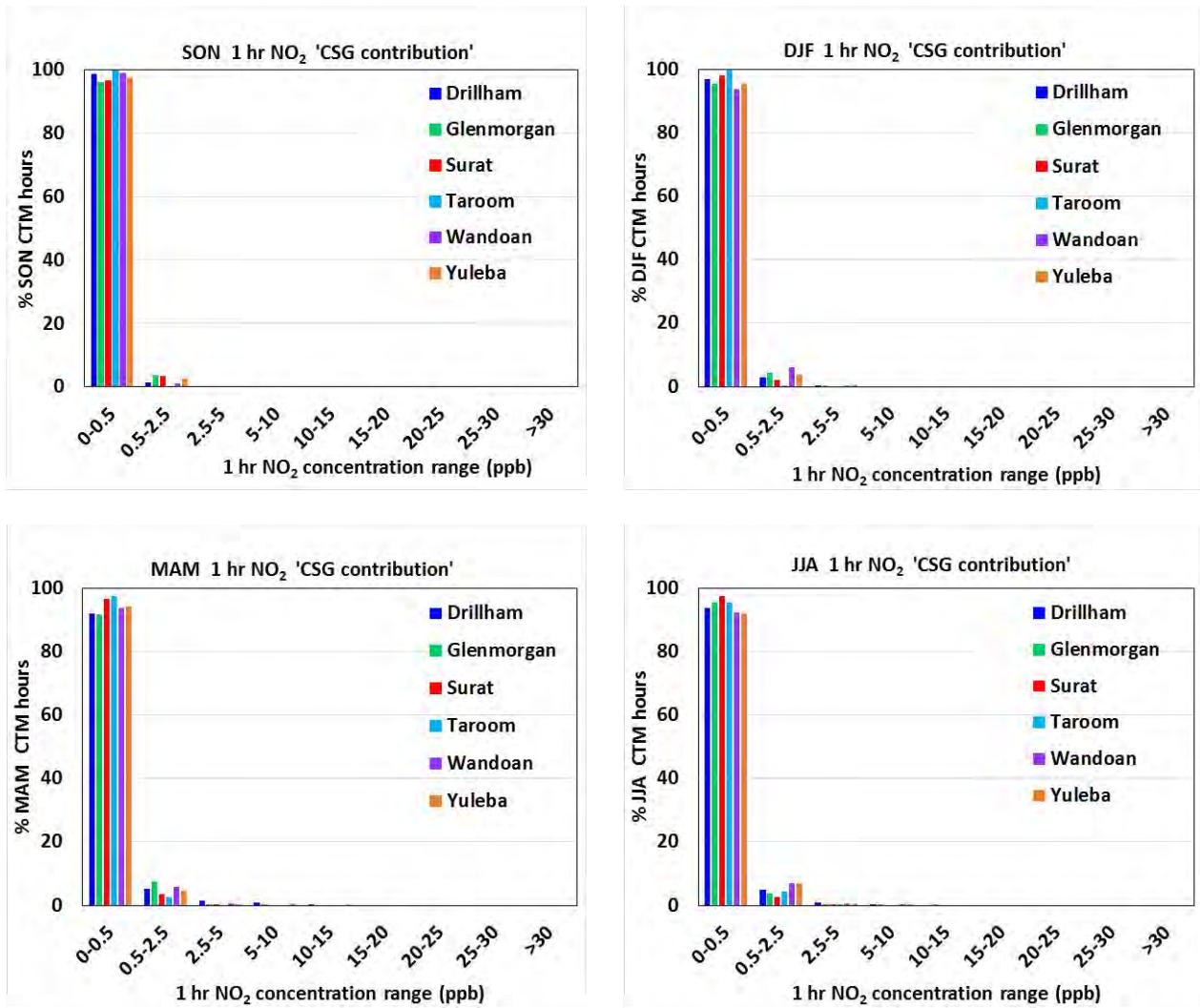


Figure G.4 The modelled contribution from the CSG-related emissions to the 1-hour average NO₂ concentration (ppb) at the Extra town sites shown as a frequency distribution for each season. The x-axis shows the concentration ranges of the contribution from the CSG-related emissions and the y-axis shows the percentage of model hours.

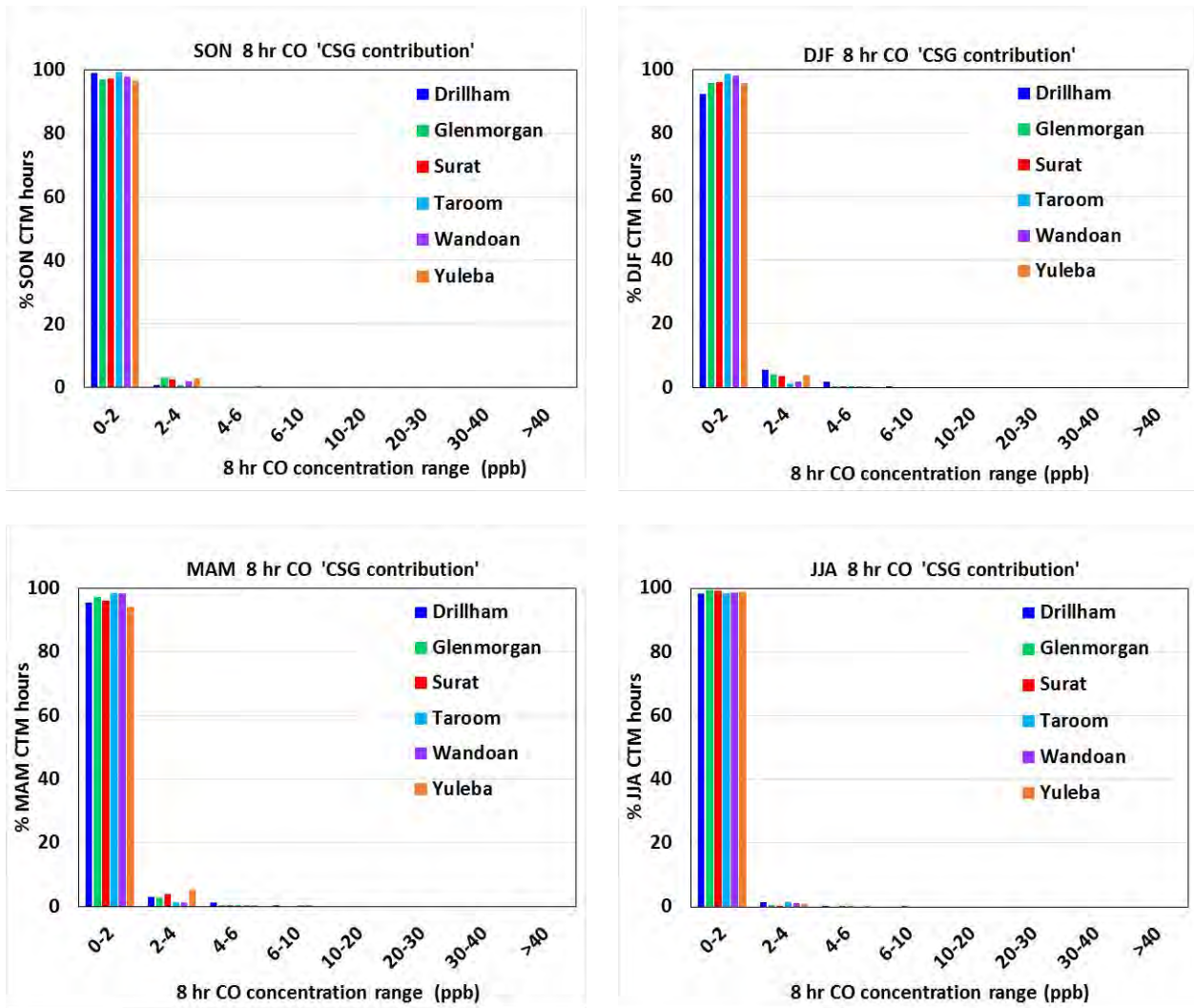


Figure G.5 The modelled contribution from the CSG-related emissions to the 8-hour average CO concentration (ppb) at the Extra town sites shown as a frequency distribution for each season. The x-axis shows the concentration ranges of the contribution from the CSG-related emissions and the y-axis shows the percentage of model hours.

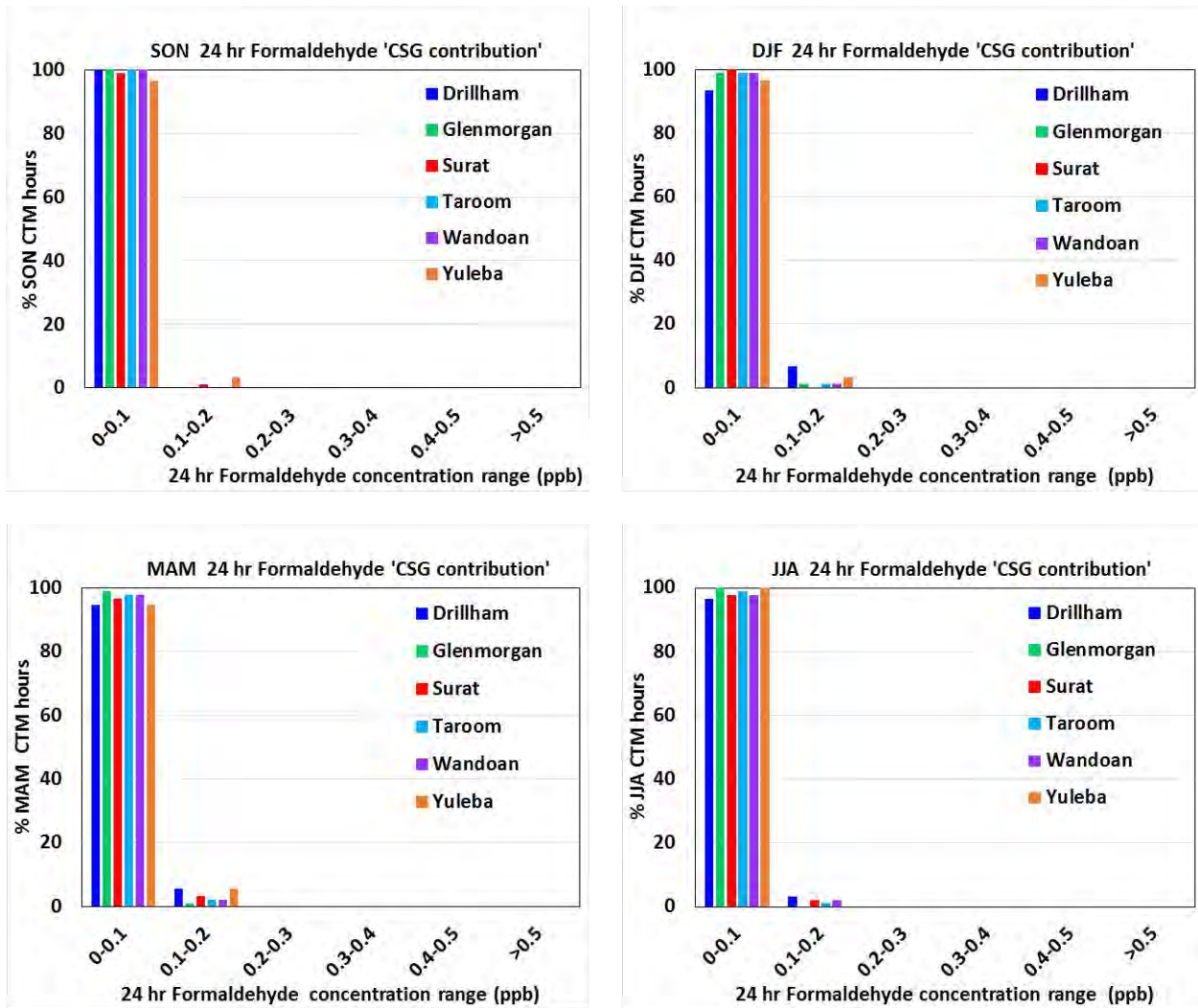


Figure G.6 The modelled contribution from the CSG-related emissions to the 24-hour average formaldehyde concentration (ppb) at the Extra town sites shown as a frequency distribution for each season. The x-axis shows the concentration ranges of the contribution from the CSG-related emissions and the y-axis shows the percentage of model hours.

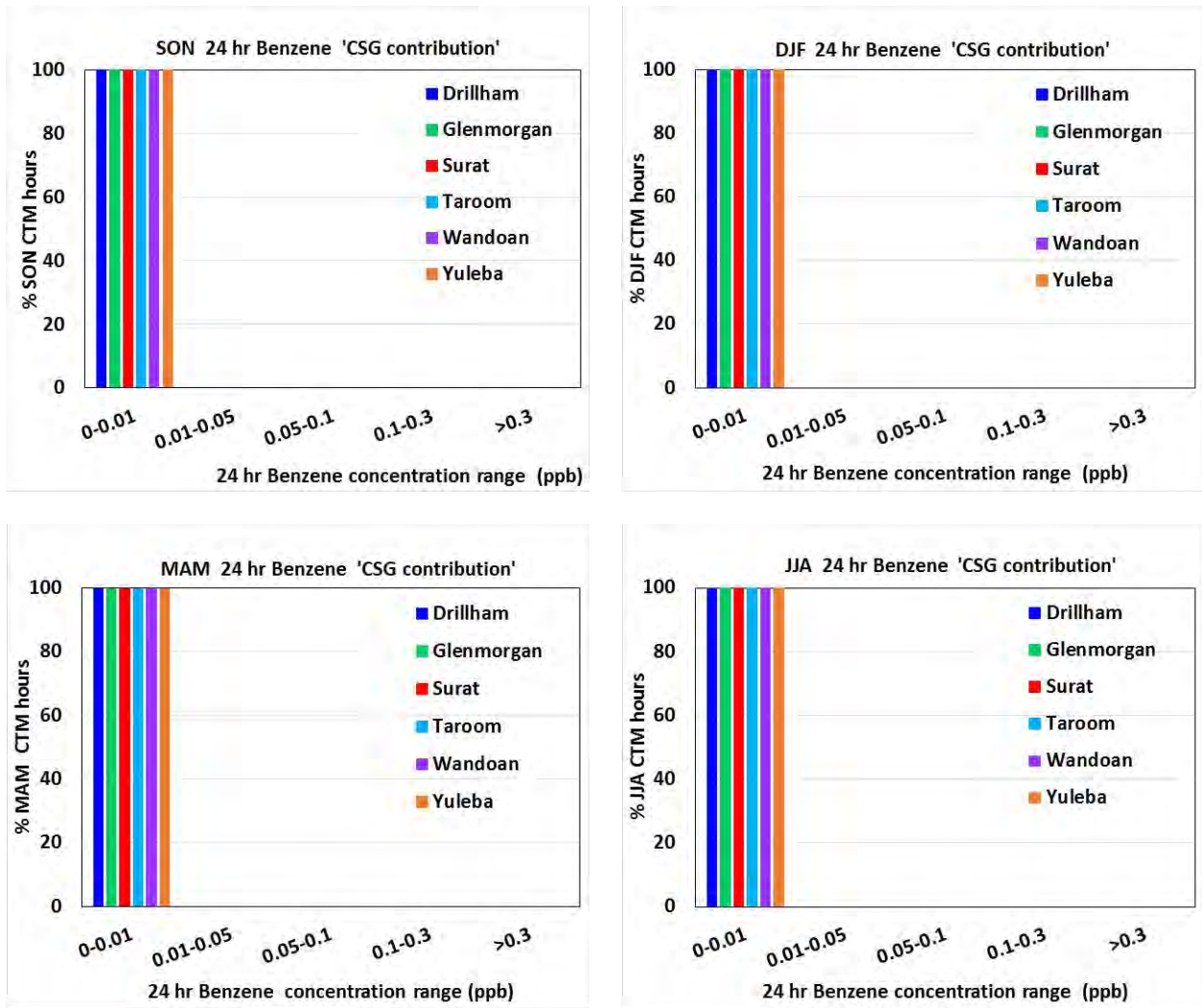


Figure G.7 The modelled contribution from the CSG-related emissions to the 24-hour average benzene concentration (ppb) at the Extra town sites shown as a frequency distribution for each season. The x-axis shows the concentration ranges of the contribution from the CSG-related emissions and the y-axis shows the percentage of model hours.

CONTACT US

t 1300 363 400
+61 3 9545 2176
e csiroenquiries@csiro.au
w www.csiro.au

FOR FURTHER INFORMATION

CSIRO Oceans and Atmosphere
Sarah Lawson
t +61 3 9239 4400
e sarah.lawson@csiro.au
w www.csiro.au/en/Research/OandA

AT CSIRO, WE DO THE EXTRAORDINARY EVERY DAY

We innovate for tomorrow and help improve today – for our customers, all Australians and the world.

Our innovations contribute billions of dollars to the Australian economy every year. As the largest patent holder in the nation, our vast wealth of intellectual property has led to more than 150 spin-off companies.

With more than 5,000 experts and a burning desire to get things done, we are Australia's catalyst for innovation.

CSIRO. WE IMAGINE. WE COLLABORATE.
WE INNOVATE.